ipcc

INTERGOVERNMENTAL PANEL ON climate change

Climate Change 2021

The Physical Science Basis

Summary for Policymakers, Technical Summary, Frequently Asked Questions and Glossary

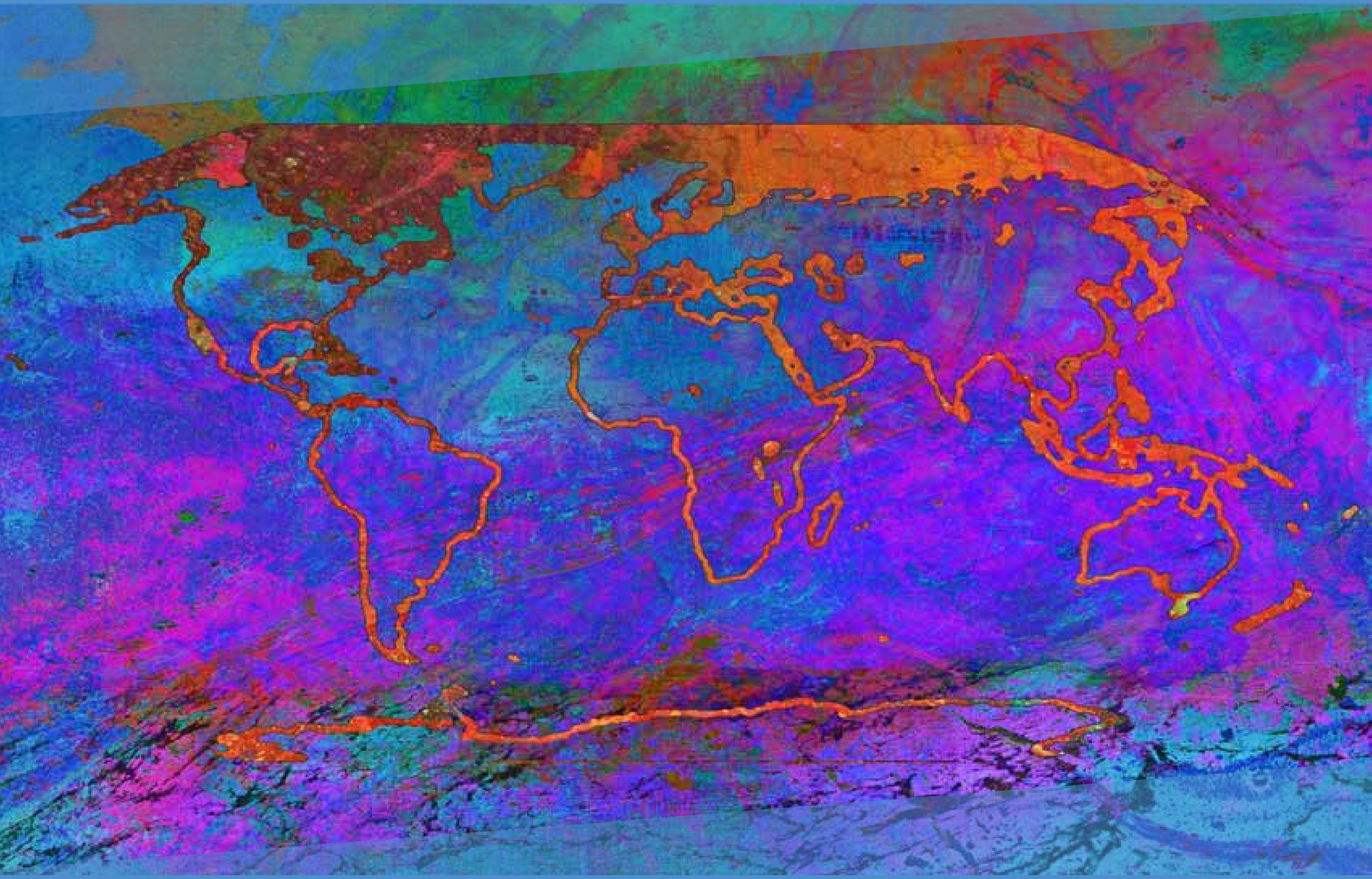

WGI

Working Group I Contribution to the
Sixth Assessment Report of the
Intergovernmental Panel on Climate Change

WMO UNEP

Climate Change 2021
The Physical Science Basis

Summary for Policymakers
Technical Summary
Frequently Asked Questions
Glossary

Part of the Working Group I Contribution to the Sixth Assessment Report of the Intergovernmental Panel on Climate Change

Edited by

Valérie Masson-Delmotte
Co-Chair Working Group I

Panmao Zhai
Co-Chair Working Group I

Anna Pirani
Head of TSU

Sarah L. Connors
Head of Science Team

Clotilde Péan
Head of Operations

Yang Chen
Senior Science officer

Leah Goldfarb
Senior Science officer

Melissa I. Gomis
Senior Science officer

J.B. Robin Matthews
Senior Science officer

Sophie Berger
Science Officer

Mengtian Huang
Science Officer

Ozge Yelekçi
Science Officer

Rong Yu
Science Officer

Baiquan Zhou
Science Officer

Elisabeth Lonnoy
Project Assistant

Thomas K. Maycock
Science Editor

Tim Waterfield
IT Officer

Katherine Leitzell
Communication Manager

Nada Caud
Outreach Manager

Working Group I Technical Support Unit

Electronic copies of this report are available from the IPCC website www.ipcc.ch

ISBN 978-92-9169-163-0

Front cover artwork: *Changing* by Alisa Singer, www.environmentalgraphiti.org © 2021 Alisa Singer.

Foreword, Preface and Dedication

Foreword

It is unequivocal that human activities have heated our climate. Recent changes are rapid, intensifying, and unprecedented over centuries to thousands of years. With each additional increment of warming, these changes will become larger, resulting in long-lasting, irreversible implications, in particular for sea level rise. United Nations Secretary-General António Guterres has stated that 'the evidence is irrefutable' and 'we see the warning signs in every continent and region'.

The Working Group I contribution to the Intergovernmental Panel on Climate Change (IPCC) Sixth Assessment Report provides a reality check on climate change. We now have a much clearer picture of the past, present and possible future climates, and this information is essential for understanding where we are headed, what can be done, and the multiple facets of a changing climate to prepare for, in every region. Unless deep reductions in greenhouse gas emissions occur in the coming decades, global warming of 1.5°C and 2°C above pre-industrial levels will be exceeded during the 21st century.

The new Working Group I Report structure integrates multiple lines of scientific evidence within each chapter and provides robust knowledge relevant for policymaking through the end-to-end assessment of key topics. This more holistic approach has resulted in a report that provides a better understanding of the climate system, for both past and future changes, with a new emphasis on climate information for regions, which is critical for informing adaptation and risk management strategies. Today, many decisions remain grounded in the experience of past climate variability. This report provides a solid basis for taking into account future changes that need to be considered in today's decisions, with increased relevance for climate services, to enhance adaptation and resilience to climate change and curb greenhouse gas emissions.

The journey of this report reflects extraordinary efforts by all contributors under exceptional circumstances. The COVID-19 pandemic, which started during the review of the Second Order Draft, disrupted the process. However, the early response of Working Group I, through the hard work of the authors, review editors, chapter scientists, the Technical Support Unit, and Bureau members, made it possible to deliver a report that meets the most stringent science quality standards, thanks to the in-depth, broad review process, with an exhaustive, robust, rigorous and transparent assessment of the latest state of climate science knowledge. We commend the additional efforts taken, including by all reviewers from the research community and government representatives who adapted to a new way of working to complete this vital report. Our particular appreciation goes to the Working Group I Co-Chairs Valérie Masson-Delmotte and Panmao Zhai for their leadership throughout the process. Their extraordinary efforts ensured that this robust and clear report is available to the world today.

This Working Group I contribution to the IPCC's Sixth Assessment Report covers important new advances in climate science that provide an invaluable input into climate negotiations and decision-making, with an emphasis on key conditions that, from a physical science basis, are needed to limit global warming and inform risk assessment and regional adaptation. The report was welcomed at the 26th Conference of the Parties to the United Nations Framework Convention on Climate Change. It will also inform the 2023 global stocktake. Unless there are deep reductions in global greenhouse gas emissions, the goal of limiting warming well below 2°C and close to 1.5°C will be out of reach.

The science is unequivocal, the changes are unprecedented, and there is no more time for delay.

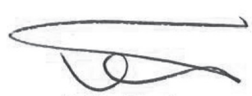

Petteri Taalas
Secretary-General
World Meteorological Organization

Inger Andersen
Executive Director
United Nations Environment Programme

Preface

The Working Group I (WGI) contribution to the Sixth Assessment Report (AR6) of the Intergovernmental Panel on Climate Change (IPCC) focuses on a full and comprehensive assessment of the physical science basis of climate change, based on evidence from more than 14,000 scientific publications available by 31 January 2021.

This Report reflects recent climate science advances resulting from progress in, and the integration of, multiple lines of evidence, including: in situ and remote observations; paleoclimate information; understanding of climate drivers and physical, chemical and biological processes and feedbacks; and global and regional climate modelling; as well as advances in methods of analyses and insights from the growing field of climate services.

The AR6 WGI Report builds on the WGI contribution to the IPCC's Fifth Assessment Report (AR5) in 2013, and the AR6 Special Reports[1] released in 2018 and 2019.

The report considers the current state of the climate in the long-term context, the understanding of human influence, the state of knowledge about possible climate futures, climate information relevant for climate-related risk assessment and regional adaptation, and the physical science basis on limiting human-induced climate change.

Scope of the Report

As part of the scoping process and approval of the outline of the IPCC Sixth Assessment Report, the WGI contribution evolved from the structure of past WGI assessment reports, reflecting developments in climate science and the assessment of global and regional climate information that is relevant to inform decision-making.

Some key new topics assessed by WGI include the global response to new illustrative emissions scenarios, physical climate storylines, low-likelihood, high-impact outcomes, and physical climate conditions that affect society and/or ecosystems (defined as climatic impact-drivers).

The integration of multiple lines of evidence strengthens the understanding of past, current and possible future changes in the climate system and the distillation of regional climate change information at regional scale. The new structure of the WGI Report is designed to facilitate this integration for end-to-end assessment of key topics and to enhance the visibility of knowledge developments for global and regional climate change. This includes climate information that is relevant for risk assessment, regional adaptation and for mitigation. It is also designed to inform decision-making without being policy prescriptive and to facilitate the integration of the WGI key findings with the other AR6 Working Group reports.

Structure of the Report

This Report consists of thirteen thematic chapters with their supporting supplementary material, ten annexes (including the report Glossary, which is developed in coordination with Working Groups II and III where relevant), an integrative Technical Summary, and a Summary for Policymakers. An innovation in this Working Group I assessment is the online Interactive Atlas (https://interactive-atlas.ipcc.ch), a novel tool for flexible spatial and temporal analyses of observed and projected climate change information, which enhances accessibility for stakeholders and users to the data assessed in the Report.

The Summary for Policymakers and Technical Summary include the line of sight, indicated in curly brackets, to the chapters and the specific sections therein where the detailed assessment can be found. In this way, these summary components of the Report provide a roadmap to the contents of the entire report and a synthesis of the major findings that is traceable to the underlying literature and assessment.

The introduction (Chapter 1) of the Report frames the WGI assessment within the broader AR6 and global climate policy context and introduces the key concepts, lines of evidence, and major developments. The remainder of the Report is structured in three segments. The first segment focuses on large-scale climate change (Chapters 2–4). These chapters provide an updated and comprehensive assessment of knowledge about the current state of the climate system, human influence and projections of future change on key large-scale indicators of the climate system. Chapter 2 assesses observed large-scale changes in the climate system in the long-term paleoclimate context. Chapter 3 updates the assessment of human influence on the climate system, considering natural variability, model performance and detection and attribution. Chapter 4 covers global climate projections spanning time horizons from the near term (2021–2040) to the mid-term (2041–2060), long term (2081–2100) and beyond.

The second segment of the report is dedicated to climate system components and processes that play key roles in global and regional climate (Chapters 5–9), including carbon and other biogeochemical cycles, energy, and water; short-lived climate forcers (SLCFs) and their link to air quality; and changes in the ocean, cryosphere and sea level. Chapter 5 addresses the assessment of the global biogeochemical budgets for carbon dioxide, methane, and nitrous

1 Global warming of 1.5°C: an IPCC special report on the impacts of global warming of 1.5°C above pre-industrial levels and related global greenhouse gas emission pathways, in the context of strengthening the global response to the threat of climate change, sustainable development, and efforts to eradicate poverty (SR1.5); Climate Change and Land: an IPCC special report on climate change, desertification, land degradation, sustainable land management, food security, and greenhouse gas fluxes in terrestrial ecosystems (SRCCL); IPCC Special Report on the Ocean and Cryosphere in a Changing Climate (SROCC).

oxide and the assessment of carbon and other biogeochemical feedbacks. Chapter 6 assesses changes in the emissions and abundances of individual SLCFs, how these changes affect Earth's energy balance through radiative forcing and feedback in the climate system, the implications of changing climate on air quality, and the implications of SLCF mitigation for climate and for air quality. Chapter 7 addresses Earth's energy budget through advances in observations, understanding and quantification of effective radiative forcing, and the assessment of feedbacks and climate sensitivity. Chapter 8 assesses observed and projected changes in the global water cycle, the physical understanding of the complexity of its response to multiple drivers, and implications for water availability. The physical processes underlying global and regional changes in the ocean, cryosphere and sea level and the understanding of observed and projected future changes since the AR5 and Special Report on the Ocean and Cryosphere in a Changing Climate are assessed in Chapter 9.

The final four chapters of the Report (Chapters 10–12 and the Atlas) are dedicated to the assessment and distillation of regional climate information from multiple lines of evidence at sub-continental to local scales (including urban climate), building on information from previous chapters on large-scale climate and process understanding, with a focus on recent and projected regional changes in mean climate, extremes, and climatic impact-drivers. Chapter 10 assesses the foundations of how regional climate information is distilled from multiple lines of evidence and the interplay between anthropogenic causes and internal variability at regional scales. Chapter 11 addresses changes in weather and climate extremes on global and regional scales, including observed changes and their attribution, as well as projected changes. Chapter 12 assesses the climatic conditions that may lead to impacts and risks across the world's regions. Changes in mean climate at regional scales, in particular observed trends and their attribution and projected future changes in temperature and precipitation, are assessed in the Atlas chapter.

The Interactive Atlas allows flexible spatial and temporal analyses of climate variables, extreme indices and climatic impact-drivers, including datasets underpinning assessment findings across report chapters and syntheses of regional changes.

Specific regional case studies are considered in different chapters, including rainfall changes in the Sahel and Western Africa, South-Western North America, and South-Eastern South America; climate information relevant for water resources in small islands, for Cape Town drought, for the Indian summer monsoon, for Mediterranean summer warming, and for the Hindu Kush Himalaya region; urban climate processes and trends; and the influence of the Arctic on mid-latitude climate.

All chapters contain Frequently Asked Questions, which are grounded in the assessment and written in language that is more accessible to a broad readership and can serve as a resource for teaching and outreach.

Each chapter is accompanied by Supplementary Material, which is available online and provides traceability and transparency for technical aspects of the assessment, such as descriptions of datasets, models or methodologies supporting chapter analyses.

The Process

This WGI Assessment Report represents the combined efforts of hundreds of leading experts in the field of climate science and has been prepared in accordance with principles and procedures of the IPCC.

A scoping meeting for the Sixth Assessment Report was held in May 2017, and the outlines for the contributions of the three Working Groups were approved at the 46th Session of the Panel in September 2017. Governments and IPCC observer organizations nominated experts for the author team. The team of 198 Coordinating Lead Authors and Lead Authors plus 36 Review Editors selected by the WGI Bureau was accepted at the 55th Session of the IPCC Bureau in January 2018. During the report preparation, a few changes have taken place to address core expertise gaps and to replace authors who were not available anymore. In addition, 615 Contributing Authors provided information to the author teams at their request.

Drafts prepared by the authors were subject to two rounds of formal review and revision followed by a final round of government comments on the Summary for Policymakers. A total of 78,007 written review comments were submitted by 1891 individual expert reviewers and 47 governments. The Review Editors for each chapter monitored the review process to ensure that all review comments received appropriate consideration. All review comments and responses are available online on the report website.

Three in-person Lead Author Meetings took place to enhance progress and coordination in the assessment process. These were particularly critical for the intense cross-chapter coordination implied by the new report outline.

We strived to foster an inclusive environment that achieves a rigorous and transparent assessment process. These efforts included greater attention to addressing implicit biases and technical considerations to enhance the participation in the process and increasing the accessibility of the assessed information.

For the first time in the IPCC, WGI recommended the implementation of FAIR (findable, accessible, interoperable, reusable) data principles in the assessment to document and curate the data assessed and included in report figures. The motivation was to increase transparency and accessibility of the assessment, support implementation of the IPCC Error Protocol, and provide for the long-term curation of the assessed digital information. This process was supported by our close collaboration with the IPCC Task Group on Data Support for Climate Change Assessments (TG-Data) established in March 2018.

The COVID-19 pandemic was declared by the World Health Organization at the start the Second Order Draft review. Following an extensive consultation process with IPCC member countries, authors and the scientific community, including editors of relevant science journals, the timeline of the report was extended by four months to balance the delays and challenges faced by authors and the scientific community with maintaining momentum and timeliness in the assessment process. The review process is critical for the rigor, objectivity and comprehensiveness of the assessment. The adjustments to the timeline facilitated broad participation from scientists and governments in the review process. Stringent scientific rigor and quality of the assessment were maintained despite the pandemic.

The fourth Lead Author Meeting, due to be held in June 2020, was replaced by extensive virtual activities to address the Second Order Draft review comments and topics that cut across multiple chapters. A final virtual Lead Author Meeting was held in February 2021 to finalize the report. Drafting meetings for the Summary for Policymakers also took place through virtual meetings.

Addressing the implications of the COVID-19 pandemic on the assessment process required innovation to facilitate international virtual collaboration, including extra support and training for participants and facilitators, support for participants with internet connectivity challenges, additional advance preparation, shorter and more focused meetings with clear agendas and objectives and duplicated to account for time zones of participants, high levels of transparency – including the provision of written summaries of meetings and decisions, and allotting time for asynchronous contributions to the discussion and decision-making process.

Documenting and understanding barriers to participation due to an increased reliance on online activities and the use of inclusive practices required priority attention in these novel conditions. We gained experience in applying methods to facilitate participatory and inclusive processes in the assessment and recognized the necessity of fostering these approaches over the course of the assessment process, both during and in-between meetings, to build a stronger community of practice within this unique international context. This will be an important legacy for future assessment cycles.

The preparation of the WGI AR6 report was also informed by recommendations from several IPCC expert meetings. The first meeting focused on assessing climate information for regions (in 2018, co-organized by WGI and WGII, and hosted at ICTP, Trieste, Italy), which provided a scoping of the Interactive Atlas. A second meeting focused on short-lived climate forcers (in 2018, co-organized by TFI and WGI, and hosted by the World Meteorological Organization in Geneva, Switzerland), which identified science advances in the understanding of emissions and climate effects of SLCFs and needs for improvements in emission inventories and methodologies. A third meeting on mitigation, sustainability, and climate stabilization scenarios (in 2019, organized by WGIII in Addis Ababa, Ethiopia), led to cross-WG coordination related to scenarios. Recommendations for clarity and readability from the 2016 IPCC Expert Meeting on Communication (organized by the IPCC Secretariat in Oslo, Norway) were taken into account in developing technical guidance, training and resources provided to authors and in particular for the preparation of the text and figures of the Frequently Asked Questions and the Summary for Policymakers.

The Summary for Policymakers was approved line-by-line during the first-ever virtual IPCC approval session, the 14th Session of IPCC Working Group I from 26 July – 06 August 2021, and the underlying Report was accepted during the 54th Session of the IPCC on the 6th August 2021.

Acknowledgements

We are very grateful for the exceptional rigor and dedication of the volunteer Coordinating Lead Authors and Lead Authors throughout this process, who delivered the most comprehensive assessment ever of our physical understanding of climate change. We thank the Review Editors for working alongside the author teams to ensure that the chapters are fully reflective of the input provided through the review process. We express our sincere appreciation to all the government and expert reviewers, including several group reviews from early-career scientists. We thank the many Contributing Authors who provided input and important support to the authors.

A special thanks goes to the Chapter Scientists of this report who went above and beyond what was expected of them: Kari Alterskjaer, Lisa Bock, Katherine Dooley, Gregory Garner, Mathias Hauser, Tim Hermans, Lijuan Hua, Carley Iles, Maialen Iturbide, Laurice Preciado Jamero, Martin Jury, Megan Kirchmeier Young, Chaincy Kuo, Hui-Wen Lai, Alice Lebehot, Elizaveta Malinina Rieger, Sebastian Milinkski, Therese Myslinski, Tamzin Palmer, Browdie Pearson, Stephane Senesi, Jérôme Servonnat, Chris Smith, David Smyth, Sabin Thazhe Purayil, Emilie Vanvyve, Tania Villasenor Jorquera, Hui Wan and Kyung-Sook Yu. Chapter scientists were recruited by and reported directly to the Coordinating Lead Author(s) and provided technical support to the chapters, including reference checking and compilation, figure drafting, traceability checking, identification of overlaps or inconsistencies across chapters, and technical editing.

We thank the Vice Chairs of the WGI Bureau for their dedication, guidance and wisdom throughout the preparation of the Report and their support for cross-Working Group coordination: Edvin Aldrian, Fatima Driouech, Gregory Flato, Jan Fuglestvedt, Muhammad I. Tariq, Carolina Vera and Noureddine Yassaa.

We gratefully acknowledge the support from the host countries and institutions of the WGI Lead Author Meetings (LAMs): China Meteorological Administration (CMA), China, for hosting the first LAM; Environment Canada, Canada, for hosting the second LAM; and Météo France, France, for hosting the third LAM. We also thank the Ministerio de Ciencia, Tecnologia, Conocimiento e Innovación and the Ministerio del Medio Ambiente, Chile, for offering to host the fourth LAM meeting that we were unable to hold in person due to the COVID-19 pandemic.

The support provided by governments and institutions, as well as through contributions to the IPCC Trust Fund, is thankfully acknowledged as it enabled the participation of the author teams in the preparation of the Report. The efficient operation of the WGI Technical Support Unit (TSU) was made possible by the generous financial support provided by the government of France and administrative and information technology support from the Université Paris Saclay (France), Institut Pierre Simon Laplace (IPSL) and the Laboratoire des Sciences du Climat et de l'Environnement (LSCE). We thank the Norwegian Environment Agency for supporting the preparation of the graphics for the Summary for Policymakers. We thank the United Nations Environment Programme Library for providing a service for authors to access literature.

The approval of the WGI Summary for Policymakers took place in an unprecedented context, with travel restrictions caused by the COVID-19 pandemic rendering an in-person IPCC Plenary session impossible. We thank the support and advice of the IPCC Executive Committee and the tireless work of the ad-hoc task group that was established to advise us as Co-Chairs in preparing for the approval session. The task group was led by IPCC Vice-Chair Ko Barrett and included WGI Vice-Chairs Fatima Driouech, Greg Flato and Edvin Aldrian; Anna Pirani and Sarah Connors of the WGI TSU; and Ermira Fida of the IPCC Secretariat. The task group prepared guidance for participants on the modalities of the session and a carefully structured meeting schedule to implement a virtual approval process.

The approval took place virtually for the first time and involved more than 186 hours of online meetings. We thank all participants for the remarkable collaborative spirit and rigorous work undertaken during the session. IPCC Vice Chairs Ko Barrett, Thelma Krug and Youba Sokona brought their unwavering support to facilitate discussions amongst authors and delegations and provided core support for the success of the approval process. We are also grateful to the Vice Chairs of WGI, as well as Mark Howden and Andy Reisinger, Vice Chairs of WGII and WGIII respectively, and Jim Skea, Co-Chair of WGIII, for their support to facilitate the discussions. The WGI TSU was joined by members of the WGII and WGIII TSUs, as well as past interns and chapter scientists to staff this Herculean coordination effort.

Our warmest thanks go to the collegial and collaborative support provided by Melinda Tignor, Elvira Poloczanska, Katja Mintenbeck, Bard Rama, Almut Niebuhr, Vincent Möller, Sina Löschke, Komila Nabiyeva, Andrés Alegría, Stefanie Langsdorf, Andrew Okem, Marlies Craig, Anka Mühle, Philisiwe Manqele, Stefan Weisfeld, Jussi Savolainen and Mallou from the Working Group II Technical Support Unit; Roger Fradera, Raphael Slade, Alaa Al Khourdajie, Minal Pathak, Sigourney Luz, Malek Belkacemi, David McCollum, Renée van Diemen, Shreya Some, Purvi Vyas, Juliette Malley and Géninha Lisboa from the Working Group III Technical Support Unit; and Noémie Le Prince-Ringuet from the Synthesis Report Technical Support Unit.

We are grateful for the close collaboration with authors and Bureau members from Working Group II and III, including as contributing authors in many parts of the report. We thank the Co-Chairs Debra Roberts, Hans-Otto Portner, Jim Skea and Priyadarshi R. Shukla for the collegial teamwork across Working Groups that has characterized the AR6. We also thank Eduardo Calvo Buendía and Kyoto Tanabe, Co-Chairs of the Task Force on Greenhouse Gas Inventories, for their support and collaboration.

We thank Hoesung Lee, Chair of the IPCC, Abdalah Mokssit, Secretary of the IPCC, and the staff of the IPCC Secretariat: Ermira Fida, Jonathan Lynn, Judith Ewa, Mxolisi Shongwe, Jennifer Lew Schneider, Jesbin Baidya, Werani Zabula, Nina Peeva, Melissa Walsh, Joelle Fernandez, Laura Biagioni and Oksana Ekzarkho for their guidance and support to implement the many facets of the IPCC process. We were grateful that we could work together extensively on communication activities. We thank Sue Escott for her tireless work to strengthen how we communicate the outcomes of the assessment.

We would like to acknowledge the support of the SHIFT Collaborative team – Stacy Barter and Michelle Colussi – and the generous support of the Canadian government for training and tools on inclusive practices in a consensus-based decision-making context, which we have been able to use for a more inclusive assessment process, including when we moved to purely online approaches. We appreciated the presence of Jessica O'Reilly and Mark Vardy, who have been with us throughout, working on an ethnographic study of how authors undertake the IPCC assessment, and we look forward to the insights from their research.

A core outcome of the report has been the development of the WGI Interactive Atlas produced by the Atlas chapter team. The Atlas is dedicated to the memory of Gemma Teresa Narisma, who co-led this innovative chapter with her extensive experience in regional climate research and outstanding leadership. The development and technical implementation have been supported with in-kind contribution from the Spanish government through the Spanish Research Council (CSIC) Instituto de Física de Cantabria, in partnership with Predictia Intelligent Data Solutions. Funding from the Spanish Research & Development program is acknowledged (ref. PID2019-111481RB-I00). We thank the modelling centres and institutions that produce and make available the datasets used in this work. The Interactive Atlas was first made available along with the rest of the Report on 9 August 2021 and was visited by more than half a million users worldwide during the first month.

The WGI TSU has initiated the process to archive the data and code from the report, building on the guidance and support from a large group of contributors. We are indebted to the members of the IPCC Task Group on Data Support for Climate Change Assessments (TG-Data) for their oversight, expert guidance and constant encouragement, including the Co-chairs of the Task Group, David Huard and Sebastian Vicuna, and members representing the WGI science community, Michio Kawamiya, Silvina Solman, José Manuel Guttierez and Nana Ama Browne Klutse. For the preparation of the figure data and code for archival, we especially thank to our dedicated contractor, Lina Sitz.

The IPCC Data Distribution Centre (DDC) has been indispensable for this effort. For the archival of figure data, we are indebted to Charlotte Pascoe, Kate Winfield, and Martin Jukes from the UK Centre for Environmental Data Analysis (CEDA). For the archival of the climate model data used as input to the report and intermediate assessed datasets, we gratefully acknowledge Martina Stockhause of the German Climate Computing Centre (DKRZ). For the transfer of metadata on archived data/code into the IPCC data catalogue, we thank MetadataWorks. Finally, we gratefully acknowledge funding

support from the Governments of the United Kingdom and Germany, without which data archival at the DDC would not have been possible.

A special thanks goes to the visual design team of the Summary for Policymakers: Tom Johansen and Angela Morelli of Information Design Lab and Jordan Harold and Irene Lorenzoni of the Tyndall Centre for Climate Change Research, as well as to Nigel Hawtin for graphical design support of the Report. We would like to thank Alisa Singer for creating the "Changing" artwork inspired by one of the scientific figures for the front cover of the Report.

Our particular appreciation goes to the WGI TSU, whose tireless dedication, professionalism and enthusiasm underpinned the production of this Report. The Report could not have been prepared without the commitment of members of the TSU, all new to the IPCC, who rose to the unprecedented Sixth Assessment Report challenge and were pivotal in all aspects of the preparation of the Report: Anna Pirani, Clotilde Péan, Sarah Connors, Yang Chen, Robin Matthews, Melissa Gomis, Sophie Berger, Leah Goldfarb, Rong Yu, Baiquan Zhou, Ozge Yelekci, Nada Caud, Katherine Leitzell, Tom Maycock, Mengtian Huang, Elisabeth Lonnoy, Tim Waterfield and Diego Cammarano. We thank our past WGI TSU team members: Wilfran Moufouma-Okia, Roz Pidcock, and Rodrigro Manzanas. We also thank the contributions of Margot Eyraud, Evéa Piedagnel, Mathilde Mousson and Felix Chavelli, who joined the TSU as interns.

We wish to express our sincere recognition to all those who contributed to the WGI assessment given the implications of undertaking this during the COVID-19 pandemic, all of whom have worked from home under such challenging conditions.

Finally, on behalf of all the participants to this unprecedented experience, we would like to thank colleagues, friends, and families who have also been part of this intense journey for their understanding and support.

This report shows that how much climate change we experience in the future depends on our decisions now, and what to prepare for. We wish that this report is widely used to provide evidence-based knowledge to inform decision-making, for teaching and training, and to enhance climate literacy worldwide.

Valérie Masson-Delmotte
IPCC Working Group I Co-Chair

Panmao Zhai
IPCC Working Group I Co-Chair

Dedication

Sir John Hougthon

(30 December 1931 – 15 April 2020)

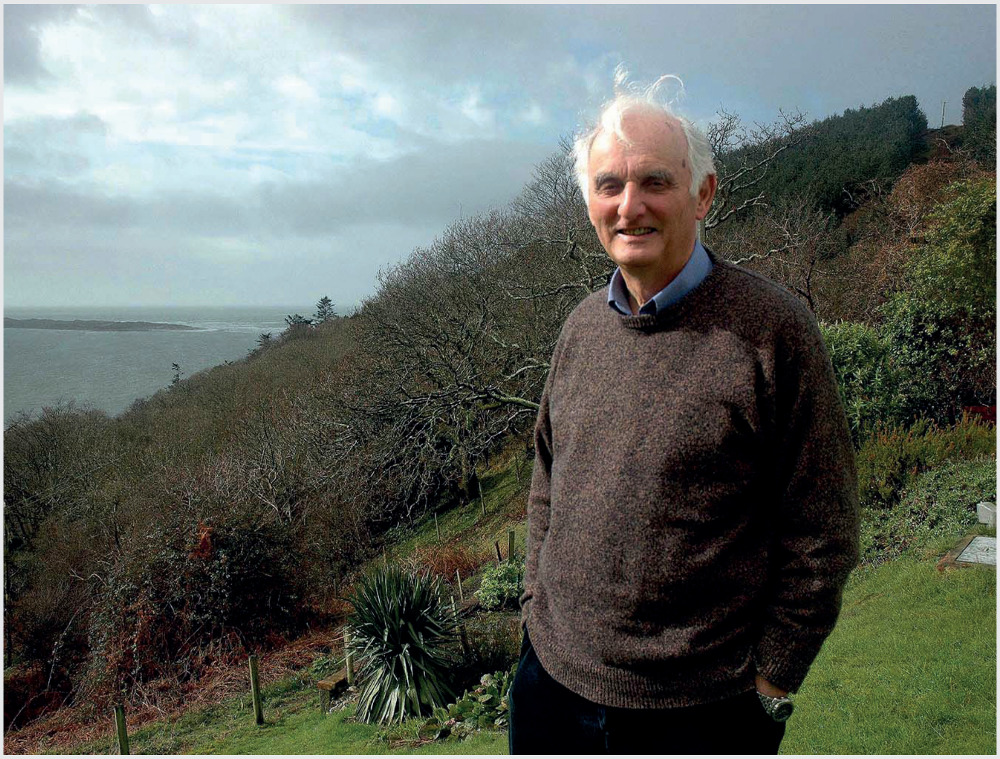

The Working Group I Contribution to the Sixth Assessment Report of the Intergovernmental Panel on Climate Change (IPCC) *Climate Change 2021: The Physical Science Basis* is dedicated to the memory of Sir John Hougthon, who was one of the key figures in the creation of the IPCC in 1988, and served as Chair and Co-Chair of Working Group I for the IPCC's first three assessment reports from 1988 to 2002.

Sir John's work was a major factor in the award of the Nobel Peace Prize to the IPCC in 2007, shared with former U.S. Vice-President Al Gore. He contributed to the development of climate science and building international cooperation based upon climate research. Sir John played a key role in ensuring a robust science-policy interface, used in the IPCC process, but his role in international scientific research extended beyond the IPCC, for instance in contributing to the establishment of the World Climate Research Programme, which he chaired from 1982 to 1984.

Sir John was a brilliant communicator among scientific colleagues, policymakers and the public at large, explaining the fact and threat of climate change with clarity and directness.

Contents

Summary for Policymakers

SPM

Summary for Policymakers

Drafting Authors:

Richard P. Allan (United Kingdom), Paola A. Arias (Colombia), Sophie Berger (France/Belgium), Josep G. Canadell (Australia), Christophe Cassou (France), Deliang Chen (Sweden), Annalisa Cherchi (Italy), Sarah L. Connors (France/United Kingdom), Erika Coppola (Italy), Faye Abigail Cruz (Philippines), Aïda Diongue-Niang (Senegal), Francisco J. Doblas-Reyes (Spain), Hervé Douville (France), Fatima Driouech (Morocco), Tamsin L. Edwards (United Kingdom), François Engelbrecht (South Africa), Veronika Eyring (Germany), Erich Fischer (Switzerland), Gregory M. Flato (Canada), Piers Forster (United Kingdom), Baylor Fox-Kemper (United States of America), Jan S. Fuglestvedt (Norway), John C. Fyfe (Canada), Nathan P. Gillett (Canada), Melissa I. Gomis (France/Switzerland), Sergey K. Gulev (Russian Federation), José Manuel Gutiérrez (Spain), Rafiq Hamdi (Belgium), Jordan Harold (United Kingdom), Mathias Hauser (Switzerland), Ed Hawkins (United Kingdom), Helene T. Hewitt (United Kingdom), Tom Gabriel Johansen (Norway), Christopher Jones (United Kingdom), Richard G. Jones (United Kingdom), Darrell S. Kaufman (United States of America), Zbigniew Klimont (Austria/Poland), Robert E. Kopp (United States of America), Charles Koven (United States of America), Gerhard Krinner (France/Germany, France), June-Yi Lee (Republic of Korea), Irene Lorenzoni (United Kingdom/Italy), Jochem Marotzke (Germany), Valérie Masson-Delmotte (France), Thomas K. Maycock (United States of America), Malte Meinshausen (Australia/Germany), Pedro M.S. Monteiro (South Africa), Angela Morelli (Norway/Italy), Vaishali Naik (United States of America), Dirk Notz (Germany), Friederike Otto (United Kingdom/Germany), Matthew D. Palmer (United Kingdom), Izidine Pinto (South Africa/Mozambique), Anna Pirani (Italy), Gian-Kasper Plattner (Switzerland), Krishnan Raghavan (India), Roshanka Ranasinghe (The Netherlands/Sri Lanka, Australia), Joeri Rogelj (United Kingdom/Belgium), Maisa Rojas (Chile), Alex C. Ruane (United States of America), Jean-Baptiste Sallée (France), Bjørn H. Samset (Norway), Sonia I. Seneviratne (Switzerland), Jana Sillmann (Norway/Germany), Anna A. Sörensson (Argentina), Tannecia S. Stephenson (Jamaica), Trude Storelvmo (Norway), Sophie Szopa (France), Peter W. Thorne (Ireland/United Kingdom), Blair Trewin (Australia), Robert Vautard (France), Carolina Vera (Argentina), Noureddine Yassaa (Algeria), Sönke Zaehle (Germany), Panmao Zhai (China), Xuebin Zhang (Canada), Kirsten Zickfeld (Canada/Germany)

Contributing Authors:

Krishna M. AchutaRao (India), Bhupesh Adhikary (Nepal), Edvin Aldrian (Indonesia), Kyle Armour (United States of America), Govindasamy Bala (India/United States of America), Rondrotiana Barimalala (South Africa/Madagascar), Nicolas Bellouin (United Kingdom/France), William Collins (United Kingdom), William D. Collins (United States of America), Susanna Corti (Italy), Peter M. Cox (United Kingdom), Frank J. Dentener (EU/The Netherlands), Claudine Dereczynski (Brazil), Alejandro Di Luca (Australia, Canada/Argentina), Alessandro Dosio (Italy), Leah Goldfarb (France/United States of America), Irina V. Gorodetskaya (Portugal/Belgium, Russian Federation), Pandora Hope (Australia), Mark Howden (Australia), A.K.M Saiful Islam (Bangladesh), Yu Kosaka (Japan), James Kossin (United States of America), Svitlana Krakovska (Ukraine), Chao Li (China), Jian Li (China), Thorsten Mauritsen (Germany/Denmark), Sebastian Milinski (Germany), Seung-Ki Min (Republic of Korea), Thanh Ngo Duc (Vietnam), Andy Reisinger (New Zealand), Lucas Ruiz (Argentina), Shubha Sathyendranath (United Kingdom/Canada, Overseas Citizen of India), Aimée B. A. Slangen (The Netherlands), Chris Smith (United Kingdom), Izuru Takayabu (Japan), Muhammad Irfan Tariq (Pakistan), Anne-Marie Treguier (France), Bart van den Hurk (The Netherlands), Karina von Schuckmann (France/Germany), Cunde Xiao (China)

This Summary for Policymakers should be cited as:

IPCC, 2021: Summary for Policymakers. In: *Climate Change 2021: The Physical Science Basis. Contribution of Working Group I to the Sixth Assessment Report of the Intergovernmental Panel on Climate Change* [Masson-Delmotte, V., P. Zhai, A. Pirani, S.L. Connors, C. Péan, S. Berger, N. Caud, Y. Chen, L. Goldfarb, M.I. Gomis, M. Huang, K. Leitzell, E. Lonnoy, J.B.R. Matthews, T.K. Maycock, T. Waterfield, O. Yelekçi, R. Yu, and B. Zhou (eds.)]. Cambridge University Press, Cambridge, United Kingdom and New York, NY, USA, pp. 3–32, doi:10.1017/9781009157896.001.

Introduction

This Summary for Policymakers (SPM) presents key findings of the Working Group I (WGI) contribution to the Intergovernmental Panel on Climate Change (IPCC) Sixth Assessment Report (AR6)[1] on the physical science basis of climate change. The report builds upon the 2013 Working Group I contribution to the IPCC's Fifth Assessment Report (AR5) and the 2018–2019 IPCC Special Reports[2] of the AR6 cycle and incorporates subsequent new evidence from climate science.[3]

This SPM provides a high-level summary of the understanding of the current state of the climate, including how it is changing and the role of human influence, the state of knowledge about possible climate futures, climate information relevant to regions and sectors, and limiting human-induced climate change.

Based on scientific understanding, key findings can be formulated as statements of fact or associated with an assessed level of confidence indicated using the IPCC calibrated language.[4]

The scientific basis for each key finding is found in chapter sections of the main Report and in the integrated synthesis presented in the Technical Summary (hereafter TS), and is indicated in curly brackets. The AR6 WGI Interactive Atlas facilitates exploration of these key synthesis findings, and supporting climate change information, across the WGI reference regions.[5]

A. The Current State of the Climate

Since AR5, improvements in observationally based estimates and information from paleoclimate archives provide a comprehensive view of each component of the climate system and its changes to date. New climate model simulations, new analyses, and methods combining multiple lines of evidence lead to improved understanding of human influence on a wider range of climate variables, including weather and climate extremes. The time periods considered throughout this section depend upon the availability of observational products, paleoclimate archives and peer-reviewed studies.

A.1 It is unequivocal that human influence has warmed the atmosphere, ocean and land. Widespread and rapid changes in the atmosphere, ocean, cryosphere and biosphere have occurred.
{2.2, 2.3, Cross-Chapter Box 2.3, 3.3, 3.4, 3.5, 3.6, 3.8, 5.2, 5.3, 6.4, 7.3, 8.3, 9.2, 9.3, 9.5, 9.6, Cross-Chapter Box 9.1} (Figure SPM.1, Figure SPM.2)

A.1.1 Observed increases in well-mixed greenhouse gas (GHG) concentrations since around 1750 are unequivocally caused by human activities. Since 2011 (measurements reported in AR5), concentrations have continued to increase in the atmosphere, reaching annual averages of 410 parts per million (ppm) for carbon dioxide (CO_2), 1866 parts per billion (ppb) for methane (CH_4), and 332 ppb for nitrous oxide (N_2O) in 2019.[6] Land and ocean have taken up a near-constant proportion (globally about 56% per year) of CO_2 emissions from human activities over the past six decades, with regional differences (*high confidence*).[7]
{2.2, 5.2, 7.3, TS.2.2, Box TS.5}

---

1 Decision IPCC/XLVI-2.

2 The three Special Reports are: Global Warming of 1.5°C: An IPCC Special Report on the impacts of global warming of 1.5°C above pre-industrial levels and related global greenhouse gas emission pathways, in the context of strengthening the global response to the threat of climate change, sustainable development, and efforts to eradicate poverty (SR1.5); Climate Change and Land: An IPCC Special Report on climate change, desertification, land degradation, sustainable land management, food security, and greenhouse gas fluxes in terrestrial ecosystems (SRCCL); IPCC Special Report on the Ocean and Cryosphere in a Changing Climate (SROCC).

3 The assessment covers scientific literature accepted for publication by 31 January 2021.

4 Each finding is grounded in an evaluation of underlying evidence and agreement. A level of confidence is expressed using five qualifiers: very low, low, medium, high and very high, and typeset in italics, for example, *medium confidence*. The following terms have been used to indicate the assessed likelihood of an outcome or result: virtually certain 99–100% probability; very likely 90–100%; likely 66–100%; about as likely as not 33–66%; unlikely 0–33%; very unlikely 0–10%; and exceptionally unlikely 0–1%. Additional terms (extremely likely 95–100%; more likely than not >50–100%; and extremely unlikely 0–5%) are also used when appropriate. Assessed likelihood is typeset in italics, for example, *very likely*. This is consistent with AR5. In this Report, unless stated otherwise, square brackets [x to y] are used to provide the assessed *very likely* range, or 90% interval.

5 The Interactive Atlas is available at https://interactive-atlas.ipcc.ch

6 Other GHG concentrations in 2019 were: perfluorocarbons (PFCs) – 109 parts per trillion (ppt) CF_4 equivalent; sulphur hexafluoride (SF_6) – 10 ppt; nitrogen trifluoride (NF_3) – 2 ppt; hydrofluorocarbons (HFCs) – 237 ppt HFC-134a equivalent; other Montreal Protocol gases (mainly chlorofluorocarbons (CFCs) and hydrochlorofluorocarbons (HCFCs)) – 1032 ppt CFC-12 equivalent). Increases from 2011 are 19 ppm for CO_2, 63 ppb for CH_4 and 8 ppb for N_2O.

7 Land and ocean are not substantial sinks for other GHGs.

A.1.2 Each of the last four decades has been successively warmer than any decade that preceded it since 1850. Global surface temperature[8] in the first two decades of the 21st century (2001–2020) was 0.99 [0.84 to 1.10] °C higher than 1850–1900.[9] Global surface temperature was 1.09 [0.95 to 1.20] °C higher in 2011–2020 than 1850–1900, with larger increases over land (1.59 [1.34 to 1.83] °C) than over the ocean (0.88 [0.68 to 1.01] °C). The estimated increase in global surface temperature since AR5 is principally due to further warming since 2003–2012 (+0.19 [0.16 to 0.22] °C). Additionally, methodological advances and new datasets contributed approximately 0.1°C to the updated estimate of warming in AR6.[10]
{2.3, Cross-Chapter Box 2.3} (Figure SPM.1)

A.1.3 The *likely* range of total human-caused global surface temperature increase from 1850–1900 to 2010–2019[11] is 0.8°C to 1.3°C, with a best estimate of 1.07°C. It is *likely* that well-mixed GHGs contributed a warming of 1.0°C to 2.0°C, other human drivers (principally aerosols) contributed a cooling of 0.0°C to 0.8°C, natural drivers changed global surface temperature by –0.1°C to +0.1°C, and internal variability changed it by –0.2°C to +0.2°C. It is *very likely* that well-mixed GHGs were the main driver[12] of tropospheric warming since 1979 and *extremely likely* that human-caused stratospheric ozone depletion was the main driver of cooling of the lower stratosphere between 1979 and the mid-1990s.
{3.3, 6.4, 7.3, TS.2.3, Cross-Section Box TS.1} (Figure SPM.2)

A.1.4 Globally averaged precipitation over land has *likely* increased since 1950, with a faster rate of increase since the 1980s (*medium confidence*). It is *likely* that human influence contributed to the pattern of observed precipitation changes since the mid-20th century and *extremely likely* that human influence contributed to the pattern of observed changes in near-surface ocean salinity. Mid-latitude storm tracks have *likely* shifted poleward in both hemispheres since the 1980s, with marked seasonality in trends (*medium confidence*). For the Southern Hemisphere, human influence *very likely* contributed to the poleward shift of the closely related extratropical jet in austral summer.
{2.3, 3.3, 8.3, 9.2, TS.2.3, TS.2.4, Box TS.6}

A.1.5 Human influence is *very likely* the main driver of the global retreat of glaciers since the 1990s and the decrease in Arctic sea ice area between 1979–1988 and 2010–2019 (decreases of about 40% in September and about 10% in March). There has been no significant trend in Antarctic sea ice area from 1979 to 2020 due to regionally opposing trends and large internal variability. Human influence *very likely* contributed to the decrease in Northern Hemisphere spring snow cover since 1950. It is *very likely* that human influence has contributed to the observed surface melting of the Greenland Ice Sheet over the past two decades, but there is only *limited evidence*, with *medium agreement*, of human influence on the Antarctic Ice Sheet mass loss.
{2.3, 3.4, 8.3, 9.3, 9.5, TS.2.5}

A.1.6 It is *virtually certain* that the global upper ocean (0–700 m) has warmed since the 1970s and *extremely likely* that human influence is the main driver. It is *virtually certain* that human-caused CO_2 emissions are the main driver of current global acidification of the surface open ocean. There is *high confidence* that oxygen levels have dropped in many upper ocean regions since the mid-20th century and *medium confidence* that human influence contributed to this drop.
{2.3, 3.5, 3.6, 5.3, 9.2, TS.2.4}

A.1.7 Global mean sea level increased by 0.20 [0.15 to 0.25] m between 1901 and 2018. The average rate of sea level rise was 1.3 [0.6 to 2.1] mm yr^{-1} between 1901 and 1971, increasing to 1.9 [0.8 to 2.9] mm yr^{-1} between 1971 and 2006, and further increasing to 3.7 [3.2 to 4.2] mm yr^{-1} between 2006 and 2018 (*high confidence*). Human influence was *very likely* the main driver of these increases since at least 1971.
{2.3, 3.5, 9.6, Cross-Chapter Box 9.1, Box TS.4}

---

8 The term 'global surface temperature' is used in reference to both global mean surface temperature and global surface air temperature throughout this SPM. Changes in these quantities are assessed with *high confidence* to differ by at most 10% from one another, but conflicting lines of evidence lead to *low confidence* in the sign (direction) of any difference in long-term trend. {Cross-Section Box TS.1}

9 The period 1850–1900 represents the earliest period of sufficiently globally complete observations to estimate global surface temperature and, consistent with AR5 and SR1.5, is used as an approximation for pre-industrial conditions.

10 Since AR5, methodological advances and new datasets have provided a more complete spatial representation of changes in surface temperature, including in the Arctic. These and other improvements have also increased the estimate of global surface temperature change by approximately 0.1°C, but this increase does not represent additional physical warming since AR5.

11 The period distinction with A.1.2 arises because the attribution studies consider this slightly earlier period. The observed warming to 2010–2019 is 1.06 [0.88 to 1.21] °C.

12 Throughout this SPM, 'main driver' means responsible for more than 50% of the change.

A.1.8 Changes in the land biosphere since 1970 are consistent with global warming: climate zones have shifted poleward in both hemispheres, and the growing season has on average lengthened by up to two days per decade since the 1950s in the Northern Hemisphere extratropics (*high confidence*).
{2.3, TS.2.6}

SPM

Human influence has warmed the climate at a rate that is unprecedented in at least the last 2000 years

Changes in global surface temperature relative to 1850–1900

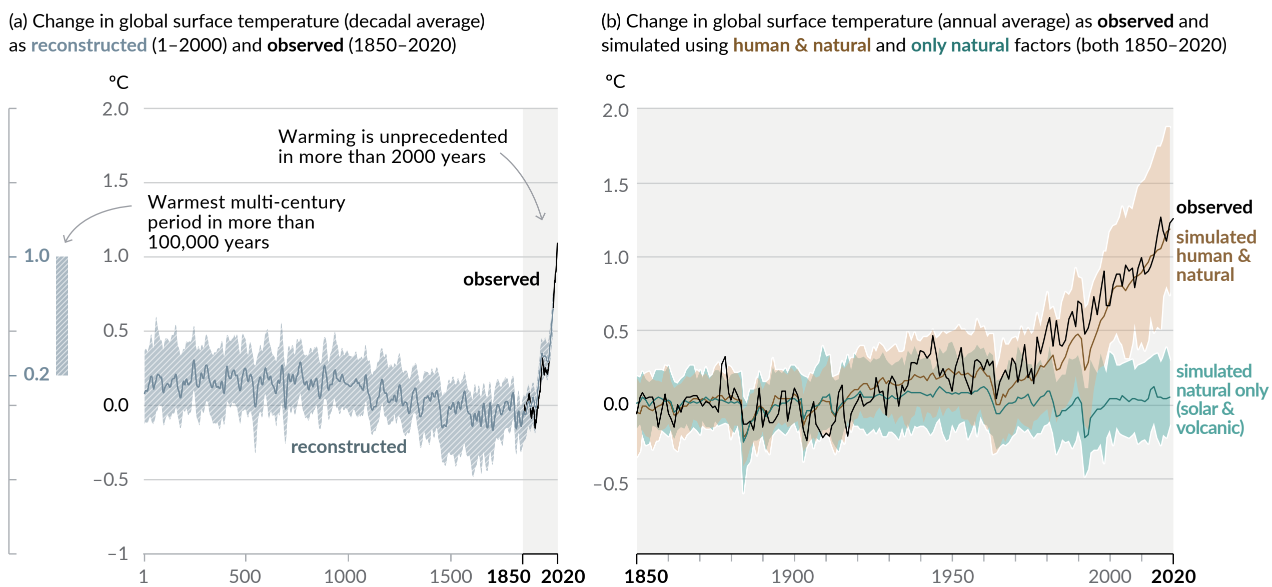

Figure SPM.1 | History of global temperature change and causes of recent warming

Panel (a) Changes in global surface temperature reconstructed from paleoclimate archives (solid grey line, years 1–2000) **and from direct observations** (solid black line, 1850–2020), both relative to 1850–1900 and decadally averaged. The vertical bar on the left shows the estimated temperature (*very likely* range) during the warmest multi-century period in at least the last 100,000 years, which occurred around 6500 years ago during the current interglacial period (Holocene). The Last Interglacial, around 125,000 years ago, is the next most recent candidate for a period of higher temperature. These past warm periods were caused by slow (multi-millennial) orbital variations. The grey shading with white diagonal lines shows the *very likely* ranges for the temperature reconstructions.

Panel (b) Changes in global surface temperature over the past 170 years (black line) relative to 1850–1900 and annually averaged, compared to Coupled Model Intercomparison Project Phase 6 (CMIP6) climate model simulations (see Box SPM.1) of the temperature response to both human and natural drivers (brown) and to only natural drivers (solar and volcanic activity, green). Solid coloured lines show the multi-model average, and coloured shades show the *very likely* range of simulations. (See Figure SPM.2 for the assessed contributions to warming).

{2.3.1; Cross-Chapter Box 2.3; 3.3; TS.2.2; Cross-Section Box TS.1, Figure 1a}

Observed warming is driven by emissions from human activities, with greenhouse gas warming partly masked by aerosol cooling

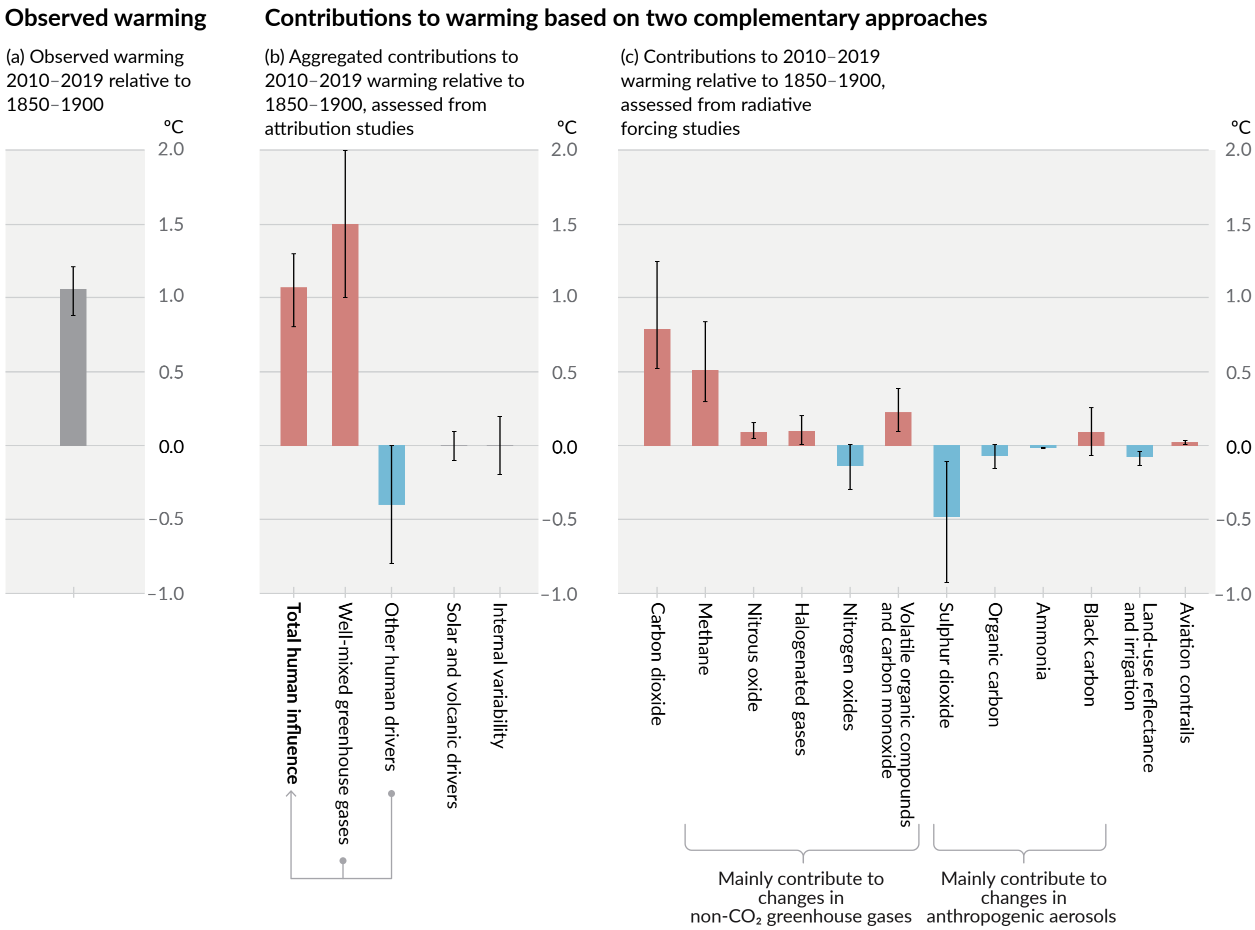

Figure SPM.2 | Assessed contributions to observed warming in 2010–2019 relative to 1850–1900

Panel (a) Observed global warming (increase in global surface temperature). Whiskers show the *very likely* range.

Panel (b) Evidence from attribution studies, which synthesize information from climate models and observations. The panel shows temperature change attributed to: total human influence; changes in well-mixed greenhouse gas concentrations; other human drivers due to aerosols, ozone and land-use change (land-use reflectance); solar and volcanic drivers; and internal climate variability. Whiskers show *likely* ranges.

Panel (c) Evidence from the assessment of radiative forcing and climate sensitivity. The panel shows temperature changes from individual components of human influence: emissions of greenhouse gases, aerosols and their precursors; land-use changes (land-use reflectance and irrigation); and aviation contrails. Whiskers show *very likely* ranges. Estimates account for both direct emissions into the atmosphere and their effect, if any, on other climate drivers. For aerosols, both direct effects (through radiation) and indirect effects (through interactions with clouds) are considered.

{Cross-Chapter Box 2.3, 3.3.1, 6.4.2, 7.3}

**A.2 The scale of recent changes across the climate system as a whole – and the present state of many aspects of the climate system – are unprecedented over many centuries to many thousands of years.
{2.2, 2.3, Cross-Chapter Box 2.1, 5.1} (Figure SPM.1)**

A.2.1 In 2019, atmospheric CO_2 concentrations were higher than at any time in at least 2 million years (*high confidence*), and concentrations of CH_4 and N_2O were higher than at any time in at least 800,000 years (*very high confidence*). Since 1750, increases in CO_2 (47%) and CH_4 (156%) concentrations far exceed – and increases in N_2O (23%) are similar to – the natural multi-millennial changes between glacial and interglacial periods over at least the past 800,000 years (*very high confidence*).
{2.2, 5.1, TS.2.2}

A.2.2 Global surface temperature has increased faster since 1970 than in any other 50-year period over at least the last 2000 years (*high confidence*). Temperatures during the most recent decade (2011–2020) exceed those of the most recent multi-century warm period, around 6500 years ago[13] [0.2°C to 1°C relative to 1850–1900] (*medium confidence*). Prior to that, the next most recent warm period was about 125,000 years ago, when the multi-century temperature [0.5°C to 1.5°C relative to 1850–1900] overlaps the observations of the most recent decade (*medium confidence*).
{2.3, Cross-Chapter Box 2.1, Cross-Section Box TS.1} (Figure SPM.1)

SPM

A.2.3 In 2011–2020, annual average Arctic sea ice area reached its lowest level since at least 1850 (*high confidence*). Late summer Arctic sea ice area was smaller than at any time in at least the past 1000 years (*medium confidence*). The global nature of glacier retreat since the 1950s, with almost all of the world's glaciers retreating synchronously, is unprecedented in at least the last 2000 years (*medium confidence*).
{2.3, TS.2.5}

A.2.4 Global mean sea level has risen faster since 1900 than over any preceding century in at least the last 3000 years (*high confidence*). The global ocean has warmed faster over the past century than since the end of the last deglacial transition (around 11,000 years ago) (*medium confidence*). A long-term increase in surface open ocean pH occurred over the past 50 million years (*high confidence*). However, surface open ocean pH as low as recent decades is unusual in the last 2 million years (*medium confidence*).
{2.3, TS.2.4, Box TS.4}

**A.3 Human-induced climate change is already affecting many weather and climate extremes in every region across the globe. Evidence of observed changes in extremes such as heatwaves, heavy precipitation, droughts, and tropical cyclones, and, in particular, their attribution to human influence, has strengthened since AR5.
{2.3, 3.3, 8.2, 8.3, 8.4, 8.5, 8.6, Box 8.1, Box 8.2, Box 9.2, 10.6, 11.2, 11.3, 11.4, 11.6, 11.7, 11.8, 11.9, 12.3} (Figure SPM.3)**

A.3.1 It is *virtually certain* that hot extremes (including heatwaves) have become more frequent and more intense across most land regions since the 1950s, while cold extremes (including cold waves) have become less frequent and less severe, with *high confidence* that human-induced climate change is the main driver[14] of these changes. Some recent hot extremes observed over the past decade would have been *extremely unlikely* to occur without human influence on the climate system. Marine heatwaves have approximately doubled in frequency since the 1980s (*high confidence*), and human influence has *very likely* contributed to most of them since at least 2006.
{Box 9.2, 11.2, 11.3, 11.9, TS.2.4, TS.2.6, Box TS.10} (Figure SPM.3)

A.3.2 The frequency and intensity of heavy precipitation events have increased since the 1950s over most land area for which observational data are sufficient for trend analysis (*high confidence*), and human-induced climate change is *likely* the main driver. Human-induced climate change has contributed to increases in agricultural and ecological droughts[15] in some regions due to increased land evapotranspiration[16] (*medium confidence*).
{8.2, 8.3, 11.4, 11.6, 11.9, TS.2.6, Box TS.10} (Figure SPM.3)

---

13 As stated in section B.1, even under the very low emissions scenario SSP1-1.9, temperatures are assessed to remain elevated above those of the most recent decade until at least 2100 and therefore warmer than the century-scale period 6500 years ago.

14 As indicated in footnote 12, throughout this SPM, 'main driver' means responsible for more than 50% of the change.

15 Agricultural and ecological drought (depending on the affected biome): a period with abnormal soil moisture deficit, which results from combined shortage of precipitation and excess evapotranspiration, and during the growing season impinges on crop production or ecosystem function in general (see Annex VII: Glossary). Observed changes in meteorological droughts (precipitation deficits) and hydrological droughts (streamflow deficits) are distinct from those in agricultural and ecological droughts and are addressed in the underlying AR6 material (Chapter 11).

16 The combined processes through which water is transferred to the atmosphere from open water and ice surfaces, bare soils and vegetation that make up the Earth's surface (Glossary).

A.3.3 Decreases in global land monsoon precipitation[17] from the 1950s to the 1980s are partly attributed to human-caused Northern Hemisphere aerosol emissions, but increases since then have resulted from rising GHG concentrations and decadal to multi-decadal internal variability (*medium confidence*). Over South Asia, East Asia and West Africa, increases in monsoon precipitation due to warming from GHG emissions were counteracted by decreases in monsoon precipitation due to cooling from human-caused aerosol emissions over the 20th century (*high confidence*). Increases in West African monsoon precipitation since the 1980s are partly due to the growing influence of GHGs and reductions in the cooling effect of human-caused aerosol emissions over Europe and North America (*medium confidence*).
{2.3, 3.3, 8.2, 8.3, 8.4, 8.5, 8.6, Box 8.1, Box 8.2, 10.6, Box TS.13}

A.3.4 It is *likely* that the global proportion of major (Category 3–5) tropical cyclone occurrence has increased over the last four decades, and it is *very likely* that the latitude where tropical cyclones in the western North Pacific reach their peak intensity has shifted northward; these changes cannot be explained by internal variability alone (*medium confidence*). There is *low confidence* in long-term (multi-decadal to centennial) trends in the frequency of all-category tropical cyclones. Event attribution studies and physical understanding indicate that human-induced climate change increases heavy precipitation associated with tropical cyclones (*high confidence*), but data limitations inhibit clear detection of past trends on the global scale.
{8.2, 11.7, Box TS.10}

A.3.5 Human influence has *likely* increased the chance of compound extreme events[18] since the 1950s. This includes increases in the frequency of concurrent heatwaves and droughts on the global scale (*high confidence*), fire weather in some regions of all inhabited continents (*medium confidence*), and compound flooding in some locations (*medium confidence*).
{11.6, 11.7, 11.8, 12.3, 12.4, TS.2.6, Table TS.5, Box TS.10}

17 The global monsoon is defined as the area in which the annual range (local summer minus local winter) of precipitation is greater than 2.5 mm day^{-1} (Glossary). Global land monsoon precipitation refers to the mean precipitation over land areas within the global monsoon.

18 Compound extreme events are the combination of multiple drivers and/or hazards that contribute to societal or environmental risk (Glossary). Examples are concurrent heatwaves and droughts, compound flooding (e.g., a storm surge in combination with extreme rainfall and/or river flow), compound fire weather conditions (i.e., a combination of hot, dry and windy conditions), or concurrent extremes at different locations.

SPM

Climate change is already affecting every inhabited region across the globe, with human influence contributing to many observed changes in weather and climate extremes

(a) Synthesis of assessment of observed change in **hot extremes** and confidence in human contribution to the observed changes in the world's regions

Type of observed change
in hot extremes

- Increase (41)
- Decrease (0)
- Low agreement in the type of change (2)
- Limited data and/or literature (2)

Confidence in human contribution
to the observed change

- ●●● High
- ●● Medium
- ● Low due to limited agreement
- ○ Low due to limited evidence

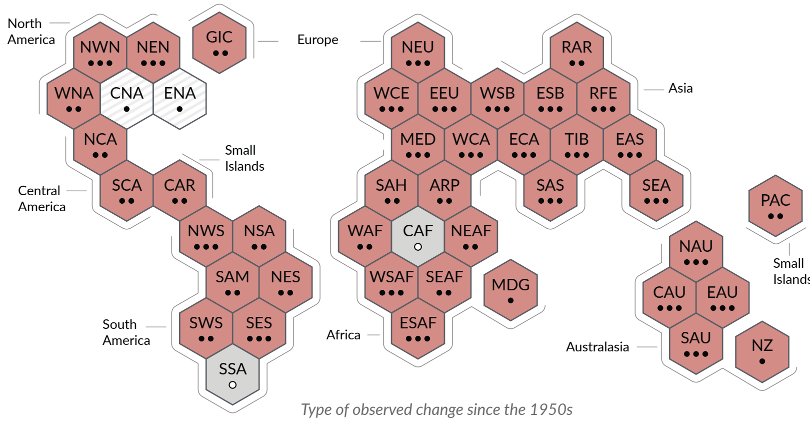

(b) Synthesis of assessment of observed change in **heavy precipitation** and confidence in human contribution to the observed changes in the world's regions

Type of observed change
in heavy precipitation

- Increase (19)
- Decrease (0)
- Low agreement in the type of change (8)
- Limited data and/or literature (18)

Confidence in human contribution
to the observed change

- ●●● High
- ●● Medium
- ● Low due to limited agreement
- ○ Low due to limited evidence

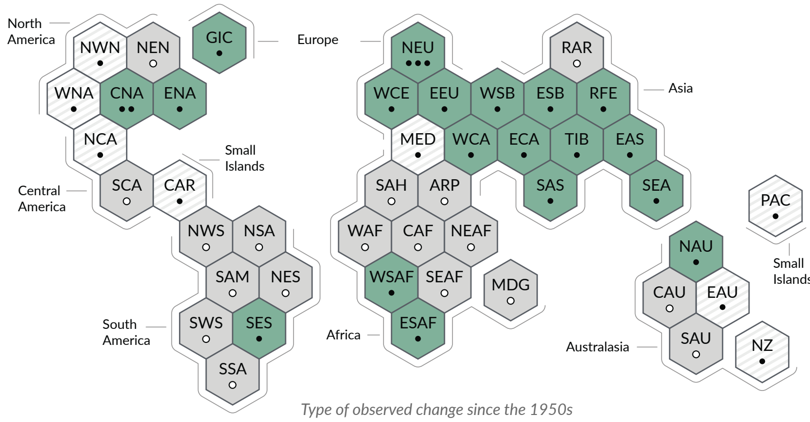

(c) Synthesis of assessment of observed change in **agricultural and ecological drought** and confidence in human contribution to the observed changes in the world's regions

Type of observed change
in agricultural and ecological drought

- Increase (12)
- Decrease (1)
- Low agreement in the type of change (28)
- Limited data and/or literature (4)

Confidence in human contribution
to the observed change

- ●●● High
- ●● Medium
- ● Low due to limited agreement
- ○ Low due to limited evidence

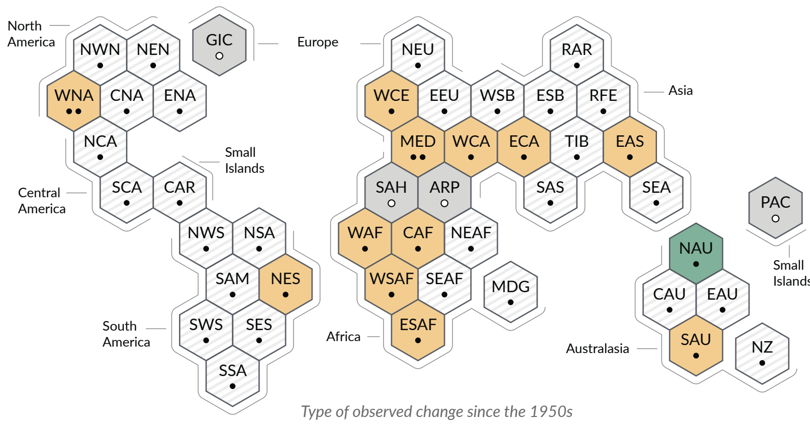

Each hexagon corresponds to one of the IPCC AR6 WGI reference regions

North-Western North America

IPCC AR6 WGI reference regions: **North America: NWN** *(North-Western North America)*, **NEN** *(North-Eastern North America)*, **WNA** *(Western North America)*, **CNA** *(Central North America)*, **ENA** *(Eastern North America)*, **Central America: NCA** *(Northern Central America)*, **SCA** *(Southern Central America)*, **CAR** *(Caribbean)*, **South America: NWS** *(North-Western South America)*, **NSA** *(Northern South America)*, **NES** *(North-Eastern South America)*, **SAM** *(South American Monsoon)*, **SWS** *(South-Western South America)*, **SES** *(South-Eastern South America)*, **SSA** *(Southern South America)*, **Europe: GIC** *(Greenland/Iceland)*, **NEU** *(Northern Europe)*, **WCE** *(Western and Central Europe)*, **EEU** *(Eastern Europe)*, **MED** *(Mediterranean)*, **Africa: MED** *(Mediterranean)*, **SAH** *(Sahara)*, **WAF** *(Western Africa)*, **CAF** *(Central Africa)*, **NEAF** *(North Eastern Africa)*, **SEAF** *(South Eastern Africa)*, **WSAF** *(West Southern Africa)*, **ESAF** *(East Southern Africa)*, **MDG** *(Madagascar)*, **Asia: RAR** *(Russian Arctic)*, **WSB** *(West Siberia)*, **ESB** *(East Siberia)*, **RFE** *(Russian Far East)*, **WCA** *(West Central Asia)*, **ECA** *(East Central Asia)*, **TIB** *(Tibetan Plateau)*, **EAS** *(East Asia)*, **ARP** *(Arabian Peninsula)*, **SAS** *(South Asia)*, **SEA** *(South East Asia)*, **Australasia: NAU** *(Northern Australia)*, **CAU** *(Central Australia)*, **EAU** *(Eastern Australia)*, **SAU** *(Southern Australia)*, **NZ** *(New Zealand)*, **Small Islands: CAR** *(Caribbean)*, **PAC** *(Pacific Small Islands)*

Figure SPM.3 | Synthesis of assessed observed and attributable regional changes

The IPCC AR6 WGI inhabited regions are displayed as **hexagons** with identical size in their approximate geographical location (see legend for regional acronyms). All assessments are made for each region as a whole and for the 1950s to the present. Assessments made on different time scales or more local spatial scales might differ from what is shown in the figure. The **colours** in each panel represent the four outcomes of the assessment on observed changes. Striped hexagons (white and light-grey) are used where there is *low agreement* in the type of change for the region as a whole, and grey hexagons are used when there is limited data and/or literature that prevents an assessment of the region as a whole. Other colours indicate at least *medium confidence* in the observed change. The **confidence level** for the human influence on these observed changes is based on assessing trend detection and attribution and event attribution literature, and it is indicated by the number of dots: three dots for *high confidence*, two dots for *medium confidence* and one dot for *low confidence* (single, filled dot: limited agreement; single, empty dot: limited evidence).

Panel (a) For hot extremes, the evidence is mostly drawn from changes in metrics based on daily maximum temperatures; regional studies using other indices (heatwave duration, frequency and intensity) are used in addition. Red hexagons indicate regions where there is at least *medium confidence* in an observed increase in hot extremes.

Panel (b) For heavy precipitation, the evidence is mostly drawn from changes in indices based on one-day or five-day precipitation amounts using global and regional studies. Green hexagons indicate regions where there is at least *medium confidence* in an observed increase in heavy precipitation.

Panel (c) Agricultural and ecological droughts are assessed based on observed and simulated changes in total column soil moisture, complemented by evidence on changes in surface soil moisture, water balance (precipitation minus evapotranspiration) and indices driven by precipitation and atmospheric evaporative demand. Yellow hexagons indicate regions where there is at least *medium confidence* in an observed increase in this type of drought, and green hexagons indicate regions where there is at least *medium confidence* in an observed decrease in agricultural and ecological drought.

For all regions, Table TS.5 shows a broader range of observed changes besides the ones shown in this figure. Note that Southern South America (SSA) is the only region that does not display observed changes in the metrics shown in this figure, but is affected by observed increases in mean temperature, decreases in frost and increases in marine heatwaves.

{11.9, Atlas 1.3.3, Figure Atlas.2, Table TS.5; Box TS.10, Figure 1}

A.4 Improved knowledge of climate processes, paleoclimate evidence and the response of the climate system to increasing radiative forcing gives a best estimate of equilibrium climate sensitivity of 3°C, with a narrower range compared to AR5. {2.2, 7.3, 7.4, 7.5, Box 7.2, 9.4, 9.5, 9.6, Cross-Chapter Box 9.1}

A.4.1 Human-caused radiative forcing of 2.72 [1.96 to 3.48] W m^{-2} in 2019 relative to 1750 has warmed the climate system. This warming is mainly due to increased GHG concentrations, partly reduced by cooling due to increased aerosol concentrations. The radiative forcing has increased by 0.43 W m^{-2} (19%) relative to AR5, of which 0.34 W m^{-2} is due to the increase in GHG concentrations since 2011. The remainder is due to improved scientific understanding and changes in the assessment of aerosol forcing, which include decreases in concentration and improvement in its calculation (*high confidence*). {2.2, 7.3, TS.2.2, TS.3.1}

A.4.2 Human-caused net positive radiative forcing causes an accumulation of additional energy (heating) in the climate system, partly reduced by increased energy loss to space in response to surface warming. The observed average rate of heating of the climate system increased from 0.50 [0.32 to 0.69] W m^{-2} for the period 1971–2006[19] to 0.79 [0.52 to 1.06] W m^{-2} for the period 2006–2018[20] (*high confidence*). Ocean warming accounted for 91% of the heating in the climate system, with land warming, ice loss and atmospheric warming accounting for about 5%, 3% and 1%, respectively (*high confidence*). {7.2, Box 7.2, TS.3.1}

A.4.3 Heating of the climate system has caused global mean sea level rise through ice loss on land and thermal expansion from ocean warming. Thermal expansion explained 50% of sea level rise during 1971–2018, while ice loss from glaciers contributed 22%, ice sheets 20% and changes in land-water storage 8%. The rate of ice-sheet loss increased by a factor of four between 1992–1999 and 2010–2019. Together, ice-sheet and glacier mass loss were the dominant contributors to global mean sea level rise during 2006–2018 (*high confidence*). {9.4, 9.5, 9.6, Cross-Chapter Box 9.1}

A.4.4 The equilibrium climate sensitivity is an important quantity used to estimate how the climate responds to radiative forcing. Based on multiple lines of evidence,[21] the *very likely* range of equilibrium climate sensitivity is between 2°C (*high confidence*) and 5°C (*medium confidence*). The AR6 assessed best estimate is 3°C with a *likely* range of 2.5°C to 4°C (*high confidence*), compared to 1.5°C to 4.5°C in AR5, which did not provide a best estimate. {7.4, 7.5, TS.3.2}

19 Cumulative energy increase of 282 [177 to 387] ZJ over 1971–2006 (1 ZJ = 10^{21} joules).

20 Cumulative energy increase of 152 [100 to 205] ZJ over 2006–2018.

21 Understanding of climate processes, the instrumental record, paleoclimates and model-based emergent constraints (Glossary).

B. Possible Climate Futures

A set of five new illustrative emissions scenarios is considered consistently across this Report to explore the climate response to a broader range of greenhouse gas (GHG), land-use and air pollutant futures than assessed in AR5. This set of scenarios drives climate model projections of changes in the climate system. These projections account for solar activity and background forcing from volcanoes. Results over the 21st century are provided for the near term (2021–2040), mid-term (2041–2060) and long term (2081–2100) relative to 1850–1900, unless otherwise stated.

Box SPM.1 | Scenarios, Climate Models and Projections

Box SPM.1.1: This Report assesses the climate response to five illustrative scenarios that cover the range of possible future development of anthropogenic drivers of climate change found in the literature. They start in 2015, and include scenarios[22] with high and very high GHG emissions (SSP3-7.0 and SSP5-8.5) and CO_2 emissions that roughly double from current levels by 2100 and 2050, respectively, scenarios with intermediate GHG emissions (SSP2-4.5) and CO_2 emissions remaining around current levels until the middle of the century, and scenarios with very low and low GHG emissions and CO_2 emissions declining to net zero around or after 2050, followed by varying levels of net negative CO_2 emissions[23] (SSP1-1.9 and SSP1-2.6), as illustrated in Figure SPM.4. Emissions vary between scenarios depending on socio-economic assumptions, levels of climate change mitigation and, for aerosols and non-methane ozone precursors, air pollution controls. Alternative assumptions may result in similar emissions and climate responses, but the socio-economic assumptions and the feasibility or likelihood of individual scenarios are not part of the assessment.
{1.6, Cross-Chapter Box 1.4, TS.1.3} (Figure SPM.4)

Box SPM.1.2: This Report assesses results from climate models participating in the Coupled Model Intercomparison Project Phase 6 (CMIP6) of the World Climate Research Programme. These models include new and better representations of physical, chemical and biological processes, as well as higher resolution, compared to climate models considered in previous IPCC assessment reports. This has improved the simulation of the recent mean state of most large-scale indicators of climate change and many other aspects across the climate system. Some differences from observations remain, for example in regional precipitation patterns. The CMIP6 historical simulations assessed in this Report have an ensemble mean global surface temperature change within 0.2°C of the observations over most of the historical period, and observed warming is within the *very likely* range of the CMIP6 ensemble. However, some CMIP6 models simulate a warming that is either above or below the assessed *very likely* range of observed warming.
{1.5, Cross-Chapter Box 2.2, 3.3, 3.8, TS.1.2, Cross-Section Box TS.1} (Figure SPM.1b, Figure SPM.2)

Box SPM.1.3: The CMIP6 models considered in this Report have a wider range of climate sensitivity than in CMIP5 models and the AR6 assessed *very likely* range, which is based on multiple lines of evidence. These CMIP6 models also show a higher average climate sensitivity than CMIP5 and the AR6 assessed best estimate. The higher CMIP6 climate sensitivity values compared to CMIP5 can be traced to an amplifying cloud feedback that is larger in CMIP6 by about 20%.
{Box 7.1, 7.3, 7.4, 7.5, TS.3.2}

Box SPM.1.4: For the first time in an IPCC report, assessed future changes in global surface temperature, ocean warming and sea level are constructed by combining multi-model projections with observational constraints based on past simulated warming, as well as the AR6 assessment of climate sensitivity. For other quantities, such robust methods do not yet exist to constrain the projections. Nevertheless, robust projected geographical patterns of many variables can be identified at a given level of global warming, common to all scenarios considered and independent of timing when the global warming level is reached.
{1.6, 4.3, 4.6, Box 4.1, 7.5, 9.2, 9.6, Cross-Chapter Box 11.1, Cross-Section Box TS.1}

---

22 Throughout this Report, the five illustrative scenarios are referred to as SSPx-y, where 'SSPx' refers to the Shared Socio-economic Pathway or 'SSP' describing the socio-economic trends underlying the scenario, and 'y' refers to the approximate level of radiative forcing (in watts per square metre, or W m^{-2}) resulting from the scenario in the year 2100. A detailed comparison to scenarios used in earlier IPCC reports is provided in Section TS.1.3, and Sections 1.6 and 4.6. The SSPs that underlie the specific forcing scenarios used to drive climate models are not assessed by WGI. Rather, the SSPx-y labelling ensures traceability to the underlying literature in which specific forcing pathways are used as input to the climate models. IPCC is neutral with regard to the assumptions underlying the SSPs, which do not cover all possible scenarios. Alternative scenarios may be considered or developed.

23 Net negative CO_2 emissions are reached when anthropogenic removals of CO_2 exceed anthropogenic emissions (Glossary).

Box SPM.1 (continued)

Future emissions cause future additional warming, with total warming dominated by past and future CO_2 emissions

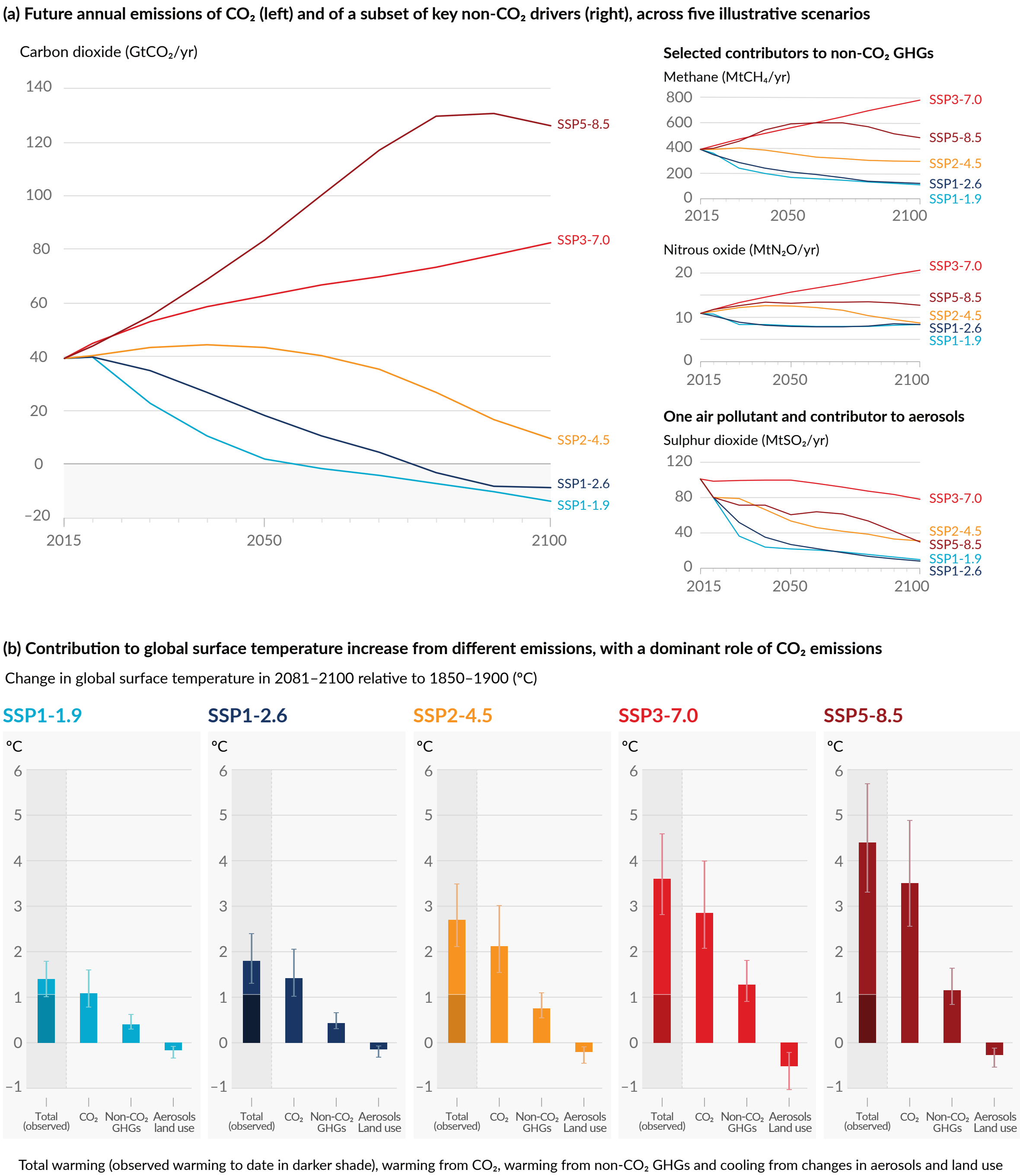

Figure SPM.4 | Future anthropogenic emissions of key drivers of climate change and warming contributions by groups of drivers for the five illustrative scenarios used in this report

The five scenarios are SSP1-1.9, SSP1-2.6, SSP2-4.5, SSP3-7.0 and SSP5-8.5.

Panel (a) Annual anthropogenic (human-caused) emissions over the 2015–2100 period. Shown are emissions trajectories for carbon dioxide (CO_2) from all sectors ($GtCO_2$/yr) (left graph) and for a subset of three key non-CO_2 drivers considered in the scenarios: methane (CH_4, $MtCH_4$/yr, top-right graph); nitrous oxide (N_2O, MtN_2O/yr, middle-right graph); and sulphur dioxide (SO_2, $MtSO_2$/yr, bottom-right graph, contributing to anthropogenic aerosols in panel (b).

Panel (b) Warming contributions by groups of anthropogenic drivers and by scenario are shown as the change in global surface temperature (°C) in 2081–2100 relative to 1850–1900, with indication of the observed warming to date. Bars and whiskers represent median values and the *very likely* range, respectively. Within each scenario bar plot, the bars represent: total global warming (°C; 'total' bar) (see Table SPM.1); warming contributions (°C) from changes in CO_2 ('CO_2' bar) and from non-CO_2 greenhouse gases (GHGs; 'non-CO_2 GHGs' bar: comprising well-mixed greenhouse gases and ozone); and net cooling from other anthropogenic drivers ('aerosols and land use' bar: anthropogenic aerosols, changes in reflectance due to land-use and irrigation changes, and contrails from aviation) (see Figure SPM.2, panel c, for the warming contributions to date for individual drivers). The best estimate for observed warming in 2010–2019 relative to 1850–1900 (see Figure SPM.2, panel a) is indicated in the darker column in the 'total' bar. Warming contributions in panel (b) are calculated as explained in Table SPM.1 for the total bar. For the other bars, the contribution by groups of drivers is calculated with a physical climate emulator of global surface temperature that relies on climate sensitivity and radiative forcing assessments.

{Cross-Chapter Box 1.4; 4.6; Figure 4.35; 6.7; Figures 6.18, 6.22 and 6.24; 7.3; Cross-Chapter Box 7.1; Figure 7.7; Box TS.7; Figures TS.4 and TS.15}

B.1 Global surface temperature will continue to increase until at least mid-century under all emissions scenarios considered. Global warming of 1.5°C and 2°C will be exceeded during the 21st century unless deep reductions in CO_2 and other greenhouse gas emissions occur in the coming decades.
{2.3, Cross-Chapter Box 2.3, Cross-Chapter Box 2.4, 4.3, 4.4, 4.5} (Figure SPM.1, Figure SPM.4, Figure SPM.8, Table SPM.1, Box SPM.1)

B.1.1 Compared to 1850–1900, global surface temperature averaged over 2081–2100 is *very likely* to be higher by 1.0°C to 1.8°C under the very low GHG emissions scenario considered (SSP1-1.9), by 2.1°C to 3.5°C in the intermediate GHG emissions scenario (SSP2-4.5) and by 3.3°C to 5.7°C under the very high GHG emissions scenario (SSP5-8.5).[24] The last time global surface temperature was sustained at or above 2.5°C higher than 1850–1900 was over 3 million years ago (*medium confidence*).
{2.3, Cross-Chapter Box 2.4, 4.3, 4.5, Box TS.2, Box TS.4, Cross-Section Box TS.1} (Table SPM.1)

Table SPM.1 | Changes in global surface temperature, which are assessed based on multiple lines of evidence, for selected 20-year time periods and the five illustrative emissions scenarios considered. Temperature differences relative to the average global surface temperature of the period 1850–1900 are reported in °C. This includes the revised assessment of observed historical warming for the AR5 reference period 1986–2005, which in AR6 is higher by 0.08 [–0.01 to +0.12] °C than in AR5 (see footnote 10). Changes relative to the recent reference period 1995–2014 may be calculated approximately by subtracting 0.85°C, the best estimate of the observed warming from 1850–1900 to 1995–2014.
{Cross-Chapter Box 2.3, 4.3, 4.4, Cross-Section Box TS.1}

	Near term, 2021–2040		Mid-term, 2041–2060		Long term, 2081–2100	
Scenario	Best estimate (°C)	*Very likely* range (°C)	Best estimate (°C)	*Very likely* range (°C)	Best estimate (°C)	*Very likely* range (°C)
SSP1-1.9	1.5	1.2 to 1.7	1.6	1.2 to 2.0	1.4	1.0 to 1.8
SSP1-2.6	1.5	1.2 to 1.8	1.7	1.3 to 2.2	1.8	1.3 to 2.4
SSP2-4.5	1.5	1.2 to 1.8	2.0	1.6 to 2.5	2.7	2.1 to 3.5
SSP3-7.0	1.5	1.2 to 1.8	2.1	1.7 to 2.6	3.6	2.8 to 4.6
SSP5-8.5	1.6	1.3 to 1.9	2.4	1.9 to 3.0	4.4	3.3 to 5.7

B.1.2 Based on the assessment of multiple lines of evidence, global warming of 2°C, relative to 1850–1900, would be exceeded during the 21st century under the high and very high GHG emissions scenarios considered in this report (SSP3-7.0 and SSP5-8.5, respectively). Global warming of 2°C would *extremely likely* be exceeded in the intermediate GHG emissions scenario (SSP2-4.5). Under the very low and low GHG emissions scenarios, global warming of 2°C is *extremely unlikely* to be exceeded (SSP1-1.9) or *unlikely* to be exceeded (SSP1-2.6).[25] Crossing the 2°C global warming level in the mid-term period (2041–2060) is *very likely* to occur under the very high GHG emissions scenario (SSP5-8.5), *likely* to occur under the high GHG emissions scenario (SSP3-7.0), and *more likely than not* to occur in the intermediate GHG emissions scenario (SSP2-4.5).[26]
{4.3, Cross-Section Box TS.1} (Table SPM.1, Figure SPM.4, Box SPM.1)

24 Changes in global surface temperature are reported as running 20-year averages, unless stated otherwise.

25 SSP1-1.9 and SSP1-2.6 are scenarios that start in 2015 and have very low and low GHG emissions, respectively, and CO_2 emissions declining to net zero around or after 2050, followed by varying levels of net negative CO_2 emissions.

26 Crossing is defined here as having the assessed global surface temperature change, averaged over a 20-year period, exceed a particular global warming level.

B.1.3 Global warming of 1.5°C relative to 1850–1900 would be exceeded during the 21st century under the intermediate, high and very high GHG emissions scenarios considered in this report (SSP2-4.5, SSP3-7.0 and SSP5-8.5, respectively). Under the five illustrative scenarios, in the near term (2021–2040), the 1.5°C global warming level is *very likely* to be exceeded under the very high GHG emissions scenario (SSP5-8.5), *likely* to be exceeded under the intermediate and high GHG emissions scenarios (SSP2-4.5 and SSP3-7.0), *more likely than not* to be exceeded under the low GHG emissions scenario (SSP1-2.6) and *more likely than not* to be reached under the very low GHG emissions scenario (SSP1-1.9).[27] Furthermore, for the very low GHG emissions scenario (SSP1-1.9), it is *more likely than not* that global surface temperature would decline back to below 1.5°C toward the end of the 21st century, with a temporary overshoot of no more than 0.1°C above 1.5°C global warming.
{4.3, Cross-Section Box TS.1} (Table SPM.1, Figure SPM.4)

B.1.4 Global surface temperature in any single year can vary above or below the long-term human-induced trend, due to substantial natural variability.[28] The occurrence of individual years with global surface temperature change above a certain level, for example 1.5°C or 2°C, relative to 1850–1900 does not imply that this global warming level has been reached.[29]
{Cross-Chapter Box 2.3, 4.3, 4.4, Box 4.1, Cross-Section Box TS.1} (Table SPM.1, Figure SPM.1, Figure SPM.8)

B.2 Many changes in the climate system become larger in direct relation to increasing global warming. They include increases in the frequency and intensity of hot extremes, marine heatwaves, heavy precipitation, and, in some regions, agricultural and ecological droughts; an increase in the proportion of intense tropical cyclones; and reductions in Arctic sea ice, snow cover and permafrost.
{4.3, 4.5, 4.6, 7.4, 8.2, 8.4, Box 8.2, 9.3, 9.5, Box 9.2, 11.1, 11.2, 11.3, 11.4, 11.6, 11.7, 11.9, Cross-Chapter Box 11.1, 12.4, 12.5, Cross-Chapter Box 12.1, Atlas.4, Atlas.5, Atlas.6, Atlas.7, Atlas.8, Atlas.9, Atlas.10, Atlas.11} (Figure SPM.5, Figure SPM.6, Figure SPM.8)

B.2.1 It is *virtually certain* that the land surface will continue to warm more than the ocean surface (*likely* 1.4 to 1.7 times more). It is *virtually certain* that the Arctic will continue to warm more than global surface temperature, with *high confidence* above two times the rate of global warming.
{2.3, 4.3, 4.5, 4.6, 7.4, 11.1, 11.3, 11.9, 12.4, 12.5, Cross-Chapter Box 12.1, Atlas.4, Atlas.5, Atlas.6, Atlas.7, Atlas.8, Atlas.9, Atlas.10, Atlas.11, Cross-Section Box TS.1, TS.2.6} (Figure SPM.5)

B.2.2 With every additional increment of global warming, changes in extremes continue to become larger. For example, every additional 0.5°C of global warming causes clearly discernible increases in the intensity and frequency of hot extremes, including heatwaves (*very likely*), and heavy precipitation (*high confidence*), as well as agricultural and ecological droughts[30] in some regions (*high confidence*). Discernible changes in intensity and frequency of meteorological droughts, with more regions showing increases than decreases, are seen in some regions for every additional 0.5°C of global warming (*medium confidence*). Increases in frequency and intensity of hydrological droughts become larger with increasing global warming in some regions (*medium confidence*). There will be an increasing occurrence of some extreme events unprecedented in the observational record with additional global warming, even at 1.5°C of global warming. Projected percentage changes in frequency are larger for rarer events (*high confidence*).
{8.2, 11.2, 11.3, 11.4, 11.6, 11.9, Cross-Chapter Box 11.1, Cross-Chapter Box 12.1, TS.2.6} (Figure SPM.5, Figure SPM.6)

B.2.3 Some mid-latitude and semi-arid regions, and the South American Monsoon region, are projected to see the highest increase in the temperature of the hottest days, at about 1.5 to 2 times the rate of global warming (*high confidence*). The Arctic is projected to experience the highest increase in the temperature of the coldest days, at about three times the rate of global warming (*high confidence*). With additional global warming, the frequency of marine heatwaves will continue to increase (*high confidence*), particularly in the tropical ocean and the Arctic (*medium confidence*).
{Box 9.2, 11.1, 11.3, 11.9, Cross-Chapter Box 11.1, Cross-Chapter Box 12.1, 12.4, TS.2.4, TS.2.6} (Figure SPM.6)

---

27 The AR6 assessment of when a given global warming level is first exceeded benefits from the consideration of the illustrative scenarios, the multiple lines of evidence entering the assessment of future global surface temperature response to radiative forcing, and the improved estimate of historical warming. The AR6 assessment is thus not directly comparable to the SR1.5 SPM, which reported *likely* reaching 1.5°C global warming between 2030 and 2052, from a simple linear extrapolation of warming rates of the recent past. When considering scenarios similar to SSP1-1.9 instead of linear extrapolation, the SR1.5 estimate of when 1.5°C global warming is first exceeded is close to the best estimate reported here.

28 Natural variability refers to climatic fluctuations that occur without any human influence, that is, internal variability combined with the response to external natural factors such as volcanic eruptions, changes in solar activity and, on longer time scales, orbital effects and plate tectonics (Glossary).

29 The internal variability in any single year is estimated to be about ±0.25°C (5–95% range, *high confidence*).

30 Projected changes in agricultural and ecological droughts are primarily assessed based on total column soil moisture. See footnote 15 for definition and relation to precipitation and evapotranspiration.

B.2.4 It is *very likely* that heavy precipitation events will intensify and become more frequent in most regions with additional global warming. At the global scale, extreme daily precipitation events are projected to intensify by about 7% for each 1°C of global warming (*high confidence*). The proportion of intense tropical cyclones (Category 4–5) and peak wind speeds of the most intense tropical cyclones are projected to increase at the global scale with increasing global warming (*high confidence*). {8.2, 11.4, 11.7, 11.9, Cross-Chapter Box 11.1, Box TS.6, TS.4.3.1} (Figure SPM.5, Figure SPM.6)

B.2.5 Additional warming is projected to further amplify permafrost thawing and loss of seasonal snow cover, of land ice and of Arctic sea ice (*high confidence*). The Arctic is *likely* to be practically sea ice-free in September[31] at least once before 2050 under the five illustrative scenarios considered in this report, with more frequent occurrences for higher warming levels. There is *low confidence* in the projected decrease of Antarctic sea ice.
{4.3, 4.5, 7.4, 8.2, 8.4, Box 8.2, 9.3, 9.5, 12.4, Cross-Chapter Box 12.1, Atlas.5, Atlas.6, Atlas.8, Atlas.9, Atlas.11, TS.2.5} (Figure SPM.8)

With every increment of global warming, changes get larger in regional mean temperature, precipitation and soil moisture

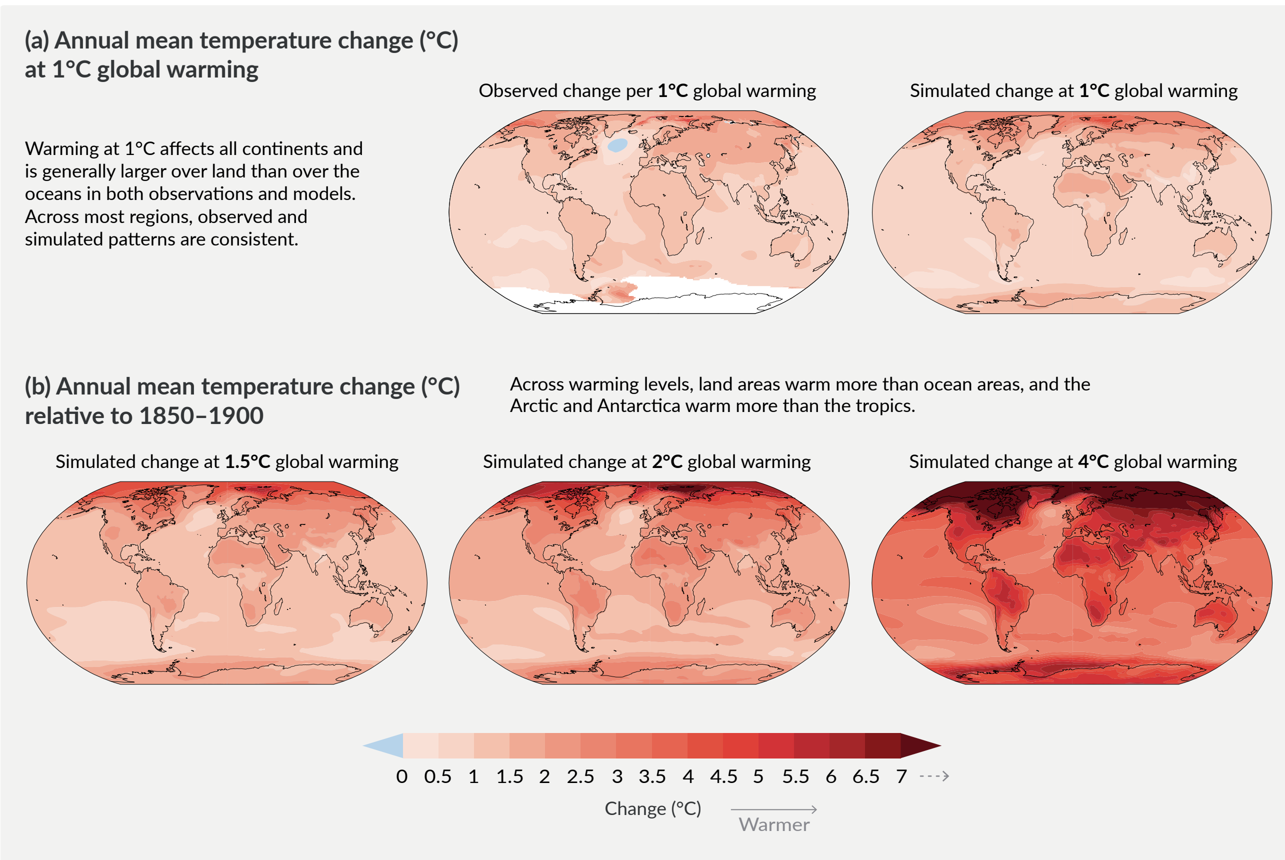

31 Monthly average sea ice area of less than 1 million km^2, which is about 15% of the average September sea ice area observed in 1979–1988.

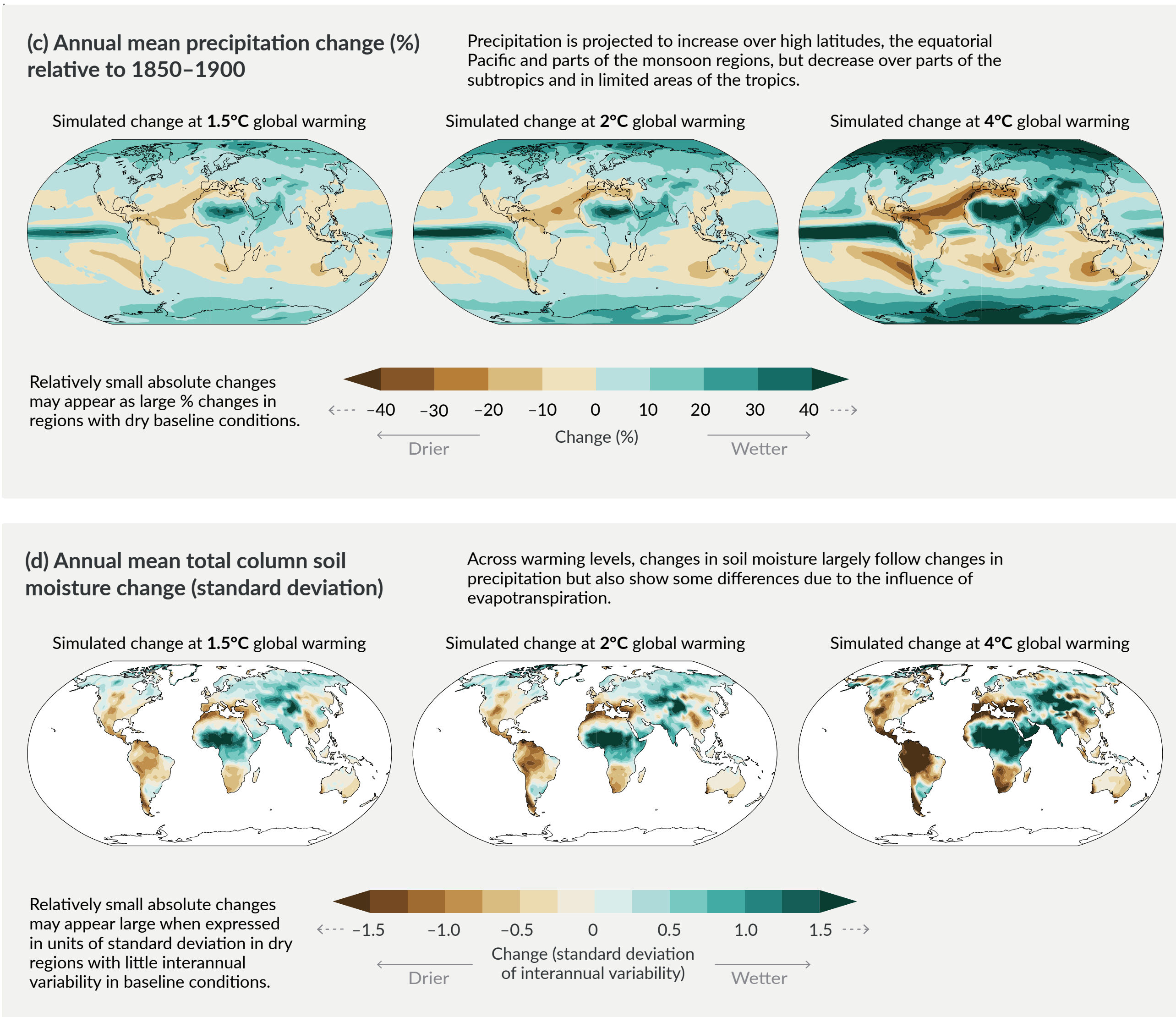

Figure SPM.5 | Changes in annual mean surface temperature, precipitation, and soil moisture

Panel (a) Comparison of observed and simulated annual mean surface temperature change. The **left map** shows the observed changes in annual mean surface temperature in the period 1850–2020 per °C of global warming (°C). The local (i.e., grid point) observed annual mean surface temperature changes are linearly regressed against the global surface temperature in the period 1850–2020. Observed temperature data are from Berkeley Earth, the dataset with the largest coverage and highest horizontal resolution. Linear regression is applied to all years for which data at the corresponding grid point is available. The regression method was used to take into account the complete observational time series and thereby reduce the role of internal variability at the grid point level. White indicates areas where time coverage was 100 years or less and thereby too short to calculate a reliable linear regression. The **right map** is based on model simulations and shows change in annual multi-model mean simulated temperatures at a global warming level of 1°C (20-year mean global surface temperature change relative to 1850–1900). The triangles at each end of the colour bar indicate out-of-bound values, that is, values above or below the given limits.

Panel (b) Simulated annual mean temperature change (°C), panel (c) precipitation change (%), and panel (d) total column soil moisture change (standard deviation of interannual variability) at global warming levels of 1.5°C, 2°C and 4°C (20-year mean global surface temperature change relative to 1850–1900). Simulated changes correspond to Coupled Model Intercomparison Project Phase 6 (CMIP6) multi-model mean change (median change for soil moisture) at the corresponding global warming level, that is, the same method as for the right map in panel (a).

In **panel (c)**, high positive percentage changes in dry regions may correspond to small absolute changes. In **panel (d)**, the unit is the standard deviation of interannual variability in soil moisture during 1850–1900. Standard deviation is a widely used metric in characterizing drought severity. A projected reduction in mean soil moisture by one standard deviation corresponds to soil moisture conditions typical of droughts that occurred about once every six years during 1850–1900. In panel (d), large changes in dry regions with little interannual variability in the baseline conditions can correspond to small absolute change. The triangles at each end of the colour bars indicate out-of-bound values, that is, values above or below the given limits. Results from all models reaching the corresponding warming level in any of the five illustrative scenarios (SSP1-1.9, SSP1-2.6, SSP2-4.5, SSP3-7.0 and SSP5-8.5) are averaged. Maps of annual mean temperature and precipitation changes at a global warming level of 3°C are available in Figure 4.31 and Figure 4.32 in Section 4.6. Corresponding maps of panels (b), (c) and (d), including hatching to indicate the level of model agreement at grid-cell level, are found in Figures 4.31, 4.32 and 11.19, respectively; as highlighted in Cross-Chapter Box Atlas.1, grid-cell level hatching is not informative for larger spatial scales (e.g., over AR6 reference regions) where the aggregated signals are less affected by small-scale variability, leading to an increase in robustness.

{Figure 1.14, 4.6.1, Cross-Chapter Box 11.1, Cross-Chapter Box Atlas.1, TS.1.3.2, Figures TS.3 and TS.5}

Projected changes in extremes are larger in frequency and intensity with every additional increment of global warming

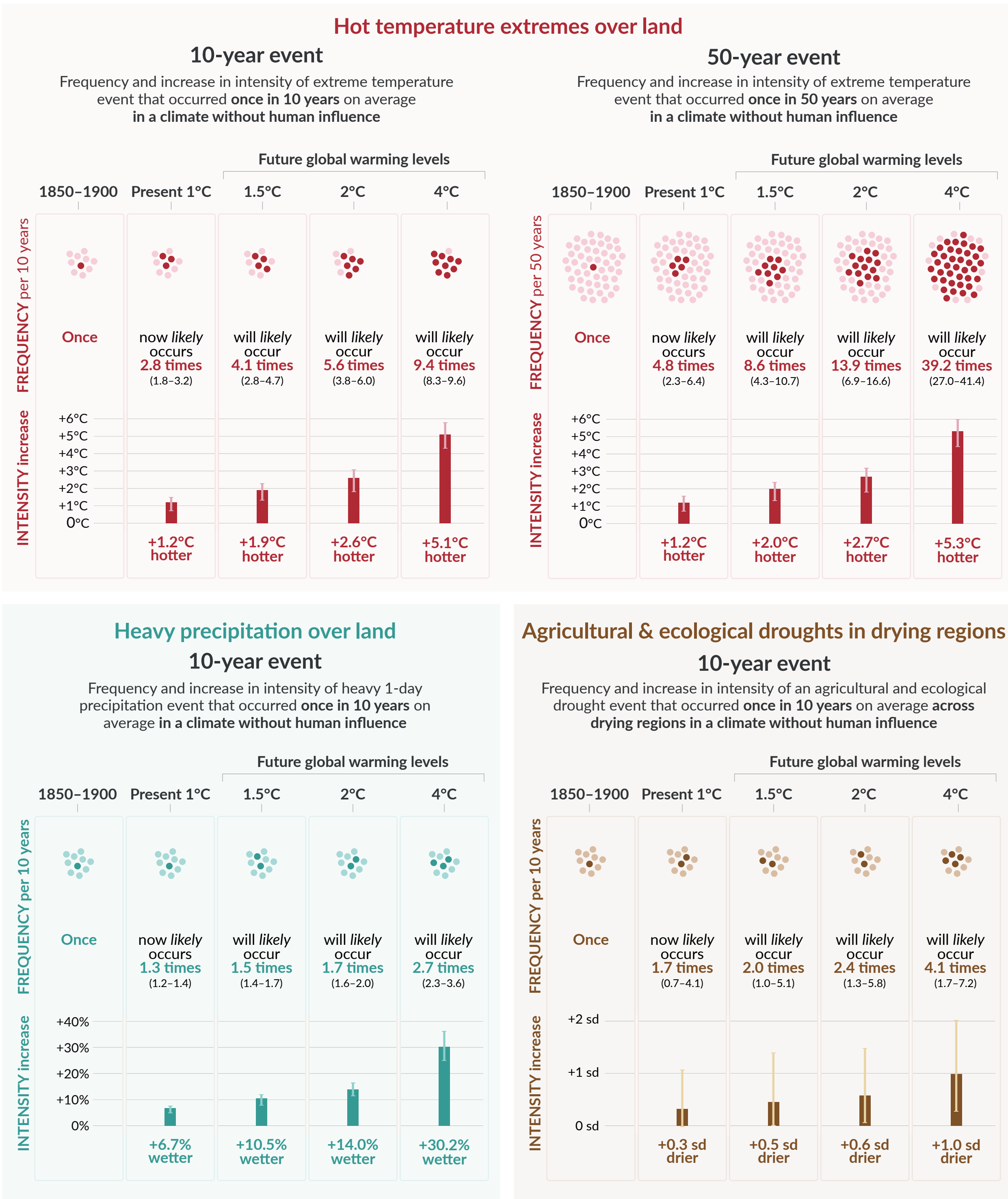

Figure SPM.6 | Projected changes in the intensity and frequency of hot temperature extremes over land, extreme precipitation over land, and agricultural and ecological droughts in drying regions

Projected changes are shown at global warming levels of 1°C, 1.5°C, 2°C, and 4°C and are relative to 1850–1900,[9] representing a climate without human influence. The figure depicts frequencies and increases in intensity of 10- or 50-year extreme events from the base period (1850–1900) under different global warming levels.

Hot temperature extremes are defined as the daily maximum temperatures over land that were exceeded on average once in a decade (10-year event) or once in 50 years (50-year event) during the 1850–1900 reference period. **Extreme precipitation events** are defined as the daily precipitation amount over land that was exceeded on average once in a decade during the 1850–1900 reference period. **Agricultural and ecological drought events** are defined as the annual average of total column soil moisture below the 10th percentile of the 1850–1900 base period. These extremes are defined on model grid box scale. For hot temperature extremes and extreme precipitation, results are shown for the global land. For agricultural and ecological drought, results are shown for drying regions only, which correspond to the AR6 regions in which there is at least *medium confidence* in a projected increase in agricultural and ecological droughts at the 2°C warming level compared to the 1850–1900 base period in the Coupled Model Intercomparison Project Phase 6 (CMIP6). These regions include Western North America, Central North America, Northern Central America, Southern Central America, Caribbean, Northern South America, North-Eastern South America, South American Monsoon, South-Western South America, Southern South America, Western and Central Europe, Mediterranean, West Southern Africa, East Southern Africa, Madagascar, Eastern Australia, and Southern Australia (Caribbean is not included in the calculation of the figure because of the too-small number of full land grid cells). The non-drying regions do not show an overall increase or decrease in drought severity. Projections of changes in agricultural and ecological droughts in the CMIP Phase 5 (CMIP5) multi-model ensemble differ from those in CMIP6 in some regions, including in parts of Africa and Asia. Assessments of projected changes in meteorological and hydrological droughts are provided in Chapter 11.

In the **'frequency' section**, each year is represented by a dot. The dark dots indicate years in which the extreme threshold is exceeded, while light dots are years when the threshold is not exceeded. Values correspond to the medians (in bold) and their respective 5–95% range based on the multi-model ensemble from simulations of CMIP6 under different Shared Socio-economic Pathway scenarios. For consistency, the number of dark dots is based on the rounded-up median. In the **'intensity' section**, medians and their 5–95% range, also based on the multi-model ensemble from simulations of CMIP6, are displayed as dark and light bars, respectively. Changes in the intensity of hot temperature extremes and extreme precipitation are expressed as degree Celsius and percentage. As for agricultural and ecological drought, intensity changes are expressed as fractions of standard deviation of annual soil moisture.

{11.1; 11.3; 11.4; 11.6; 11.9; Figures 11.12, 11.15, 11.6, 11.7, and 11.18}

B.3 Continued global warming is projected to further intensify the global water cycle, including its variability, global monsoon precipitation and the severity of wet and dry events.
{4.3, 4.4, 4.5, 4.6, 8.2, 8.3, 8.4, 8.5, Box 8.2, 11.4, 11.6, 11.9, 12.4, Atlas.3} (Figure SPM.5, Figure SPM.6)

B.3.1 There is strengthened evidence since AR5 that the global water cycle will continue to intensify as global temperatures rise (*high confidence*), with precipitation and surface water flows projected to become more variable over most land regions within seasons (*high confidence*) and from year to year (*medium confidence*). The average annual global land precipitation is projected to increase by 0–5% under the very low GHG emissions scenario (SSP1-1.9), 1.5–8% for the intermediate GHG emissions scenario (SSP2-4.5) and 1–13% under the very high GHG emissions scenario (SSP5-8.5) by 2081–2100 relative to 1995–2014 (*likely* ranges). Precipitation is projected to increase over high latitudes, the equatorial Pacific and parts of the monsoon regions, but decrease over parts of the subtropics and limited areas in the tropics in SSP2-4.5, SSP3-7.0 and SSP5-8.5 (*very likely*). The portion of the global land experiencing detectable increases or decreases in seasonal mean precipitation is projected to increase (*medium confidence*). There is *high confidence* in an earlier onset of spring snowmelt, with higher peak flows at the expense of summer flows in snow-dominated regions globally.
{4.3, 4.5, 4.6, 8.2, 8.4, Atlas.3, TS.2.6, TS.4.3, Box TS.6} (Figure SPM.5)

B.3.2 A warmer climate will intensify very wet and very dry weather and climate events and seasons, with implications for flooding or drought (*high confidence*), but the location and frequency of these events depend on projected changes in regional atmospheric circulation, including monsoons and mid-latitude storm tracks. It is *very likely* that rainfall variability related to the El Niño–Southern Oscillation is projected to be amplified by the second half of the 21st century in the SSP2-4.5, SSP3-7.0 and SSP5-8.5 scenarios.
{4.3, 4.5, 4.6, 8.2, 8.4, 8.5, 11.4, 11.6, 11.9, 12.4, TS.2.6, TS.4.2, Box TS.6} (Figure SPM.5, Figure SPM.6)

B.3.3 Monsoon precipitation is projected to increase in the mid- to long term at the global scale, particularly over South and South East Asia, East Asia and West Africa apart from the far west Sahel (*high confidence*). The monsoon season is projected to have a delayed onset over North and South America and West Africa (*high confidence*) and a delayed retreat over West Africa (*medium confidence*).
{4.4, 4.5, 8.2, 8.3, 8.4, Box 8.2, Box TS.13}

B.3.4 A projected southward shift and intensification of Southern Hemisphere summer mid-latitude storm tracks and associated precipitation is *likely* in the long term under high GHG emissions scenarios (SSP3-7.0, SSP5-8.5), but in the near term the effect of stratospheric ozone recovery counteracts these changes (*high confidence*). There is *medium confidence* in a continued poleward shift of storms and their precipitation in the North Pacific, while there is *low confidence* in projected changes in the North Atlantic storm tracks.
{4.4, 4.5, 8.4, TS.2.3, TS.4.2}

B.4 Under scenarios with increasing CO_2 emissions, the ocean and land carbon sinks are projected to be less effective at slowing the accumulation of CO_2 in the atmosphere.
{4.3, 5.2, 5.4, 5.5, 5.6} (Figure SPM.7)

B.4.1 While natural land and ocean carbon sinks are projected to take up, in absolute terms, a progressively larger amount of CO_2 under higher compared to lower CO_2 emissions scenarios, they become less effective, that is, the proportion of emissions taken up by land and ocean decrease with increasing cumulative CO_2 emissions. This is projected to result in a higher proportion of emitted CO_2 remaining in the atmosphere (*high confidence*).
{5.2, 5.4, Box TS.5} (Figure SPM.7)

B.4.2 Based on model projections, under the intermediate GHG emissions scenario that stabilizes atmospheric CO_2 concentrations this century (SSP2-4.5), the rates of CO_2 taken up by the land and ocean are projected to decrease in the second half of the 21st century (*high confidence*). Under the very low and low GHG emissions scenarios (SSP1-1.9, SSP1-2.6), where CO_2 concentrations peak and decline during the 21st century, the land and ocean begin to take up less carbon in response to declining atmospheric CO_2 concentrations (*high confidence*) and turn into a weak net source by 2100 under SSP1-1.9 (*medium confidence*). It is *very unlikely* that the combined global land and ocean sink will turn into a source by 2100 under scenarios without net negative emissions (SSP2-4.5, SSP3-7.0, SSP5-8.5).[32]
{4.3, 5.4, 5.5, 5.6, Box TS.5, TS.3.3}

B.4.3 The magnitude of feedbacks between climate change and the carbon cycle becomes larger but also more uncertain in high CO_2 emissions scenarios (*very high confidence*). However, climate model projections show that the uncertainties in atmospheric CO_2 concentrations by 2100 are dominated by the differences between emissions scenarios (*high confidence*). Additional ecosystem responses to warming not yet fully included in climate models, such as CO_2 and CH_4 fluxes from wetlands, permafrost thaw and wildfires, would further increase concentrations of these gases in the atmosphere (*high confidence*).
{5.4, Box TS.5, TS.3.2}

The proportion of CO_2 emissions taken up by land and ocean carbon sinks is smaller in scenarios with higher cumulative CO_2 emissions

Total cumulative CO_2 emissions **taken up by land and ocean** (colours) and remaining in the atmosphere (grey) under the five illustrative scenarios from 1850 to 2100

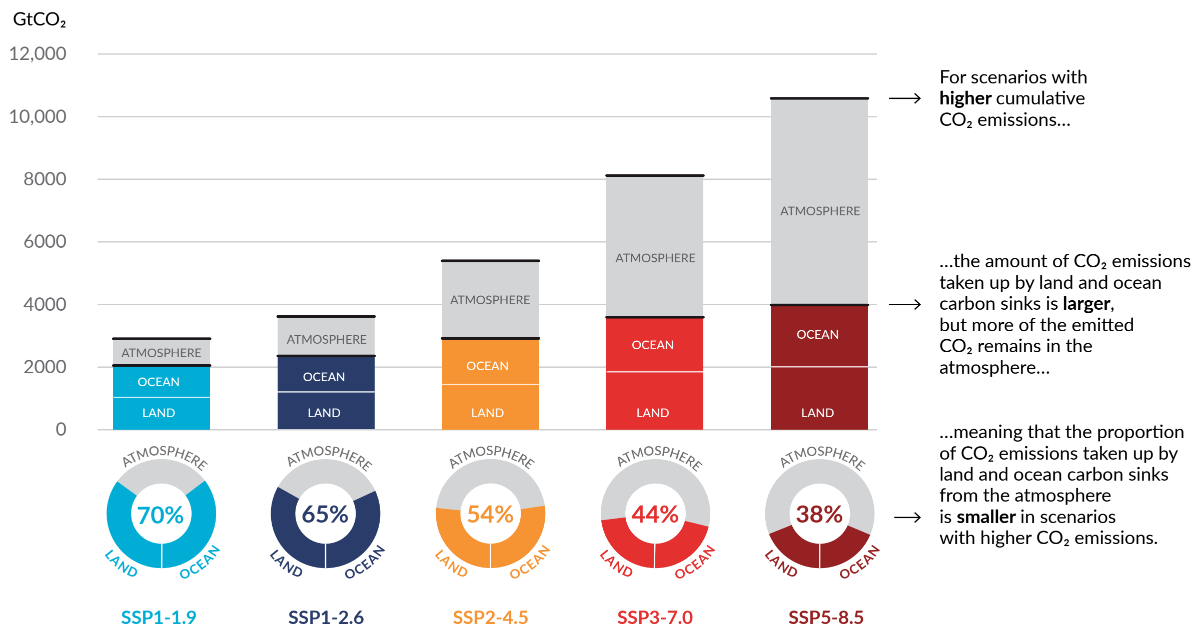

Figure SPM.7 | Cumulative anthropogenic CO_2 emissions taken up by land and ocean sinks by 2100 under the five illustrative scenarios

The cumulative anthropogenic (human-caused) carbon dioxide (CO_2) emissions taken up by the land and ocean sinks under the five illustrative scenarios (SSP1-1.9, SSP1-2.6, SSP2-4.5, SSP3-7.0 and SSP5-8.5) are simulated from 1850 to 2100 by Coupled Model Intercomparison Project Phase 6 (CMIP6) climate models in the concentration-driven simulations. Land and ocean carbon sinks respond to past, current and future emissions; therefore, cumulative sinks from 1850 to 2100 are presented here. During the historical period (1850–2019) the observed land and ocean sink took up 1430 $GtCO_2$ (59% of the emissions).

32 These projected adjustments of carbon sinks to stabilization or decline of atmospheric CO_2 are accounted for in calculations of remaining carbon budgets.

The bar chart illustrates the projected amount of cumulative anthropogenic CO_2 emissions ($GtCO_2$) between 1850 and 2100 remaining in the atmosphere (grey part) and taken up by the land and ocean (coloured part) in the year 2100. **The doughnut chart** illustrates the proportion of the cumulative anthropogenic CO_2 emissions taken up by the land and ocean sinks and remaining in the atmosphere in the year 2100. Values in % indicate the proportion of the cumulative anthropogenic CO_2 emissions taken up by the combined land and ocean sinks in the year 2100. The overall anthropogenic carbon emissions are calculated by adding the net global land-use emissions from the CMIP6 scenario database to the other sectoral emissions calculated from climate model runs with prescribed CO_2 concentrations.[33] Land and ocean CO_2 uptake since 1850 is calculated from the net biome productivity on land, corrected for CO_2 losses due to land-use change by adding the land-use change emissions, and net ocean CO_2 flux.

{5.2.1; Table 5.1; 5.4.5; Figure 5.25; Box TS.5; Box TS.5, Figure 1}

B.5 Many changes due to past and future greenhouse gas emissions are irreversible for centuries to millennia, especially changes in the ocean, ice sheets and global sea level.
{2.3, Cross-Chapter Box 2.4, 4.3, 4.5, 4.7, 5.3, 9.2, 9.4, 9.5, 9.6, Box 9.4} (Figure SPM.8)

B.5.1 Past GHG emissions since 1750 have committed the global ocean to future warming (*high confidence*). Over the rest of the 21st century, *likely* ocean warming ranges from 2–4 (SSP1-2.6) to 4–8 times (SSP5-8.5) the 1971–2018 change. Based on multiple lines of evidence, upper ocean stratification (*virtually certain*), ocean acidification (*virtually certain*) and ocean deoxygenation (*high confidence*) will continue to increase in the 21st century, at rates dependent on future emissions. Changes are irreversible on centennial to millennial time scales in global ocean temperature (*very high confidence*), deep-ocean acidification (*very high confidence*) and deoxygenation (*medium confidence*).
{4.3, 4.5, 4.7, 5.3, 9.2, TS.2.4} (Figure SPM.8)

B.5.2 Mountain and polar glaciers are committed to continue melting for decades or centuries (*very high confidence*). Loss of permafrost carbon following permafrost thaw is irreversible at centennial time scales (*high confidence*). Continued ice loss over the 21st century is *virtually certain* for the Greenland Ice Sheet and *likely* for the Antarctic Ice Sheet. There is *high confidence* that total ice loss from the Greenland Ice Sheet will increase with cumulative emissions. There is *limited evidence* for low-likelihood, high-impact outcomes (resulting from ice-sheet instability processes characterized by deep uncertainty and in some cases involving tipping points) that would strongly increase ice loss from the Antarctic Ice Sheet for centuries under high GHG emissions scenarios.[34]
{4.3, 4.7, 5.4, 9.4, 9.5, Box 9.4, Box TS.1, TS.2.5}

B.5.3 It is *virtually certain* that global mean sea level will continue to rise over the 21st century. Relative to 1995–2014, the *likely* global mean sea level rise by 2100 is 0.28–0.55 m under the very low GHG emissions scenario (SSP1-1.9); 0.32–0.62 m under the low GHG emissions scenario (SSP1-2.6); 0.44–0.76 m under the intermediate GHG emissions scenario (SSP2-4.5); and 0.63–1.01 m under the very high GHG emissions scenario (SSP5-8.5); and by 2150 is 0.37–0.86 m under the very low scenario (SSP1-1.9); 0.46–0.99 m under the low scenario (SSP1-2.6); 0.66–1.33 m under the intermediate scenario (SSP2-4.5); and 0.98–1.88 m under the very high scenario (SSP5-8.5) (*medium confidence*).[35] Global mean sea level rise above the *likely* range – approaching 2 m by 2100 and 5 m by 2150 under a very high GHG emissions scenario (SSP5-8.5) (*low confidence*) – cannot be ruled out due to deep uncertainty in ice-sheet processes.
{4.3, 9.6, Box 9.4, Box TS.4} (Figure SPM.8)

B.5.4 In the longer term, sea level is committed to rise for centuries to millennia due to continuing deep-ocean warming and ice-sheet melt and will remain elevated for thousands of years (*high confidence*). Over the next 2000 years, global mean sea level will rise by about 2 to 3 m if warming is limited to 1.5°C, 2 to 6 m if limited to 2°C and 19 to 22 m with 5°C of warming, and it will continue to rise over subsequent millennia (*low confidence*). Projections of multi-millennial global mean sea level rise are consistent with reconstructed levels during past warm climate periods: *likely* 5–10 m higher than today around 125,000 years ago, when global temperatures were *very likely* 0.5°C–1.5°C higher than 1850–1900; and *very likely* 5–25 m higher roughly 3 million years ago, when global temperatures were 2.5°C–4°C higher (*medium confidence*).
{2.3, Cross-Chapter Box 2.4, 9.6, Box TS.2, Box TS.4, Box TS.9}

---

33 The other sectoral emissions are calculated as the residual of the net land and ocean CO_2 uptake and the prescribed atmospheric CO_2 concentration changes in the CMIP6 simulations. These calculated emissions are net emissions and do not separate gross anthropogenic emissions from removals, which are included implicitly.

34 Low-likelihood, high-impact outcomes are those whose probability of occurrence is low or not well known (as in the context of deep uncertainty) but whose potential impacts on society and ecosystems could be high. A tipping point is a critical threshold beyond which a system reorganizes, often abruptly and/or irreversibly. (Glossary) {1.4, Cross-Chapter Box 1.3, 4.7}

35 To compare to the 1986–2005 baseline period used in AR5 and SROCC, add 0.03 m to the global mean sea level rise estimates. To compare to the 1900 baseline period used in Figure SPM.8, add 0.16 m.

SPM

Human activities affect all the major climate system components, with some responding over decades and others over centuries

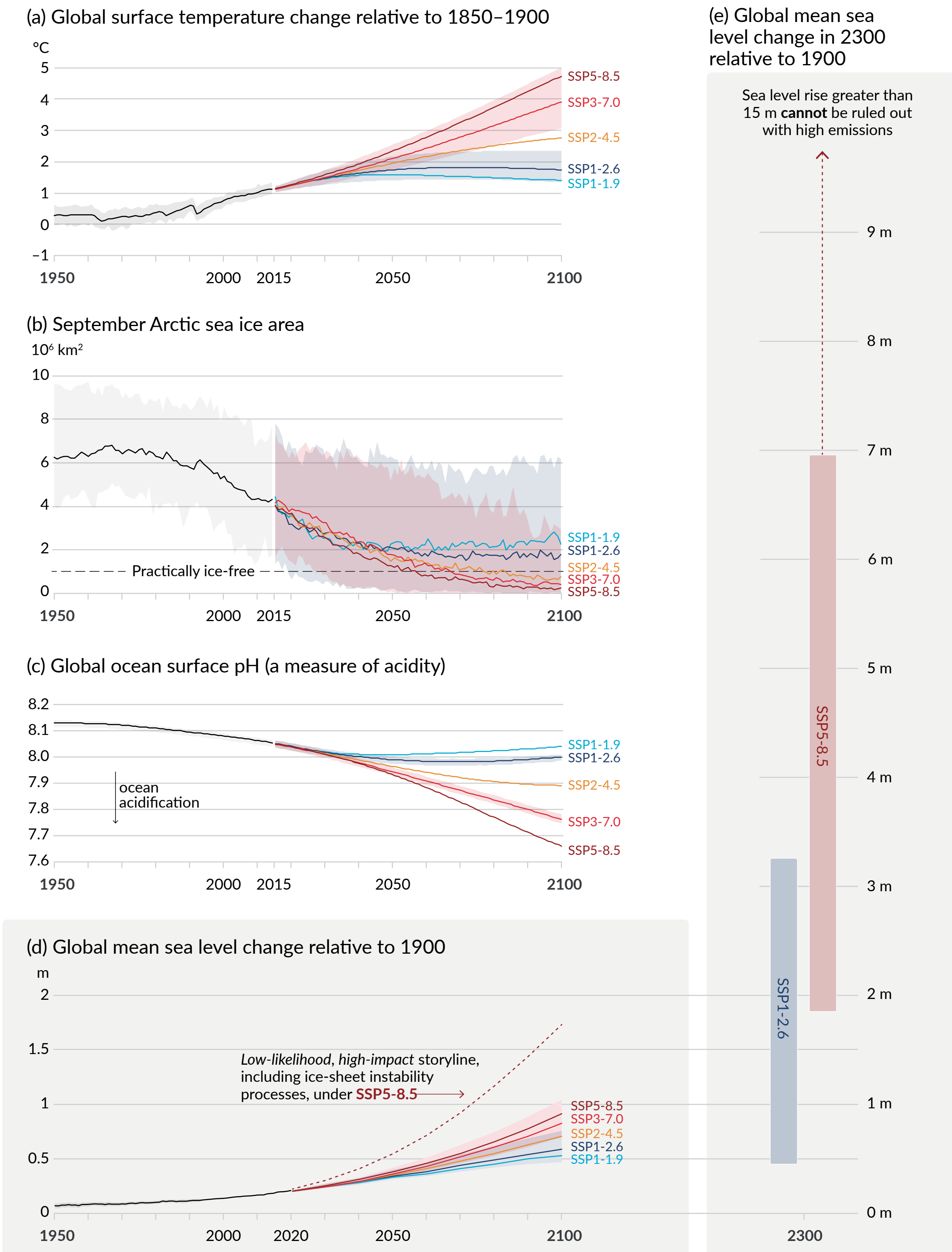

Figure SPM.8 | Selected indicators of global climate change under the five illustrative scenarios used in this Report

The projections for each of the five scenarios are shown in colour. Shades represent uncertainty ranges – more detail is provided for each panel below. The black curves represent the historical simulations (panels a, b, c) or the observations (panel d). Historical values are included in all graphs to provide context for the projected future changes.

Panel (a) Global surface temperature changes in °C relative to 1850–1900. These changes were obtained by combining Coupled Model Intercomparison Project Phase 6 (CMIP6) model simulations with observational constraints based on past simulated warming, as well as an updated assessment of equilibrium climate sensitivity (see Box SPM.1). Changes relative to 1850–1900 based on 20-year averaging periods are calculated by adding 0.85°C (the observed global surface temperature increase from 1850–1900 to 1995–2014) to simulated changes relative to 1995–2014. *Very likely* ranges are shown for SSP1-2.6 and SSP3-7.0.

Panel (b) September Arctic sea ice area in 10^6 km^2 based on CMIP6 model simulations. *Very likely* ranges are shown for SSP1-2.6 and SSP3-7.0. The Arctic is projected to be practically ice-free near mid-century under intermediate and high GHG emissions scenarios.

Panel (c) Global ocean surface pH (a measure of acidity) based on CMIP6 model simulations. *Very likely* ranges are shown for SSP1-2.6 and SSP3-7.0.

Panel (d) Global mean sea level change in metres, relative to 1900. The historical changes are observed (from tide gauges before 1992 and altimeters afterwards), and the future changes are assessed consistently with observational constraints based on emulation of CMIP, ice-sheet, and glacier models. *Likely* ranges are shown for SSP1-2.6 and SSP3-7.0. Only *likely* ranges are assessed for sea level changes due to difficulties in estimating the distribution of deeply uncertain processes. The dashed curve indicates the potential impact of these deeply uncertain processes. It shows the 83rd percentile of SSP5-8.5 projections that include low-likelihood, high-impact ice-sheet processes that cannot be ruled out; because of *low confidence* in projections of these processes, this curve does not constitute part of a *likely* range. Changes relative to 1900 are calculated by adding 0.158 m (observed global mean sea level rise from 1900 to 1995–2014) to simulated and observed changes relative to 1995–2014.

Panel (e) Global mean sea level change at 2300 in metres relative to 1900. Only SSP1-2.6 and SSP5-8.5 are projected at 2300, as simulations that extend beyond 2100 for the other scenarios are too few for robust results. The 17th–83rd percentile ranges are shaded. The dashed arrow illustrates the 83rd percentile of SSP5-8.5 projections that include low-likelihood, high-impact ice-sheet processes that cannot be ruled out.

Panels (b) and (c) are based on single simulations from each model, and so include a component of internal variability. Panels (a), (d) and (e) are based on long-term averages, and hence the contributions from internal variability are small.

{4.3; Figures 4.2, 4.8, and 4.11; 9.6; Figure 9.27; Figures TS.8 and TS.11; Box TS.4, Figure 1}

C. Climate Information for Risk Assessment and Regional Adaptation

Physical climate information addresses how the climate system responds to the interplay between human influence, natural drivers and internal variability. Knowledge of the climate response and the range of possible outcomes, including low-likelihood, high impact outcomes, informs climate services, the assessment of climate-related risks, and adaptation planning. Physical climate information at global, regional and local scales is developed from multiple lines of evidence, including observational products, climate model outputs and tailored diagnostics.

C.1 Natural drivers and internal variability will modulate human-caused changes, especially at regional scales and in the near term, with little effect on centennial global warming. These modulations are important to consider in planning for the full range of possible changes.
{1.4, 2.2, 3.3, Cross-Chapter Box 3.1, 4.4, 4.6, Cross-Chapter Box 4.1, Box 7.2, 8.3, 8.5, 9.2, 10.3, 10.4, 10.6, 11.3, 12.5, Atlas.4, Atlas.5, Atlas.8, Atlas.9, Atlas.10, Atlas.11, Cross-Chapter Box Atlas.2}

C.1.1 The historical global surface temperature record highlights that decadal variability has both enhanced and masked underlying human-caused long-term changes, and this variability will continue into the future (*very high confidence*). For example, internal decadal variability and variations in solar and volcanic drivers partially masked human-caused surface global warming during 1998–2012, with pronounced regional and seasonal signatures (*high confidence*). Nonetheless, the heating of the climate system continued during this period, as reflected in both the continued warming of the global ocean (*very high confidence*) and in the continued rise of hot extremes over land (*medium confidence*).
{1.4, 3.3, Cross-Chapter Box 3.1, 4.4, Box 7.2, 9.2, 11.3, Cross-Section Box TS.1} (Figure SPM.1)

C.1.2 Projected human-caused changes in mean climate and climatic impact-drivers (CIDs),[36] including extremes, will be either amplified or attenuated by internal variability (*high confidence*).[37] Near-term cooling at any particular location with respect to present climate could occur and would be consistent with the global surface temperature increase due to human influence (*high confidence*).
{1.4, 4.4, 4.6, 10.4, 11.3, 12.5, Atlas.5, Atlas.10, Atlas.11, TS.4.2}

---

36 Climatic impact-drivers (CIDs) are physical climate system conditions (e.g., means, events, extremes) that affect an element of society or ecosystems. Depending on system tolerance, CIDs and their changes can be detrimental, beneficial, neutral, or a mixture of each across interacting system elements and regions (Glossary). CID types include heat and cold, wet and dry, wind, snow and ice, coastal and open ocean.

37 The main internal variability phenomena include El Niño–Southern Oscillation, Pacific Decadal Variability and Atlantic Multi-decadal Variability through their regional influence.

C.1.3 Internal variability has largely been responsible for the amplification and attenuation of the observed human-caused decadal-to-multi-decadal mean precipitation changes in many land regions (*high confidence*). At global and regional scales, near-term changes in monsoons will be dominated by the effects of internal variability (*medium confidence*). In addition to the influence of internal variability, near-term projected changes in precipitation at global and regional scales are uncertain because of model uncertainty and uncertainty in forcings from natural and anthropogenic aerosols (*medium confidence*).
{1.4, 4.4, 8.3, 8.5, 10.3, 10.4, 10.5, 10.6, Atlas.4, Atlas.8, Atlas.9, Atlas.10, Atlas.11, Cross-Chapter Box Atlas.2, TS.4.2, Box TS.6, Box TS.13}

C.1.4 Based on paleoclimate and historical evidence, it is *likely* that at least one large explosive volcanic eruption would occur during the 21st century.[38] Such an eruption would reduce global surface temperature and precipitation, especially over land, for one to three years, alter the global monsoon circulation, modify extreme precipitation and change many CIDs (*medium confidence*). If such an eruption occurs, this would therefore temporarily and partially mask human-caused climate change.
{2.2, 4.4, Cross-Chapter Box 4.1, 8.5, TS.2.1}

C.2 With further global warming, every region is projected to increasingly experience concurrent and multiple changes in climatic impact-drivers. Changes in several climatic impact-drivers would be more widespread at 2°C compared to 1.5°C global warming and even more widespread and/or pronounced for higher warming levels.
{8.2, 9.3, 9.5, 9.6, Box 10.3, 11.3, 11.4, 11.5, 11.6, 11.7, 11.9, Box 11.3, Box 11.4, Cross-Chapter Box 11.1, 12.2, 12.3, 12.4, 12.5, Cross-Chapter Box 12.1, Atlas.4, Atlas.5, Atlas.6, Atlas.7, Atlas.8, Atlas.9, Atlas.10, Atlas.11} (Table SPM.1, Figure SPM.9)

C.2.1 All regions[39] are projected to experience further increases in hot climatic impact-drivers (CIDs) and decreases in cold CIDs (*high confidence*). Further decreases are projected in permafrost; snow, glaciers and ice sheets; and lake and Arctic sea ice (*medium* to *high confidence*).[40] These changes would be larger at 2°C global warming or above than at 1.5°C (*high confidence*). For example, extreme heat thresholds relevant to agriculture and health are projected to be exceeded more frequently at higher global warming levels (*high confidence*).
{9.3, 9.5, 11.3, 11.9, Cross-Chapter Box 11.1, 12.3, 12.4, 12.5, Cross-Chapter Box 12.1, Atlas.4, Atlas.5, Atlas.6, Atlas.7, Atlas.8, Atlas.9, Atlas.10, Atlas.11, TS.4.3} (Table SPM.1, Figure SPM.9)

C.2.2 At 1.5°C global warming, heavy precipitation and associated flooding are projected to intensify and be more frequent in most regions in Africa and Asia (*high confidence*), North America (*medium* to *high confidence*)[40] and Europe (*medium confidence*). Also, more frequent and/or severe agricultural and ecological droughts are projected in a few regions in all inhabited continents except Asia compared to 1850–1900 (*medium confidence*); increases in meteorological droughts are also projected in a few regions (*medium confidence*). A small number of regions are projected to experience increases or decreases in mean precipitation (*medium confidence*).
{11.4, 11.5, 11.6, 11.9, Atlas.4, Atlas.5, Atlas.7, Atlas.8, Atlas.9, Atlas.10, Atlas.11, TS.4.3} (Table SPM.1)

C.2.3 At 2°C global warming and above, the level of confidence in and the magnitude of the change in droughts and heavy and mean precipitation increase compared to those at 1.5°C. Heavy precipitation and associated flooding events are projected to become more intense and frequent in the Pacific Islands and across many regions of North America and Europe (*medium* to *high confidence*).[40] These changes are also seen in some regions in Australasia and Central and South America (*medium confidence*). Several regions in Africa, South America and Europe are projected to experience an increase in frequency and/or severity of agricultural and ecological droughts with *medium* to *high confidence*;[40] increases are also projected in Australasia, Central and North America, and the Caribbean with *medium confidence*. A small number of regions in Africa, Australasia, Europe and North America are also projected to be affected by increases in hydrological droughts, and several regions are projected to be affected by increases or decreases in meteorological droughts, with more regions displaying an increase (*medium confidence*). Mean precipitation is projected to increase in all polar, northern European and northern North American regions, most Asian regions and two regions of South America (*high confidence*).
{11.4, 11.6, 11.9, Cross-Chapter Box 11.1, 12.4, 12.5, Cross-Chapter Box 12.1, Atlas.5, Atlas.7, Atlas.8, Atlas.9, Atlas.11, TS.4.3} (Table SPM.1, Figure SPM.5, Figure SPM.6, Figure SPM.9)

---

38 Based on 2500 year reconstructions, eruptions more negative than -1 W m^{-2} occur on average twice per century.

39 Regions here refer to the AR6 WGI reference regions used in this Report to summarize information in sub-continental and oceanic regions. Changes are compared to averages over the last 20–40 years unless otherwise specified. {1.4, 12.4, Atlas.1}.

40 The specific level of confidence or likelihood depends on the region considered. Details can be found in the Technical Summary and the underlying Report.

C.2.4 More CIDs across more regions are projected to change at 2°C and above compared to 1.5°C global warming (*high confidence*). Region-specific changes include intensification of tropical cyclones and/or extratropical storms (*medium confidence*), increases in river floods (*medium* to *high confidence*),[40] reductions in mean precipitation and increases in aridity (*medium* to *high confidence*),[40] and increases in fire weather (*medium* to *high confidence*).[40] There is *low confidence* in most regions in potential future changes in other CIDs, such as hail, ice storms, severe storms, dust storms, heavy snowfall and landslides.
{11.7, 11.9, Cross-Chapter Box 11.1, 12.4, 12.5, Cross-Chapter Box 12.1, Atlas.4, Atlas.6, Atlas.7, Atlas.8, Atlas.10, TS.4.3.1, TS.4.3.2, TS.5} (Table SPM.1, Figure SPM.9)

C.2.5 It is *very likely* to *virtually certain*[40] that regional mean relative sea level rise will continue throughout the 21st century, except in a few regions with substantial geologic land uplift rates. Approximately two-thirds of the global coastline has a projected regional relative sea level rise within ±20% of the global mean increase (*medium confidence*). Due to relative sea level rise, extreme sea level events that occurred once per century in the recent past are projected to occur at least annually at more than half of all tide gauge locations by 2100 (*high confidence*). Relative sea level rise contributes to increases in the frequency and severity of coastal flooding in low-lying areas and to coastal erosion along most sandy coasts (*high confidence*).
{9.6, 12.4, 12.5, Cross-Chapter Box 12.1, Box TS.4, TS.4.3} (Figure SPM.9)

C.2.6 Cities intensify human-induced warming locally, and further urbanization together with more frequent hot extremes will increase the severity of heatwaves (*very high confidence*). Urbanization also increases mean and heavy precipitation over and/or downwind of cities (*medium confidence*) and resulting runoff intensity (*high confidence*). In coastal cities, the combination of more frequent extreme sea level events (due to sea level rise and storm surge) and extreme rainfall/riverflow events will make flooding more probable (*high confidence*).
{8.2, Box 10.3, 11.3, 12.4, Box TS.14}

C.2.7 Many regions are projected to experience an increase in the probability of compound events with higher global warming (*high confidence*). In particular, concurrent heatwaves and droughts are *likely* to become more frequent. Concurrent extremes at multiple locations, including in crop-producing areas, become more frequent at 2°C and above compared to 1.5°C global warming (*high confidence*).
{11.8, Box 11.3, Box 11.4, 12.3, 12.4, Cross-Chapter Box 12.1, TS.4.3} (Table SPM.1)

Multiple climatic impact-drivers are projected to change in all regions of the world

Climatic impact-drivers (CIDs) are physical climate system conditions (e.g., means, events, extremes) that affect an element of society or ecosystems. Depending on system tolerance, CIDs and their changes can be detrimental, beneficial, neutral, or a mixture of each across interacting system elements and regions. The CIDs are grouped into seven types, which are summarized under the icons in the figure. All regions are projected to experience changes in at least 5 CIDs. Almost all (96%) are projected to experience changes in at least 10 CIDs and half in at least 15 CIDs. For many CID changes, there is wide geographical variation, and so each region is projected to experience a specific set of CID changes. Each bar in the chart represents a specific geographical set of changes that can be explored in the WGI Interactive Atlas.

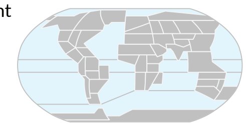

interactive-atlas.ipcc.ch

Number of land & coastal regions (a) and **open-ocean regions** (b) where each **climatic impact-driver** (CID) is projected to **increase** or **decrease** with ***high** confidence* (dark shade) or ***medium** confidence* (light shade)

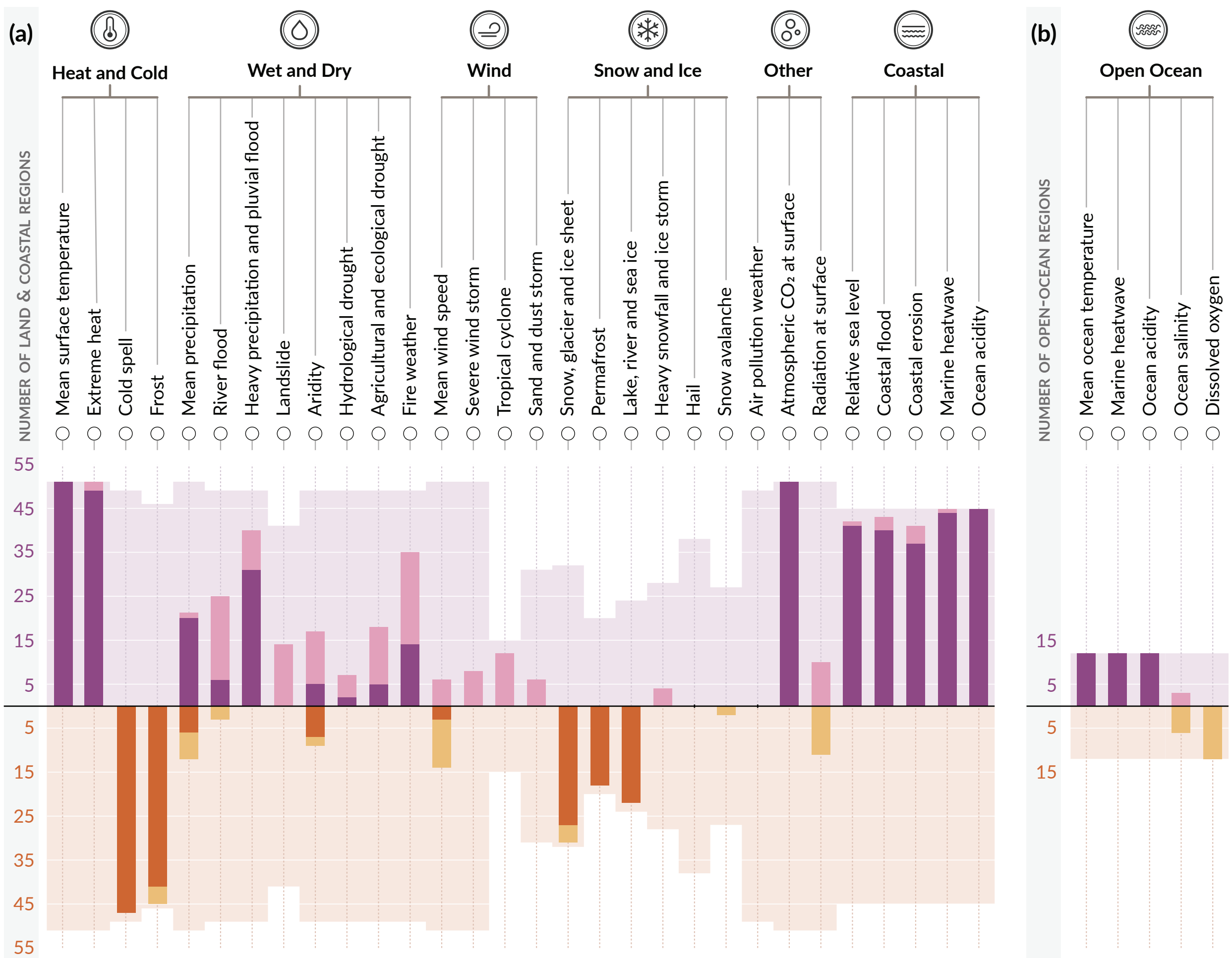

BAR CHART LEGEND

- Regions with ***high** confidence* **increase**
- Regions with ***medium** confidence* **increase**
- Regions with ***high** confidence* **decrease**
- Regions with ***medium** confidence* **decrease**

LIGHTER-SHADED ‘ENVELOPE’ LEGEND

The height of the lighter shaded ‘envelope’ behind each bar represents the maximum number of regions for which each CID is relevant. The envelope is symmetrical about the x-axis showing the maximum possible number of relevant regions for CID increase (upper part) or decrease (lower part).

ASSESSED FUTURE CHANGES

Changes refer to a 20–30 year period centred around 2050 and/or consistent with 2°C global warming compared to a similar period within 1960–2014 or 1850–1900.

Figure SPM.9 | Synthesis of the number of AR6 WGI reference regions where climatic impact-drivers are projected to change

A total of 35 climatic impact-drivers (CIDs) grouped into seven types are shown: heat and cold; wet and dry; wind; snow and ice; coastal; open ocean; and other. For each CID, the bar in the graph below displays the number of AR6 WGI reference regions where it is projected to change. The **colours** represent the direction of change and the level of confidence in the change: purple indicates an increase while brown indicates a decrease; darker and lighter shades refer to *high* and *medium confidence*, respectively. Lighter background colours represent the maximum number of regions for which each CID is broadly relevant.

Panel (a) shows the 30 CIDs relevant to the **land and coastal regions**, while **panel (b)** shows the five CIDs relevant to the **open-ocean regions**. Marine heatwaves and ocean acidity are assessed for coastal ocean regions in panel (a) and for open-ocean regions in panel (b). Changes refer to a 20–30-year period centred around 2050 and/or consistent with 2°C global warming compared to a similar period within 1960–2014, except for hydrological drought and agricultural and ecological drought, which is compared to 1850–1900. Definitions of the regions are provided in Sections 12.4 and Atlas.1 and the Interactive Atlas (see https://interactive-atlas.ipcc.ch/).

{11.9, 12.2, 12.4, Atlas.1, Table TS.5, Figures TS.22 and TS.25} (Table SPM.1)

C.3 Low-likelihood outcomes, such as ice-sheet collapse, abrupt ocean circulation changes, some compound extreme events, and warming substantially larger than the assessed *very likely* range of future warming, cannot be ruled out and are part of risk assessment.
{1.4, Cross-Chapter Box 1.3, 4.3, 4.4, 4.8, Cross-Chapter Box 4.1, 8.6, 9.2, Box 9.4, 11.8, Box 11.2, Cross-Chapter Box 12.1} (Table SPM.1)

C.3.1 If global warming exceeds the assessed *very likely* range for a given GHG emissions scenario, including low GHG emissions scenarios, global and regional changes in many aspects of the climate system, such as regional precipitation and other CIDs, would also exceed their assessed *very likely* ranges (*high confidence*). Such low-likelihood, high-warming outcomes are associated with potentially very large impacts, such as through more intense and more frequent heatwaves and heavy precipitation, and high risks for human and ecological systems, particularly for high GHG emissions scenarios.
{Cross-Chapter Box 1.3, 4.3, 4.4, 4.8, Box 9.4, Box 11.2, Cross-Chapter Box 12.1, TS.1.4, Box TS.3, Box TS.4} (Table SPM.1)

C.3.2 Low-likelihood, high-impact outcomes[34] could occur at global and regional scales even for global warming within the *very likely* range for a given GHG emissions scenario. The probability of low-likelihood, high-impact outcomes increases with higher global warming levels (*high confidence*). Abrupt responses and tipping points of the climate system, such as strongly increased Antarctic ice-sheet melt and forest dieback, cannot be ruled out (*high confidence*).
{1.4, 4.3, 4.4, 4.8, 5.4, 8.6, Box 9.4, Cross-Chapter Box 12.1, TS.1.4, TS.2.5, Box TS.3, Box TS.4, Box TS.9} (Table SPM.1)

C.3.3 If global warming increases, some compound extreme events[18] with low likelihood in past and current climate will become more frequent, and there will be a higher likelihood that events with increased intensities, durations and/or spatial extents unprecedented in the observational record will occur (*high confidence*).
{11.8, Box 11.2, Cross-Chapter Box 12.1, Box TS.3, Box TS.9}

C.3.4 The Atlantic Meridional Overturning Circulation is *very likely* to weaken over the 21st century for all emissions scenarios. While there is *high confidence* in the 21st century decline, there is only *low confidence* in the magnitude of the trend. There is *medium confidence* that there will not be an abrupt collapse before 2100. If such a collapse were to occur, it would *very likely* cause abrupt shifts in regional weather patterns and water cycle, such as a southward shift in the tropical rain belt, weakening of the African and Asian monsoons and strengthening of Southern Hemisphere monsoons, and drying in Europe.
{4.3, 8.6, 9.2, TS2.4, Box TS.3}

C.3.5 Unpredictable and rare natural events not related to human influence on climate may lead to low-likelihood, high-impact outcomes. For example, a sequence of large explosive volcanic eruptions within decades has occurred in the past, causing substantial global and regional climate perturbations over several decades. Such events cannot be ruled out in the future, but due to their inherent unpredictability they are not included in the illustrative set of scenarios referred to in this Report
{2.2, Cross-Chapter Box 4.1, Box TS.3} (Box SPM.1)

D. Limiting Future Climate Change

Since AR5, estimates of remaining carbon budgets have been improved by a new methodology first presented in SR1.5, updated evidence, and the integration of results from multiple lines of evidence. A comprehensive range of possible future air pollution controls in scenarios is used to consistently assess the effects of various assumptions on projections of climate and air pollution. A novel development is the ability to ascertain when climate responses to emissions reductions would become discernible above natural climate variability, including internal variability and responses to natural drivers.

D.1 From a physical science perspective, limiting human-induced global warming to a specific level requires limiting cumulative CO_2 emissions, reaching at least net zero CO_2 emissions, along with strong reductions in other greenhouse gas emissions. Strong, rapid and sustained reductions in CH_4 emissions would also limit the warming effect resulting from declining aerosol pollution and would improve air quality.
{3.3, 4.6, 5.1, 5.2, 5.4, 5.5, 5.6, Box 5.2, Cross-Chapter Box 5.1, 6.7, 7.6, 9.6} (Figure SPM.10, Table SPM.2)

D.1.1 This Report reaffirms with *high confidence* the AR5 finding that there is a near-linear relationship between cumulative anthropogenic CO_2 emissions and the global warming they cause. Each 1000 $GtCO_2$ of cumulative CO_2 emissions is assessed to *likely* cause a 0.27°C to 0.63°C increase in global surface temperature with a best estimate of 0.45°C.[41] This is a narrower range compared to AR5 and SR1.5. This quantity is referred to as the transient climate response to cumulative CO_2 emissions (TCRE). This relationship implies that reaching net zero anthropogenic CO_2 emissions[42] is a requirement to stabilize human-induced global temperature increase at any level, but that limiting global temperature increase to a specific level would imply limiting cumulative CO_2 emissions to within a carbon budget.[43] {5.4, 5.5, TS.1.3, TS.3.3, Box TS.5} (Figure SPM.10)

Every tonne of CO_2 emissions adds to global warming

Global surface temperature increase since 1850–1900 (°C) as a function of cumulative CO_2 emissions ($GtCO_2$)

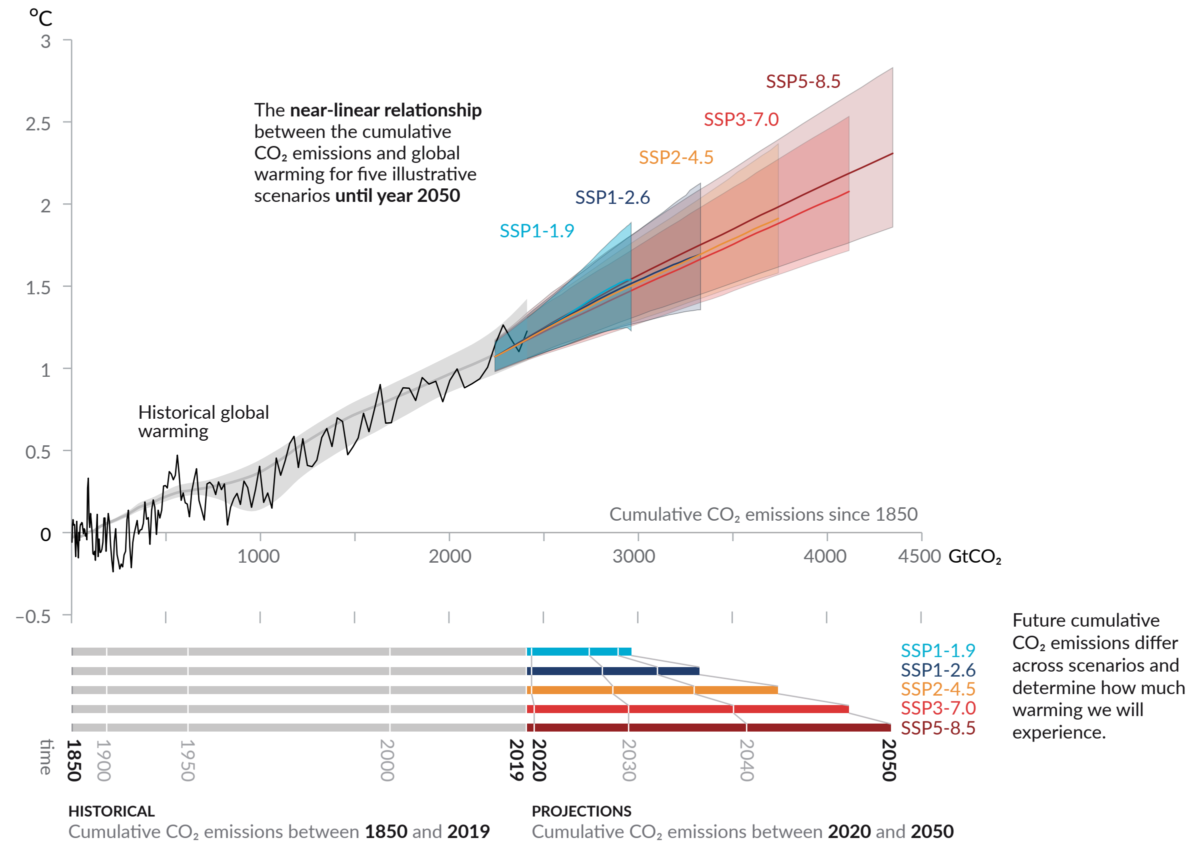

Figure SPM.10 | Near-linear relationship between cumulative CO_2 emissions and the increase in global surface temperature

Top panel: Historical data (thin black line) shows observed global surface temperature increase in °C since 1850–1900 as a function of historical cumulative carbon dioxide (CO_2) emissions in $GtCO_2$ from 1850 to 2019. The grey range with its central line shows a corresponding estimate of the historical human-caused surface warming (see Figure SPM.2). Coloured areas show the assessed *very likely* range of global surface temperature projections, and thick coloured central lines show the median estimate as a function of cumulative CO_2 emissions from 2020 until year 2050 for the set of illustrative scenarios (SSP1-1.9, SSP1-2.6, SSP2-4.5, SSP3-7.0, and SSP5-8.5; see Figure SPM.4). Projections use the cumulative CO_2 emissions of each respective scenario, and the projected global warming includes the contribution from all anthropogenic forcers. The relationship is illustrated over the domain of cumulative CO_2 emissions for which there is *high confidence* that the transient climate response to cumulative CO_2 emissions (TCRE) remains constant, and for the time period from 1850 to 2050 over which global CO_2 emissions remain net positive under all illustrative scenarios, as there is *limited evidence* supporting the quantitative application of TCRE to estimate temperature evolution under net negative CO_2 emissions.

Bottom panel: Historical and projected cumulative CO_2 emissions in $GtCO_2$ for the respective scenarios.

{Section 5.5, Figure 5.31, Figure TS.18}

---

41 In the literature, units of °C per 1000 PgC (petagrams of carbon) are used, and the AR6 reports the TCRE ***likely*** range as 1.0°C to 2.3°C per 1000 PgC in the underlying report, with a best estimate of 1.65°C.

42 The condition in which anthropogenic carbon dioxide (CO_2) emissions are balanced by anthropogenic CO_2 removals over a specified period (Glossary).

43 The term 'carbon budget' refers to the maximum amount of cumulative net global anthropogenic CO_2 emissions that would result in limiting global warming to a given level with a given probability, taking into account the effect of other anthropogenic climate forcers. This is referred to as the total carbon budget when expressed starting from the pre-industrial period, and as the remaining carbon budget when expressed from a recent specified date (Glossary). Historical cumulative CO_2 emissions determine to a large degree warming to date, while future emissions cause future additional warming. The remaining carbon budget indicates how much CO_2 could still be emitted while keeping warming below a specific temperature level.

D.1.2 Over the period 1850–2019, a total of 2390 ± 240 (*likely* range) $GtCO_2$ of anthropogenic CO_2 was emitted. Remaining carbon budgets have been estimated for several global temperature limits and various levels of probability, based on the estimated value of TCRE and its uncertainty, estimates of historical warming, variations in projected warming from non-CO_2 emissions, climate system feedbacks such as emissions from thawing permafrost, and the global surface temperature change after global anthropogenic CO_2 emissions reach net zero.
{5.1, 5.5, Box 5.2, TS.3.3} (Table SPM.2)

Table SPM.2 | Estimates of historical carbon dioxide (CO_2) emissions and remaining carbon budgets. Estimated remaining carbon budgets are calculated from the beginning of 2020 and extend until global net zero CO_2 emissions are reached. They refer to CO_2 emissions, while accounting for the global warming effect of non-CO_2 emissions. Global warming in this table refers to human-induced global surface temperature increase, which excludes the impact of natural variability on global temperatures in individual years.
{Table 3.1, 5.5.1, 5.5.2, Box 5.2, Table 5.1, Table 5.7, Table 5.8, Table TS.3}

Global Warming Between 1850–1900 and 2010–2019 (°C)		Historical Cumulative CO_2 Emissions from 1850 to 2019 ($GtCO_2$)					
1.07 (0.8–1.3; likely range)		2390 (± 240; likely range)					
Approximate global warming relative to 1850–1900 until temperature limit (°C)[a]	Additional global warming relative to 2010–2019 until temperature limit (°C)	Estimated remaining carbon budgets from the beginning of 2020 ($GtCO_2$) *Likelihood of limiting global warming to temperature limit*[b]					Variations in reductions in non-CO_2 emissions[c]
		17%	*33%*	*50%*	*67%*	*83%*	
1.5	0.43	900	650	500	400	300	Higher or lower reductions in accompanying non-CO_2 emissions can increase or decrease the values on the left by 220 $GtCO_2$ or more
1.7	0.63	1450	1050	850	700	550	
2.0	0.93	2300	1700	1350	1150	900	

[a] Values at each 0.1°C increment of warming are available in Tables TS.3 and 5.8.

[b] This likelihood is based on the uncertainty in transient climate response to cumulative CO_2 emissions (TCRE) and additional Earth system feedbacks and provides the probability that global warming will not exceed the temperature levels provided in the two left columns. Uncertainties related to historical warming (±550 $GtCO_2$) and non-CO_2 forcing and response (±220 $GtCO_2$) are partially addressed by the assessed uncertainty in TCRE, but uncertainties in recent emissions since 2015 (±20 $GtCO_2$) and the climate response after net zero CO_2 emissions are reached (±420 $GtCO_2$) are separate.

[c] Remaining carbon budget estimates consider the warming from non-CO_2 drivers as implied by the scenarios assessed in SR1.5. The Working Group III Contribution to AR6 will assess mitigation of non-CO_2 emissions.

D.1.3 Several factors that determine estimates of the remaining carbon budget have been re-assessed, and updates to these factors since SR1.5 are small. When adjusted for emissions since previous reports, estimates of remaining carbon budgets are therefore of similar magnitude compared to SR1.5 but larger compared to AR5 due to methodological improvements.[44]
{5.5, Box 5.2, TS.3.3} (Table SPM.2)

D.1.4 Anthropogenic CO_2 removal (CDR) has the potential to remove CO_2 from the atmosphere and durably store it in reservoirs (*high confidence*). CDR aims to compensate for residual emissions to reach net zero CO_2 or net zero GHG emissions or, if implemented at a scale where anthropogenic removals exceed anthropogenic emissions, to lower surface temperature. CDR methods can have potentially wide-ranging effects on biogeochemical cycles and climate, which can either weaken or strengthen the potential of these methods to remove CO_2 and reduce warming, and can also influence water availability and quality, food production and biodiversity[45] (*high confidence*).
{5.6, Cross-Chapter Box 5.1, TS.3.3}

D.1.5 Anthropogenic CO_2 removal (CDR) leading to global net negative emissions would lower the atmospheric CO_2 concentration and reverse surface ocean acidification (*high confidence*). Anthropogenic CO_2 removals and emissions are partially

44 Compared to AR5, and when taking into account emissions since AR5, estimates in AR6 are about 300–350 $GtCO_2$ larger for the remaining carbon budget consistent with limiting warming to 1.5°C; for 2°C, the difference is about 400–500 $GtCO_2$.

45 Potential negative and positive effects of CDR for biodiversity, water and food production are methods-specific and are often highly dependent on local context, management, prior land use, and scale. IPCC Working Groups II and III assess the CDR potential and ecological and socio-economic effects of CDR methods in their AR6 contributions.

compensated by CO_2 release and uptake respectively, from or to land and ocean carbon pools (*very high confidence*). CDR would lower atmospheric CO_2 by an amount approximately equal to the increase from an anthropogenic emission of the same magnitude (*high confidence*). The atmospheric CO_2 decrease from anthropogenic CO_2 removals could be up to 10% less than the atmospheric CO_2 increase from an equal amount of CO_2 emissions, depending on the total amount of CDR (*medium confidence*).
{5.3, 5.6, TS.3.3}

D.1.6 If global net negative CO_2 emissions were to be achieved and be sustained, the global CO_2-induced surface temperature increase would be gradually reversed but other climate changes would continue in their current direction for decades to millennia (*high confidence*). For instance, it would take several centuries to millennia for global mean sea level to reverse course even under large net negative CO_2 emissions (*high confidence*).
{4.6, 9.6, TS.3.3}

D.1.7 In the five illustrative scenarios, simultaneous changes in CH_4, aerosol and ozone precursor emissions, which also contribute to air pollution, lead to a net global surface warming in the near and long term (*high confidence*). In the long term, this net warming is lower in scenarios assuming air pollution controls combined with strong and sustained CH_4 emissions reductions (*high confidence*). In the low and very low GHG emissions scenarios, assumed reductions in anthropogenic aerosol emissions lead to a net warming, while reductions in CH_4 and other ozone precursor emissions lead to a net cooling. Because of the short lifetime of both CH_4 and aerosols, these climate effects partially counterbalance each other, and reductions in CH_4 emissions also contribute to improved air quality by reducing global surface ozone (*high confidence*).
{6.7, Box TS.7} (Figure SPM.2, Box SPM.1)

D.1.8 Achieving global net zero CO_2 emissions, with anthropogenic CO_2 emissions balanced by anthropogenic removals of CO_2, is a requirement for stabilizing CO_2-induced global surface temperature increase. This is different from achieving net zero GHG emissions, where metric-weighted anthropogenic GHG emissions equal metric-weighted anthropogenic GHG removals. For a given GHG emissions pathway, the pathways of individual GHGs determine the resulting climate response,[46] whereas the choice of emissions metric[47] used to calculate aggregated emissions and removals of different GHGs affects what point in time the aggregated GHGs are calculated to be net zero. Emissions pathways that reach and sustain net zero GHG emissions defined by the 100-year global warming potential are projected to result in a decline in surface temperature after an earlier peak (*high confidence*).
{4.6, 7.6, Box 7.3, TS.3.3}

D.2 Scenarios with very low or low GHG emissions (SSP1-1.9 and SSP1-2.6) lead within years to discernible effects on greenhouse gas and aerosol concentrations and air quality, relative to high and very high GHG emissions scenarios (SSP3-7.0 or SSP5-8.5). Under these contrasting scenarios, discernible differences in trends of global surface temperature would begin to emerge from natural variability within around 20 years, and over longer time periods for many other climatic impact-drivers (*high confidence*).
{4.6, 6.6, 6.7, Cross-Chapter Box 6.1, 9.6, 11.2, 11.4, 11.5, 11.6, Cross-Chapter Box 11.1, 12.4, 12.5} (Figure SPM.8, Figure SPM.10)

D.2.1 Emissions reductions in 2020 associated with measures to reduce the spread of COVID-19 led to temporary but detectable effects on air pollution (*high confidence*) and an associated small, temporary increase in total radiative forcing, primarily due to reductions in cooling caused by aerosols arising from human activities (*medium confidence*). Global and regional climate responses to this temporary forcing are, however, undetectable above natural variability (*high confidence*). Atmospheric CO_2 concentrations continued to rise in 2020, with no detectable decrease in the observed CO_2 growth rate (*medium confidence*).[48]
{Cross-Chapter Box 6.1, TS.3.3}

D.2.2 Reductions in GHG emissions also lead to air quality improvements. However, in the near term,[49] even in scenarios with strong reduction of GHGs, as in the low and very low GHG emissions scenarios (SSP1-2.6 and SSP1-1.9), these improvements

46 A general term for how the climate system responds to a radiative forcing (Glossary).

47 The choice of emissions metric depends on the purposes for which gases or forcing agents are being compared. This Report contains updated emissions metric values and assesses new approaches to aggregating gases.

48 For other GHGs, there was insufficient literature available at the time of the assessment to assess detectable changes in their atmospheric growth rate during 2020.

49 Near term: 2021–2040.

are not sufficient in many polluted regions to achieve air quality guidelines specified by the World Health Organization (*high confidence*). Scenarios with targeted reductions of air pollutant emissions lead to more rapid improvements in air quality within years compared to reductions in GHG emissions only, but from 2040, further improvements are projected in scenarios that combine efforts to reduce air pollutants as well as GHG emissions, with the magnitude of the benefit varying between regions (*high confidence*).
{6.6, 6.7, Box TS.7}.

D.2.3 Scenarios with very low or low GHG emissions (SSP1-1.9 and SSP1-2.6) would have rapid and sustained effects to limit human-caused climate change, compared with scenarios with high or very high GHG emissions (SSP3-7.0 or SSP5-8.5), but early responses of the climate system can be masked by natural variability. For global surface temperature, differences in 20-year trends would *likely* emerge during the near term under a very low GHG emissions scenario (SSP1-1.9), relative to a high or very high GHG emissions scenario (SSP3-7.0 or SSP5-8.5). The response of many other climate variables would emerge from natural variability at different times later in the 21st century (*high confidence*).
{4.6, Cross-Section Box TS.1} (Figure SPM.8, Figure SPM.10)

D.2.4 Scenarios with very low and low GHG emissions (SSP1-1.9 and SSP1-2.6) would lead to substantially smaller changes in a range of CIDs[36] beyond 2040 than under high and very high GHG emissions scenarios (SSP3-7.0 and SSP5-8.5). By the end of the century, scenarios with very low and low GHG emissions would strongly limit the change of several CIDs, such as the increases in the frequency of extreme sea level events, heavy precipitation and pluvial flooding, and exceedance of dangerous heat thresholds, while limiting the number of regions where such exceedances occur, relative to higher GHG emissions scenarios (*high confidence*). Changes would also be smaller in very low compared to low GHG emissions scenarios, as well as for intermediate (SSP2-4.5) compared to high or very high GHG emissions scenarios (*high confidence*).
{9.6, 11.2, 11.3, 11.4, 11.5, 11.6, 11.9, Cross-Chapter Box 11.1, 12.4, 12.5, TS.4.3}

Technical Summary

TS

Technical Summary

Coordinating Authors:

Paola A. Arias (Colombia), Nicolas Bellouin (United Kingdom/France), Erika Coppola (Italy), Richard G. Jones (United Kingdom), Gerhard Krinner (France/Germany, France), Jochem Marotzke (Germany), Vaishali Naik (United States of America), Matthew D. Palmer (United Kingdom), Gian-Kasper Plattner (Switzerland), Joeri Rogelj (United Kingdom/Belgium), Maisa Rojas (Chile), Jana Sillmann (Norway/Germany), Trude Storelvmo (Norway), Peter W. Thorne (Ireland/United Kingdom), Blair Trewin (Australia)

Authors:

Krishna Achuta Rao (India), Bhupesh Adhikary (Nepal), Richard P. Allan (United Kingdom), Kyle Armour (United States of America), Govindasamy Bala (India/United States of America), Rondrotiana Barimalala (South Africa/Madagascar), Sophie Berger (France/Belgium), Josep G. Canadell (Australia), Christophe Cassou (France), Annalisa Cherchi (Italy), William Collins (United Kingdom), William D. Collins (United States of America), Sarah L. Connors (France/United Kingdom), Susanna Corti (Italy), Faye Cruz (Philippines), Frank J. Dentener (EU/The Netherlands), Claudine Dereczynski (Brazil), Alejandro Di Luca (Australia, Canada/Argentina), Aida Diongue Niang (Senegal), Francisco J. Doblas-Reyes (Spain), Alessandro Dosio (Italy), Hervé Douville (France), François Engelbrecht (South Africa), Veronika Eyring (Germany), Erich Fischer (Switzerland), Piers Forster (United Kingdom), Baylor Fox-Kemper (United States of America), Jan S. Fuglestvedt (Norway), John C. Fyfe (Canada), Nathan P. Gillett (Canada), Leah Goldfarb (France/United States of America), Irina Gorodetskaya (Portugal/Russian Federation, Belgium), Jose Manuel Gutierrez (Spain), Rafiq Hamdi (Belgium), Ed Hawkins (United Kingdom), Helene T. Hewitt (United Kingdom), Pandora Hope (Australia), AKM Saiful Islam (Bangladesh), Christopher Jones (United Kingdom), Darrell S. Kaufman (United States of America), Robert E. Kopp (United States of America), Yu Kosaka (Japan), James Kossin (United States of America), Svitlana Krakovska (Ukraine), June-Yi Lee (Republic of Korea), Jian Li (China), Thorsten Mauritsen (Sweden, Denmark), Thomas K. Maycock (United States of America), Malte Meinshausen (Australia/Germany), Seung-Ki Min (Republic of Korea), Pedro M. S. Monteiro (South Africa), Thanh Ngo-Duc (Vietnam), Friederike Otto (United Kingdom/Germany), Izidine Pinto (South Africa/Mozambique), Anna Pirani (Italy), Krishnan Raghavan (India), Roshanka Ranasinghe (The Netherlands/Sri Lanka, Australia), Alex C. Ruane (United States of America), Lucas Ruiz (Argentina), Jean-Baptiste Sallée (France), Bjørn H. Samset (Norway), Shubha Sathyendranath (UK/Canada, United Kingdom, Overseas Citizen of India), Sonia I. Seneviratne (Switzerland), Anna A. Sörensson (Argentina), Sophie Szopa (France), Izuru Takayabu (Japan), Anne-Marie Treguier (France), Bart van den Hurk (The Netherlands), Robert Vautard (France), Karina von Schuckmann (France/Germany), Sönke Zaehle (Germany), Xuebin Zhang (Canada), Kirsten Zickfeld (Canada/Germany)

Contributing Authors:
Guðfinna Aðalgeirsdóttir (Iceland), Lincoln M. Alves (Brazil), Terje Berntsen (Norway), Sara M. Blichner (Norway), Lisa Bock (Germany), Gregory G. Garner (United States of America), Joelle Gergis (Australia), Sergey K. Gulev (Russian Federation), Mathias Hauser (Switzerland), Flavio Lehner (United States of America/Switzerland), Chao Li (China), Marianne T. Lund (Norway), Daniel J. Lunt (United Kingdom), Sebastian Milinski (Germany), Gemma Teresa Narisma (Philippines), Zebedee R. J. Nicholls (Australia), Dirk Notz (Germany), Sophie Nowicki (United States of America/France, United States of America), Bette Otto-Bliesner (United States of America), Brodie Pearson (United States of America/United Kingdom), Adam S. Phillips (United States of America), James Renwick (New Zealand), Stéphane Sénési (France), Lucas Silva (Portugal/Switzerland), Aimee B. A. Slangen (The Netherlands), Thomas F. Stocker (Switzerland), Claudia Tebaldi (United States of America), Laurent Terray (France), Sabin Thazhe Purayil (India), Andrew Turner (United Kingdom), Steven Turnock (United Kingdom), Carolina Vera (Argentina), Cunde Xiao (China), Panmao Zhai (China)

Review Editors:
Valérie Masson-Delmotte (France), Gregory M. Flato (Canada), Noureddine Yassa (Algeria)

TS

This Technical Summary should be cited as:
Arias, P.A., N. Bellouin, E. Coppola, R.G. Jones, G. Krinner, J. Marotzke, V. Naik, M.D. Palmer, G.-K. Plattner, J. Rogelj, M. Rojas, J. Sillmann, T. Storelvmo, P.W. Thorne, B. Trewin, K. Achuta Rao, B. Adhikary, R.P. Allan, K. Armour, G. Bala, R. Barimalala, S. Berger, J.G. Canadell, C. Cassou, A. Cherchi, W. Collins, W.D. Collins, S.L. Connors, S. Corti, F. Cruz, F.J. Dentener, C. Dereczynski, A. Di Luca, A. Diongue Niang, F.J. Doblas-Reyes, A. Dosio, H. Douville, F. Engelbrecht, V. Eyring, E. Fischer, P. Forster, B. Fox-Kemper, J.S. Fuglestvedt, J.C. Fyfe, N.P. Gillett, L. Goldfarb, I. Gorodetskaya, J.M. Gutierrez, R. Hamdi, E. Hawkins, H.T. Hewitt, P. Hope, A.S. Islam, C. Jones, D.S. Kaufman, R.E. Kopp, Y. Kosaka, J. Kossin, S. Krakovska, J.-Y. Lee, J. Li, T. Mauritsen, T.K. Maycock, M. Meinshausen, S.-K. Min, P.M.S. Monteiro, T. Ngo-Duc, F. Otto, I. Pinto, A. Pirani, K. Raghavan, R. Ranasinghe, A.C. Ruane, L. Ruiz, J.-B. Sallée, B.H. Samset, S. Sathyendranath, S.I. Seneviratne, A.A. Sörensson, S. Szopa, I. Takayabu, A.-M. Tréguier, B. van den Hurk, R. Vautard, K. von Schuckmann, S. Zaehle, X. Zhang, and K. Zickfeld, 2021: Technical Summary. In *Climate Change 2021: The Physical Science Basis. Contribution of Working Group I to the Sixth Assessment Report of the Intergovernmental Panel on Climate Change* [Masson-Delmotte, V., P. Zhai, A. Pirani, S.L. Connors, C. Péan, S. Berger, N. Caud, Y. Chen, L. Goldfarb, M.I. Gomis, M. Huang, K. Leitzell, E. Lonnoy, J.B.R. Matthews, T.K. Maycock, T. Waterfield, O. Yelekçi, R. Yu, and B. Zhou (eds.)]. Cambridge University Press, Cambridge, United Kingdom and New York, NY, USA, pp. 33–144. doi:10.1017/9781009157896.002.

Table of Contents

Introduction

The Working Group I (WGI) contribution to the Intergovernmental Panel on Climate Change (IPCC) Sixth Assessment Report (AR6) assesses the physical science basis of climate change. As part of that contribution, this Technical Summary (TS) is designed to bridge between the comprehensive assessment of the WGI Chapters and its Summary for Policymakers (SPM). It is primarily built from the Executive Summaries of the individual chapters and Atlas and provides a synthesis of key findings based on multiple lines of evidence (e.g., analyses of observations, models, paleoclimate information and understanding of physical, chemical and biological processes and components of the climate system). All the findings and figures here are supported by and traceable to the underlying chapters, with relevant chapter sections indicated in curly brackets.

Throughout this Technical Summary, key assessment findings are reported using the IPCC calibrated uncertainty language (Chapter 1, Box 1.1). Two calibrated approaches are used to communicate the degree of certainty in key findings, which are based on author teams' evaluations of underlying scientific understanding:

1) Confidence[1] is a qualitative measure of the validity of a finding, based on the type, amount, quality and consistency of evidence (e.g., data, mechanistic understanding, theory, models, expert judgment) and the degree of agreement.
2) Likelihood[2] provides a quantified measure of confidence in a finding expressed probabilistically (e.g., based on statistical analysis of observations or model results, or both, and expert judgement by the author team or from a formal quantitative survey of expert views, or both).

Where there is sufficient scientific confidence, findings can also be formulated as statements of fact without uncertainty qualifiers. Throughout IPCC reports, the calibrated language is clearly identified by being typeset in italics.

The context and progress in climate science (Section TS.1) is followed by a Cross-Section Box TS.1 on global surface temperature change. Section TS.2 provides information about past and future large-scale changes in all components of the climate system. Section TS.3 summarizes knowledge and understanding of climate forcings, feedbacks and responses. Infographic TS.1 uses a storyline approach to integrate findings on possible climate futures. Finally, Section TS.4 provides a synthesis of climate information at regional scales.[3] The list of acronyms used in the WGI Report is in Annex VIII.

Text at the beginning of a section presented in dark blue with a blue vertical bar at the left, as shown here, provides a summary of the findings discussed in that section.

The AR6 WGI Report promotes best practices in traceability and reproducibility, including through adoption of the Findable, Accessible, Interoperable, and Reusable (FAIR) principles for scientific data. Each chapter has a data table (in its Supplementary Material) documenting the input data and code used to generate its figures and tables. In addition, a collection of data and code from the report has been made freely-available online via long-term archives.[4]

These FAIR principles are central to the WGI Interactive Atlas[5], an online tool that complements the WGI Report by providing flexible spatial and temporal analyses of past, observed and projected climate change information. It comprises a regional information component that supports many of the chapters of the Report and a regional synthesis component that supports the Technical Summary and Summary for Policymakers.

Regarding the representation of robustness and uncertainty in maps, the method chosen for the AR6[6] differs from the method used in the Fifth Assessment Report (AR5). This choice is based on new research on the visualization of uncertainty and on user surveys.

1 In this Technical Summary, the following summary terms are used to describe the available evidence: limited, medium, or robust; and for the degree of agreement: low, medium, or high. A level of confidence is expressed using five qualifiers: very low, low, medium, high, and very high, and typeset in italics, e.g., *medium confidence*. For a given evidence and agreement statement, different confidence levels can be assigned, but increasing levels of evidence and degrees of agreement are correlated with increasing confidence (see Chapter 1, Box 1.1 for more details).

2 In this Technical Summary, the following terms are used to indicate the assessed likelihood of an outcome or a result: virtually certain 99–100% probability, very likely 90–100%, likely 66–100%, about as likely as not 33–66%, unlikely 0–33%, very unlikely 0–10%, exceptionally unlikely 0–1%. Additional terms (extremely likely: 95–100%, more likely than not >50–100%, and extremely unlikely 0–5%) may also be used when appropriate. Assessed likelihood is typeset in italics, e.g., *very likely* (see Chapter 1, Box 1.1 for more details). Throughout the WGI report and unless stated otherwise, uncertainty is quantified using 90% uncertainty intervals. The 90% uncertainty interval, reported in square brackets [x to y], is estimated to have a 90% likelihood of covering the value that is being estimated. The range encompasses the median value, and there is an estimated 10% combined likelihood of the value being below the lower end of the range (x) and above its upper end (y). Often, the distribution will be considered symmetric about the corresponding best estimate, but this is not always the case. In this Report, an assessed 90% uncertainty interval is referred to as a '*very likely* range'. Similarly, an assessed 66% uncertainty interval is referred to as a '*likely* range'.

3 The regional traceback matrices that provide the location of the assessment findings synthesized in Section TS.4 are in the Supplementary Material (SM) of Chapter 10.

4 Data archive is available at https://catalogue.ceda.ac.uk/uuid/3234e9111d4f4354af00c3aaecd879b7.

5 https://interactive-atlas.ipcc.ch/

6 The AR6 figures use one of the following approaches. For observations, the absence of 'x' symbols shows areas with statistical significance, while the presence of 'x' indicates non-significance. For model projections, the method offers two approaches with varying complexity. In the simple approach, *high agreement* (≥80%) is indicated with no overlay, and diagonal lines (///) show *low agreement* (<80%); In the advanced approach, areas with no overlay display robust signal (≥66% of models show change greater than the variability threshold and ≥80% of all models agree on the sign of change), reverse diagonal lines (\\\) show no robust signal, and crossed lines show conflicting signals (i.e., significant change but *low agreement*). Cross-Chapter Box Atlas.1 provides more information on the AR6 method for visualizing robustness and uncertainty on maps.

Box TS.1 | Core Concepts Central to This Report

This box provides short descriptions of key concepts that are relevant to the AR6 WGI assessment, with a focus on their use in the Technical Summary and the Summary for Policymakers. The Glossary (Annex VII) includes more information on these concepts along with definitions of many other important terms and concepts used in this Report.

Characteristics of Climate Change Assessment

Global warming: Global warming refers to the change of global surface temperature relative to a baseline depending upon the application. Specific global warming levels, such as 1.5°C, 2°C, 3°C or 4°C, are defined as changes in global surface temperature relative to the years 1850–1900 as the baseline (the earliest period of reliable observations with sufficient geographic coverage). They are used to assess and communicate information about global and regional changes, linking to scenarios and used as a common basis for Working Group II (WGII) and Working Group III (WGIII) assessments. (Section TS.1.3, Cross-Section Box TS.1) {1.4.1, 1.6.2, 4.6.1, Cross-Chapter Boxes 1.5, 2.3, 11.1, and 12.1, Atlas Sections 3–11, Glossary}

Emergence: Emergence refers to the experience or appearance of novel conditions of a particular climate variable in a given region. This concept is often expressed as the ratio of the change in a climate variable relative to the amplitude of natural variations of that variable (often termed a 'signal-to-noise' ratio, with emergence occurring at a defined threshold of this ratio). Emergence can be expressed in terms of a time or a global warming level at which the novel conditions appear and can be estimated using observations or model simulations. (Sections TS.1.2.3 and TS.4.2) {1.4.2, FAQ 1.2, 7.5.5, 10.3, 10.4, 12.5.2, Cross-Chapter Box Atlas.1, Glossary}

Cumulative carbon dioxide (CO_2) emissions: The total net amount of CO_2 emitted into the atmosphere as a result of human activities. Given the nearly linear relationship between cumulative CO_2 emissions and increases in global surface temperature, cumulative CO_2 emissions are relevant for understanding how past and future CO_2 emissions affect global surface temperature. A related term – remaining carbon budget – is used to describe the total net amount of CO_2 that could be released in the future by human activities while keeping global warming to a specific global warming level, such as 1.5°C, taking into account the warming contribution from non-CO_2 forcers as well. The remaining carbon budget is expressed from a recent specified date, while the total carbon budget is expressed starting from the pre-industrial period. (Sections TS.1.3 and TS.3.3) {1.6.3, 5.5, Glossary}

Net zero CO_2 emissions: A condition that occurs when the amount of CO_2 emitted into the atmosphere by human activities equals the amount of CO_2 removed from the atmosphere by human activities over a specified period of time. Net negative CO_2 emissions occur when anthropogenic removals exceed anthropogenic emissions. (Section TS.3.3) {Box 1.4, Glossary}

Human Influence on the Climate System

Earth's energy imbalance: In a stable climate, the amount of energy that Earth receives from the Sun is approximately in balance with the amount of energy that is lost to space in the form of reflected sunlight and thermal radiation. 'Climate drivers', such as an increase in greenhouse gases or aerosols, interfere with this balance, causing the system to either gain or lose energy. The strength of a climate driver is quantified by its effective radiative forcing (ERF), measured in W m^{-2}. Positive ERF leads to warming, and negative ERF leads to cooling. That warming or cooling in turn can change the energy imbalance through many positive (amplifying) or negative (dampening) climate feedbacks. (Sections TS.2.2, TS.3.1 and TS.3.2) {2.2.8, 7.2, 7.3, 7.4, Box 7.1, Box 7.2, Glossary}

Attribution: Attribution is the process of evaluating the relative contributions of multiple causal factors to an observed change in climate variables (e.g., global surface temperature, global mean sea level), or to the occurrence of extreme weather or climate-related events. Attributed causal factors include human activities (such as increases in greenhouse gas concentration and aerosols, or land-use change) or natural external drivers (solar and volcanic influences), and in some cases internal variability. (Sections TS.1.2.4 and TS.2, Box TS.10) {Cross-Working Group Box: Attribution in Chapter 1; 3.5; 3.8; 10.4; 11.2.4; Glossary}

Committed change, long-term commitment: Changes in the climate system, resulting from past, present and future human activities, which will continue long into the future (centuries to millennia) even with strong reductions in greenhouse gas emissions. Some aspects of the climate system, including the terrestrial biosphere, the deep ocean and the cryosphere, respond much more slowly than surface temperatures to changes in greenhouse gas concentrations. As a result, there are already substantial committed changes associated with past greenhouse gas emissions. For example, global mean sea level will continue to rise for thousands of years, even if future CO_2 emissions are reduced to net zero and global warming halted, as excess energy due to past emissions continues to propagate into the deep ocean and as glaciers and ice sheets continue to melt. (Section TS.2.1, Box TS.4, Box TS.9) {1.2.1, 1.3, Box 1.2, Cross-Chapter Box 5.3}

Box TS.1 (continued)

Climate Information for Regional Climate Change and Risk Assessment

Distillation: The process of synthesizing information about climate change from multiple lines of evidence obtained from a variety of sources, taking into account user context and values. It leads to an increase in the usability, usefulness and relevance of climate information, enhances stakeholder trust, and expands the foundation of evidence used in climate services. It is particularly relevant in the context of co-producing regional-scale climate information to support decision-making. (Section TS.4.1, Box TS.11) {10.1, 10.5, 12.6}

(Climate change) risk: The concept of risk is a key aspect of how the IPCC assesses and communicates to decision-makers about the potential for adverse consequences for human or ecological systems, recognizing the diversity of values and objectives associated with such systems. In the context of climate change, risks can arise from potential impacts of climate change as well as human responses to climate change. WGI contributes to the common IPCC risk framing through the assessment of relevant climate information, including climatic impact-drivers and low-likelihood, high-impact outcomes. (Sections TS.1.4 and TS.4.1, Box TS.4) {Cross-Chapter Boxes 1.3 and 12.1, Glossary}

Climatic impact-drivers: Physical climate system conditions (e.g., means, events, extremes) that can be directly connected with having impacts on human or ecological systems are described as 'climatic impact-drivers' (CIDs) without anticipating whether their impacts are detrimental (i.e., as for hazards in the context of climate change risks) or provide potential opportunities. A range of indices may capture the sector- or application-relevant characteristics of a climatic impact-driver and can reflect exceedances of identified tolerance thresholds. (Sections TS.1.4 and TS.4.3) {12.1–12.3, FAQ 12.1, Glossary}

Storylines: The term storyline is used both in connection to scenarios (related to a future trajectory of emissions or socio-economic developments) or to describe plausible trajectories of weather and climate conditions or events, especially those related to high levels of risk. Physical climate storylines are introduced in AR6 to explore uncertainties in climate change and natural climate variability, to develop and communicate integrated and context-relevant regional climate information, and to address issues with deep uncertainty[7], including low-likelihood, high-impact outcomes. (Section TS.1.4, Box TS.3, Infographic TS.1) {1.4.4, Box 10.2, Glossary}

Low-likelihood, high impact outcomes: Outcomes/events whose probability of occurrence is low or not well known (as in the context of deep uncertainty) but whose potential impacts on society and ecosystems could be high. To better inform risk assessment and decision-making, such low-likelihood outcomes are considered if they are associated with very large consequences and may therefore constitute material risks, even though those consequences do not necessarily represent the most likely outcome. (Section TS.1.4, Box TS.3, Figure TS.6) {1.4.4, 4.8, Cross Chapter Box 1.3, Glossary}

As part of the AR6 cycle, the IPCC produced three Special Reports in 2018 and 2019: the Special Report on Global Warming of 1.5°C (SR1.5), the Special Report on the Ocean and Cryosphere in a Changing Climate (SROCC), and the Special Report on Climate Change and Land (SRCCL).

The AR6 WGI Report provides a full and comprehensive assessment of the physical science basis of climate change that builds on the previous assessments and these Special Reports and considers new information and knowledge from the recent scientific literature[8], including longer observational datasets and new scenarios and model results.

The structure of the AR6 WGI Report is designed to enhance the visibility of knowledge developments and to facilitate the integration of multiple lines of evidence, thereby improving confidence in findings. The Report has been peer-reviewed by the scientific community and governments (Annex X provides the Expert Reviewer list). The substantive introduction provided by Chapter 1 is followed by a first set of chapters dedicated to large-scale climate knowledge (Chapters 2–4), which encompasses observations and paleoclimate evidence, causes of observed changes, and projections; these are complemented by Chapter 11 for large-scale changes in extremes. The second set of chapters (Chapters 5–9) is orientated around the understanding of key climate system components and processes, including the global cycles of carbon, energy and water; short-lived climate forcers and their link to air quality; and the ocean, cryosphere and sea level change. The last set of chapters (Chapters 10–12 and the Atlas) is dedicated to the assessment and distillation of regional climate information from multiple lines of evidence at sub-continental to local scales (including urban climate), with a focus on recent and projected regional changes in mean climate, extremes, and climatic impact-drivers. The new online

7 Although not a core concept of the WGI Report, deep uncertainty is used in the Technical Summary in the following sense: 'A situation of deep uncertainty exists when experts or stakeholders do not know or cannot agree on: (1) appropriate conceptual models that describe relationships among key driving forces in a system; (2) the probability distributions used to represent uncertainty about key variables and parameters; and/or (3) how to weigh and value desirable alternative outcomes' (Lempert et al., 2003). Lempert, R. J., Popper, S. W., and Bankes, S. C. (2003). *Shaping the next one hundred years: New methods for quantitative long-term strategy analysis (MR-1626-RPC)*. Santa Monica, CA: The RAND Pardee Center.

8 The assessment covers scientific literature accepted for publication by 31 January 2021.

Interactive Atlas allows users to interact in a flexible manner through maps, time series and summary statistics with climate information for a set of updated WGI reference regions. The Report also includes 34 Frequently Asked Questions and answers for the general public (https://www.ipcc.ch/report/ar6/wg1/faqs).

Together, this Technical Summary and the underlying chapters aim at providing a comprehensive picture of knowledge progress since the WGI contribution to AR5. Multiple lines of scientific evidence confirm that the climate is changing due to human influence. Important advances in the ability to understand past, present and possible future changes should result in better-informed decision-making.

Some of the new results and main updates to key findings in this Report compared to AR5, SR1.5, SRCCL, and SROCC are summarized below. Relevant Technical Summary sections with further details are shown in parentheses after each bullet point.

Selected Updates and/or New Results since AR5

- **Human influence[9] on the climate system is now an established fact:** The Fourth Assessment Report (AR4) stated in 2007 that 'warming of the climate system is unequivocal', and AR5 stated in 2013 that 'human influence on the climate system is clear'. Combined evidence from across the climate system strengthens this finding. It is unequivocal that the increase of CO_2, methane (CH_4) and nitrous oxide (N_2O) in the atmosphere over the industrial era is the result of human activities and that human influence is the main driver[10] of many changes observed across the atmosphere, ocean, cryosphere and biosphere. (Sections TS.1.2, TS.2.1 and TS.3.1)
- **Observed global warming to date:** A combination of improved observational records and a series of very warm years since AR5 have resulted in a substantial increase in the estimated level of global warming to date. The contribution of changes in observational understanding alone between AR5 and AR6 leads to an increase of about 0.1°C in the estimated warming since 1850–1900. For the decade 2011–2020, the increase in global surface temperature since 1850–1900 is assessed to be 1.09 [0.95 to 1.20] °C.[11] Estimates of crossing times of global warming levels and estimates of remaining carbon budgets are updated accordingly. (Section TS.1.2, Cross-Section Box TS.1)
- **Paleoclimate evidence:** The AR5 assessed that many of the changes observed since the 1950s are unprecedented over decades to millennia. Updated paleoclimate evidence strengthens this assessment; over the past several decades, key indicators of the climate system are increasingly at levels unseen in centuries to millennia and are changing at rates unprecedented in at least the last 2000 years. (Box TS.2, Section TS.2)
- **Updated assessment of recent warming:** The AR5 reported a smaller rate of increase in global mean surface temperature over the period 1998–2012 than the rate calculated since 1951. Based on updated observational datasets showing a larger trend over 1998–2012 than earlier estimates, there is now *high confidence* that the observed 1998–2012 global surface temperature trend is consistent with ensembles of climate model simulations, and there is now *very high confidence* that the slower rate of global surface temperature increase observed over this period was a temporary event induced by internal and naturally forced variability that partly offset the anthropogenic surface warming trend over this period, while heat uptake continued to increase in the ocean. Since 2012, strong warming has been observed, with the past five years (2016–2020) being the hottest five-year period in the instrumental record since at least 1850 (*high confidence*). (Section TS.1.2, Cross-Section Box TS.1)
- **Magnitude of climate system response:** In this Report, it has been possible to reduce the long-standing uncertainty ranges for metrics that quantify the response of the climate system to radiative forcing, such as the equilibrium climate sensitivity (ECS) and the transient climate response (TCR), due to substantial advances (e.g., a 50% reduction in the uncertainty range of cloud feedbacks) and improved integration of multiple lines of evidence, including paleoclimate information. Improved quantification of ERF, the climate system radiative response, and the observed energy increase in the Earth system over the past five decades demonstrate improved consistency between independent estimates of climate drivers, the combined climate feedbacks, and the observed energy increase relative to AR5. (Section TS.3.2)
- **Improved constraints on projections of future climate change:** For the first time in an IPCC report, the assessed future change in global surface temperature is consistently constructed by combining scenario-based projections (which AR5 focused on) with observational constraints based on past simulations of warming as well as the updated assessment of ECS and TCR. In addition, initialized forecasts have been used for the period 2019–2028. The inclusion of these lines of evidence reduces the assessed uncertainty for each scenario. (Section TS.1.3, Cross-Section Box TS.1)
- **Air quality:** The AR5 assessed that projections of air quality are driven primarily by precursor emissions, including CH_4. New scenarios explore a diversity of future options in air pollution management. The AR6 reports rapid recent shifts in the geographical distribution of some of these precursor emissions, confirms the AR5 finding, and shows higher warming effects of short-lived climate forcers in scenarios with the highest air pollution. (Sections TS.1.3 and TS.2.2, Box TS.7)
- **Effects of short-lived climate forcers on global warming:** The AR5 assessed the radiative forcing for emitted compounds. The AR6 has extended this by assessing the emissions-based ERFs

9 Human influence on the climate system refers to human-driven activities that lead to changes in the climate system due to perturbations of Earth's energy budget (also called anthropogenic forcing). Human influence results from emissions of greenhouse gases, aerosols and tropospheric ozone precursors, ozone-depleting substances, and land-use change.

10 Throughout this Technical Summary, 'main driver' means responsible for more than 50% of the change.

11 Throughout the WGI report and unless stated otherwise, uncertainty is quantified using 90% uncertainty intervals. The 90% uncertainty interval, reported in square brackets [x to y], is estimated to have a 90% likelihood of covering the value that is being estimated. The range encompasses the median value and there is an estimated 10% combined likelihood of the value being below the lower end of the range (x) and above its upper end (y). Often the distribution will be considered symmetric about the corresponding best estimate, but this is not always the case. In this Report, an assessed 90% uncertainty interval is referred to as a '*very likely* range'. Similarly, an assessed 66% uncertainty interval is referred to as a '*likely* range'.

also accounting for aerosol–cloud interactions. The best estimates of ERF attributed to sulphur dioxide (SO_2) and CH_4 emissions are substantially greater than in AR5, while that of black carbon is substantially reduced. The magnitude of uncertainty in the ERF due to black carbon emissions has also been reduced relative to AR5. (Section TS.3.1)

- **Global water cycle:** The AR5 assessed that anthropogenic influences have *likely* affected the global water cycle since 1960. The dedicated chapter in AR6 (Chapter 8) concludes with *high confidence* that human-caused climate change has driven detectable changes in the global water cycle since the mid-20th century, with a better understanding of the response to aerosol and greenhouse gas changes. The AR6 further projects with *high confidence* an increase in the variability of the water cycle in most regions of the world and under all emissions scenarios. (Box TS.6)
- **Extreme events:** The AR5 assessed that human influence had been detected in changes in some climate extremes. A dedicated chapter in AR6 (Chapter 11) concludes that it is now an established fact that human-induced greenhouse gas emissions have led to an increased frequency and/or intensity of some weather and climate extremes since 1850, in particular for temperature extremes. Evidence of observed changes and attribution to human influence has strengthened for several types of extremes since AR5, in particular for extreme precipitation, droughts, tropical cyclones and compound extremes (including fire weather). (Sections TS.1.2 and TS.2.1, Box TS.10)

Selected Updates and/or New Results Since AR5 and SR1.5

- **Timing of crossing 1.5°C global warming:** Slightly different approaches are used in SR1.5 and in this Report. SR1.5 assessed a *likely* range of 2030 to 2052 for reaching a global warming level of 1.5°C (for a 30-year period), assuming a continued, constant rate of warming. In AR6, combining the larger estimate of global warming to date and the assessed climate response to all considered scenarios, the central estimate of crossing 1.5°C of global warming (for a 20-year period) occurs in the early 2030s, in the early part of the *likely* range assessed in SR1.5, assuming no major volcanic eruption. (Section TS.1.3, Cross-Section Box TS.1)
- **Remaining carbon budgets:** The AR5 had assessed the transient climate response to cumulative emissions of CO_2 to be *likely* in the range of 0.8°C to 2.5°C per 1000 GtC (1 Gigatonne of carbon, GtC, = 1 Petagram of carbon, PgC, = 3.664 Gigatonnes of carbon dioxide, $GtCO_2$), and this was also used in SR1.5. The assessment in AR6, based on multiple lines of evidence, leads to a narrower *likely* range of 1.0°C–2.3°C per 1000 GtC. This has been incorporated in updated estimates of remaining carbon budgets (see Section TS.3.3.1), together with methodological improvements and recent observations. (Sections TS.1.3 and TS.3.3)
- **Effect of short-lived climate forcers on global warming in coming decades:** The SR1.5 stated that reductions in emissions of cooling aerosols partially offset greenhouse gas mitigation effects for two to three decades in pathways limiting global warming to 1.5°C. The AR6 assessment updates the AR5 assessment of the net cooling effect of aerosols and confirms that changes in short-lived climate forcers will *very likely* cause further warming in the next two decades across all scenarios. (Section TS.1.3, Box TS.7)
- **COVID-19:** Temporary emissions reductions in 2020 associated with COVID-19 containment led to small and positive net radiative effect (warming influence). However, global and regional climate responses to this forcing are undetectable above internal climate variability due to the temporary nature of emissions reductions. (Section TS.3.3)

Selected Updates and/or New Results Since AR5, SRCCL and SROCC

- **Atmospheric concentration of methane:** The SRCCL reported a resumption of atmospheric CH_4 concentration growth since 2007. The AR6 reports a faster growth over 2014–2019 and assesses growth since 2007 to be largely driven by emissions from the fossil fuels and agriculture (dominated by livestock) sectors. (Section TS.2.2)
- **Land and ocean carbon sinks:** The SRCCL assessed that the persistence of the land carbon sink is uncertain due to climate change. The AR6 finds that land and ocean carbon sinks are projected to continue to grow until 2100 with increasing atmospheric concentrations of CO_2, but the fraction of emissions taken up by land and ocean is expected to decline as the CO_2 concentration increases, with a much larger uncertainty range for the land sink. The AR5, SR1.5 and SRCCL assessed carbon dioxide removal options and scenarios. The AR6 finds that the carbon cycle response is asymmetric for pulse emissions or removals, which means that CO_2 emissions would be more effective at raising atmospheric CO_2 than CO_2 removals are at lowering atmospheric CO_2. (Section TS.3.3, Box TS.5)
- **Ocean stratification increase[12]:** Refined analyses of available observations in the AR6 lead to a reassessment of the rate of increase of the global stratification in the upper 200 m to be double that estimated in SROCC from 1970 to 2018. (Section TS.2.4)
- **Projected ocean oxygen loss:** Future subsurface oxygen decline in new projections assessed in WGI AR6 is substantially greater in 2080–2099 than assessed in SROCC. (Section TS.2.4)
- **Ice loss from glaciers and ice sheets:** Since SROCC, globally resolved glacier changes have improved estimates of glacier mass loss over the past 20 years, and estimates of the Greenland and Antarctic Ice Sheet loss have been extended to 2020. (Section TS.2.5)
- **Observed global mean sea level change:** new observation-based estimates published since SROCC lead to an assessed sea level rise estimate from 1901 to 2018 that is now consistent with the sum of individual components and consistent with closure of the global energy budget. (Box TS.4)

12 Increased stratification reduces the vertical exchange of heat, salinity, oxygen, carbon and nutrients. Stratification is an important indicator for ocean circulation.

- **Projected global mean sea level change:** The AR6 projections of global mean sea level are based on projections from ocean thermal expansion and land ice contribution estimates, which are consistent with the assessed ECS and assessed changes in global surface temperature. They are underpinned by new land ice model intercomparisons and consideration of processes associated with *low confidence* to characterize the deep uncertainty in future ice loss from Antarctica. The AR6 projections based on new models and methods are broadly consistent with SROCC findings. (Box TS.4)

TS.1 A Changing Climate

This section introduces the assessment of the physical science basis of climate change in the AR6 and presents the climate context in which this assessment takes place, recent progress in climate science and the relevance of global and regional climate information for impact and risk assessments. The future emissions scenarios and global warming levels, used to integrate assessments across this Report, are introduced and their applications for future climate projections are briefly addressed. Paleoclimate science provides a long-term context for observed climate change of the past 150 years and the projected changes in the 21st century and beyond (Box TS.2). The assessment of past, current and future global surface temperature changes relative to the standard baselines and reference periods[13] used throughout this Report is summarized in Cross-Section Box TS.1.

TS1.1 Context of a Changing Climate

This Report assesses new scientific evidence relevant for a world whose climate system is rapidly changing, overwhelmingly due to human influence. The five IPCC assessment cycles since 1990 have comprehensively and consistently laid out the rapidly accumulating evidence of a changing climate system, with the Fourth Assessment Report in 2007 being the first to conclude that warming of the climate system is unequivocal. Sustained changes have been documented in all major elements of the climate system: the atmosphere, land, cryosphere, biosphere and ocean (Section TS.2). Multiple lines of evidence indicate the recent large-scale climatic changes are unprecedented in a multi-millennial context and that they represent a millennial-scale commitment for the slow-responding elements of the climate system, resulting in continued worldwide loss of ice, increase in ocean heat content, sea level rise and deep ocean acidification (Box TS.2; Section TS.2). {1.2.1, 1.3, Box 1.2, 2.2, 2.3, Figure 2.34, 5.1, 5.3, 9.2, 9.4–9.6, Appendix 1.A}

Earth's climate system has evolved over many millions of years, and evidence from natural archives provides a long-term perspective on observed changes and projected changes over the coming centuries. These reconstructions of past climate also show that atmospheric CO_2 concentrations and global surface temperature are strongly coupled (Figure TS.1), based on evidence from a variety of proxy records over multiple time scales (Box TS.2, Section TS.2). Levels of global warming (see Core Concepts Box) that have not been seen in millions of years could be reached by 2300, depending on the emissions pathway that is followed (Section TS.1.3). For example, there is *medium confidence* that, by 2300, an intermediate scenario[14] used in this Report leads to global surface temperatures of [2.3°C to 4.6°C] higher than 1850–1900, similar to the mid-Pliocene Warm

13 Several baselines or reference periods are used consistently throughout this Report. Baseline refers to a period against which anomalies (i.e., differences from the average value for the baseline period) are calculated. Examples include the 1750 baseline (used for anthropogenic radiative forcings), the 1850–1900 baseline (an approximation for pre-industrial global surface temperature from which global warming levels are calculated) and the 1995–2014 baseline (used for many climate model projections). A reference period indicates a time period over which various statistics are calculated (e.g., the near-term reference period, 2021–2040). Paleo reference periods are listed in Box TS.2. {1.4.1, Cross-Chapter Boxes 1.2 and 2.1}

14 Please refer to Section TS.1.3.1 for an overview of the climate change scenarios used in this Report.

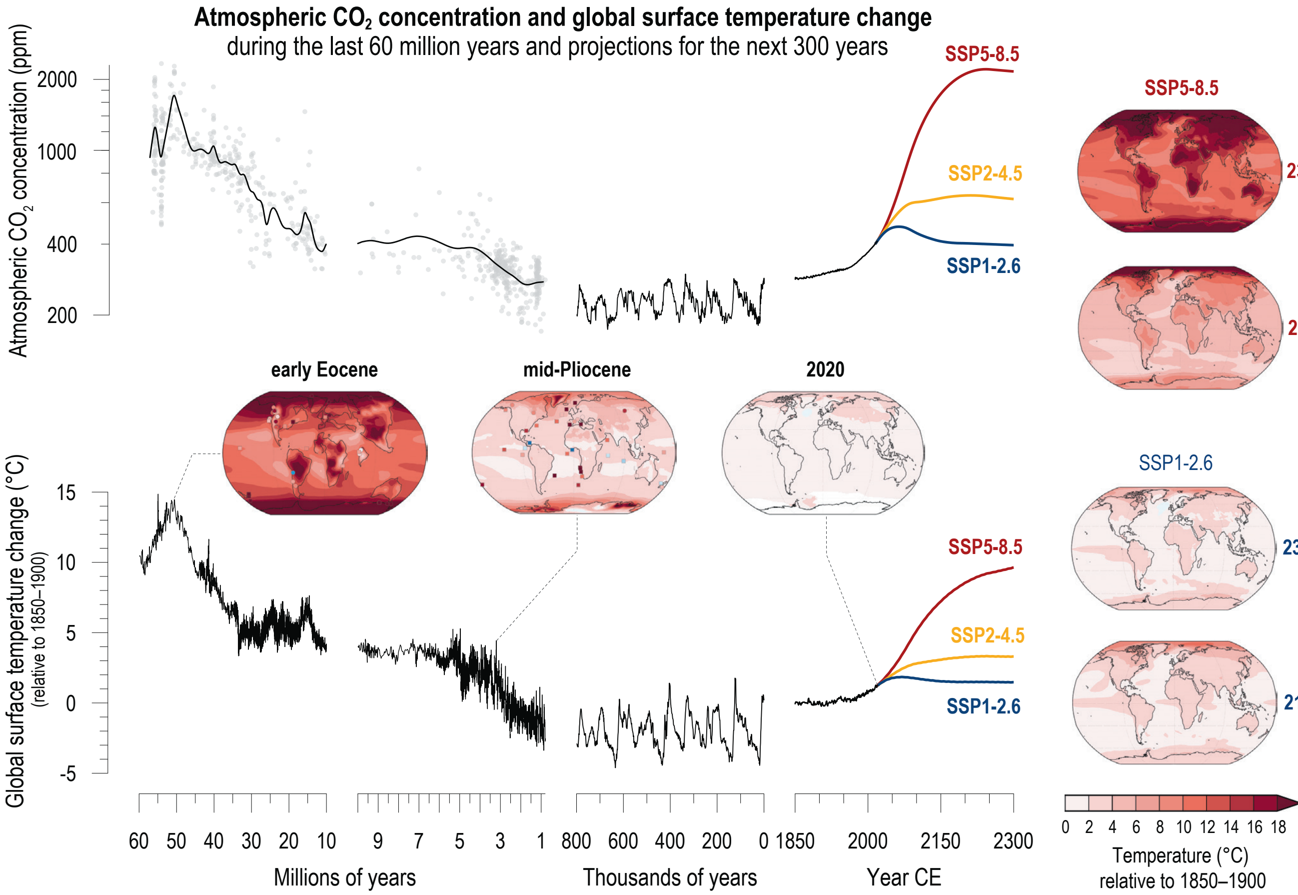

Figure TS.1 | Changes in atmospheric CO_2 and global surface temperature (relative to 1850–1900) from the deep past to the next 300 years. *The intent of this figure is to show that CO_2 and temperature covary, both in the past and into the future, and that projected CO_2 and temperatures are similar to those only from many millions of years ago.* CO_2 concentrations from millions of years ago are reconstructed from multiple proxy records (grey dots are data from Section 2.2.3.1, Figure 2.3 shown with cubic-spline fit). CO_2 levels for the last 800,000 years through the mid-20th century are from air trapped in polar ice; recent values are from direct air measurements. Global surface temperature prior to 1850 is estimated from marine oxygen isotopes, one of multiple sources of evidence used to assess paleo temperatures in this Report. Temperature of the past 170 years is the AR6 assessed mean. CO_2 levels and global surface temperature change for the future are shown for three Shared Socio-economic Pathway (SSP) scenarios through 2300 CE, using Earth system model emulators calibrated to the assessed global surface temperatures. Their smooth trajectories do not account for inter-annual to inter-decadal variability, including transient response to potential volcanic eruptions. Global maps for two paleo reference periods are based on Coupled Model Intercomparison Project Phase 6 (CMIP6) and pre-CMIP6 multi-model means, with site-level proxy data for comparison (squares and circles are marine and terrestrial, respectively). The map for 2020 is an estimate of the total observed warming since 1850–1900. Global maps at right show two SSP scenarios at 2100 (2081–2100) and at 2300 (2281–2300; map from CMIP6 models; temperature assessed in 4.7.1). A brief account of the major climate forcings associated with past global temperature changes is in Cross-Chapter Box 2.1. (Section TS.1.3, Figure TS.9, Cross-Section Box TS.1, Box TS.2) {1.2.1.2; Figures 1.14 and 1.5; 2.2.3; 2.3.1.1; 2.3.1.1.1; Figures 2.4 and 2.5; Cross-Chapter Box 2.1, Figure 1; 4.5.1; 4.7.1; Cross-Chapter Box 4.1; Cross-Chapter Box 7.1; Figure 7.13}

Period [2.5°C to 4°C], about 3.2 million years ago, whereas the high CO_2 emissions scenario SSP5-8.5 leads to temperatures of [6.6°C to 14.1°C] by 2300, which overlaps with the Early Eocene Climate Optimum [10°C to 18°C], about 50 million years ago. {Cross-Chapter Boxes 2.1 and 2.4, 2.3.1, 4.3.1.1, 4.7.1.2, 7.4.4.1}

Understanding of the climate system's fundamental elements is robust and well established. Scientists in the 19th century identified the major natural factors influencing the climate system. They also hypothesized the potential for anthropogenic climate change due to CO_2 emitted by combustion of fossil fuels (petroleum, coal, natural gas). The principal natural drivers of climate change, including changes in incoming solar radiation, volcanic activity, orbital cycles and changes in global biogeochemical cycles, have been studied systematically since the early 20th century. Other major anthropogenic drivers, such as atmospheric aerosols (fine solid particles or liquid droplets), land-use change and non-CO_2 greenhouse gases, were identified by the 1970s. Since systematic scientific assessments began in the 1970s, the influence of human activities on the warming of the climate system has evolved from theory to established fact (see also Section TS.2). The evidence for human influence on recent climate change strengthened from the IPCC First Assessment Report in 1990 to the IPCC Fifth Assessment Report in 2013/14, and is now even stronger in this assessment (Sections TS.1.2.4 and TS.2). Changes across a greater number of climate system components, including changes in regional climate and extremes can now be attributed to human influence (see Sections TS.2 and TS.4). {1.3.1–1.3.5, 3.1, 11.2, 11.9}

Box TS.2 | Paleoclimate

Paleoclimate evidence is integrated within multiple lines of evidence across the WGI Report to more fully understand the climate system. Paleo evidence extends instrument-based observations of climate variables and climate drivers back in time, providing the long-term context needed to gauge the extent to which recent and potential future changes are unusual (Section TS.2, Figure TS.1). Pre-industrial climate states complement evidence from climate model projections by providing real-world examples of climate characteristics for past global warming levels, with empirical evidence for how the slow-responding components of the climate system operate over centuries to millennia – the time scale for committed climate change (Core Concepts Box, Box TS.4, Box TS.9). Information about the state of the climate system during well-described paleoclimate reference periods helps narrow the uncertainty range in the overall assessment of Earth's sensitivity to climate forcing (Section TS.3.2.1). {Cross-Chapter Box 2.1, FAQ 1.3, FAQ 2.1}

Paleoclimate reference periods. Over the long evolution of Earth's climate, several periods have received extensive research attention as examples of distinct climate states and rapid climate transitions (Box TS.2, Figure 1). These paleoclimate reference periods represent the present geological era (Cenozoic; past 65 million years) and are used across chapters to help structure the assessment of climate changes prior to industrialization. Cross-Chapter Box 2.1 describes the reference periods, along with a brief account of their climate forcings, and lists where each is discussed in other chapters. Cross-Chapter Box 2.4 summarizes information on one of the reference periods, the mid-Pliocene Warm Period. The Interactive Atlas includes model output from the World Climate Research Programme Coupled Model Intercomparison Project Phase 6 (CMIP6) for four of the paleoclimate reference periods.

Three selected global climate indicators covary across multiple paleoclimate reference periods

(a)

Reference period (*See Interactive Atlas for climate model output)	Age	CO_2 (ppm)	Temperature (°C)	Sea level (m)
Recent past	1995–2014 CE	360 ⟶ 397	0.66 to 1.00	0.15 to 0.25
Approximate pre-industrial	1850–1900 CE	286 ⟶ 296	–0.15 to +0.11	–0.03 to 0.00
Last Millennium	850–1850 CE	278 to 285	–0.14 ~ 0.24	–0.05 to 0.03
Mid-Holocene*	6.5–5.5 ka	260 to 268	0.2 to 1.0	–3.5 to +0.5
Last Deglacial Transition	18–11 ka	193 ⟶ 271	not assessed	–120 ⟶ –50
Last Glacial Maximum*	23–19 ka	188 to 194	–5 to –7	–134 to –125
Last Interglacial*	129–116 ka	266 to 282	0.5 to 1.5	5 to 10
Mid-Pliocene Warm Period*	3.3–3.0 Ma	360 to 420	2.5 to 4.0	5 to 25
Early Eocene	53–49 Ma	1150 to 2500	10 to 18	70 to 76
Paleocene-Eocene Thermal Maximum	55.9–55.7 Ma	900 ⟶ 2000	10 to 25	not assessed

X to Y: *very likely* range (caveats in Figure 2.34)
X → Y: start to end of period, with no stated uncertainty
X ~ Y: lowest and highest values, with not stated uncertainty

lower 1850–1900 higher

(b)

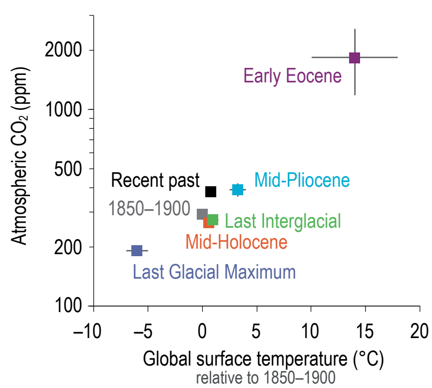

Box TS.2, Figure 1 | Paleoclimate and recent reference periods, with selected key indicators. *The intent of this figure is to list the paleoclimate reference periods used in this Report, to summarize three key global climate indicators, and compare CO_2 with global temperature over multiple periods.* **(a)** Three large-scale climate indicators (atmospheric CO_2, global surface temperature relative to 1850–1900, and global mean sea level relative to 1900), based on assessments in Chapter 2, with confidence levels ranging from *low* to *very high*. **(b)** Comparison between global surface temperature (relative to 1850–1900) and atmospheric CO_2 concentration (shown on a log scale) for multiple reference periods (mid-points with 5–95% ranges). {2.2.3, 2.3.1.1, 2.3.3.3, Figure 2.34}

Paleoclimate models and reconstructions. Climate models that target paleoclimate reference periods have been featured by the IPCC since the First Assessment Report. Under the framework of CMIP6-PMIP4 (Paleoclimate Modelling Intercomparison Project), new protocols for model intercomparisons have been developed for multiple paleoclimate reference periods. These modelling efforts have led to improved understanding of the climate response to different external forcings, including changes in Earth's orbital and plate movements, solar irradiance, volcanism, ice-sheet size and atmospheric greenhouse gases. Likewise, quantitative reconstructions of climate variables from proxy records that are compared with paleoclimate simulations have improved as the number of study sites and variety of proxy types have expanded, and as records have been compiled into new regional and global datasets. {1.3.2, 1.5.1, Cross-Chapter Boxes 2.1 and 2.4}

Global surface temperature. Since AR5, updated climate forcings, improved models, new understanding of the strengths and weaknesses of a growing array of proxy records, better chronologies and more robust proxy data products have led to better agreement between models and reconstructions. For global surface temperature, the mid-point of the AR6-assessed range and the median of the model-simulated temperatures differ by an average of 0.5°C across five reference periods; they overlap within their

TS

Box TS.2 (continued)

90% ranges in four of five cases, which together span from about 6 [5 to 7]°C colder during the Last Glacial Maximum to about 14 [10 to 18] °C warmer during the Early Eocene, relative to 1850–1900 (Box TS.2, Figure 2a). Changes in temperature by latitude in response to multiple forcings show that polar amplification (stronger warming at high latitudes than the global average) is a prominent feature of the climate system across multiple climate states, and the ability of models to simulate this polar amplification in past warm climates has improved since AR5 (*high confidence*). Over the past millennium, and especially since about 1300 CE, simulated global surface temperature anomalies are well within the uncertainty of reconstructions (*medium confidence*), except for some short periods immediately following large volcanic eruptions, for which different forcing datasets disagree (Box TS.2, Figure 2b). {2.3.1.1, 3.3.3.1, 3.8.2.1, 7.4.4.1.2}

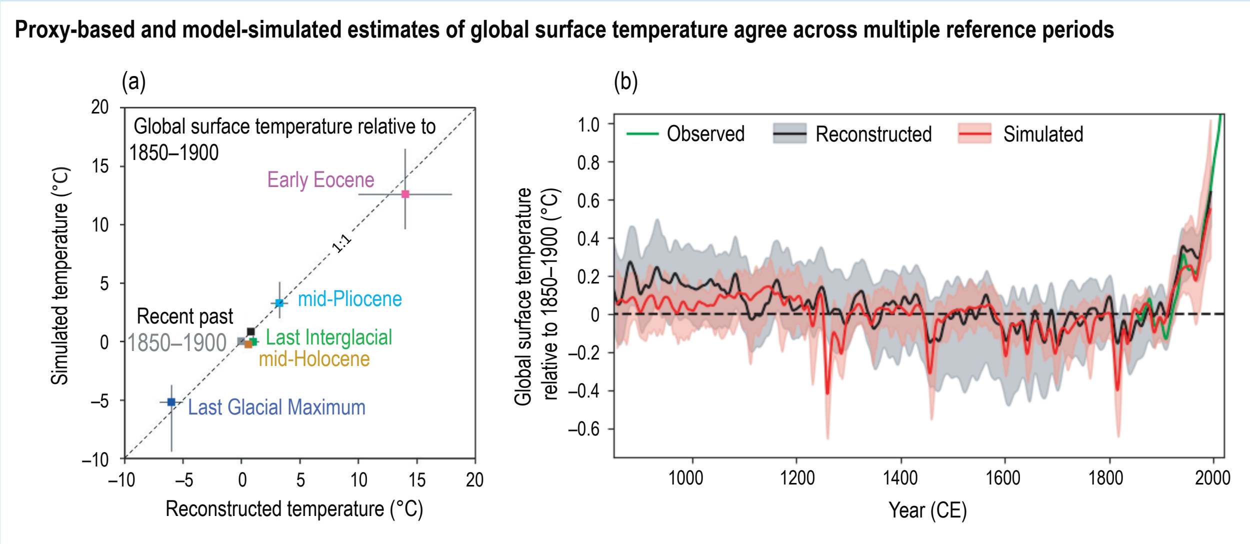

Box TS.2, Figure 2 | Global surface temperature as estimated from proxy records (reconstructed) and climate models (simulated). *The intent of this figure is to show the agreement between observations and models of global temperatures during paleo reference periods.* **(a)** For individual paleoclimate reference periods. **(b)** For the last millennium, with instrumental temperature (AR6 assessed mean, 10-year smoothed). Model uncertainties in (a) and (b) are 5–95% ranges of multi-model ensemble means; reconstructed uncertainties are 5–95% ranges (*medium confidence*) of (a) midpoints and (b) multi-method ensemble median. {2.3.1.1, Figure 2.34, Figure 3.2c, Figure 3.44}

Equilibrium climate sensitivity. Paleoclimate data provide evidence to estimate equilibrium climate sensitivity (ECS[15]) (Section TS.3.2.1). In AR6, refinements in paleo data for paleoclimate reference periods indicate that ECS is *very likely* greater than 1.5°C and *likely* less than 4.5°C, which is largely consistent with other lines of evidence and helps narrow the uncertainty range of the overall assessment of ECS. Some of the CMIP6 climate models that have either high (>5°C) or low (<2°C) ECS also simulate past global surface temperature changes outside the range of proxy-based reconstructions for the coldest and warmest reference periods. Since AR5, independent lines of evidence, including proxy records from past warm periods and glacial–interglacial cycles, indicate that sensitivity to forcing increases as temperature increases (Section TS.3.2.2). {7.4.3.2, 7.5.3, 7.5.6, Table 7.11}

Water cycle. New hydroclimate reconstructions and model-data comparisons have improved the understanding of the causes and effects of long-term changes in atmospheric and ocean circulation, including monsoon variability and modes of variability (Box TS.13, Section TS.4.2). Climate models are able to reproduce decadal drought variability on large regional scales, including the severity, persistence and spatial extent of past megadroughts known from proxy records (*medium confidence*). Some long-standing discrepancies remain, however, such as the magnitude of African monsoon precipitation during the early Holocene (the past 11,700 years), suggesting continuing knowledge gaps. Paleoclimate evidence shows that, in relatively high CO_2 climates such as the Pliocene, Walker circulation over the equatorial Pacific Ocean weakens, supporting the *high confidence* model projections of weakened Walker cells by the end of the 21st century. {3.3.2, 8.3.1.6, 8.4.1.6, 8.5.2.1, 9.2}

15 In this Report, equilibrium climate sensitivity is defined as the equilibrium (steady state) change in the surface temperature following a doubling of the atmospheric carbon dioxide (CO_2) concentration from pre-industrial conditions.

Box TS.2 (continued)

Sea level and ice sheets. Although past and future global warming differ in their forcings, evidence from paleoclimate records and modelling show that ice-sheet mass and global mean sea level (GMSL) responded dynamically over multiple millennia (*high confidence*). This evidence helps to constrain estimates of the committed GMSL response to global warming (Box TS.4). For example, under a past global warming levels of around [2.5°C to 4°C] relative to 1850–1900, like during the mid-Pliocene Warm Period, sea level was [5 to 25 m] higher than 1900 (*medium confidence*); under past global warming levels of [10°C to 18°C], like during the Early Eocene, the planet was essentially ice free (*high confidence*). Constraints from these past warm periods, combined with physical understanding, glaciology and modelling, indicate a committed long-term GMSL rise over 10,000 years, reaching about 8 to 13 m for sustained peak global warming of 2°C and up to 28 to 37 m for 5°C, which exceeds the AR5 estimate. {2.3.3.3, 9.4.1.4, 9.4.2.6, 9.6.2, 9.6.3.5}

Ocean. Since AR5, better integration of paleo-oceanographic data with modelling along with higher-resolution analyses of transient changes have improved understanding of long-term ocean processes. Low-latitude sea surface temperatures at the Last Glacial Maximum cooled more than previously inferred, resolving some inconsistencies noted in AR5. This paleo context supports the assessment that ongoing increase in ocean heat content (OHC) represents a long-term commitment (see Core Concepts Box), essentially irreversible on human time scales (*high confidence*). Estimates of past global OHC variations generally track those of sea surface temperatures around Antarctica, underscoring the importance of Southern Ocean processes in regulating deep-ocean temperatures. Paleoclimate data, along with other evidence of glacial–interglacial changes, show that Antarctic Circumpolar flow strengthened and that ventilation of Antarctic Bottom Water accelerated during warming intervals, facilitating release of CO_2 stored in the deep ocean to the atmosphere. Paleo evidence suggests significant reduction of deep-ocean ventilation associated with meltwater input during times of peak warmth. {2.3.1.1, 2.3.3.1, 9.2.2, 9.2.3.2}

Carbon cycle. Past climate states were associated with substantial differences in the inventories of the various carbon reservoirs, including the atmosphere (Section TS.2.2). Since AR5, the quantification of carbon stocks has improved due to the development of novel sedimentary proxies and stable-isotope analyses of air trapped in polar ice. Terrestrial carbon storage decreased markedly during the Last Glacial Maximum by 300–600 PgC, possibly by 850 PgC when accounting for interactions with the lithosphere and ocean sediments, a larger reduction than previously estimated, owing to a colder and drier climate. At the same time, the storage of remineralized carbon in the ocean interior increased by as much as 750–950 PgC, sufficient to balance the removal of carbon from the atmosphere (200 PgC) and terrestrial biosphere reservoirs combined (*high confidence*). {5.1.2.2}

TS.1.2 Progress in Climate Science

TS.1.2.1 Observation-based Products and their Assessments

Observational capabilities have continued to improve and expand overall since AR5, enabling improved consistency between independent estimates of climate drivers, the combined climate feedbacks, and the observed energy and sea level increase. Satellite climate records and improved reanalyses are used as an additional line of evidence for assessing changes at the global and regional scales. However, there have also been reductions in some observational data coverage or continuity and limited access to data resulting from data policy issues. Natural archives of past climate, such as tropical glaciers, have also been subject to losses (in part due to anthropogenic climate change). {1.5.1, 1.5.2, 10.2.2}

Earth system observations are an essential driver of progress in our understanding of climate change. Overall, capabilities to observe the physical climate system have continued to improve and expand. Improvements are particularly evident in ocean observing networks and remote-sensing systems. Records from several recently instigated satellite measurement techniques are now long enough to be relevant for climate assessments. For example, globally distributed, high-vertical-resolution profiles of temperature and humidity in the upper troposphere and stratosphere can be obtained from the early 2000s using global navigation satellite systems, leading to updated estimates of recent atmospheric warming. Improved measurements of ocean heat content, warming of the land surface, ice-sheet mass loss and sea level changes allow a better closure of the global energy and sea level budgets relative to AR5. For surface and balloon-based networks, apparent regional data reductions result from a combination of data policy issues, data curation/provision challenges, and real cessation of observations, and are to an extent counter-balanced by improvements elsewhere. Limited observational records of extreme events and spatial data gaps currently limit the assessment of some observed regional climate change. {1.5.1, 2.3.2, 7.2.2, Box 7.2, Cross-Chapter Box 9.1, 9.6.1, 10.2.2, 10.6, 11.2, 12.4}

New paleoclimate reconstructions from natural archives have enabled more robust reconstructions of the spatial and temporal patterns of past climate changes over multiple time scales (Box TS.2). However, paleoclimate archives, such as tropical glaciers and modern natural archives used for calibration (e.g., corals and trees), are rapidly disappearing owing to a host of pressures, including increasing temperatures (*high confidence*). Substantial quantities of past instrumental observations of weather and other climate variables, over both land and ocean, which could fill gaps in existing datasets, remain un-digitized or inaccessible. These include measurements of temperature (air and sea surface), rainfall, surface pressure, wind strength and direction, sunshine amount and many other variables dating back into the 19th century. {1.5.1}

Reanalyses combine observations and models (e.g., a numerical weather prediction model) using data assimilation techniques to provide a spatially complete, dynamically consistent estimate of multiple variables describing the evolving climate state. Since AR5, new reanalyses have been developed for the atmosphere and the ocean with various combinations of increased resolution, extended records, more consistent data assimilation and larger availability of uncertainty estimates. Limitations remain, for example, in how reanalyses represent global-scale changes to the water cycle. Regional reanalyses use high-resolution, limited-area models constrained by regional observations and with boundary conditions from global reanalyses. There is *high confidence* that regional reanalyses better represent the frequencies of extremes and variability in precipitation, surface air temperature and surface wind than global reanalyses and provide estimates that are more consistent with independent observations than dynamical downscaling approaches. {1.5.2, 10.2.1.2, Annex I}

TS.1.2.2 Climate Model Performance

This report assesses results from climate models participating in the Coupled Model Intercomparison Project Phase 6 (CMIP6) of the World Climate Research Programme. These models include new and better representation of physical, chemical and biological processes, as well as higher resolution, compared to climate models considered in previous IPCC Assessment Reports. This has improved the simulation of the recent mean state of most large-scale indicators of climate change and many other aspects across the climate system. Some differences from observations remain, for example in regional precipitation patterns. Projections of the increase in global surface temperature, the pattern of warming, and global mean sea level rise from previous IPCC Assessment Reports and other studies are broadly consistent with subsequent observations, especially when accounting for the difference in radiative forcing scenarios used for making projections and the radiative forcings that actually occurred.

The CMIP6 historical simulations assessed in this report have an ensemble mean global surface temperature change within 0.2°C of the observations over most of the historical period, and observed warming is within the *very likely* range of the CMIP6 ensemble. However, some CMIP6 models simulate a warming that is either above or below the assessed *very likely* range of observed warming. The information about how well models simulate past warming, as well as other insights from observations and theory, are used to assess projections of global warming (see Cross-Section Box TS.1). Increasing horizontal resolution in global climate models improves the representation of small-scale features and the statistics of daily precipitation (*high confidence*). Earth system models, which include additional biogeochemical feedbacks, often perform as well as their lower-complexity global climate model counterparts, which do not account for these additional feedbacks (*medium confidence*). {1.3.6, 1.5.3, 3.1, 3.5.1, 3.8.2, 4.3.1, 4.3.4, 7.5, 8.5.1, 9.6.3.1}

Climate model simulations coordinated and collected as part of the World Climate Research Programme's Coupled Model Intercomparison Project Phase 6 (CMIP6), complemented by a range of results from the previous phase (CMIP5), constitute a key line of evidence supporting this Report. The latest generation of CMIP6 models have an improved representation of physical processes relative to previous generations, and a wider range of Earth system models now represent biogeochemical cycles. Higher-resolution models that better capture smaller-scale processes are also increasingly becoming available for climate change research (Figure TS.2, Panels a and b). Results from coordinated regional climate modelling initiatives, such as the Coordinated Regional Climate Downscaling Experiment (CORDEX) complement and add value to the CMIP global models, particularly in complex topography zones, coastal areas and small islands, as well as for extremes. {1.5.3, 1.5.4, 2.8.2, FAQ 3.3, 6.2.2, 6.4, 6.4.5, 8.5.1, 10.3.3, Atlas.1.4}

Projections of the increase in global surface temperature and the pattern of warming from previous IPCC Assessment Reports and other studies are broadly consistent with subsequent observations (*limited evidence, high agreement*), especially when accounting for the difference in radiative forcing scenarios used for making projections and the radiative forcings that actually occurred (Figure TS.3). The AR5 and SROCC projections of GMSL for the 2007–2018 period have been shown to be consistent with observed trends in GMSL and regional weighted mean tide gauges. {1.3.6, 9.6.3.1}

For most large-scale indicators of climate change, the simulated recent mean climate from CMIP6 models underpinning this assessment have improved compared to the CMIP5 models used in AR5 (*high confidence*). This is evident from the performance of 18 simulated atmospheric and land large-scale indicators of climate change between the three generations of models (CMIP3, CMIP5, and CMIP6) when benchmarked against reanalysis and observational data (Figure TS.2, Panel c). Earth system models, characterized by additional biogeochemical feedbacks, often perform at least as well as related, more constrained, lower-complexity models lacking these feedbacks (*medium confidence*). {3.8.2, 10.3.3.3}

The CMIP6 multi-model mean global surface temperature change from 1850–1900 to 2010–2019 is close to the best estimate of the observed warming. However, some CMIP6 models simulate a warming that is below or above the assessed *very likely* range. The CMIP6 models also reproduce surface temperature variations over the past millennium, including the cooling that follows periods of intense volcanism (*medium confidence*). For upper air temperature, an overestimation of the upper tropical troposphere warming by about 0.1°C per decade between 1979 and 2014 persists in most CMIP5 and CMIP6 models (*medium confidence*), whereas the differences between simulated and improved satellite-derived estimates of change in global mean temperature through the depth of the stratosphere have decreased. {3.3.1}

Some CMIP6 models demonstrate an improvement in how clouds are represented. CMIP5 models commonly displayed a negative shortwave cloud radiative effect that was too weak in the present climate. These errors have been reduced, especially over the Southern Ocean, due to a more realistic simulation of supercooled liquid droplets with sufficient numbers and an associated increase in the cloud optical depth. Because a negative cloud optical depth feedback in response to surface warming results from 'brightening' of clouds via active phase change from ice to liquid cloud particles (increasing their shortwave cloud radiative effect), the extratropical cloud shortwave feedback in CMIP6 models tends to be less negative, leading to a better agreement with observational estimates (*medium confidence*). CMIP6 models generally represent more processes that drive aerosol–cloud interactions than the previous generation of climate models, but there is only *medium confidence* that those enhancements improve their fitness-for-purpose of simulating radiative forcing of aerosol–cloud interactions. {6.4, 7.4.2, FAQ 7.2}

CMIP6 models still have deficiencies in simulating precipitation patterns, particularly in the tropical ocean. Increasing horizontal resolution in global climate models improves the representation of small-scale features and the statistics of daily precipitation (*high confidence*). There is *high confidence* that high-resolution global, regional and hydrological models provide a better representation of land surfaces, including topography, vegetation and land-use change, which can improve the accuracy of simulations of regional changes in the terrestrial water cycle. {3.3.2, 8.5.1, 10.3.3, 11.2.3}

There is *high confidence* that climate models can reproduce the recent observed mean state and overall warming of temperature extremes globally and in most regions, although the magnitude of the trends may differ. There is *high confidence* in the ability of models to capture the large-scale spatial distribution of precipitation extremes over land. The overall performance of CMIP6 models in simulating the intensity and frequency of extreme precipitation is similar to that of CMIP5 models (*high confidence*). {Cross-Chapter Box 3.2, 11.3.3, 11.4.3}

The structure and magnitude of multi-model mean ocean temperature biases have not changed substantially between CMIP5 and CMIP6 (*medium confidence*). Since AR5, there is improved consistency between recent observed estimates and model simulations of changes in upper (<700 m) ocean heat content. The mean zonal and overturning circulations of the Southern Ocean and the mean overturning circulation of the North Atlantic (AMOC) are broadly reproduced by CMIP5 and CMIP6 models. {3.5.1, 3.5.4, 9.2.3, 9.3.2, 9.4.2}

CMIP6 models better simulate the sensitivity of Arctic sea ice area to anthropogenic CO_2 emissions, and thus better capture the time evolution of the satellite-observed Arctic sea ice loss (*high confidence*). The ability to model ice-sheet processes has improved substantially since AR5. As a consequence, there is *medium confidence* in the representation of key processes related to surface-mass balance and retreat of the grounding-line (the junction between a grounded ice sheet and an ice shelf, where the ice starts to float) in the absence of instabilities. However, there remains *low confidence* in simulations of ice-sheet instabilities, ice-shelf disintegration and basal melting owing to their high sensitivity to both uncertain oceanic forcing and uncertain boundary conditions and parameters. {1.5.3, 2.3.2, 3.4.1, 3.4.2, 3.8.2, 9.3.1, 9.3.2, 9.4.1, 9.4.2}

CMIP6 models are able to reproduce most aspects of the spatial structure and variance of the El Niño–Southern Oscillation (ENSO) and Indian Ocean Basin and Dipole modes of variability (*medium confidence*). However, despite a slight improvement in CMIP6, some underlying processes are still poorly represented. Models reproduce observed spatial features and variance of the Southern Annular Mode (SAM) and Northern Annular Mode (NAM) very well (*high confidence*). The summertime SAM trend is well captured, with CMIP6 models outperforming CMIP5 models (*medium confidence*). By contrast, the cause of the NAM trend towards its positive phase is not well understood. In the Tropical Atlantic basin, which contains the Atlantic Zonal and Meridional modes, major biases in modelled mean state and variability remain. Model performance is limited in reproducing sea surface temperature anomalies for decadal modes of variability, despite improvements from CMIP5 to CMIP6 (*medium confidence*) (see also Section TS.1.4.2.2, Table TS.4). {3.7.3–3.7.7}

Earth system models (ESMs) simulate globally averaged land carbon sinks within the range of observation-based estimates (*high confidence*), but global-scale agreement masks large regional disagreements. There is also *high confidence* that the ESMs simulate the weakening of the global net flux of CO_2 into the ocean during the 1990s, as well as the strengthening of the flux from 2000. {3.6}

Two important quantities used to estimate how the climate system responds to changes in greenhouse gas (GHG) concentrations are the equilibrium climate sensitivity (ECS) and transient climate response (TCR[16]). The CMIP6 ensemble has broader ranges of ECS and TCR values than CMIP5 (see Section TS.3.2 for the assessed range). These higher sensitivity values can, in some models, be traced to changes in extratropical cloud feedbacks (*medium confidence*). To combine evidence from CMIP6 models and independent assessments of ECS and TCR, various emulators are used throughout the report. Emulators are a broad class of simple climate models or statistical methods that reproduce the behaviour of complex ESMs to represent key characteristics of the climate system, such as global surface temperature and sea level projections. The main application of emulators in AR6 is to extrapolate insights from ESMs and observational constraints to produce projections from a larger set of emissions scenarios, which is achieved due to their computational efficiency. These emulated projections are also used for scenario classification in WGIII. {Box 4.1, 4.3.4, 7.4.2, 7.5.6, Cross-Chapter Box 7.1, FAQ 7.2}

16 In this Report, transient climate response is defined as the surface temperature response for the hypothetical scenario in which atmospheric carbon dioxide (CO_2) increases at 1% yr^{-1} from pre-industrial to the time of a doubling of atmospheric CO_2 concentration.

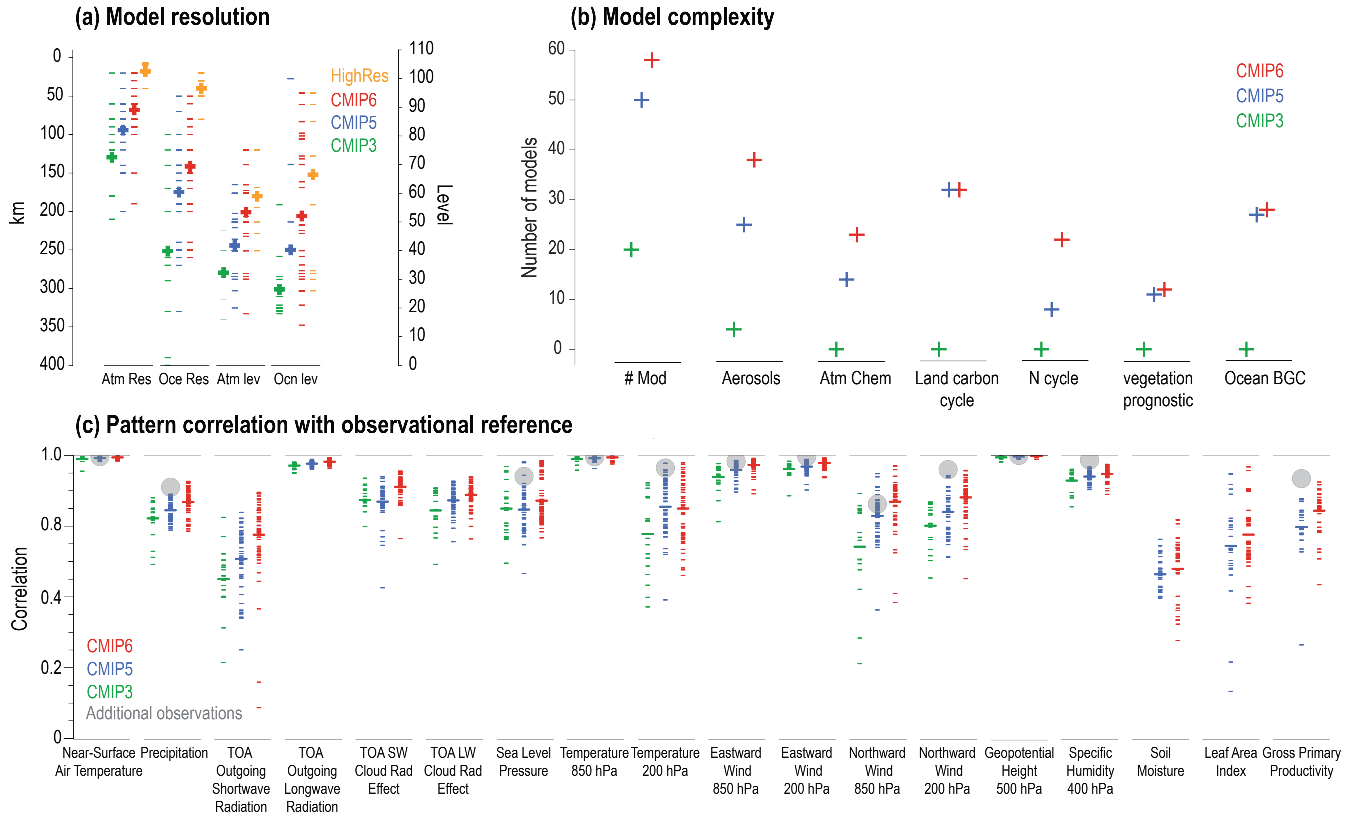

Figure TS.2 | Progress in climate models. *The intent of this figure is to show present improvements in climate models in resolution, complexity and representation of key variables.* **(a)** Evolution of model horizontal resolution and vertical levels (based on Figure 1.19). **(b)** Evolution of inclusion of processes and resolution from Coupled Model Intercomparison Project Phase 3 (CMIP3), Phase 5 (CMIP5) and Phase 6 (CMIP6; Annex II). **(c)** Centred pattern correlations between models and observations for the annual mean climatology over the period 1980–1999. Results are shown for individual CMIP3 (cyan), CMIP5 (blue) and CMIP6 (red) models (one ensemble member is used) as short lines, along with the corresponding ensemble averages (long lines). The correlations are shown between the models and the primary reference observational data set (from left to right: ERA5, GPCP-SG, CERES-EBAF, CERES-EBAF, CERES-EBAF, CERES-EBAF, JR-55, ERA5, ERA5, ERA5, ERA5, ERA5, ERA5, AIRS, ERA5, ESACCI-Soilmoisture, LAI3g, MTE). In addition, the correlation between the primary reference and additional observational data sets (from left to right: NCEP, GHCN, -, -, -, -, ERA5, HadISST, NCEP, NCEP, NCEP, NCEP, NCEP, NCEP, ERA5, NCEP, -, -, FLUXCOM) are shown (solid grey circles) if available. To ensure a fair comparison across a range of model resolutions, the pattern correlations are computed after regridding all datasets to a resolution of 4° in longitude and 5° in latitude. (Expanded from Figure 3.43; produced with ESMValTool version 2). {Figure 3.43}

TS.1.2.3 Understanding Climate Variability and Emerging Changes

Observed changes in climate are unequivocal at the global scale and are increasingly apparent on regional and local spatial scales. Both the rate of long-term change and the amplitude of year-to-year variations differ between regions and across climate variables, thus influencing when changes emerge or become apparent compared to natural variations (see Emergence in Core Concepts Box). The signal of temperature change has emerged more clearly in tropical regions, where year-to-year variations tend to be small over land, than in regions with greater warming but larger year-to-year variations (*high confidence*) (Figure TS.3). Long-term changes in other variables have emerged in many regions, such as for some weather and climate extremes and Arctic sea ice area. {1.4.2, Cross-Chapter Box 3.1, 9.3.1, 11.3.2, 12.5.2}

Observational datasets have been extended and improved since AR5, providing stronger evidence that the climate is changing and allowing better estimates of natural climate variability on decadal time scales. There is *very high confidence* that the slower rate of global surface temperature change observed over 1998–2012 compared to 1951–2012 was temporary, and was, with *high confidence*, induced by internal variability (particularly Pacific Decadal Variability) and variations in solar irradiance and volcanic forcing that partly offset the anthropogenic warming over this period. Global ocean heat content continued to increase throughout this period, indicating continuous warming of the entire climate system (*very high confidence*). Hot extremes also continued to increase during this period over land (*high confidence*). Even in a continually warming climate, periods of reduced and increased trends in global surface temperature at decadal time scales will continue to occur in the 21st century (*very high confidence*). {Cross-Chapter Box 3.1, 3.3.1, 3.5.1, 4.6.2, 11.3.2}

Since AR5, the increased use of 'large ensembles', or multiple simulations with the same climate model but using different initial conditions, supports improved understanding of the relative roles of internal variability and forced change in the climate system. Simulations and understanding of modes of climate variability, including teleconnections, have improved since AR5 (*medium confidence*), and larger ensembles allow a better quantification of uncertainty in projections due to internal climate variability. {1.4.2, 1.5.3, 1.5.4, 4.2, 4.4.1, Box 4.1, 8.5.2, 10.3.4, 10.4}

Changes in regional climate can be detected even though natural climate variations can temporarily increase or obscure anthropogenic climate change on decadal time scales. While anthropogenic forcing has contributed to multi-decadal mean precipitation changes in several regions, internal variability can delay emergence of the anthropogenic signal in long-term precipitation changes in many land regions (*high confidence*). {10.4}

Mean temperatures and heat extremes have emerged above natural variability in almost all land regions with *high confidence*. Changes in temperature-related variables, such as regional temperatures, growing season length, extreme heat and frost, have already occurred, and there is *medium confidence* that many of these changes are attributable to human activities. Several impact-relevant changes have not yet emerged from natural variability but will emerge sooner or later in this century depending on the emissions scenario (*high confidence*). Ocean acidification and deoxygenation have already emerged over most of the global open ocean, as has a reduction in Arctic sea ice (*high confidence*). {9.3.1, 9.6.4, 11.2, 11.3, 12.4, 12.5, Atlas.3–Atlas.11}

TS.1.2.4 Understanding of Human Influence

The evidence for human influence on recent climate change has strengthened progressively from the IPCC Second Assessment Report to AR5 and is even stronger in this assessment, including for regional scales and for extremes. Human influence in the IPCC context refers to the human activities that lead to or contribute to a climate response, such as the human-induced emissions of greenhouse gases that subsequently alter the atmosphere's radiative

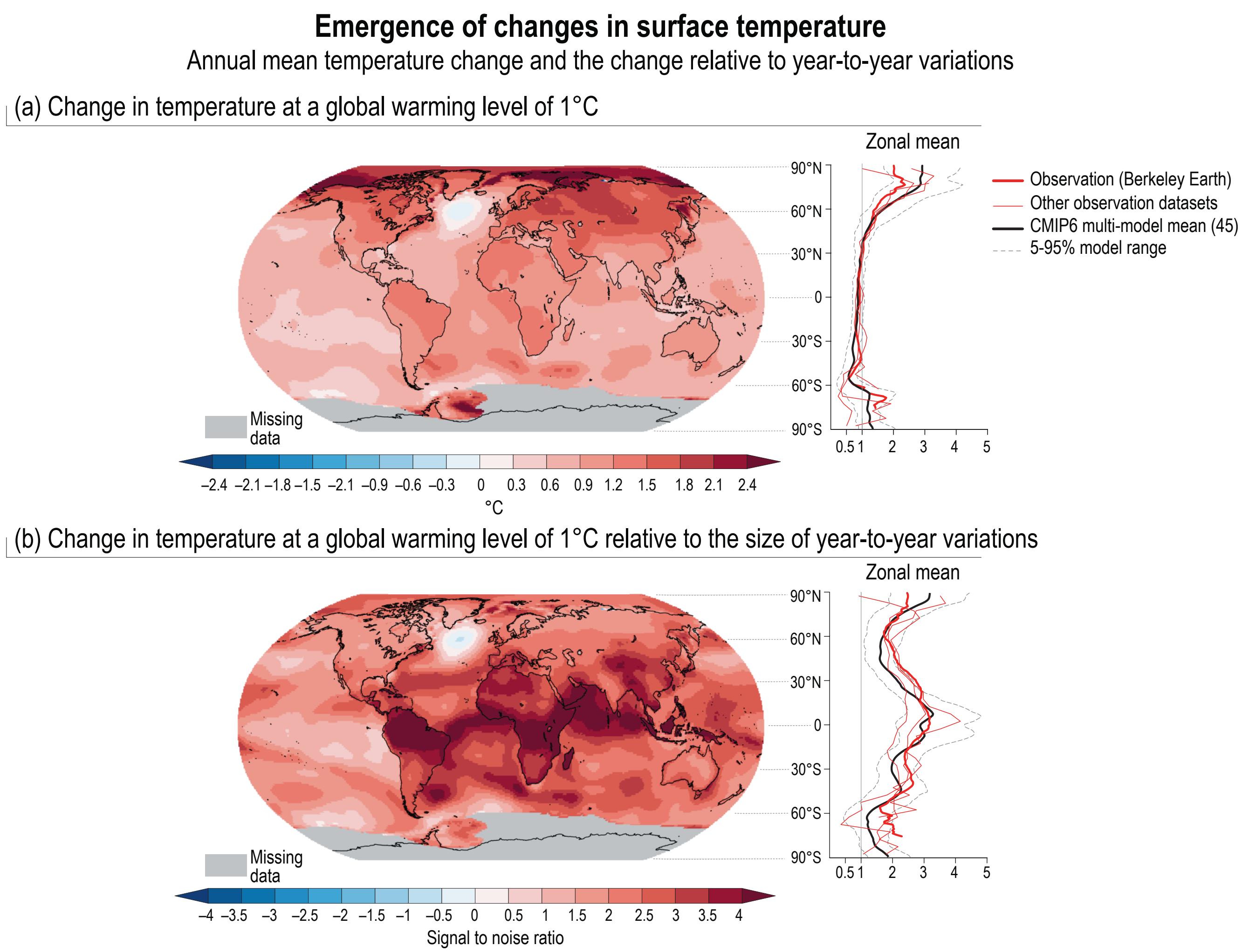

Figure TS.3 | Emergence of changes in temperature over the historical period. *The intent of this figure is to show how observed changes in temperature have emerged and that the emergence pattern agrees with model simulations.* The observed change in temperature at a global warming level of 1°C **(a),** and the signal-to-noise ratio (the change in temperature at a global warming level of 1°C, divided by the size of year-to-year variations, (**b**)) using data from Berkeley Earth. The right panels show the zonal means of the maps and include data from different observational datasets (red) and the Coupled Model Intercomparison Project Phase 6 (CMIP6) simulations (black, including the 5–95% range) processed in the same way as the observations. {1.4.2, 10.4.3}

properties, resulting in warming of the atmosphere, ocean and land components of the climate system. Other human activities influencing climate include the emission of aerosols and other short-lived climate forcers, and land-use change such as urbanization. Progress in our understanding of human influence is gained from longer observational datasets, improved paleoclimate information, a stronger warming signal since AR5, and improvements in climate models, physical understanding and attribution techniques (see Core Concepts Box). Since AR5, the attribution to human influence has become possible across a wider range of climate variables and climatic impact-drivers (CIDs, see Core Concepts Box). New techniques and analyses drawing on several lines of evidence have provided greater confidence in attributing changes in regional weather and climate extremes to human influence (*high confidence*). {1.3, 1.5.1, Appendix 1.A, 3.1–3.8, 5.2, 6.4.2, 7.3.5, 7.4.4, 8.3.1, 10.4, Cross-Chapter Box 10.3, 11.2–11.9, 12.4}

Combining the evidence from across the climate system increases the level of confidence in the attribution of observed climate change to human influence and reduces the uncertainties associated with assessments based on single variables. {Cross-Chapter Box 10.3}

Since AR5, the accumulation of energy in the Earth system has become established as a robust measure of the rate of global climate change on interannual-to-decadal time scales. The rate of accumulation of energy is equivalent to Earth's energy imbalance and can be quantified by changes in the global energy inventory for all components of the climate system, including global ocean heat uptake, warming of the atmosphere, warming of the land and melting of ice. Compared to changes in global surface temperature, Earth's energy imbalance (see Core Concepts Box) exhibits less variability, enabling more accurate identification and estimation of trends. {Box 7.2 and Section 7.2}

Identifying the human-induced components contributing to the energy budget provides an implicit estimate of the human influence on global climate change (Sections TS.2 and TS.3.1). {Cross-Working Group Box: Attribution in Chapter 1, 3.8, 7.2.2, Box 7.2, Cross-Chapter Box 9.1}

Regional climate changes can be moderated or amplified by regional forcing from land-use and land-cover changes or from aerosol concentrations and other short-lived climate forcers (SLCFs). For example, the difference in observed warming trends between cities and their surroundings can partly be attributed to urbanization (*very high confidence*). While established attribution techniques provide confidence in our assessment of human influence on large-scale climate changes (as described in Section TS.2), new techniques developed since AR5, including attribution of individual events, have provided greater confidence in attributing changes in climate extremes to climate change (Box TS.10). Multiple attribution approaches support the contribution of human influence to several regional multi-decadal mean precipitation changes (*high confidence*). Understanding about past and future changes in weather and climate extremes has increased due to better observation-based datasets, physical understanding of processes, an increasing proportion of scientific literature combining different lines of evidence, and improved accessibility to different types of climate models (*high confidence*) (see Sections TS.2 and TS.4). {Cross-Working Group Box: Attribution in Chapter 1, 1.5, 3.2, 3.5, 5.2, 6.4.3, 8.3, 9.6, 10.1, 10.2, 10.3.3, 10.4.1, 10.4.2, 10.4.3, 10.5, 10.6, Cross-Chapter Box 10.3, Box 10.3, 11.1.6, 11.2–11.9, 12.4}

TS.1.3 Assessing Future Climate Change

Various frameworks can be used to assess future climatic changes and to synthesize knowledge across climate change assessment in WGI, WGII and WGIII. These frameworks include: (i) scenarios, (ii) global warming levels and (iii) cumulative CO_2 emissions (see Core Concepts Box). The latter two offer scenario- and path-independent approaches to assess future projections. Additional choices, for instance with regard to common reference periods and time windows for which changes are assessed, can further help to facilitate integration across the WGI report and across the whole AR6 (see Section TS.1.1). {1.4.1, 1.6, Cross-Chapter Box 1.4, 4.2.2, 4.2.4, Cross-Chapter Box 11.1}

TS.1.3.1 Climate Change Scenarios

A core set of five illustrative scenarios based on the Shared Socio-economic Pathways (SSPs) are used consistently across this Report: SSP1-1.9, SSP1-2.6, SSP2-4.5, SSP3-7.0, and SSP5-8.5. These scenarios cover a broader range of greenhouse gas and air pollutant futures than assessed in earlier WGI reports, and they include high-CO_2 emissions pathways without climate change mitigation as well as new low-CO_2 emissions pathways (Figure TS.4). In these scenarios, differences in air pollution control and variations in climate change mitigation stringency strongly affect anthropogenic emissions trajectories of SLCFs. Modelling studies relying on the Representative Concentration Pathways (RCPs) used in AR5 complement the assessment based on SSP scenarios, for example at the regional scale.

A comparison of simulations from CMIP5 using the RCPs with SSP-based simulations from CMIP6 shows that about half of the increase in simulated warming in CMIP6 versus CMIP5 arises because higher climate sensitivity is more prevalent in CMIP6 model versions; the other half arises from higher radiative forcing in nominally corresponding scenarios (e.g., RCP8.5 and SSP5-8.5; *medium confidence*). The feasibility or likelihood of individual scenarios is not part of this assessment, which focuses on the climate response to a large range of emissions scenarios. {1.5.4, 1.6, Cross-Chapter Box 1.4, 4.2, 4.3, 4.6, 6.6, 6.7, Cross-Chapter Box 7.1, Atlas.2.1}

Climate change projections with climate models require information about future emissions or concentrations of greenhouse gases, aerosols, ozone-depleting substances, and land use over time (Figure TS.4). This information can be provided by scenarios, which are internally consistent projections of these quantities based on assumptions of how socio-economic systems could evolve over the 21st century. Emissions from natural sources, such as the ocean and

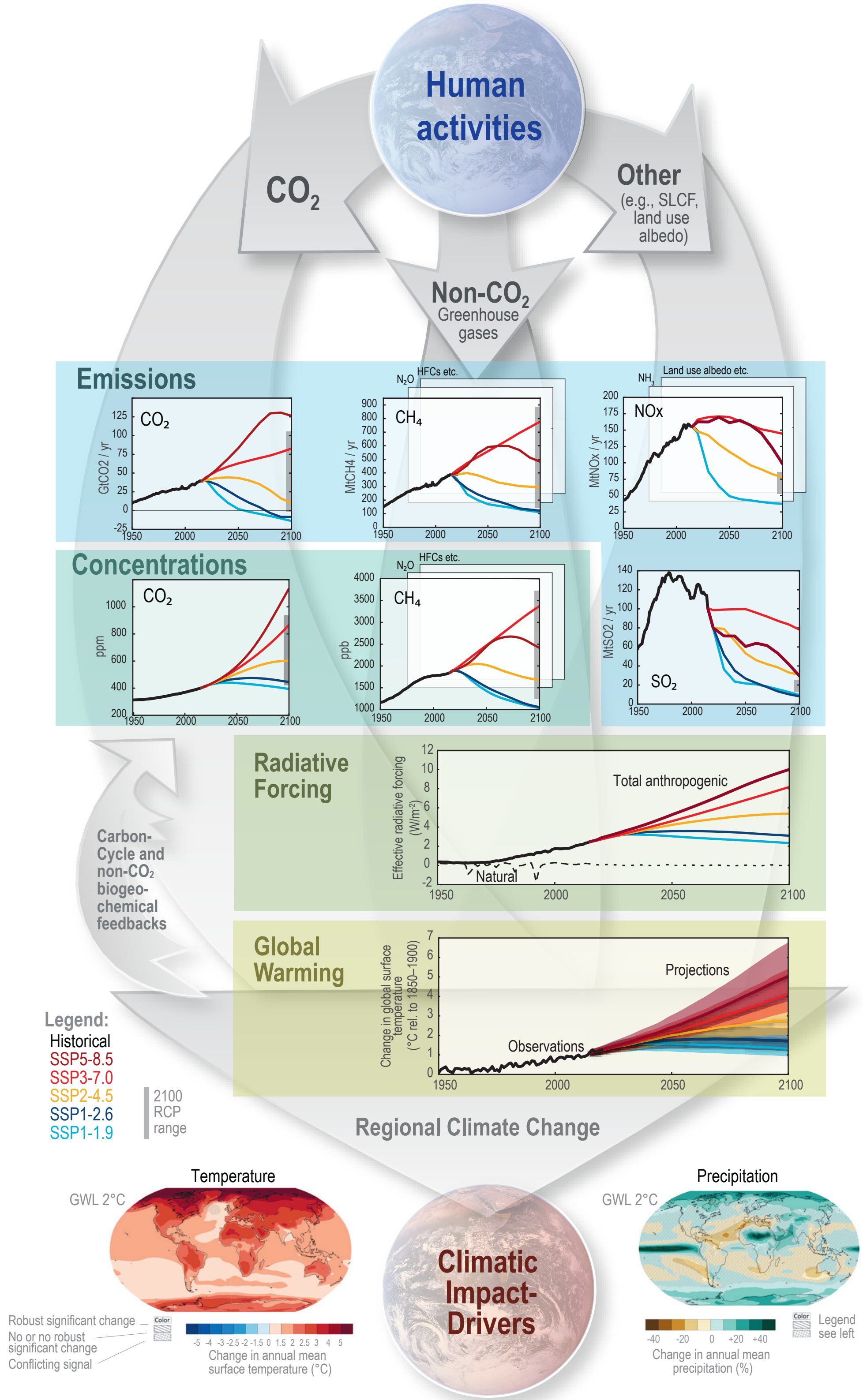

Figure TS.4 | The climate change cause–effect chain: *The intent of this figure is to illustrate the process chain starting from anthropogenic emissions, to changes in atmospheric concentration, to changes in Earth's energy balance ('forcing'), to changes in global climate and ultimately regional climate and climatic impact-drivers*. Shown is the core set of five Shared Socio-economic Pathway (SSP) scenarios as well as emissions and concentration ranges for the previous Representative Concentration Pathway (RCP) scenarios in year 2100; carbon dioxide (CO_2) emissions ($GtCO_2$ yr^{-1}), panel top left; methane (CH_4) emissions (middle) and sulphur dioxide (SO_2), nitrogen oxide (NOx) emissions (all in Mt yr^{-1}), top right; concentrations of atmospheric CO_2 (ppm) and CH_4 (ppb), second row left and right; effective radiative forcing for both anthropogenic and natural forcings (W m^{-2}), third row; changes in global surface air temperature (°C) relative to 1850–1900, fourth row; maps of projected temperature change (°C) (left) and changes in annual-mean precipitation (%) (right) at a global warming level (GWL) of 2°C relative to 1850–1900 (see also Figure TS.5), bottom row. Carbon cycle and non-CO_2 biogeochemical feedbacks will also influence the ultimate response to anthropogenic emissions (arrows on the left). {1.6.1, Cross-Chapter Box 1.4, 4.2.2, 4.3.1, 4.6.1, 4.6.2} the land biosphere, are usually assumed to be constant, or to evolve in response to changes in anthropogenic forcings or to projected climate change. Natural forcings, such as past changes in solar irradiance and historical volcanic eruptions, are represented in model simulations covering the historical era. Future simulations assessed in this Report account for projected changes in solar irradiance and for the long-term mean background forcing from volcanoes, but not for individual volcanic eruptions. Scenarios have a long history in IPCC as a method for systematically examining possible futures and following the cause–effect chain: from anthropogenic emissions, to changes in atmospheric concentrations, to changes in Earth's energy balance ('forcing'), to changes in global climate and ultimately regional climate and climatic impact-drivers (Figure TS.4, Section TS.2, Infographic TS.1). {1.5.4, 1.6.1, 4.2.2, 4.4.4, Cross-Chapter Box 4.1, 11.1}

The uncertainty in climate change projections that results from assessing alternative socio-economic futures, the so-called scenario uncertainty, is explored through the use of scenario sets. Designed to span a wide range of possible future conditions, these scenarios do not intend to match how events actually unfold in the future, and they do not account for impacts of climate change on the socio-economic pathways. Besides scenario uncertainty, climate change projections are also subject to climate response uncertainty (i.e., the uncertainty related to our understanding of the key physical processes and structural uncertainties in climate models) and irreducible and intrinsic uncertainties related to internal variability. Depending on the spatial and temporal scales of the projection, and on the variable of interest, the relative importance of these different uncertainties may vary substantially. {1.4.3, 1.6, 4.2.5, Box 4.1, 8.5.1}

Scenarios in AR6 cover a broader range of emissions futures than considered in AR5, including high CO_2 emissions scenarios without climate change mitigation as well as a low CO_2 emissions scenario reaching net zero CO_2 emissions (see Core Concepts Box) around mid-century. In this Report, a core set of five illustrative scenarios is used to explore climate change over the 21st century and beyond (Section TS.2). They are labelled SSP1-1.9, SSP1-2.6, SSP2-4.5, SSP3-7.0, and SSP5-8.5[17] and span a wide range of radiative forcing levels in 2100. They start in 2015 and include scenarios with high and very high GHG emissions and CO_2 emissions that roughly double from current levels by 2100 and 2050, respectively (SSP3-7.0 and SSP5-8.5); scenarios with intermediate GHG emissions and CO_2 emissions remaining around current levels until the middle of the century (SSP2-4.5); and scenarios with very low and low GHG emissions and CO_2 emissions declining to net zero around or after 2050, followed by varying levels of net negative CO_2 emissions (SSP1-1.9 and SSP1-2.6). These SSP scenarios offer unprecedented detail of input data for ESM simulations and allow for a more comprehensive assessment of climate drivers and responses, in particular because some aspects, such as the temporal evolution of pollutants, emissions or changes in land use and land cover, span a broader range in the SSP scenarios than in the RCPs used in AR5. Modelling studies utilizing the RCPs complement the assessment based on SSP scenarios, for example, at the regional scale (Section TS.4). Scenario extensions are based on assumptions about the post-2100 evolution of emissions or of radiative forcing that are independent from the modelling of socio-economic dynamics, which does not extend beyond 2100. To explore specific dimensions, such as air pollution or temporary overshoot of a given warming level, scenario variants are used in addition to the core set. {1.6.1, Cross-Chapter Box 1.4, 4.2.2, 4.2.6, 4.7.1, Cross-Chapter Box 7.1}

SSP1-1.9 represents the low end of future emissions pathways, leading to warming below 1.5°C in 2100 and limited temperature overshoot of 1.5°C over the course of the 21st century (see Figure TS.6). At the opposite end of the range, SSP5-8.5 represents the very high warming end of future emissions pathways from the literature. SSP3-7.0 has overall lower GHG emissions than SSP5-8.5 but, for example, CO_2 emissions still almost double by 2100 compared to today's levels. SSP2-4.5 and SSP1-2.6 represent scenarios with stronger climate change mitigation and thus lower GHG emissions. SSP1-2.6 was designed to limit warming to below 2°C. Infographic TS.1 presents a narrative depiction of SSP-related climate futures. No likelihood is attached to the scenarios assessed in this Report, and the feasibility of specific scenarios in relation to current trends is best informed by the WGIII contribution to AR6. In the scenario literature, the plausibility of some scenarios with high CO_2 emissions, such as RCP8.5 or SSP5-8.5, has been debated in light of recent developments in the energy sector. However, climate projections from these scenarios can still be valuable because the concentration levels reached in RCP8.5 or SSP5-8.5 and corresponding simulated climate futures cannot be ruled out. That is because of uncertainty in carbon-cycle feedbacks which, in nominally lower emissions trajectories, can result in projected concentrations that are higher than the central concentration levels typically used to drive model projections. {1.6.1; Cross-Chapter Box 1.4; 4.2.2, 5.4; SROCC; Chapter 3 in WGIII}

The socio-economic narratives underlying SSP-based scenarios differ in their assumed level of air pollution control. Together with variations in climate change mitigation stringency, this difference strongly affects anthropogenic emissions trajectories of SLCFs, some of which are also air pollutants. SSP1 and SSP5 assume strong pollution control, projecting a decline of global emissions of ozone precursors (except methane; CH_4) and of aerosols and most of their precursors in the mid- to long term. The reductions due to air pollution controls are further strengthened in scenarios that assume a marked decarbonization, such as SSP1-1.9 or SSP1-2.6. SSP2-4.5 is a medium pollution-control scenario with air pollutant emissions following current trends, and SSP3-7.0 is a weak pollution-control scenario with strong increases in emissions of air pollutants over the 21st century. Methane emissions in SSP-based scenarios vary with the overall climate change mitigation stringency, declining rapidly in SSP1-1.9 and SSP1-2.6 but declining only after 2070 in SSP5-8.5. SSP trajectories span a wider range of air pollutant emissions than considered in the RCP scenarios (see Figure TS.4), reflecting the potential for large regional differences in their assumed pollution

17 Throughout this Report, scenarios are referred to as SSPx-y, where "SSPx" refers to the Shared Socio-economic Pathway or "SSP" describing the socio-economic trends underlying the scenario, and "y" refers to the approximate target level of radiative forcing (in W m^{-2}) resulting from the scenario in the year 2100.

policies. Their effects on climate and air pollution are assessed in Box TS.7. {4.4.4, 6.6.1, Figure 6.4, 6.7.1, Figure 6.19}

Since the RCPs are also labelled by the level of radiative forcing they reach in 2100, they can in principle be related to the core set of AR6 scenarios (Figure TS.4). However, the RCPs and SSP-based scenarios are not directly comparable. First, the gas-to-gas compositions differ; for example, the SSP5-8.5 scenario has higher CO_2 but lower CH_4 concentrations compared to RCP8.5. Second, the projected 21st-century trajectories may differ, even if they result in the same radiative forcing by 2100. Third, the overall effective radiative forcing (see Core Concepts Box) may differ, and tends to be higher for the SSPs compared to RCPs that share the same nominal stratospheric-temperature-adjusted radiative forcing label. Comparing the differences between CMIP5 and CMIP6 projections (Cross-Section Box TS.1) that were driven by RCPs and SSP-based scenarios, respectively, indicates that about half of the difference in simulated warming arises because of higher climate sensitivity being more prevalent in CMIP6 model versions; the remainder arises from higher ERF in nominally corresponding scenarios (e.g., RCP8.5 and SSP5-8.5; *medium confidence*) (see Section TS.1.2.2). In SSP1-2.6 and SSP2-4.5, changes in ERF also explain about half of the changes in the range of warming (*medium confidence*). For SSP5-8.5, higher climate sensitivity is the primary reason behind the upper end of the CMIP6-projected warming being higher than for RCP8.5 in CMIP5 (*medium confidence*). Note that AR6 uses multiple lines of evidence beyond CMIP6 results to assess global surface temperature under various scenarios (see Cross-Section Box TS.1 for the detailed assessment). {1.6, 4.2.2, 4.6.2.2, Cross-Chapter Box 7.1}

Earth system models can be driven by anthropogenic CO_2 emissions ('emissions-driven' runs), in which case atmospheric CO_2 concentration is a projected variable; or by prescribed time-varying atmospheric concentrations ('concentration-driven' runs). In emissions-driven runs, changes in climate feed back on the carbon cycle and interactively modify the projected CO_2 concentration in each ESM, thus adding the uncertainty in the carbon cycle response to climate change to the projections. Concentration-driven simulations are based on a central estimate of carbon cycle feedbacks, while emissions-driven simulations help quantify the role of feedback uncertainty. The differences in the few ESMs for which both emissions and concentration-driven runs were available for the same scenario are small and do not affect the assessment of global surface temperature projections discussed in Cross-Section Box TS.1 and Section TS.2 (*high confidence*). By the end of the 21st century, emissions-driven simulations are on average around 0.1°C cooler than concentration-driven runs, reflecting the generally lower CO_2 concentrations simulated by the emissions-driven ESMs, and have a spread about 0.1°C greater, reflecting the range of simulated CO_2 concentrations. However, these carbon cycle–climate feedbacks do affect the transient climate response to cumulative CO_2 emissions (TCRE[18]), and their quantification is crucial for the assessment of remaining carbon budgets consistent with global warming levels simulated by ESMs (see Section TS.3). {1.6.1, Cross-Chapter Box 1.4, 4.2, 4.3.1, 5.4.5, Cross-Chapter Box 7.1}

TS.1.3.2 Global Warming Levels and Cumulative CO_2 Emissions

Quantifying geographical response patterns of climate change at various global warming levels (GWLs), such as 1.5°C or 2°C above the 1850–1900 period, is useful for characterizing changes in mean climate, extremes and climatic impact-drivers. Global warming levels are used in this Report as a dimension of integration independent of the timing when the warming level is reached and of the emissions scenario that led to the warming. For many climate variables the response pattern for a given GWL is consistent across different scenarios. However, this is not the case for slowly responding processes, such as ice-sheet and glacier mass loss, deep ocean warming, and the related sea level rise. The response of these variables depends on the time it takes to reach the GWL, differs if the warming is reached in a transient warming state or after a temporary overshoot of the warming level, and will continue to evolve, over centuries to millennia, even after global warming has stabilized. Different GWLs correspond closely to specific cumulative CO_2 emissions due to their near-linear relationship with global surface temperature. This Report uses 1.0°C, 1.5°C, 2.0°C, 3.0°C and 4.0°C above 1850–1900 conditions as a primary set of GWLs. {1.6.2, 4.2.4, 4.6.1, 5.5, Cross-Chapter Box 11.1, Cross-chapter Box 12.1}

For many indicators of climate change, such as seasonal and annual mean and extreme surface air temperatures and precipitation, the geographical patterns of changes are well estimated by the level of global surface warming, independently of the details of the emissions pathways that caused the warming, or the time at which the level of warming is attained. GWLs, defined as a global surface temperature increase of, for example, 1.5°C or 2°C relative to the mean of 1850–1900, are therefore a useful way to integrate climate information independently of specific scenarios or time periods. {1.6.2, 4.2.4, 4.6.1, 11.2.4, Cross-Chapter Box 11.1}

The use of GWLs allows disentangling the contribution of changes in global warming from regional aspects of the climate response, as scenario differences in response patterns at a given GWL are often smaller than model uncertainty and internal variability. The relationship between the GWL and response patterns is often linear, but integration of information can also be done for non-linear changes, like the frequency of heat extremes. The requirement is that the relationship to the GWL is broadly independent of the scenario and relative contribution of radiative forcing agents. {1.6, 11.2.4, Cross-Chapter Box 11.1}

The GWL approach to integration of climate information also has some limitations. Variables that are quick to respond to warming, like temperature and precipitation, including extremes, sea ice area, permafrost and snow cover, show little scenario dependence for a given GWL, whereas slow-responding variables such as glacier and ice-sheet mass, warming of the deep ocean and their contributions to sea level rise, have substantial dependency on the trajectory of

18 The transient surface temperature change per unit of cumulative CO_2 emissions, usually 1000 GtC.

warming taken to reach the GWL. A given GWL can also be reached for different balances between anthropogenic forcing agents, such as long-lived greenhouse gas and SLCF emissions, and the response patterns may depend on this balance. Finally, there is a difference in the response even for temperature-related variables if a GWL is reached in a rapidly warming transient state or in an equilibrium state when the land–sea warming contrast is less pronounced. In this Report, the climate responses at different GWLs are calculated based on climate model projections for the 21st century (see Figure TS.5), which are mostly not in equilibrium. The SSP1-1.9 scenario allows assessing the response to a GWL of about 1.5°C after a (relatively) short-term stabilization by the end of the 21st century. {4.6.2, 9.3.1.1, 9.5.2.3, 9.5.3.3, 11.2.4, Cross-Chapter Box 11.1, Cross-Chapter Box 12.1}

Global warming levels are highly relevant as a dimension of integration across scientific disciplines and socio-economic actors and are motivated by the long-term goal in the Paris Agreement of 'holding the increase in the global average temperature to well below 2°C above pre-industrial levels and to pursue efforts to limit the temperature increase to 1.5°C above pre-industrial levels'. The evolution of aggregated impacts with temperature levels has also been widely used and embedded in the WGII assessment. This includes the 'Reasons for Concern' (RFC) and other 'burning ember' diagrams in IPCC WGII. The RFC framework has been further expanded in SR1.5, SROCC and SRCCL by explicitly looking at the differential impacts between half-degree GWLs and the evolution of risk for different socio-economic assumptions. {1.4.4, 1.6.2, 11.2.4, 12.5.2, Cross-Chapter Box 11.1, Cross-Chapter Box 12.1}

SR1.5 concluded that 'climate models project robust differences in regional climate characteristics between present-day and global warming of 1.5°C, and between 1.5°C and 2°C'. This Report adopts a set of common GWLs across which climate projections, impacts, adaptation challenges and climate change mitigation challenges can be integrated, within and across the three Working Groups, relative to 1850–1900. The core set of GWLs in this Report are 1.0°C (close to present day conditions), 1.5°C, 2.0°C, 3.0°C and 4.0°C. {1.4, 1.6.2, Cross-Chapter Box 1.2, Table 1.5, Cross-Chapter Box 11.1}

Connecting Scenarios and Global Warming Levels

In this Report, scenario-based climate projections are translated into GWLs by aggregating the ESM model response at specific GWLs across scenarios (see Figure TS.5 and Figure TS.6). The climate response pattern for the 20-year period around when individual simulations reach a given GWL are averaged across all models and scenarios that reach that GWL. The best estimate and *likely* range of the timing of when a certain GWL is reached under a particular scenario (or 'GWL-crossing time'), however, is based not only on CMIP6 output, but on a combined assessment taking into account the observed warming to date, CMIP6 output and additional lines of evidence (see Cross-Section Box TS.1). {4.3.4, Cross-Chapter Box 11.1, Atlas.2, Interactive Atlas}

Global warming levels are closely related to cumulative CO_2 (and in some cases CO_2-equivalent) emissions. This Report confirms the assessment of the WGI contribution to AR5 and SR1.5 that a near-linear relationship exists between cumulative CO_2 emissions and the

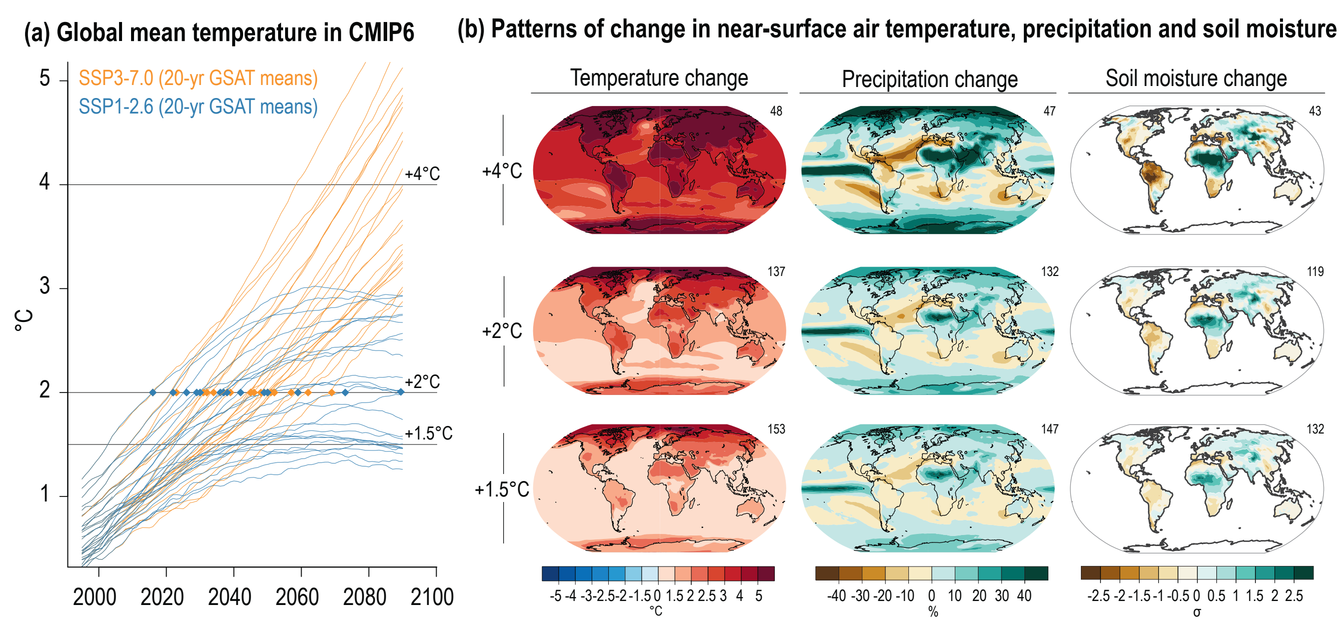

Figure TS.5 | Scenarios, global warming levels, and patterns of change. *The intent of this figure is to show how scenarios are linked to global warming levels (GWLs) and to provide examples of the evolution of patterns of change with global warming levels.* **(a)** Illustrative example of GWLs defined as global surface temperature response to anthropogenic emissions in unconstrained Coupled Model Intercomparison Project Phase 6 (CMIP6) simulations, for two illustrative scenarios (SSP1-2.6 and SSP3-7.0). The time when a given simulation reaches a GWL, for example, +2°C, relative to 1850–1900 is taken as the time when the central year of a 20-year running mean first reaches that level of warming. See the dots for +2°C, and how not all simulations reach all levels of warming. The assessment of the timing when a GWL is reached takes into account additional lines of evidence and is discussed in Cross-Section Box TS.1. **(b)** Multi-model, multi-simulation average response patterns of change in near-surface air temperature, precipitation (expressed as percentage change) and soil moisture (expressed in standard deviations of interannual variability) for three GWLs. The number to the top right of the panels shows the number of model simulations averaged across including all models that reach the corresponding GWL in any of the five Shared Socio-economic Pathways (SSPs). See Section TS.2 for discussion. {Cross-Chapter Box 11.1} resulting increase in global surface temperature (Section TS.3.2). This implies that continued CO_2 emissions will cause further warming and associated changes in all components of the climate system. For declining cumulative CO_2 emissions (i.e., if negative net emissions are achieved), the relationship is less strong for some components, such as the hydrological cycle. The WGI report uses cumulative CO_2 emissions to compare climate response across scenarios and provides a link to the emissions pathways assessment in WGIII. The advantage of using cumulative CO_2 emissions is that it is an inherent emissions scenario characteristic rather than an outcome of the scenario-based projections, where uncertainties in the cause–effect chain from emissions to temperature change are important (Figure TS.4), for example, the uncertainty in ERF and TCR. Cumulative CO_2 emissions can also provide a link to the assessments of mitigation options. Cumulative CO_2 emissions do not carry information about non-CO_2 emissions, although these can be included with specific emissions metrics to estimate CO_2-equivalent emissions. (Section TS.3.3) {1.3.2, 1.6, 4.6.2, 5.5, 7.6}

TS.1.4 From Global to Regional Climate Information for Impact and Risk Assessment

The AR6 WGI Report has an expanded focus on regional information supported by the increased availability of coordinated regional climate model ensemble projections and improvements in the sophistication and resolution of global and regional climate models (*high confidence*). Multiple lines of evidence can be used to construct climate information on a global to regional scale and can be further distilled in a co-production process to meet user needs (*high confidence*). To better support risk assessment, a common risk framework across all three Working Groups has been implemented in AR6, and low-likelihood but high-impact outcomes are explicitly addressed in WGI by using physical climate storylines (see Core Concepts Box).

Climatic impact-drivers are physical climate system conditions (e.g., means, events, extremes) that affect an element of society or ecosystems. They are the WGI contribution to the risk framing without anticipating whether their impact provides potential opportunities or is detrimental (i.e., as for hazards). Many global and regional climatic impact-drivers have a direct relation to global warming levels (*high confidence*). {1.4.4, 1.5.2–1.5.4, Cross-Chapter Box 1.3, 4.8, 10.1, 10.5.1, Box 10.2, Cross-Chapter Box 10.3, 11.2.4, 11.9, Box 11.2, Cross-Chapter Box 11.1, 12.1–12.3, 12.6, Cross-Chapter Boxes 12.1 and 12.2, Atlas.1.3.3–1.3.4, Atlas.1.4, Atlas.1.4.4}

Climate change is a global phenomenon, but manifests differently in different regions. The impacts of climate change are generally experienced at local, national and regional scales, and these are also the scales at which decisions are typically made. Robust climate change information is increasingly available at regional scales for impact and risk assessments. Depending on the climate information context, geographical regions in AR6 may refer to larger areas, such as sub-continents and oceanic regions, or to typological regions, such as monsoon regions, coastlines, mountain ranges or cities, as used in Section TS.4. A new set of standard AR6 WGI reference regions has also been included in this Report (Figure TS.6, bottom panels). {1.4.5, 10.1, 11.9, 12.1–12.4, Atlas.1.3.3–1.3.4}

Global and regional climate models are important sources of climate information at the regional scale. Since AR5, a more comprehensive assessment of past and future evolution of a range of climate variables on a regional scale has been enabled by the increased availability of coordinated ensemble regional climate model projections and improvements in the level of sophistication and resolution of global and regional climate models. This has been complemented by observational, attribution and sectoral-vulnerability studies informing, for instance, about impact-relevant tolerance thresholds. {10.3.3, 11.9, 12.1, 12.3, 12.6, Atlas.3–Atlas.11}

Multiple lines of evidence derived from observations, model simulations and other approaches can be used to construct climate information on a regional scale as described in detail in Sections TS.4.1.1 and TS.4.1.2. Depending on the phenomena and specific context, these sources and methodologies include theoretical understanding of the relevant processes, drivers and feedbacks of climate at regional scale; trends in observed data from multiple datasets; and the attribution of these trends to specific drivers. Furthermore, simulations from different model types (including global and regional climate models, emulators, statistical downscaling methods, etc.) and experiments (e.g., CMIP, CORDEX, and large ensembles of single-model simulations with different initial conditions), attribution methodologies and other relevant local knowledge (e.g., indigenous knowledge) are utilized (see Box TS.11). {1.5.3, 1.5.4, Cross-Chapter Box 7.1, 10.2–10.6, 11.2, Atlas.1.4, Cross-Chapter Box 10.3}

From the multiple lines of evidence, climate information can be distilled in a co-production process that involves users, related stakeholders and producers of climate information, considering the specific context of the question at stake, the underlying values and the challenge of communicating across different communities. The co-production process is an essential part of climate services, which are discussed in Section TS.4.1.2. {10.5, 12.6, Cross-Chapter Box 12.2}

With the aim of informing decision-making at local or regional scales, a common risk framework has been implemented in AR6. Methodologies have been developed to construct more impact- and risk-relevant climate change information tailored to regions and stakeholders. Physical storyline approaches are used in order to build climate information based on multiple lines of evidence, and which can explicitly address physically plausible, but low-likelihood, high-impact outcomes and uncertainties related to climate variability for consideration in risk assessments (Figure TS.6). {Cross-Chapter Box 1.3, 4.8, Box 9.4, 10.5, Box 10.2, Box 11.2, 12.1–12.3, 12.6, Glossary}

The climatic impact-driver framework developed in AR6 supports an assessment of changing climate conditions that are relevant for sectoral impacts and risk assessment. Climatic impact-drivers (CIDs) are physical climate system conditions (e.g., means, extremes,

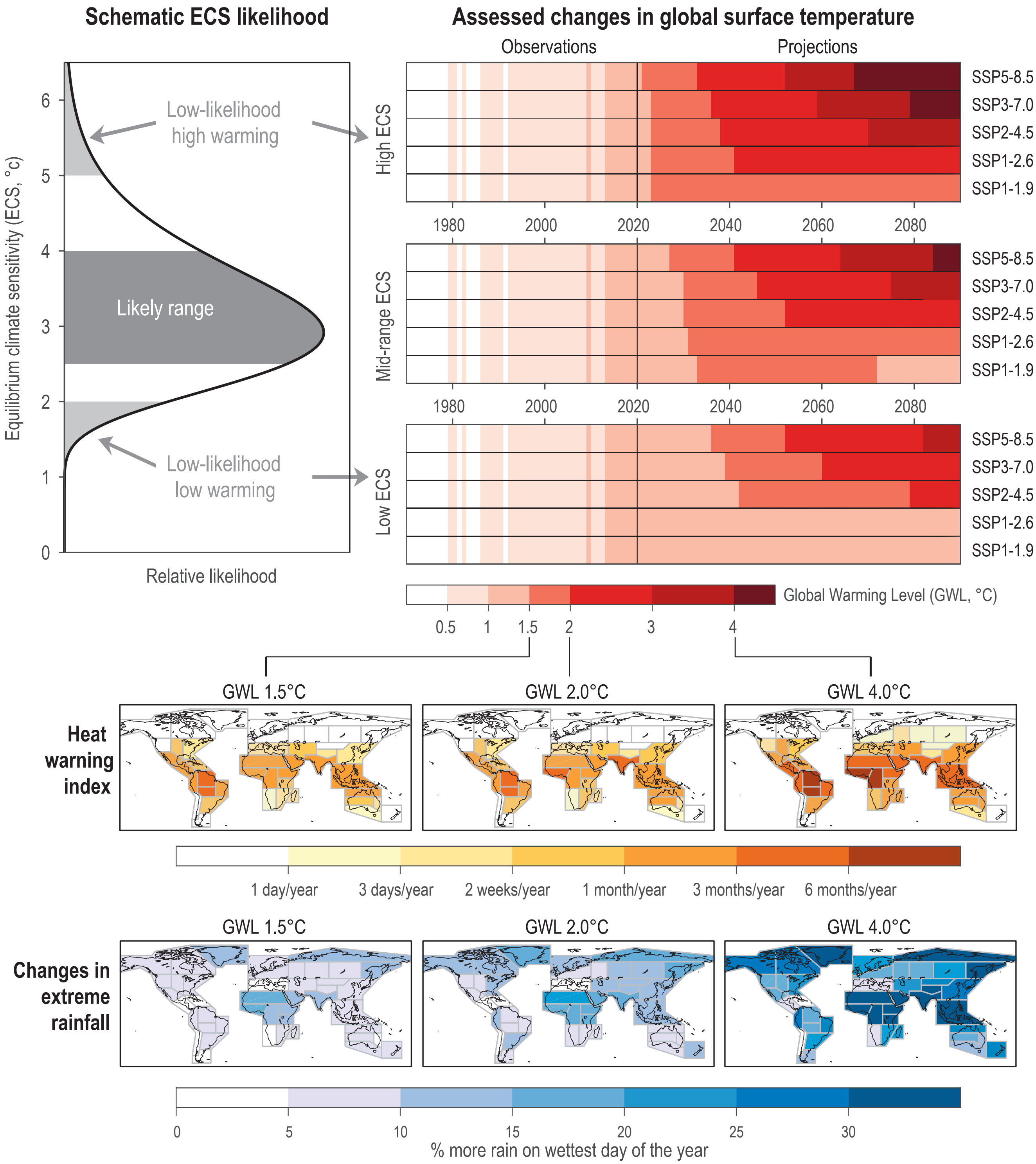

Figure TS.6 | A graphical abstract for key aspects of the Technical Summary. *The intent of this figure is to summarize many different aspects of the Technical Summary related to observed and projected changes in global temperature and associated regional changes in climatic impact-drivers relevant for impact and risk assessment.* **Top left:** a schematic representation of the likelihood for equilibrium climate sensitivity (ECS), consistent with the AR6 assessment (see Chapter 7 and Section TS.3). ECS values above 5°C and below 2°C are termed low-likelihood, high warming (LLHW) and low-likelihood, low warming, respectively (Box TS.3). **Top right:** Observed (see Cross-Section Box TS.1) and projected global surface temperature changes, shown as global warming levels (GWLs) relative to 1850–1900, using the assessed 95% (top), 50% (middle) and 5% (bottom) likelihood time series (see Chapter 4 and Section TS.2). **Bottom panels** show maps of Coupled Model Intercomparison Project Phase 6 (CMIP6) median projections of two climatic impact-drivers (CIDs, see Section TS.1.4) at three different GWLs (columns for 1.5, 2 and 4°C) for the AR6 land regions (see Chapters 1, 10, and Atlas and Section TS.4). The heat warning index is the number of days per year averaged across each region at which a heat warning for human health at level 'danger' would be issued according to the U.S. National Oceanic and Atmospheric Administration (NOAA) (NOAA HI41, see Chapter 12 and Annex VI). The maps of extreme rainfall changes show the percentage change in the amount of rain falling on the wettest day of a year (Rx1day, relative to 1995–2014, see Chapter 11) averaged across each region when the respective GWL is reached. Additional CIDs are discussed in Section TS.4. {1.4.4, Box 4.1, 7.5, 11.4.3, 12.4} events) that affect an element of society or ecosystems and are thus a potential priority for providing climate information. For instance, the heat index used by the U.S. National Oceanic and Atmospheric Administration (NOAA HI) for issuing heat warnings is a CID index that can be associated with adverse human health impacts due to heat stress (see Figure TS.6). Depending on system tolerance, CIDs and their changes can be detrimental (i.e., hazards in the risk framing), beneficial, neutral, or a mixture of each across interacting system elements, regions and sectors (aligning with WGII Sectoral Chapters 2–8). Each sector is affected by multiple CIDs, and each CID affects multiple sectors. Climate change has already altered CID profiles and resulted in shifting magnitude, frequency, duration, seasonality and spatial extent of associated indices (*high confidence*) (see regional details in Section TS.4.3). {12.1–12.4, Table 12.1, Table 12.2, Annex VI}

Many global- and regional-scale CIDs, including extremes, have a direct relation to global warming levels (GWLs) and can thus inform the hazard component of 'Representative Key Risks' and 'Reasons for Concern' assessed by AR6 WGII. These include heat, cold, wet and dry hazards, both mean and extremes; cryospheric hazards (snow cover, ice extent, permafrost) and oceanic hazards (marine heatwaves) (*high confidence*) (Figure TS.6). Establishing links between specific GWLs with tipping points and irreversible behaviour is challenging due to model uncertainties and lack of observations, but their occurrence cannot be excluded, and their likelihood of occurrence generally increases at greater warming levels (Box TS.1, Section TS.9). {11.2.4, Box 11.2, Cross-Chapter Boxes 11.1 and 12.1}

Cross-Section Box TS.1: Global Surface Temperature Change

This box synthesizes the outcomes of the assessment of past, current and future global surface temperature. Global mean surface temperature (GMST) and global surface air temperature (GSAT) are the two primary metrics of global surface temperature used to estimate global warming in IPCC reports. GMST merges sea surface temperature (SST) over the ocean and 2 m air temperature over land and sea ice areas and is used in most paleo, historical and present-day observational estimates. The GSAT metric is 2 m air temperature over all surfaces and is the diagnostic generally used from climate models. Changes in GMST and GSAT over time differ by at most 10% in either direction (*high confidence*), but conflicting lines of evidence from models and direct observations, combined with limitations in theoretical understanding, lead to *low confidence* in the sign of any difference in long-term trend. Therefore, long-term changes in GMST/GSAT are presently assessed to be identical, with expanded uncertainty in GSAT estimates. Hence the term global surface temperature is used in reference to both quantities in the text of the TS and SPM. {Cross-Chapter Box 2.3}

Global surface temperature has increased by 0.99 [0.84 to 1.10] °C from 1850–1900 to the first two decades of the 21st century (2001–2020) and by 1.09 [0.95 to 1.20] °C from 1850–1900 to 2011–2020. Temperatures as high as during the most recent decade (2011–2020) exceed the warmest centennial-scale range reconstructed for the present interglacial, around 6500 years ago [0.2°C to 1°C] (*medium confidence*). The next most recent warm period was about 125,000 years ago during the last interglacial when the multi-centennial temperature range [0.5°C to 1.5°C] encompasses the 2011–2020 values (*medium confidence*). The *likely* range of human-induced change in global surface temperature in 2010–2019 relative to 1850–1900 is 0.8°C to 1.3°C, with a central estimate of 1.07°C, encompassing the best estimate of observed warming for that period, which is 1.06°C with a *very likely* range of [0.88°C to 1.21°C], while the *likely* range of the change attributable to natural forcing is only –0.1°C to +0.1°C.

Compared to 1850–1900, average global surface temperature over the period 2081–2100 is *very likely* to be higher by [1.0°C to 1.8°C] in the low CO_2 emissions scenario SSP1-1.9 and by [3.3°C to 5.7°C] in the high CO_2 emissions scenario SSP5-8.5. In all scenarios assessed here except SSP5-8.5, the central estimate of 20-year averaged global surface warming crossing the 1.5°C level lies in the early 2030s, which is in the early part of the *likely* range (2030–2052) assessed in SR1.5. It is *more likely than not* that under SSP1-1.9, global surface temperature relative to 1850–1900 will remain below 1.6°C throughout the 21st century, implying a potential temporary overshoot of 1.5°C global warming of no more than 0.1°C. Global surface temperature in any individual year could exceed 1.5°C relative to 1850–1900 by 2030 with a likelihood between 40% and 60% across the scenarios considered here (*medium confidence*). A 2°C increase in global surface temperature relative to 1850–1900 will be crossed under SSP5-8.5 but is *extremely unlikely* to be crossed under SSP1-1.9. Periods of reduced and increased global surface temperature trends at decadal time scales will continue to occur in the 21st century (*very high confidence*). The effect of strong mitigation on 20-year global surface temperature trends would be *likely* to emerge during the near term (2021–2040), assuming no major volcanic eruptions occur. (Figure TS.8, Cross-Section Box TS.1, Figure 1) {2.3, 3.3, 4.3, 4.4, 4.5, 4.6, 7.3}

Surface Temperature History

Dataset innovations, particularly more comprehensive representation of polar regions, and the availability of new datasets have led to an assessment of increased global surface temperature change relative to the directly equivalent estimates reported in AR5. The contribution of changes in observational understanding alone between AR5 and AR6 in assessing temperature changes from 1850–1900

Cross-Section Box TS.1 (continued)

to 1986–2005 is estimated at 0.08 [–0.01 to 0.12] °C. Global surface temperature increased from 1850–1900 to 1995–2014 by 0.85 [0.69 to 0.95] °C, between 1850–1900 and the first two decades of the 21st century (2001–2020) by 0.99 [0.84 to 1.20] °C, and to the most recent decade (2011–2020) by 1.09 [0.95 to 1.20] °C. Each of the last four decades has in turn been warmer than any decade that preceded it since 1850. Temperatures have increased faster over land than over the ocean since 1850–1900, with warming to 2011–2020 of 1.59 [1.34 to 1.83] °C over land and 0.88 [0.68 to 1.01] °C over the ocean. {2.3.1, Cross-Chapter Box 2.3}

Global surface temperature during the period 1850–1900 is used as an approximation for pre-industrial conditions for consistency with AR5 and AR6 Special Reports, whilst recognizing that radiative forcings have a baseline of 1750 for the start of anthropogenic influences. It is *likely* that there was a net anthropogenic forcing of 0.0–0.3 Wm^{-2} in 1850–1900 relative to 1750 (*medium confidence*), and from the period around 1750 to 1850–1900, there was a change in global surface temperature of around 0.1°C (*likely* range –0.1 to +0.3°C, *medium confidence*), with an anthropogenic component of 0.0°C to 0.2°C (*likely* range, *medium confidence*). {Cross-Chapter Box 1.2, 7.3.5}

Global surface temperature has evolved over geological time (Figure TS.1, Box TS.2). Beginning approximately 6500 years ago, global surface temperature generally decreased, culminating in the coldest multi-century interval of the post-glacial period (since roughly 7000 years ago), which occurred between around 1450 and 1850 (*high confidence*). Over the last 50 years, global surface temperature has increased at an observed rate unprecedented in at least the last two thousand years (*high confidence*). Temperatures as high as during the most recent decade (2011–2020) exceed the warmest centennial-scale range reconstructed for the present interglacial, around 6500 years ago [0.2°C to 1°C] (*medium confidence*). The next most recent warm period was about 125,000 years ago during the Last Interglacial when the multi-centennial temperature range [0.5°C to 1.5°C] encompasses the 2011–2020 values (*medium confidence*) (Cross-Section Box TS.1, Figure 1). During the mid-Pliocene Warm Period, around 3.3–3.0 million years ago, global surface temperature was 2.5°C to 4°C warmer (*medium confidence*). {2.3.1, Cross-Chapter Box 2.1 and 2.4}

Current Warming

There is *very high confidence* that the CMIP6 model ensemble reproduces observed global surface temperature trends and variability since 1850 with errors small enough to allow for detection and attribution of human-induced warming. The CMIP6 multi-model mean global surface warming between 1850–1900 and 2010–2019 is close to the best estimate of observed warming, though some CMIP6 models simulate a warming that is outside the assessed *very likely* observed range. {3.3.1}

The *likely* range of human-induced change in global surface temperature in 2010–2019 relative to 1850–1900 is 0.8°C to 1.3°C, with a central estimate of 1.07°C (Figure Cross-Section Box TS.1, Figure 1), encompassing the best estimate of observed warming for that period, which is 1.06°C with a *very likely* range of [0.88°C to 1.21°C], while the *likely* range of the change attributable to natural forcing is only –0.1°C to +0.1°C. This assessment is consistent with an estimate of the human-induced global surface temperature rise based on assessed ranges of perturbations to the top of the atmosphere (effective radiative forcing) and with metrics of feedbacks of the climate response (equilibrium climate sensitivity and the transient climate response). Over the same period, well-mixed greenhouse gas forcing *likely* warmed global surface temperature by 1.0°C to 2.0°C, while aerosols and other anthropogenic forcings *likely* cooled global surface temperature by 0.0°C to 0.8°C. {2.3.1, 3.3.1, 7.3.5, Cross-Chapter Box 7.1}

The observed slower increase in global surface temperature (relative to preceding and following periods) in the 1998–2012 period, sometimes referred to as 'the hiatus', was temporary (*very high confidence*). The increase in global surface temperature during the 1998–2012 period is also greater in the data sets used in the AR6 assessment than in those available at the time of AR5. Using these updated observational data sets and a like-for-like consistent comparison of simulated and observed global surface temperature, all observed estimates of the 1998–2012 trend lie within the *very likely* range of CMIP6 trends. Furthermore, the heating of the climate system continued during this period, as reflected in the continued warming of the global ocean (*very high confidence*) and in the continued rise of hot extremes over land (*medium confidence*). Since 2012, global surface temperature has risen strongly, with the past five years (2016–2020) being the hottest five-year period between 1850 and 2020 (*high confidence*). {2.3.1, 3.3.1, 3.5.1, Cross-Chapter Box 3.1}

Future Changes in Global Surface Temperature

The AR6 assessment of future change in global surface temperature is, for the first time in an IPCC report, explicitly constructed by combining new projections for the SSP scenarios with observational constraints based on past simulated warming as well as the AR6-updated assessment of equilibrium climate sensitivity and transient climate response. In addition, climate forecasts initialized from the observed climate state have been used for the period 2019–2028. The inclusion of additional lines of evidence has reduced the assessed uncertainty ranges for each scenario (Cross-Section Box TS.1, Figure 1). {4.3.1, 4.3.4, Box 4.1, 7.5}

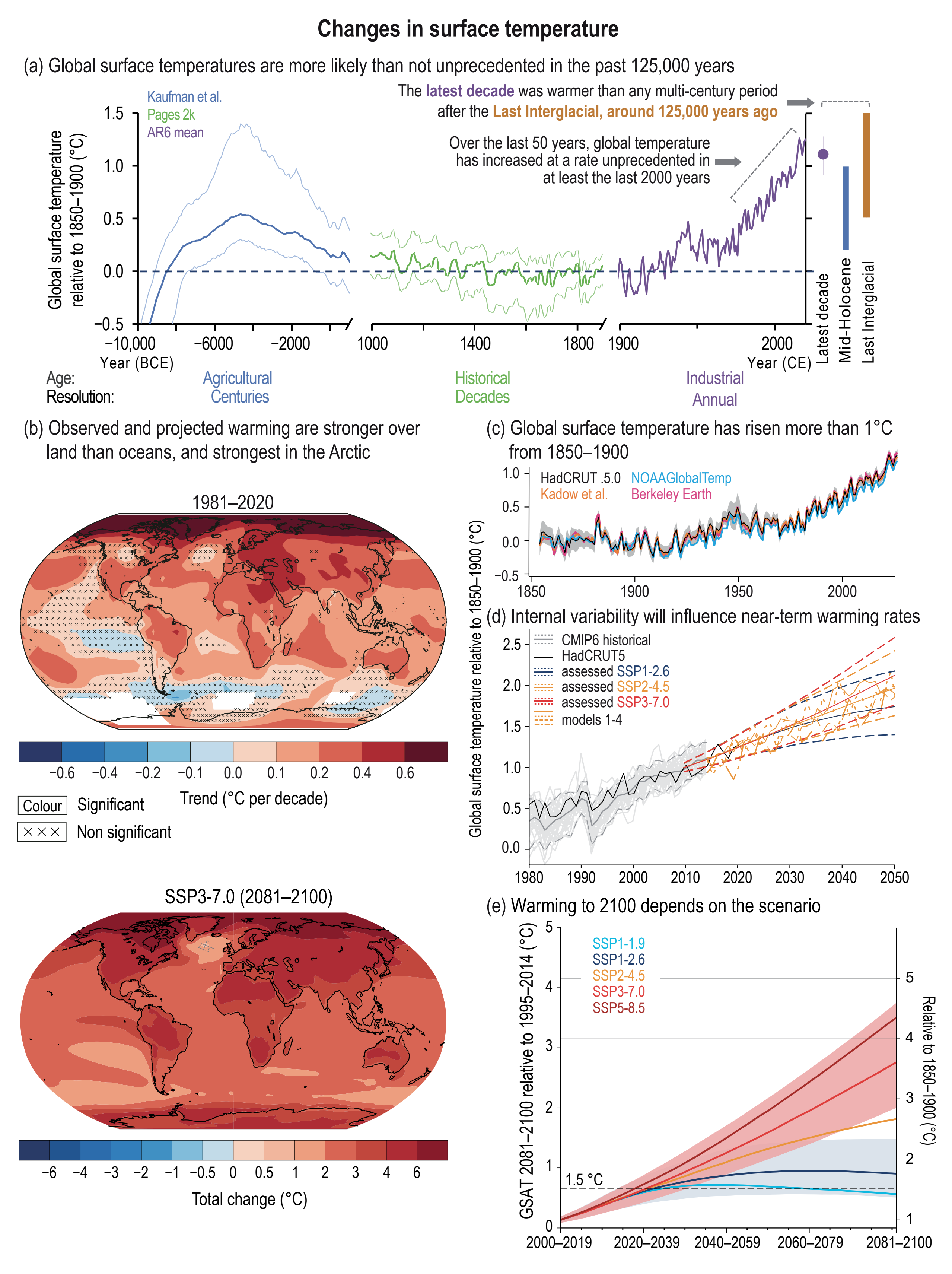

Cross-Section Box TS.1, Figure 1 | Earth's surface temperature history and future with key findings annotated within each panel.

Cross-Section Box TS.1 (continued)

Cross-Section Box TS.1, Figure 1 (continued): *The intent of this figure is to show global surface temperature observed changes from the Holocene to now, and projected changes.* **(a)** Global surface temperature over the Holocene divided into three time scales: (i) 12,000 to 1000 years ago (10,000 BCE to 1000 CE) in 100-year time steps, (ii) 1000 to 1900 CE, 10-year smooth, and (iii) 1900 to 2020 CE (mean of four datasets in panel c). Bold lines show the median of the multi-method reconstruction, with 5% and 95% percentiles of the ensemble members (thin lines). Vertical bars are 5–95th percentile ranges of estimated global surface temperature for the Last Interglacial and mid-Holocene (*medium confidence*) (Section 2.3.1.1). All temperatures are relative to 1850–1900. **(b)** Spatially resolved trends (°C per decade) for (upper map) HadCRUTv5 over 1981–2020, and (lower map, total change) multi-model mean projected changes from 1995–2014 to 2081–2100 in the SST3-7.0 scenario. Observed trends have been calculated where data are present in both the first and last decade and for at least 70% of all years within the period using ordinary least squares. Significance is assessed with autoregressive AR(1) model correction and denoted by stippling. Hatched areas in the lower map show areas of conflicting model evidence on significance of changes. **(c)** Temperature from instrumental data for 1850–2020, including annually resolved averages for the four global surface temperature datasets assessed in Section 2.3.1.1.3 (see text for references). The grey shading shows the uncertainty associated with the HadCRUTv5 estimate. All temperatures are relative to the 1850–1900 reference period. **(d)** Recent past and 2015–2050 evolution of annual mean global surface temperature change relative to 1850–1900, from HadCRUTv5 (black), Coupled Model Intercomparison Project Phase 6 (CMIP6) historical simulations (up to 2014, in grey, ensemble mean solid, 5% and 95% percentiles dashed, individual models thin), and CMIP6 projections under scenario SSP2-4.5, from four models that have an equilibrium climate sensitivity near the assessed central value (thick yellow). Solid thin coloured lines show the assessed central estimate of 20-year change in global surface temperature for 2015–2050 under three scenarios, and dashed thin coloured lines the corresponding 5% and 95% quantiles. **(e)** Assessed projected change in 20-year running mean global surface temperature for five scenarios (central estimate solid, *very likely* range shaded for SSP1-2.6 and SSP3-7.0), relative to 1995–2014 (left y-axis) and 1850–1900 (right y-axis). The y-axis on the right-hand side is shifted upward by 0.85°C, the central estimate of the observed warming for 1995–2014, relative to 1850–1900. The right y-axis in (e) is the same as the y-axis in (d). {2.3, 4.3, 4.4}

During the near term (2021–2040), a 1.5°C increase in global surface temperature, relative to 1850–1900, is *very likely* to occur in scenario SSP5-8.5, *likely* to occur in scenarios SSP2-4.5 and SSP3-7.0, and *more likely than not* to occur in scenarios SSP1-1.9 and SSP1-2.6. The time of crossing a warming level is defined here as the midpoint of the first 20-year period during which the average global surface temperature exceeds the level. In all scenarios assessed here except SSP5-8.5, the central estimate of crossing the 1.5°C level lies in the early 2030s. This is in the early part of the *likely* range (2030–2052) assessed in SR1.5, which assumed continuation of the then-current warming rate; this rate has been confirmed in the AR6. Roughly half of this difference arises from a larger historical warming diagnosed in AR6. The other half arises because for central estimates of climate sensitivity, most scenarios show stronger warming over the near term than was estimated as 'current' in SR1.5 (*medium confidence*). When considering scenarios similar to SSP1-1.9 instead of linear extrapolation, the SR1.5 estimate of when 1.5°C global warming is crossed is close to the central estimate reported here. (Cross-Section Box TS.1, Table 1) {2.3.1, Cross-Chapter Box 2.3, 3.3.1, 4.3.4, Box 4.1}

It is *more likely than not* that under SSP1-1.9, global surface temperature relative to 1850–1900 will remain below 1.6°C throughout the 21st century, implying a potential temporary overshoot of 1.5°C global warming of no more than 0.1°C. If climate sensitivity lies near the lower end of the assessed *very likely* range, crossing the 1.5°C warming level is avoided in scenarios SSP1-1.9 and SSP1-2.6 (*medium confidence*). Global surface temperature in any individual year, in contrast to the 20-year average, could by 2030 exceed 1.5°C relative to 1850–1900 with a likelihood between 40% and 60%, across the scenarios considered here (*medium confidence*). (Cross-Section Box TS.1, Table 1) {4.3.4, 4.4.1, Box 4.1, 7.5}

During the 21st century, a 2°C increase in global surface temperature relative to 1850–1900 will be crossed under SSP5-8.5 and SSP3-7.0, is *extremely likely* to be crossed under SSP2-4.5, but is *unlikely* to be crossed under SSP1-2.6 and *extremely unlikely* to be crossed under SSP1-1.9. For the mid-term period 2041–2060, this 2°C global warming level is *very likely* to be crossed under SSP5-8.5, *likely* to be crossed under SSP3-7.0, and *more likely than not* to be crossed under SSP2-4.5. (Cross-Section Box TS.1, Table 1) {4.3.4}

Events of reduced and increased global surface temperature trends at decadal time scales will continue to occur in the 21st century but will not affect the centennial-scale warming (*very high confidence*). If strong mitigation is applied from 2020 onward as reflected in SSP1-1.9, its effect on 20-year trends in global surface temperature would *likely* emerge during the near term (2021–2040), measured against an assumed non-mitigation scenario such as SSP3-7.0 or SSP5-8.5. All statements about crossing the 1.5°C level assume that no major volcanic eruption occurs during the near term (Cross-Section Box TS.1, Table 1). {2.3.1, Cross-Chapter Box 2.3, 4.3.4, 4.4.1, 4.6.3, Box 4.1}

Compared to 1850–1900, average global surface temperature over the period 2081–2100 is *very likely* to be higher by [1.0°C to 1.8°C] in the low CO_2 emissions scenario SSP1-1.9 and by [3.3°C to 5.7°C] in the high CO_2 emissions scenario SSP5-8.5. For the scenarios SSP1-2.6, SSP2-4.5, and SSP3-7.0, the corresponding *very likely* ranges are [1.3°C to 2.4°C], [2.1°C to 3.5°C], and [2.8°C to 4.6°C], respectively. The uncertainty ranges for the period 2081–2100 continue to be dominated by the uncertainty in equilibrium climate sensitivity and transient climate response (*very high confidence*) (Cross-Section Box TS.1, Table 1). {4.3.1, 4.3.4, 4.4.1, 7.5}

The CMIP6 models project a wider range of global surface temperature change than the assessed range (*high confidence*); furthermore, the CMIP6 global surface temperature increase tends to be larger than that in CMIP5 (*very high confidence*). {4.3.1, 4.3.4, 4.6.2, 7.5.6}

Cross-Section Box TS.1 (continued)

Cross-Section Box TS.1, Table 1 | Assessment results for 20-year averaged change in global surface temperature based on multiple lines of evidence. The change is displayed in °C relative to the 1850–1900 reference period for selected time periods (first three rows), and as the first 20-year period during which the average global surface temperature change exceeds the specified level relative to the period 1850–1900 (last four rows). The entries give both the central estimate and, in parentheses, the *very likely* (5–95%) range. An entry n.c. means that the global warming level is not crossed during the period 2021–2100.

	SSP1-1.9	SSP1-2.6	SSP2-4.5	SSP3-7.0	SSP5-8.5
Near term, 2021–2040	1.5 [1.2 to 1.7]	1.5 [1.2 to 1.8]	1.5 [1.2 to 1.8]	1.5 [1.2 to 1.8]	1.6 [1.3 to 1.9]
Mid-term, 2041–2060	1.6 [1.2 to 2.0]	1.7 [1.3 to 2.2]	2.0 [1.6 to 2.5]	2.1 [1.7 to 2.6]	2.4 [1.9 to 3.0]
Long term, 2081–2100	1.4 [1.0 to 1.8]	1.8 [1.3 to 2.4]	2.7 [2.1 to 3.5]	3.6 [2.8 to 4.6]	4.4 [3.3 to 5.7]
1.5°C	2025–2044 [2013–2032 to n.c.]	2023–2042 [2012–2031 to n.c.]	2021–2040 [2012–2031 to 2037–2056]	2021–2040 [2013–2032 to 2033–2052]	2018–2037 [2011–2030 to 2029–2048]
2°C	n.c. [n.c. to n.c.]	n.c. [2031–2050 to n.c.]	2043–2062 [2028–2047 to 2075–2094]	2037–2056 [2026–2045 to 2053–2072]	2032–2051 [2023–2042 to 2044–2063]
3°C	n.c. [n.c. to n.c.]	n.c. [n.c. to n.c.]	n.c. [2061–2080 to n.c.]	2066–2085 [2050–2069 to n.c.]	2055–2074 [2042–2061 to 2074–2093]
4°C	n.c. [n.c. to n.c.]	n.c. [n.c. to n.c.]	n.c. [n.c. to n.c.]	n.c. [2070–2089 to n.c.]	2075–2094 [2058–2077 to n.c.]

TS.2 Large-scale Climate Change: Mean Climate, Variability and Extremes

This section summarizes knowledge about observed and projected large-scale climate change (including variability and extremes), drivers and attribution of observed changes to human activities. It describes observed and projected large-scale changes associated with major components of the climate system: atmosphere, ocean (including sea level change), land, biosphere and cryosphere, and the carbon, energy and water cycles. In each subsection, reconstructed past changes, observed and attributed recent changes, and projected near- and long-term changes to mean climate, variability and extremes are presented, where possible, in an integrated way. See Section TS.1.3.1 for information on the scenarios used for projections.

TS.2.1 Changes Across the Global Climate System

In addition to global surface temperature (Cross-Section Box TS.1), a wide range of indicators across all components of the climate system are changing rapidly (Figure TS.7), with many at levels unseen in millennia. The observed changes provide a coherent picture of a warming world, many aspects of which have now been formally attributed to human influence, and human influence on the atmosphere, ocean, and land components of the climate system, taken together, is assessed as unequivocal for the first time in an IPCC assessment report (Table TS.1, Figure TS.7).

It is *virtually certain* that global surface temperature rise and associated changes can be limited through rapid and substantial reductions in global GHG emissions. Continued GHG emissions greatly increase the likelihood of potentially irreversible changes in the global climate system (Box TS.9), in particular with respect to the contribution of ice sheets to global sea level change (*high confidence*). {2.3, 3.8, 4.3, 4.6, 4.7, 7.2–7.4, Cross-Chapter Box 7.1, 9.2–9.6}

Earth system model simulations of the historical period since 1850 are only able to reproduce the observed changes in key climate indicators when anthropogenic forcings are included (Figure TS.7). Taken together with numerous formal attribution studies across an even broader range of indicators and theoretical understanding, this underpins the unequivocal attribution of observed warming of the atmosphere, ocean, and land to human influence (Table TS.1). {2.3, 3.8}

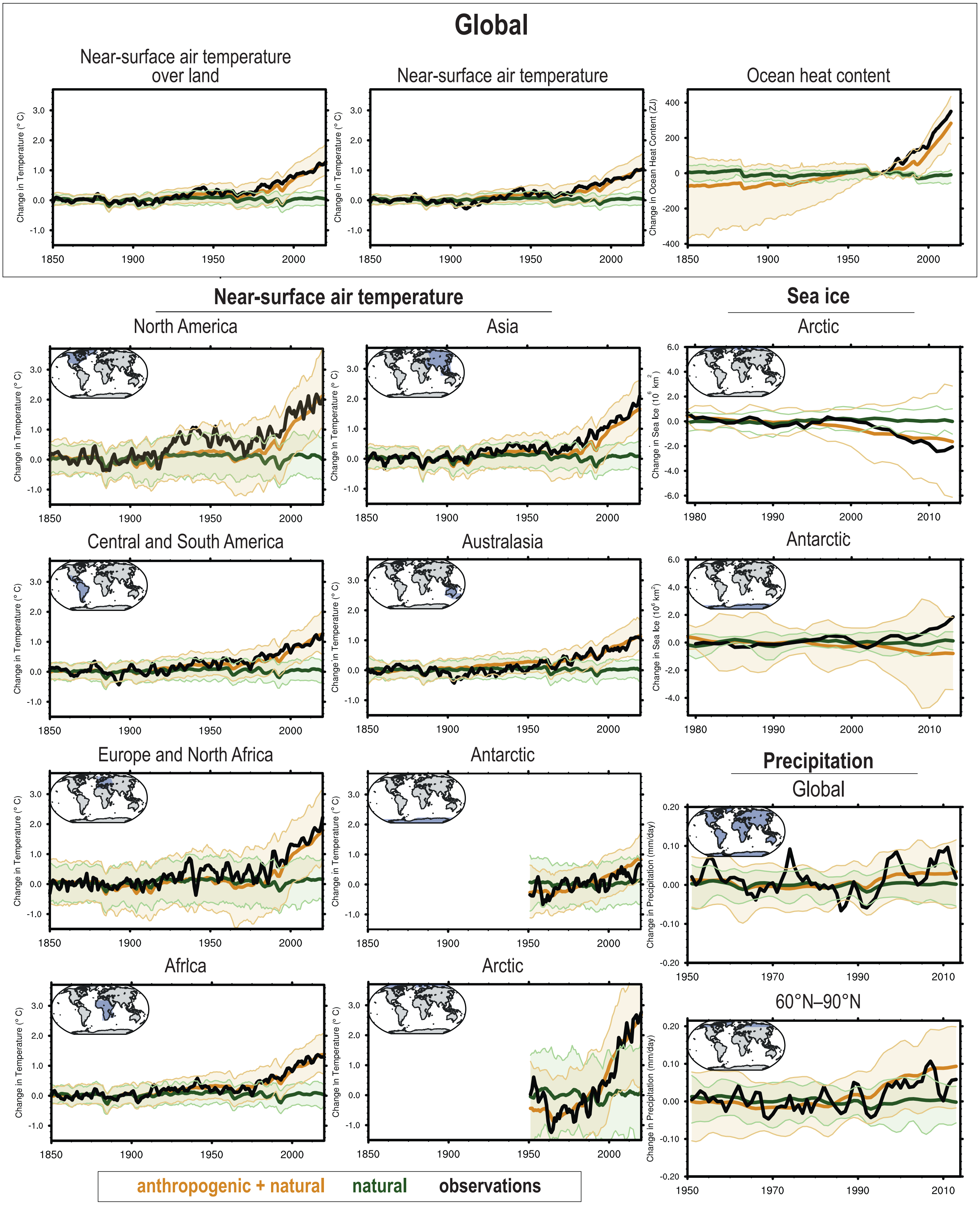

Figure TS.7 | Simulated and observed changes compared to the 1850–1900 average in key large-scale indicators of climate change across the climate system, for continents, ocean basins and globally up to 2014. *The intent of this figure is to compare the observed and simulated changes over the historical period for a range of variables and regions, with and without anthropogenic forcings, for attribution.* Black lines show observations, orange lines and shading show the multi-model mean and 5–95th percentile ranges for Coupled Model Intercomparison Project Phase 6 (CMIP6) historical simulations including anthropogenic and natural forcing, and green lines and shading show corresponding ensemble means and 5–95th percentile ranges for CMIP6 natural-only simulations. Observations after 2014 (including, for example, a strong subsequent decrease of Antarctic sea ice area that leads to no significant overall trend since 1979) are not shown because the CMIP6 historical simulations end in 2014. A 3-year running mean smoothing has been applied to all observational time series. {3.8, Figure 3.41}

Table TS.1 | Assessment of observed changes in large-scale indicators of mean climate across climate system components and their attribution to human influence. The colour coding indicates the assessed confidence in/likelihood of the human contribution as a driver or main driver[19] (main driver is specified in that case) where available (see colour key). Otherwise, explanatory text is provided in cells with white background. The relevant chapter section with more detailed information is listed in each table cell.

Change in Indicator	Observed Change Assessment	Human Contribution Assessment
Atmosphere and Water Cycle		
Warming of global mean surface air temperature since 1850–1900	{2.3.1, Cross-Chapter Box 2.3}	*Likely* range of human contribution (0.8°C–1.3°C) encompasses observed warming (0.9°C–1.2°C) {3.3.1}
Warming of the troposphere since 1979	{2.3.1}	Main driver {3.3.1}
Cooling of the lower stratosphere	Since mid-20th century {2.3.1}	Main driver 1979–mid-1990s {3.3.1}
Large-scale precipitation and upper troposphere humidity changes since 1979	{2.3.1}	{3.3.2, 3.3.3}
Expansion of the zonal mean Hadley Circulation since the 1980s	{2.3.1}	Southern Hemisphere {3.3.3}
Ocean		
Ocean heat content increase since the 1970s	{2.3.3, 2.3.4, 9.2.1, Cross-Chapter Box 9.1}	Main driver {3.5.1}
Salinity changes since the mid-20th century	{2.3.3, 2.3.4, 9.2.2}	{3.5.2}
Global mean sea level rise since 1971	{2.3.3, 9.6.1}	Main driver {3.5.3}
Cryosphere		
Arctic sea ice loss since 1979	{2.3.2, 9.3.1}	Main driver {3.4.1}
Reduction in Northern Hemisphere spring snow cover since 1950	{2.3.2, 9.5.3}	{3.4.2}
Greenland Ice Sheet mass loss since 1990s	{2.3.2, 9.4.1}	{3.4.3}
Antarctic Ice Sheet mass loss since 1990s	{2.3.2, 9.4.2}	*Limited evidence* and *medium agreement* {3.4.3}
Retreat of glaciers	{2.3.2, 9.5.1}	Main driver {3.4.3}
Carbon Cycle		
Increased amplitude of the seasonal cycle of atmospheric CO_2 since the early 1960s	{2.3.4}	Main driver {3.6.1}
Acidification of the global surface ocean	{SROCC, 5.3.2, Cross-Chapter Box 5.3}	Main driver {3.6.2}
Land Climate (Extremes, see Table TS.12)		
Mean 2 m land warming since 1850–1900 (about 40% larger than global mean warming)	{2.3.1}	Main driver {3.3.1}
Synthesis		
Warming of the global climate system since pre-industrial times	{2.3.5}	{3.8.1}

See text description | *medium confidence* | *likely/high confidence* | *very likely* | *extremely likely* | *virtually certain* | *fact*

Future climate change across a range of atmospheric, cryospheric, oceanic and biospheric indicators depends upon future emissions pathways. Outcomes for a broad range of indicators increasingly diverge through the 21st century across the different SSPs (Section TS.1.3.1, Figure TS.8). Due to the slow response of the deep ocean and ice sheets, this divergence continues long after 2100, and 21st century emissions choices will have implications for GMSL rise for centuries to millennia. Furthermore, it is *likely* that at least one large volcanic eruption will occur during the 21st century. Such an eruption would reduce global surface temperature for several years, decrease land precipitation, alter monsoon circulation and modify extreme precipitation, at both global and regional scales. {4.3, 4.7, 9.4, 9.6, Cross-Chapter Box 4.1}

19 Throughout this Technical Summary, 'main driver' means responsible for more than 50% of the change.

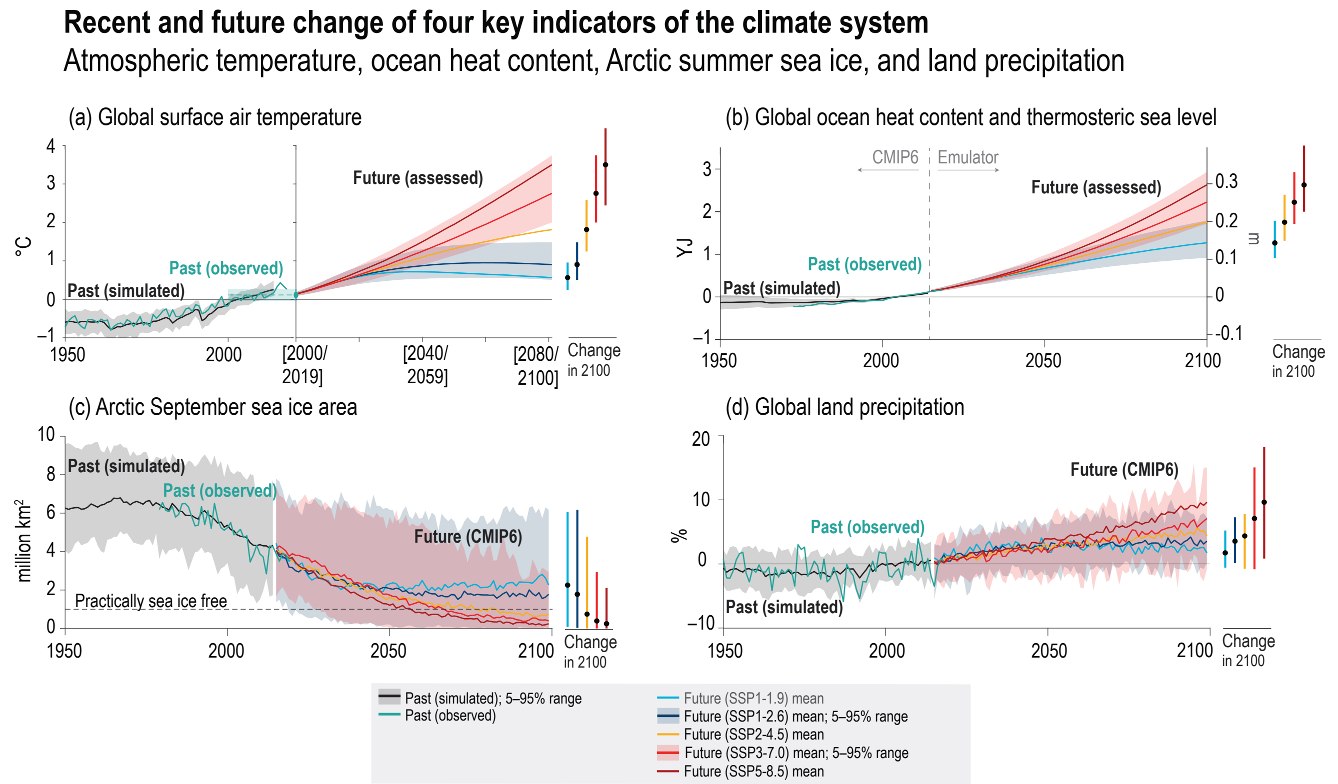

Figure TS.8 | Observed, simulated and projected changes compared to the 1995–2014 average in four key indicators of the climate system through to 2100 differentiated by Shared Socio-economic Pathway (SSP) scenario. *The intent of this figure is to show how future emissions choices impact key, iconic large-scale indicators and to highlight that our collective choices matter.* Past simulations are based on the Coupled Model Intercomparison Project Phase 6 (CMIP6) multi-model ensemble. Future projections are based on the assessed ranges based upon multiple lines of evidence for **(a)** global surface temperature (Cross-Section Box TS.1) and **(b)** global ocean heat content and the associated thermosteric sea level contribution to global mean sea level change (right-hand axis) using a climate model emulator (Cross-Chapter Box 7.1), and CMIP6 simulations for **(c)** Arctic September sea ice and **(d)** global land precipitation. Projections for SSP1-1.9 and SSP1-2.6 show that reduced greenhouse gas emissions lead to a stabilization of global surface temperature, Arctic sea ice area and global land precipitation over the 21st century. Projections for SSP1-2.6 show that emissions reductions have the potential to substantially reduce the increase in ocean heat content and thermosteric sea level rise over the 21st century but that some increase is unavoidable. The brackets in the x axis in panel (a) indicate assessed 20-year-mean periods. {4.3, Figure 4.2, 9.3, 9.6, Figure 9.6}

Observational records show changes in a wide range of climate extremes that have been linked to human influence on the climate system (Table TS.2). In many cases, the frequency and intensity of future changes in extremes can be directly linked to the magnitude of future projected warming. Changes in extremes have been widespread over land since the 1950s, including a *virtually certain* global increase in extreme air temperatures and a *likely* intensification in global-scale extreme precipitation. It is *extremely likely* that human influence is the main contributor to the observed increase (decrease) in the likelihood and severity of hot (cold) extremes (Table TS.2). The frequency of extreme temperature and precipitation events in the current climate will change with warming, with warm extremes becoming more frequent (*virtually certain*), cold extremes becoming less frequent (*extremely likely*) and precipitation extremes becoming more frequent in most locations (*very likely*). {9.6.4, 11.2, 11.3, 11.4, 11.6, 11.7, 11.8, 11.9, Box 9.2}

Table TS.2 | Summary table on observed changes in extremes, their attribution since 1950 (except where stated otherwise), and projected changes at +1.5°C, +2°C and +4°C of global warming, on global and continental scales. An increase in warm/hot extremes refers to warmer and/or more frequent hot days and nights and warm spells/heatwaves, over most land areas. A decrease in cold extremes refers to warmer and/or fewer cold days and nights and cold spells/cold waves, over most land areas. Drought events are relative to a predominant fraction of land area. For tropical cyclones, observed changes and attribution refer to Categories 3–5, while projected changes refer to Categories 4–5. Tables 11.1 and 11.2 are more detailed versions of this table, containing, in particular, information on regional scales. In general, higher warming levels also imply stronger projected changes for indicators where the confidence level does not depend on the warming level and the table does not explicitly quantify the global sensitivity. See also Box TS.10. {9.6, Box 9.2, 11.3, 11.7}

Change in Indicator	Observed (since 1950)	Attributed (since 1950)	Projected at GWL (°C)		
			+1.5	+2	+4
Warm/hot extremes: Frequency or intensity	↑	✓ Main driver	↑	↑	↑
Cold extremes: Frequency or intensity	↓	✓ Main driver	↓	↓	↓
Heavy precipitation events: Frequency, intensity and/or amount	↑ Over majority of land regions with good observational coverage	✓ Main driver of the observed intensification of heavy precipitation in land regions	↑ in most land regions	↑	↑ in most land regions
Agricultural and ecological droughts: Intensity and/or frequency	↑ in some regions	✓ in some regions	↑ in more regions compared to observed changes	↑ in more regions compared to 1.5°C of global warming	↑ in more regions compared to 2°C of global warming
Precipitation associated with tropical cyclones	↑	✓	↑ Rate +11%	↑ Rate +14%	↑ Rate +28%
Tropical cyclones: Proportion of intense cyclones	↑	✓	↑ +10%	↑ +13%	↑ +20%
Compound events: Co-occurrent heatwaves and droughts	↑ (Frequency)	✓ (Frequency)	↑ (Frequency and intensity increases with warming)		
Marine heatwaves: Intensity & frequency	↑ (since 1900)	✓ (since 2006)	↑ Strongest in tropical and Arctic Ocean		
Extreme sea levels: Frequency	↑ (since 1960)	✓	↑ (Scenario-based assessment for 21st century)		

medium confidence *likely/high confidence* *very likely* *extremely likely* *virtually certain*

TS.2.2 Changes in the Drivers of the Climate System

Since 1750, changes in the drivers of the climate system are dominated by the warming influence of increases in atmospheric GHG concentrations and a cooling influence from aerosols, both resulting from human activities. In comparison there has been negligible long-term influence from solar activity and volcanoes. Concentrations of CO_2, methane (CH_4), and nitrous oxide (N_2O) have increased to levels unprecedented in at least 800,000 years, and there is *high confidence* that current CO_2 concentrations have not been experienced for at least 2 million years. Global mean concentrations of anthropogenic aerosols peaked in the late 20th century and have slowly declined since in northern mid-latitudes, although they continue to increase in South Asia and East Africa (*high confidence*).

The total anthropogenic effective radiative forcing (ERF) in 2019, relative to 1750, was 2.72 [1.96 to 3.48] W m^{-2} (*medium confidence*) and has *likely* been growing at an increasing rate since the 1970s. {2.2, 6.4, 7.2, 7.3}

Solar activity since 1900 was high but not exceptional compared to the past 9000 years (*high confidence*). The average magnitude and variability of volcanic aerosols since 1900 has not been unusual compared to at least the past 2500 years (*medium confidence*). However, sporadic strong volcanic eruptions can lead to temporary drops in global surface temperature lasting 2–5 years. {2.2.1, 2.2.2, 2.2.8, Cross-Chapter Box 4.1}

Atmospheric CO_2 concentrations have changed substantially over millions of years (Figure TS.1). Current levels of atmospheric CO_2 have not been experienced for at least 2 million years (*high

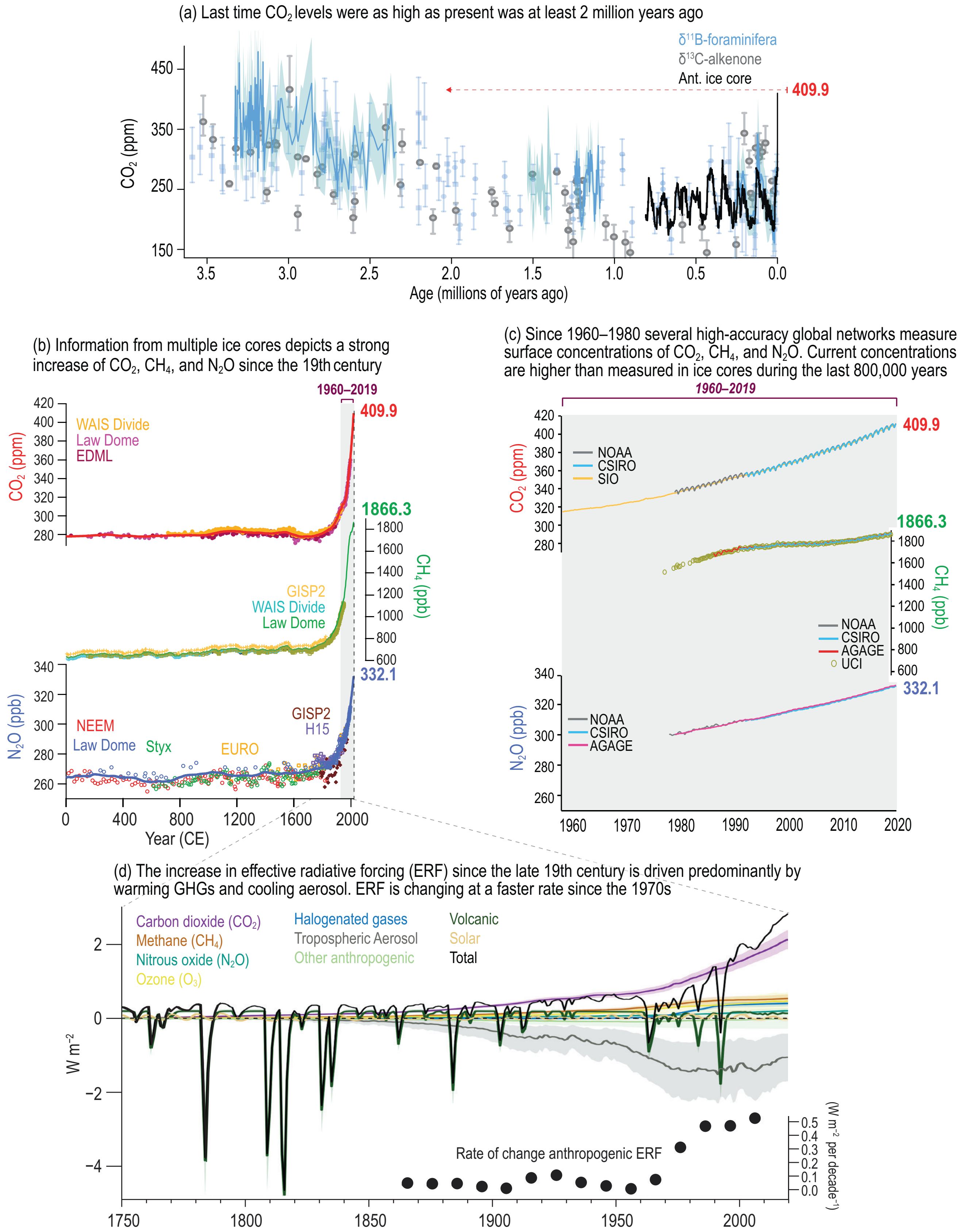

Figure TS.9 | Changes in well-mixed greenhouse gas (WMGHG) concentrations and effective radiative forcing (EFR). *The intent of this figure is to show that the changes of the main drivers of climate system over the industrial period are exceptional in a long-term context.* **(a)** Changes in carbon dioxide (CO_2) from proxy records over the past 3.5 million years. **(b)** Changes in all three WMGHGs from ice core records over the Common Era. **(c)** Directly observed WMGHG changes since the mid-20th century. **(d)** Evolution of ERF and components since 1750. Further details on data sources and processing are available in the associated FAIR data table. {2.2, Figures 2.3, 2.4 and 2.10} *confidence*, Figure TS.9a). Over 1750–2019, CO_2 increased by 131.6 ± 2.9 ppm (47.3%). The centennial rate of change of CO_2 since 1850 has no precedent in at least the past 800,000 years (Figure TS.9), and the fastest rates of change over the last 56 million years were at least a factor of four lower (*low confidence*) than over 1900–2019. Several networks of high-accuracy surface observations show that concentrations of CO_2 have exceeded 400 ppm, reaching 409.9 (± 0.3) ppm in 2019 (Figure TS.9c). The ERF from CO_2 in 2019 (relative to 1750) was 2.16 Wm^{-2}. {2.2.3, 5.1.2, 5.2.1, 7.3}

By 2019, concentrations of CH_4 reached 1866.3 (± 3.3) ppb (Figure TS.9c). The increase since 1750 of 1137 ± 10 ppb (157.8%) far exceeds the range over multiple glacial–interglacial transitions of the past 800,000 years (*high confidence*). In the 1990s, CH_4 concentrations plateaued, but started to increase again around 2007 at an average rate of 7.6 ± 2.7 ppb yr^{-1} (2010–2019; *high confidence*). There is *high confidence* that this recent growth is largely driven by emissions from fossil fuel exploitation, livestock, and waste, with ENSO driving multi-annual variability of wetland and biomass burning emissions. In 2019, ERF from CH_4 was 0.54 Wm^{-2}. {2.2.3, 5.2.2, 7.3}

Since 1750, N_2O increased by 62.0 ± 6.0 ppb, reaching a level of 332.1 (± 0.4) ppb in 2019. The increase since 1750 is of comparable magnitude to glacial–interglacial fluctuations of the past 800,000 years (Figure TS.9c). N_2O concentration trends since 1980 are largely driven by a 30% increase in emissions from the expansion and intensification of global agriculture (*high confidence*). By 2019 its ERF was 0.21 W m^{-2}. {2.2.3, 5.2.3}

Halogenated gases consist of chlorofluorocarbons (CFCs), hydrochlorofluorocarbons (HCFCs), hydrofluorocarbons (HFCs) and other gases, many of which can deplete stratospheric ozone and warm the atmosphere. In response to controls on production and consumption mandated by the Montreal Protocol on Substances that Deplete the Ozone Layer and its amendments, the atmospheric abundances of most CFCs have continued to decline since AR5. Abundances of HFCs, which are replacements for CFCs and HCFCs, are increasing (*high confidence*), though increases of the major HCFCs have slowed in recent years. The ERF from halogenated components in 2019 was 0.41 Wm^{-2}. {2.2.4, 6.3.4, 7.3.2}

Tropospheric aerosols mainly act to cool the climate system, directly by reflecting solar radiation, and indirectly by enhancing cloud reflectance. Ice cores show increases in aerosols across the Northern Hemisphere mid-latitudes since 1700 and reductions since the late 20th century (*high confidence*). Aerosol optical depth (AOD), derived from satellite- and ground-based radiometers, has decreased since 2000 over the mid-latitude continents of both hemispheres, but increased over South Asia and East Africa (*high confidence*). Trends in AOD are more pronounced from sub-micrometre aerosols for which the anthropogenic contribution is particularly large. Global carbonaceous aerosol budgets and trends remain poorly characterized due to limited observations, but black carbon (BC), a warming aerosol component, is declining in several regions of the Northern Hemisphere (*low confidence*). Total aerosol ERF in 2019, relative to 1750, is –1.1 [–1.7 to –0.4] W m^{-2} (*medium confidence*) and *more likely than not* became less negative since the late 20th century, with *low confidence* in the magnitude of post-2014 changes due to conflicting evidence (Section TS.3.1). {2.2.6, 6.2.1, 6.3.5, 6.4.1, 7.3.3}

There is *high confidence* that tropospheric ozone has been increasing from 1750 in response to anthropogenic changes in ozone precursor emissions (nitrogen oxides, carbon monoxide, non-methane volatile organic compounds, and methane), but with *medium confidence* in the magnitude of this change, due to limited observational evidence and knowledge gaps. Since the mid-20th century, tropospheric ozone surface concentrations have increased by 30–70% across the Northern Hemisphere (*medium confidence*); since the mid-1990s, free tropospheric ozone has increased by 2–7% per decade in most northern mid-latitude regions and 2–12% per decade in sampled tropical regions. Future changes in surface ozone concentrations will be primarily driven by changes in precursor emissions rather than climate change (*high confidence*). Stratospheric ozone has declined between 60°S–60°N by 2.2% from 1964–1980 to 2014–2017 (*high confidence*), with the largest declines during 1980–1995. The strongest loss of stratospheric ozone continues to occur in austral spring over Antarctica (ozone hole), with emergent signs of recovery after 2000. The 1750–2019 ERF for total (stratospheric and tropospheric) ozone is 0.47 [0.24 to 0.71] W m^{-2}, which is dominated by tropospheric ozone changes. {2.2.5, 6.3.2, 7.3.2, 7.3.5}

The global mean abundance of hydroxyl (OH) radical, or 'oxidizing capacity', chemically regulates the lifetimes of many SLCFs, and therefore the radiative forcing of CH_4, ozone, secondary aerosols and many halogenated species. Model estimates suggest no significant change in oxidizing capacity from 1850 to 1980 (*low confidence*). Increases of about 9% over 1980–2014 computed by ESMs and carbon cycle models are not confirmed by observationally constrained inverse models, rendering an overall *medium confidence* in stable OH or positive trends since the 1980s, and implying that OH is not the primary driver of recent observed growth in CH_4. {6.3.6, Cross-Chapter Box 5.2}

Land use and land-cover change exert biophysical and biogeochemical effects. There is *medium confidence* that the biophysical effects of land-use change since 1750, most notably the increase in global albedo, have had an overall cooling on climate, whereas biogeochemical effects (i.e., changes in GHG and volatile organic compound emissions or sinks) led to net warming. Overall land-use and land-cover ERF is estimated at –0.2 [–0.3 to –0.1] W m^{-2}. {2.2.7, 7.3.4, SRCCL Section 2.5}

The total anthropogenic ERF in 2019 relative to 1750 was 2.72 [1.96 to 3.48] W m^{-2} (Figure TS.9), dominated by GHGs (positive ERF) and partially offset by aerosols (negative ERF). The rate of change of ERF *likely* has increased since the 1970s, mainly due to growing CO_2 concentrations and less negative aerosol ERF (Section TS.3.1). {2.2.8, 7.3}

TS.2.3 Upper Air Temperatures and Atmospheric Circulation

The effects of human-induced climate change have been clearly identified in observations of atmospheric temperature and some aspects of atmospheric circulation, and these effects are *likely* to intensify in the future. Tropospheric warming and stratospheric cooling are *virtually certain* to continue with continued net emissions of greenhouse gases. Several aspects of the atmospheric circulation have *likely* changed since the mid-20th century, and human influence has *likely* contributed to the observed poleward expansion of the Southern Hemisphere Hadley Cell and *very likely* contributed to the observed poleward shift of the Southern Hemisphere extratropical jet in summer. It is *likely* that the mid-latitude jet will shift poleward and strengthen, accompanied by a strengthening of the storm track in the Southern Hemisphere by 2100 under the high CO_2 emissions scenarios. It is *likely* that the proportion of intense tropical cyclones has increased over the last four decades and that this cannot be explained entirely by natural variability. There is *low confidence* in observed recent changes in the total number of extratropical cyclones over both hemispheres. The proportion of tropical cyclones that are intense is expected to increase (*high confidence*), but the total global number of tropical cyclones is expected to decrease or remain unchanged (*medium confidence*). {2.3, 3.3, 4.3, 4.4, 4.5, 8.3, 8.4, 11.7}

The troposphere has warmed since at least the 1950s, and it is *virtually certain* that the stratosphere has cooled. It is *very likely* that human-induced increases in GHGs were the main driver of tropospheric warming since 1979. It is *extremely likely* that anthropogenic forcing, both from increases in GHG concentrations and depletion of

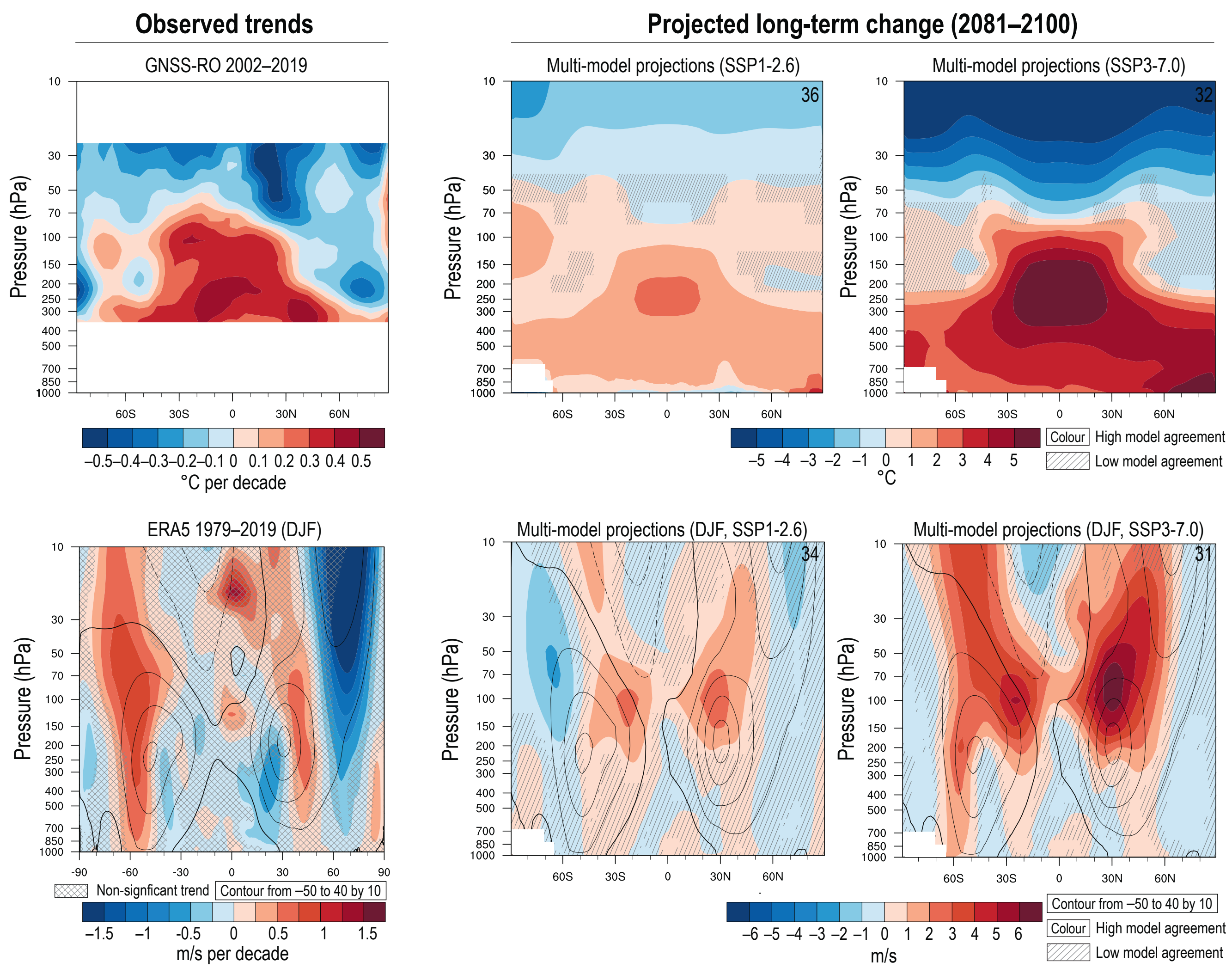

Figure TS.10 | Observed and projected upper air temperature and circulation changes. *The intent of this figure is to visualize upper air temperature and circulation changes and the similarity between observed and projected changes.* **Upper panels: (Left)** Zonal cross-section of temperature trends for 2002–2019 in the upper troposphere region for the ROM SAF radio-occultation dataset. **(Middle)** Change in the annual and zonal mean atmospheric temperature (°C) in 2081–2100 in SSP1-2.6 relative to 1995–2014 for 36 Coupled Model Intercomparison Project Phase 6 (CMIP6) models. **(Right)** the same in SSP3-7.0 for 32 models. **Lower panels: (Left)** Long-term mean (thin black colour) and linear trend (colour) of zonal mean December–January–February (DJF) zonal winds for ERA5. **(Middle)** multi-model mean change in annual and zonal mean wind (m s^{-1}) in 2081–2100 in SSP1-2.6 relative to 1995–2014 based on 34 CMIP6 models. The 1995–2014 climatology is shown in contours with spacing of 10 m s^{-1}. **(Right)** the same for SSP3-7.0 for 31 models. {2.3.1; Figures 2.12 and 2.18; 4.5.1; Figure 4.2.6} stratospheric ozone due to ozone-depleting substances, was the main driver of upper stratospheric cooling since 1979. It is *very likely* that global mean stratospheric cooling will be larger for scenarios with higher atmospheric CO_2 concentrations. In the tropics, since at least 2001 (when new techniques permit more robust quantification), the upper troposphere has warmed faster than the near-surface (*medium confidence*) (Figure TS.10). There is *medium confidence* that most CMIP5 and CMIP6 models overestimate the observed warming in the upper tropical troposphere over the period 1979–2014, in part because they overestimate tropical SST warming. It is *likely* that future tropical upper tropospheric warming will be larger than at the tropical surface. {2.3.1, 3.3.1, 4.5.1}

The Hadley Circulation has *likely* widened since at least the 1980s, predominantly in the Northern Hemisphere, although there is only *medium confidence* in the extent of the changes. This has been accompanied by a strengthening of the Hadley Circulation in the Northern Hemisphere (*medium confidence*). It is *likely* that human influence has contributed to the poleward expansion of the zonal mean Hadley cell in the Southern Hemisphere since the 1980s, which is projected to further expand with global warming (*high confidence*). There is *medium confidence* that the observed poleward expansion in the Northern Hemisphere is within the range of internal variability. {2.3.1, 3.3.3, 8.4.3}

Since the 1970s, near-surface average winds have *likely* weakened over land. Over the ocean, near-surface average winds *likely* strengthened over 1980–2000, but divergent estimates lead to *low confidence* thereafter. Extratropical storm tracks have *likely* shifted poleward since the 1980s. There is *low confidence* in projected poleward shifts of the Northern Hemisphere mid-latitude jet and storm tracks due to large internal variability and structural uncertainty in model simulations. There is *medium confidence* in a projected decrease in the frequency of atmospheric blocking over Greenland and the North Pacific in boreal winter in 2081–2100 under the SSP3-7.0 and SSP5-8.5 scenarios. There is *high confidence* that Southern Hemisphere storm tracks and associated precipitation have migrated polewards over recent decades, especially in the austral summer and autumn, associated with a trend towards more positive phases of the Southern Annular Mode (SAM) (Section TS.4.2.2) and the strengthening and southward shift of the Southern Hemisphere extratropical jet in austral summer. In the long term (2081–2100), the Southern Hemisphere mid-latitude jet is *likely* to shift poleward and strengthen under the SSP5-8.5 scenario relative to 1995–2014, accompanied by an increase in the SAM (Section TS.4.2.2). It is *likely* that wind speeds associated with extratropical cyclones will strengthen in the Southern Hemisphere storm track for SSP5-8.5. There is *low confidence* in the potential role of Arctic warming and sea ice loss on historical or projected mid-latitude atmospheric variability. {2.3.1, 3.3.3, 3.7.2, 4.3.3, 4.4.3, 4.5.1, 4.5.3, 8.2.2, 8.3.2, Cross-Chapter Box 10.1}

It is *likely* that the proportion of major (Category 3–5) tropical cyclones (TCs) and the frequency of rapid TC intensification events have increased over the past four decades. The average location of peak TC wind-intensity has *very likely* migrated poleward in the western North Pacific Ocean since the 1940s, and TC forward translation speed has *likely* slowed over the contiguous USA since 1900. It is *likely* that the poleward migration of TCs in the western North Pacific and the global increase in TC intensity rates cannot be explained entirely by natural variability. There is *high confidence* that average peak TC wind speeds and the proportion of Category 4–5 TCs will increase with warming and that peak winds of the most intense TCs will increase. There is *medium confidence* that the average location where TCs reach their maximum wind-intensity will migrate poleward in the western North Pacific Ocean, while the total global frequency of TC formation will decrease or remain unchanged with increasing global warming. {11.7.1}

There is *low confidence* in observed recent changes in the total number of extratropical cyclones over both hemispheres. There is also *low confidence* in past-century trends in the number and intensity of the strongest extratropical cyclones over the Northern Hemisphere due to the large interannual-to-decadal variability and temporal and spatial heterogeneities in the volume and type of assimilated data in atmospheric reanalyses, particularly before the satellite era. Over the Southern Hemisphere, it is *likely* that the number of extratropical cyclones with low central pressures (<980 hPa) has increased since 1979. The frequency of intense extratropical cyclones is projected to decrease (*medium confidence*). Projected changes in the intensity depend on the resolution of climate models (*medium confidence*). There is *medium confidence* that wind speeds associated with extratropical cyclones will change following changes in the storm tracks. {2.3.1, 3.3.3, 4.5.1, 4.5.3, 8.3.2, 8.4.2, 11.7.2}

Box TS.3 | Low-likelihood, High-warming Storylines

Future global warming exceeding the assessed *very likely* range cannot be ruled out and is potentially associated with the highest risks for society and ecosystems. Such low-likelihood, high-warming storylines tend to exhibit substantially greater changes in the intensity of regional drying and wetting than the multi-model mean. Even at levels of warming within the *very likely* range, global and regional low-likelihood outcomes might occur, such as large precipitation changes, additional sea level rise associated with collapsing ice sheets (see Box TS.4), or abrupt ocean circulation changes. While there is *medium confidence* that the Atlantic Meridional Overturning Circulation (AMOC) will not experience an abrupt collapse before 2100, if it were to occur, it would *very likely* cause abrupt shifts in regional weather patterns and water cycle. The probability of these low-likelihood outcomes increases with higher global warming levels. If the real-world climate sensitivity lies at the high end of the assessed range, then global and regional changes substantially outside the *very likely* range projections occur for a given emissions scenario. With increasing global warming, some very rare extremes and some compound events (multivariate or concurrent extremes) with low likelihood in past and current climate will become more frequent, and there is a higher chance that events unprecedented in the observational record occur (*high confidence*). Finally, low-likelihood, high-impact outcomes may also arise from a series of very large volcanic eruptions that could substantially alter the 21st century climate trajectory compared to SSP-based Earth system model (ESM) projections. {Cross-Chapter Box 4.1, 4.3, 4.4, 4.8, 7.3, 7.4, 7.5, 8.6, 9.2, 9.6, Box 9.4, Box 11.2, Cross-Chapter Box 12.1}

Previous IPCC reports largely focused their assessment on the projected *very likely* range of future surface warming and associated climate change. However, a comprehensive risk assessment also requires considering the potentially larger changes in the physical climate system that are *unlikely* or *very unlikely* but possible and potentially associated with the highest risks for society and ecosystems (Figure TS.6). Since AR5, the development of physical climate storylines of high warming has emerged as a useful approach for exploring the future risk space that lies outside of the IPCC *very likely* range projections. {4.8}

Uncertainty in the true values of equilibrium climate sensitivity (ECS) and transient climate response (TCR) dominate uncertainty in projections of future warming under moderate to strong emissions scenarios (Section TS.3.2). A real-world ECS higher than the assessed *very likely* range (2°C–5°C) would require a strong historical aerosol cooling and/or a trend towards stronger warming from positive feedbacks linked to changes in SST patterns (pattern effects), combined with a strong positive cloud feedback and substantial biases in paleoclimate reconstructions – each of which is assessed as either *unlikely* or *very unlikely*, but not ruled out. Since CMIP6 contains several ESMs that exceed the upper bound of the assessed *very likely* range in future surface warming, these models can be used to develop low-likelihood, high warming storylines to explore risks and vulnerabilities, even in the absence of a quantitative assessment of likelihood. {4.3.4, 4.8, 7.3.2, 7.4.4, 7.5.2, 7.5.5, 7.5.7}

CMIP6 models with surface warming outside, or close to, the upper bound of the *very likely* range exhibit patterns of large widespread temperature and precipitation changes that differ substantially from the multi-model mean in all scenarios. For SSP5-8.5, the high-warming models exhibit widespread warming of more than 6°C over most extratropical land regions and parts of the Amazon. In the Arctic, annual mean temperatures increase by more than 10°C relative to present-day, corresponding to about 30% more than the best estimate of warming. Even for SSP1-2.6, high-warming models show on average 2°C–3°C warming relative to present-day conditions over much of Eurasia and North America (about 40% more than the best estimate of warming) and more than 4°C warming relative to the present over the Arctic in 2081–2100 (Box TS.3, Figure 1). Such a high global warming storyline would imply that the remaining carbon budget consistent with a 2°C warming is smaller than the assessed *very likely* range. Put another way, even if a carbon budget that *likely* limits warming to 2°C is met, a low-likelihood, high-warming storyline would result in warming of 2.5°C or more. {4.8}

CMIP6 models with global warming close to the upper bound of the assessed *very likely* warming range tend to exhibit greater changes in the intensity of regional drying and wetting than the multi-model mean. Furthermore, these model projections show a larger area of drying and tend to show a larger fraction of strong precipitation increases than the multi-model mean. However, regional precipitation changes arise from both thermodynamic and dynamic processes so that the most pronounced global warming levels are not necessarily associated with the strongest precipitation response. Abrupt human-caused changes to the water cycle cannot be ruled out. Positive land surface feedbacks, involving vegetation and dust, can contribute to abrupt changes in aridity, but there is only *low confidence* that such changes will occur during the 21st century. Continued Amazon deforestation, combined with a warming climate, raises the probability that this ecosystem will cross a tipping point into a dry state during the 21st century (*low confidence*). (See also Box TS.9). {4.8, 8.6.2}

Box TS.3 (continued)

While there is *medium confidence* that the projected decline in the AMOC (Section TS.2.4) will not involve an abrupt collapse before 2100, such a collapse might be triggered by an unexpected meltwater influx from the Greenland Ice Sheet. If an AMOC collapse were to occur, it would *very likely* cause abrupt shifts in the regional weather patterns and water cycle, such as a southward shift in the tropical rain belt, and could result in weakening of the African and Asian monsoons, strengthening of Southern Hemisphere monsoons, and drying in Europe. (See also Boxes TS.9 and TS.13). {4.7.2, 8.6.1, 9.2.3}

Very rare extremes and compound or concurrent events, such as the 2018 concurrent heatwaves across the Northern Hemisphere, are often associated with large impacts. The changing climate state is already altering the likelihood of extreme events, such as decadal droughts and extreme sea levels, and will continue to do so under future warming. Compound events and concurrent extremes contribute to increasing probability of low-likelihood, high-impact outcomes and will become more frequent with increasing global warming (*high confidence*). Higher warming levels increase the likelihood of events unprecedented in the observational record. {9.6.4, Box 11.2}

Finally, low likelihood storylines need not necessarily relate solely to the human-induced changes in climate. A low-likelihood, high-impact outcome, consistent with historical precedent in the past 2500 years, would be to see several large volcanic eruptions that could greatly alter the 21st century climate trajectory compared to SSP-based Earth system model projections. {Cross-Chapter Box 4.1}

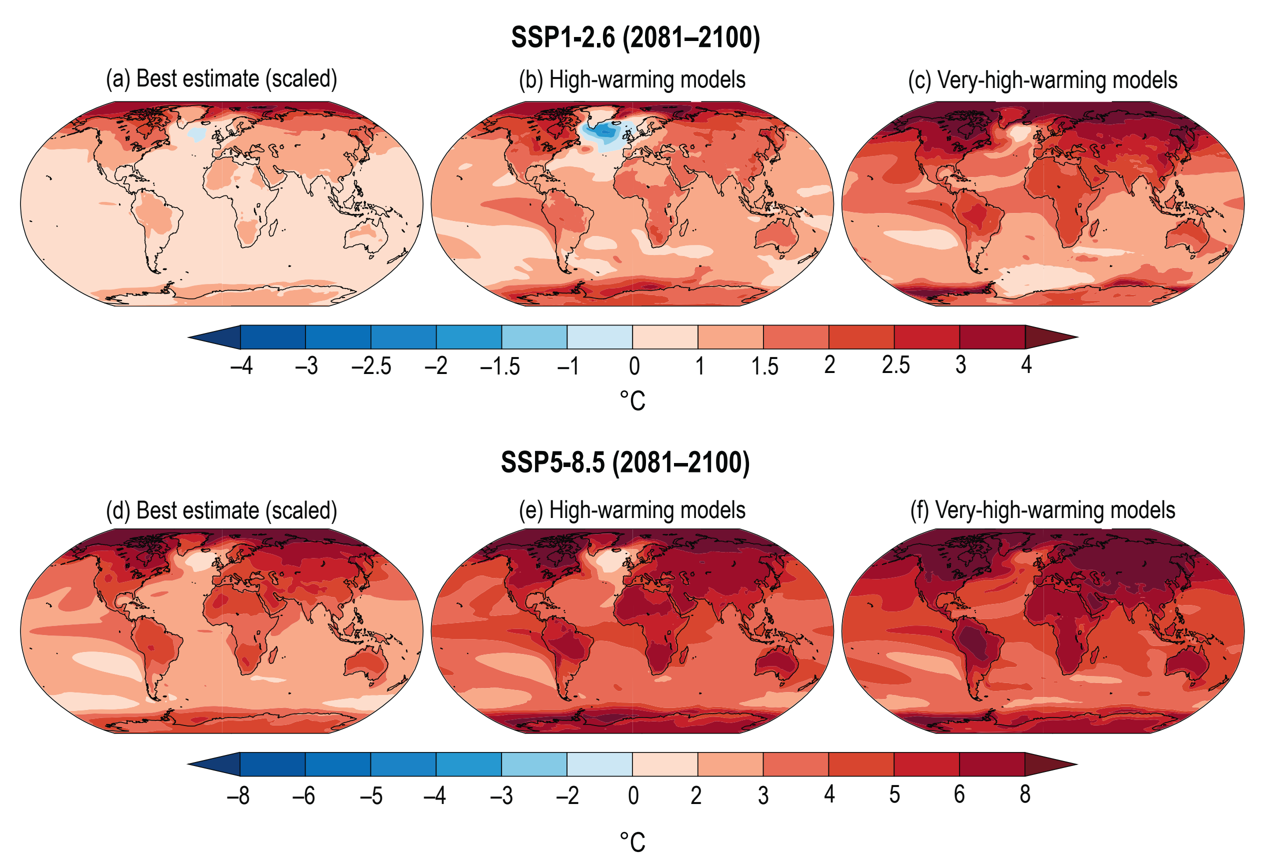

Box TS.3, Figure 1 | High-warming storylines. *The intent of this figure is to illustrate high warming storylines compared to the CMIP6 multi-model-mean.* **(a)** Coupled Model Intercomparison Project Phase 6 (CMIP6) multi-model mean linearly scaled to the assessed best global surface temperature estimate for SSP1-2.6 in 2081–2100 relative to 1995–2014, **(b)** mean across five high-warming models with global surface temperature changes nearest to the upper bound of the assessed very likely range, and **(c)** mean across five very high-warming models with global surface temperature changes higher than the assessed *very likely*. **(d–f)** Same as (a–c) but for SSP5-8.5. Note the different colour bars in (a–c) and (d–f). {4.7, Figure 4.41}

TS.2.4 The Ocean

Observations, models and paleo-evidence indicate that recently observed changes in the ocean are unprecedented for centuries to millennia (*high confidence*). Over the past four to six decades, it is *virtually certain* that the global ocean has warmed, with human influence *extremely likely* the main driver since the 1970s, making climate change irreversible over centuries to millennia (*medium confidence*). It is *virtually certain* that upper ocean salinity contrasts have increased since the 1950s and *extremely likely* that human influence has contributed. It is *virtually certain* that upper ocean stratification has increased since 1970 and that sea water pH has declined globally over the last 40 years, with human influence being the main driver of the observed surface open ocean acidification (*virtually certain*). A long-term increase in surface open ocean pH occurred over the past 50 million years (*high confidence*), and surface ocean pH as low as recent times is uncommon in the last 2 million years (*medium confidence*). There is *high confidence* that marine heatwaves have become more frequent in the 20th century, and most of those since 2006 have been attributed to anthropogenic warming (*very likely*). There is *high confidence* that oxygen levels have dropped in many regions since the mid 20th century and that the geographic range of many marine organisms has changed over the last two decades.

The amount of ocean warming observed since 1971 will *likely* at least double by 2100 under a low warming scenario (SSP1-2.6) and will increase by 4–8 times under a high warming scenario (SSP5-8.5). Stratification (*virtually certain*), acidification (*virtually certain*), deoxygenation (*high confidence*) and marine heatwave frequency (*high confidence*) will continue to increase in the 21st century. While there is *low confidence* in 20th century AMOC change, it is *very likely* that AMOC will decline over the 21st century (Figure TS.11). {2.3, 3.5, 3.6, 4.3.2, 5.3, 7.2, 9.2, Box 9.2, 12.4}

It is *virtually certain* that the global ocean has warmed since at least 1971, representing about 90% of the increase in the global energy inventory (Section TS.3.1). The ocean is currently warming faster than at any other time since at least the last deglacial transition (*medium confidence*), with warming extending to depths well below 2000 m (*very high confidence*). It is *extremely likely* that human influence was the main driver of this recent ocean warming. Ocean warming will continue over the 21st century (*virtually certain*), and will *likely* continue until at least to 2300 even for low CO_2 emissions scenarios. Ocean warming is irreversible over centuries to millennia (*medium confidence*), but the magnitude of warming is scenario-dependent from about the mid-21st century (*medium confidence*). The warming will not be globally uniform, with heat primarily stored in Southern Ocean water-masses and weaker warming in the subpolar North Atlantic (*high confidence*). Limitations in the understanding of feedback mechanisms limit our confidence in future ocean warming close to Antarctica and how this will affect sea ice and ice shelves. {2.3.3, 3.5.1, 4.7.2, 7.2.2, 9.2.2, 9.2.3, 9.2.4, 9.3.2, 9.6.1, Cross-Chapter Box 9.1}

Global mean SST has increased since the beginning of the 20th century by 0.88 [0.68 to 1.01] °C, and it is *virtually certain* it will continue to increase throughout the 21st century, with increasing hazards to marine ecosystems (*medium confidence*). Marine heatwaves have become more frequent over the 20th century (*high confidence*), approximately doubling in frequency (*high confidence*) and becoming more intense and longer since the 1980s (*medium confidence*). Most of the marine heatwaves over 2006–2015 have been attributed to anthropogenic warming (*very likely*). Marine heatwaves will continue to increase in frequency, with a *likely* global increase of 2–9 times in 2081–2100 compared to 1995–2014 under SSP1-2.6, and 3–15 times under SSP5-8.5 (Figure TS.11a), with the largest changes in the tropical and Arctic ocean. {2.3.1, Cross-Chapter Box 2.3, 9.2.1, Box 9.2, 12.4.8}

Observed upper-ocean stratification (0–200 m) has increased globally since at least 1970 (*virtually certain*). Based on recent refined analyses of the available observations, there is *high confidence* that it increased by 4.9 ± 1.5% from 1970–2018, which is about twice as much as assessed in SROCC, and will continue to increase throughout the 21st century at a rate depending on the emissions scenario (*virtually certain*). {2.3.3, 9.2.1}

It is *virtually certain* that since 1950 near-surface high-salinity regions have become more saline, while low-salinity regions have become fresher, with *medium confidence* that this is linked to an intensification of the hydrological cycle (Box TS.6). It is *extremely likely* that human influence has contributed to this salinity change and that the large-scale pattern will grow in amplitude over the 21st century (*medium confidence*). {2.3.3, 3.5.2, 9.2.2, 12.4.8}

The AMOC was relatively stable during the past 8000 years (*medium confidence*). There is *low confidence* in the quantification of AMOC changes in the 20th century because of *low agreement* in quantitative reconstructed and simulated trends, missing key processes in both models and measurements used for formulating proxies, and new model evaluations. Direct observational records since the mid-2000s are too short to determine the relative contributions of internal variability, natural forcing and anthropogenic forcing to AMOC change (*high confidence*). An AMOC decline over the 21st century is *very likely* for all SSP scenarios (Figure TS.11b); a possible abrupt decline is assessed further in Box TS.3. {2.3.3, 3.5.4, 4.3.2, 8.6.1, 9.2.3, Cross-Chapter Box 12.3}

There is *high confidence* that many ocean currents will change in the 21st century in response to changes in wind stress. There is *low confidence* in 21st century change of Southern Ocean circulation, despite *high confidence* that it is sensitive to changes in wind patterns and increased ice-shelf melt. Western boundary currents and subtropical gyres have shifted poleward since 1993 (*medium confidence*). Subtropical gyres, the East Australian Current Extension, the Agulhas Current, and the Brazil Current are projected to intensify in the 21st century in response to changes in wind stress, while the Gulf Stream and the Indonesian Throughflow are projected to weaken (*medium confidence*). All of the four main eastern boundary upwelling systems are projected to weaken at low latitudes and intensify at high latitudes in the 21st century (*high confidence*). {2.3.3, 9.2.3}

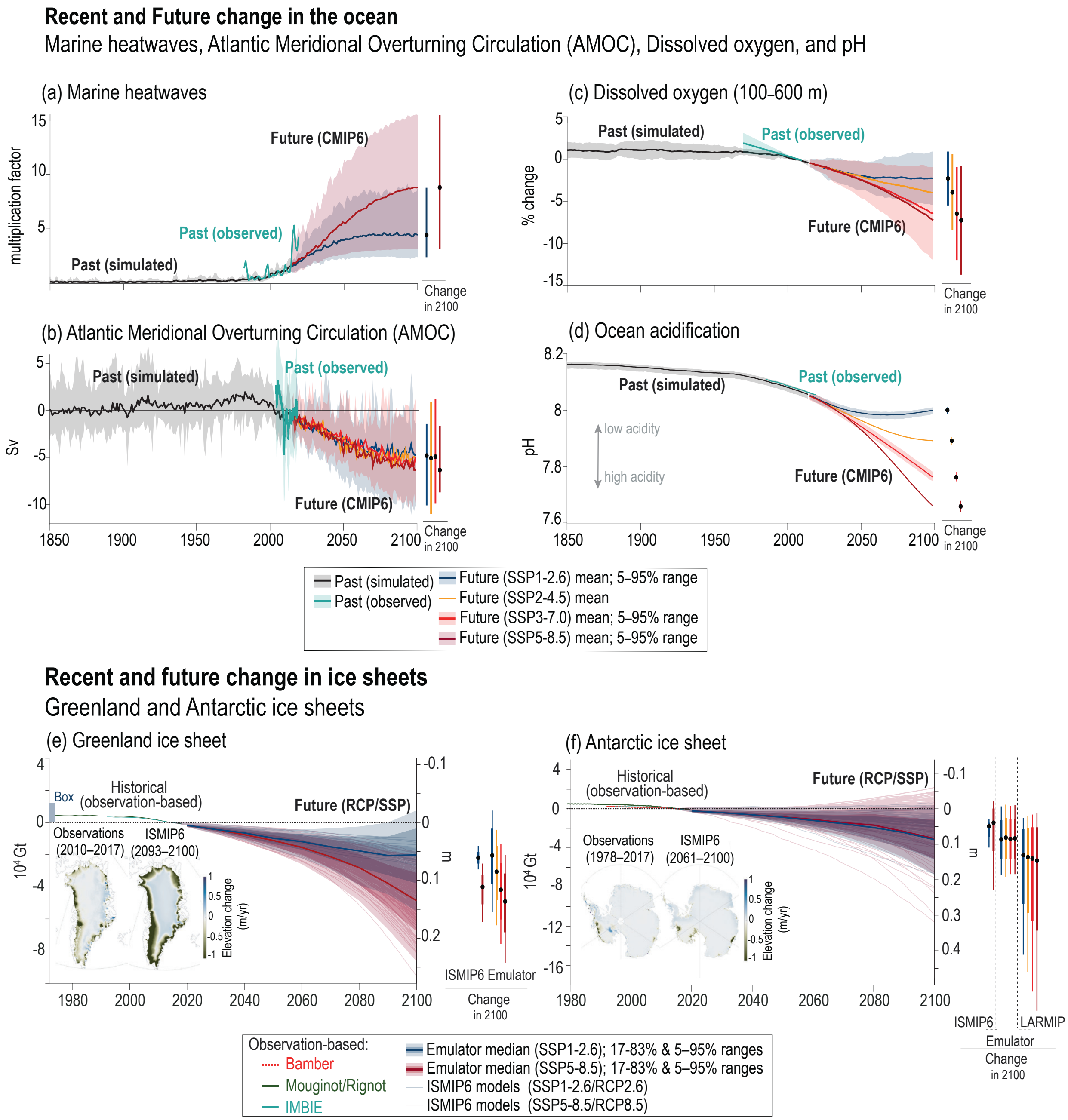

Figure TS.11 | Past and future ocean and ice-sheet changes. *The intent of this figure is to show that observed and projected time series of many ocean and cryosphere indicators are consistent.* Observed and simulated historical changes and projected future changes under varying greenhouse gas emissions scenarios. Simulated and projected ocean changes are shown as Coupled Model Intercomparison Project Phase 6 (CMIP6) ensemble mean, and 5–95% range (shading) is provided for scenarios SSP1-2.6 and SSP3-7.0 (except in panel a where the range is provided for scenario SSP1-2.6 and SSP5-8.5). Mean and 5–95% range in 2100 are shown as vertical bars on the right-hand side of each panel. **(a)** Change in multiplication factor in surface ocean marine heatwave days relative to 1995–2014 (defined as days exceeding the 99th percentile in sea surface temperature (SST) from 1995–2014 distribution). Assessed observational change span 1982–2019 from AVHRR satellite SST. **(b)** Atlantic Meridional Overturning Circulation (AMOC) transport relative to 1995–2014 (defined as maximum transport at 26°N). Assessed observational change spans 2004–2018 from the RAPID array smoothed with a 12-month running mean (shading around the mean shows the 12-month running standard deviation around the mean). **(c)** Global mean percent change in ocean oxygen (100–600 m depth), relative to 1995–2014. Assessed observational trends and *very likely* range are from the SROCC assessment, and span 1970–2010 centred on 2005. **(d)** Global mean surface pH. Assessed observational change spans 1985–2019, from the CMEMS SOCAT-based reconstruction (shading around the global mean shows the 90% confidence interval). **(e), (f)**: Ice sheet mass changes. Projected ice-sheet changes are shown as median, 5–95% range (light shading), and 17–83% range (dark shading) of cumulative mass loss and sea level equivalent from ISMIP6 emulation under SSP1-2.6 and SSP5-8.5 (shading and bold line), with individual emulated projections as thin lines. Median (dot), 17–83% range (thick vertical bar), and 5–95% range (thin vertical bar) in 2100 are shown as vertical bars on the right-hand side of each panel, from ISMIP6, ISMIP6 emulation, and LARMIP-2. Observation-based estimates: For Greenland (e), for 1972–2018 (Mouginot), for 1992–2016 (Bamber), for 1992–2020 (IMBIE) and total estimated mass loss range for 1840–1972 (Box). For Antarctica (f), estimates based on satellite data combined with simulated surface mass balance and glacial isostatic adjustment for 1992–2020 (IMBIE), 1992–2016 (Bamber), and 1979–2017 (Rignot). Left inset maps: mean Greenland elevation changes 2010–2017 derived from CryoSat-2 radar altimetry (e) and mean Antarctica elevation changes 1978–2017 derived from restored analogue radar records (f). Right inset maps: ISMIP6 model mean (2093–2100) projected changes under the MIROC5 climate model for the RCP8.5 scenario. {2.3.3; 2.3.4; 3.5.4; 4.3.2; 5.3.2; 5.3.3; 5.6.3; 9.2.3; 9.4.1; 9.4.2; Box 9.2; Box 9.2, Figure 1; Figures 9.10, 9.17 and 9.18}

It is *virtually certain* that surface pH has declined globally over the last 40 years and that the main driver is uptake of anthropogenic CO_2. Ocean acidification and associated reductions in the saturation state of calcium carbonate – a constituent of skeletons or shells of a variety of marine organisms – is expected to increase in the 21st century under all emissions scenarios (*high confidence*). A long-term increase in surface open ocean pH occurred over the past 50 million years (*high confidence*), and surface ocean pH as low as recent times is uncommon in the last 2 million years (*medium confidence*). There is *very high confidence* that present-day surface pH values are unprecedented for at least 26,000 years and current rates of pH change are unprecedented since at least that time. Over the past 2–3 decades, a pH decline in the ocean interior has been observed in all ocean basins (*high confidence*) (Figure TS.11d). {2.3.3, 2.3.4, 3.6.2, 4.3.2, 5.3.2, 5.3.3, 5.6.3, 12.4.8}

Open-ocean deoxygenation and expansion of oxygen minimum zones have been observed in many areas of the global ocean since the mid 20th century (*high confidence*), in part due to human influence (*medium confidence*). Deoxygenation is projected to continue to increase with ocean warming (*high confidence*) (Figure TS.11c). Higher climate sensitivity and reduced ocean ventilation in CMIP6 compared to CMIP5 results in substantially greater projections of subsurface (100–600 m) oxygen decline than reported in SROCC for the period 2080–2099. {2.3.3, 2.3.4, Cross-Chapter Box 2.4, 3.6.2, 5.3.3, 12.4.8}

Over at least the last two decades, the geographic range of many marine organisms has shifted towards the poles and towards greater depths (*high confidence*), indicative of shifts towards cooler waters. The range of a smaller subset of organisms has shifted equatorward and to shallower depths (*high confidence*). Phenological metrics associated with the life cycles of many organisms have also changed over the last two decades or longer (*high confidence*). Since the changes in the geographical range of organisms and their phenological metrics have been observed to differ with species and location, there is the possibility of disruption to major marine ecosystems. {2.3.4}

TS.2.5 The Cryosphere

Over recent decades, widespread loss of snow and ice has been observed, and several elements of the cryosphere are now in states unseen in centuries (*high confidence*). Human influence was *very likely* the main driver of observed reductions in Arctic sea ice since the late 1970s (with late-summer sea ice loss *likely* unprecedented for at least 1000 years) and the widespread retreat of glaciers (unprecedented in at least the last 2,000 years, *medium confidence*). Furthermore, human influence *very likely* contributed to the observed Northern Hemisphere spring snow cover decrease since 1950.

By contrast, Antarctic sea ice area experienced no significant net change since 1979, and there is only *low confidence* in its projected changes. The Arctic Ocean is projected to become practically sea ice-free in late summer under high CO_2 emissions scenarios by the end of the 21st century (*high confidence*). It is *virtually certain* that further warming will lead to further reductions of Northern Hemisphere snow cover, and there is *high confidence* that this is also the case for near-surface permafrost volume.

Glaciers will continue to lose mass at least for several decades even if global temperature is stabilized (*very high confidence*), and mass loss over the 21st century is *virtually certain* for the Greenland Ice Sheet and *likely* for the Antarctic Ice Sheet. Deep uncertainty persists with respect to the possible evolution of the Antarctic Ice Sheet within the 21st century and beyond, in particular due to the potential instability of the West Antarctic Ice Sheet. {2.3, 3.4, 4.3, 8.3, 9.3–9.6, Box 9.4, 12.4}

Current Arctic sea ice coverage levels (both annual and late summer) are at their lowest since at least 1850 (*high confidence*), and for late summer for the past 1000 years (*medium confidence*). Since the late 1970s, Arctic sea ice area and thickness have decreased in both summer and winter, with sea ice becoming younger, thinner and more dynamic (*very high confidence*). It is *very likely* that anthropogenic forcing, mainly due to greenhouse gas increases, was the main driver of this loss, although new evidence suggests that anthropogenic aerosol forcing has offset part of the greenhouse gas-induced losses since the 1950s (*medium confidence*). The annual Arctic sea ice area minimum will *likely* fall below 1 million km^2 at least once before 2050 under all assessed SSP scenarios. This practically sea ice-free state will become the norm for late summer by the end of the 21st century in high CO_2 emissions scenarios (*high confidence*). Arctic summer sea ice varies approximately linearly with global surface temperature, implying that there is no tipping point and observed/projected losses are potentially reversible (*high confidence*). {2.3.2, 3.4.1, 4.3.2, 9.3.1, 12.4.9}

For Antarctic sea ice, there is no significant trend in satellite-observed sea ice area from 1979 to 2020 in both winter and summer, due to regionally opposing trends and large internal variability. Due to mismatches between model simulations and observations, combined with a lack of understanding of reasons for substantial inter-model spread, there is *low confidence* in model projections of future Antarctic sea ice changes, particularly at the regional level. {2.3.2, 3.4.1, 9.3.2}

In permafrost regions, increases in ground temperatures in the upper 30 m over the past three to four decades have been widespread (*high confidence*). For each additional 1°C of warming (up to 4°C above the 1850–1900 level), the global volume of perennially frozen ground to 3 m below the surface is projected to decrease by about 25% relative to the present volume (*medium confidence*). However, these decreases may be underestimated due to an incomplete representation of relevant physical processes in ESMs (*low confidence*). Seasonal snow cover is treated in Section TS.2.6. {2.3.2, 9.5.2, 12.4.9}

There is *very high confidence* that, with few exceptions, glaciers have retreated since the second half of the 19th century; this behaviour is unprecedented in at least the last 2000 years (*medium* *confidence*). Mountain glaciers *very likely* contributed 67.2 [41.8 to 92.6] mm to the observed GMSL change between 1901 and 2018. This retreat has occurred at increased rates since the 1990s, with human influence *very likely* being the main driver. Under RCP2.6 and RCP8.5, respectively, glaciers are projected to lose 18% ± 13% and 36% ± 20% of their current mass over the 21st century (*medium confidence*). {2.3.2, 3.4.3, 9.5.1, 9.6.1}

The Greenland Ice Sheet was smaller than at present during the Last Interglacial period (roughly 125,000 years ago) and the mid-Holocene (roughly 6,000 years ago) (*high confidence*). After reaching a recent maximum ice mass at some point between 1450 and 1850, the ice sheet retreated overall, with some decades *likely* close to equilibrium (i.e., mass loss approximately equalling mass gained). It is *virtually certain* that the Greenland Ice Sheet has lost mass since the 1990s, with human influence a contributing factor (*medium confidence*). There is *high confidence* that annual mass changes have been consistently negative since the early 2000s. Over the period 1992–2020, Greenland *likely* lost 4890 ± 460 Gt of ice, contributing 13.5 ± 1.3 mm to GMSL rise. There is *high confidence* that Greenland ice mass losses are increasingly dominated by surface melting and runoff, with large interannual variability arising from changes in surface mass balance. Projections of future Greenland ice-mass loss (Box TS.4, Table 1; Figure TS.11e) are dominated by increased surface melt under all emissions scenarios (*high confidence*). Potential irreversible long-term loss of the Greenland Ice Sheet, and of parts of the Antarctic Ice Sheet, is assessed in Box TS.9. {2.3.2, 3.4.3, 9.4.1, 9.4.2, 9.6.3, Atlas.11.2}

It is *likely* that the Antarctic Ice Sheet has lost 2670 ± 530 Gt, contributing 7.4 ± 1.5 mm to GMSL rise over 1992–2020. The total Antarctic ice mass losses were dominated by the West Antarctic Ice Sheet, with combined West Antarctic and Peninsula annual loss rates increasing since about 2000 (*very high confidence*). Furthermore, it is *very likely* that parts of the East Antarctic Ice Sheet have lost mass since 1979. Since the 1970s, snowfall has *likely* increased over the western Antarctic Peninsula and eastern West Antarctica, with large spatial and interannual variability over the rest of Antarctica. Mass losses from West Antarctic outlet glaciers, mainly induced by ice shelf basal melt (*high confidence*), outpace mass gain from increased snow accumulation on the continent (*very high confidence*). However, there is only *limited evidence*, with *medium agreement*, of anthropogenic forcing of the observed Antarctic mass loss since 1992 (with *low confidence* in process attribution). Increasing mass loss from ice shelves and inland discharge will *likely* continue to outpace increasing snowfall over the 21st century (Figure TS.11f). Deep uncertainty persists with respect to the possible evolution of the Antarctic Ice Sheet along high-end mass-loss storylines within the 21st century and beyond, primarily related to the abrupt and widespread onset of marine ice sheet instability and marine ice cliff instability. (See also Boxes TS.3 and TS.4). {2.3.2, 3.4.3, 9.4.2, 9.6.3, Box 9.4, Atlas.11.1}

Box TS.4 | Sea Level

Global mean sea level (GMSL) increased by 0.20 [0.15 to 0.25] m over the period 1901 to 2018, with a rate of rise that has accelerated since the 1960s to 3.7 [3.2 to 4.2] mm yr^{-1} for the period 2006–2018 (*high confidence*). Human activities were *very likely* the main driver of observed GMSL rise since 1971, and new observational evidence leads to an assessed sea level rise over the period 1901 to 2018 that is consistent with the sum of individual components contributing to sea level rise, including expansion due to ocean warming and melting of glaciers and ice sheets (*high confidence*). It is *virtually certain* that GMSL will continue to rise over the 21st century in response to continued warming of the climate system (Box TS.4, Figure 1). Sea level responds to greenhouse gas (GHG) emissions more slowly than global surface temperature, leading to weaker scenario dependence over the 21st century than for global surface temperature (*high confidence*). This slow response also leads to long-term committed sea level rise, associated with ongoing ocean heat uptake and the slow adjustment of the ice sheets, that will continue over the centuries and millennia following cessation of emissions (*high confidence*) (Box TS.9). By 2100, GMSL is projected to rise by 0.28–0.55 m (*likely* range) under SSP1-1.9 and 0.63–1.01 m (*likely* range) under SSP5-8.5 relative to the 1995–2014 average (*medium confidence*). Under the higher CO_2 emissions scenarios, there is deep uncertainty in sea level projections for 2100 and beyond associated with the ice-sheet responses to warming. In a low-likelihood, high-impact storyline and a high CO_2 emissions scenario, ice-sheet processes characterized by deep uncertainty could drive GMSL rise up to about 5 m by 2150. Given the long-term commitment, uncertainty in the timing of reaching different GMSL rise levels is an important consideration for adaptation planning. {2.3, 3.4, 3.5, 9.6, Box 9.4, Cross-Chapter Box 9.1, Table 9.5}

GMSL change is driven by warming or cooling of the ocean (and the associated expansion/contraction) and changes in the amount of ice and water stored on land. Paleo-evidence shows that GMSL has been about 70 m higher and 130 m lower than present within the past 55 million years and was *likely* 5 to 10 m higher during the Last Interglacial (Box TS.2, Figure 1). Sea level observations show that GMSL rose by 0.20 [0.15 to 0.25] m over the period 1901–2018 at an average rate of 1.7 [1.3 to 2.2] mm yr^{-1}. New analyses and paleo-evidence since AR5 show this rate is *very likely* faster than during any century over at least the last three millennia (*high confidence*). Since AR5, there is strengthened evidence for an increase in the rate of GMSL rise since the mid-20th century, with an average rate of 2.3 [1.6–3.1] mm yr^{-1} over the period 1971–2018 increasing to 3.7 [3.2–4.2] mm yr^{-1} for the period 2006–2018 (*high confidence*). {2.3.3, 9.6.1, 9.6.2}

Box TS.4 (continued)

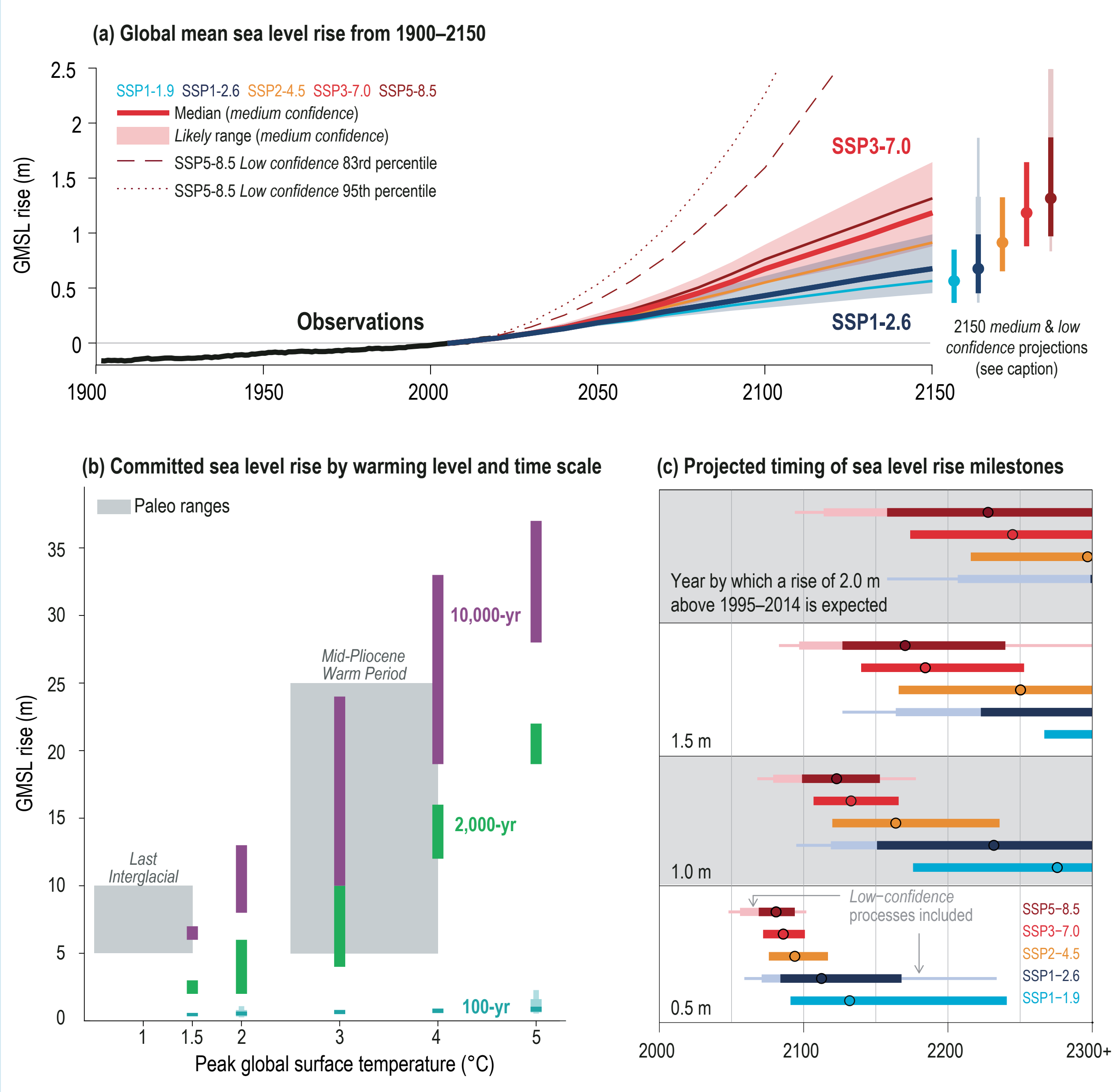

Box TS.4, Figure 1 | Global mean sea level (GMSL) change on different time scales and under different scenarios. *The intent of this figure is to (i) show the century-scale GMSL projections in the context of the 20th century observations, (ii) illustrate 'deep uncertainty' in projections by considering the timing of GMSL rise milestones, and (iii) show the long-term commitment associated with different warming levels, including the paleo evidence to support this.* **(a)** GMSL change from 1900 to 2150, observed (1900–2018) and projected under the SSP scenarios (2000–2150), relative to a 1995–2014 baseline. Solid lines show median projections. Shaded regions show *likely* ranges for SSP1-2.6 and SSP3-7.0. Dotted and dashed lines show respectively the 83rd and 95th percentile *low confidence* projections for SSP5-8.5. Bars at right show *likely* ranges for SSP1-1.9, SSP1-2.6, SSP2-4.5, SSP3-7.0 and SSP5-8.5 in 2150. Lightly shaded thick/thin bars show 17th–83rd/5th–95th percentile *low-confidence* ranges in 2150 for SSP1-2.6 and SSP5-8.5, based upon projection methods incorporating structured expert judgement and marine ice cliff instability. *Low confidence* range for SSP5-8.5 in 2150 extends to 4.8/5.4 m at the 83rd/95th percentile. **(b)** GMSL change on 100- (blue), 2000- (green) and 10,000-year (magenta) time scales as a function of global surface temperature, relative to 1850–1900. For 100-year projections, GMSL is projected for the year 2100, relative to a 1995–2014 baseline, and temperature anomalies are average values over 2081–2100. For longer-term commitments, warming is indexed by peak warming above 1850–1900 reached after cessation of emissions. Shaded regions show paleo-constraints on global surface temperature and GMSL for the Last Interglacial and mid-Pliocene Warm Period. Lightly shaded thick/thin blue bars show 17th–83rd/5th–95th percentile *low confidence* ranges for SSP1-2.6 and SSP5-8.5 in 2100, plotted at 2°C and 5°C. **(c)** Timing of exceedance of GMSL thresholds of 0.5, 1.0, 1.5 and 2.0 m, under different SSPs. Lightly shaded thick/thin bars show 17th–83rd/5th–95th percentile *low-confidence* ranges for SSP1-2.6 and SSP5-8.5. {4.3.2, 9.6.1, 9.6.2, 9.6.3, Box 9.4}

Box TS.4 (continued)

GMSL will continue to rise throughout the 21st century (Box TS.4, Figure 1a). Considering only those processes in whose projections we have at least *medium confidence*, relative to the period 1995–2014, GMSL is projected to rise between 0.18 m (0.15–0.23 m, *likely range*; SSP1-1.9) and 0.23 m (0.20–0.30 m, *likely range*; SSP5-8.5) by 2050. By 2100, the projected rise is between 0.38 m (0.28–0.55 m, *likely range*; SSP1-1.9) and 0.77 m (0.63–1.01 m, *likely range*; SSP5-8.5) {Table 9.9}. The methods, models and scenarios used for sea level projections in the AR6 are updated from those employed by SROCC, with contributions informed by the latest model projections described in the ocean and cryosphere Sections (Sections TS.2.4 and TS.2.5). Despite these differences, the sea level projections are broadly consistent with those of SROCC. {4.3.2, 9.6.3}

Importantly, *likely* range projections do not include those ice-sheet-related processes whose quantification is highly uncertain or that are characterized by deep uncertainty. Higher amounts of GMSL rise before 2100 could be caused by earlier-than-projected disintegration of marine ice shelves, the abrupt, widespread onset of marine ice sheet instability (MISI) and marine ice cliff instability (MICI) around Antarctica, and faster-than-projected changes in the surface mass balance and dynamical ice loss from Greenland (Box TS.4, Figure 1). In a low-likelihood, high-impact storyline and a high CO_2 emissions scenario, such processes could in combination contribute more than one additional meter of sea level rise by 2100 (Box TS.3). {4.3.2, 9.6.3, Box 9.4}

Beyond 2100, GMSL will continue to rise for centuries to millennia due to continuing deep ocean heat uptake and mass loss from ice sheets, and will remain elevated for thousands of years (*high confidence*). By 2150, considering only those processes in whose projections we have at least *medium confidence* and assuming no acceleration in ice-mass flux after 2100, GMSL is projected to rise between 0.6 m (0.4–0.9 m, *likely* range, SSP1-1.9) and 1.3 m (1.0–1.9 m, *likely* range) (SSP5-8.5), relative to the period 1995–2014 based on the SSP scenario extensions. Under high CO_2 emissions, processes in which there is *low confidence*, such as MICI, could drive GMSL rise up to about 5 m by 2150 (Box TS.4, Figure 1a). By 2300, GMSL will rise 0.3–3.1 m under low CO_2 emissions (SSP1-2.6) (*low confidence*). Under high CO_2 emissions (SSP5-8.5), projected GMSL rise is between 1.7 and 6.8 m by 2300 in the absence of MICI and by up to 16 m considering MICI (*low confidence*). Over 2000 years, there is *medium agreement* and *limited evidence* that committed GMSL rise is projected to be about 2–3 m with 1.5°C peak warming, 2–6 m with 2°C of peak warming, 4–10 m with 3°C of peak warming, 12–16 m with 4°C of peak warming, and 19–22 m with 5°C of peak warming. {9.6.3}

Looking at uncertainty in time provides an alternative perspective on uncertainty in future sea level rise (Box TS.4, Figure 1c). For example, considering only *medium confidence* processes, GMSL rise is likely to exceed 0.5 m between about 2080 and 2170 under SSP1-2.6 and between about 2070 and 2090 under SSP5-8.5. Given the long-term commitment, uncertainty in the timing of reaching different levels of GMSL rise is an important consideration for adaptation planning. {9.6.3}

At regional scales, additional processes come into play that modify the local sea level change relative to GMSL, including vertical land motion, ocean circulation and density changes, and gravitational, rotational, and deformational effects arising from the redistribution of water and ice mass between land and the ocean. These processes give rise to a spatial pattern that tends to increase sea level rise at the low latitudes and reduce sea level rise at high latitudes. However, over the 21st century, the majority of coastal locations have a median projected regional sea level rise within ±20% of the projected GMSL change (*medium confidence*). Further details on regional sea level change and extremes are provided in Section TS.4. {9.6.3}

Box TS.5 | The Carbon Cycle

The continued growth of atmospheric CO_2 concentrations over the industrial era is unequivocally due to emissions from human activities. Ocean and land carbon sinks slow the rise of CO_2 in the atmosphere. Projections show that while land and ocean sinks absorb more CO_2 under high emissions scenarios than low emissions scenarios, the fraction of emissions removed from the atmosphere by natural sinks decreases with higher concentrations (*high confidence*). Projected ocean and land sinks show similar responses for a given scenario, but the land sink has a much higher interannual variability and wider model spread. The slowed growth rates of the carbon sinks projected for the second half of this century are linked to strengthening carbon–climate feedbacks and stabilization of atmospheric CO_2 under medium-to-no-mitigation and high-mitigation scenarios, respectively (see FAQ 5.1). {5.2, 5.4}

Box TS.5 (continued)

Carbon sinks for anthropogenic CO_2 are associated with mainly physical ocean and biospheric land processes that drive the exchange of carbon between multiple land, ocean and atmospheric reservoirs. These exchanges are driven by increasing atmospheric CO_2, but are modulated by changes in climate (Box TS.5, Figure 1c,d). The Northern and Southern Hemispheres dominate the land and ocean sinks, respectively (Box TS.5, Figure 1). Ocean circulation and thermodynamic processes also play a critical role in coupling the global carbon and energy (heat) cycles. There is *high confidence* that this ocean carbon–heat nexus is an important basis for one of the most important carbon–climate metrics, the transient climate response to cumulative CO_2 emissions (TCRE; Section TS.3.2.1) used to determine the remaining carbon budget. {5.1, 5.2, 5.5, 9.2, Cross-Chapter Box 5.3}

Based on multiple lines of evidence using interhemispheric gradients of CO_2 concentrations, isotopes, and inventory data, it is unequivocal that the growth in CO_2 in the atmosphere since 1750 (see Section TS.2.2) is due to the direct emissions from human activities. The combustion of fossil fuels and land-use change for the period 1750–2019 resulted in the release of 700 ± 75 PgC (*likely* range, 1 PgC = 10^{15} g of carbon) to the atmosphere, of which about 41% ± 11% remains in the atmosphere today (*high confidence*). Of the total anthropogenic CO_2 emissions, the combustion of fossil fuels was responsible for about 64% ± 15%, growing to an 86% ± 14% contribution over the past 10 years. The remainder resulted from land-use change. During the last decade (2010–2019), average annual anthropogenic CO_2 emissions reached the highest levels in human history at 10.9 ± 0.9 PgC yr^{-1} (*high confidence*). Of these emissions, 46% accumulated in the atmosphere (5.1 ± 0.02 PgC yr^{-1}), 23% (2.5 ± 0.6 PgC yr^{-1}) was taken up by the ocean and 31% (3.4 ± 0.9 PgC yr^{-1}) was removed by terrestrial ecosystems (*high confidence*). {5.2.1, 5.2.2, 5.2.3}

The ocean (*high confidence*) and land (*medium confidence*) sinks of CO_2 have increased with anthropogenic emissions over the past six decades (Box TS.5, Figure 1). This coherence between emissions and the growth in ocean and land sinks has resulted in the airborne fraction of anthropogenic CO_2 remaining at 44 ± 10% over the past 60 years (*high confidence*). Interannual and decadal variability of the ocean and land sinks indicate that they are sensitive to changes in the growth rate of emissions as well as climate variability and are therefore also sensitive to climate change (*high confidence*). {5.2.1}

The land CO_2 sink is driven by carbon uptake by vegetation, with large interannual variability, for example, linked to the El Niño–Southern Oscillation (ENSO). Since the 1980s, carbon fertilization from rising atmospheric CO_2 has increased the strength of the net land CO_2 sink (*medium confidence*). During the historical period, the growth of the ocean sink has been primarily determined by the growth rate of atmospheric CO_2. However, there is *medium confidence* that changes to physical and chemical processes in the ocean and in the land biosphere, which govern carbon feedbacks, are already modifying the characteristics of variability, particularly the seasonal cycle of CO_2, in both the ocean and land. However, changes to the multi-decadal trends in the sinks have not yet been observed. {2.3.4, 3.6.1, 5.2.1}

In AR6, ESM projections are assessed with CO_2 concentrations by 2100 from about 400 ppm (SSP1-1.9) to above 1100 ppm (SSP5-8.5). Most simulations are performed with prescribed atmospheric CO_2 concentrations, which already account for a central estimate of climate–carbon feedback effects. Carbon dioxide emissions-driven simulations account for uncertainty in these feedbacks, but do not significantly change the projected global surface temperature changes (*high confidence*). Although land and ocean sinks absorb more CO_2 under high emissions than low emissions scenarios, the fraction of emissions removed from the atmosphere decreases (*high confidence*). This means that the more CO_2 that is emitted, the less efficient the ocean and land sinks become (*high confidence*), an effect which compensates for the logarithmic relationship between CO_2 and its radiative forcing, which means that for each unit increase in additional atmospheric CO_2 the effect on global temperature decreases. (Box TS.5, Figure 1f,g). {4.3.1, 5.4.5, 5.5.1.2}

Ocean and land sinks show similar responses for a given scenario, but the land sink has a much higher interannual variability and wider model spread. Under SSP3-7.0 and SSP5-8.5, the initial growth of both sinks in response to increasing atmospheric concentrations of CO_2 is subsequently limited by emerging carbon–climate feedbacks (*high confidence*) (Box TS.5, Figure 1f). Projections show that the ocean and land sinks will stop growing from the second part of the 21st century under all emissions scenarios, but with different drivers for different emissions scenarios. Under SSP3-7.0 and SSP5-8.5, the weakening growth rate of the ocean CO_2 sink in the second half of the century is primarily linked to the strengthening positive feedback from reduced carbonate buffering capacity, ocean warming and altered ocean circulation (e.g., AMOC changes). In contrast, for SSP1-1.9, SSP1-2.6 and SSP2-4.5, the weakening growth rate of the ocean carbon sink is a response to the stabilizing or declining atmospheric CO_2 concentrations. Under SSP1-1.9, models project that combined land and ocean sinks will turn into a weak source by 2100 (*medium confidence*). Under high CO_2 emissions scenarios, it is *very likely* that the land carbon sink will grow more slowly due to warming and drying from the mid-21st century, but it is *very unlikely* that it will switch from being a sink to a source before 2100.

Box TS.5 (continued)

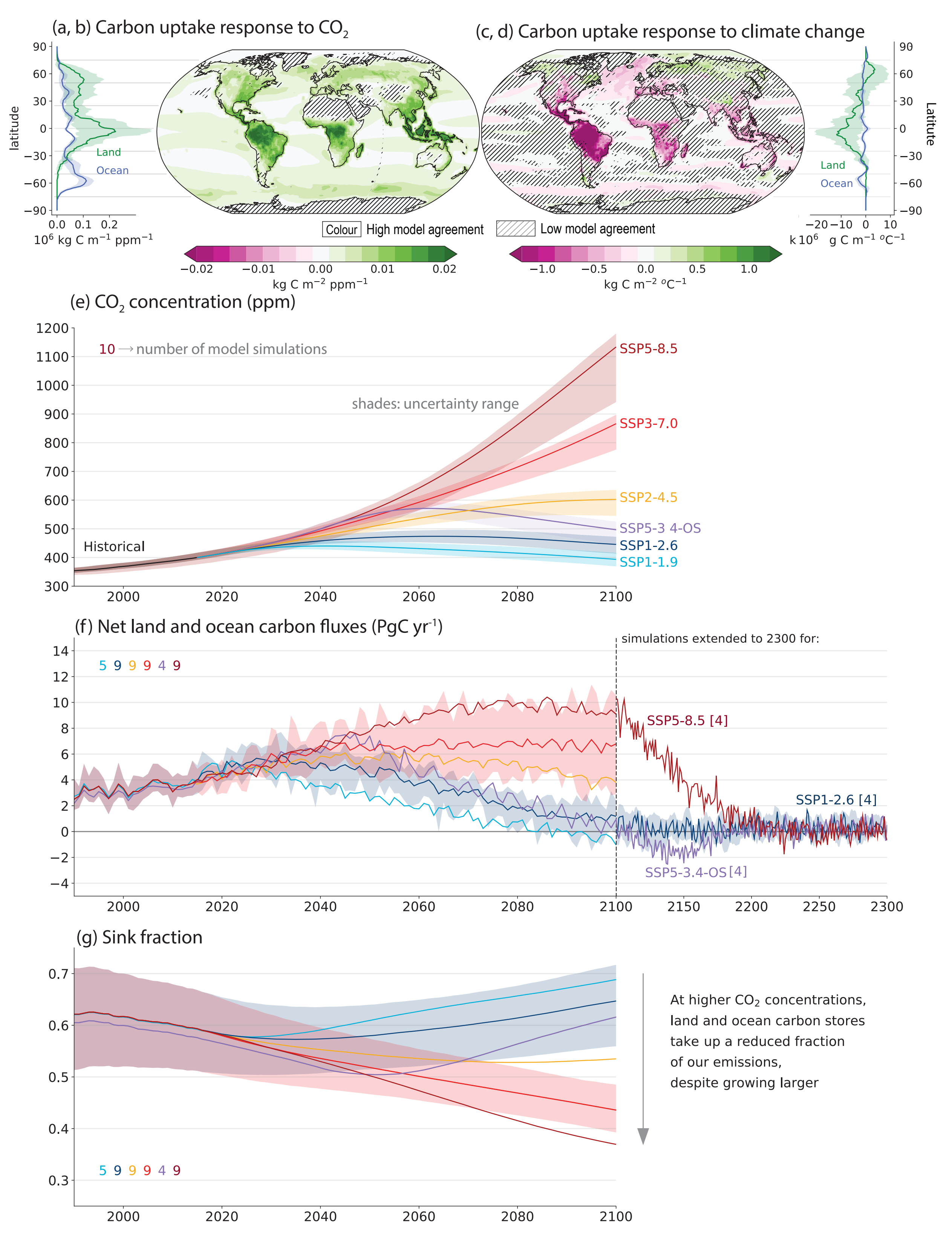

Box TS.5, Figure 1 | Carbon cycle processes and projections.

Box TS.5 (continued)

Box TS.5, Figure 1 (continued): *The intent of this figure is to show the response of the carbon cycle to carbon dioxide (CO_2) emissions and climate and its role in determining future CO_2 levels through projected changes to sinks and sink fractions.* The figure shows changes in carbon storage in response to elevated CO_2 **(a, b)** and the response to climate warming **(c, d)**. Maps show spatial patterns of changes in carbon uptake during simulations with 1% per year increase in CO_2 (Section 5.4.5.5), and zonal mean plots show distribution of carbon changes is dominated by the land (green lines) in the tropics and Northern Hemisphere and ocean (blue lines) in the Southern Hemisphere. Hatching indicates regions where fewer than 80% of models agree on the sign of response. **(e)** Future CO_2 projections: projected CO_2 concentrations in the Shared Socio-economic Pathway (SSP) scenarios in response to anthropogenic emissions, results from coupled Earth system models for SSP5-8.5 and from the MAGICC7 emulator for other scenarios (Section 4.3.1). **(f)** Future carbon fluxes: projected combined land and ocean fluxes (positive downward) up to 2100 for the SSP scenarios, and extended to 2300 for available scenarios, 5–95% uncertainty plumes shown for SSP1-2.6 and SSP3-7.0 (Sections 4.3.2.4, 5.4.5.4 and 5.4.10). The numbers near the top show the number of model simulations used. **(g)** Sink fraction: the fraction of cumulative emissions of CO_2 removed by land and ocean sinks. The sink fraction is smaller under conditions of higher emissions. {Figure 4.3; 5.4.5; Figures 5.25, 5.27 and 5.30}

Climate change alone is expected to increase land carbon accumulation in the high latitudes (not including permafrost, which is assessed in Sections TS.2.5 and TS.3.2.2), but also to lead to a counteracting loss of land carbon in the tropics (*medium confidence*). Earth system model projections show that the overall uncertainty of atmospheric CO_2 by 2100 is still dominated by the emissions pathway, but carbon–climate feedbacks (see Section TS.3.3.2) are important, with increasing uncertainties in high emissions pathways (Box TS.5, Figure 1e). {4.3.2, 5.4.1, 5.4.2, 5.4.4, 5.4.5, 11.6, 11.9, Cross-Chapter Box 5.1, Cross-Chapter Box 5.3}

Under three SSP scenarios with long-term extensions until 2300 (SSP5-8.5, SSP5-3.4-OS, SSP1-2.6), ESMs project a change of the land from a sink to a source (*medium confidence*). The scenarios make simplified assumptions about emissions reductions, with SSP1-2.6 and SSP5-3.4-OS reaching about 400 ppm by 2300, while SSP5-8.5 exceeds 2000 ppm. Under high emissions, the transition is warming-driven, whereas it is linked to the decline in atmospheric CO_2 under net negative CO_2 emissions. The ocean remains a sink throughout the period to 2300 except under very large net negative emissions. The response of the natural aspects of the carbon cycle to carbon dioxide removal is further developed in Section TS.3.3.2. {5.4.9}

TS.2.6 Land Climate, Including Biosphere and Extremes

Land surface air temperatures have risen faster than the global surface temperature since the 1850s, and it is *virtually certain* that this differential warming will persist into the future. It is *virtually certain* that the frequency and intensity of hot extremes and the intensity and duration of heatwaves have increased since 1950 and will further increase in the future even if global warming is stabilized at 1.5°C. The frequency and intensity of heavy precipitation events have increased over a majority of those land regions with good observational coverage (*high confidence*) and will *extremely likely* increase over most land regions with additional global warming.

Over the past half century, key aspects of the biosphere have changed in ways that are consistent with large-scale warming: climate zones have shifted poleward, and the growing season length in the Northern Hemisphere extratropics has increased (*high confidence*). The amplitude of the seasonal cycle of atmospheric CO_2 poleward of 45°N has increased since the 1960s (*very high confidence*), with increasing productivity of the land biosphere due to the increasing atmospheric CO_2 concentration as the main driver (*medium confidence*). Global-scale vegetation greenness has increased since the 1980s (*high confidence*). {2.3, 3.6, 4.3, 4.5, 5.2, 11.3, 11.4, 11.9, 12.4}

Observed temperatures over land have increased by 1.59 [1.34–1.83] °C between the period 1850–1900 and 2011–2020. Warming of the land is about 45% larger than for global surface temperature and about 80% larger than warming of the ocean surface. Warming of the land surface during the period 1971–2018 contributed about 5% of the increase in the global energy inventory (Section TS.3.1), nearly twice the estimate in AR5 (*high confidence*). It is *virtually certain* that the average surface warming over land will continue to be higher than over the ocean throughout the 21st century. The warming pattern will *likely* vary seasonally, with northern high latitudes warming more during winter than summer (*medium confidence*). {2.3.1, 4.3.1, 4.5.1, 7.2.2, Box 7.2, Cross-Chapter Box 9.1, 11.3, Atlas 11.2}

The frequency and intensity of hot extremes (warm days and nights) and the intensity and duration of heatwaves have increased globally and in most regions since 1950, while the frequency and intensity of cold extremes have decreased (*virtually certain*). There is *high confidence* that the increases in frequency and severity of hot extremes are due to human-induced climate change. Some recent extreme events would have been *extremely unlikely* to occur without human influence on the climate system. It is *virtually certain* that further changes in hot and cold extremes will occur throughout the 21st century in nearly all inhabited regions, even if global warming is stabilized at 1.5°C (Table TS.2, Figure TS.12a). {1.3, Cross-Chapter Box 3.2, 11.1.4, 11.3.2, 11.3.4, 11.3.5, 11.9, 12.4}

Greater warming over land alters key water cycle characteristics (Box TS.6). The rates of change in mean precipitation and runoff, and their variability, increase with global warming (Figure TS.12e,f). Human-induced climate change has contributed to increases in agricultural and ecological droughts in some regions due to increases in evapotranspiration (*medium confidence*). More regions are affected by increases in agricultural and ecological droughts with increasing global warming (*high confidence*; see also Figure TS.12c).

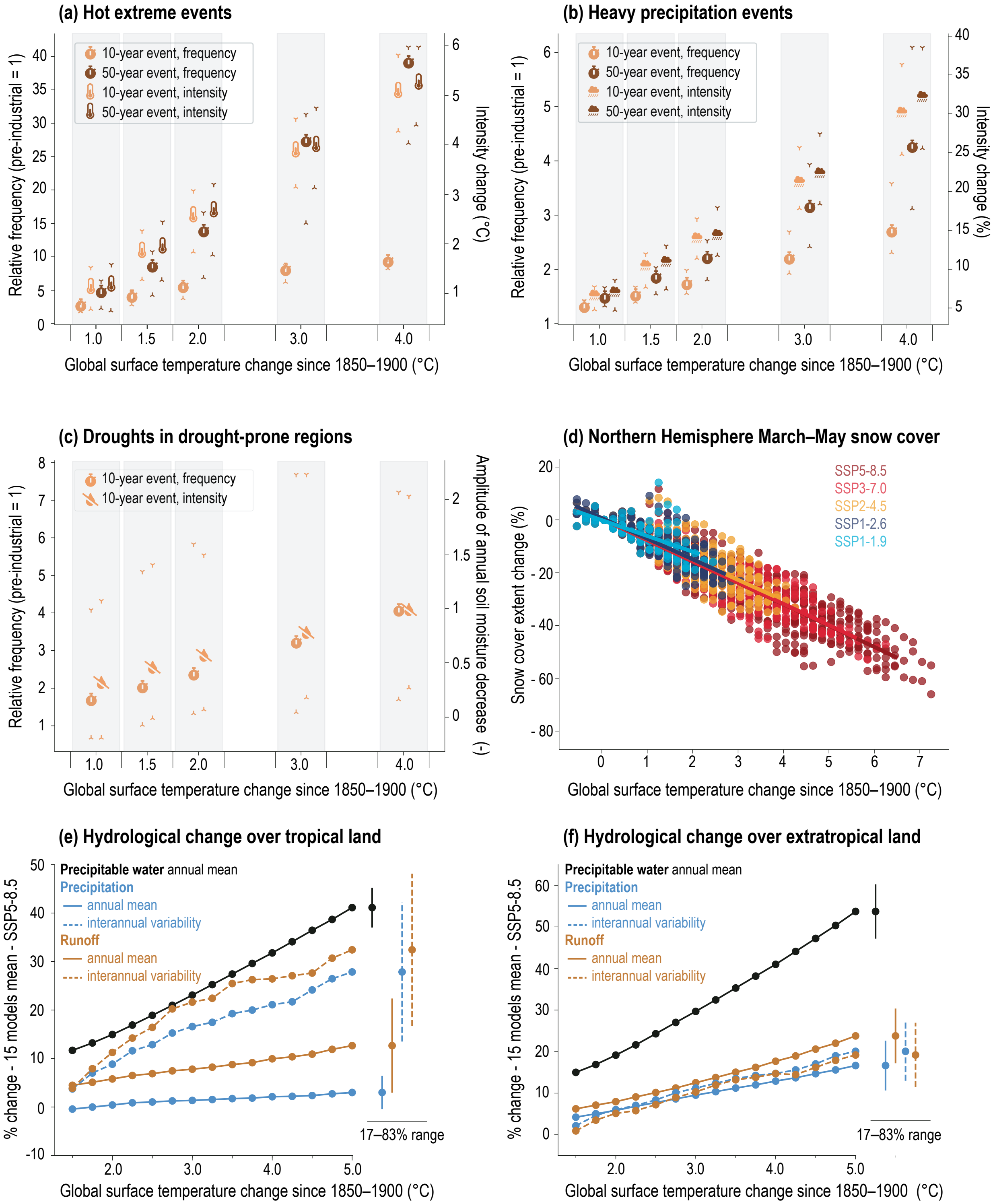

Figure TS.12 | Land-related changes relative to the 1850-1900 as a function of global warming levels. *The intent of this figure is to show that extremes and mean land variables change consistently with warming levels and to show the changes with global warming levels of water cycle indicators (i.e., precipitation and runoff) over tropical and extratropical land in terms of mean and interannual variability (interannual variability increases at a faster rate than the mean).* **(a)** Changes in the frequency (left scale) and intensity (in °C, right scale) of daily hot extremes occurring every 10 and 50 years. **(b)** as (a), but for daily heavy precipitation extremes, with intensity change in %. **(c)** Changes in 10-year droughts aggregated over drought-prone regions (WNA, CNA, NCA, SCA, NSA, NES, SAM, SWS, SSA, WCE, MED, WSAF, ESAF, MDG, SAU, and EAU; for definitions of these regions, see Figure Atlas.2), with drought intensity (right scale) represented by the change of annual mean soil moisture, normalized with respect to interannual variability. Limits of the 5%–95% confidence interval are shown in panels (a–c). **(d)** Changes in Northern Hemisphere spring (March–April–May) snow cover extent relative to 1850–1900; (e,f) Relative change (%) in annual mean of total precipitable water (grey line), precipitation (red solid lines), runoff (blue solid lines) and in standard deviation (i.e., variability) of precipitation (red dashed lines) and runoff (blue dashed lines) averaged over **(e)** tropical and **(f)** extratropical land as function of global warming levels. Coupled Model Intercomparison Project Phase 6 (CMIP6) models that reached a 5°C warming level above the 1850–1900 average in the 21st century in SSP5-8.5 have been used. Precipitation and runoff variability are estimated by respective standard deviation after removing linear trends. Error bars show the 17–83% confidence interval for the warmest +5°C global warming level. {Figures 8.16, 9.24, 11.6, 11.7, 11.12, 11.15, 11.18 and Atlas.2}

There is *low confidence* that the increase of plant water-use efficiency due to higher atmospheric CO_2 concentration alleviates extreme agricultural and ecological droughts in conditions characterized by limited soil moisture and increased atmospheric evaporative demand. {2.3.1, Cross-Chapter Box 5.1, 8.2.3, 8.4.1, 11.2.4, 11.4, 11.6, Box 11.1}

Northern Hemisphere spring snow cover has decreased since at least 1978 (*very high confidence*), and there is *high confidence* that trends in snow cover loss extend back to 1950. It is *very likely* that human influence contributed to these reductions. Earlier onset of snowmelt has contributed to seasonally dependent changes in streamflow (*high confidence*). A further decrease of Northern Hemisphere seasonal snow cover extent is *virtually certain* under further global warming (Figure TS.12d). {2.3.2, 3.4.2, 8.3.2. 9.5.3, 12.4, 9.2, 11.2, Atlas 8.2}

The frequency and intensity of heavy precipitation events have increased over a majority of land regions with good observational coverage since 1950 (*high confidence,* Box TS.6, Table TS.2). Human influence is *likely* the main driver of this change (Table TS.2). It is *extremely likely* that on most land regions heavy precipitation will become more frequent and more intense with additional global warming (Table TS.2, Figure TS.12b). The projected increase in heavy precipitation extremes translates to an increase in the frequency and magnitude of pluvial floods (*high confidence*) (Table TS.2). {Cross-Chapter Box 3.2, 8.4.1, 11.4.2, 11.4.4, 11.5.5, 12.4}

The probability of compound extreme events has *likely* increased due to human-induced climate change. Concurrent heatwaves and droughts have become more frequent over the last century, and this trend will continue with higher global warming (*high confidence*). The probability of compound flooding (storm surge, extreme rainfall and/or river flow) has increased in some locations and will continue to increase due to both sea level rise and increases in heavy precipitation, including changes in precipitation intensity associated with tropical cyclones (*high confidence*). {11.8.1, 11.8.2, 11.8.3}

Changes in key aspects of the terrestrial biosphere, such as an increase of the growing season length in much of the Northern Hemisphere extratropics since the mid-20th century (*high confidence*), are consistent with large-scale warming. At the same time an increase in the amplitude of the seasonal cycle of atmospheric CO_2 poleward of 45°N since the early 1960s (*high confidence*) and a global-scale increase in vegetation greenness of the terrestrial surface since the early 1980s (*high confidence*) have been observed. Increasing atmospheric CO_2, warming at high latitudes, and land management interventions have contributed to the observed greening trend, but there is *low confidence* in their relative roles. There is *medium confidence* that increased plant growth associated with CO_2 fertilization is the main driver of the observed increase in amplitude of the seasonal cycle of atmospheric CO_2 in the Northern Hemisphere. Reactive nitrogen, ozone and aerosols affect terrestrial vegetation and carbon cycle through deposition and effects on large-scale radiation (*high confidence*), but the magnitude of these effects on the land carbon sink, ecosystem productivity and indirect CO_2 forcing remains uncertain. {2.3.4, 3.6.1, 5.2.1, 6.4.5, 12.3.7, 12.4}

Over the last century, there has been a poleward and upslope shift in the distribution of many land species (*very high confidence*) as well as increases in species turnover within many ecosystems (*high confidence*). There is *high confidence* that the geographical distribution of climate zones has shifted in many parts of the world in the last half century. The SRCCL concluded that continued warming will exacerbate desertification processes (*medium confidence*) and that ecosystems will become increasingly exposed to climates beyond those that they are currently adapted to (*high confidence*). There is *medium confidence* that climate change will increase disturbance by, for example, fire and tree mortality, across several ecosystems. Increases are projected in drought, aridity and fire weather in some regions (Section TS.4.3; *high confidence*). There is *low confidence* in the magnitude of these changes, but the probability of crossing uncertain regional thresholds (e.g., fires, forest dieback) increases with further warming (*high confidence*). The response of biogeochemical cycles to the anthropogenic perturbation can be abrupt at regional scales, and irreversible on decadal to century time scales (*high confidence*). {2.3.4, 5.4.3, 5.4.9, 11.6, 11.8, 12.5, SRCCL 2.2, SRCCL 2.5, SR1.5 3.4}

Box TS.6 | Water Cycle

Human-caused climate change has driven detectable changes in the global water cycle since the mid-20th century (*high confidence*), and it is projected to cause substantial further changes at both global and regional scales (*high confidence*).

Global land precipitation has *likely* increased since 1950, with a faster increase since the 1980s (*medium confidence*). Atmospheric water vapour has increased throughout the troposphere since at least the 1980s (*likely*). Annual global land precipitation will increase over the 21st century as global surface temperature increases (*high confidence*). Human influence has been detected in amplified surface salinity and precipitation minus evaporation (P–E) patterns over the ocean (*high confidence*).

The severity of very wet and very dry events increase in a warming climate (*high confidence*), but changes in atmospheric circulation patterns affect where and how often these extremes occur. Water cycle variability and related extremes are projected to increase faster than mean changes in most regions of the world and under all emissions scenarios (*high confidence*).

Over the 21st century, the total land area subject to drought will increase and droughts will become more frequent and severe (*high confidence*). Near-term projected changes in precipitation are uncertain mainly because of internal variability, model uncertainty and uncertainty in forcings from natural and anthropogenic aerosols (*medium confidence*).

Over the 21st century and beyond, abrupt human-caused changes to the water cycle cannot be excluded (*medium confidence*). {2.3, 3.3, 4.3, 4.4, 4.5, 4.6, 8.2, 8.3, 8.4, 8.5, 8.6, 11.4, 11.6, 11.9}

There is *high confidence* that the global water cycle has intensified since at least 1980 expressed by, for example, increased atmospheric moisture fluxes and amplified precipitation minus evaporation patterns. Global land precipitation has *likely* increased since 1950, with a faster increase since the 1980s (*medium confidence*), and a *likely* human contribution to patterns of change, particularly for increases in high-latitude precipitation over the Northern Hemisphere. Increases in global mean precipitation are determined by a robust response to global surface temperature (*very likely* 2–3% per °C) that is partly offset by fast atmospheric adjustments to atmospheric heating by greenhouse gases (GHGs) and aerosols (Section TS.3.2.2). The overall effect of anthropogenic aerosols is to reduce global precipitation through surface radiative cooling effects (*high confidence*). Over much of the 20th century, opposing effects of GHGs and aerosols on precipitation have been observed for some regional monsoons (*high confidence*) (Box TS.13). Global annual precipitation over land is projected to increase on average by 2.4% (–0.2% to +4.7% *likely* range) under SSP1-1.9, 4.6% (1.5% to 8.3% *likely* range) under SSP2-4.5, and 8.3% (0.9% to 12.9% *likely* range) under SSP5-8.5 by 2081–2100 relative to 1995–2014 (Box TS.6, Figure 1). Inter-model differences and internal variability contribute to a substantial range in projections of large-scale and regional water cycle changes (*high confidence*). The occurrence of volcanic eruptions can alter the water cycle for several years (*high confidence*). Projected patterns of precipitation change exhibit substantial regional differences and seasonal contrast as global surface temperature increases over the 21st century (Box TS.6, Figure 1). {2.3.1, 3.3.2, 3.3.3, 3.5.2, 4.3.1, 4.4.1, 4.5.1, 4.6.1, Cross-Chapter Box 4.1, 8.2.1, 8.2.2, 8.2.3, Box 8.1, 8.3.2.4, 8.4.1, 8.5.2, 10.4.2}

Global total column water vapour content has *very likely* increased since the 1980s, and it is *likely* that human influence has contributed to tropical upper tropospheric moistening. Near-surface specific humidity has increased over the ocean (*likely*) and land (*very likely*) since at least the 1970s, with a detectable human influence (*medium confidence*). Human influence has been detected in amplified surface salinity and precipitation minus evaporation (P–E) patterns over the ocean (*high confidence*). It is *virtually certain* that evaporation will increase over the ocean and *very likely* that evapotranspiration will increase over land, with regional variations under future surface warming (Box TS.6, Figure 1). There is *high confidence* that projected increases in precipitation amount and intensity will be associated with increased runoff in northern high latitudes (Box TS.6, Figure 1). In response to cryosphere changes (Section TS.2.5), there have been changes in streamflow seasonality, including an earlier occurrence of peak streamflow in high-latitude and mountain catchments (*high confidence*). Projected runoff (Box TS.6, Figure 1c) is typically decreased by contributions from small glaciers because of glacier mass loss, while runoff from larger glaciers will generally increase with increasing global warming levels until their mass becomes depleted (*high confidence*). {2.3.1, 3.3.2, 3.3.3, 3.5.2, 8.2.3, 8.4.1, 11.5}

Box TS.6 (continued)

Warming over land drives an increase in atmospheric evaporative demand and in the severity of drought events (*high confidence*). Greater warming over land than over the ocean alters atmospheric circulation patterns and reduces continental near-surface relative humidity, which contributes to regional drying (*high confidence*). A *very likely* decrease in relative humidity has occurred over much of the global land area since 2000. Projected increases in evapotranspiration due to growing atmospheric water demand will decrease soil moisture over the Mediterranean region, south-western North America, South Africa, South-Western South America and south-western Australia (*high confidence*) (Box TS.6, Figure 1). Some tropical regions are also projected to experience enhanced aridity, including the Amazon basin and Central America (*high confidence*). The total land area subject to increasing drought frequency and severity will expand (*high confidence*), and in the Mediterranean, South-Western South America, and Western North America, future aridification will far exceed the magnitude of change seen in the last millennium (*high confidence*). {4.5.1, 8.2.2, 8.2.3, 8.4.1, Box 8.2, 11.6, 11.9}

Land-use change and water extraction for irrigation have influenced local and regional responses in the water cycle (*high confidence*). Large-scale deforestation *likely* decreases evapotranspiration and precipitation and increases runoff over the deforested regions relative to the regional effects of climate change (*medium confidence*). Urbanization increases local precipitation (*medium confidence*) and runoff intensity (*high confidence*) (Box TS.14). Increased precipitation intensities have enhanced groundwater recharge, most notably in tropical regions (*medium confidence*). There is *high confidence* that groundwater depletion has occurred since at least the start of the 21st century, as a consequence of groundwater withdrawals for irrigation in agricultural areas in drylands. {8.2.3, 8.3.1, 11.1.6, 11.4, 11.6, FAQ 8.1}

Water cycle variability and related extremes are projected to increase faster than mean changes in most regions of the world and under all emissions scenarios (*high confidence*). A warmer climate increases moisture transport into weather systems, which intensifies wet seasons and events (*high confidence*). The magnitudes of projected precipitation increases and related extreme events depend on model resolution and the representation of convective processes (*high confidence*). Increases in near-surface atmospheric moisture capacity of about 7% per 1°C of warming lead to a similar response in the intensification of heavy precipitation from sub-daily up to seasonal time scales, increasing the severity of flood hazards (*high confidence*). The average and maximum rain-rates associated with tropical and extratropical cyclones, atmospheric rivers and severe convective storms will therefore also increase with future warming (*high confidence*). For some regions, there is *medium confidence* that peak tropical cyclone rain-rates will increase by more than 7% per 1°C of warming due to increased low-level moisture convergence caused by increases in wind intensity. In the tropics year-round and in the summer season elsewhere, interannual variability of precipitation and runoff over land is projected to increase at a faster rate than changes in seasonal mean precipitation (Figure TS.12e,f) (*medium confidence*). Sub-seasonal precipitation variability is also projected to increase, with fewer rainy days but increased daily mean precipitation intensity over many land regions (*high confidence*). {4.5.3, 8.2.3, 8.4.1, 8.4.2, 8.5.1, 8.5.2, 11.4, 11.5, 11.7, 11.9}

Box TS.6 (continued)

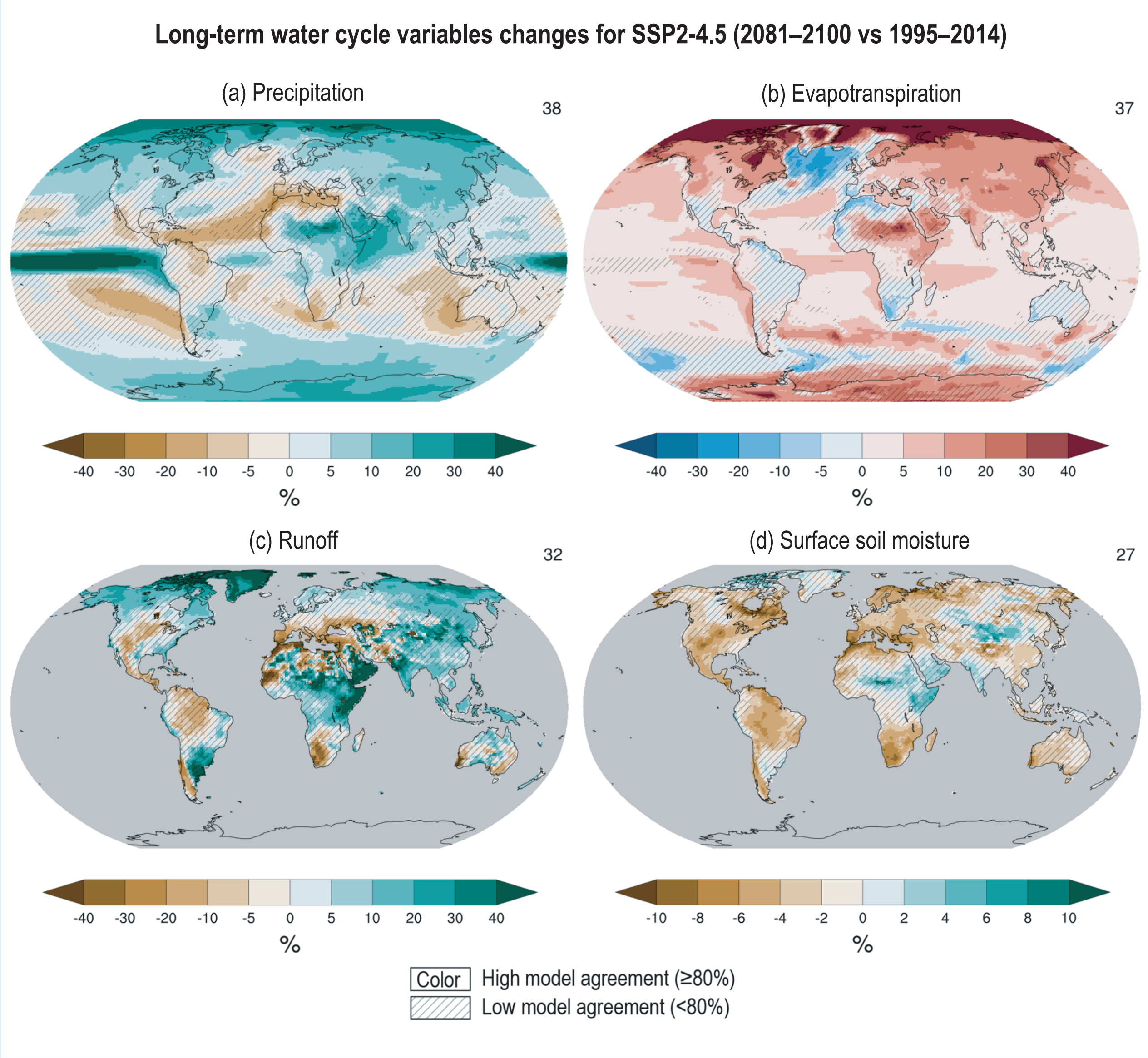

Box TS.6, Figure 1 | Projected water cycle changes. *The intent of this figure is to give a geographical overview of changes in multiple components of the global water cycle using an intermediate emissions scenario. Important key message: without drastic reductions in greenhouse gas emissions, human-induced global warming will be associated with widespread changes in all components of the water cycle.* Long-term (2081–2100) projected annual mean changes (%) relative to present-day (1995–2014) in the SSP2-4.5 emissions scenario for **(a)** precipitation, **(b)** surface evapotranspiration, **(c)** total runoff and **(d)** surface soil moisture. Numbers in top right of each panel indicate indicate the number of Coupled Model Intercomparison Project Phase 6 (CMIP6) models used for estimating the ensemble mean. For other scenarios, please refer to relevant figures in Chapter 8. Uncertainty is represented using the simple approach: No overlay indicates regions with high model agreement, where ≥80% of models agree on sign of change; diagonal lines indicate regions with low model agreement, where <80% of models agree on sign of change. For more information on the simple approach, please refer to the Cross-Chapter Box Atlas.1. {8.4.1; Figures 8.14, 8.17, 8.18, and 8.19}

Infographic TS.1 | Climate Futures

Climate futures

The climate change that people will experience this century and beyond depends on our **greenhouse gases emissions**, how much **global warming this will cause** and the **response of the climate system** to this warming.

Emissions pathways

Different social and economic developments can lead to substantially different future emissions of carbon dioxide (CO_2), other greenhouse gases and air pollutants for the rest of the century.

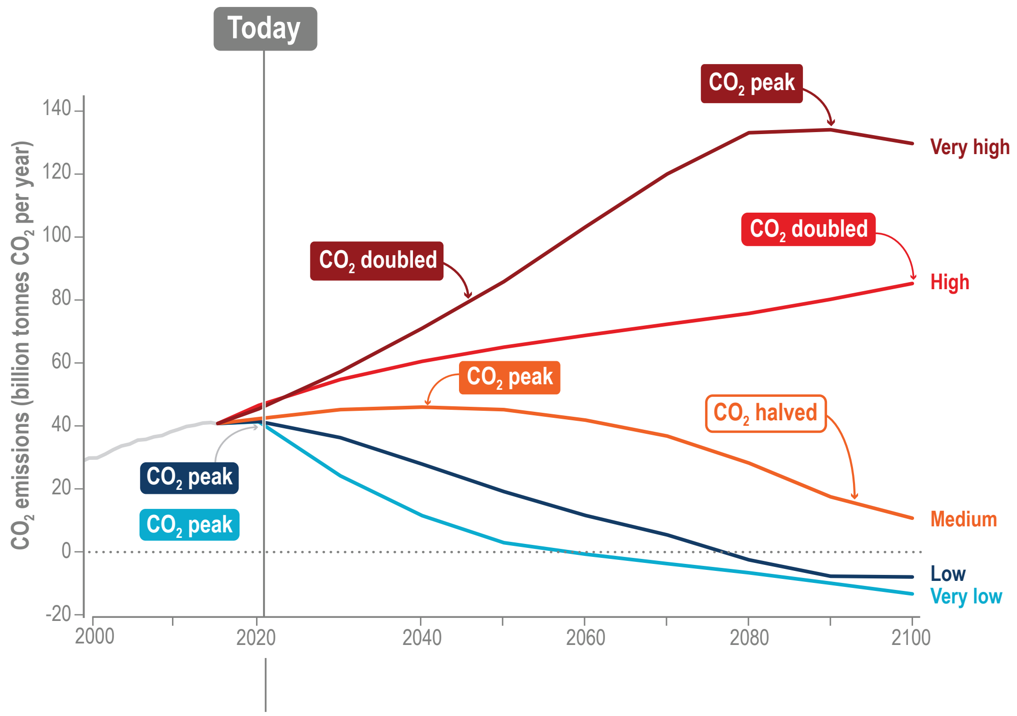

Effect on surface temperature

For temperature to stabilize, CO_2 emissions need to reach net zero.

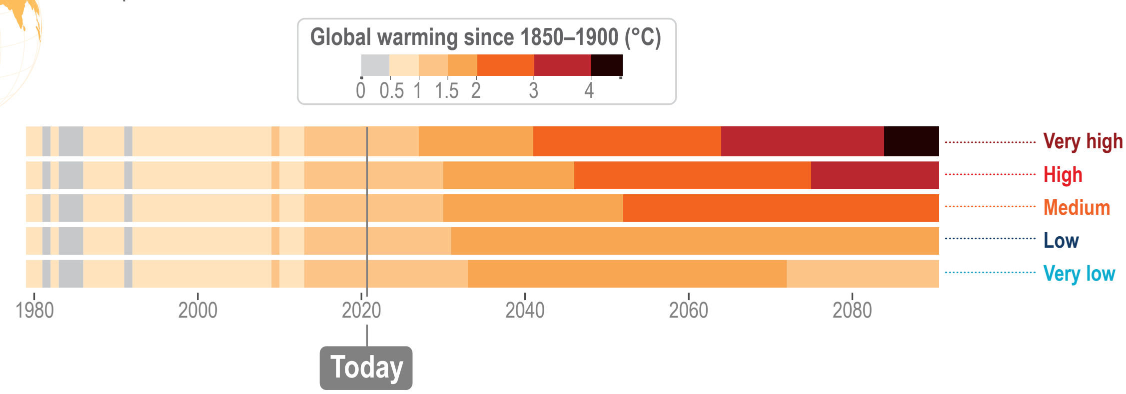

Short-term effect: Natural variability

Over short time scales (typically a decade), natural variability can temporarily dampen or accentuate global warming trends resulting from emissions.

Infographic TS.1 | Climate Futures. *The intent of this figure is to show possible climate futures: The climate change that people will experience this century and beyond depends on our greenhouse gas emissions, how much global warming this will cause and the response of the climate system to this warming.*

(top left) Annual emissions of CO_2 for the five core Shared Socio-economic Pathway (SSP) scenarios (very low: SSP1-1.9, low: SSP1-2.6, intermediate: SSP2-4.5, high: SSP3-7.0, very high: SSP5-8.5).**(bottom left)** Projected warming for each of these emissions scenarios.

Climate futures

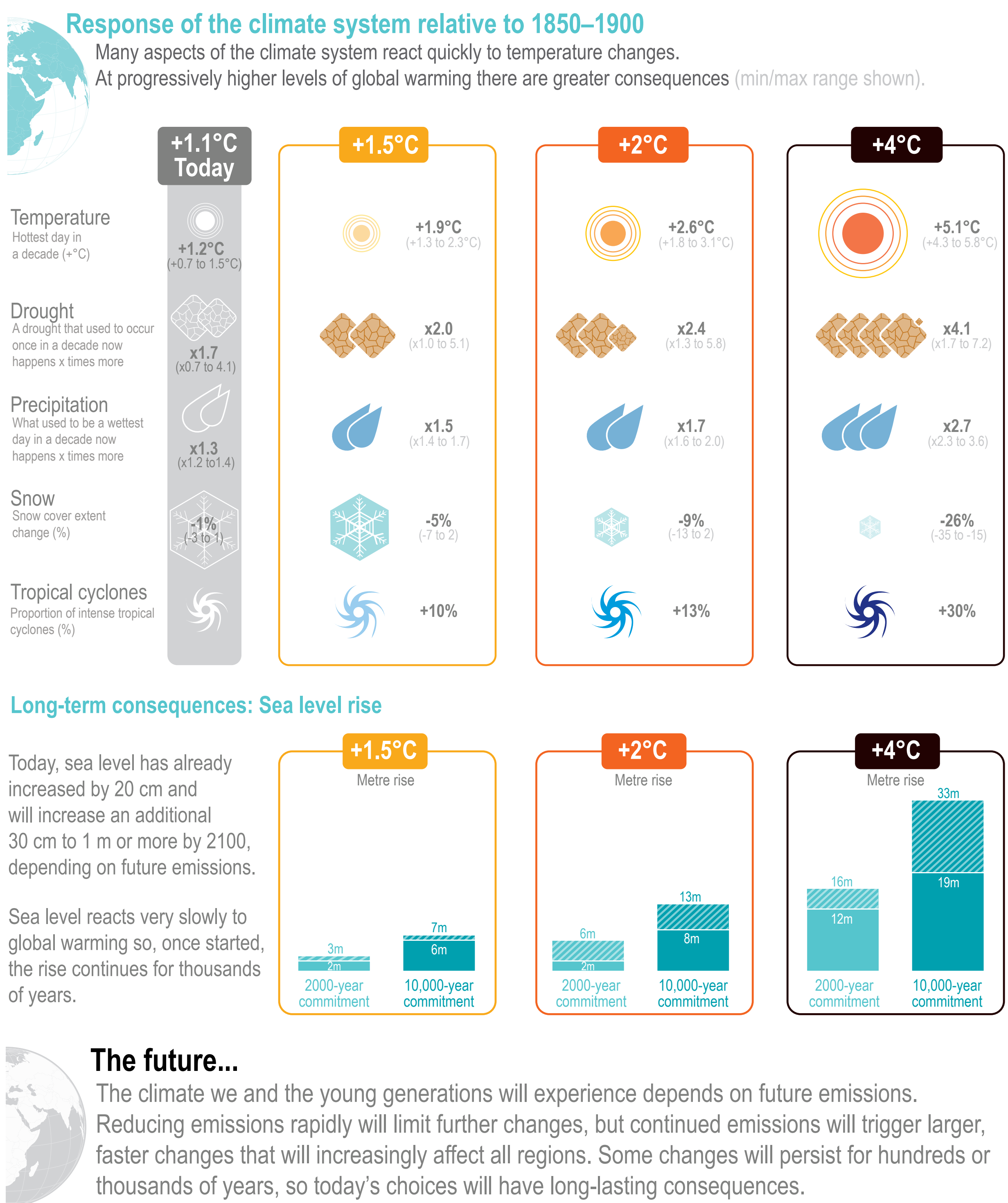

(top right) Response of some selected climate variables to four levels of global warming (°C). Changes in the 'Today' column are based on a global warming level of 1°C.
(bottom right) The long-term effect of each global warming level on sea level. See Section TS.1.3.1 for more detail on the SSP climate change scenarios.
This infographic builds from several figures in the Technical Summary: Figure TS.4 (for top left panel), Figure TS.6 (bottom left), Figure TS.12 (top right) and Box TS.4, Figure 1b (bottom right).

TS

TS.3 Understanding the Climate System Response and Implications for Limiting Global Warming

This section summarizes advances in our knowledge of Earth's energy budget, including the time evolution of forcings and climate feedbacks that lead to the climate system responses summarized in Section TS.2. It assesses advances since AR5 and SR1.5 in the estimation of remaining carbon budgets, the Earth system response to carbon dioxide removal, and the quantification of metrics that allow comparisons of the relative effects of different forcing agents. The section also highlights: future climate and air pollution responses due to projected changes in short-lived climate forcers (SLCFs); the state of understanding of the climate response to potential interventions related to solar radiation modification (SRM); and irreversibility, tipping points and abrupt changes in the climate system.

TS.3.1 Radiative Forcing and Energy Budget

Since AR5, the accumulation of energy in the Earth system, quantified by observations of warming of the ocean, atmosphere, and land and melting of ice, has become established as a robust measure of the rate of global climate change on interannual-to-decadal time scales. Compared to changes in global surface temperature, the increase in the global energy inventory exhibits less variability, and thus better indicates underlying climate trends.

The global energy inventory increased by 282 [177 to 387] zettajoules (ZJ, equal to 10^{21} Joules) for the period 1971–2006 and 152 [100 to 205] ZJ for the period 2006–2018 (Figure TS.13), with more than 90% accounted for

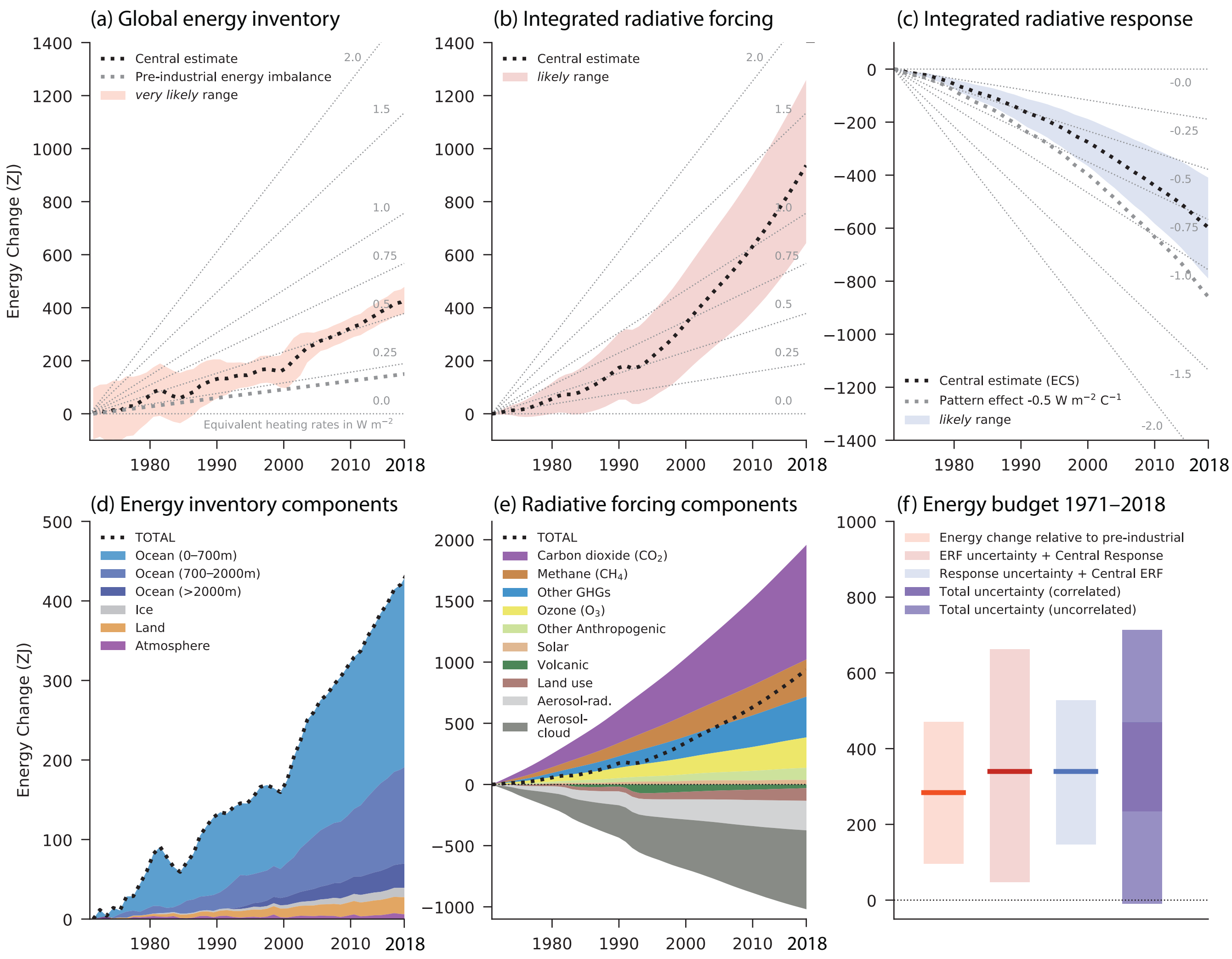

Figure TS.13 | Estimates of the net cumulative energy change (ZJ = 10^{21} Joules) for the period 1971–2018 associated with (a) observations of changes in the global energy inventory, (b) integrated radiative forcing, and (c) integrated radiative response. *The intent is to show assessed changes in energy budget and effective radiative forcings (ERFs).* Black dotted lines indicate the central estimate with *likely* and *very likely* ranges as indicated in the legend. The grey dotted lines indicate the energy change associated with an estimated 1850–1900 Earth energy imbalance of 0.2 W m^{-2} (panel a) and an illustration of an assumed pattern effect of –0.5 W m^{-2} °C^{-1} (panel c). Background grey lines indicate equivalent heating rates in W m^{-2} per unit area of Earth's surface. Panels **(d)** and **(e)** show the breakdown of components, as indicated in the legend, for the global energy inventory and integrated radiative forcing, respectively. Panel **(f)** shows the global energy budget assessed for the period 1971–2018, that is, the consistency between the change in the global energy inventory relative to 1850–1900 and the implied energy change from integrated radiative forcing plus integrated radiative response under a number of different assumptions, as indicated in the figure legend, including assumptions of correlated and uncorrelated uncertainties in forcing plus response. Shading represents the *very likely* range for observed energy change relative to 1850–1900 and *likely* range for all other quantities. Forcing and response time series are expressed relative to a baseline period of 1850–1900. {Box 7.2, Figure 1}

by ocean warming. To put these numbers in context, the 2006–2018 average Earth energy imbalance is equivalent to approximately 20 times the annual rate of global energy consumption in 2018. The accumulation of energy is driven by a positive total anthropogenic effective radiative forcing (ERF) relative to 1750.

The best estimate ERF of 2.72 W m^{-2} has increased by 0.43 W m^{-2} relative to that given in AR5 (for 1750–2014) due to an increase in the greenhouse gas ERF that is partly compensated by a more negative aerosol ERF compared to AR5. The greenhouse gas ERF has been revised due to changes in atmospheric concentrations and updates to forcing efficiencies, while the revision to aerosol ERF is due to increased understanding of aerosol–cloud interactions and is supported by improved agreement between different lines of evidence. Improved quantifications of ERF, the climate system radiative response, and the observed energy increase in the Earth system for the period 1971–2018 demonstrate improved closure of the global energy budget (i.e., the extent to which the sum of the integrated forcing and the integrated radiative response equals the energy gain of the Earth system) compared to AR5 (*high confidence*). (See FAQ 7.1). {7.2.2, 7.3.5, 7.5.2, Box 7.2, Table 7.1}

The global energy inventory change for the period 1971–2006 corresponds to an Earth energy imbalance (Box TS.1) of 0.50 [0.32 to 0.69] W m^{-2}, increasing to 0.79 [0.52 to 1.06] W m^{-2} for the period 2006–2018. Ocean heat uptake is by far the largest contribution and accounts for 91% of the total energy change. Land warming, melting of ice and warming of the atmosphere account for about 5%, 3% and 1% of the total change, respectively. More comprehensive analysis of inventory components, cross-validation of satellite and in situ-based estimates of the global energy imbalance, and closure of the global sea level budget have led to a strengthened assessment relative to AR5. (*high confidence*) {7.2.2, 7.5.2.3, Box 7.2, Table 7.1, 9.6.1, Cross-Chapter Box 9.1, Table 9.5}

As in AR5, the perturbations to Earth's top-of-atmosphere energy budget are quantified using ERFs (see also Section TS.2.2). These include any consequent adjustments to the climate system (e.g., from changes in atmospheric temperatures, clouds and water vapour as shown in Figure TS.14), but exclude any surface temperature response. Since AR5, ERFs have been estimated for a larger number of forcing agents and shown to be more closely related to the temperature response than the stratospheric-temperature-adjusted radiative forcing. (*high confidence*) {7.3.1}

Improved quantifications of ERF, the climate system radiative response, and the observed energy increase in the Earth system for the period 1971–2018 demonstrate improved closure of the global energy budget relative to AR5 (Figure TS.13). Combining the *likely* range of ERF over this period with the central estimate of radiative response gives an expected energy gain of 340 [47 to 662] ZJ. Both estimates are consistent with an independent observation-based assessment of the global energy increase of 284 [96 to 471] ZJ (*very likely range*), expressed relative to the estimated 1850–1900 Earth energy imbalance. (*high confidence*) {7.2.2, 7.3.5, Box 7.2}

The assessed greenhouse gas ERF over the 1750–2019 period (Section TS.2.2) has increased by +0.59 W m^{-2} over AR5 estimates for 1750–2011. This increase includes +0.34 W m^{-2} from increases in atmospheric concentrations of well-mixed greenhouse gases (including halogenated species) since 2011, +0.15 W m^{-2} from upwards revisions of their radiative efficiencies and +0.10 W m^{-2} from re-evaluation of the ozone and stratospheric water vapour ERF. {7.3.2, 7.3.4, 7.3.5}

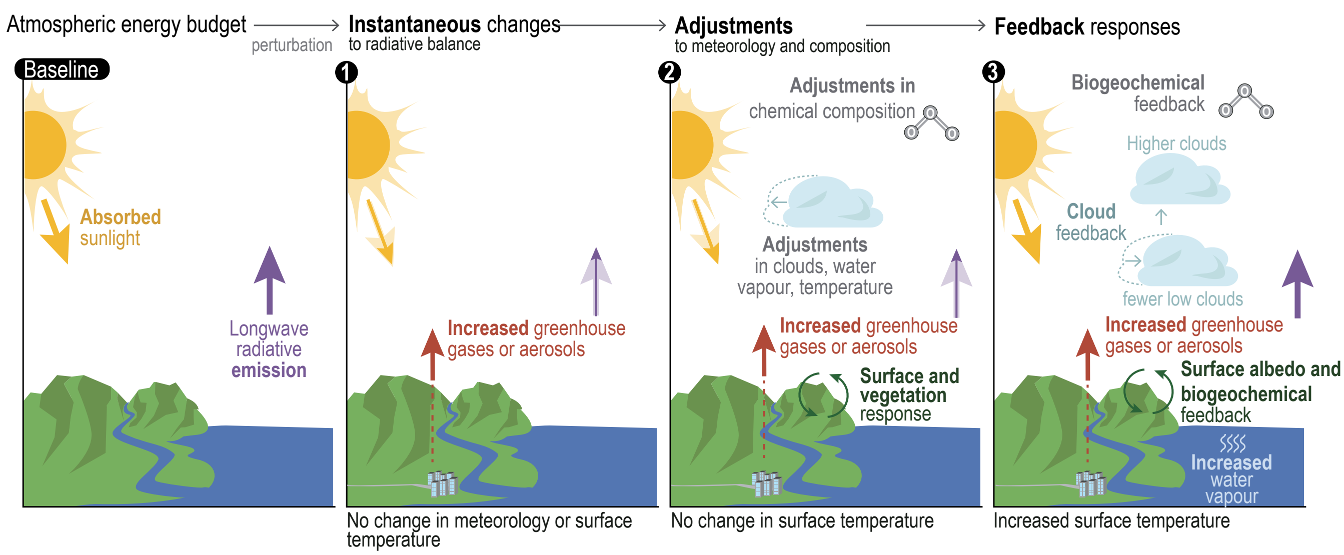

Figure TS.14 | Schematic representation of changes in the top-of-atmosphere (TOA) radiation budget following a perturbation. *The intent of this figure is to illustrate the concept of adjustments in the climate system following a perturbation in the radiation budget.* The baseline TOA energy budget **(a)** responds instantaneously to perturbations **(b)**, leading to adjustments in the atmospheric meteorology and composition and land surface that are independent of changes in surface temperature **(c)**. Surface temperature changes (here using an increase as an example) lead to physical, biogeophysical and biogeochemical feedback processes **(d)**. Long-term feedback processes, such as those involving ice sheets, are not shown here. {adapted from Figure 7.2; FAQ 7.2, Figure 1; and Figure 8.3}

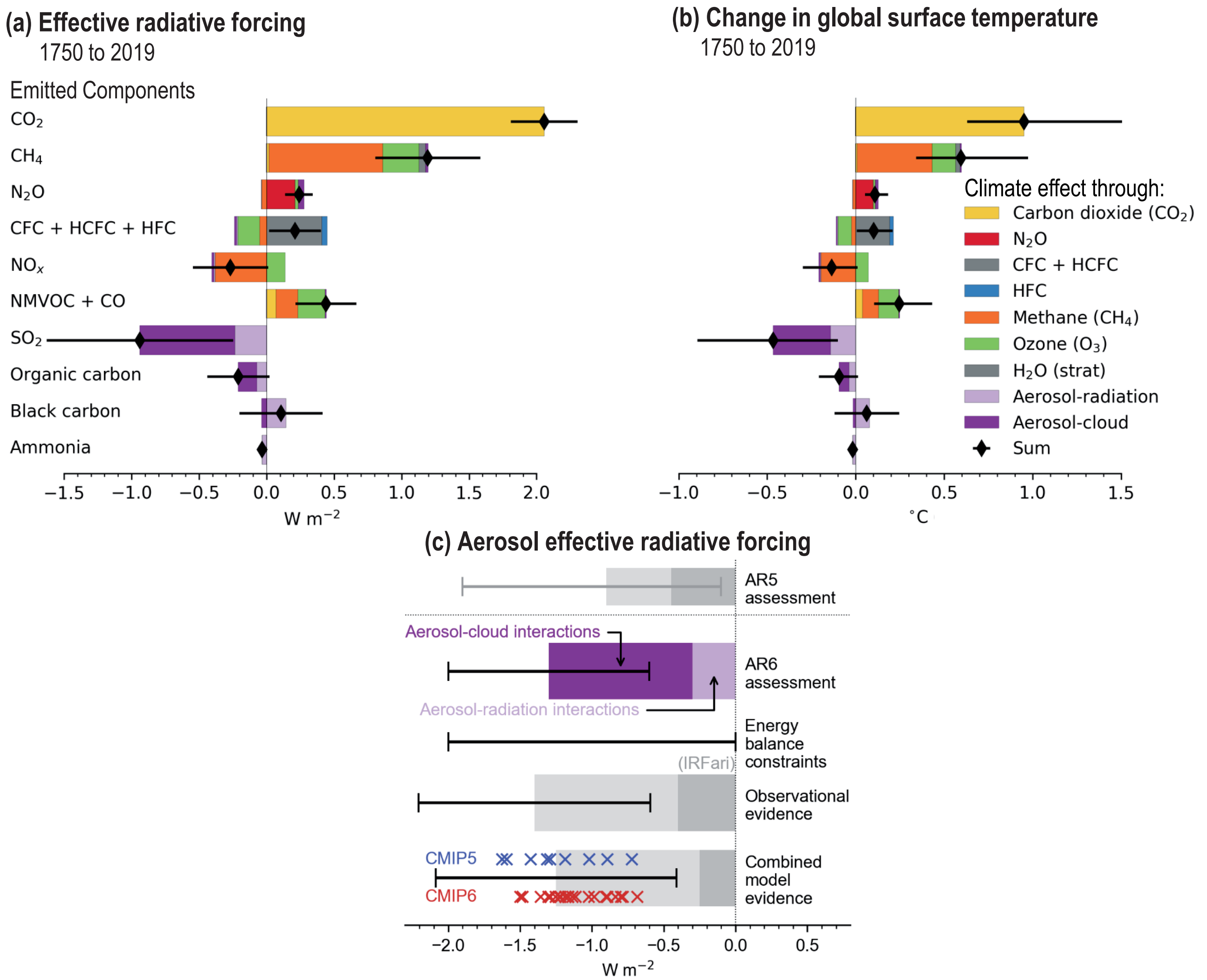

Figure TS.15 | Contribution to (a) effective radiative forcing (ERF) and (b) global surface temperature change from component emissions for 1750–2019 based on Coupled Model Intercomparison Project Phase 6 (CMIP6) models and (c) net aerosol ERF for 1750–2014 from different lines of evidence. *The intent of this figure is to show advances since AR5 in the understanding of (a) emissions-based ERF, (b) global surface temperature response for short-lived climate forcers as estimated in Chapter 6, and (c) aerosol ERF from different lines of evidence as assessed in Chapter 7.* **In panel (a),** ERFs for well-mixed greenhouse gases (WMGHGs) are from the analytical formulae. ERFs for other components are multi-model means based on Earth system model simulations that quantify the effect of individual components. The derived emissions-based ERFs are rescaled to match the concentration-based ERFs in Figure 7.6. Error bars are 5–95% and for the ERF account for uncertainty in radiative efficiencies and multi-model error in the means. **In panel (b),** the global mean temperature response is calculated from the ERF time series using an impulse response function. **In panel (c),** the AR6 assessment is based on energy balance constraints, observational evidence from satellite retrievals, and climate model-based evidence. For each line of evidence, the assessed best-estimate contributions from ERF due to aerosol–radiation interactions (ERFari) and aerosol–cloud interactions (ERFaci) are shown with darker and paler shading, respectively. Estimates from individual CMIP Phase 5 (CMIP5) and CMIP6 models are depicted by blue and red crosses, respectively. The observational assessment for ERFari is taken from the instantaneous forcing due to aerosol–radiation interactions (IRFari). Uncertainty ranges are given in black bars for the total aerosol ERF and depict *very likely* ranges. {6.4.2, Figure 6.12, 7.3.3, Cross-Chapter Box 7.1, Table 7.8, Figure 7.5}

For CO_2, CH_4, N_2O, and chlorofluorocarbons, there is now evidence to quantify the effect on ERF of tropospheric adjustments. The assessed ERF for a doubling of CO_2 compared to 1750 levels (3.9 ± 0.5 Wm^{-2}) is larger than in AR5. For CO_2, the adjustments include the physiological effects on vegetation. The reactive well-mixed greenhouse gases (CH_4, N_2O, and halocarbons) cause additional chemical adjustments to the atmosphere through changes in ozone and aerosols (Figure TS.15a). The ERF due to CH_4 emissions is 1.19 [0.81 to 1.58] W m^{-2}, of which 0.35 [0.16 to 0.54] W m^{-2} is attributed to chemical adjustments mainly via ozone. These chemical adjustments also affect the emissions metrics (Section TS.3.3.3). Changes in sulphur dioxide (SO_2) emissions make the dominant contribution to the ERF from aerosol–cloud interactions (*high confidence*). Over the 1750–2019 period, the contributions from the emitted compounds to global surface temperature changes broadly match their contributions to the ERF (*high confidence*) (Figure TS.15b). Since a peak in emissions-induced SO_2 ERF has already occurred recently (Section TS.2.2) and since there is a delay in the full global surface temperature response owing to the thermal inertia in the climate system, changes in SO_2 emissions have a slightly larger contribution to global surface temperature change compared with changes in CO_2 emissions, relative to their respective contributions to ERF. {6.4.2, 7.3.2}

Aerosols contributed an ERF of –1.3 [–2.0 to –0.6] W m^{-2} over the period 1750 to 2014 (*medium confidence*). The ERF due to aerosol–cloud interactions (ERFaci) contributes most to the magnitude of the total aerosol ERF (*high confidence*) and is assessed to be –1.0 [–1.7 to –0.3] W m^{-2} (*medium confidence*), with the remainder due to aerosol–radiation interactions (ERFari), assessed to be –0.3 [–0.6 to 0.0] W m^{-2} (*medium confidence*). There has been an increase in the estimated magnitude – but a reduction in the uncertainty – of the total aerosol ERF relative to AR5, supported by a combination of increased process-understanding and progress in modelling and observational analyses (Figure TS.15c). Effective radiative forcing estimates from these separate lines of evidence are now consistent with each other, in contrast to AR5, and support the assessment that it is *virtually certain* that the total aerosol ERF is negative. Compared to AR5, the assessed magnitude of ERFaci has increased, while that of ERFari has decreased. {7.3.3, 7.3.5}

TS.3.2 Climate Sensitivity and Earth System Feedbacks

TS.3.2.1 Equilibrium Climate Sensitivity, Transient Climate Response, and Transient Climate Response to Cumulative Carbon-dioxide Emissions

Since AR5, substantial quantitative progress has been made in combining new evidence of Earth's climate sensitivity with improvements in the understanding and quantification of Earth's energy imbalance, the instrumental record of global surface temperature change, paleoclimate change from proxy records, climate feedbacks and their dependence on time scale and climate state. A key advance is the broad agreement across these multiple lines of evidence, supporting a best estimate of equilibrium climate sensitivity of 3°C, with a *very likely* range of 2°C to 5°C. The *likely* range of 2.5°C to 4°C is narrower than the AR5 *likely* range of 1.5°C to 4.5°C. {7.4, 7.5}

Constraints on equilibrium climate sensitivity (ECS) and transient climate response (TCR) (see Glossary) are based on four main lines of evidence: feedback process understanding, climate change and variability seen within the instrumental record, paleoclimate evidence, and so-called 'emergent constraints', whereby a relationship between an observable quantity and either ECS or TCR established within an ensemble of models is combined with observations to derive a constraint on ECS or TCR. In reports up to and including the IPCC Third Assessment Report, ECS and TCR derived directly from ESMs were the primary line of evidence. However, since AR4, historical warming and paleoclimates provided useful additional evidence (Figure TS.16a). This Report differs from previous reports in not directly using climate model estimates of ECS and TCR in the assessed ranges of climate sensitivity. {1.5, 7.5}

It is now clear that when estimating ECS and TCR, the dependence of feedbacks on time scales and the climate state must be accounted for. Feedback processes are expected to become more positive overall (more amplifying of global surface temperature changes) on multi-decadal time scales as the spatial pattern of surface warming evolves and global surface temperature increases, leading to an ECS that is higher than was inferred in AR5 based on warming over the instrumental record (*high confidence*). Historical surface temperature change since 1870 has shown relatively little warming in several key regions of positive feedbacks, including the eastern equatorial Pacific Ocean and the Southern Ocean, while showing greater warming in key regions of negative feedbacks, including the western Pacific warm pool. Based on process understanding, climate modelling, and paleoclimate reconstructions of past warm periods, it is expected that future warming will become enhanced over the eastern Pacific Ocean (*medium confidence*) and Southern Ocean (*high confidence*) on centennial time scales. This new understanding, along with updated estimates of historical temperature change, ERF, and energy imbalance, reconciles previously disparate ECS estimates. {7.4.4, 7.5.2, 7.5.3}

The AR6 best estimate of ECS is 3°C, the *likely* range is 2.5°C to 4°C and the *very likely* range is 2°C to 5°C. There is a high level of agreement among the four main lines of evidence listed above (Figure TS.16b), and altogether it is *virtually certain* that ECS is larger than 1.5°C, but currently it is not possible to rule out ECS values above 5°C. Therefore, the 5°C upper end of the *very likely* range is assessed with *medium confidence* and the other bounds with *high confidence*. {7.5.5}

Based on process understanding, warming over the instrumental record, and emergent constraints, the best estimate of TCR is 1.8°C, the *likely* range is 1.4°C to 2.2°C and the *very likely* range is 1.2°C to 2.4°C. There is a high level of agreement among the different lines of evidence (Figure TS.16c) (*high confidence*). {7.5.5}

On average, CMIP6 models have higher mean ECS and TCR values than the CMIP5 generation of models and also have higher mean values and wider spreads than the assessed best estimates and *very likely* ranges within this Report. These higher mean ECS and TCR values can be traced to a positive net cloud feedback that is larger in CMIP6 by about 20%. The broader ECS and TCR ranges from CMIP6 also lead the models to project a range of future warming that is wider than the assessed future warming range, which is based on multiple lines of evidence (Cross-Section Box TS.1). However, some of the high-sensitivity CMIP6 models (Section TS.1.2.2) are less consistent with observed recent changes in global warming and with paleoclimate proxy records than models with ECS within the *very likely* range. Similarly, some of the low-sensitivity models are less consistent with the paleoclimate data. The CMIP6 models with the highest ECS and TCRs values provide insights into low-likelihood, high-impact futures, which cannot be excluded based on currently available evidence (Cross-Section Box TS.1). {4.3.1, 4.3.4, 7.4.2, 7.5.6}

Uncertainties regarding the true value of ECS and TCR are the dominant source of uncertainty in global temperature projections over the 21st century under moderate to high GHG concentrations scenarios. For scenarios that reach net zero CO_2 emissions (Section TS.3.3), the uncertainty in the ERF values of aerosol and other SLCFs contribute substantial uncertainty in projected temperature. Global ocean heat uptake is a smaller source of uncertainty in centennial warming. {7.5.7}

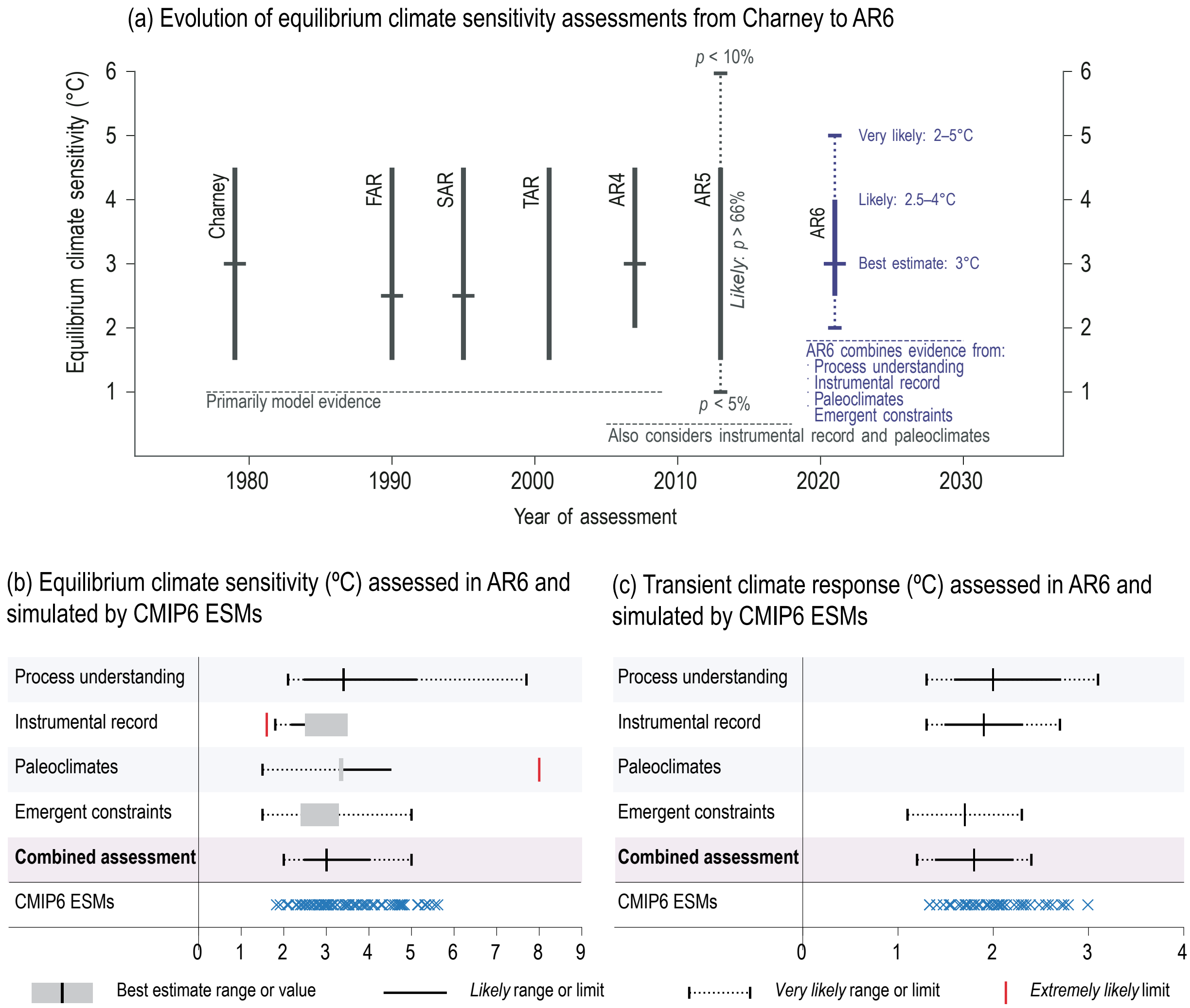

Figure TS.16 | (a) Evolution of equilibrium climate sensitivity (ECS) assessments from the Charney Report through a succession of IPCC Assessment Reports to AR6, and lines of evidence and combined assessment for (b) ECS and (c) transient climate response (TCR) in AR6. *The intent of this figure is to show the progression in estimates of ECS, including uncertainty and the lines of evidence used for assessment, and to show the lines of assessment used to assess ECS and TCR in AR6.* **In panel (a),** the lines of evidence considered are listed below each assessment. Best estimates are marked by horizontal bars, *likely* ranges by vertical bars, and *very likely* ranges by dotted vertical bars. **In panel (b) and (c),** assessed ranges are taken from Tables 7.13 and 7.14 for ECS and TCR respectively. Note that for the ECS assessment based on both the instrumental record and paleoclimates, limits (i.e., one-sided distributions) are given, which have twice the probability of being outside the maximum/minimum value at a given end, compared to ranges (i.e., two tailed distributions) which are given for the other lines of evidence. For example, the *extremely likely* limit of greater than 95% probability corresponds to one side of the *very likely* (5% to 95%) range. Best estimates are given as either a single number or by a range represented by grey box. Coupled Model Intercomparison Project Phase 6 (CMIP6) Earth system model (ESM) values are not directly used as a line of evidence but are presented on the figure for comparison. {1.5, 7.5; Tables 7.13 and 7.14; Figure 7.18}

The transient climate response to cumulative CO_2 emissions (TCRE) is the ratio between globally averaged surface temperature increase and cumulative CO_2 emissions (see Glossary). This Report reaffirms with *high confidence* the finding of AR5 that there is a near-linear relationship between cumulative CO_2 emissions and the increase in global average temperature caused by CO_2 over the course of this century for global warming levels up to at least 2°C relative to 1850–1900. The TCRE falls *likely* in the 1.0°C–2.3°C per 1000 PgC range, with a best estimate of 1.65°C per 1000 PgC. This is equivalent to a 0.27°C–0.63°C range with a best estimate of 0.45°C when expressed in units per 1000 $GtCO_2$. This range is about 15% narrower than the 0.8°–2.5°C per 1000 PgC assessment of AR5 because of a better integration of evidence across chapters, in particular the assessment of TCR. Beyond this century, there is *low confidence* that the TCRE alone remains an accurate predictor of temperature changes in scenarios of very low or net negative CO_2 emissions because of uncertain Earth system feedbacks that can result in further changes in temperature or a path dependency of warming as a function of cumulative CO_2 emissions. {4.6.2, 5.4, 5.5.1}

TS.3.2.2 Earth System Feedbacks

The combined effect of all climate feedback processes is to amplify the climate response to forcing (*virtually certain*). While major advances in the understanding of cloud processes have increased the level of confidence and decreased the uncertainty range for the cloud feedback by about 50% compared to AR5, clouds remain the largest contribution to overall uncertainty in climate feedbacks (*high confidence*). Uncertainties in the ECS and other climate sensitivity metrics, such as the TCR and TCRE, are the dominant source of uncertainty in global temperature projections over the 21st century under moderate to high GHG emissions scenarios. CMIP6 models have higher mean values and wider spreads in ECS and TCR than the assessed best estimates and *very likely* ranges within this Report, leading the models to project a range of future warming that is wider than the assessed future warming range (Section TS.2.2). {7.1, 7.4.2, 7.5}

Earth system feedbacks can be categorized into three broad groups: physical feedbacks, biogeophysical and biogeochemical feedbacks, and feedbacks associated with ice sheets. In previous assessments, the ECS has been associated with a distinct set of physical feedbacks (Planck response, water vapour, lapse rate, surface albedo, and cloud feedbacks). In this assessment, a more general definition of ECS is adopted whereby all biogeophysical and biogeochemical feedbacks that do not affect the atmospheric concentration of CO_2 are included. These include changes in natural CH_4 emissions, natural aerosol emissions, N_2O, ozone, and vegetation, which all act on time scales of years to decades and are therefore relevant for temperature change over the 21st century. Because the total biogeophysical and non-CO_2 biogeochemical feedback is assessed to have a central value that is near zero (*low confidence*), including it does not affect the assessed ECS but does contribute to the net feedback uncertainty. The biogeochemical feedbacks that affect the atmospheric concentration of CO_2 are not included because ECS is defined as the response to a sustained doubling of CO_2. Moreover, the long-term feedbacks associated with ice sheets are not included in the ECS owing to their long time scales of adjustment. {5.4, 6.4, 7.4, 7.5, Box 7.1}

The net effect of changes in clouds in response to global warming is to amplify human-induced warming, that is, the net cloud feedback is positive (*high confidence*). Compared to AR5, major advances in the understanding of cloud processes have increased the level of confidence and decreased the uncertainty range in the cloud feedback by about 50% (Figure TS.17a). An assessment of the low-altitude cloud feedback over the subtropical ocean, which was previously the major source of uncertainty in the net cloud feedback, is improved owing to a combined use of climate model simulations, satellite observations, and explicit simulations of clouds, altogether leading to strong evidence that this type of cloud amplifies global warming. The net cloud feedback is assessed to be +0.42 [–0.10 to 0.94] W m^{-2} °C^{-1}. A net negative cloud feedback is *very unlikely*. The CMIP5 and CMIP6 ranges of cloud feedback are similar to this assessed range, with CMIP6 having a slightly more positive median cloud feedback (*high confidence*). The surface albedo feedback and combined water vapour-lapse rate feedback are positive (Figure TS.17a), with *high confidence* in the estimated value of each based on multiple lines of evidence, including observations, models and theory (Box TS.6). {7.4.2, Figure 7.14, Table 7.10}

Natural sources and sinks of non-CO_2 greenhouse gases such as methane (CH_4) and nitrous oxide (N_2O) respond both directly and indirectly to atmospheric CO_2 concentration and climate change, and thereby give rise to additional biogeochemical feedbacks in the climate system. Many of these feedbacks are only partially understood and are not yet fully included in ESMs. There is *medium confidence* that the net response of natural ocean and land CH_4 and N_2O sources to future warming will be increased emissions, but the magnitude and timing of the responses of each individual process is known with *low confidence*. {5.4.7}

Non-CO_2 biogeochemical feedbacks induced from changes in emissions, abundances or lifetimes of SLCFs mediated by natural processes or atmospheric chemistry are assessed to decrease ECS (Figure TS.17b). These non-CO_2 biogeochemical feedbacks are estimated from ESMs, which since AR5 have advanced to include a consistent representation of biogeochemical cycles and atmospheric chemistry. However, process-level understanding of many biogeochemical feedbacks involving SLCFs, particularly natural emissions, is still emerging, resulting in *low confidence* in the magnitude and sign of the feedbacks. The central estimate of the total biogeophysical and non-CO_2 biogeochemical feedback is assessed to be –0.01 [–0.27 to +0.25] W m^{-2} °C^{-1} (Figure TS.17a). {5.4.7, 5.4.8, 6.2.2, 6.4.5, 7.4, Table 7.10}

The combined effect of all known radiative feedbacks (physical, biogeophysical, and non-CO_2 biogeochemical) is to amplify the base climate response (in the absence of feedbacks), also known as the Planck temperature response[20] (*virtually certain*). Combining these feedbacks with the Planck response, the net climate feedback parameter is assessed to be –1.16 [–1.81 to –0.51] W m^{-2} °C^{-1}, which is slightly less negative than that inferred from the overall ECS assessment. The combined water vapour and lapse rate feedback makes the largest single contribution to global warming, whereas the cloud feedback remains the largest contribution to overall uncertainty. Due to the state-dependence of feedbacks, as evidenced from paleoclimate observations and from models, the net feedback parameter will increase (become less negative) as global temperature increases. Furthermore, on long time scales the ice-sheet feedback parameter is *very likely* positive, promoting additional warming on millennial time scales as ice sheets come into equilibrium with the forcing. (*high confidence*) {7.4.2, 7.4.3, Figure 7.14, Table 7.10}

The carbon cycle provides for additional feedbacks on climate owing to the sensitivity of land–atmosphere and ocean–atmosphere carbon fluxes and storage to changes in climate and in atmospheric CO_2 (Figure TS.17c). Because of the time scales associated with land and ocean carbon uptake, these feedbacks are known to be scenario dependent. Feedback estimates deviate from linearity in scenarios of stabilizing or reducing concentrations. With *high confidence*, increased atmospheric CO_2 will lead to increased land and ocean carbon uptake, acting as a negative feedback on climate change. It is *likely* that a warmer climate will lead to reduced land and ocean carbon uptake, acting as a positive feedback (Box TS.5). {4.3.2, 5.4.1–5}

20 For reference, the Planck temperature response for a doubling of atmospheric CO_2 is approximately 1.2°C at equilibrium.

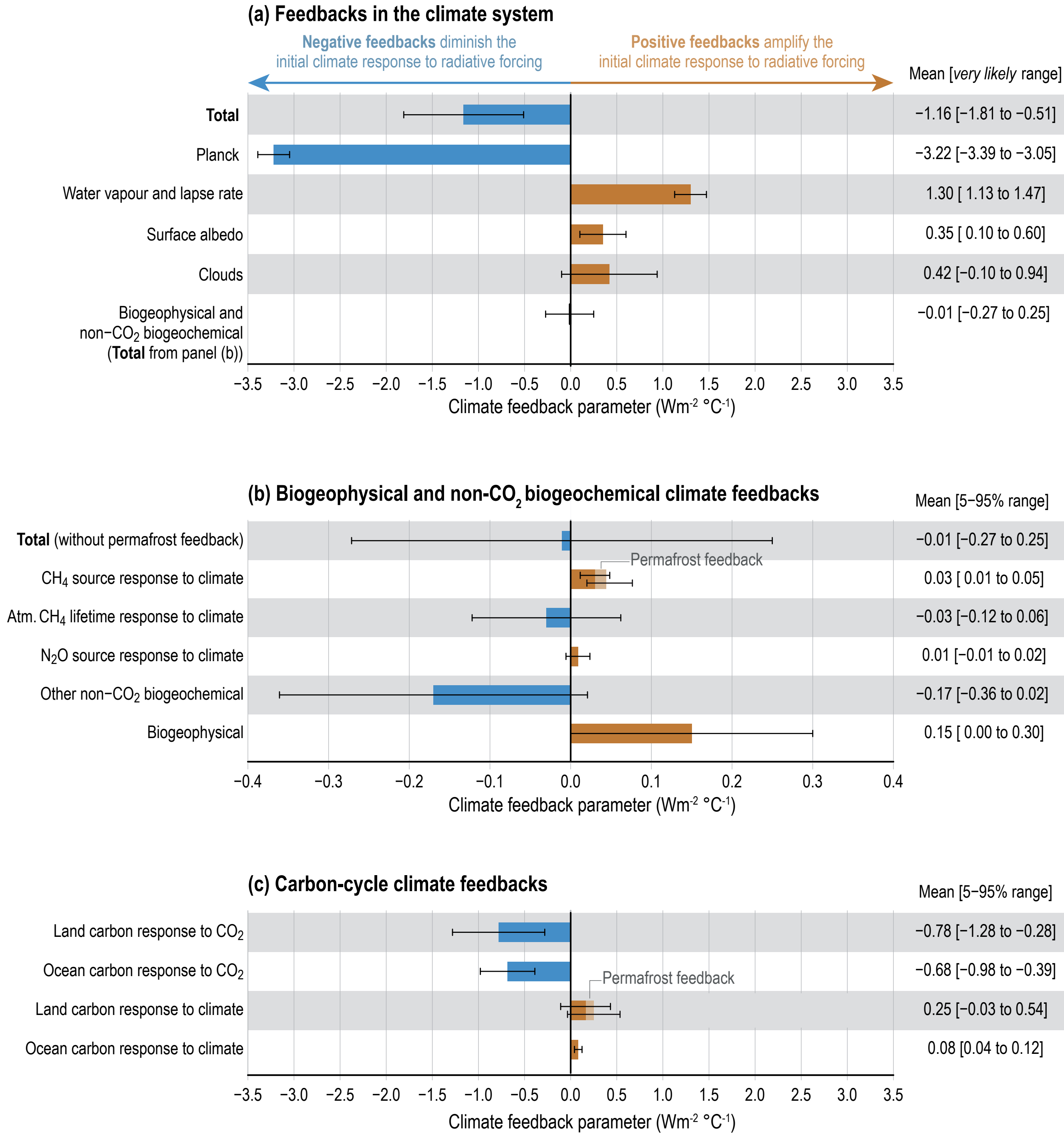

Figure TS.17 | An overview of physical and biogeochemical feedbacks in the climate system. *The intent of this figure is to summarize assessed estimates of physical, biogeophysical and biogeochemical feedbacks on global temperature based on Chapters 5, 6 and 7.* **(a)** Synthesis of physical, biogeophysical and non-carbon dioxide (CO_2) biogeochemical feedbacks that are included in the definition of equilibrium climate sensitivity (ECS) assessed in this Technical Summary. These feedbacks have been assessed using multiple lines of evidence including observations, models and theory. The net feedback is the sum of the Planck response, water vapour and lapse rate, surface albedo, cloud, and biogeophysical and non-CO_2 biogeochemical feedbacks. Bars denote the mean feedback values, and uncertainties represent *very likely* ranges; **(b)** Estimated values of individual biogeophysical and non-CO_2 biogeochemical feedbacks. The atmospheric methane (CH_4) lifetime and other non-CO_2 biogeochemical feedbacks have been calculated using global Earth system model simulations from AerChemMIP, while the CH_4 and nitrous oxide (N_2O) source responses to climate have been assessed for the year 2100 using a range of modelling approaches using simplified radiative forcing equations. The estimates represent the mean and 5–95% range. The level of confidence in these estimates is *low* owing to the large model spread. **(c)** Carbon-cycle feedbacks as simulated by models participating in the C4MIP of the Coupled Model Intercomparison Project Phase 6 (CMIP6). An independent estimate of the additional positive carbon-cycle climate feedbacks from permafrost thaw, which is not considered in most C4MIP models, is added. The estimates represent the mean and 5–95% range. Note that these feedbacks act through modifying the atmospheric concentration of CO_2 and thus are not included in the definition of ECS, which assumes a doubling of CO_2, but are included in the definition and assessed range of the transient climate response to cumulative CO_2 emissions (TCRE). {5.4.7, 5.4.8, Box 5.1, Figure 5.29, 6.4.5, Table 6.9, 7.4.2, Table 7.10}

Thawing terrestrial permafrost will lead to carbon release (*high confidence*), but there is *low confidence* in the timing, magnitude and the relative roles of CO_2 versus CH_4 as feedback processes. An ensemble of models projects CO_2 release from permafrost to be 3–41 PgC per 1°C of global warming by 2100, leading to warming strong enough that it must be included in estimates of the remaining carbon budget but weaker than the warming from fossil fuel burning. However, the incomplete representation of important processes, such as abrupt thaw, combined with weak observational constraints, only allow *low confidence* in both the magnitude of these estimates and in how linearly proportional this feedback is to the amount of global warming. There is emerging evidence that permafrost thaw and thermokarst give rise to increased CH_4 and N_2O emissions, which leads to the combined radiative forcing from permafrost thaw being larger than from CO_2 emissions only. However, the quantitative understanding of these additional feedbacks is low, particularly for N_2O. These feedbacks, as well as potential additional carbon losses due to climate-induced fire feedback are not routinely included in Earth system models. {Box 5.1, 5.4.3, 5.4.7, 5.4.8}

TS.3.3 Temperature Stabilization, Net Zero Emissions and Mitigation

TS.3.3.1 Remaining Carbon Budgets and Temperature Stabilization

The near-linear relationship between cumulative CO_2 emissions and maximum global surface temperature increase caused by CO_2 implies that stabilizing human-induced global temperature increase at any level requires net anthropogenic CO_2 emissions to become zero. This near-linear relationship further implies that mitigation requirements for limiting warming to specific levels can be quantified in terms of a carbon budget (*high confidence*). Remaining carbon budget estimates have been updated since AR5 with methodological improvements, resulting in larger estimates that are consistent with SR1.5. Several factors, including estimates of historical warming, future emissions from thawing permafrost, variations in projected non-CO_2 warming, and the global surface temperature change after cessation of CO_2 emissions, affect the exact value of carbon budgets (*high confidence*). {1.3.5, Box 1.2, 4.7.1, 5.5}

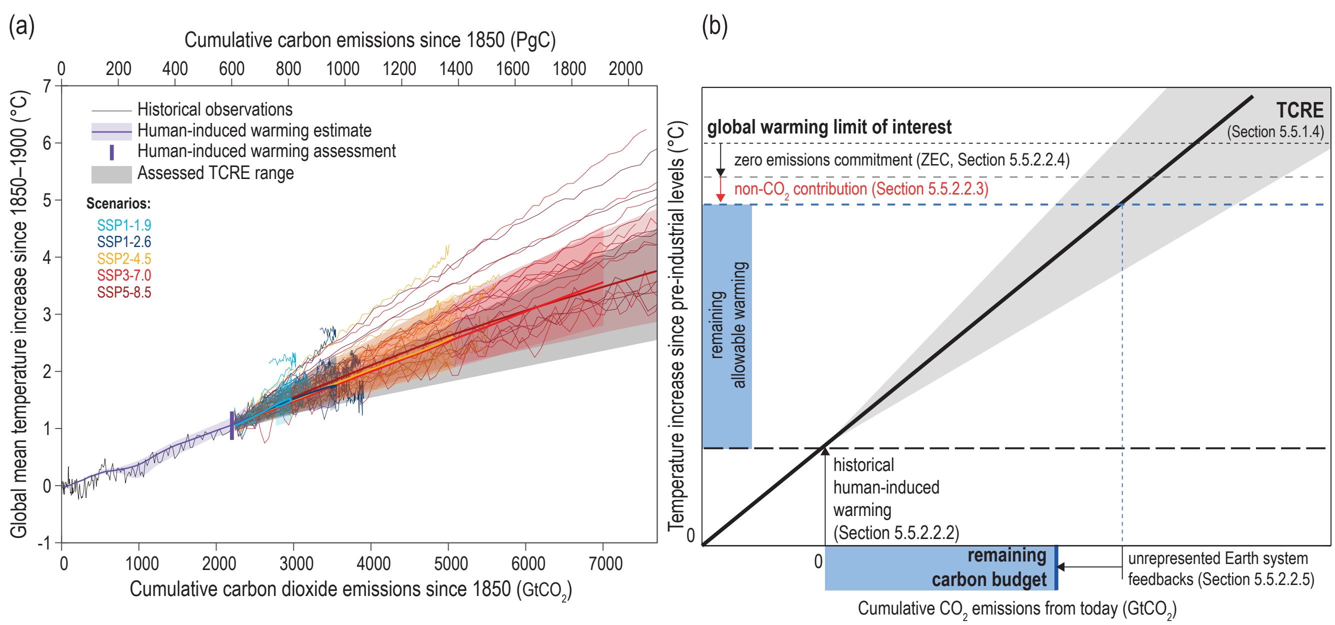

Figure TS.18 | Illustration of (a) relationship between cumulative emissions of carbon dioxide (CO_2) and global mean surface air temperature increase and (b) the assessment of the remaining carbon budget from its constituting components based on multiple lines of evidence. *The intent of this figure is to show (i) the proportionality between cumulative CO_2 emissions and global surface air temperature in observations and models as well as the assessed range of the transient climate response to cumulative CO_2 emissions (TCRE), and (ii) how information is combined to derive remaining carbon budgets consistent with limiting warming to a specific level.* Carbon budgets consistent with various levels of additional warming are provided in Table 5.8 and should not be read from the illustrations in either panel. **In panel (a)** thin black line shows historical CO_2 emissions together with the assessed global surface temperature increase from 1850–1900 as assessed in Chapter 2 (Box 2.3). The orange-brown range with its central line shows the estimated human-induced share of historical warming. The vertical orange-brown line shows the assessed range of historical human-induced warming for the 2010–2019 period relative to 1850–1900 (Chapter 3). The grey cone shows the assessed *likely* range for the TCRE (Section 5.5.1.4), starting from 2015. Thin coloured lines show Coupled Model Intercomparison Project Phase 6 (CMIP6) simulations for the five scenarios of the WGI core set (SSP1-1.9, light blue; SSP1-2.6, blue; SSP2-4.5, yellow; SSP3-7.0, red; SSP5-8.5, maroon), starting from 2015 and until 2100. Diagnosed carbon emissions are complemented with estimated land-use change emissions for each respective scenario. Coloured areas show the Chapter 4 assessed *very likely* range of global surface temperature projections and thick coloured central lines show the median estimate, for each respective scenario. These temperature projections are expressed relative to cumulative CO_2 emissions that are available for emissions-driven CMIP6 ScenarioMIP experiments for each respective scenario. **For panel (b),** the remaining allowable warming is estimated by combining the global warming limit of interest with the assessed historical human-induced warming (Section 5.5.2.2.2), the assessed future potential non-CO_2 warming contribution (Section 5.5.2.2.3) and the zero emissions commitment (ZEC; Section 5.5.2.2.4). The remaining allowable warming (vertical blue bar) is subsequently combined with the assessed TCRE (Sections 5.5.1.4 and 5.5.2.2.1) and contribution of unrepresented Earth system feedbacks (Section 5.5.2.2.5) to provide an assessed estimate of the remaining carbon budget (horizontal blue bar, Table 5.8). Note that contributions in panel (b) are illustrative and are not to scale. For example, the central ZEC estimate was assessed to be zero. {Box 2.3, 5.2.1, 5.2.2, Figure 5.31}

Limiting further climate change would require substantial and sustained reductions of GHG emissions. Without net zero CO_2 emissions, and a decrease in the net non-CO_2 forcing (or sufficient net negative CO_2 emissions to offset any further warming from net non-CO_2 forcing), the climate system will continue to warm. There is *high confidence* that mitigation requirements for limiting warming to specific levels over this century can be estimated using a carbon budget that relates cumulative CO_2 emissions to global mean temperature increase (Figure TS.18, Table TS.3). For the period 1850–2019, a total of 2390 ± 240 $GtCO_2$ of anthropogenic CO_2 has been emitted. Remaining carbon budgets (starting from 1 January 2020) for limiting warming to 1.5°C, 1.7°C and 2.0°C are estimated at 500 $GtCO_2$, 850 $GtCO_2$ and 1350 $GtCO_2$, respectively, based on the 50th percentile of TCRE. For the 67th percentile, the respective values are 400 $GtCO_2$, 700 $GtCO_2$ and 1150 $GtCO_2$. The remaining carbon budget estimates for different temperature limits assume that non-CO_2 emissions are mitigated consistent with the median reductions found in scenarios in the literature as assessed in SR1.5, but they may vary by an estimated ±220 $GtCO_2$ depending on how deeply future non-CO_2 emissions are assumed to be reduced (Table TS.3). {5.5.2, 5.6, Box 5.2, 7.6}

There is *high confidence* that several factors, including estimates of historical warming, future emissions from thawing permafrost, and variations in projected non-CO_2 warming, affect the value of carbon budgets but do not change the conclusion that global CO_2 emissions would need to decline to net zero to halt global warming. Estimates may vary by ±220 $GtCO_2$ depending on the level of non-CO_2 emissions at the time global anthropogenic CO_2 emissions reach net zero levels. This variation is referred to as non-CO_2 scenario uncertainty and will be further assessed in the AR6 Working Group III Contribution. Geophysical uncertainties surrounding the climate response to these non-CO_2 emissions result in an additional uncertainty of at least ±220 $GtCO_2$, and uncertainties in the level of historical warming result in a ±550 $GtCO_2$ uncertainty. {5.4, 5.5.2}

Table TS.3 | Estimates of remaining carbon budgets and their uncertainties. Assessed estimates are provided for additional human-induced warming, expressed as global surface temperature, since the recent past (2010–2019), *likely* amounted to 0.8° to 1.3°C with a best estimate of 1.07°C relative to 1850–1900. Historical CO_2 emissions between 1850 and 2014 have been estimated at about 2180 ± 240 $GtCO_2$ (1-sigma range), while since 1 January 2015, an additional 210 $GtCO_2$ has been emitted until the end of 2019. $GtCO_2$ values to the nearest 50. {Table 3.1, 5.5.1, 5.5.2, Box 5.2, Table 5.1, Table 5.7, Table 5.8}

Global surface temperature change since 2010–2019	Global surface temperature change since 1850–1900[a]	Estimated remaining carbon budgets starting from 1 January 2020 and subject to variations and uncertainties quantified in the columns on the right					Scenario variation	Geophysical uncertainties[d]			
°C	°C	Percentiles of TCRE[b] $GtCO_2$					Non-CO_2 scenario variation[c]	Non-CO_2 forcing and response uncertainty	Historical temperature uncertainty[a]	Zero CO_2 emissions commitment uncertainty	Recent emissions uncertainty[e]
		17th	33rd	50th	67th	83rd	$GtCO_2$	$GtCO_2$	$GtCO_2$	$GtCO_2$	$GtCO_2$
0.43	1.5	900	650	500	400	300	Values can vary by at least ±220 due to choices related to non-CO_2 emissions mitigation	Values can vary by at least ±220 due to uncertainty in the warming response to future non-CO_2 emissions	±550	±420	±20
0.53	1.6	1200	850	650	550	400					
0.63	1.7	1450	1050	850	700	550					
0.73	1.8	1750	1250	1000	850	650					
0.83	1.9	2000	1450	1200	1000	800					
0.93	2	2300	1700	1350	1150	900					

[a] Human-induced global surface temperature increase between 1850–1900 and 2010–2019 is assessed at 0.8–1.3°C (*likely* range; Cross-Section Box TS.1) with a best estimate of 1.07°C. Combined with a central estimate of TCRE (1.65°C per 1000 PgC) this uncertainty in isolation results in a potential variation of remaining carbon budgets of ±550 $GtCO_2$, which, however, is not independent of the assessed uncertainty of TCRE and thus not fully additional.

[b] TCRE: transient climate response to cumulative emissions of carbon dioxide, assessed to fall *likely* between 1.0–2.3°C per 1000 PgC with a normal distribution, from which the percentiles are taken. Additional Earth system feedbacks are included in the remaining carbon budget estimates as discussed in Section 5.5.2.2.5.

[c] Estimates assume that non-CO_2 emissions are mitigated consistent with the median reductions found in scenarios in the literature as assessed in SR1.5. Non-CO_2 scenario variations indicate how much remaining carbon budget estimates vary due to different scenario assumptions related to the future evolution of non-CO_2 emissions in mitigation scenarios from SR1.5 that reach net zero CO_2 emissions. This variation is additional to the uncertainty in TCRE. The Working Group III Contribution to AR6 will reassess the potential for non-CO_2 mitigation based on literature since SR1.5.

[d] Geophysical uncertainties reported in these columns and TCRE uncertainty are not statistically independent, as uncertainty in TCRE depends on uncertainty in the assessment of historical temperature, non-CO_2 versus CO_2 forcing, and uncertainty in emissions estimates. These estimates cannot be formally combined, and these uncertainty variations are not directly additional to the spread of remaining carbon budgets due to TCRE uncertainty reported in columns three to seven.

[e] Recent emissions uncertainty reflects the ±10% uncertainty in the historical CO_2 emissions estimate since 1 January 2015.

Methodological improvements and new evidence result in updated remaining carbon budget estimates. The assessment in AR6 applies the same methodological improvements as in SR1.5, which uses a recent observed baseline for historic temperature change and cumulative emissions. Changes compared to SR1.5 are therefore small: the assessment of new evidence results in updated median remaining carbon budget estimates for limiting warming to 1.5°C and 2°C being the same and about 60 $GtCO_2$ smaller, respectively, after accounting for emissions since SR1.5. Meanwhile, remaining carbon budgets for limiting warming to 1.5°C would be about 300–350 $GtCO_2$ larger if evidence and methods available at the time of AR5 would be used. If a specific remaining carbon budget is exceeded, this results in a lower probability of keeping warming below a specified temperature level and higher irreversible global warming over decades to centuries, or alternatively a need for net negative CO_2 emissions or further reductions in non-CO_2 greenhouse gases after net zero CO_2 is achieved to return warming to lower levels in the long term. {5.5.2, 5.6, Box 5.2}

Based on idealized model simulations that explore the climate response once CO_2 emissions have been brought to zero, the magnitude of the zero CO_2 emissions commitment (ZEC, see Glossary) is assessed to be *likely* smaller than 0.3°C for time scales of about half a century and cumulative CO_2 emissions broadly consistent with global warming of 2°C. However, there is *low confidence* about its sign on time scales of about half a century. For lower cumulative CO_2 emissions, the range would be smaller yet with equal uncertainty about the sign. If the ZEC is positive on decadal time scales, additional warming leads to a reduction in the estimates of remaining carbon budgets, and vice versa if it is negative. {4.7.1, 5.5.2}

Permafrost thaw is included in estimates together with other feedbacks that are often not captured by models. Limitations in modelling studies combined with weak observational constraints only allow *low confidence* in the magnitude of these estimates (Section TS.3.2.2). Despite the large uncertainties surrounding the quantification of the effect of additional Earth system feedback processes, such as emissions from wetlands and permafrost thaw, these feedbacks represent identified additional risk factors that scale with additional warming and mostly increase the challenge of limiting warming to specific temperature levels. These uncertainties do not change the basic conclusion that global CO_2 emissions would need to decline to net zero to halt global warming. {5.4.8, 5.5.2, Box 5.1}

TS.3.3.2 Carbon Dioxide Removal

Deliberate carbon dioxide removal (CDR) from the atmosphere has the potential to compensate for residual CO_2 emissions to reach net zero CO_2 emissions or to generate net negative CO_2 emissions. In the same way that part of current anthropogenic net CO_2 emissions are taken up by land and ocean carbon stores, net CO_2 removal will be partially counteracted by CO_2 release from these stores (*very high confidence*). Asymmetry in the carbon cycle response to simultaneous CO_2 emissions and removals implies that a larger amount of CO_2 would need to be removed to compensate for an emission of a given magnitude to attain the same change in atmospheric CO_2 (*medium confidence*). CDR methods have wide-ranging side-effects that can either weaken or strengthen the carbon sequestration and cooling potential of these methods and affect the achievement of sustainable development goals (*high confidence*). {4.6.3, 5.6}

Carbon dioxide removal (CDR) refers to anthropogenic activities that deliberately remove CO_2 from the atmosphere and durably store it in geological, terrestrial or ocean reservoirs, or in products. Carbon dioxide is removed from the atmosphere by enhancing biological or geochemical carbon sinks or by direct capture of CO_2 from air. Emissions pathways that limit global warming to 1.5°C or 2°C typically assume the use of CDR approaches in combination with GHG emissions reductions. CDR approaches could be used to compensate for residual emissions from sectors that are difficult or costly to decarbonize. CDR could also be implemented at a large scale to generate global net negative CO_2 emissions (i.e., anthropogenic CO_2 removals exceeding anthropogenic emissions), which could compensate for earlier emissions as a way to meet long-term climate stabilization goals after a temperature overshoot. This Report assesses the effects of CDR on the carbon cycle and climate. Co-benefits and trade-offs for biodiversity, water and food production are briefly discussed for completeness, but a comprehensive assessment of the ecological and socio-economic dimensions of CDR options is left to the WGII and WGIII reports. {4.6.3, 5.6}

CDR methods have the potential to sequester CO_2 from the atmosphere (*high confidence*). In the same way part of current anthropogenic net CO_2 emissions are taken up by land and ocean carbon stores, net CO_2 removal will be partially counteracted by CO_2 release from these stores, such that the amount of CO_2 sequestered by CDR will not result in an equivalent drop in atmospheric CO_2 (*very high confidence*). The fraction of CO_2 removed from the atmosphere that is not replaced by CO_2 released from carbon stores – a measure of CDR effectiveness – decreases slightly with increasing amounts of removal (*medium confidence*) and decreases strongly if CDR is applied at lower atmospheric CO_2 concentrations (*medium confidence*). The reduction in global surface temperature is approximately linearly related to cumulative CO_2 removal (*high confidence*). Because of this near-linear relationship, the amount of cooling per unit CO_2 removed is approximately independent of the rate and amount of removal (*medium confidence*). {4.6.3, 5.6.2.1, Figure 5.32, Figure 5.34}

Due to non-linearities in the climate system, the century-scale climate–carbon cycle response to a CO_2 removal from the atmosphere is not always equal and opposite to its response to a simultaneous CO_2 emission (*medium* confidence). For CO_2 emissions of 100 PgC released from a state in equilibrium with pre-industrial atmospheric CO_2 levels, CMIP6 models simulate that 27± 6% (mean ± 1 standard deviation) of emissions remain in the atmosphere 80–100 years after the emissions, whereas for removals of 100 PgC only 23 ± 6% of removals remain out of the atmosphere. This asymmetry implies that an extra amount of CDR is required to compensate for a positive emission of a given magnitude to attain the same change in atmospheric CO_2. Due to *low agreement* between models, there

TS

is *low confidence* in the sign of the asymmetry of the temperature response to CO_2 emissions and removals. {4.6.3, 5.6.2.1, Figure 5.35}

Simulations with ESMs indicate that under scenarios where CO_2 emissions gradually decline, reach net zero and become net negative during the 21st century (e.g., SSP1-2.6), land and ocean carbon sinks begin to weaken in response to declining atmospheric CO_2 concentrations, and the land sink eventually turns into a source (Figure TS.19). This sink-to-source transition occurs decades to a few centuries after CO_2 emissions become net negative. The ocean remains a sink of CO_2 for centuries after emissions become net negative. Under scenarios with large net negative CO_2 emissions (e.g., SSP5-3.4-OS) and rapidly declining CO_2 concentrations, the land source is larger than for SSP1-2.6 and the ocean also switches to a source. While the general response is robust across models, there is *low confidence* in the timing of the sink-to-source transition and the magnitude of the CO_2 source in scenarios with net negative CO_2 emissions. Carbon dioxide removal could reverse some aspects climate change if CO_2 emissions become net negative, but some changes would continue in their current direction for decades to millennia. For instance, sea level rise due to ocean thermal expansion would not reverse for several centuries to millennia (*high confidence*) (Box TS.4). {4.6.3, 5.4.10, 5.6.2.1, Figure 5.30, Figure 5.33}

Carbon dioxide removal methods have a range of side effects that can either weaken or strengthen the carbon sequestration and cooling potential of these methods and affect the achievement of sustainable development goals (*high confidence*). Biophysical and biogeochemical side-effects of CDR methods are associated with changes in surface albedo, the water cycle, emissions of CH_4 and N_2O, ocean acidification and marine ecosystem productivity (*high confidence*). These side-effects and associated Earth system feedbacks can decrease carbon uptake and/or change local and regional climate and in turn limit the CO_2 sequestration and cooling potential of specific CDR methods (*medium confidence*). Deployment of CDR, particularly on land, can also affect water quality and quantity, food production and biodiversity (*high confidence*). These effects are often highly dependent on local context, management regime, prior land use, and scale (*high confidence*). The largest co-benefits are obtained with methods that seek to restore natural ecosystems or improve soil carbon sequestration (*medium confidence*). The climate and biogeochemical effects of terminating CDR are expected to be small for most CDR methods (*medium confidence*). {4.6.3, 5.6.2.2, Figure 5.36, 8.4.3, 8.6.3}

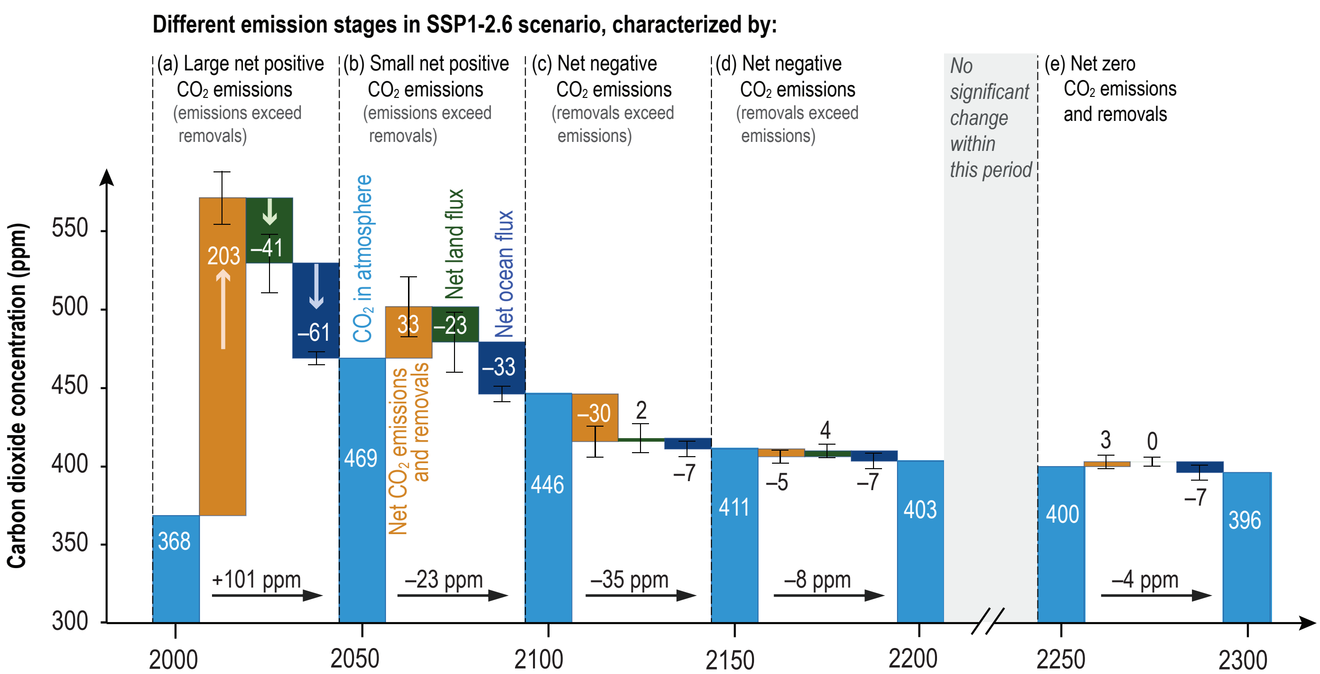

Figure TS.19 | Carbon sink response in a scenario with net carbon dioxide (CO_2) removal from the atmosphere. *The intent of this figure is to show how atmospheric CO_2 evolves under negative emissions and its dependence on the negative emissions technologies. It also shows the evolution of the ocean and land sinks.* Shown are CO_2 flux components from concentration-driven Earth system model (ESM) simulations during different emissions stages of SSP1–2.6 and its long-term extension. **(a)** Large net positive CO_2 emissions, **(b)** small net positive CO_2 emissions, **(c–d)** net negative CO_2 emissions, and **(e)** net zero CO_2 emissions. Positive flux components act to raise the atmospheric CO_2 concentration, whereas negative components act to lower the CO_2 concentration. Net CO_2 emissions and land and ocean CO_2 fluxes represent the multi-model mean and standard deviation (error bar) of four ESMs (CanESM5, UKESM1, CESM2-WACCM, IPSL-CM6a-LR) and one Earth system model of intermediate complexity (Uvic ESCM). Net CO_2 emissions are calculated from concentration-driven ESM simulations as the residual from the rate of increase in atmospheric CO_2 and land and ocean CO_2 fluxes. Fluxes are accumulated over each 50-year period and converted to concentration units (parts per million, or ppm). {5.6.2.1, Figure 5.33}

TS.3.3.3 Relating Different Forcing Agents

When including other GHGs, the choice of emissions metric affects the quantification of net zero GHG emissions and their resulting temperature outcome (*high confidence*). Reaching and sustaining net zero GHG emissions typically leads to a peak and decline in temperatures when quantified with the global warming potential over a 100-year period (GWP-100). Carbon-cycle responses are more robustly accounted for in emissions metrics compared to AR5 (*high confidence*). New emissions metric approaches can be used to generate equivalent cumulative emissions of CO_2 for short-lived greenhouse gases based on their rate of emissions. {7.6.2}

Over 10- to 20-year time scales, the temperature response to a single year's worth of current emissions of short-lived climate forcers (SLCFs) is at least as large as that of CO_2, but because the effects of SLCFs decay rapidly over the first few decades after emission, the net long-term temperature response to a single year's worth of emissions is predominantly determined by cumulative CO_2 emissions.

Emissions reductions in 2020 associated with COVID-19 containment led to small and positive global ERF; however, global and regional climate responses to the forcing are undetectable above internal variability due to the temporary nature of emissions reductions. {6.6, Cross-Chapter Box 6.1}

The relative climate effects of different forcing agents are typically quantified using emissions metrics that compare the effects of an idealised pulse of 1 kg of some climate forcing agent against a reference climate forcing agent, almost always CO_2. The two most prominent pulse emissions metrics are the global warming potential (GWP) and global temperature change potential (GTP) (see Glossary). The climate responses to CO_2 emissions by convention include the effects of warming on the carbon cycle, so for consistency these also need to be determined for non-CO_2 emissions. The methodology for doing this has been placed on a more robust scientific footing compared to AR5 (*high confidence*). Methane from fossil fuel sources has slightly higher emissions metric values than those from biogenic sources since it leads to additional fossil CO_2 in the atmosphere (*high confidence*). Updates to the chemical adjustments for CH_4 and N_2O emissions (Section TS.3.1) and revisions in their lifetimes result in emissions metrics for GWP and GTP that are slightly lower than in AR5 (*medium confidence*). Emissions metrics for the entire suite of GHGs assessed in the AR6 have been calculated for various time horizons. {7.6.1, Table 7.15, Table 7.SM.7}

New emissions metric approaches, such as GWP* and Combined-GTP (CGTP), relate changes in the emissions rate of short-lived greenhouse gases to equivalent cumulative emissions of CO_2 (CO_2-e). Global surface temperature response from aggregated emissions of short-lived greenhouse gases over time is determined by multiplying these cumulative CO_2-e by TCRE (see Section TS.3.2.1). When GHGs are aggregated using standard metrics such as GWP or GTP, cumulative CO_2-e emissions are not necessarily proportional to future global surface temperature outcomes (*high confidence*) {7.6.1, Box 7.3}

Emissions metrics are needed to aggregate baskets of gases to determine net zero GHG emissions. Generally, achieving net zero CO_2 emissions and declining non-CO_2 radiative forcing would halt human-induced warming. Reaching net zero GHG emissions quantified by GWP-100 typically leads to declining temperatures after net zero GHGs emissions are achieved if the basket includes short-lived gases, such as CH_4. Net zero GHG emissions defined by CGTP or GWP* imply net zero CO_2 and other long-lived GHG emissions and constant (CGTP) or gradually declining (GWP*) emissions of short-lived gases. The warming evolution resulting from net zero GHG emissions defined in this way corresponds approximately to reaching net zero CO_2 emissions, and would thus not lead to declining temperatures after net zero GHG emissions are achieved but to an approximate temperature stabilization (*high confidence*). The choice of emissions metric hence affects the quantification of net zero GHG emissions, and therefore the resulting temperature outcome of reaching and sustaining net zero GHG emissions levels (*high confidence*). {7.6.1.4, 7.6.2, 7.6.3}

As pointed out in AR5, ultimately, it is a matter for policymakers to decide which emissions metric is most applicable to their needs. This Report does not recommend the use of any specific emissions metric, as the most appropriate metric depends on the policy goal and context (see Chapter 7, Section 7.6). A detailed assessment of GHG metrics to support climate change mitigation and associated policy contexts is provided in the WGIII contribution to the AR6.

The global surface temperature response following a climate change mitigation measure that affects emissions of both short- and long-lived climate forcers depends on their lifetimes, their ERFs, how fast and for how long the emissions are reduced, and the thermal inertia in the climate system. Mitigation, relying on emissions reductions and implemented through new legislation or technology standards, implies that emissions reductions occur year after year. Global temperature response to a year's worth of current emissions from different sectors informs about the mitigation potential (Figure TS.20). Over 10- to 20-year time scales, the influence of SLCFs is at least as large as that of CO_2, with sectors producing the largest warming being fossil fuel production and distribution, agriculture, and waste management. Because the effects of the SLCFs decay rapidly over the first few decades after emission, the net long-term temperature effect from a single year's worth of current emissions is predominantly determined by CO_2. Fossil fuel combustion for energy, industry and land transportation are the largest contributing sectors on a 100-year time scale (*high confidence*). Current emissions of CO_2, N_2O and SLCFs from East Asia and North America are the largest regional contributors to additional net future warming on both short (*medium confidence*) and long time scales (10 and 100 years, respectively) (*high confidence*). {6.6.1, 6.6.2, Figure 6.16}

COVID-19 restrictions led to detectable reductions in global anthropogenic emissions of nitrogen oxides (NO_x) (about 35% in April 2020) and fossil CO_2 (7%, with estimates ranging from 5.8% to 13.0%), driven largely by reduced emissions from the transportation

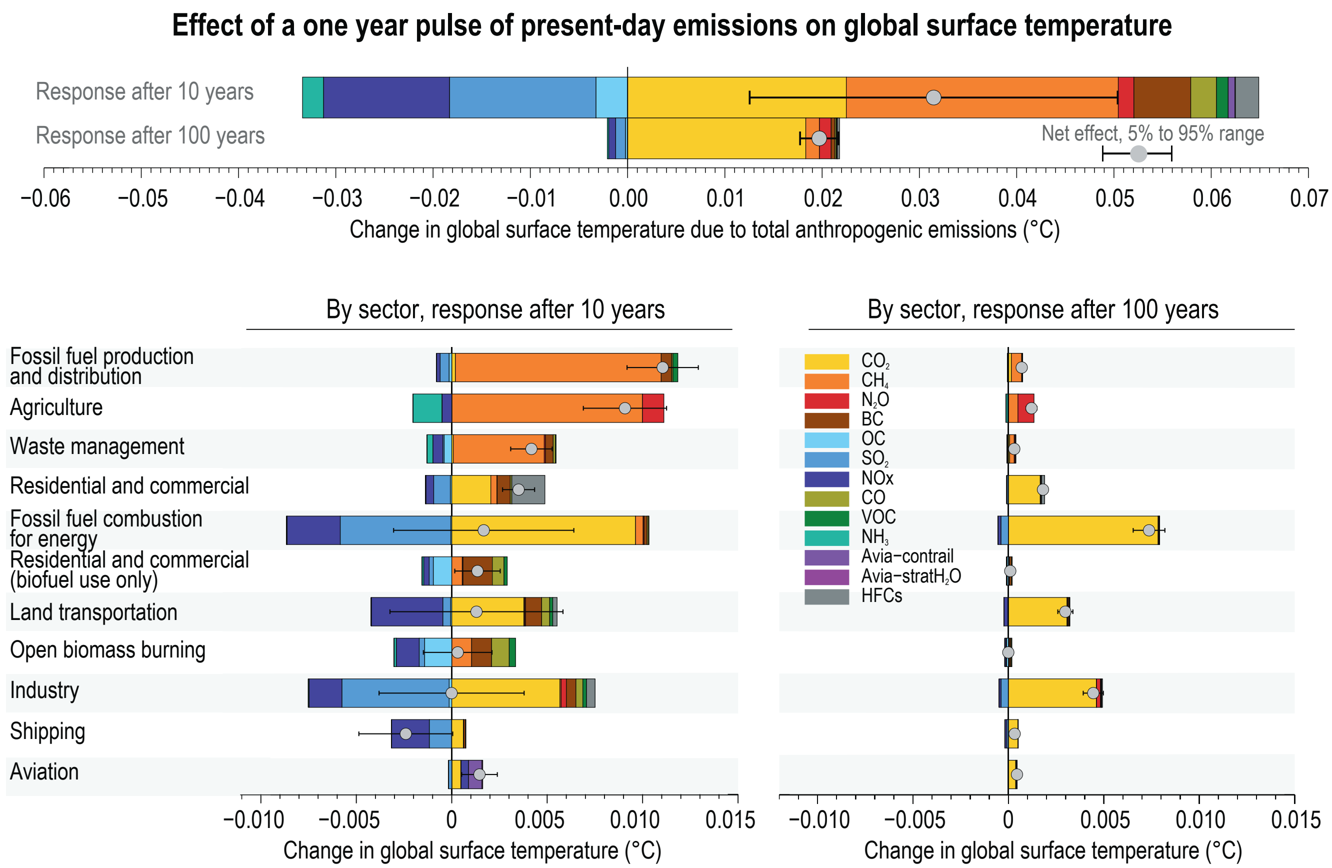

Figure TS.20 | Global surface temperature change 10 and 100 years after a one-year pulse of present-day emissions. *The intent of this figure is to show the sectoral contribution to present-day climate change by specific climate forcers, including carbon dioxide (CO_2) as well as short-lived climate forcers (SLCFs).* The temperature response is broken down by individual species and shown for total anthropogenic emissions **(top)**, and sectoral emissions on 10-year **(left)** and 100-year time scales **(right)**. Sectors are sorted by (high-to-low) net temperature effect on the 10-year time scale. Error bars in the top panel show the 5–95% range in net temperature effect due to uncertainty in radiative forcing only (calculated using a Monte Carlo approach and best estimate uncertainties from the literature). Emissions for 2014 are from the Coupled Model Intercomparison Project Phase 6 (CMIP6) emissions dataset, except for hydrofluorocarbons (HFCs) and aviation H_2O, which rely on other datasets (see Section 6.6.2 for more details). CO_2 emissions are excluded from open biomass burning and residential biofuel use. {6.6.2, Figure 6.16}

sector (*medium confidence*). There is *high confidence* that, with the exception of surface ozone, reductions in pollutant precursors contributed to temporarily improved air quality in most regions of the world. However, these reductions were lower than what would be expected from sustained implementation of policies addressing air quality and climate change (*medium confidence*). Overall, the net global ERF from COVID-19 containment was likely small and positive for 2020 (with a temporary peak value less than 0.2 W m^{-2}), thus temporarily adding to the total anthropogenic climate influence, with positive forcing (warming influence) from aerosol changes dominating over negative forcings (cooling influence) from CO_2, NO_x and contrail cirrus changes. Consistent with this small net radiative forcing, and against a large component of internal variability, Earth system models show no detectable effect on global or regional surface temperature or precipitation (*high confidence*). {Cross Chapter Box 6.1}

Box TS.7 | Climate and Air Quality Responses to Short-lived Climate Forcers in Shared Socio-economic Pathways

Future changes in emissions of short-lived climate forcers (SLCFs) are expected to cause an additional global mean warming, with a large diversity in the end-of-century response across the WGI core set of Shared Socio-economic Pathways (SSPs), depending upon the level of climate change and air pollution mitigation (Box TS.7, Figure 1). This additional warming is either due to reductions in cooling aerosols for air pollution regulation or due to increases in methane (CH_4), ozone and hydrofluorocarbons (HFCs). This additional warming is stable after 2040 in SSPs associated with lower global air pollution as long as CH_4 emissions are also mitigated, but the overall warming induced by SLCF changes is higher in scenarios in which air quality continues to deteriorate (induced by growing fossil fuel use and limited air pollution control) (*high confidence*).

Sustained CH_4 mitigation reduces global surface ozone, contributing to air quality improvements, and also reduces surface temperature in the longer term, but only sustained CO_2 emissions reductions allow long-term climate stabilization (*high confidence*). Future changes in air quality (near-surface ozone and particulate matter, or PM) at global and local scales are predominantly driven by changes in ozone and aerosol precursor emissions rather than climate (*high confidence*). Air quality improvements driven by rapid decarbonization strategies, as in SSP1-1.9 and SSP1-2.6, are not sufficient in the near term to achieve air quality guidelines set by the World Health Organization in some highly polluted regions (*high confidence*). Additional policies (e.g., access to clean energy, waste management) envisaged to attain United Nations Sustainable Development Goals bring complementary SLCF reduction. {4.4.4, 6.6.3, 6.7.3, Box 6.2}

The net effect of SLCF emissions changes on temperature will depend on how emissions of warming and cooling SLCFs will evolve in the future. The magnitude of the cooling effect of aerosols remains the largest uncertainty in the effect of SLCFs in future climate projections. Since the SLCFs have undergone large changes over the past two decades, the temperature and air pollution responses are estimated relative to the year 2019 instead of 1995–2014.

Temperature Response

In the next two decades, it is *very likely* that SLCF emissions changes will cause a warming relative to 2019, across the WGI core set of SSPs (see Section TS.1.3.1), in addition to the warming from long-lived GHGs. The net effect of SLCF and HFC changes in global surface temperature across the SSPs is a *likely* warming of 0.06°C–0.35°C in 2040 relative to 2019. This near-term global mean warming linked to SLCFs is quite similar in magnitude across the SSPs due to competing effects of warming (CH_4, ozone) and cooling (aerosols) forcers (Box TS.7, Figure 1). There is greater diversity in the end-of-century response among the scenarios. SLCF changes in scenarios with no climate change mitigation (SSP3-7.0 and SSP5-8.5) will cause a warming in the *likely* range of 0.4°C–0.9°C in 2100 relative to 2019 due to increases in CH_4, tropospheric ozone and HFC levels. For the stringent climate change and pollution mitigation scenarios (SSP1-1.9 and SSP1-2.6), the cooling from reductions in CH_4, ozone and HFCs partially balances the warming from reduced aerosols, primarily sulphate, and the overall SLCF effect is a *likely* increase in global surface temperature of 0.0°C–0.3°C in 2100, relative to 2019. With intermediate climate change and air pollution mitigations, SLCFs in SSP2-4.5 add a *likely* warming of 0.2°C–0.5°C to global surface temperature change in 2100, with the largest warming resulting from reductions in aerosols. {4.4.4, 6.7.3}

Assuming implementation and efficient enforcement of both the Kigali Amendment to the Montreal Protocol on Substances that Deplete the Ozone Layer and current national plans result in limiting emissions (as in SSP1-2.6), the effects of HFCs on global surface temperature, relative to 2019, would remain below +0. 02°C from 2050 onwards versus about +0.04°C–0.08°C in 2050 and +0.1°C–0.3°C in 2100 considering only national HFC regulations decided prior to the Kigali Amendment (as in SSP5-8.5) (*medium confidence*). {6.6.3, 6.7.3}

Air Quality Responses

Air pollution projections range from strong reductions in global surface ozone and PM (e.g., SSP1-2.6, with stringent mitigation of both air pollution and climate change) to no improvement and even degradation (e.g., SSP3-7.0 without climate change mitigation and with only weak air pollution control) (*high confidence*). Under the SSP3-7.0 scenario, PM levels are projected to increase until 2050 over large parts of Asia, and surface ozone pollution is projected to worsen over all continental areas through 2100 (*high confidence*). In SSP5-8.5, a scenario without climate change mitigation but with stringent air pollution control, PM levels decline through 2100, but high CH_4 levels hamper the decline in global surface ozone at least until 2080 (*high confidence*). {6.7.1}

Box TS.7 (continued)

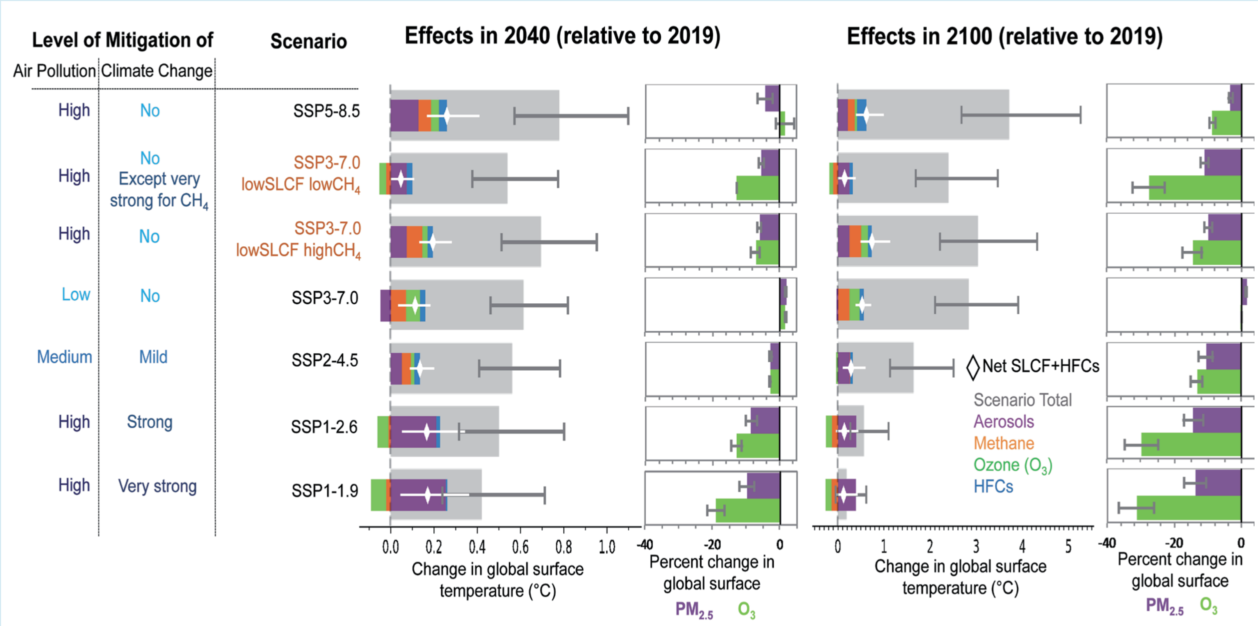

Box TS.7, Figure 1 | Effects of short-lived climate forcers (SLCFs) on global surface temperature and air pollution across the WGI core set of Shared Socio-economic Pathways (SSPs). *The intent of this figure is to show the climate and air quality (surface ozone and particulate matter smaller than 2.5 microns in diameter, or $PM_{2.5}$) response to SLCFs in the SSP scenarios for the near and long-term.* Effects of net aerosols, tropospheric ozone, hydrofluorocarbons (HFCs; with lifetimes less than 50 years), and methane (CH_4) are compared with those of total anthropogenic forcing for 2040 and 2100 relative to year 2019. The global surface temperature changes are based on historical and future evolution of effective radiative forcing (ERF) as assessed in Chapter 7 of this Report. The temperature responses to the ERFs are calculated with a common impulse response function (RT) for the climate response, consistent with the metric calculations in Chapter 7 (Box 7.1). The RT has an equilibrium climate sensitivity of 3.0°C for a doubling of atmospheric CO_2 concentration (feedback parameter of -1.31 W m^{-2} °C^{-1}). The scenario total (grey bar) includes all anthropogenic forcings (long- and short-lived climate forcers, and land-use changes). Uncertainties are 5–95% ranges. The global changes in air pollutant concentrations (ozone and $PM_{2.5}$) are based on multimodel Coupled Model Intercomparison Project Phase 6 (CMIP6) simulations and represent changes in five-year mean surface continental concentrations for 2040 and 2098 relative to 2019. Uncertainty bars represent inter-model ±1 standard deviation. {6.7.2, 6.7.3, Figure 6.24}

Box TS.8 | Earth System Response to Solar Radiation Modification

Since AR5, further modelling work has been conducted on aerosol-based solar radiation modification (SRM) options such as stratospheric aerosol injection, marine cloud brightening, and cirrus cloud thinning[21] and their climate and biogeochemical effects. These investigations have consistently shown that SRM could offset some of the effects of increasing greenhouse gases on global and regional climate, including the carbon and water cycles (*high confidence*). However, there would be substantial residual or overcompensating climate change at the regional scales and seasonal time scales (*high confidence*), and large uncertainties associated with aerosol–cloud–radiation interactions persist. The cooling caused by SRM would increase the global land and ocean CO_2 sinks (*medium confidence*), but this would not stop CO_2 from increasing in the atmosphere or affect the resulting ocean acidification under continued anthropogenic emissions (*high confidence*). It is *likely* that abrupt water cycle changes will occur if SRM techniques are implemented rapidly. A sudden and sustained termination of SRM in a high CO_2 emissions scenario would cause rapid climate change (*high confidence*). However, a gradual phase-out of SRM combined with emissions reduction and carbon dioxide removal (CDR) would avoid these termination effects (*medium confidence*). {4.6.3, 5.6.3. 6.4.6, 8.6.3}.

21 Although cirrus cloud thinning aims to cool the planet by increasing longwave emissions to space, it is included in the portfolio of SRM options for consistency with AR5 and SR1.5. {4.6.3.3}

Box TS.8 (continued)

Solar radiation modification (SRM) refers to deliberate, large-scale climate intervention options that are studied as potential supplements to deep mitigation, for example, in scenarios that overshoot climate stabilization goals. SRM options aim to offset some of the warming effects of GHG emissions by modification of Earth's shortwave radiation budget. Following SR1.5, the SRM assessed in this Report also includes some options, such as cirrus cloud thinning, that alter the longwave radiation budget.

SRM contrasts with climate change mitigation activities, such as emissions reductions and CDR, as it introduces a 'mask' to the climate change problem by altering Earth's radiation budget, rather than attempting to address the root cause of the problem, which is the increase in GHGs in the atmosphere. By masking only the climate effects of GHG emissions, SRM does not address other issues related to atmospheric CO_2 increase, such as ocean acidification. This Report assesses physical understanding of the Earth system response to proposed SRM, and the assessment is based primarily on idealized climate model simulations. There are other important considerations, such as risk to human and natural systems, perceptions, ethics, cost, governance, and trans-boundary issues and their relationship to the United Nations Sustainable Development Goals – issues that the WGII (Chapter 16) and WGIII (Chapter 14) Reports address. {4.6.3}

SRM options include those that increase surface albedo, brighten marine clouds by increasing the amount of cloud condensation nuclei, or reduce the optical depth of cirrus clouds by seeding them with ice nucleating particles. However, the most commonly studied approaches attempt to mimic the cooling effects of major volcanic eruptions by injecting reflective aerosols (e.g., sulphate aerosols) or their precursors (e.g., sulphur dioxide) into the stratosphere. {4.6.3, 5.6.3, 6.4.6}

SRM could offset some effects of greenhouse gas-induced warming on global and regional climate, but there would be substantial residual and overcompensating climate change at the regional scale and seasonal time scales (*high confidence*). Since AR5, more modelling work has been conducted with more sophisticated treatment of aerosol-based SRM approaches, but the uncertainties in cloud–aerosol–radiation interactions are still large (*high confidence*). Modelling studies suggest that it is possible to stabilize multiple large-scale temperature indicators simultaneously by tailoring the deployment strategy of SRM options (*medium confidence*) but with large residual or overcompensating regional and seasonal climate changes. {4.6.3}

SRM approaches targeting shortwave radiation are *likely* to reduce global mean precipitation, relative to future CO_2 emissions scenarios, if all global mean warming is offset. In contrast, cirrus cloud thinning, targeting longwave radiation, is expected to cause an increase in global mean precipitation (*medium confidence*). If shortwave approaches are used to offset global mean warming, the magnitude of reduction in regional precipitation minus evapotranspiration (P–E) (Box TS.5), which is more relevant to freshwater availability, is smaller than precipitation decrease because of simultaneous reductions in both precipitation and evapotranspiration (*medium confidence*). {4.6.3, 8.2.1, 8.6.3}.

If SRM is used to cool the planet, it would cause a reduction in plant and soil respiration and slow the reduction of ocean carbon uptake due to warming (*medium confidence*). The result would be an enhancement of the global land and ocean CO_2 sinks (*medium confidence*) and a slight reduction in atmospheric CO_2 concentration relative to unmitigated climate change. However, SRM would not stop CO_2 from increasing in the atmosphere or affect the resulting ocean acidification under continued anthropogenic emissions (*high confidence*). {5.6.3}

The effect of stratospheric aerosol injection on global temperature and precipitation is projected by models to be detectable after one to two decades, which is similar to the time scale for the emergence of the benefits of emissions reductions. A sudden and sustained termination of SRM in a high GHG emissions scenario would cause rapid climate change and a reversal of the SRM effects on the carbon sinks (*high confidence*). It is also *likely* that a termination of strong SRM would drive abrupt changes in the water cycle globally and regionally, especially in the tropical regions by shifting the Inter-tropical Convergence Zone and Hadley cells. At the regional scale, non-linear responses cannot be excluded, due to changes in evapotranspiration. However, a gradual phase-out of SRM combined with emissions reductions and CDR would avoid larger rates of changes (*medium confidence*). {4.6.3, 5.6.3, 8.6.3}.

Box TS.9 | Irreversibility, Tipping Points and Abrupt Changes

The present rates of response of many aspects of the climate system are proportionate to the rate of recent temperature change, but some aspects may respond disproportionately. Some climate system components are slow to respond, such as the deep ocean overturning circulation and the ice sheets (Box TS.4). It is *virtually certain* that irreversible, committed change is already underway for the slow-to-respond processes as they come into adjustment for past and present emissions.

The paleoclimate record indicates that tipping elements exist in the climate system where processes undergo sudden shifts toward a different sensitivity to forcing, such as during a major deglaciation, where 1°C degree of temperature change might correspond to a large or small ice-sheet mass loss during different stages (Box TS.2). For global climate indicators, evidence for abrupt change is limited, but deep ocean warming, acidification and sea level rise are committed to ongoing change for millennia after global surface temperatures initially stabilize and are irreversible on human time scales (*very high confidence*). At the regional scale, abrupt responses, tipping points and even reversals in the direction of change cannot be excluded (*high confidence*). Some regional abrupt changes and tipping points could have severe local impacts, such as unprecedented weather, extreme temperatures and increased frequency of droughts and forest fires.

Models that exhibit such tipping points are characterized by abrupt changes once the threshold is crossed, and even a return to pre-threshold surface temperatures or to atmospheric carbon dioxide concentrations does not guarantee that the tipping elements return to their pre-threshold state. Monitoring and early warning systems are being put into place to observe tipping elements in the climate system. {1.3, 1.4.4, 1.5, 4.3.2, Table 4.10, 5.3.4, 5.4.9, 7.5.3, 9.2.2, 9.2.4, 9.4.1, 9.4.2, 9.6.3, Cross-chapter Box 12.1}

Understanding of multi-decadal reversibility (i.e., the system returns to the previous climate state within multiple decades after the radiative forcing is removed) has improved since AR5 for many atmospheric, land surface and sea ice climate metrics following sea surface temperature recovery. Some processes suspected of having tipping points, such as the Atlantic Meridional Overturning Circulation (AMOC), have been found to often undergo recovery after temperature stabilization with a time delay (*low confidence*). However, substantial irreversibility is further substantiated for some cryosphere changes, ocean warming, sea level rise, and ocean acidification. {4.7.2, 5.3.3, 5.4.9, 9.2.2, 9.2.4, 9.4.1, 9.4.2, 9.6.3}

Some climate system components are slow to respond, such as the deep ocean overturning circulation and the ice sheets. It is *likely* that under stabilization of global warming at 1.5°C, 2.0°C or 3.0°C relative to 1850–1900, the AMOC will continue to weaken for several decades by about 15%, 20% and 30% of its strength and then recover to pre-decline values over several centuries (*medium confidence*). At sustained warming levels between 2°C and 3°C, there is *limited evidence* that the Greenland and West Antarctic ice sheets will be lost almost completely and irreversibly over multiple millennia; both the probability of their complete loss and the rate of mass loss increases with higher surface temperatures (*high confidence*). At sustained warming levels between 3°C and 5°C, near-complete loss of the Greenland Ice Sheet and complete loss of the West Antarctic Ice Sheet is projected to occur irreversibly over multiple millennia (*medium confidence*); with substantial parts or all of Wilkes Subglacial Basin in East Antarctica lost over multiple millennia (*low confidence*). Early-warning signals of accelerated sea level rise from Antarctica could possibly be observed within the next few decades. For other hazards (e.g., ice-sheet behaviour, glacier mass loss and global mean sea level change, coastal floods, coastal erosion, air pollution, and ocean acidification) the time and/or scenario dimensions remain critical, and a simple and robust relationship with global warming level cannot be established (*high confidence*). {4.3.2, 4.7.2, 5.4.3, 5.4.5, 5.4.8, 8.6, 9.2, 9.4, Box 9.3, Cross-Chapter Box 12.1}

For global climate indicators, evidence for abrupt change is limited. For global warming up to 2°C above 1850–1900 levels, paleoclimate records do not indicate abrupt changes in the carbon cycle (*low confidence*). Despite the wide range of model responses, uncertainty in atmospheric CO_2 by 2100 is dominated by future anthropogenic emissions rather than uncertainties related to carbon–climate feedbacks (*high confidence*). There is no evidence of abrupt change in climate projections of global temperature for the next century: there is a near-linear relationship between cumulative CO_2 emissions and maximum global mean surface air temperature increase caused by CO_2 over the course of this century for global warming levels up to at least 2°C relative to 1850–1900. The increase in global ocean heat content (Section TS.2.4) will likely continue until at least 2300 even for low emissions scenarios, and global mean sea level will continue to rise for centuries to millennia following cessation of emissions (Box TS.4) due to continuing deep ocean heat uptake and mass loss of the Greenland and Antarctic ice sheets (*high confidence*). {2.2.3; Cross-Chapter Box 2.1; 5.1.1; 5.4; Cross-Chapter Box 5.1; Figures 5.3, 5.4, 5.25, and 5.26; 9.2.2; 9.2.4}

The response of biogeochemical cycles to anthropogenic perturbations can be abrupt at regional scales and irreversible on decadal to century time scales (*high confidence*). The probability of crossing uncertain regional thresholds increases with climate change (*high

Box TS.9 (continued)

confidence). It is *very unlikely* that gas clathrates (mostly methane) in deeper terrestrial permafrost and subsea clathrates will lead to a detectable departure from the emissions trajectory during this century. Possible abrupt changes and tipping points in biogeochemical cycles lead to additional uncertainty in 21st century atmospheric GHG concentrations, but future anthropogenic emissions remain the dominant uncertainty (*high confidence*). There is potential for abrupt water cycle changes in some high emissions scenarios, but there is no overall consistency regarding the magnitude and timing of such changes. Positive land surface feedbacks, including vegetation, dust, and snow, can contribute to abrupt changes in aridity, but there is only *low confidence* that such changes will occur during the 21st century. Continued Amazon deforestation, combined with a warming climate, raises the probability that this ecosystem will cross a tipping point into a dry state during the 21st century (*low confidence*). (Section TS.3.2.2) {5.4.3, 5.4.5, 5.4.8, 5.4.9, 8.6.2, 8.6.3, Cross-Chapter Box 12.1}

TS.4 Regional Climate Change

This section focuses on how to generate regional climate change information and its relevance for climate services; the drivers of regional climate variability and change and how they are being affected by anthropogenic factors; and observed, attributed and projected changes in climate, including extreme events and climatic impact-drivers (CIDs), across all regions of the world. There is a small set of CID changes common to all land or ocean regions and a specific set of changes from a broader range of CIDs seen in each region. This regional diversity results from regional climate being determined by a complex interplay between the seasonal-to-multi-decadal variation of large-scale modes of climate variability, external natural and anthropogenic forcings, local climate processes and related feedbacks.

TS.4.1 Generation and Communication of Regional Climate Change Information

Climate change information at regional scale is generated using a range of data sources and methodologies. Multi-model ensembles and models with a range of resolutions are important data sources, and discarding models that fundamentally misrepresent relevant processes improves the credibility of ensemble information related to these processes. A key methodology is distillation – combining lines of evidence and accounting for stakeholder context and values – which helps ensure the information is relevant, useful and trusted for decision-making (see Core Concepts Box) (*high confidence*).

Since AR5, physical climate storylines have emerged as a complementary approach to ensemble projections for generating more accessible climate information and promoting a more comprehensive treatment of risk. They have been used as part of the distillation process within climate services to generate the required context-relevant, credible and trusted climate information.

Since AR5, climate change information produced for climate services has increased significantly due to scientific and technological advancements and growing user awareness, requirements, and demand (*very high confidence*). The decision-making context, level of user engagement, and co-production between scientists, practitioners and users are important determinants of the type of climate service developed and its utility in supporting adaptation, mitigation and risk management decisions. {10.3, 10.6, Cross-Chapter Box 10.3, 12.6, Cross-Chapter Box 12.2}

TS.4.1.1 Sources and Methodologies for Generating Regional Climate Information

Climate change information at regional scale is generated using a range of data sources and methodologies (Section TS.1.4). Understanding of observed regional climate change and variability is based on the availability and analysis of multiple observational datasets that are suitable for evaluating the phenomena of interest (e.g., extreme events), including accounting for observational uncertainty (Section TS.1.2.1). These datasets are combined with climate model simulations of observed changes and events to attribute causes of those changes and events to large- and regional-scale anthropogenic and natural drivers and to assess the performance of the models. Future simulations with many climate models (multi-model ensembles) are then used to generate and quantify ranges of projected regional climate responses (Section TS.4.2). Discarding models that fundamentally misrepresent relevant processes improves the credibility of regional climate information generated from these ensembles (*high confidence*). However, multi-model mean and ensemble spread are not a full measure of the range of projection uncertainty and are not sufficient to characterize low-likelihood, high-impact changes (Box TS.3) or situations where different models simulate substantially different or even opposite changes (*high confidence*). Large single-model ensembles are now available and provide a more comprehensive spectrum of possible changes associated with internal variability (*high confidence*) (Section TS.1.2.3). {1.5.1, 1.5.4, 10.2, 10.3.3, 10.3.4, 10.4.1, 10.6.2, 11.2, Box 11.2, Cross-Chapter Box 11.1, 12.4, Atlas.1.4.1}

Depending on the region of interest, representing regionally important forcings (e.g., aerosols, land-use change and ozone concentrations) and feedbacks (e.g., between snow and albedo, soil moisture and temperature, or soil moisture and precipitation) in climate models is a prerequisite for them to reproduce past regional trends to underpin the reliability of future projections (*medium confidence*) (Section TS.1.2.2). In some cases, even the sign of a projected change in regional climate cannot be trusted if relevant regional processes are not represented, for example, for variables such as precipitation and wind speed (*medium confidence*). In some regions, either geographical (e.g., Central Africa, Antarctica) or typological (e.g., mountainous areas, Small Islands and cities), and for certain phenomena, fewer observational records are available or accessible, which limits the assessment of regional climate change in these cases. {1.5.1, 1.5.3, 1.5.4, 8.5.1, 10.2, 10.3.3, 10.4.1, 11.1.6, 11.2, 12.4, Atlas.8.3, Atlas.11.1.5, Cross-Chapter Box Atlas.2}

Methodologies such as statistical downscaling, bias adjustment and weather generators are beneficial as an interface between climate model projections and impact modelling and for deriving user-relevant indicators (*high confidence*). However, the performance of these techniques depends on that of the driving climate model: in particular, bias adjustment cannot overcome all consequences of unresolved or strongly misrepresented physical processes, such as large-scale circulation biases or local feedbacks (*medium confidence*). {10.3.3, Cross-Chapter Box 10.2, 12.2, Atlas.2.2}

Box TS.10 | Event Attribution

The attribution of observed changes in extremes to human influence (including greenhouse gas and aerosol emissions and land-use changes) has substantially advanced since AR5, in particular for extreme precipitation, droughts, tropical cyclones, and compound extremes (*high confidence*). There is *limited evidence* for windstorms and convective storms. Some recent hot extreme events would have been *extremely unlikely* to occur without human influence on the climate system. (Section TS.1) {Cross-Working Group Box: Attribution in Chapter 1, 11.2, 11.3, 11.4, 11.6, 11.7, 11.8}

Since AR5, the attribution of extreme weather events has emerged as a growing field of climate research with an increasing body of literature. It provides evidence that greenhouse gases and other external forcings have affected individual extreme weather events by disentangling anthropogenic drivers from natural variability. Event attribution is now an important line of evidence for assessing changes in extremes on regional scales. (Section TS.1) {Cross-Working Group Box: Attribution, 11.1.4}

The regional extremes and events that have been studied are geographically uneven (Section TS.4.1). A few events, for example, extreme rainfall events in the United Kingdom, heatwaves in Australia, or Hurricane Harvey that hit Texas in 2017, have been heavily studied. Many highly impactful extreme weather events have not been studied in the event attribution framework, particularly in the developing world where studies are generally lacking. This is due to various reasons, including lack of observational data, lack of reliable climate models, and lack of scientific capacity. While the events that have been studied are not representative of all extreme events that have occurred, and results from these studies may also be subject to selection bias, the large number of event attribution studies provide evidence that changes in the properties of these local and individual events are in line with expected consequences of human influence on the climate and can be attributed to external drivers. {Cross-Working Group Box: Attribution, 11.1.4, 11.2.2}

It is *very likely* that human influence is the main contributor to the observed increase in the intensity and frequency of hot extremes and the observed decrease in the intensity and frequency of cold extremes on continental scales. Some specific recent hot extreme events would have been *extremely unlikely* to occur without human influence on the climate system. Changes in aerosol concentrations have *likely* slowed the increase in hot extremes in some regions, in particular from 1950–1980. No-till farming, irrigation and crop expansion have similarly attenuated increases in summer hot extremes in some regions, such as central North America (*medium confidence*). {11.3.4}

Human influence has contributed to the intensification of heavy precipitation in three continents where observational data are most abundant: North America, Europe and Asia (*high confidence*). On regional scales, evidence of human influence on extreme precipitation is limited, but new evidence from attributing individual heavy precipitation events found that human influence was a significant driver of the events. {11.4.4}

There is *low confidence* that human influence has affected trends in meteorological droughts in most regions, but *medium confidence* that they have contributed to the severity of some specific events. There is *medium confidence* that human-induced climate change has contributed to increasing trends in the probability or intensity of recent agricultural and ecological droughts, leading to an increase of the affected land area. {11.6.4}

Event attribution studies of specific strong tropical cyclones provide *limited evidence* for anthropogenic effects on tropical cyclone intensifications so far, but *high confidence* for increases in precipitation. There is *high confidence* that anthropogenic climate change contributed to extreme rainfall amounts during Hurricane Harvey (in 2017) and other intense tropical cyclones. {11.7.3}

Box TS.10 (continued)

The number of evident attribution studies on compound events is limited. There is *medium confidence* that weather conditions that promote wildfires have become more probable in southern Europe, northern Eurasia, the USA, and Australia over the last century. In Australia a number of event attribution studies show that there is *medium confidence* of increase in fire weather conditions due to human influence. {11.8.3, 12.4.3.2}

Climate change is already affecting every inhabited region across the globe, with human influence contributing to many observed changes in weather and climate extremes

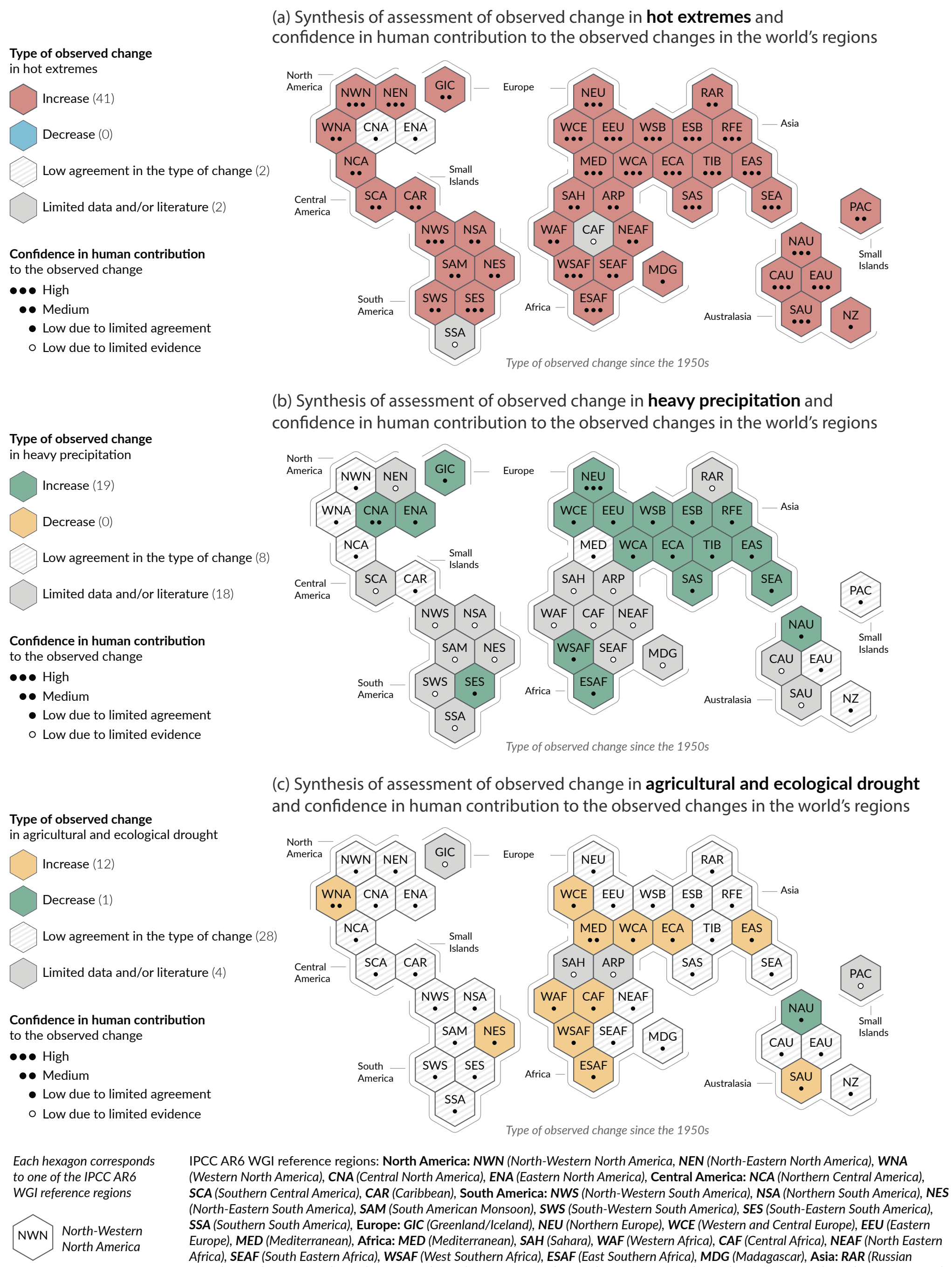

IPCC AR6 WGI reference regions: **North America: *NWN*** *(North-Western North America),* ***NEN*** *(North-Eastern North America),* ***WNA*** *(Western North America),* ***CNA*** *(Central North America),* ***ENA*** *(Eastern North America),* **Central America: *NCA*** *(Northern Central America),* ***SCA*** *(Southern Central America),* ***CAR*** *(Caribbean),* **South America: *NWS*** *(North-Western South America),* ***NSA*** *(Northern South America),* ***NES*** *(North-Eastern South America),* ***SAM*** *(South American Monsoon),* ***SWS*** *(South-Western South America),* ***SES*** *(South-Eastern South America),* ***SSA*** *(Southern South America),* **Europe: *GIC*** *(Greenland/Iceland),* ***NEU*** *(Northern Europe),* ***WCE*** *(Western and Central Europe),* ***EEU*** *(Eastern Europe),* ***MED*** *(Mediterranean),* **Africa: *MED*** *(Mediterranean),* ***SAH*** *(Sahara),* ***WAF*** *(Western Africa),* ***CAF*** *(Central Africa),* ***NEAF*** *(North Eastern Africa),* ***SEAF*** *(South Eastern Africa),* ***WSAF*** *(West Southern Africa),* ***ESAF*** *(East Southern Africa),* ***MDG*** *(Madagascar),* **Asia: *RAR*** *(Russian Arctic),* ***WSB*** *(West Siberia),* ***ESB*** *(East Siberia),* ***RFE*** *(Russian Far East),* ***WCA*** *(West Central Asia),* ***ECA*** *(East Central Asia),* ***TIB*** *(Tibetan Plateau),* ***EAS*** *(East Asia),* ***ARP*** *(Arabian Peninsula),* ***SAS*** *(South Asia),* ***SEA*** *(South East Asia),* **Australasia: *NAU*** *(Northern Australia),* ***CAU*** *(Central Australia),* ***EAU*** *(Eastern Australia),* ***SAU*** *(Southern Australia),* ***NZ*** *(New Zealand),* **Small Islands: *CAR*** *(Caribbean),* ***PAC*** *(Pacific Small Islands)*

Box TS.10, Figure 1 | Synthesis of assessed observed and attributable regional changes.

Box TS.10 (continued)

Box TS.10, Figure 1 (continued): The IPCC AR6 WGI inhabited regions are displayed as **hexagons** of identical sizes in their approximate geographical location (see legend for regional acronyms). All assessments are made for each region as a whole and for the 1950s to the present. Assessments made on different time scales or more local spatial scales might differ from what is shown in the figure. The **colours** in each panel represent the four outcomes of the assessment on observed changes. Striped hexagons (white and light-grey) are used where there is *low agreement* in the type of change for the region as a whole, and grey hexagons are used when there is limited data and/or literature that prevents an assessment of the region as a whole. Other colours indicate at least *medium confidence* in the observed change. The **confidence level** for the human influence on these observed changes is based on assessing trend detection and attribution and event attribution literature, and it is indicated by the number of dots: three dots for *high confidence*, two dots for *medium confidence* and one dot for *low confidence* (single, filled dot: limited agreement; single, empty dot: *limited evidence*).

Panel (a) For hot extremes, the evidence is mostly drawn from changes in metrics based on daily maximum temperatures; regional studies using other indices (heatwave duration, frequency and intensity) are used in addition. Red hexagons indicate regions where there is at least *medium confidence* in an observed increase in hot extremes.

Panel (b) For heavy precipitation, the evidence is mostly drawn from changes in indices based on one-day or five-day precipitation amounts using global and regional studies. Green hexagons indicate regions where there is at least *medium confidence* in an observed increase in heavy precipitation.

Panel (c) Agricultural and ecological droughts are assessed based on observed and simulated changes in total column soil moisture, complemented by evidence on changes in surface soil moisture, water balance (precipitation minus evapotranspiration) and indices driven by precipitation and atmospheric evaporative demand. Yellow hexagons indicate regions where there is at least *medium confidence* in an observed increase in this type of drought and green hexagons indicate regions where there is at least *medium confidence* in an observed decrease in agricultural and ecological drought.

For all regions, Table TS.5 shows a broader range of observed changes besides the ones shown in this figure. Note that Southern South America (SSA) is the only region that does not display observed changes in the metrics shown in this figure, but is affected by observed increases in mean temperature, decreases in frost and increases in marine heatwaves.

(Table TS.5) {11.9, Atlas 1.3.3, Figure Atlas.2}

TS.4.1.2 Regional Climate Information Distillation and Climate Services

The construction of regional climate information involves people with a variety of backgrounds, from various disciplines, who have different sets of experiences, capabilities and values. The process of synthesizing climate information from different lines of evidence from a number of sources, taking into account the context of a user vulnerable to climate variability and change and the values of all relevant actors, is called distillation. Distillation is conditioned by the sources available, the actors involved, and the context, which all depend heavily on the regions considered, and is framed by the question being addressed. Distilling regional climate information from multiple lines of evidence and taking the user context into account increases fitness, usefulness, relevance and trust in that information for use in climate services (Box TS.11) and decision-making (*high confidence*). {1.2.3, 10.1.4, 10.5, Cross-Chapter Box 10.3, 12.6}

The distillation process can vary substantially, as it needs to consider multiple lines of evidence on all physically plausible outcomes (especially when they are contrasting) relevant to a specific decision required in response to a changing climate. Confidence in the distilled regional climate information is enhanced when there is agreement across multiple lines of evidence, so the outcome can be limited if these are inconsistent or contradictory. For example, in the Mediterranean region the agreement between different lines of evidence, such as observations, projections by regional and global models, and understanding of the underlying mechanisms, provides *high confidence* in summer warming that exceeds the global average (see Box TS.12). In a less clear-cut case for Cape Town, South Africa, despite consistency among global model future projections, there is *medium confidence* in a projected future drier climate due to the lack of consistency in links between increasing greenhouse gases, changes in a key mode of variability (the Southern Annular Mode) and drought in Cape Town among different observation periods and in model simulations. {10.5.3, 10.6, 10.6.2, 10.6.4, Cross-Chapter Box 10.3, 12.4}

Since AR5, physical climate storyline approaches have emerged as a complementary instrument to provide a different perspective, or additional climate information, to facilitate communication of the information or provide a more flexible consideration of risk. Storylines that condition climatic events and processes on a set of plausible but distinct large-scale climatic changes enable the exploration of uncertainties in regional climate projections. For example, they can explicitly address low-likelihood, high-impact outcomes, which would be less emphasized in a probabilistic approach, and can be embedded in a user's risk landscape, taking account of socio-economic factors as well as physical climate changes. Storylines can also be used to communicate climate information by narrative elements describing and contextualizing the main climatological features and the relevant consequences in the user context and, as such, can be used as part of a climate information distillation process. {1.4.4., Box 10.2, 11.2, Box 11.2, Cross-Chapter Box 12.2}

Box TS.11 | Climate Services

Climate services involve providing climate information to assist decision-making, for example, about how extreme rainfall will change to inform improvements in urban drainage. Since AR5, there has been a significant increase in the range and diversity of climate service activities (*very high confidence*). The level of user-engagement, co-design and co-production are factors determining the utility of climate services, while resource limitations for these activities constrain their full potential. {12.6, Cross-Chapter Box 12.2}

Climate services include engagement from users and providers and an effective access mechanism; they are responsive to user needs and based on integrating scientifically credible information and relevant expertise. Climate services are being developed across regions, sectors, time scales and user-groups and include a range of knowledge brokerage and integration activities. These involve identifying knowledge needs; compiling, translating and disseminating knowledge; coordinating networks and building capacity through informed decision-making; analysis, evaluation and development of policy; and personal consultation.

Since AR5, climate change information produced in climate service contexts has increased significantly due to scientific and technological advancements and growing user awareness, requirements and demand (*very high confidence*). Climate services are growing rapidly and are highly diverse in their practices and products. The decision-making context, level of user engagement and co-production between scientists, practitioners and intended users are important determinants of the type of climate service developed and their utility for supporting adaptation, mitigation and risk management decisions. They require different types of user–producer engagement depending on what the service aims to deliver (*high confidence*), and these fall into three broad categories: website-based services, interactive group activities and focused relationships.

Realization of the full potential of climate services is often hindered by limited resources for the co-design and co-production process, including sustained engagement between scientists, service providers and users (*high confidence*). Further challenges relate to the development and provision of climate services, generation of climate service products, communication with users, and evaluation of their quality and socio-economic benefit. (Section TS.4.1) {1.2.3, 10.5.4, 12.6, Cross-Chapter Box 12.2, Glossary}

Box TS.12 | Multiple Lines of Evidence for Assessing Regional Climate Change and the Interactive Atlas

A key novel element in the AR6 is the Working Group I Atlas, which includes the Interactive Atlas (https://interactive-atlas.ipcc.ch/). The Interactive Atlas provides the ability to explore much of the observational and climate model data used as lines of evidence in this assessment to generate regional climate information. {Atlas.2}

A significant innovation in the AR6 WGI Report is the Atlas. Part of its remit is to provide region-by-region assessment on changes in mean climate and to link with other WGI chapters to generate climate change information for the regions. An important component is the new online interactive tool, the Interactive Atlas, with flexible spatial and temporal analyses of much of the observed, simulated past and projected future climate change data underpinning the WGI assessment. This includes the ability to generate global maps and a number of regionally aggregated products (time series, scatter plots, tables, etc.) for a range of observations and ensemble climate change projections of variables (such as changes in the climatic impact-drivers summarized in Table TS.5) from the Coupled Model Intercomparison Project Phases 5 and 6 (CMIP5, CMIP6) and the Coordinated Regional Climate Downscaling Experiment (CORDEX). The data can be displayed and summarized under a range of SSP-RCP scenarios and future time slices and also for different global warming levels, relative to several different baseline periods. The maps and various statistics can be generated for annual mean trends and changes or for any user-specified season. A new set of WGI reference regions is used for the regional summary statistics and applied widely throughout the report (with the regions, along with aggregated datasets and the code to generate these, available at the ATLAS GitHub: https://github.com/IPCC-WG1/Atlas).

Box TS.12, Figure 1 shows how the Interactive Atlas products, together with other lines of evidence, can be used to generate climate information for an illustrative example of the Mediterranean summer warming. The lines of evidence include the understanding of relevant mechanisms, dynamic and thermodynamic processes and the effect of aerosols in this case (Box TS.12, Figure 1a); trends in observational datasets (which can have different spatial and temporal coverage; Box TS.12, Figure 1b, c); and attribution of these trends and temperature projections from global and regional climate models at different resolutions, including single-model initial-condition large ensembles (SMILEs; Box TS.12, Figure 1d, e). Taken together, this evidence shows there is *high confidence* that the

Box TS.12 (continued)

projected Mediterranean summer temperature increase will be larger than the global mean, with consistent results from CMIP5 and CMIP6 (Box TS.12, Figure 1e). However, CMIP6 results project both more pronounced warming than CMIP5 for a given emissions scenario and time period and a greater range of changes (Box TS.12, Figure 1d). {10.6.4, Atlas.2, Atlas.8.4}

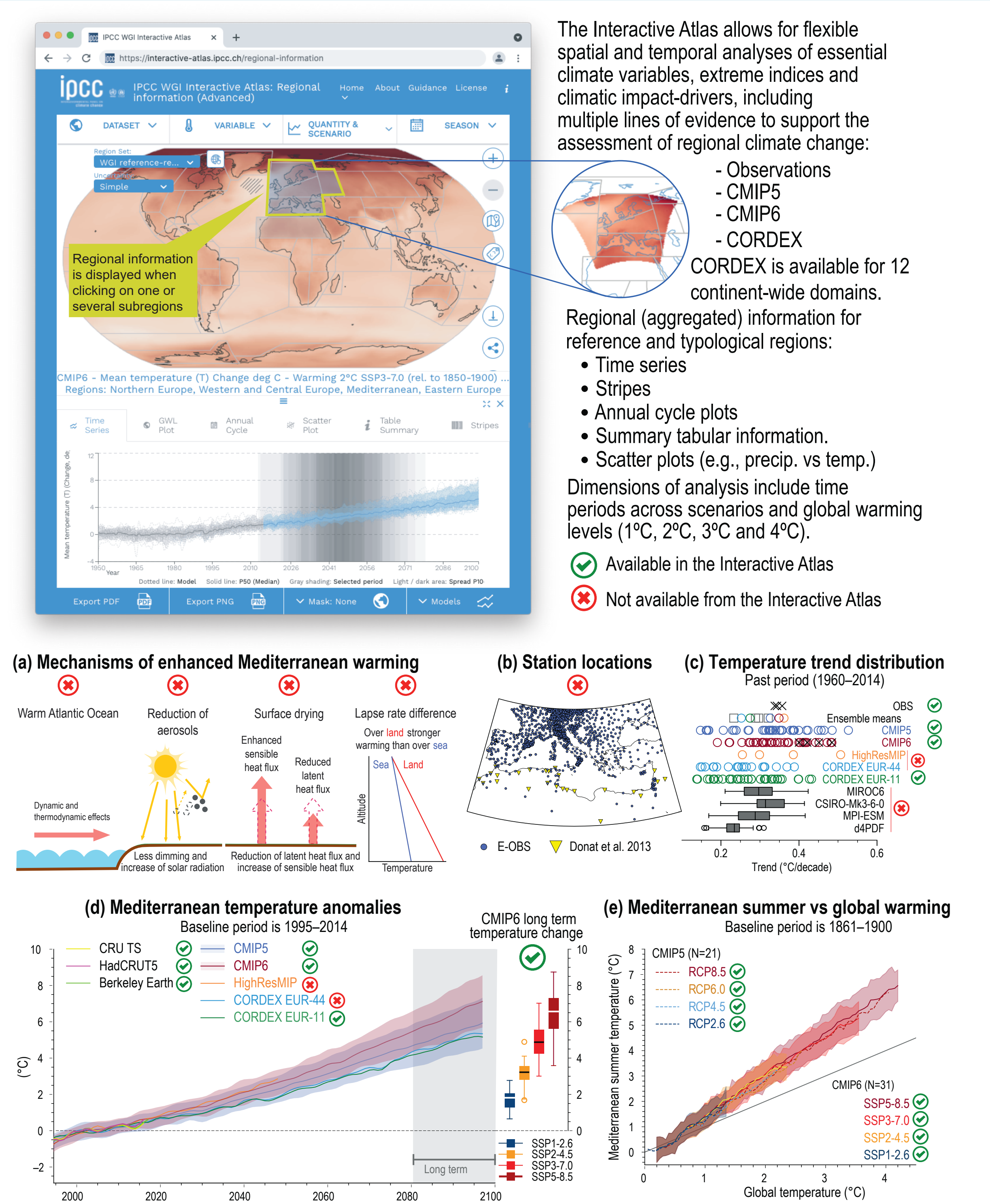

Box TS.12, Figure 1 | Example of generating regional climate information from multiple lines of evidence for the case of Mediterranean summer warming.

Box TS.12 (continued)

Box TS.12, Figure 1 (continued): *The intent of this figure is to provide an example of using different lines of evidence to assess the confidence in or likelihood of a projected change in regional climate and which of these lines of evidence are available to view and explore in the Interactive Atlas.* **(a)** Mechanisms and feedbacks involved in enhanced Mediterranean summer warming. **(b)** Locations of observing stations from different datasets. **(c)** Distribution of 1960–2014 summer temperature trends (°C per decade) for observations (black crosses), CMIP5 (blue circles), CMIP6 (red circles), HighResMIP (orange circles), CORDEX EUR-44 (light blue circles), CORDEX EUR-11 (green circles), and selected single model initial-condition large ensembles (SMILEs; grey boxplots, MIROC6, CSIRO-Mk3-6-0, MPI-ESM and d4PDF). **(d)** Time series of area averaged (25°N–50°N, 10°W–40°E) land point summer temperature anomalies (°C, baseline period is 1995–2014): the boxplot shows long term (2081–2100) temperature changes of different CMIP6 scenarios in respect to the baseline period. **(e)** Projected Mediterranean summer warming in comparison to global annual mean warming of CMIP5 (RCP2.6, RCP4.5, RCP6.0 and RCP8.5) and CMIP6 (SSP1-2.6, SSP2-4.5, SSP3-7.0 and SSP5-8.5) ensemble means (lines) and spread (shading). {Figure 10.20, Figure 10.21, Figure Atlas.8}

TS.4.2 Drivers of Regional Climate Variability and Change

Anthropogenic forcing, including GHGs and aerosols, but also regional land use and irrigation have all affected observed regional climate changes (*high confidence*) and will continue to do so in the future (*high confidence*), with various degrees of influence and response times, depending on warming levels, the nature of the forcing and the relative importance of internal variability.

Since the late 19th century, major modes of variability (MoVs) exhibited fluctuations in frequency and magnitude at multi-decadal time scales, but no sustained trends outside the range of internal variability (Table TS.4). An exception is the Southern Annular Mode (SAM), which has become systematically more positive (*high confidence*) and is projected to be more positive in all seasons, except for December–January–February (DJF), in high CO_2 emissions scenarios (*high confidence*). The influence of stratospheric ozone forcing on the SAM trend has been reduced since the early 2000s compared to earlier decades, contributing to the weakening of its positive trend as observed over 2000–2019 (*medium confidence*).

In the near term, projected changes in most of the MoVs and related teleconnections will *likely* be dominated by internal variability. In the long term, it is *very likely* that the precipitation variance related to El Niño–Southern Oscillation will increase. Physical climate storylines, including the complex interplay between climate drivers, MoVs, and local and remote forcing, increase confidence in the understanding and use of observed and projected regional changes. {2.4, 3.7, 4.3, 4.4, 4.5, 6.4, 8.3, 8.4, 10.3, 10.4, 11.3}

TS.4.2.1 Regional Fingerprints of Anthropogenic and Natural Forcing

While anthropogenic forcing has contributed to multi-decadal mean precipitation changes in several regions, internal variability can delay emergence of the anthropogenic signal in long-term precipitation changes in many land regions (*high confidence*). At the regional scale, the effect of human-induced GHG forcing on extreme temperature is moderated or amplified by soil moisture feedback, snow/ice-albedo feedback, regional forcing from land-use/land-cover changes, forcing from aerosol concentrations, or decadal/multi-decadal natural variability. Changes in local and remote aerosol forcings lead to south–north gradients of the effective radiative forcing (hemispherical asymmetry). Along latitudes, it is more uniform, with strong amplification of the temperature response towards the Arctic (*medium confidence*). The decrease of SO_2 emissions since the 1980s reduces the damping effect of aerosols, leading to a faster increase in surface air temperature that is most pronounced at mid- and high latitudes of the Northern Hemisphere, where the largest emissions reductions have taken place (*medium confidence*). {1.3, 3.4.1, 6.3.4, 6.4.1, 6.4.3, 8.3.1, 8.3.2, Box 8.1, 10.4.2, 10.6, 11.1.6, 11.3}

Multi-decadal dimming and brightening trends in incoming solar radiation at Earth's surface occurred at widespread locations (*high confidence*). Multi-decadal variation in anthropogenic aerosol emissions are thought to be a major contributor (*medium confidence*), but multi-decadal variability in cloudiness may also have played a role. Volcanic eruptions affect regional climate through their spatially heterogeneous effect on the radiative budget as well as through triggering dynamical responses by favouring a given phase from some MoVs, for instance. {1.4.1, Cross-Chapter Box 1.2, 2.2.1, 2.2.2, 3.7.1, 3.7.3, 4.3.1, 4.4.1, 4.4.4, Cross-Chapter Box 4.1, 7.2.2, 8.5.2, 10.1.4, 11.1.6, 11.3.1}

Historical urbanization affects the observed warming trends in cities and their surroundings (*very high confidence*). Future urbanization will amplify the projected air temperature under different background climates, with a strong effect on minimum temperatures that could be as large as the global warming signal (*very high confidence*) (Box TS.14). Irrigation and crop expansion have attenuated increases in summer hot extremes in some regions, such as central North America (*medium confidence*) (Box TS.6). {Box 10.3, 11.1.6, 11.3}

TS.4.2.2 Modes of Variability and Regional Teleconnections

Modes of variability (Annex IV, Table TS.4) have existed for millennia or longer (*high confidence*), but there is *low confidence* in detailed reconstructions of most of them prior to direct instrumental records. MoVs are treated as a main source of uncertainties associated with internal dynamics, as they can either accentuate or dampen, even mask, the anthropogenically forced responses. {2.4, 8.5.2, 10.4, 10.6, 11.1.5, Atlas.3.1}

Since the late 19th century, major MoVs (Table TS.4) show no sustained trends, exhibiting fluctuations in frequency and magnitude at multi-decadal time scales, except for the Southern Annular Mode (SAM), which has become systematically more positive (*high confidence*) (Table TS.4). It is *very likely* that human influence has contributed to this trend from the 1970s to the 1990s, and to the associated strengthening and southward shift of the Southern Hemispheric extratropical jet in austral summer. The influence of stratospheric ozone forcing on the SAM trend has been reduced since the early 2000s compared to earlier decades, contributing to the weakening of its positive trend observed over 2000–2019 (*medium confidence*). By contrast, the cause of the Northern Annular Mode (NAM) trend toward its positive phase since the 1960s and associated northward shifts of Northern Hemispheric extratropical jet and storm track in boreal winter is not well understood. The evaluation of model performance on simulating MoVs is assessed in Section TS.1.2.2. {2.3.3, 2.4, 3.3.3, 3.7.1, 3.7.2}

In the near term, the forced change in SAM in austral summer is *likely* to be weaker than observed during the late 20th century under all five SSPs assessed. This is because of the opposing influence in the near to mid-term from stratospheric ozone recovery and increases in other greenhouse gases on the Southern Hemisphere summertime mid-latitude circulation (*high confidence*). In the near term, forced changes in the SAM in austral summer are therefore *likely* to be smaller than changes due to natural internal variability. In the long term (2081–2100) under the SSP5-8.5 scenario, the SAM index is *likely* to increase in all seasons relative to 1995–2014. The CMIP6 multi-model ensemble projects a long-term (2081–2100) increase in the boreal wintertime NAM index under SSP3-7.0 and SSP5-8.5, but regional associated changes may deviate from a simple shift in the mid-latitude circulation due to a modified teleconnection resulting from interaction with a modified mean background state. {4.3.3, 4.4.3, 4.5.1, 4.5.3, 8.4.2}

Human influence has not affected the principal tropical modes of interannual climate variability (Table TS.4) and their associated regional teleconnections beyond the range of internal variability (*high confidence*). It is *virtually certain* that the El Niño–Southern Oscillation (ENSO) will remain the dominant mode of interannual variability in a warmer world. There is no consensus from models for a systematic change in amplitude of ENSO sea surface temperature (SST) variability over the 21st century in any of the SSP scenarios assessed (*medium confidence*). However, it is *very likely* that rainfall variability related to ENSO will be enhanced significantly by the latter half of the 21st century in the SSP2-4.5, SSP3-7.0 and SSP5-8.5 scenarios, regardless of the amplitude changes in SST variability related to the mode. It is *very likely* that rainfall variability related to changes in the strength and spatial extent of ENSO teleconnections will lead to significant changes at regional scale. {3.7.3, 3.7.4, 3.7.5, 4.3.3, 4.5.3, 8.4.2, 10.3.3}

Modes of decadal and multi-decadal variability over the Pacific and Atlantic Ocean exhibit no significant changes in variance over the period of observational records (*high confidence*). There is *medium confidence* that anthropogenic and volcanic aerosols contributed to observed temporal evolution in the Atlantic Multi-decadal Variability (AMV) and associated regional teleconnections, especially since the 1960s, but there is *low confidence* in the magnitude of this influence and the relative contributions of natural and anthropogenic forcings. Internal variability is the main driver of Pacific Decadal Variability (PDV) observed since the start of the instrumental records (*high confidence*), despite some modelling evidence for potential external influence. There is *medium confidence* that the AMV will undergo a shift towards a negative phase in the near term. {2.4, 3.7.6, 3.7.7, 8.5.2, 4.4.3}

Table TS.4 | Summary of the assessments on modes of variability (MoVs) and associated teleconnections. (a) Assessments on observed changes since the start of instrumental records, Coupled Model Intercomparison Project Phases 5 and 6 (CMIP5 and CMIP6) model performance, human influence on the observed changes, and near-term (2021–2040) and mid- to long-term (2041–2100) changes. Curves schematically illustrate the assessed overall changes, with the horizontal axis indicating time, and are not intended to precisely represent the time evolution. **(b)** Fraction of surface air temperature (SAT) and precipitation (pr) variance explained at interannual time scale by each MoV for each AR6 region (numbers in each cell; in percent). Values correspond to the average of significant explained variance fractions based on HadCRUT, GISTEMP, BerkeleyEarth and CRU-TS (for SAT) and GPCC and CRU-TS (for precipitation). Significance is tested based on F-statistics at the 95% level confidence, and a slash indicates that the value is not significant in more than half of the available data sets. The colour scale corresponds to the sign and values of the explained variance as shown at the bottom. The corresponding anomaly maps are shown in Annex IV. DJF: December–January–February. MAM: March–April–May. JJA: June–July–August. SON: September–October–November. In (b), Northern Annular Mode (NAM) and El Niño–Southern Oscillation (ENSO) teleconnections are evaluated for 1959–2019, Southern Annular Mode (SAM) for 1979–2019, Indian Ocean Basin (IOB), Indian Ocean Dipole (IOD), Atlantic Zonal Mode (AZM) and Atlantic Meridional Mode (AMM) for 1958–2019, and Pacific Decadal Variability (PDV) and Atlantic Multi-decadal Variability (AMV) for 1900–2019. All data are linearly detrended prior to computation. (Section TS.1.2.2) {2.4, 3.7, 4.3.3, 4.4.3, 4.5.3, Table Atlas.1, Annex IV}

(a) Assessments on MoV.

	NAM	SAM	ENSO	IOB	IOD	AZM	AMM	PDV	AMV
Past changes since the start of observations	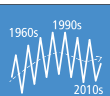 Boreal winter	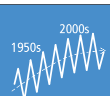 Austral summer	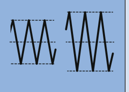 1400–1850 Since 1950s	Within proxy-inferred variability range	Within proxy-inferred variability range	*Limited evidence*	*Limited evidence*	Dominated by multi-decadal fluctuations	Dominated by multi-decadal fluctuations
	{2.4.1.1}	{2.4.1.2}	{2.4.2}	{2.4.3}	{2.4.3}	{2.4.4}	{2.4.4}	{2.4.5}	{2.4.6}
CMIP5 and CMIP6 model performance	High performance	High performance	Medium performance	Medium performance	Medium performance	Low performance	Low performance	Medium performance	Medium performance
	{3.7.1}	{3.7.2}	{3.7.3}	{3.7.4}	{3.7.4}	{3.7.5}	{3.7.5}	{3.7.6}	{3.7.7}
Human influence on the observed changes	No robust evidence	Contributed through GHG (all seasons) & ozone (DJF)	*Low agreement*	No robust evidence	Not detected	No robust evidence	No robust evidence	Not detected	Contributed through aerosols
	{3.7.1}	{3.7.2}	{3.7.3}	{3.7.4}	{3.7.4}	{3.7.5}	{3.7.5}	{3.7.6}	{3.7.7}
Near-term future changes (2021–2040)	Internal variability dominates	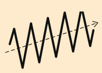 All seasons except DJF	Internal variability dominates	No robust evidence	No robust evidence	No robust evidence	No robust evidence	*Limited evidence*	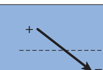 Phase shift from + to –
	{4.4.3.1}	{4.4.3.1}	{4.4.3.2}	{4.4.3.3}	{4.4.3.3}	{4.4.3.4}	{4.4.3.4}	{4.4.3.5}	{4.4.3.6}
Mid-to-long-term future changes (2041–2100)	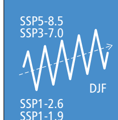	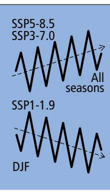	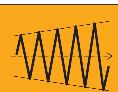 Increase in precipitation variance	No robust evidence	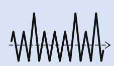 increase in extreme positive events	No robust evidence	No robust evidence	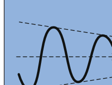 Decrease in variance	No changes
	{4.3.3.1; 4.5.3.1}	{4.3.3.1; 4.5.3.1}	{4.3.3.2; 4.5.3.2}	{4.5.3.3}	{4.5.3.3}	{4.5.3.4}	{4.5.3.4}	{4.5.3.5}	{4.5.3.6}

low confidence · *medium confidence* · *high confidence*

more likely than not · *likely* · *very likely*

Table TS.4 (continued): (b) Regional climate anomalies associated with MoV.

Mode		NAM		SAM		ENSO		IOB		IOD		AZM		AMM		PDV		AMV	
Season		DJF		DJF		DJF		MAM		SON		JJA		JJA		annual		annual	
Variable		SAT	pr	SAT	pr	SAT	pr	SAT	pr	SAT	pr	SAT	pr	SAT	pr	SAT	pr	SAT	pr
Africa	Mediterranean	28	58			7												19	
	Sahara	58						14				10	19		12		9	12	25
	Western Africa	25					15	45				21		10			6	6	23
	Central Africa	19	8		10	14		50				13					10	14	11
	North Eastern Africa	19	7				14	36			32					7		7	
	South Eastern Africa					14	22	36			57			10			4	9	
	West Southern Africa					49	26	27	16	8						4	12	5	
	East Southern Africa			13		75	34	35	7							4	6		
	Madagascar					24		24	7	11	10			9				5	
Asia	West Siberia	45					7						9						11
	East Siberia	52														3			11
	Russian Far East	8	10			11		6										5	5
	West Central Asia								15		21						4		
	East Central Asia								38										
	Tibetan Plateau		15							15	7		11			6	5	9	
	East Asia					7	20		23				9				9	13	
	South Asia	9						12			8			8				5	
	South East Asia					39	31	73	6		48					5	12		7
	Arabian Peninsula	32						10	24		20						5	13	7
Australasia	Northern Australia					21	13	38			19				7	7	7		
	Central Australia			14		21	12	18		22	20		7		7	6	5		
	East Australia			22		20	11	18		9	8		7			7	8		
	Southern Australia						11			23	40		8				3		
	New Zealand			16															
Central & South America	Southern Central America					21	16	33		10	11			17		6		6	7
	North-Western South America		7	14	16	82	17	54		18				13	16	7	8		
	Northern South America	7				56	58	61					22	17	24	9	12	7	
	North-Eastern South America					25		58	19	9	12				8				
	South American Monsoon					54		31		22	7				6	7			
	South-Western South America				10	16	14	17		10	16					8			
	South-Eastern South America						21		13	21	10		12				5		6
	Southern South America				23					13	7								9
Europe	Mediterranean	28	58			7												19	
	Western and Central Europe	28	18							13	10						4		8
	Eastern Europe	35										7							
	Northern Europe	53	32															6	
North America	Northern Central America			10	26	13	27	18				7	12	15	12		6	19	
	Western North America															4		6	5
	Central North America	17			12		17					8					3	9	6
	Eastern North America	12										11	9			4		9	4
	North-Eastern North America	18	26									8					10	9	4
	North-Western North America		14			10	8	17								8	4		
Small Islands	Caribbean				10	15	18	26	8		10			17	12	7			5
	Pacific																		
Polar Terrestrial Regions	Greenland/Iceland	42	8												7			44	
	Russian Arctic	25	10														6	11	8
	West Antarctica											8		21					
	East Antarctica			38															

colder — warmer

40 30 20 0 20 30 40

Temperature anomalies and explained variance (%)

drier — wetter

40 30 20 0 20 30 40

Precipitation anomalies and explained variance (%)

Not significant in >50% of available data sets

Data unavailable in >50% of data sets

TS.4.2.3 Interplay Between Drivers of Climate Variability and Change at Regional Scales

Anthropogenic forcing has been a major driver of regional mean temperature change since 1950 in many sub-continental regions of the world (*virtually certain*). At regional scales, internal variability is stronger, and uncertainties in observations, models and external forcing are all larger than at the global scale, hindering a robust assessment of the relative contributions of greenhouse gases, stratospheric ozone, and different aerosol species in most of the cases. Multiple lines of evidence, combining multi-model ensemble global projections with those coming from single-model initial-condition large ensembles, show that internal variability is largely contributing to the delayed or absent emergence of the anthropogenic signal in long-term regional mean precipitation changes (*high confidence*). Internal variability in ocean dynamics dominates regional patterns on annual to decadal time scales (*high confidence*). The anthropogenic signal in regional sea level change will emerge in most regions by 2100 (*medium confidence*). {9.2.4, 9.6.1, 10.4.1, 10.4.2, 10.4.3}

Regional climate change is subject to the complex interplay between multiple external forcings and internal variability. Time evolution of mechanisms operating at different time scales can modify the amplitude of the regional-scale response of temperature, and both the amplitude and sign of the response of precipitation, to anthropogenic forcing (*high confidence*). These mechanisms include non-linear temperature, precipitation and soil moisture feedbacks; slow and fast responses of SST patterns; and atmospheric circulation changes to increasing GHGs. Land-use and aerosol forcings and land–atmosphere feedback play important roles in modulating regional changes, for instance in weather and climate extremes (*high confidence*). These can also lead to a higher warming of extreme

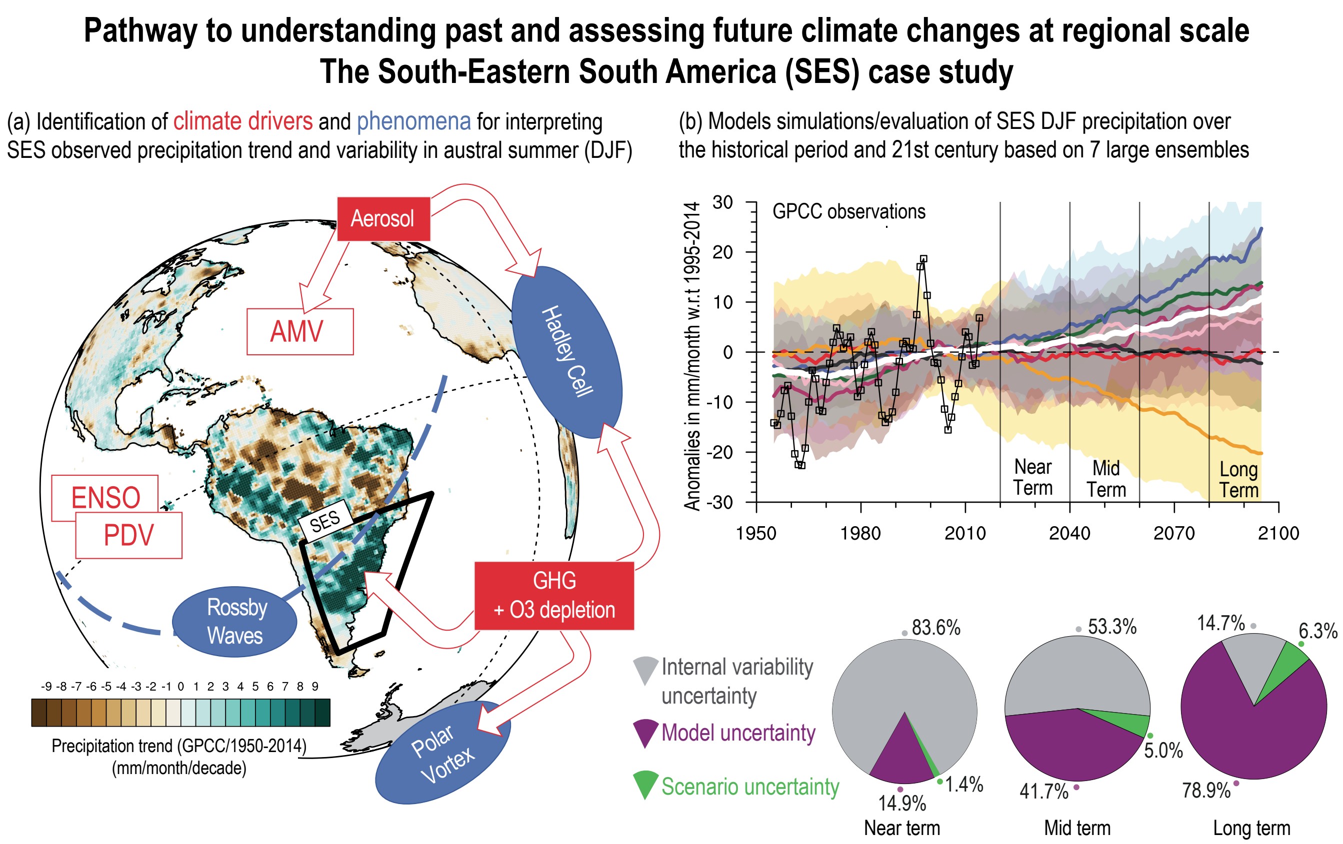

Figure TS.21 | Example of the interplay between drivers of climate variability and change at regional scale to understand past and projected changes. *The figure intent is to show an illustrative pathway for understanding past, and anticipating future, climate change at regional scale in the presence of uncertainties.* **(a)** Identification of the climate drivers and their influences on climate phenomena contributing through teleconnection to South-Eastern South America (SES) summer (December–January–February; DJF) precipitation variability and trends observed over 1950–2014. Drivers (red squares) include modes of variability as well as external forcing. Observed precipitation linear trend from GPCC is shown on continents (green-brown colour bar in mm month^{-1} per decade) and the SES AR6 WGI reference region is outlined with the thick black contour. Climate phenomena leading to local effects on SES are schematically presented (blue ovals). **(b)** Time series of decadal precipitation anomalies for DJF SES simulated from seven large ensembles of historical plus RCP8.5 simulations over 1950–2100. Shading corresponds to the 5–95th range of climate outcomes given from each large ensemble for precipitation (in mm month^{-1}) and thick coloured lines stand for their respective ensemble mean. The thick time series in white corresponds to the multi-model multi-member ensemble mean, with model contribution being weighted according to their ensemble size. GPCC observation is shown in the light black line with squares over 1950–2014, and the 1995–2014 baseline period has been retained for calculation of anomalies in all datasets. **(c)** Quantification of the respective weight (in percent) between the individual sources of uncertainties (internal in grey, model in magenta and scenario in green) at near-term, mid-term and long-term temporal windows defined in AR6 and highlighted in (b) for SES DJF precipitation. All computations are done with respect to 1995–2014, taken as the reference period, and the scenario uncertainty is estimated from Coupled Model Intercomparison Project Phase 5 (CMIP5) using the same set of models as for the large ensembles that have run different Representative Concentration Pathway (RCP) scenarios. {Figure 10.12a} temperatures compared to mean temperature (*high confidence*), and possibly cooling in some regions (*medium confidence*). The soil moisture–temperature feedback was shown to be relevant for past and present-day heatwaves based on observations and model simulations. {10.4.3, 11.1.6, 11.3.1}

South-Eastern South America (SES) is one of the AR6 WGI reference regions (outlined with black thick contour in Figure TS.21a), and it is used here as an illustrative example of the interplay between drivers of climate variability and change at regional scale. Austral summer (DJF) precipitation positive trends have been observed over the region during 1950–2014. Drivers of this change include MoVs, such as AMV, ENSO, and PDV, as well as external forcing, like GHG increases and ozone depletion together with aerosols (as illustrated in Figure TS.21a). Modes of variability and external forcing collectively affect climate phenomena, such as the Hadley cell width and strength, Rossby waves activity emerging from the large-scale tropical SST anomalies, and the Southern Hemisphere polar vortex, which are relevant for the region. In fact, local changes over SES in terms of moisture convergence, ascending motion and storm-track locations depend on these climate phenomena, and they are overall responsible for the observed precipitation trends. Projections suggest continuing positive trends in rainfall over SES in the near-term in response to GHG emissions scenarios. Multi-model mean and ensemble spread are not sufficient to characterize situations where different models simulate substantially different or even opposite changes (*high confidence*). In such cases, physical climate storylines addressing possible outcomes for climate phenomena shown to play a role in the variability of the region of interest can aid the interpretation of projection uncertainties. In addition, single-model initial-condition large ensembles of many realizations of internal variability are required to separate internal variability from forced changes (*high confidence*) and to partition the different sources of uncertainties as a function of future assessed periods. {10.3.4, 10.4.2, Figure 10.12a}

Box TS.13 | Monsoons

Global land monsoon precipitation decreased from the 1950s to the 1980s, partly due to anthropogenic aerosols, but has increased since then in response to GHG forcing and large-scale multi-decadal variability (*medium confidence*). Northern Hemispheric anthropogenic aerosols weakened the regional monsoon circulations in South Asia, East Asia and West Africa during the second half of the 20th century, thereby offsetting the expected strengthening of monsoon precipitation in response to GHG-induced warming (*high confidence*).

During the 21st century, global land monsoon precipitation is projected to increase in response to GHG warming in all time horizons and scenarios (*high confidence*). Over South and South East Asia, East Asia and the central Sahel, monsoon precipitation is projected to increase, whereas over North America and the far western Sahel it is projected to decrease (*medium confidence*). There is *low confidence* in projected precipitation changes in the South American and Australian-Maritime Continent monsoons. At global and regional scales, near-term monsoon changes will be dominated by the effects of internal variability (*medium confidence*). {2.3, Cross-Chapter Box 2.4, 3.3, 4.4, 4.5, 8.2, 8.3, 8.4, 8.5, Box 8.1, Box 8.2, 10.6}

Global Monsoon

Paleoclimate records indicate that during warm climates, like the mid-Pliocene Warm Period, monsoon systems were stronger (*medium confidence*). In the instrumental records, global summer monsoon precipitation intensity has *likely* increased since the 1980s, dominated by Northern Hemisphere summer trends and large multi-decadal variability. Contrary to the expected increase of precipitation under global warming, the Northern Hemisphere monsoon regions experienced declining precipitation from the 1950s to 1980s, which is partly attributable to the influence of anthropogenic aerosols (*medium confidence*) (Box TS.13, Figure 1). {2.3.1, Cross-Chapter Box 2.4, 3.3.2, 3.3.3}

With continued global warming, it is *likely* that global land monsoon precipitation will increase during this century (Box TS.13, Figure 1), particularly in the Northern Hemisphere, although the monsoon circulation is projected to weaken. A slowdown of the tropical circulation with global warming can partly offset the warming-induced strengthening of precipitation in monsoon regions (*high confidence*). In the near term, global monsoon changes are *likely* to be dominated by the effects of internal variability and model uncertainties (*medium confidence*). In the long term, global monsoon rainfall change will feature a robust north–south asymmetry characterized by a greater increase in the Northern Hemisphere than in the Southern Hemisphere and an east–west asymmetry characterized by enhanced Asian–African monsoons and a weakened North American monsoon (*medium confidence*). {4.4.1, 4.5.1, 8.4.1}

Regional Monsoons

Paleoclimate reconstructions indicate stronger monsoons in the Northern Hemisphere but weaker ones in the Southern Hemisphere during warm periods, particularly for the South and South East Asian, East Asian, and North and South American monsoons, with the opposite occurring during cold periods (*medium confidence*). It is *very likely* that Northern Hemispheric anthropogenic aerosols weakened the regional monsoon circulations in South Asia, East Asia and West Africa during the second half of the 20th century,

Box TS.13 (continued)

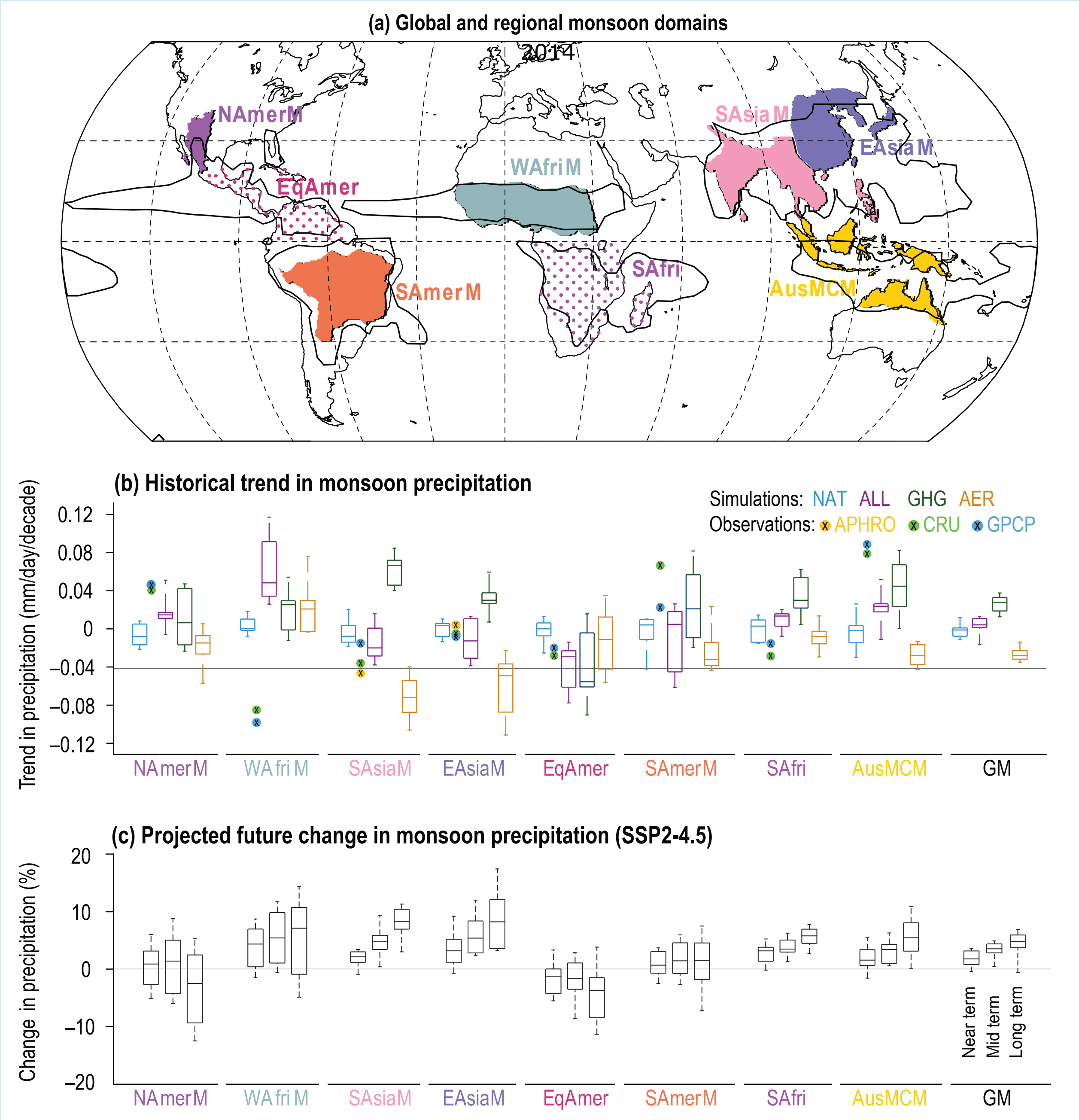

Box TS.13, Figure 1 | Global and regional monsoons: past trends and projected changes. *The intent of this figure is to show changes in precipitation over regional monsoon domains in terms of observed past trends, how greenhouse gases and aerosols relate to these changes, and in terms of future projections in one intermediate emissions scenario in the near, medium and long term.* **(a)** Global (black contour) and regional monsoons (colour shaded) domains. The global monsoon (*GM*) is defined as the area with local summer-minus-winter precipitation rate exceeding 2.5 mm day^{-1} (see Annex V). The regional monsoon domains are defined based on published literature and expert judgement (see Annex V) and accounting for the fact that the climatological summer monsoon rainy season varies across the individual regions. Assessed regional monsoons are South and South East Asia (*SAsiaM, Jun–July–August–September*), East Asia (*EAsiaM, June–July–August*), West Africa (*WAfriM, June–July–August–September*), North America (*NAmerM, July–August–-September*), South America (*SAmerM, December–January–February*), Australia and Maritime Continent Monsoon (*AusMCM, December–January–February*). Equatorial South America (*EqSAmer*) and South Africa (*SAfri*) regions are also shown, as they receive unimodal summer seasonal rainfall although their qualification as monsoons is subject to discussion. **(b)** Global and regional monsoons precipitation trends based on DAMIP CMIP6 simulations with both natural and anthropogenic (ALL), greenhouse gas only (GHG), aerosols only (AER) and natural only (NAT) radiative forcing. Weighted ensemble means are based on nine Coupled model Intercomparison Project Phase 6 (CMIP6) models contributing to the MIP (with at least three members). Observed trends computed from CRU, GPCP and APHRO (only for *SAsiaM* and *EAsiaM*) datasets are shown as well. **(c)** Percentage change in projected seasonal mean precipitation over global and regional monsoons domain in the near term (2021–2040), mid-term (2041–2060), and long term (2081–2100) under SSP2-4.5 based on 24 CMIP6 models. {Figures 8.11 and 8.22}

Box TS.13 (continued)

thereby offsetting the expected strengthening of monsoon precipitation in response to GHG-induced warming (Box TS.13, Figure 1). Multiple lines of evidence explain this contrast over South Asia, with the observed trends dominated by the effects of aerosols, while future projections are mostly driven by GHG increases. The recent partial recovery and enhanced intensity of monsoon precipitation over West Africa is related to the growing influence of GHGs with an additional contribution due to the reduced cooling effect of anthropogenic aerosols, emitted largely from North America and Europe (*medium confidence*). For other regional monsoons, that is, North and South America and Australia, there is *low confidence* in the attribution of recent changes in precipitation (Box TS.13, Figure 1) and winds. {2.3.1, 8.3.1, 8.3.2, Box 8.1, 10.6.3}

Projections of regional monsoons during the 21st century indicate contrasting (region-dependent) and uncertain precipitation and circulation changes. The annual contrast between the wettest and driest month of the year is *likely* to increase by 3–5% per degree Celsius in most monsoon regions in terms of precipitation, precipitation minus evaporation, and runoff (*medium confidence*). For the North American monsoon, projections indicate a decrease in precipitation, whereas increased monsoon rainfall is projected over South and South East Asia and over East Asia (*medium confidence*) (Box TS.13, Figure 1). West African monsoon precipitation is projected to increase over the central Sahel and decrease over the far western Sahel (*medium confidence*). There is *low confidence* in projected precipitation changes in the South American and Australian-Maritime Continent regional monsoons (for both magnitude and sign) (Box TS.13, Figure 1). There is *medium confidence* that the monsoon season will be delayed in the Sahel and *high confidence* that it will be delayed in North and South America. {8.2.2, 8.4.2.4, Box 8.2}

Building the Assessment from Multiple Lines of Evidence

Large natural variability of monsoon precipitation across different time scales, found in both paleoclimate reconstructions and instrumental measurements, poses an inherent challenge for robust quantification of future changes in precipitation at regional and smaller spatial scales. At both global and regional scales, there is *medium confidence* that internal variability contributes the largest uncertainty related to projected changes, at least in the near term (2021–2040). A collapse of the Atlantic Meridional Overturning Circulation could weaken the African and Asian monsoons but strengthen the Southern Hemisphere monsoons (*high confidence*). {4.4.4, 4.5.1, Cross-Chapter Box 4.1, 8.5.2, 8.6.1, 9.2.3, 10.6.3}

Overall, long-term (2081–2100) future changes in regional monsoons like the South and South East Asian monsoon are generally consistent across global (including high-resolution) and regional climate models and are supported by theoretical arguments. Uncertainties in simulating the observed characteristics of regional monsoon precipitation are related to varying complexities of regional monsoon processes and their responses to external forcing, internal variability, and deficiencies in representing monsoon warm rain processes, organized tropical convection, heavy orographic rainfall and cloud–aerosol interactions. {8.3.2, 8.5.1, 10.3.3, 10.6.3}

TS.4.3 Regional Climate Change and Implications for Climate Extremes and Climatic Impact-Drivers

Current climate in all regions is already distinct from the climate of the early or mid-20th century with respect to several climatic impact-drivers (CIDs), resulting in shifting magnitude, frequency, duration, seasonality and spatial extent of associated climate indices (*high confidence*). It is *very likely* that mean temperatures have increased in all land regions and will continue to increase at rates greater than the global average (*high confidence*). The frequency of heat and cold extremes have increased and decreased, respectively. These changes are attributed to human influence in almost all regions (*medium* to *high confidence*) and will continue through the 21st century (*high confidence*). In particular, extreme heat would exceed critical thresholds for health, agriculture and other sectors more frequently by the mid 21st century with 2°C of global warming (*high confidence*).

Relative sea level rise is *very likely* to *virtually certain* (depending on the region) to continue during the 21st century, contributing to increased coastal flooding in low-lying areas (*high confidence*) and coastal erosion along most sandy coasts (*high confidence*). Sea level will continue to rise beyond 2100 (*high confidence*) (Box TS.4).

Every region of the world will experience concurrent changes in multiple CIDs by mid-century or at 2°C global warming and above (*high confidence*). Even for the current climate, climate change-induced shifts in CID distributions and event probabilities, some of which have occurred over recent decades, are relevant for risk assessments. {11.9, 12.1, 12.2, 12.4, 12.5, Atlas.3–Atlas.11}

An overview of changes in regional CIDs (introduced in Section TS.1) is given in Table TS.5, which summarizes multiple lines of evidence on regional climate change derived from observed trends, attribution of these trends and future projections. The level of confidence and the amplitude in the projected direction of change in CIDs at a given time horizon depends on climate change mitigation efforts over the 21st century. It is evident from Table TS.5 that many heat, cold, snow and ice, coastal, and oceanic CID changes are projected with *high confidence* in most regions starting from a global warming level (GWL) of 2°C, indicating worldwide challenges. Changes in many other regional CIDs have higher confidence later in the 21st century or at higher GWLs (*high confidence*), and another small subset are projected with *high confidence* for the 1.5°C GWL. This section focuses on the 2°C GWL and mid-century time period because the signal emerges from natural variability for a wider range of CIDs at this higher warming level. Figure TS.22 shows the geographical location of regions belonging to one of five groups characterized by a specific combination of changing CIDs. The Regional Synthesis component of the Interactive Atlas provides comprehensive synthesis information about changes in all of the individual CIDs across all of the AR6 WGI reference regions. {10.5, Cross-Chapter Box 10.3, 11.1, 11.9, Box 11.1, 12.1, 12.2, 12.4, 12.5}

Table TS.5 | Summary of confidence for climatic impact-driver changes in each AR6 WGI reference region (illustrated in Figure TS.25) across multiple lines of evidence for observed, attributed and projected directional changes. The colours represent their projected aggregate characteristic changes for the mid-21st century, considering scenarios RCP4.5, SSP2-4.5, SRES A1B, or above (RCP6.0, RCP8.5, SSP3-7.0, SSP5-8.5, SRES A2), which approximately encompasses global warming levels of 2.0°C to 2.4°C. Arrows indicate *medium* to *high confidence* trends derived from observations, and asterisks indicate *medium* and *high confidence* in attribution of observed changes. (North Africa is not an AR6 WGI reference region, but assessment here is based upon the African portion of the Mediterranean reference region). {Tables 12.3–12.11 and Tables 11.4–11.21}

	Climatic Impact-driver																													
	Heat and Cold				Wet and Dry								Wind				Snow and Ice						Coastal and Oceanic					Other		
	Mean air temperature	Extreme heat	Cold spell	Frost	Mean precipitation	River flood	Heavy precipitation and pluvial flood	Landslide	Aridity	Hydrological drought	Agricultural and ecological drought	Fire weather	Mean wind speed	Severe wind storm	Tropical cyclone	Sand and dust storm	Snow, glacier and ice sheet	Permafrost	Lake, river and sea ice	Heavy snowfall and ice storm	Hail	Snow avalanche	Relative sea level	Coastal flood	Coastal erosion	Marine heatwave	Ocean and lake acidity	Air pollution weather	Atmospheric CO_2 at surface	Radiation at surface
Africa																														
North Africa	↗	↗ ***	↘ ***						↗	↗	↗			3									↗		4	↗	↗		↗	
Sahara	↗	↗ **	↘ **																				↗		4	↗	↗		↗	
Western Africa	↗	↗ **	↘ **		1	↗			↗ 1	↗ 1	↗ 1												↗		4	↗	↗		↗	
Central Africa	↗				↘ 1,2						↗												↗		4	↗	↗		↗	
North Eastern Africa	↗	↗ **	↘ **		↘				1	1	1						↘						↗		4	↗	↗		↗	
South Eastern Africa	↗	↗ **							1	1	1				3		↘						↗		4	↗	↗		↗	
West Southern Africa	↗	↗ ***	↘ ***		↘	↗	↗				↗												↗		4	↗	↗		↗	
East Southern Africa	↗	↗ ***	↘ ***		↘	↗	↗				↗				3								↗		4,5	↗	↗		↗	
Madagascar	↗	↗	↘												3								↗		4,5	↗	↗		↗	

Note: There are several region-specific qualifiers/exceptions attached to some of the directions of change/confidence levels indicated above. {12.4}

Key for observational trend evidence ↗ Past upward trend (*medium* or *higher confidence*) ↘ Past downward trend (*medium or higher confidence*)

Key for attribution evidence *** *High confidence* (or more) ** *Medium confidence*

Key for level of confidence in future changes *High confidence* of increase (or more) | *Medium confidence* of increase (or more) | *Low confidence* in direction of change | *Medium confidence* of decrease | *High confidence* of decrease | Not broadly relevant

Table TS.5 (continued)

	Heat and Cold: Mean air temperature	Heat and Cold: Extreme heat	Heat and Cold: Cold spell	Heat and Cold: Frost	Wet and Dry: Mean precipitation	Wet and Dry: River flood	Wet and Dry: Heavy precipitation and pluvial flood	Wet and Dry: Landslide	Wet and Dry: Aridity	Wet and Dry: Hydrological drought	Wet and Dry: Agricultural and ecological drought	Wet and Dry: Fire weather	Wind: Mean wind speed	Wind: Severe wind storm	Wind: Tropical cyclone	Wind: Sand and dust storm	Snow and Ice: Snow, glacier and ice sheet	Snow and Ice: Permafrost	Snow and Ice: Lake, river and sea ice	Snow and Ice: Heavy snowfall and ice storm	Snow and Ice: Hail	Snow and Ice: Snow avalanche	Coastal and Oceanic: Relative sea level	Coastal and Oceanic: Coastal flood	Coastal and Oceanic: Coastal erosion	Coastal and Oceanic: Marine heatwave	Coastal and Oceanic: Ocean and lake acidity	Other: Air pollution weather	Other: Atmospheric CO_2 at surface	Other: Radiation at surface
Asia																														
Arabian Peninsula	↗	↗ ***	↘ **	↘																			↗		1	↗			↗	
West Central Asia	↗	↗ ***	↘ ***	↘	5		↗		↗		↗		↘				↘						↗		1,2	↗			↗	
West Siberia	↗	↗ ***	↘ ***	↘	↗		↗						↘				↗	↘											↗	
East Siberia	↗	↗ ***	↘ ***	↘	↗		↗						↘				↗	↘											↗	
Russian Far East	↗	↗ ***	↘ ***	↘	↗		↗										↗	↘					↗		1,2	↗	↗		↗	
East Asia	↗	↗ ***	↘ ***	↘			↗			↗	↗		↘		↗ 3				↘				↗		1,2	↗			↗	
East Central Asia	↗	↗ ***	↘ ***				↗				↗		↘					↘	↘											
Tibetan Plateau	↗	↗ ***	↘ ***	↘			↗						↘					↘											↗	
South Asia	↗	↗ ***	↘ ***	↘	↘		↗						↘				↘	↘					↗		1	↗				
South East Asia	↗	↗ ***	↘ ***		4		↗								↗ 3								↗		1,2	↗			↗	

Note: There are several region-specific qualifiers/exceptions attached to some of the directions of change/confidence levels indicated above. {12.4}

Key for observational trend evidence ↗ Past upward trend (*medium* or *higher confidence*) ↘ Past downward trend (*medium or higher confidence*)

Key for attribution evidence *** *High confidence* (or more) ** *Medium confidence*

Key for level of confidence in future changes *High confidence* of increase (or more) | *Medium confidence* of increase (or more) | *Low confidence* in direction of change | *Medium confidence* of decrease | *High confidence* of decrease | Not broadly relevant

Table TS.5 (continued)

	Climatic Impact-driver																													
	Heat and Cold				Wet and Dry								Wind				Snow and Ice						Coastal and Oceanic					Other		
	Mean air temperature	Extreme heat	Cold spell	Frost	Mean precipitation	River flood	Heavy precipitation and pluvial flood	Landslide	Aridity	Hydrological drought	Agricultural and ecological drought	Fire weather	Mean wind speed	Severe wind storm	Tropical cyclone	Sand and dust storm	Snow, glacier and ice sheet	Permafrost	Lake, river and sea ice	Heavy snowfall and ice storm	Hail	Snow avalanche	Relative sea level	Coastal flood	Coastal erosion	Marine heatwave	Ocean and lake acidity	Air pollution weather	Atmospheric CO_2 at surface	Radiation at surface
Australasia																														
Northern Australia		↗ ***	↘ ***	↘			↗				↘				↘ 5								↗		7	↗	↗		↗	
Central Australia	↗	↗ ***	↘ ***	↘																			↗		7	↗	↗		↗	
Eastern Australia	↗	↗ ***	↘ ***	↘																			↗		7	↗	↗		↗	
Southern Australia	↗	↗ ***	↘ ***	↘	1				↗ 3	↗	↗	↗ **	7				↘						↗		7	↗	↗		↗	
New Zealand	↗	↗	↘ **		2				4				8				↘ 6						↗		7	↗	↗		↗	

Note: There are several region-specific qualifiers/exceptions attached to some of the directions of change/confidence levels indicated above. {12.4}

Key for observational trend evidence ↗ Past upward trend (*medium* or *higher confidence*) ↘ Past downward trend (*medium or higher confidence*)

Key for attribution evidence *** *High confidence* (or more) ** *Medium confidence*

Key for level of confidence in future changes *High confidence* of increase (or more) | *Medium confidence* of increase (or more) | *Low confidence* in direction of change | *Medium confidence* of decrease | *High confidence* of decrease | Not broadly relevant

Table TS.5 (continued)

	Climatic Impact-driver																													
	Heat and Cold				Wet and Dry								Wind				Snow and Ice						Coastal and Oceanic					Other		
	Mean air temperature	Extreme heat	Cold spell	Frost	Mean precipitation	River flood	Heavy precipitation and pluvial flood	Landslide	Aridity	Hydrological drought	Agricultural and ecological drought	Fire weather	Mean wind speed	Severe wind storm	Tropical cyclone	Sand and dust storm	Snow, glacier and ice sheet	Permafrost	Lake, river and sea ice	Heavy snowfall and ice storm	Hail	Snow avalanche	Relative sea level	Coastal flood	Coastal erosion	Marine heatwave	Ocean and lake acidity	Air pollution weather	Atmospheric CO_2 at surface	Radiation at surface
Central and South America																														
Southern Central America	↗	↗ **	↘ **												2								↗		3	↗	↗		↗	
North-Western South America	↗	↗ ***	↘ ***																				↗		3,4	↗	↗		↗	
Northern South America	↗	↗ **	↘ **												2								↗		3,4	↗	↗		↗	
South American Monsoon	↗	↗ **	↘ **			↗ 1																							↗	
North-Eastern South America	↗	↗ **	↘ **		↘						↗												↗		3,4	↗	↗		↗	
South-Western South America	↗	↗ **	↘ **	↘					↗														↗		3	↗	↗		↗	
South-Eastern South America	↗	↗ ***	↘ ***	↘	↗		↗			↘													↗		3	↗	↗		↗	
Southern South America	↗			↘																			↗		3	↗	↗		↗	

Note: There are several region-specific qualifiers/exceptions attached to some of the directions of change/confidence levels indicated above. {12.4}

Key for observational trend evidence ↗ Past upward trend (*medium* or *higher confidence*) ↘ Past downward trend (*medium or higher confidence*)

Key for attribution evidence *** *High confidence* (or more) ** *Medium confidence*

Key for level of confidence in future changes *High confidence* of increase (or more) | *Medium confidence* of increase (or more) | *Low confidence* in direction of change | *Medium confidence* of decrease | *High confidence* of decrease | Not broadly relevant

Table TS.5 (continued)

	Climatic Impact-driver																													
	Heat and Cold				Wet and Dry								Wind				Snow and Ice						Coastal and Oceanic					Other		
	Mean air temperature	Extreme heat	Cold spell	Frost	Mean precipitation	River flood	Heavy precipitation and pluvial flood	Landslide	Aridity	Hydrological drought	Agricultural and ecological drought	Fire weather	Mean wind speed	Severe wind storm	Tropical cyclone	Sand and dust storm	Snow, glacier and ice sheet	Permafrost	Lake, river and sea ice	Heavy snowfall and ice storm	Hail	Snow avalanche	Relative sea level	Coastal flood	Coastal erosion	Marine heatwave	Ocean and lake acidity	Air pollution weather	Atmospheric CO_2 at surface	Radiation at surface
Europe																														
Mediterranean	↗	↗ ***	↘ ***			↘	5			↗ **	↗ **		↘ 6	7			↘						↗		2	↗	↗		↗	
Western and Central Europe	↗	↗ ***	↘ ***		↗	↗	↗	4			↗		↘				↘	↘					↗		2	↗	↗		↗	
Eastern Europe	↗	↗ ***	↘ ***		↗		↗						↘				↘												↗	
Northern Europe	↗	↗ ***	↘ ***		↗	↘ 1	↗ ***			↘			↘				↘	↘					↗	8	2,3	↗	↗		↗	
North America																														
North Central America	↗	↗ **	↘ **						↗			↗											↗	↗	2	↗	↗		↗	
Western North America	↗	↗ **	↘ **		3		5	5	4,7		↗ 6,7 **	↗ 6.7	↘	8		↗ 6	↘ 1		↘	1		1	↗	↗ 5	2	↗	↗		↗	
Central North America	↗				↗		↗ **		7		7	7	↘	8		4	↘		↘				↗	↗	2	↗	↗		↗	
Eastern North America	↗				↗ 5		↗					7	↘	8			↘ 1		↘	1		1	↗	↗	2	↗	↗		↗	
North-Eastern North America	↗	↗ ***	↘ ***	↘	5				5		6,7	6,7		8			↘ 1,6	↘	↘			1	4	↗ 4,6	2,6	↗	↗		↗	
North-Western North America	↗	↗ ***	↘ ***	↘	5			6	5		6,7	↗ 6,7		8			↘ 1	↘	↘			1,6	↗ 9	↗	2	↗	↗		↗	

Note: There are several region-specific qualifiers/exceptions attached to some of the directions of change/confidence levels indicated above. {12.4}

Key for observational trend evidence ↗ Past upward trend (*medium* or *higher confidence*) ↘ Past downward trend (*medium or higher confidence*)

Key for attribution evidence *** *High confidence* (or more) ** *Medium confidence*

Key for level of confidence in future changes *High confidence* of increase (or more) | *Medium confidence* of increase (or more) | *Low confidence* in direction of change | *Medium confidence* of decrease | *High confidence* of decrease | Not broadly relevant

Table TS.5 (continued)

	Climatic Impact-driver																													
	Heat and Cold				Wet and Dry								Wind				Snow and Ice						Coastal and Oceanic					Other		
	Mean air temperature	Extreme heat	Cold spell	Frost	Mean precipitation	River flood	Heavy precipitation and pluvial flood	Landslide	Aridity	Hydrological drought	Agricultural and ecological drought	Fire weather	Mean wind speed	Severe wind storm	Tropical cyclone	Sand and dust storm	Snow, glacier and ice sheet	Permafrost	Lake, river and sea ice	Heavy snowfall and ice storm	Hail	Snow avalanche	Relative sea level	Coastal flood	Coastal erosion	Marine heatwave	Ocean and lake acidity	Air pollution weather	Atmospheric CO_2 at surface	Radiation at surface
Small Islands																														
Caribbean	↗	↗ **													5								↗		6	↗	↗		↗	
Pacific	↗	↗ **1			2		3		4						5								↗		6	↗	↗		↗	
Polar Terrestrial Regions																														
Greenland and Iceland	↗	↗ **	↘ **			↗	↗		↘ 3			2,3					↘ 1	↘	↘				↗ 5				↗		↗	
Arctic North Europe	↗	↗				↗			↘ 3			2,3					↘ 1	↘	↘				↗ 6		7		↗		↗	
Russian Arctic	↗	↗ **	↘ **			↗			↘ 3			2,3					↘ 1,4		↘						7		↗		↗	
Arctic North-Western North America	↗					↗			↘ 3			2,3					↘ 1,4	↘	↘						7		↗		↗	
Arctic North-East North America	↗	↗				↗			↘ 3			2,3					↘ 1,4	↘	↘				↘				↗		↗	
West Antarctica																	↘ 1,4										↗		↗	
East Antarctica																											↗		↗	

Note: There are several region-specific qualifiers/exceptions attached to some of the directions of change/confidence levels indicated above. {12.4}

Key for observational trend evidence ↗ Past upward trend (*medium* or *higher confidence*) ↘ Past downward trend (*medium or higher confidence*)

Key for attribution evidence *** *High confidence* (or more) ** *Medium confidence*

Key for level of confidence in future changes *High confidence* of increase (or more) | *Medium confidence* of increase (or more) | *Low confidence* in direction of change | *Medium confidence* of decrease | *High confidence* of decrease | Not broadly relevant

Table TS.5 (continued)

	Climatic Impact-driver					
	Mean ocean temperature	Marine heatwave	Ocean acidity	Ocean salinity	Dissolved oxygen	Sea ice
Oceans						
Arctic Ocean	↗		↗			↘ ***
South Pacific Ocean	↗	↗	↗			
Equatorial Pacific Ocean	↗	↗	↗			
North Pacific Ocean	↗	↗	↗			
South Atlantic Ocean	↗	↗	↗			
Equatorial Atlantic Ocean	↗	↗	↗			
North Atlantic Ocean	↗	↗	↗			
Equatorial Indian Ocean	↗	↗	↗			
South Indian Ocean	↗	↗	↗			
Arabian Sea	↗	↗	↗			
Bay of Bengal	↗	↗	↗			
Southern Ocean						

Note: There are several region-specific qualifiers/exceptions attached to some of the directions of change/confidence levels indicated above. {12.4}

Key for observational trend evidence ↗ Past upward trend (*medium* or *higher confidence*) ↘ Past downward trend (*medium or higher confidence*)

Key for attribution evidence *** *High confidence* (or more) ** *Medium confidence*

Key for level of confidence in future changes *High confidence* of increase (or more) | *Medium confidence* of increase (or more) | *Low confidence* in direction of change | *Medium confidence* of decrease | *High confidence* of decrease | Not broadly relevant

Notes:

Africa (projections)

1. Contrasted regional signal: drying in western portions and wetting in eastern portions
2. *Likely* increase over the Ethiopian Highlands
3. *Medium confidence* of decrease in frequency and increase in intensity
4. Along sandy coasts and in the absence of sufficient sediment supply from terrestrial or offshore sources
5. Substantial parts of the East Southern Africa and Madagascar coast are projected to prograde if present-day ambient shoreline change rates continue

Asia (projections)

1. Along sandy coasts and in the absence of additional sediment sinks/sources or any physical barriers to shoreline retreat.
2. Substantial parts of the coasts in these regions are projected to prograde if present-day ambient shoreline change rates continue
3. Tropical cyclones decrease in number but increase in intensity
4. *High confidence* of decrease in Indonesia (Atlas.5.4.5)
5. *Medium confidence* of decreasing in summer and increasing in winter

Australasia (projections)

1. *High confidence* of decrease in the south-west of the state of Western Australia
2. *Medium confidence* of decrease in north and east and increase in south and west
3. *High confidence* of increase in the south-west of the state of Western Australia
4. *Medium confidence* of increase in the north and east and decrease in south and west
5. *Low confidence* of increasing intensity, and *high confidence* of decreasing occurrence
6. *High confidence* of decrease in glacier volume, *medium confidence* of decrease in snow
7. Along sandy coasts and in the absence of additional sediment sinks/sources or any physical barriers to shoreline retreat

Central and South America (projections)

1. Increase in extreme flow in the Amazon basin
2. Tropical cyclones decrease in number but increase in intensity
3. Along sandy coasts and in the absence of additional sediment sinks/sources or any physical barriers to shoreline retreat.
4. Substantial parts of the North-Western South America, Northern South America and North-Eastern South America coasts are projected to prograde if present-day ambient shoreline change rates continue

Europe (projections)

1. Excluding southern United Kingdom
2. Along sandy coasts and in the absence of additional sediment sinks/sources or any physical barriers to shoreline retreat
3. The Baltic Sea shoreline is projected prograde if present-day ambient shoreline change rates continue.
4. For the Alps, conditions conducive to landslides are expected to increase
5. *Low confidence* of decrease in the southernmost part of the region
6. General decrease except in Aegean Sea
7. *Medium confidence* of decrease in frequency and increase in intensities
8. Except in the Northern Baltic Sea region

North America (projections)

1. Snow may increase in some high elevations and during the cold season and decrease in other seasons and at lower elevations
2. Along sandy coasts and in the absence of additional sediment sinks/sources or any physical barriers to shoreline retreat.
3. Increasing in northern regions and decreasing toward the south
4. Decreasing in northern regions and increasing toward the south
5. Higher confidence in northern regions and lower toward the south
6. Higher confidence in southern regions and lower toward the north
7. Higher confidence in increase for some climatic impact-driver indices during summertime
8. Increase in convective conditions but decrease in winter extratropical cyclones
9. Relative sea level rise reduced given land uplift in Southern Alaska

Small Islands (projections)

1. *Very high confidence* in the direction of change, but *low* to *medium confidence* in the magnitude of change due to model uncertainty
2. Decrease in eastern Pacific and southern Pacific subtropics, but increase in parts of western and equatorial Pacific; with seasonal variation in future changes
3. *High confidence* in increase in extreme rain frequency and intensity in western tropical Pacific; *low confidence* in magnitude of change due to model bias
4. Increase in southern Pacific
5. Increase in intensity; decrease in frequency except over central North Pacific.
6. Along sandy coasts and in the absence of additional sediment sinks/sources or any physical barriers to shoreline retreat.

Polar Terrestrial Regions (projections)

1. Snow may increase in some high elevations and during the cold season and decrease in other seasons and at lower elevations
2. Higher confidence in southern regions and lower toward the north
3. Higher confidence in increase for some climatic impact-driver indices during summertime
4. Glaciers decline even as some regional snow climatic impact-driver indices increase
5. Decreasing in west and increasing in east
6. Except for Northern Baltic Sea coasts where relative sea levels fall
7. Along sandy coasts and in the absence of additional sediment sinks/sources or any physical barriers to shoreline retreat

While changes in climatic impact-drivers are projected everywhere, there is a specific combination of changes each region would experience

(a) World regions grouped into five clusters, each one based on a combination of changes in climatic impact-drivers

Assessed future changes: Changes refer to a 20–30 year period centred around 2050 and/or consistent with 2°C global warming compared to a similar period within 1960–2014 or 1850–1900.

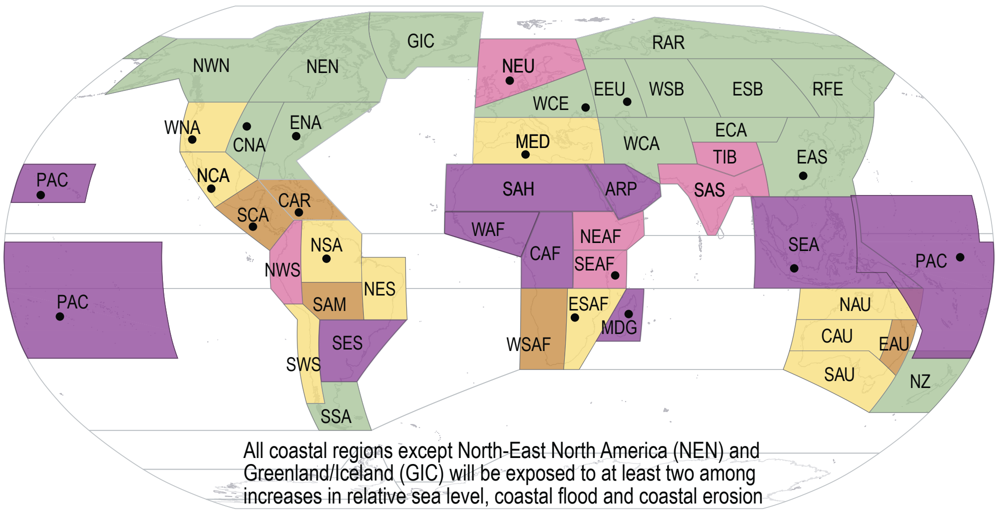

1) Hotter and drier

2) Hotter and drier and in some regions wetter extremes

3) Hotter and wetter extremes and in some regions more precipitation or fire weather

4) Hotter and wetter and in some regions more flooding

5) Hotter and in some regions wetter extremes or more precipitation

6) Increase in Tropical cyclones intensity or Severe winds

Combinations of future changes in climatic impact-drivers (CIDs)

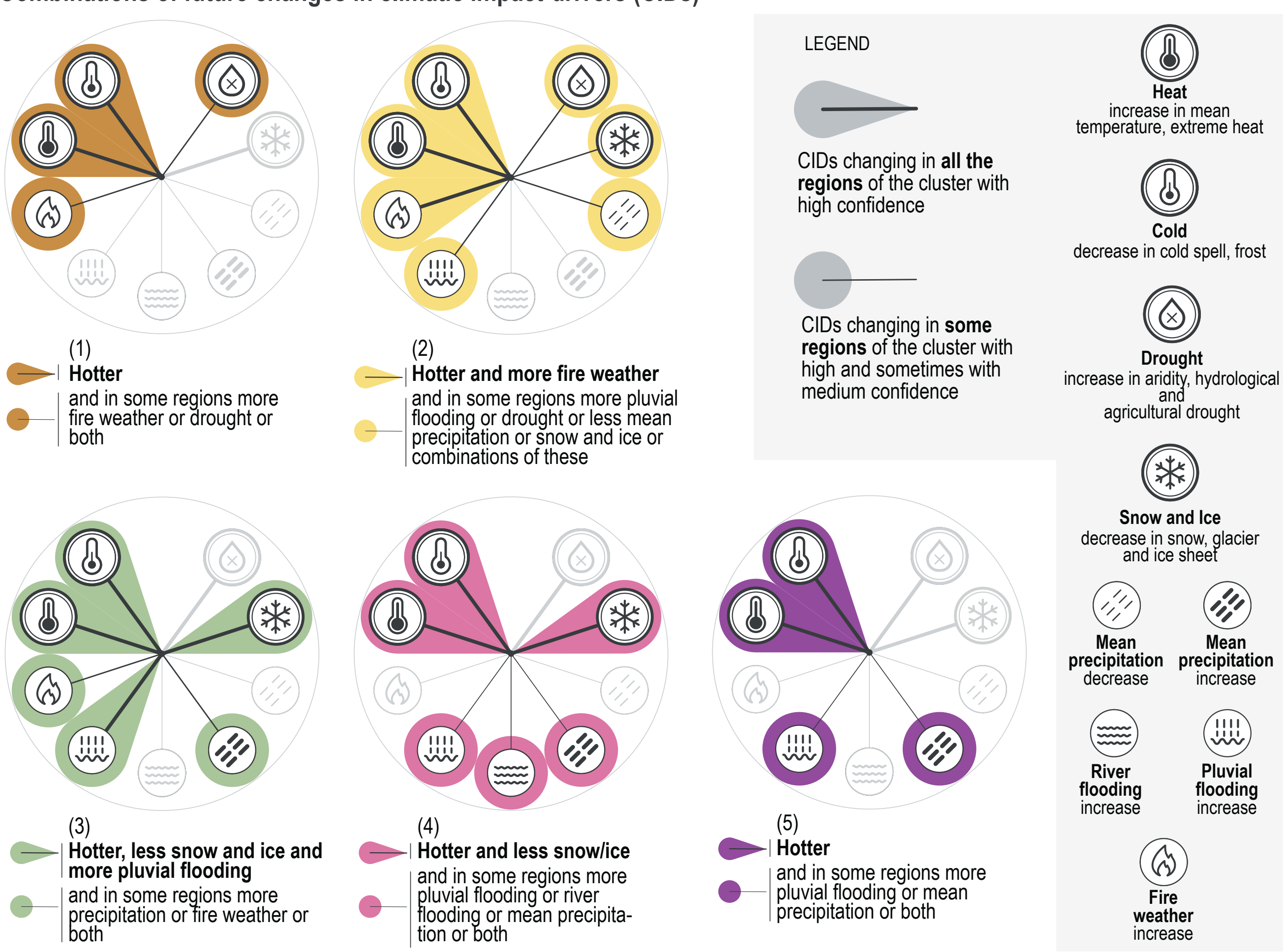

(b) Number of land & coastal regions (i) and **open-ocean regions** (ii) where each **climatic impact-driver** (CID) is projected to **increase** or **decrease** with ***high*** *confidence* (dark shade) or ***medium*** *confidence* (light shade)

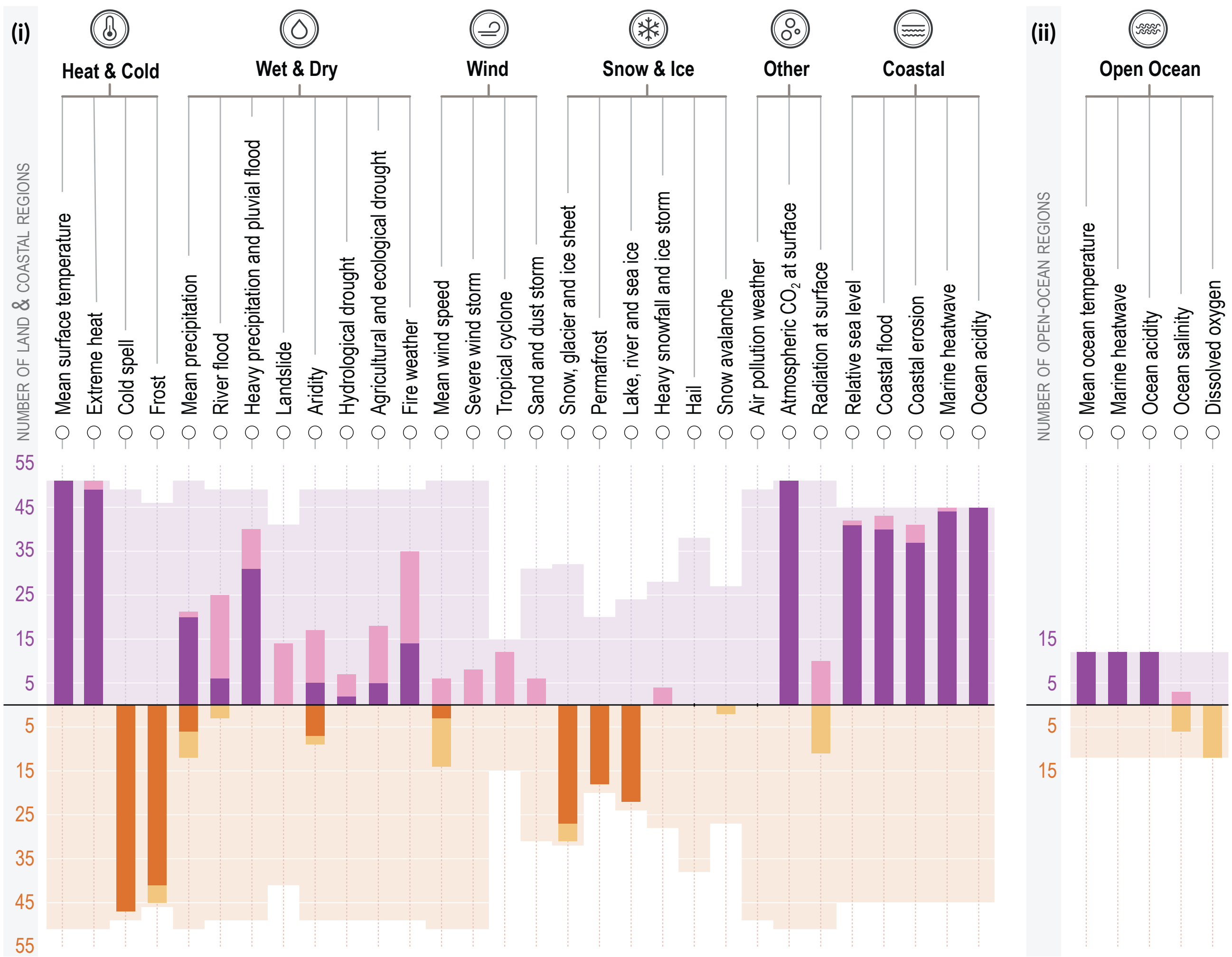

BAR CHART LEGEND

- Regions with ***high*** *confidence* **increase**
- Regions with ***medium*** *confidence* **increase**
- Regions with ***high*** *confidence* **decrease**
- Regions with ***medium*** *confidence* **decrease**

LIGHTER-SHADED 'ENVELOPE' LEGEND

The height of the lighter shaded 'envelope' behind each bar represents the maximum number of regions for which each CID is relevant. The envelope is symmetrical about the x-axis showing the maximum possible number of relevant regions for CID increase (upper part) or decrease (lower part).

Climatic impact-drivers (CIDs) are physical climate system conditions (e.g., means, events, extremes) that affect an element of society or ecosystems. Depending on system tolerance, CIDs and their changes can be detrimental, beneficial, neutral, or a mixture of each across interacting system elements and regions. The CIDs are grouped into seven types, which are summarized under the icons in sub-panels (i) and (ii). All regions are projected to experience changes in at least 5 CIDs. Almost all (96%) are projected to experience changes in at least 10 CIDs and half in at least 15 CIDs. For many CID changes, there is wide geographical variation, and so each region is projected to experience a specific set of CID changes. Each bar in the chart represents a specific geographical set of changes that can be explored in the WGI Interactive Atlas.

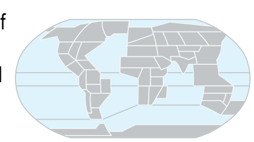

interactive-atlas.ipcc.ch

Figure TS.22 | Synthesis of the geographical distribution of climatic impact-drivers changes and the number of AR6 WGI reference regions where they are projected to change.

Figure TS.22 (continued): Panel (a) shows the geographical location of regions belonging to one of five groups characterized by a specific combination of changing climatic impact-drivers (CIDs). The five groups are represented by the five different colours, and the CID combinations associated with each group are represented in the corresponding 'fingerprint' and text below the map. Each fingerprint comprises a set of CIDs projected to change with *high confidence* in every region in the group and a second set of CIDs, one or more of which are projected to change in each region with *high* or *medium confidence*. The CID combinations follow a progression from those becoming hotter and drier (group 1) to those becoming hotter and wetter (group 5). In between (groups 2–4), the CIDs that change include some becoming drier and some wetter and always include a set of CIDs which are getting hotter. Tropical cyclones and severe wind CID changes are represented on the map with black dots in the regions affected. Regions affected by coastal CID changes are described by text on the map. The five groups are chosen to provide a reasonable level of detail for each region while not overwhelming the map with a full summary of all aspects of the assessment, which is available in Table TS.5 and can be visualized in the Regional Synthesis component of the Interactive Atlas. The CID changes summarized in the figure represent *high* and *medium confidence* changes for the mid-21st century, considering scenarios SSP2-4.5, RCP4.5, SRES A1B, or above (SSP3-7.0, SSP5-8.5, RCP6.0, RCP8.5, SRES A2), which approximately encompasses global warming levels of 2.0°C to 2.4°C.

The bar chart in **panel (b)** shows the numbers of regions where each CID is increasing or decreasing with *medium* or *high confidence* for all land regions and ocean regions listed in Table TS.5. The colours represent the direction of change and the level of confidence in the change: purple indicates an increase while brown indicates a decrease; darker and lighter shades refer to *high* and *medium confidence*, respectively. Lighter background colours represent the maximum number of regions for which each CID is broadly relevant. Sub-panel (i) shows the 30 CIDs relevant to the land and coastal regions while sub-panel (ii) shows the 5 CIDs relevant to the open ocean regions. Marine heatwaves and ocean acidity are assessed for coastal ocean regions in panel (i) and for open ocean regions in panel (ii). Changes refer to a 20- to 30-year period centred around 2050 and/or consistent with 2°C global warming compared to a similar period within 1960–2014, except for hydrological drought and agricultural and ecological drought, which is compared to 1850–1900. Definitions of the regions are provided in Atlas.1, the Interactive Atlas (https://interactive-atlas.ipcc.ch/) and Chapter 12. (Table TS.5, Figure TS.24) {11.9, 12.2, 12.4, Atlas.1}

TS.4.3.1 Common Regional Changes in Climatic Impact-Drivers

Heat and cold: Changes in temperature-related CIDs such as mean temperatures, growing season length, and extreme heat and frost have already occurred (*high confidence*), and many of these changes have been attributed to human activities (*medium confidence*). Over all land regions with sufficient data (i.e., all except Antarctica), observed changes in temperature have already clearly emerged outside the range of internal variability, relative to 1850–1900 (Figure TS.23). In tropical regions, recent past temperature distributions have already shifted to a range different to that of the early 20th century (*high confidence*) (Section TS.1.2.4). Most land areas have *very likely* warmed by at least 0.1°C per decade since 1960, and faster in recent decades. On regional-to-continental scales, trends of increased frequency of hot extremes and decreased frequency of cold extremes are generally consistent with the global-scale trends in mean temperature (*high confidence*). In a few regions, trends are difficult to assess due to limited data availability. {2.3.1.1, 11.3, 11.9, 12.4, Atlas.3.1}

Warming trends observed in recent decades are projected to continue over the 21st century and over most land regions at a rate higher than the global average (*high confidence*). For given global warming levels, model projections from CMIP6 show future regional warming changes that are similar to those projected by CMIP5. However, projected regional warming in CMIP6 for given time periods and emissions scenarios has a wider range with a higher upper limit compared to CMIP5 because of the higher climate sensitivity in some CMIP6 models and differences in the forcings. {Atlas.3–Atlas.11}

Under RCP8.5/SSP5-8.5, it is *likely* that most land areas will experience further warming of at least 4°C compared to a 1995–2014 baseline by the end of the 21st century, and in some areas significantly more. At increasing warming levels, extreme heat will exceed critical thresholds for health, agriculture and other sectors more frequently (*high confidence*), and it is *likely* that cold spells will become less frequent towards the end of the century. For example, by the end of the 21st century, dangerous humid heat thresholds, such as the National Oceanic and Atmospheric Administration (NOAA) heat index (HI) threshold of 41°C, will be exceeded much more frequently under the SSP5-8.5 scenario than under SSP1-2.6 and will affect many regions (*high confidence*). In many tropical regions, the number of days per year where a heat index of 41°C is exceeded would increase by more than 100 days relative to the recent past under SSP5-8.5, while this increase will be limited to less than 50 days under SSP1-2.6 (*high confidence*) (Figure TS.6). The number of days per year where temperature exceeds 35°C would increase by more than 150 days in many tropical areas, such as the Amazon basin and South East Asia, by the end of century for the SSP5-8.5 scenario, while it is expected to increase by less than 60 days in these areas under SSP1-2.6 (except for the Amazon Basin) (*high confidence*) (Figure TS.24). {4.6.1, 11.3, 11.9, 12.4, 12.5.2, Atlas}

Wet and dry: Compared to the global scale, precipitation internal variability is stronger at the regional scale while uncertainties in observations, models and external forcing are all larger. However, GHG forcing has driven increased contrasts in precipitation amounts between wet and dry seasons and weather regimes over tropical land areas (*medium confidence*), with a detectable precipitation increase in the northern high latitudes (*high confidence*) (Box TS.6). The frequency and intensity of heavy precipitation events have increased over a majority of land regions with good observational coverage (*high confidence*). A majority of land areas have experienced decreases in available water in dry seasons due to human-induced climate change associated with changes in evapotranspiration (*medium confidence*). Global hydrological models project a larger fraction of land areas to be affected by an increase rather than by a decrease in river floods (*medium confidence*). Extreme precipitation and pluvial flooding will increase in many regions around the world on almost all continents (*high confidence*), but regional changes in river floods are more uncertain than changes in pluvial floods because complex hydrological processes, including land cover and human water management, are involved. {8.2.2.1, 8.3.1, Box 8.2, 10.4.1, 11.5, 11.6, 11.9, 12.4, 12.5.1, Atlas.3.1}

Wind: Mean wind speed has decreased over most land areas with good observational coverage (*medium confidence*). It is *likely* that the global proportion of major tropical cyclone (TC) intensities (Categories 3–5) over the past four decades has increased. The proportion of intense TCs, average peak TC wind speeds, and peak wind speeds of the most intense TCs will increase on the global scale with increasing global warming (*high confidence*). {11.7.1}

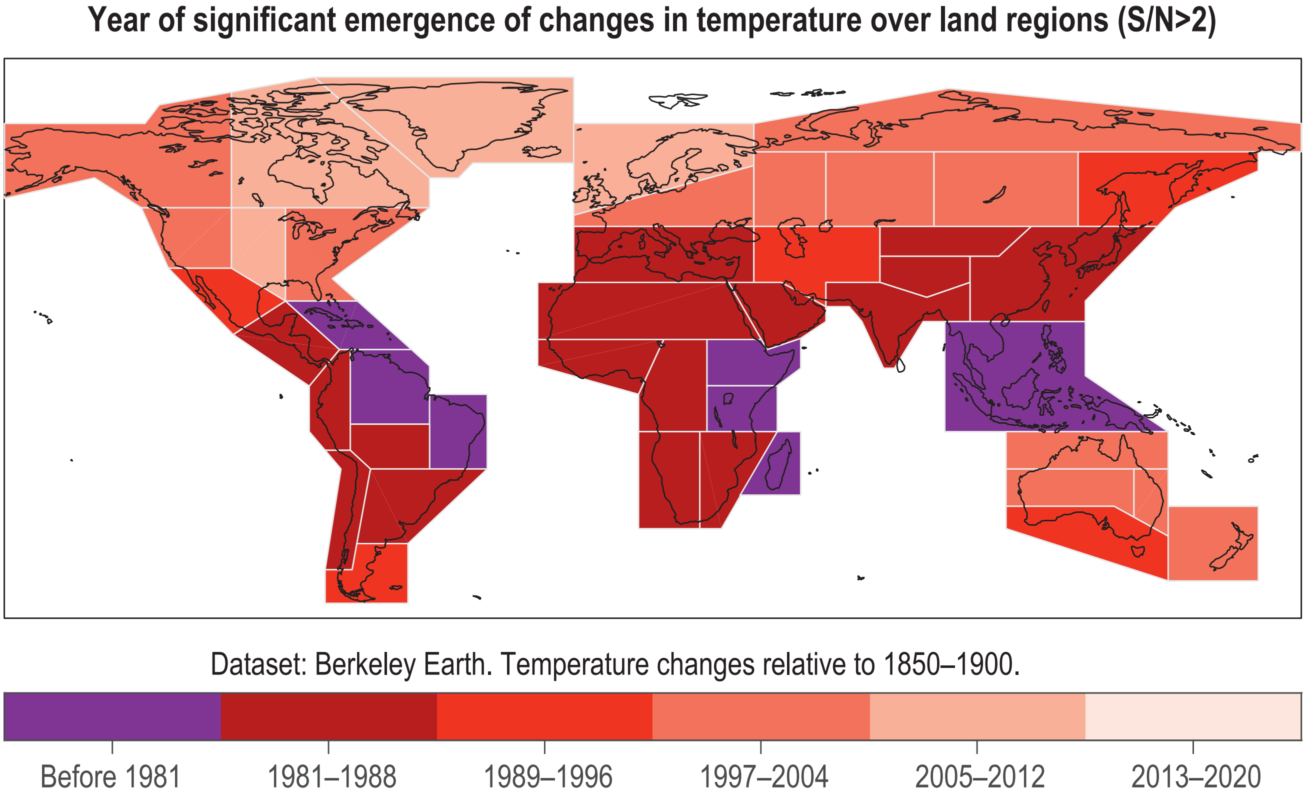

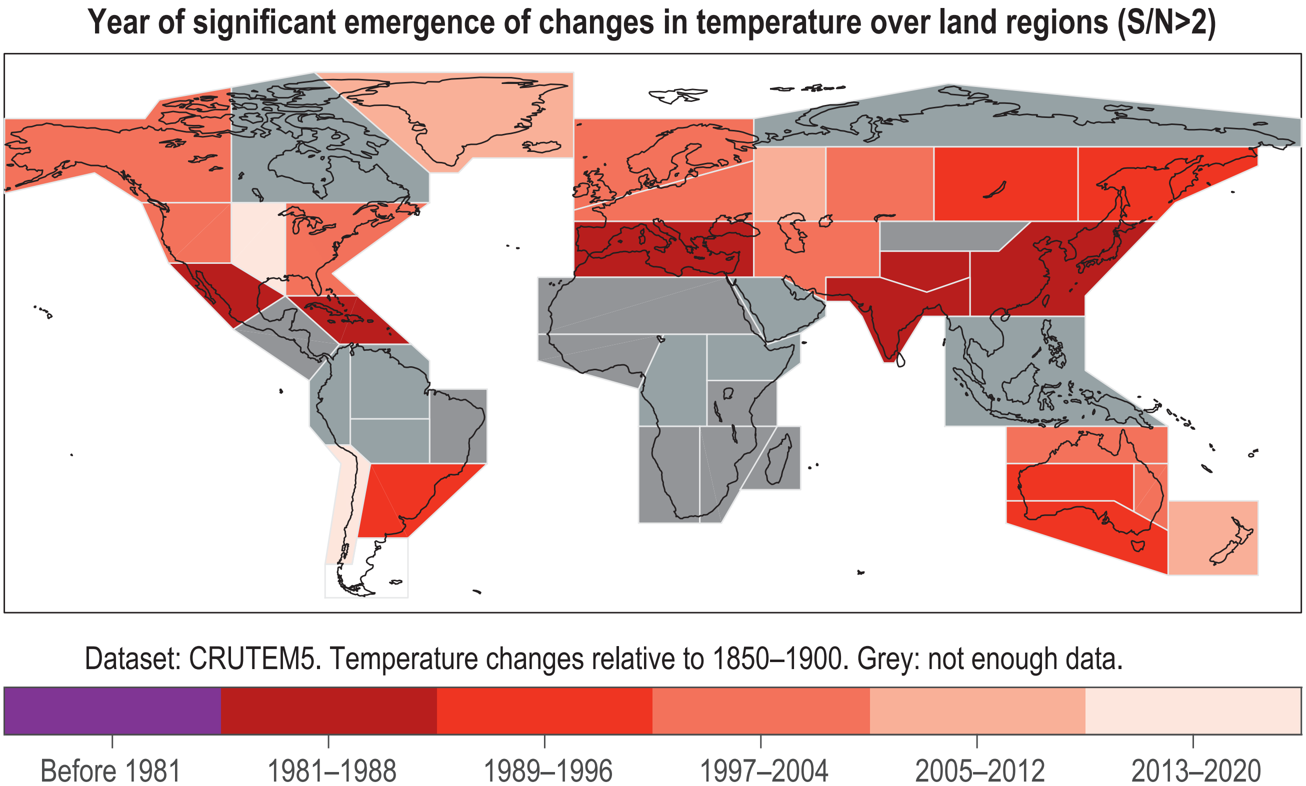

Figure TS.23 | Time period during which the signals of temperature change in observed data aggregated over the reference regions emerged from the noise of annual variability in the respective aggregated data, using a signal-to-noise ratio of two as the threshold for emergence. *The intent of this figure is to show, for the AR6 WGI reference regions, when a signal of annual mean surface temperature change emerged from the noise of annual variability in two global datasets and thus also provide some information on observational uncertainty.* Emergence time is calculated for two global observational datasets: **(a)** Berkeley Earth and **(b)** CRUTEM5. Regions in the CRUTEM5 map are shaded grey when data are available over less than 50% of the area of the region. (Section TS.1.2.4) {Figure Atlas.11}

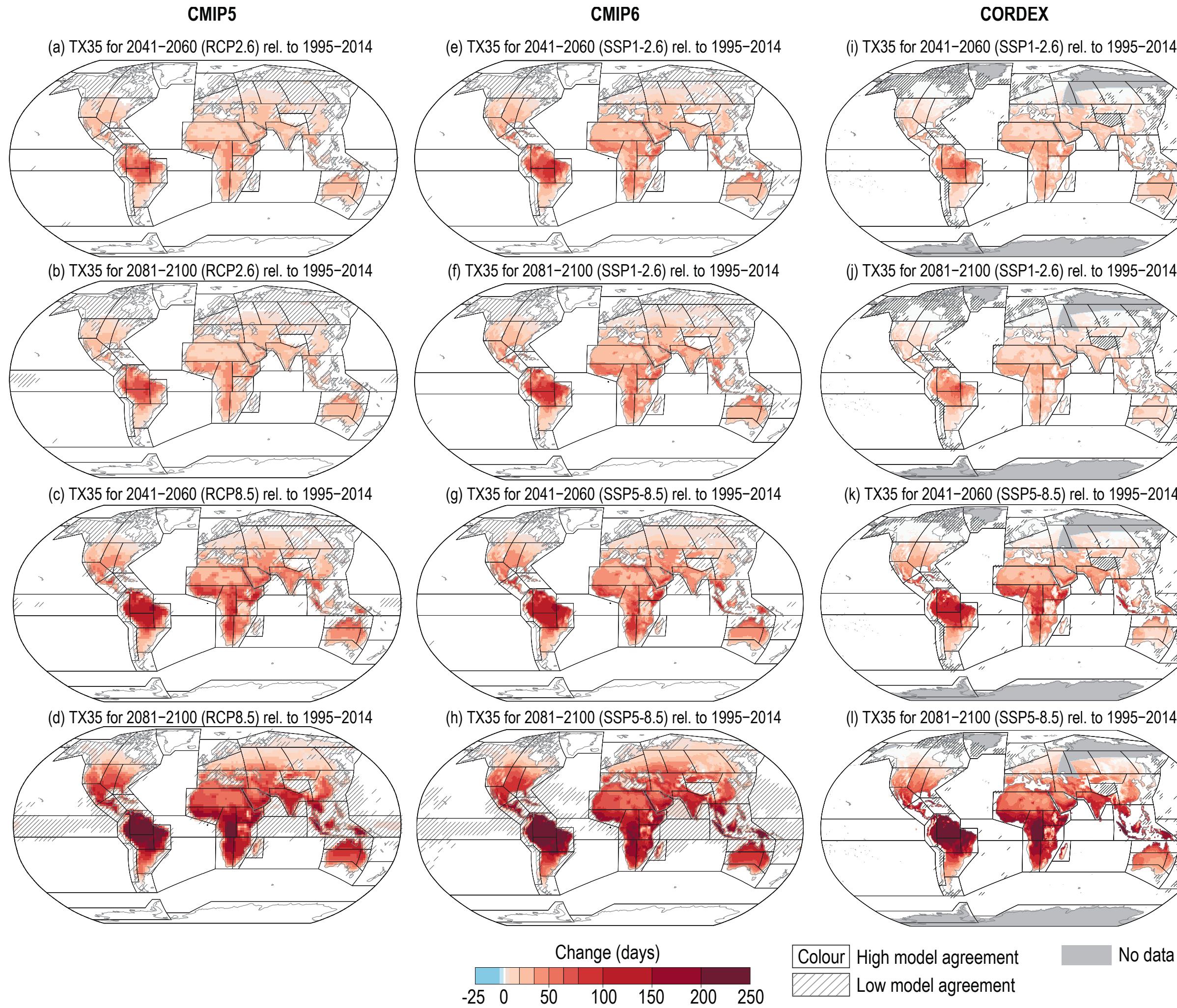

Figure TS.24 | Projected change in the mean number of days per year with maximum temperature exceeding 35°C for Coupled Model Intercomparison Project Phase 5 (CMIP5; first column), Phase 6 (CMIP6; second column) and Coordinated Regional Climate Downscaling Experiment (CORDEX; third column) ensembles. *The intent of this figure is to show that there is a consistent message about the patterns of projected change in extreme daily temperatures from the CMIP5, CMIP6 and CORDEX ensembles.* The map shows the median change in the number of days per year between the mid-century (2041–2060) or end-century (2081–2100) and historical (1995–2014) periods for the CMIP5 and CORDEX RCP8.5 and RCP2.6 scenario ensembles and the CMIP6 SSP5-8.5 and SSP1-2.6 scenario ensembles. Hatching indicates areas where less than 80% of the models agree on the sign of change. {Interactive Atlas}

Snow and ice: Many aspects of the cryosphere either have seen significant changes in the recent past or will see them during the 21st century (*high confidence*). Glaciers will continue to shrink and permafrost to thaw in all regions where they are present (*high confidence*). Also, it is *virtually certain* that snow cover will experience a decline over most land regions during the 21st century, in terms of water equivalent, extent and annual duration. There is *high confidence* that the global warming-induced earlier onset of spring snowmelt and increased melting of glaciers have already contributed to seasonal changes in streamflow in high-latitude and low-elevation mountain catchments. Nevertheless, it is *very likely* that some high-latitude regions will experience an increase in winter snow water equivalent due to the effect of increased snowfall prevailing over warming-induced increased snowmelt. (Section TS.2.5) {8.2.2.1, 8.3.1, Box 8.2, 9.4, 9.5.1, 9.5.2, 12.4, Atlas.4–Atlas.9, Atlas.11}

Coastal and oceanic: There is *high confidence* that SST will increase in all oceanic regions except the North Atlantic. Regional sea level change has been the main driver of changes in extreme sea levels across the quasi-global tide gauge network over the 20th century (*high confidence*). With the exception of a few regions with substantial land uplift, relative sea level rise is *very likely to virtually certain* (depending on the region) to continue during the 21st century, contributing to increased coastal flooding in low-lying areas (*high confidence*) and coastal erosion along most sandy coasts (*high confidence*) over the 21st century. In the open ocean, acidification, changes in sea ice, and deoxygenation have already emerged in many areas (*high confidence*). Marine heatwaves are also expected to increase around the globe over the 21st century (*high confidence*). (Section TS.2.4) {Box 9.2, 9.2.1.1, 9.6, 9.6.4, 9.6.4.2, 12.4}

Other variables and concurrent CID changes: It is *virtually certain* that atmospheric CO_2 and oceanic pH will increase in all climate scenarios, until net zero CO_2 emissions are achieved (Section TS.2.2). In nearly all regions, there is *low confidence* in changes in hail, ice storms, severe storms, dust storms, heavy snowfall, and avalanches, although this does not indicate that these CIDs will not be affected by climate change. For such CIDs, observations are often short-term or lack homogeneity, and models often do not have sufficient resolution or accurate parametrizations to adequately simulate them over climate change time scales. The probability of compound events has increased in the past due to human-induced climate change and will *likely* continue to increase with further global warming, including for concurrent heatwaves and droughts, compound flooding, and the possibility of connected sectors experiencing multiple regional extreme events at the same time (for example, in multiple breadbaskets) (*high confidence*). {5.3.4.2, 11.8, Box 11.3, Box 11.4, 12.4}

TS.4.3.2 Region-by-Region Changes in Climatic Impact-Drivers

This section provides a continental synthesis of changes in CIDs, some examples of which are presented in Figure TS.25.

With 2°C global warming, and as early as the mid-21st century, a wide range of CIDs, particularly related to the water cycle and storms, are expected to show simultaneous region-specific changes relative to the recent past with *high* or *medium confidence*. In a number of regions (Southern Africa, the Mediterranean, North Central America, Western North America, the Amazon regions, South-Western South America, and Australia), increases in one or more of drought, aridity and fire weather (*high confidence*) will affect a wide range of sectors, including agriculture, forestry, health and ecosystems. In another group of regions (North-Western, Central and Eastern North America, Arctic regions, North-Western South America, Northern, Western and Central and Eastern Europe, Siberia, Central, South and East Asia, Southern Australia and New Zealand), decreases in snow and/or ice or increases in pluvial/river flooding (*high confidence*) will affect sectors such as winter tourism, energy production, river transportation and infrastructure. {11.9, 12.3, 12.4, 12.5, Table 12.2}

TS.4.3.2.1 Africa

Additional regional changes in Africa, besides those described in Section TS.4.3.1, include a projected decrease in total precipitation in the northernmost and southernmost regions (*high confidence*), with Western Africa having a west-to-east pattern of decreasing-to-increasing precipitation (*medium confidence*). Increases in heavy precipitation that can lead to pluvial floods (*high confidence*) are projected for most African regions, even as increasing dry CIDs (aridity; hydrological, agricultural and ecological droughts; fire weather) are projected in the western part of Western Africa, Southern Africa and Northern Africa and the Mediterranean regions (*medium* to *high confidence*). {8.4, 11.3, 11.6, 11.9, 12.4, Atlas.4}

In addition to the main changes summarized above and in Section TS.4.3.1, additional details per CID are given below.

Heat and cold: Observed and projected increases in mean temperature and a shift toward heat extreme characteristics are broadly similar to the generic pattern described in Section TS.4.3.1. {2.3.1.1.2, 11.3, 11.9, 12.4.1.1, Atlas.4.2, Atlas.4.4}

Wet and dry: Mean precipitation changes have been observed over Africa, but the historical trends are not spatially coherent (*high confidence*). North Eastern Africa, East Southern Africa and Central Africa have experienced a decline in rainfall since about 1980 and parts of West Africa an increase (*high confidence*). Increases in the frequency and/or the intensity of heavy rainfall have been observed in East and West Southern Africa, and the eastern Mediterranean region (*medium confidence*). Increasing trends in river flood occurrence can be identified beyond 1980 in East and West Southern Africa (*medium confidence*) and Western Africa (*high confidence*). However, Northern Africa and West Southern Africa are *likely* to have a reduction in precipitation. Over West Africa, rainfall is projected to decrease in the western Sahel subregion and increase along the Guinea Coast subregion (*medium confidence*). Rainfall is projected to increase over Eastern Africa (*medium confidence*). {8.3.1.6, 11.4, 11.9, 12.4.1.2, Atlas.4.2, Atlas.4.4, Atlas.4.5}

Precipitation declines and aridity trends in Western Africa, Central Africa, Southern Africa and the Mediterranean co-occur with trends towards increased agricultural and ecological droughts in the same regions (*medium confidence*). Trends towards increased hydrological droughts have been observed in the Mediterranean (*high confidence*) and Western Africa (*medium confidence*). These trends correspond with projected regional increases in aridity and fire weather conditions (*high confidence*). {8.3.1.6, 8.4.1.6, 11.6, 11.9, 12.4.1.2}

Wind: Mean wind, extreme winds and the wind energy potential in North Africa and the Mediterranean are projected to decrease across all scenarios (*high confidence*). Over Western Africa and Southern Africa, a future significant increase in wind speed and wind energy potential is projected (*medium confidence*). There is a projected decrease in the frequency of tropical cyclones making landfall over Madagascar, East Southern Africa and East Africa (*medium confidence*). {12.4.1.3}

Snow and ice: There is *high confidence* that African glaciers and snow have very significantly decreased in the last decades and that this trend will continue in the 21st century. {12.4.1.4}

Coastal and oceanic: Relative sea level has increased at a higher rate than GMSL around Africa over the last 3 decades. The present day 1-in-100-year extreme total water level (ETWL) is between 0.1 m and 1.2 m around Africa, with values around 1 m or above along the East and West Southern and Central Eastern Africa coasts. Satellite-derived shoreline retreat rates up to 1 m yr^{-1} have been observed around the continent from 1984 to 2015, except in South Eastern Africa, which has experienced a shoreline progradation (growth) rate of 0.1 m yr^{-1} over the same period. {12.4.1.5}

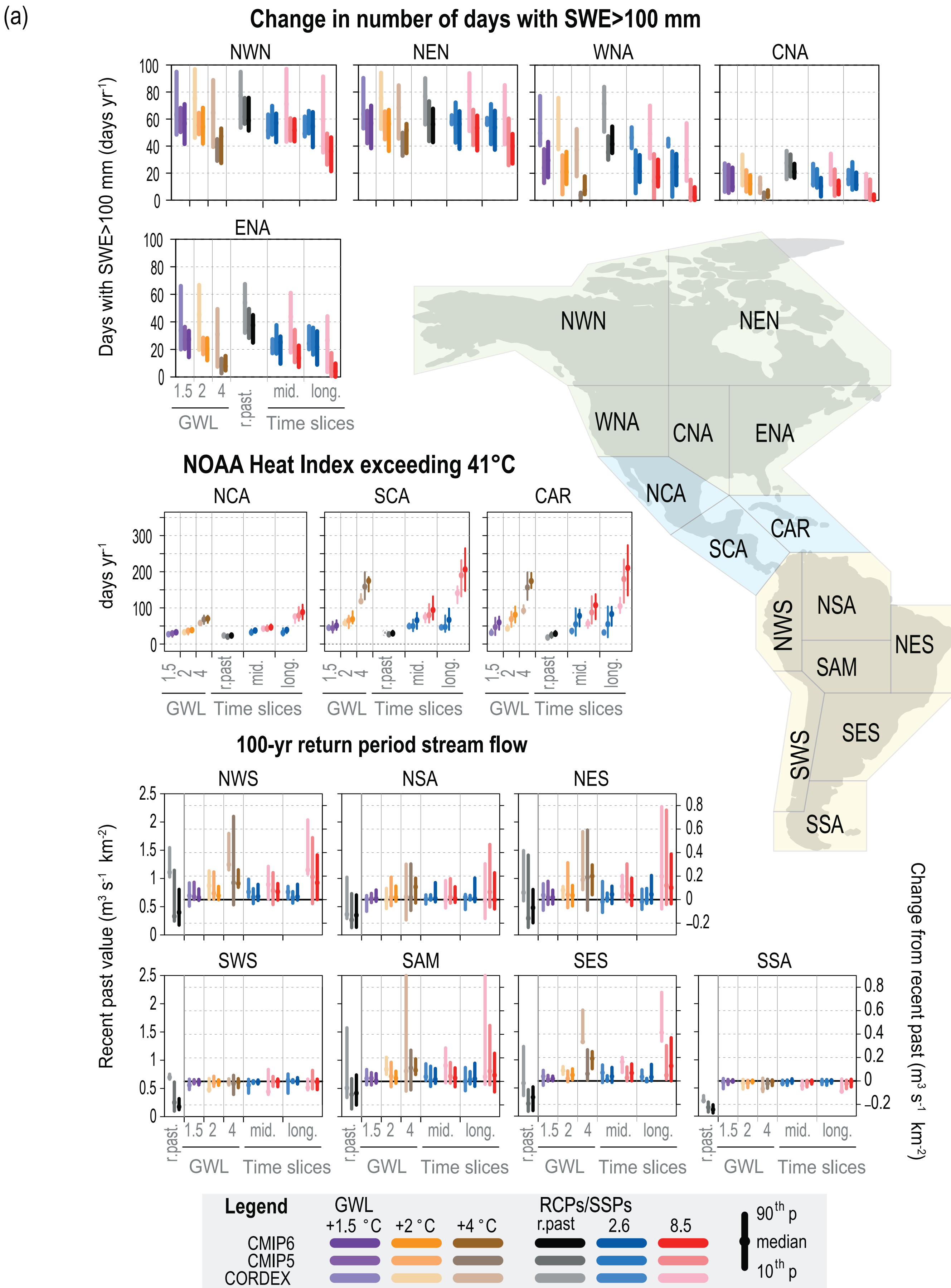
(a)
Change in number of days with SWE>100 mm
NWN
NEN
WNA
CNA
ENA
Days with SWE>100 mm (days yr⁻¹)
1.5 2 4
r.past.
mid. long.
GWL
Time slices
NWN
NEN
WNA
CNA
ENA
NCA
SCA
CAR
NWS
NSA
NES
SAM
SES
SWS
SSA
NOAA Heat Index exceeding 41°C
NCA
SCA
CAR
days yr⁻¹
GWL Time slices
100-yr return period stream flow
NWS
NSA
NES
SWS
SAM
SES
SSA
Recent past value (m³ s⁻¹ km⁻²)
Change from recent past (m³ s⁻¹ km⁻²)
Legend
GWL
+1.5 °C
+2 °C
+4 °C
RCPs/SSPs
r.past
2.6
8.5
CMIP6
CMIP5
CORDEX
90th p
median
10th p

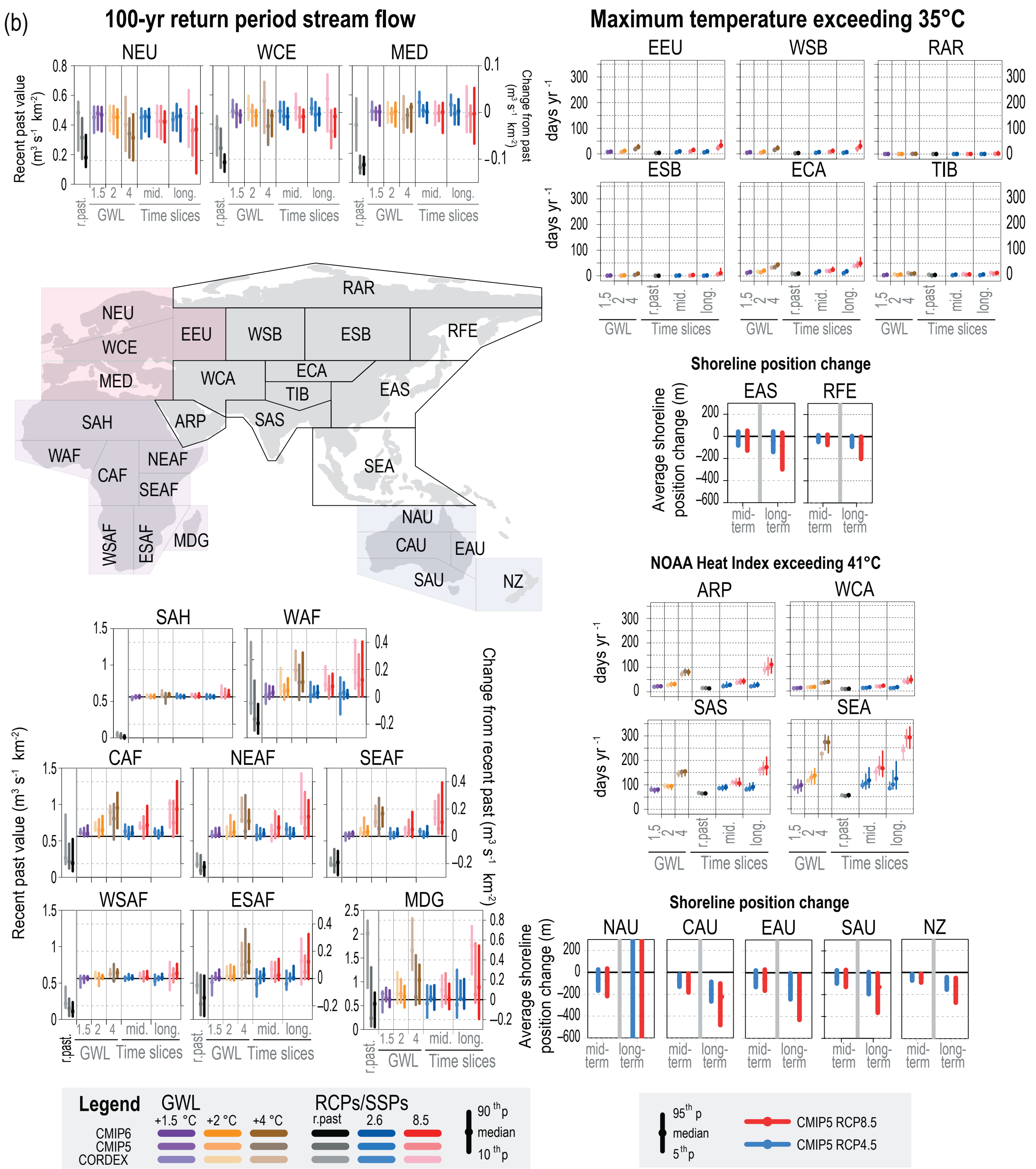

Figure TS.25 | Distribution of projected changes in selected climatic impact-driver (CID) indices for selected regions for Coupled Model Intercomparison Project Phases 5 and 6 (CMIP6, CMIP5) and Coordinated Regional Downscaling Experiment (CORDEX) model ensembles. *The intent of this figure is to show that many CID projections for multiple global warming levels and scenarios time slices are available for all the AR6 WGI reference regions and are based on both global (CMIP5, CMIP6) and regional (CORDEX) model ensembles.* Different indices are shown for different region: for Eastern Europe and North Asia, the mean number of days per year with maximum temperature exceeding 35°C; for Central America, the Caribbean, South West Asia, South Asia and South East Asia, the mean number of days per year with the National Oceanic and Atmospheric Administration (NOAA) Heat Index exceeding 41°C; for Australasia, East Asia and Russian Far East, the average shoreline position change; for South America, Europe and Africa, the mean change in 1-in-100-year river discharge per unit catchment area ($m^3\ s^{-1}\ km^{-2}$); and for North America, the median change in the number of days with snow water equivalent (SWE) over 100 mm. For each box plot, the changes or the climatological values are reported with respect to, or compared to, the recent past (1995–2014) period for 1.5°C, 2°C and 4°C global warming levels and for mid-century (2041–2060) or end-century (2081–2100) periods for the CMIP5 and CORDEX RCP8.5 and RCP2.6 and CMIP6 SSP5-8.5 and SSP1-2.6 scenarios ensembles. {Figures 12.5, 12.6, 12.9, 12.SM.1, 12.SM.2, and 12.SM.6}

TS.4.3.2.2 Asia

Due to the high climatological and geographical heterogeneity of Asia, some assessment findings below are summarized over five sub-continental areas comprising one or more of the AR6 WGI reference regions (Box TS.12): East Asia (EAS+ECA), North Asia (WSB+ESB+RFE), South Asia (SAS), South East Asia (SEA) and South West Asia (ARP+WCA).

Additional regional changes in Asia, besides those features described in Section TS.4.3.1, include historical trends of annual precipitation that show considerable regional differences (*high confidence*). East Asian Monsoon precipitation has changed, with drying in the north and wetting in the south since the 1950s, and annual mean precipitation totals *very likely* have increased over most territories of North Asia since the mid-1970s (*high confidence*). South Asian summer monsoon precipitation decreased over several areas since the mid-20th century (*high confidence*) but is *likely* to increase during the 21st century, with enhanced interannual variability. (Box TS.13)

Increases in precipitation and river floods are projected over much of Asia: in the annual mean precipitation in East, North, South and South East Asia (*high confidence*); for extremes in East, South, West Central, North and South East Asia (*high confidence*) and Arabian Peninsula (*medium confidence*); and for river floods in East, South and South East Asia and East Siberia (*medium confidence*). Aridity in East and West Central Asia is projected to increase, especially beyond the middle of the 21st century and global warming levels beyond 2°C (*medium confidence*). Fire weather seasons are projected to lengthen and intensify everywhere except South East Asia, Tibetan Plateau and Arabian Peninsula (*medium confidence*).

Surface wind speeds have been decreasing in Asia (*high confidence*), but there is a large uncertainty in future trends, with *medium confidence* that mean wind speeds will decrease in North Asia, East Asia and Tibetan Plateau and that tropical cyclones will have decreasing frequency and increasing intensity overall in South East and East Asia.

Over North Asia, increases in permafrost temperature and its thawing have been observed over recent decades (*high confidence*). Future projections indicate continuing decline in seasonal snow duration, glacial mass, and permafrost area by mid-century (*high confidence*). Snow-covered areas and snow volumes will decrease in most regions of the Hindu Kush Himalaya (HKH) during the 21st century, and snowline elevations will rise (*high confidence*) and glacier volumes are *likely* to decline with greater mass loss in higher CO_2 emissions scenarios. Heavy snowfall is increasing in East Asia and North Asia (*medium confidence*) but with *limited evidence* on future changes in hail and snow avalanches. **{2.3, 8.3, 8.4, 9.5, 9.6, 10.6, Box 10.4, 11.4, 11.5, 11.7, 11.9, 12.4.2, Atlas.3.1, Atlas.5, Atlas.5.2, Atlas.5.3, Atlas.5.4, Atlas.5.5}**

In addition to the main changes summarized above and in Section TS.4.3.1, further details are given below.

Heat and cold: Over all regions of Asia, observed and projected increases in mean temperature and a shift toward heat extreme characteristics are broadly similar to the generic pattern described in Section TS.4.3.1. Over South East Asia, annual mean surface temperature will *likely* increase by a slightly smaller amount than the global average. {Atlas.5.4.4}

Wet and dry: Over East Asia, historical trends of annual precipitation show considerable regional differences but with increases over north-west China and South Korea (*high confidence*). Daily precipitation extremes have increased over part of the region (*high confidence*). Extreme hydrological drought frequency has increased in a region extending from south-west to north-east China, with projected increases of agricultural and ecological drought for 4°C GWL and fire weather for 2°C and above (*medium confidence*). {8.3.2, 8.4.2, 11.4.4, 11.4.5, 11.9, 12.4.2.2, Atlas.5.1.2}

Over North Asia, annual mean precipitation totals have *very likely* increased, causing more intense flooding events, and there is *medium confidence* that the number of dry days has decreased. Concurrently, total soil moisture is projected to decline extensively (*medium confidence*). {8.3.1.3, 8.4.1.6, 11.4.5, 11.5.2, 11.5.5, 12.4.2.2, Atlas.5.2.2}

Over South Asia, the summer monsoon precipitation decreased over several areas since the mid-20th century (*high confidence*), while it increased in parts of the western HKH and decreased over eastern-central HKH (*medium confidence*). The frequency of heavy precipitation and flood events has increased over several areas during the last few decades (*medium confidence*). {8.3.1.3, 8.3.2.4.1, 8.4.1.5, 8.4.2.4.1, 10.6.3.3, 10.6.3.5, 10.6.3.6, 10.6.3.8, Cross-Chapter Box 10.4, 11.4.1, 11.4.2, 11.4.5, 11.5.5, 12.4.2.2, Box 10.4, Atlas 5.3.2}

Over South East Asia, mean precipitation trends are not spatially coherent or consistent across datasets and seasons (*high confidence*). Most of the region has experienced an increase in rainfall intensity but with a reduced number of wet days (*medium confidence*). Rainfall is projected to increase in the northern parts of South East Asia and decrease in areas in the Maritime Continent (*medium confidence*). {8.4.1, 11.4.2, 11.5.5, 11.9, 12.4.2.2, Atlas.3.1, Atlas.5.4.2, Atlas.5.4.4}

Over South West Asia, an observed annual precipitation decline over the Arabian Peninsula since the 1980s of 6.3 mm per decade is contrasted with observed increases between 1.3 mm and 4.8 mm per decade during 1960–2013 over the elevated part of eastern West Central Asia (*very high confidence*), along with an increase of the frequency and intensity of extreme precipitation. {Figure 8.19, Figure 8.20, 8.3.1.6, 8.4.1.6, 11.9, Table 11.2A, 12.4.2.2, Atlas.5.5}

Wind: Over East Asia, the terrestrial near-surface wind speed has decreased and is projected to decrease further in the future (*medium confidence*). Since the mid 1980's, there has been an increase in the number and intensification rate of intense TCs (*medium confidence*), with a significant north-westward shift in tracks and a northward shift in their average latitude, increasing exposure over East China, the Korean Peninsula and the Japanese Archipelago (*medium confidence*). {11.7.1, 12.4.2.3}

Over North Asia, there is *medium confidence* for a decreasing trend in wind speed during 1979–2018 and for projected continuing decreases of terrestrial near-surface wind speed. {2.3.1.4.4, 12.4.2.3}

Over South East Asia, although there is no significant long-term trend in the number of TCs, fewer but more extreme TCs have affected the Philippines during 1951–2013. {11.7.4, 12.4.2.3}

Snow and ice: Over East Asia, decreases have been observed in the frequency, and increases in the mean intensity, of snowfall in north-western, north-eastern and south-eastern China and the eastern Tibetan Plateau since the 1960s. Heavy snowfall is projected to occur more frequently in some parts of Japan (*medium confidence*). {12.4.2.4, Atlas.5.1.2}

Over North Asia, seasonal snow duration and extent have decreased in recent decades (*high confidence*), and maximum snow depth *likely* has increased since the mid-1970s, particularly over the south of the Russian Far East. {2.3.2.5, 8.3.1.7.2, 9.5, 12.4.2.4, Atlas.5.2, Atlas.5.4}

Over South Asia, snow cover has reduced over most of the HKH since the early 21st century, and glaciers have thinned, retreated, and lost mass since the 1970s (*high confidence*), although the Karakoram glaciers have either slightly gained mass or are in an approximately balanced state (*medium confidence*). {8.3.1.7.1, Cross-Chapter Box 10.4}

Over South West Asia, mountain permafrost degradation at high altitudes has increased the instability of mountain slopes in the past decade (*medium confidence*). More than 60% of glacier mass in the Caucasus is projected to disappear under RCP8.5 emissions by the end of the 21st century (*medium confidence*). {9.5.1, 9.5.3, 12.4.2.4}

Coastal and oceanic: Over the last three decades, relative sea level has increased at a rate higher than GMSL around Asia (*high confidence*). Gross coastal area loss and shoreline retreat has been observed over 1984–2015, but with localized shoreline progradation in the Russian Far East, East and South East Asia. {12.4.2.5}

Projections show that regional mean sea level continues to rise (*high confidence*), ranging from 0.4–0.5 m under SSP1-2.6 to 0.8–1.0 m under SSP5-8.5 for 2081–2100 relative to 1995–2014 (median values). This will contribute to more frequent coastal flooding and higher ETWL in low-lying areas and coastal erosion along sandy beaches (*high confidence*). There is *high confidence* that compound effects of climate change, land subsidence, and human factors will lead to higher flood levels and prolonged inundation in the Mekong Delta and other Asian coasts. {9.6.1, 9.6.3, 12.4.2.5}

TS.4.3.2.3 Australasia

Additional regional changes in Australasia, besides those features described in Section TS.4.3.1, include a significant decrease in April to October rainfall in the south-west of the state of Western Australia, observed from 1910 to 2019 and attributable to human influence (*high confidence*), which is *very likely* to continue in future. Agricultural and ecological droughts and hydrological droughts have increased over Southern Australia (*medium confidence*), and meteorological droughts have decreased over Northern and Central Australia (*medium confidence*). Relative sea level has increased over the period 1993–2018 at a rate higher than GMSL around Australasia (*high confidence*). Sandy shorelines have retreated around the region, except in Southern Australia, where a shoreline progradation rate of 0.1 m yr^{-1} has been observed.

In the future, heavy precipitation and pluvial flooding are *very likely* to increase over Northern Australia and Central Australia, and they are *likely* to increase elsewhere in Australasia for global warming levels (GWLs) exceeding 2°C and with *medium confidence* for a 2°C GWL. Agricultural and ecological droughts are projected to increase in Southern and Eastern Australia (*medium confidence*) for a 2°C GWL. Fire weather is projected to increase throughout Australia (*high confidence*) and New Zealand (*medium confidence*). Snowfall is expected to decrease throughout the region at high altitudes in both Australia (*high confidence*) and New Zealand (*medium confidence*), with glaciers receding in New Zealand (*high confidence*). {11.4, Table 11.6, 12.3, 12.4.3, Atlas.6.4, Atlas.6.5}

In addition to the main changes summarized above and in Section TS.4.3.1, further details are given below.

Heat and cold: Observed and projected increases in mean temperature and a shift toward heat extreme characteristics are broadly similar to the generic pattern described in Section TS.4.3.1. {11.9, 12.4.3.1, Atlas.6}

Wet and dry: There is *medium confidence* that heavy precipitation has increased in Northern Australia since 1950. Annual mean precipitation is projected to increase in the south and west of New Zealand (*medium confidence*) and is projected to decrease in south-west Southern Australia (*high confidence*), Eastern Australia (*medium confidence*), and in the north and east of New Zealand (*medium confidence*) for a GWL of 2°C. There is *medium confidence* that river flooding will increase in New Zealand and Australia, with higher increases in Northern Australia. Aridity is projected to increase with *medium confidence* in Southern Australia (*high confidence* in south-west Southern Australia), Eastern Australia (*medium confidence*) and in the north and east of New Zealand (*medium confidence*) for GWLs around 2°C. {11.4, 11.9, Table 11.6, 12.4.3.2, Atlas.6.2}

Wind: Mean wind speeds are projected to increase in parts of north-eastern Australia (*medium confidence*) by the end of the 21st century

TS

under high CO_2 emissions scenarios. TCs in north-eastern and north Australia are projected to decrease in number (*high confidence*) but increase in intensity except for 'east coast lows' (*low confidence*). {12.4.3.3}

Snow and ice: Observations in Australia show that the snow season length has decreased by 5% in the last five decades. Furthermore, the date of peak snowfall in Australia has advanced by 11 days over the last 5 decades. Glacier ice volume in New Zealand has decreased by 33% from 1977 to 2018. {12.4.3.4, Atlas.6.2}

Coastal and oceanic: Observed changes in marine heatwaves (MHWs) over the 20th century in the region show an increase in their occurrence frequency, except along the south-east coast of New Zealand, an increase in duration per event, and the total number of MHW days per decade, with the change being stronger in the Tasman Sea than elsewhere. The present day 1-in-100-year ETWL is between 0.5–2.5 m around most of Australia, except the north-western coast where 1-in-100-year ETWL can be as high as 6–7 m. {Box 9.1, 12.3.1.5, 12.4.3.5}

TS.4.3.2.4 Central and South America

Additional regional changes in Central and South America, besides those features described in Section TS.4.3.1, include increases in mean and extreme precipitation in South-Eastern South America since the 1960s (*high confidence*) (Section TS.4.2.3). Decreasing trends in mean precipitation and increasing trends in agricultural and ecological drought are observed over North-Eastern South America (*medium confidence*). The intensity and frequency of extreme precipitation and pluvial floods is projected to increase over South-Eastern South America, Southern South America, Northern South America, South American Monsoon and North-Eastern South America (*medium confidence*) for a 2°C GWL and above. Increases of agricultural and ecological drought are projected in South America Monsoon and Southern South America, and fire weather is projected to increase over several regions (Northern South America, the South American Monsoon, North-Eastern South America and South-Western South America) (*high confidence*). {8.3, 8.4, 11.3, 11.4, 11.9, Table 11.13, Table 11.14, Table 11.15, 12.4.4.2, Atlas.7.1, Atlas.7.2}

In addition to the main changes summarized above and in Section TS.4.3.1, further details are given below.

Heat and cold: Observed and projected increases in mean temperature and a shift toward heat extreme characteristics are broadly similar to the generic pattern described in Section TS.4.3.1. {11.3.2, 11.3.5, Table 11.13, 12.4.4.1, Atlas.7.1.2, Atlas.7.2.2, Atlas.7.2.4}

Wet and dry: Mean precipitation is projected to change in a dipole pattern with increases in North-Western and South-Eastern South America and decreases in North-Eastern and South-Western South America (*high confidence*) and with further decreases in Northern South America and Southern Central America (*medium confidence*). In Northern South America and Southern Central America, aridity and agricultural and ecological droughts are increasing with *medium confidence*. Fire weather is projected to increase over Southern Central America and Southern South America with *medium confidence*. {8.3.1.3, 8.4.2.4.5, 11.4.2, 11.9, Table 11.14, Table 11.15, 12.4.4.2, Atlas.7.2.2, Atlas.7.2.4}

Wind: Climate projections indicate an increase in mean wind speed and in wind power potential over the Amazonian region (Northern South America, South American Monsoon, North-Eastern South America) (*medium confidence*). {12.4.4.3}

Snow and ice: Glacier volume loss and permafrost thawing will *likely* continue in the Andes Cordillera under all climate scenarios, causing important reductions in river flow and potentially high-magnitude glacial lake outburst floods. {9.5.1.1, 12.4.4.4}

Coastal and oceanic: Around Central and South America, relative sea level has increased at a higher rate than GMSL in the South Atlantic and the subtropical North Atlantic, and at a rate lower than GMSL in the East Pacific over the last 3 decades. The present day 1-in-100-year ETWL is highest in Southern and South-Western South America subregions, where it can be as large as 5 to 6 m. Satellite observations for 1984–2015 show shoreline retreat rates along the sandy coasts of Southern Central America, South-Eastern South America and Southern South America, while shoreline progradation rates have been observed in North-Western South America and Northern South America. Over the period 1982–2016, the coastlines experienced at least one MHW per year, and more along the Pacific coast of North Central America and the Atlantic coast of South-Eastern South America. {12.4.4.5}

TS.4.3.2.5 Europe

Additional regional changes in Europe, besides those features described in Section TS.4.3.1, include observed increases in pluvial flooding in Northern Europe and hydrological and agricultural/ecological droughts in the Mediterranean (*high confidence*), which have been attributed to human influence with *high* and *medium confidence*, respectively. Increased mean precipitation amounts at high latitudes in boreal winter and reduced summer precipitation in southern Europe are projected starting from a 2°C GWL (*high confidence*). Aridity, agricultural and hydrological droughts and fire weather conditions will increase in the Mediterranean region starting from 2°C GWL (*high confidence*). Pluvial flooding will increase everywhere with *high confidence* except for *medium confidence* in the Mediterranean; in Western and Central Europe this also applies to river flooding starting from a 2°C GWL (*high confidence*). Most periglacial processes in Northern Europe are projected to disappear by the end of the 21st century, even for a low warming scenario (*medium confidence*). {8.3, 11.3, 11.9, 12.4.5, 12.5.2, Atlas.8.2, Atlas.8.4}

In addition to the main changes summarized above and in Section TS.4.3.1, further details are given below.

Heat and cold: Observed and projected increases in mean temperature and a shift toward heat extreme characteristics are broadly similar to the generic pattern described in Section TS.4.3.1. {11.3, 11.9, 12.4.5.1, 12.5.2, Atlas.8.2, Atlas.8.4}

Wet and dry: There is *medium confidence* that annual mean precipitation has increased in Northern Europe, West and Central Europe, and Eastern Europe since the early 20th century and *high confidence* for increases in extreme precipitation. In the European Mediterranean, the magnitude and sign of observed land precipitation trends depend on time period and exact study region (*medium confidence*). There is *medium confidence* that river floods will decrease in Northern, Eastern and southern Europe for high warming levels. {8.3.1.3, 11.3, 11.9, 12.4.5.2, Atlas.8.2, Atlas.8.4}

Wind: Mean wind speed over land has decreased (*medium confidence*), but the role of human-induced climate change has not been established. There is *high confidence* that mean wind speeds will decrease in Mediterranean areas and *medium confidence* for such decreases in Northern Europe for GWLs exceeding 2°C. The frequency of Medicanes (tropical-like cyclones in the Mediterranean) is projected to decrease (*medium confidence*). {11.9, 12.4.5.3}

Snow and ice: In the Alps, snow cover will decrease below elevations of 1500–2000 m throughout the 21st century (*high confidence*). A reduction of glacier ice volume is projected in the European Alps and Scandinavia with *high confidence* and with *medium confidence* for the timing and mass change rates. {9.5.2, 12.4.5.4}

Coastal and oceanic: Over the last three decades, relative sea level has increased at a lower rate than GMSL in the sub-polar North Atlantic coasts of Europe. The present-day 1-in-100-year ETWL is between 0.5–1.5 m in the Mediterranean basin and 2.5–5.0 m in the western Atlantic European coasts, around the United Kingdom and along the North Sea coast, and lower at 1.5–2.5 m along the Baltic Sea coast. Satellite-derived shoreline change estimates over 1984–2015 indicate shoreline retreat rates of around 0.5 m yr^{-1} along the sandy coasts of Central Europe and the Mediterranean and more or less stable shorelines in Northern Europe. Over the period 1982–2016, the coastlines of Europe experienced on average more than 2.0 MHW per year, with the eastern Mediterranean and Scandinavia experiencing 2.5–3 MHWs per year. {12.4.5.5}

TS.4.3.2.6 North America

Additional regional changes in North America, besides those features described in Section TS.4.3.1, include changes in North American wet and dry CIDs, which are largely organized by the north-east (more wet) to south-west (more dry) pattern of mean precipitation change, although heavy precipitation increases are widespread (*high confidence*). Increasing evaporative demand will expand agricultural and ecological drought and fire weather (particularly in summertime) in Central North America, Western North America and Northern Central America (from *medium* to *high confidence*). Severe wind storms, tropical cyclones and dust storms in North America are shifting toward more extreme characteristics (*medium confidence*), and both observations and projections point to strong changes in the seasonal and geographic range of snow and ice conditions in the coming decades (*very high confidence*). General findings for relative sea level, coastal flooding and erosion will not apply for areas with substantial land uplift around the Hudson Bay and Southern Alaska. {8.4, 11.4, 11.5, 11.7, 11.9, 12.4, Atlas.9.4}

In addition to the main changes summarized above and in Section TS.4.3.1, further details are given below.

Heat and cold: Observed and projected increases in mean temperature and a shift toward heat extreme characteristics are broadly similar to the generic pattern described in Section TS.4.3.1. {11.3, 11.9, 12.4.6.1, Atlas.9.2, Atlas.9.4}

Wet and dry: Annual precipitation increased over parts of Eastern and Central North America during 1960–2015 (*high confidence*) and has decreased in parts of south-western United States and north-western Mexico (*medium confidence*). River floods are projected to increase for all North American regions other than Northern Central America (*medium confidence*). {8.4.2.4, 11.4, 11.5, 11.9, 12.4.6.2, Atlas.9.2, Atlas.9.4}

Agricultural and ecological drought increases have been observed in Western North America (*medium confidence*), and aridity is projected to increase in the south-western United States and Northern Central America, with lower summer soil moisture across much of the continental interior (*medium confidence*). {8.4.1, 11.6.2, 12.4.6.2}

Wind: Projections indicate a greater number of the most intense TCs, with slower translation speeds and higher rainfall potential for Mexico's Pacific Coast, the Gulf Coast and the United States East Coast (*medium confidence*). Mean wind speed and wind power potential are projected to decrease in Western North America (*high confidence*), with differences between global and regional models lending *low confidence* elsewhere. {11.4, 11.7, 12.4.6.3}

Snow and ice: It is *likely* that some high-latitude regions will experience an increase in winter snow water equivalent due to the snowfall increase prevailing over the warming trend. At sustained GWLs between 3°C and 5°C, nearly all glacial mass in Western Canada and Western North America will disappear (*medium confidence*). {9.5.1, 9.5.3, 12.4.6.4, Atlas.9.4}

Coastal and oceanic: Around North America, relative sea level has increased over the last three decades at a rate lower than GMSL in the subpolar North Atlantic and in the East Pacific, while it has increased at a rate higher than GMSL in the subtropical North Atlantic. Observations indicate that episodic coastal flooding is increasing along many coastlines in North America. Shoreline retreat rates of around 1 m yr^{-1} have been observed during 1984–2015 along the sandy coasts of North-Western North America and Northern Central

America, while portions of the United States Gulf Coast have seen a retreat rate approaching 2.5 m yr^{-1}. Sandy shorelines along Eastern North America and Western North America have remained more or less stable during 1984–2014, but a shoreline progradation rate of around 0.5 m yr^{-1} has been observed in North-Eastern North America. {12.4.6.5}

TS.4.3.2.7 Small Islands

Additional regional changes in Small Islands, besides those features described in Section TS.4.3.1, include a *likely* decrease in rainfall during boreal summer in the Caribbean and in some parts of the Pacific islands poleward of 20° latitude in both the Northern and Southern Hemispheres. These drying trends will *likely* continue in coming decades. Fewer but more intense tropical cyclones are projected starting from a 2°C GWL (*medium confidence*). {9.6, 11.3, 11.4, 11.7, 11.9, 12.4.7, Atlas.10.2, Atlas.10.4, Cross-Chapter Box Atlas.2}

In addition to the main changes summarized above and in Section TS.4.3.1, further details are given below.

Heat and cold: It is *very likely* that most Small Islands have warmed over the period of instrumental records, and continued temperature increases in the 21st century will further increase heat stress in these regions. {11.3.2, 11.9, 12.4.7.1, Atlas.10.2, Atlas.10.4, Cross-Chapter Box Atlas.2}

Wet and dry: Observed and projected rainfall trends vary spatially across the Small Islands. Higher evapotranspiration under a warming climate can partially offset future increases or amplify future reductions in rainfall, resulting in increased aridity as well as more severe agricultural and ecological drought in the Caribbean (*medium confidence*). {11.4.2, 11.9, 12.4.7.2, Atlas.10.2, Atlas.10.4, Cross-Chapter Box Atlas.2}

Wind: Global changes indicate that Small Islands will face fewer but more intense TCs, with spatial inconsistency in projections given poleward shifts in TC tracks (*medium confidence*). {11.7.1.2, 11.7.1.5, 12.4.7.3}

Coastal and oceanic: Continued relative sea level rise is *very likely* in the ocean around Small Islands and, along with storm surges and waves, will exacerbate coastal inundation with the potential to increase saltwater intrusion into aquifers in small islands. Shoreline retreat is projected along sandy coasts of most small islands (*high confidence*). {9.6.3.3, 12.4.7.4, Cross-Chapter Box Atlas.2}

TS.4.3.2.8 Polar

It is *virtually certain* that surface warming in the Arctic will continue to be more pronounced than the global average warming over the 21st century. An intensification of the polar water cycle will increase mean precipitation, with precipitation intensity becoming stronger and more *likely* to be rainfall rather than snowfall (*high confidence*). Permafrost warming, loss of seasonal snow cover, and glacier melt will be widespread (*high confidence*). There is *high confidence* that both the Greenland and Antarctic ice sheets have lost mass since 1992 and will continue to lose mass throughout this century under all emissions scenarios. Relative sea level and coastal flooding are projected to increase in areas other than regions with substantial land uplift (*medium confidence*). {2.3, 3.4, 4.3, 4.5, 7.4, 8.2, 8.4, Box 8.2, 9.5, 12.4.9, Atlas.11.1, Atlas.11.2}

In addition to the main changes summarized above and in Section TS.4.3.1, further details are given below.

Heat and cold: Changes in Antarctica showed larger spatial variability, with *very likely* warming in the Antarctic Peninsula since the 1950s and no overall trend in East Antarctica. Less warming and weaker polar amplification are projected as *very likely* over the Antarctic than in the Arctic, with a weak polar amplification projected as *very likely* by the end of the 21st century. {4.3.1, 4.5.1, 7.4.4, 12.4.9.1, Atlas.11.1, Atlas.11.2}

Wet and dry: Recent decades have seen a general decrease in Arctic aridity (*high confidence*), with increased moisture transport leading to higher precipitation, humidity and streamflow and a corresponding decrease in dry days. Antarctic precipitation showed a positive trend during the 20th century. The water cycle is projected to intensify in both polar regions, leading to higher precipitation totals (and a shift to more heavy precipitation) and higher fraction of precipitation falling as rain. In the Arctic, this will result in higher river flood potential and earlier meltwater flooding, altering seasonal characteristics of flooding (*high confidence*). A lengthening of the fire season (*medium confidence*) and encroachment of fire regimes into tundra regions (*high confidence*) are projected. {8.2.3, 8.4.1, Box 8.2, 9.4.1, 9.4.2, 12.4.9.2, Atlas.11.1, Atlas.11.2}

Wind: There is *medium confidence* in mean wind decrease over the Russian Arctic and Arctic North-East North America, but *low confidence* of changes in other Arctic regions and Antarctica. {12.4.9.3}

Snow and ice: Reductions in spring snow cover extent have occurred across the Northern Hemisphere since at least 1978 (*very high confidence*). Permafrost warming and thawing have been widespread in the Arctic since the 1980s (*high confidence*), causing strong heterogeneity in surface conditions. There is *high confidence* in future glacier- and ice-sheet loss, permafrost warming, decreasing permafrost extent and decreasing seasonal duration and extent of snow cover in the Arctic. Decline in seasonal sea ice coverage along the majority of the Arctic coastline in recent decades is projected to continue, contributing to an increase in coastal hazards (including open water storm surge, coastal erosion and flooding). {2.3.2, 3.4.2, 3.4.3, 9.4.1, 9.4.2, 9.5, 12.4.6, 12.4.9, Atlas.11.2}

Coastal and oceanic: Higher sea levels contribute to *high confidence* for projected increases of Arctic coastal flooding and higher coastal erosion (aided by sea ice loss) (*medium confidence*), with lower confidence for those regions with substantial land uplift (Arctic North-East North America and Greenland). {12.4.9.5}

TS.4.3.2.9 Ocean

The Indian Ocean, western equatorial Pacific Ocean and western boundary currents have warmed faster than the global average (*very high confidence*), with the largest changes in the frequency of marine heatwaves (MHWs) projected in the western tropical Pacific and the Arctic Ocean (*medium confidence*). The Pacific and Southern Ocean are projected to freshen and the Atlantic to become more saline (*medium confidence*). Anthropogenic warming is *very likely* to further decrease ocean oxygen concentrations, and this deoxygenation is expected to persist for thousands of years (*medium confidence*). Arctic sea ice losses are projected to continue, leading to a practically ice-free Arctic in September by the end of the 21st century under high CO_2 emissions scenarios (*high confidence*). {2.3, 5.3, 9.2, 9.3, Box 9.2, 12.3.6, 12.4.8}

In addition to the main changes summarized above and in Section TS.4.3.1, further details are given below.

Ocean surface temperature: The Southern Ocean, the eastern equatorial Pacific, and the North Atlantic Ocean have warmed more slowly than the global average or slightly cooled. Global warming of 2°C above 1850–1900 levels would result in the exceedance of numerous hazard thresholds for pathogens, seagrasses, mangroves, kelp forests, rocky shores, coral reefs and other marine ecosystems (*medium confidence*). {9.2.13, 12.4.8}

Marine heatwaves: Moderate increases in MHW frequency are projected for mid-latitudes, and only small increases are projected for the Southern Ocean (*medium confidence*). Under the SSP5-8.5 scenario, permanent MHWs (more than 360 days per year) are projected to occur in the 21st century in parts of the tropical ocean, the Arctic Ocean, and around 45°S; however, the occurrence of such permanent MHWs can be largely avoided under the SSP1-2.6 scenario. {Box 9.2, 12.4.8}

Ocean acidity: With the rising CO_2 concentration, the ocean surface pH has declined globally over the past four decades (*virtually certain*). {2.3.3.5, 5.3.3.2, 12.4.8}

Ocean salinity: At the basin scale, it is *very likely* that the Pacific and the Southern Ocean have freshened while the Atlantic has become more saline. {2.3.3.2, 9.2.2.2, 12.4.8}

Dissolved oxygen: In recent decades, low oxygen zones in ocean ecosystems have expanded. {2.3.4.2, 5.3.3.2, 12.4.8}

Sea ice: Arctic perennial sea ice is being replaced by thin, seasonal ice, with earlier spring melt and delayed fall freeze up. There is no clear trend in the Antarctic sea ice area over the past few decades and *low confidence* in its future change. {2.3.2.1.1, 9.3.1.1, 12.4.8, 12.4.9}

TS.4.3.2.10 Other Typological Domains

Some types of regions found in different continents face common climate challenges regardless of their location. These include biodiversity hot spots that will *very likely* see even more extreme heat and droughts, mountain areas where a projected raising in the freezing level height will alter snow and ice conditions (*high confidence*), and tropical forests that are increasingly prone to fire weather (*medium confidence*). {8.4, Box 8.2, 9.5, 12.3, 12.4}

Biodiversity hotspots located around the world will each face unique challenges in CID changes. Heat, drought and length of dry season, wildfire weather, sea surface temperature and deoxygenation are relevant drivers to terrestrial and freshwater ecosystems and have marked increasing trends. {12.3, 12.4.10.1}

Desert and semi-arid areas are strongly affected by CIDs such as extreme heat, drought and dust storms, with large-scale aridity trends contributing to expanding drylands in some regions (*high confidence*). {12.3, 12.4.10.3}

Average warming in mountain areas varies with elevation, but the pattern is not globally uniform (*medium confidence*). Extreme precipitation is projected to increase in major mountainous regions (*medium* to *high confidence* depending on location), with potential cascading consequences of floods, landslides and lake outbursts in all scenarios (*medium confidence*). {8.4.1.5, Box 8.2, 9.5.1.3, 9.5.3.3, 9.5.2.3, Cross-Chapter Box 10.4, 11.5.5, 12.3, 12.4.1–12.4.6, 12.4.10.4}

Most tropical forests are challenged by a mix of emerging warming trends that are particularly large in comparison to historical variability (*medium confidence*). Water cycle changes bring prolonged drought, longer dry seasons and increased fire weather to many tropical forests (*medium confidence*). {10.5, 12.3, 12.4}

Box TS.14 | Urban Areas

With global warming, urban areas and cities will be affected by more frequent occurrences of extreme climate events, such as heatwaves, with more hot days and warm nights as well as sea level rise and increases in tropical cyclone storm surge and rainfall intensity that will increase the probability of coastal city flooding (*high confidence*). {Box 10.3, 11.3, 11.5, 12.3, 12.4}

Urban areas have special interactions with the climate system, for instance in terms of heat islands and altering the water cycle, and thereby will be more affected by extreme climate events such as extreme heat (*high confidence*). With global warming, increasing relative sea level compounded by increasing tropical cyclone storm surge and rainfall intensity will increase the probability of coastal city flooding (*high confidence*). Arctic coastal settlements are particularly exposed to climate change due to sea ice retreat (*high confidence*). Improvements in urban climate modelling and climate monitoring networks have contributed to understanding the mutual interaction between regional and urban climate (*high confidence*). {Box 10.3, 11.3, 11.5, 12.3, 12.4}

Despite having a negligible effect on global surface temperature (*high confidence*), urbanization has exacerbated the effects of global warming through its contribution to the observed warming trend in and near cities, particularly in annual mean minimum temperature (*very high confidence*) and increases in mean and extreme precipitation over and downwind of the city, especially in the afternoon and early evening (*medium confidence*). {2.3, Box 10.3, 11.3, 11.4, 12.3, 12.4}

Combining climate change projections with urban growth scenarios, future urbanization will amplify (*very high confidence*) the projected local air temperature increase, particularly by strong influence on minimum temperatures, which is approximately comparable in magnitude to global warming (*high confidence*). Compared to present day, large implications are expected from the combination of future urban development and more frequent occurrence of extreme climate events, such as heatwaves, with more hot days and warm nights adding to heat stress in cities (*very high confidence*). {Box 10.2, 11.3, 12.4}

Both sea levels and air temperatures are projected to rise in most coastal settlements (*high confidence*). There is *high confidence* in an increase in pluvial flood potential in urban areas where extreme precipitation is projected to increase, especially at high global warming levels. {11.4, 11.5, 12.4}

Frequently Asked Questions

FAQ

Frequently Asked Questions

Coordinating Editors:

Sophie Berger (France/Belgium), Sarah L. Connors (France/United Kingdom)

Drafting Authors:

Richard P. Allan (United Kingdom), Paola A. Arias (Colombia), Kyle Armour (United States of America), Terje Berntsen (Norway), Lisa Bock (Germany), Ruth Cerezo-Mota (Mexico), Kim Cobb (United States of America), Alejandro Di Luca (Australia, Canada/Argentina), Paul Edwards (United States of America), Tamsin L. Edwards (United Kingdom), Seita Emori (Japan), François Engelbrecht (South Africa), Veronika Eyring (Germany), Piers Forster (United Kingdom), Baylor Fox- Kemper (United States of America), Sandro Fuzzi (Italy), John C. Fyfe (Canada), Nathan P. Gillett (Canada), Nicholas R. Golledge (New Zealand/United Kingdom), Melissa I. Gomis (France/Switzerland), William J. Gutowski (United States of America), Rafiq Hamdi (Belgium), Mathias Hauser (Switzerland), Ed Hawkins (United Kingdom), Nigel Hawtin (United Kingdom), Darrell S. Kaufman (United States of America), Megan Kirchmeier-Young (Canada/ United States of America), Charles Koven (United States of America), June-Yi Lee (Republic of Korea), Sophie Lewis (Australia), Jochem Marotzke (Germany), Valérie Masson-Delmotte (France), Thorsten Mauritsen (Sweden/Denmark), Thomas K. Maycock (United States of America), Shayne McGregor (Australia), Sebastian Milinski (Germany), Olaf Morgenstern (New Zealand/Germany), Swapna Panickal (India), Joeri Rogelj (United Kingdom/Belgium), Maisa Rojas (Chile), Alex C. Ruane (United States of America), Bjørn H. Samset (Norway), Trude Storelvmo (Norway), Sophie Szopa (France), Jessica Tierney (United States of America), Russell S. Vose (United States of America), Masahiro Watanabe (Japan), Sönke Zaehle (Germany), Xuebin Zhang (Canada), Kirsten Zickfeld (Canada/Germany)

These Frequently Asked Questions have been extracted from the chapters of the underlying report and are compiled here. When referencing specific FAQs, please reference the corresponding chapter in the report from where the FAQ originated (e.g., FAQ 3.1 is part of Chapter 3).

Table of Contents

Frequently Asked Questions

Frequently Asked Questions

FAQ 1.1 | Do We Understand Climate Change Better Now Compared to When the IPCC Started?

Yes, much better. The first IPCC report, released in 1990, concluded that human-caused climate change would soon become evident, but could not yet confirm that it was already happening. Today, evidence is overwhelming that the climate has indeed changed since the pre-industrial era and that human activities are the principal cause of that change. With much more data and better models, we also understand more about how the atmosphere interacts with the ocean, ice, snow, ecosystems and land surfaces of the Earth. Computer climate simulations have also improved dramatically, incorporating many more natural processes and providing projections at much higher resolutions.

Since the first IPCC report in 1990, large numbers of new instruments have been deployed to collect data in the air, on land, at sea and from outer space. These instruments measure temperature, clouds, winds, ice, snow, ocean currents, sea level, soot and dust in the air, and many other aspects of the climate system. New satellite instruments have also provided a wealth of increasingly fine-grained data. Additional data from older observing systems and even hand-written historical records are still being incorporated into observational datasets, and these datasets are now better integrated and adjusted for historical changes in instruments and measurement techniques. Ice cores, sediments, fossils, and other new evidence from the distant past have taught us much about how Earth's climate has changed throughout its history.

Understanding of climate system processes has also improved. For example, in 1990 very little was known about how the deep ocean responds to climate change. Today, reconstructions of deep-ocean temperatures extend as far back as 1871. We now know that the oceans absorb most of the excess energy trapped by greenhouse gases and that even the deep ocean is warming up. As another example, in 1990, relatively little was known about exactly how or when the gigantic ice sheets of Greenland and Antarctica would respond to warming. Today, much more data and better models of ice-sheet behaviour reveal unexpectedly high melt rates that will lead to major changes within this century, including substantial sea level rise (FAQ 9.2).

The major natural factors contributing to climate change on time scales of decades to centuries are volcanic eruptions and variations in the sun's energy output. Today, data show that changes in incoming solar energy since 1900 have contributed only slightly to global warming, and they exhibit a slight downward trend since the 1970s. Data also show that major volcanic eruptions have sometimes cooled the entire planet for relatively short periods of time (typically several years) by erupting aerosols (tiny airborne particles) high into the atmosphere.

The main human causes of climate change are the heat-absorbing greenhouse gases released by fossil fuel combustion, deforestation, and agriculture, which warm the planet; and aerosols such as sulphate from burning coal, which have a short-term cooling effect that partially counteracts human-caused warming. Since 1990, we have more and better observations of these human factors as well as improved historical records, resulting in more precise estimates of human influence on the climate system (FAQ 3.1).

While most climate models in 1990 focused on the atmosphere, using highly simplified representations of oceans and land surfaces, today's Earth system simulations include detailed models of oceans, ice, snow, vegetation and many other variables. An important test of models is their ability to simulate Earth's climate over the period of instrumental records (since about 1850). Several rounds of such testing have taken place since 1990, and the testing itself has become much more rigorous and extensive. As a group and at large scales, models have predicted the observed changes well in these tests (FAQ 3.3). Since there is no way to do a controlled laboratory experiment on the actual Earth, climate model simulations can also provide a kind of 'alternate Earth' to test what would have happened without human influence. Such experiments show that the observed warming would not have occurred without human influence.

Finally, physical theory predicts that human influence on the climate system should produce specific patterns of change, and we see those patterns in both observations and climate simulations. For example, nights are warming faster than days, less heat is escaping to space, and the lower atmosphere (troposphere) is warming but the upper atmosphere (stratosphere) has cooled. These confirmed predictions are all evidence of changes driven primarily by increases in GHG concentrations rather than natural causes.

FAQ 1.1 (continued)

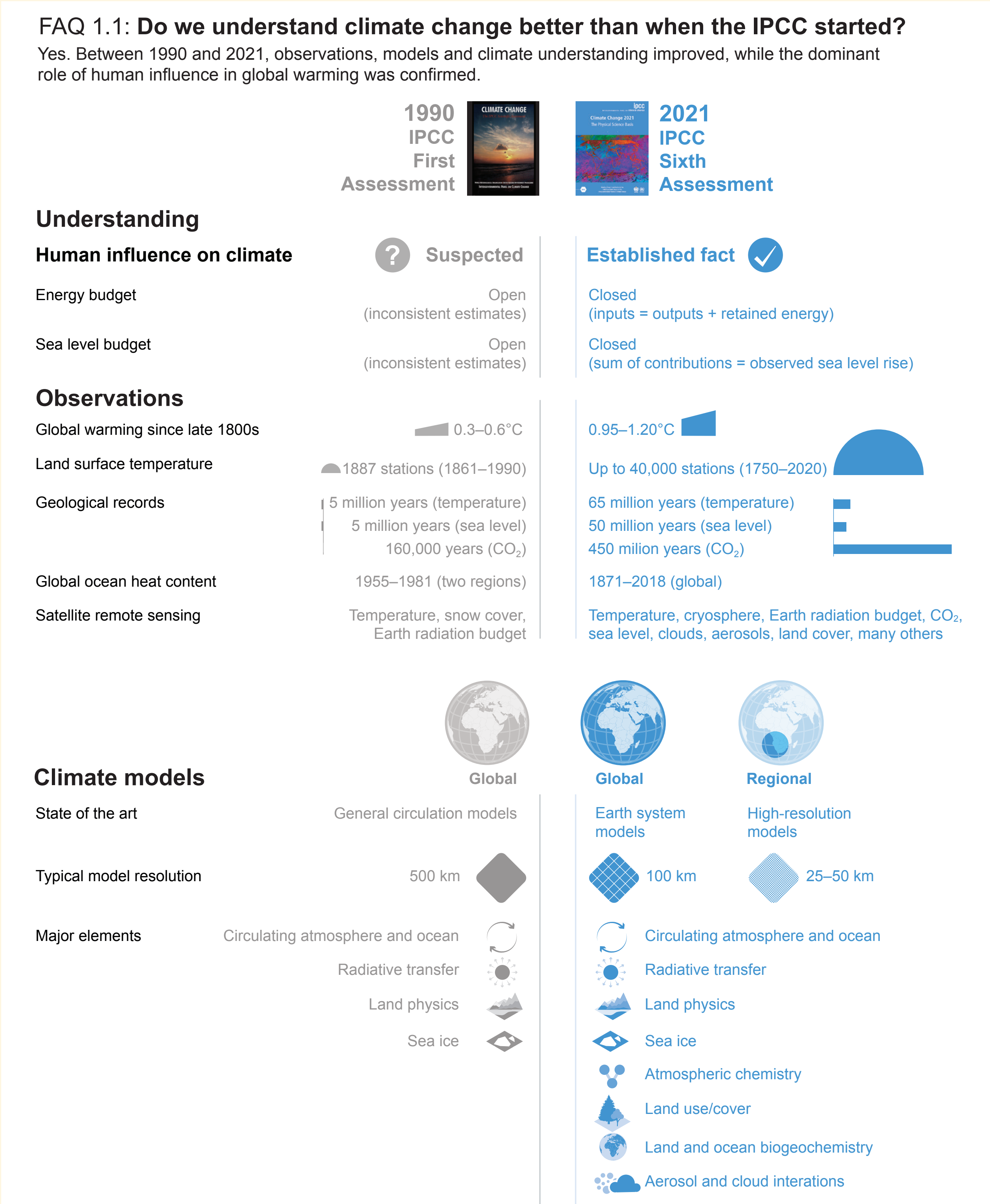

FAQ 1.1, Figure 1 | Sample elements of climate understanding, observations and models as assessed in the IPCC First Assessment Report (1990) and Sixth Assessment Report (2021). Many other advances since 1990, such as key aspects of theoretical understanding, geological records and attribution of change to human influence, are not included in this figure because they are not readily represented in this simple format. Fuller explanations of the history of climate knowledge are available in the introductory chapters of the IPCC Fourth and Sixth assessment reports.

FAQ

Frequently Asked Questions

FAQ 1.2 | Where Is Climate Change Most Apparent?

The signs of climate change are unequivocal at the global scale and are increasingly apparent on smaller spatial scales. The high northern latitudes show the largest temperature increase, with clear effects on sea ice and glaciers. The warming in the tropical regions is also apparent because the natural year-to-year variations in temperature there are small. Long-term changes in other variables such as rainfall and some weather and climate extremes have also now become apparent in many regions.

It was first noticed that the planet's land areas were warming in the 1930s. Although increasing atmospheric carbon dioxide (CO_2) concentrations were suggested as part of the explanation, it was not certain at the time whether the observed warming was part of a long-term trend or a natural fluctuation: global warming had not yet become apparent. But the planet continued to warm, and by the 1980s the changes in temperature had become obvious or, in other words, the *signal* had *emerged*.

Imagine you had been monitoring temperatures at the same location for the past 150 years. What would you have experienced? When would the warming have become noticeable in your data? The answers to these questions depend on where on the planet you are.

Observations and climate model simulations both demonstrate that the largest long-term warming trends are in the high northern latitudes and the smallest warming trends over land are in tropical regions. However, the year-to-year variations in temperature are smallest in the tropics, meaning that the changes there are also apparent, relative to the range of past experiences (FAQ 1.2, Figure 1).

Changes in temperature also tend to be more apparent over land areas than over the open ocean and are often most apparent in regions which are more vulnerable to climate change. It is expected that future changes will continue to show the largest signals at high northern latitudes, but with the most apparent warming in the tropics. The tropics also stand to benefit the most from climate change mitigation in this context, as limiting global warming will also limit how far the climate shifts relative to past experience.

Changes in other climate variables have also become apparent at smaller spatial scales. For example, changes in average rainfall are becoming clear in some regions, but not in others, mainly because natural year-to-year variations in precipitation tend to be large relative to the magnitude of the long-term trends. However, extreme rainfall is becoming more intense in many regions, potentially increasing the impacts from inland flooding (FAQ 8.2). Sea levels are also clearly rising on many coastlines, increasing the impacts of inundation from coastal storm surges, even without any increase in the number of storms reaching land. A decline in the amount of Arctic sea ice is apparent, both in the area covered and in its thickness, with implications for polar ecosystems.

When considering climate-related impacts, it is not necessarily the size of the change that is most important. Instead, it can be the rate of change or it can also be the size of the change relative to the natural variations of the climate to which ecosystems and society are adapted. As the climate is pushed further away from past experiences and enters an unprecedented state, the impacts can become larger, along with the challenge of adapting to them.

How and when a long-term trend becomes distinguishable from shorter-term natural variations depends on the aspect of climate being considered (e.g., temperature, rainfall, sea ice or sea level), the region being considered, the rate of change, and the magnitude and timing of natural variations. When assessing the local impacts from climate change, both the size of the change and the amplitude of natural variations matter.

FAQ 1.2 (continued)

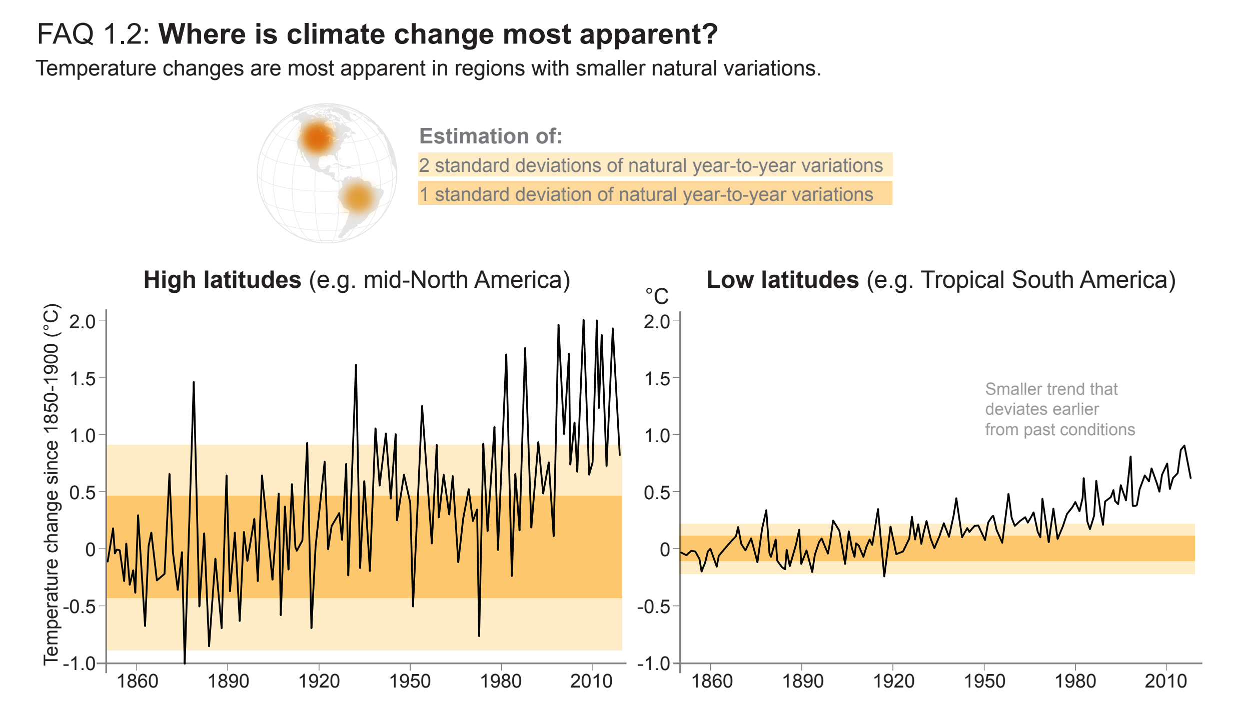

FAQ 1.2, Figure 1 | Observed variations in regional temperatures since 1850 (data from Berkeley Earth). Regions in high latitudes, such as mid-North America (40°N–64°N, 140°W–60°W, **left**), have warmed by a larger amount than regions at lower latitudes, such as tropical South America (10°S–10°N, 84°W–16°W, **right**), but the natural variations are also much larger at high latitudes (darker and lighter shading represents 1 and 2 standard deviations, respectively, of natural year-to-year variations). The signal of observed temperature change emerged earlier in tropical South America than mid-North America even though the changes were of a smaller magnitude. (Note that those regions were chosen because of the longer length of their observational record; see Figure 1.14 for more regions).

FAQ

Frequently Asked Questions

FAQ 1.3 | What Can Past Climate Teach Us About the Future?

In the past, the Earth has experienced prolonged periods of elevated greenhouse gas concentrations that caused global temperatures and sea levels to rise. Studying these past warm periods informs us about the potential long-term consequences of increasing greenhouse gases in the atmosphere.

Rising greenhouse gas concentrations are driving profound changes to the Earth system, including global warming, sea level rise, increases in climate and weather extremes, ocean acidification, and ecological shifts (FAQ 2.2 and FAQ 7.1). The vast majority of instrumental observations of climate began during the 20th century, when greenhouse gas emissions from human activities became the dominant driver of changes in Earth's climate (FAQ 3.1).

As scientists seek to refine our understanding of Earth's climate system and how it may evolve in coming decades to centuries, past climate states provide a wealth of insights. Data about these past states help to establish the relationship between natural climate drivers and the history of changes in global temperature, global sea levels, the carbon cycle, ocean circulation, and regional climate patterns, including climate extremes. Guided by such data, scientists use Earth system models to identify the chain of events underlying the transitions between past climatic states (FAQ 3.3). This is important because during present-day climate change, just as in past climate changes, some aspects of the Earth system (e.g., surface temperature) respond to changes in greenhouse gases on a time scale of decades to centuries, while others (e.g., sea level and the carbon cycle) respond over centuries to millennia (FAQ 5.3). In this way, past climate states serve as critical benchmarks for climate model simulations, improving our understanding of the sequences, rates, and magnitude of future climate change over the next decades to millennia.

Analyzing previous warm periods caused by natural factors can help us understand how key aspects of the climate system evolve in response to warming. For example, one previous warm-climate state occurred roughly 125,000 years ago, during the Last Interglacial period, when slight variations in the Earth's orbit triggered a sequence of changes that caused about 1°C–2°C of global warming and about 2–8 m of sea level rise relative to the 1850–1900, even though atmospheric carbon dioxide concentrations were similar to 1850–1900 values (FAQ 1.3, Figure 1). Modelling studies highlight that increased summer heating in the higher latitudes of the Northern Hemisphere during this time caused widespread melting of snow and ice, reducing the reflectivity of the planet and increasing the absorption of solar energy by the Earth's surface. This gave rise to global-scale warming, which led in turn to further ice loss and sea level rise. These self-reinforcing positive *feedback cycles* are a pervasive feature of Earth's climate system, with clear implications for future climate change under continued greenhouse gas emissions. In the case of sea level rise, these cycles evolved over several centuries to millennia, reminding us that the rates and magnitude of sea level rise in the 21st century are just a fraction of the sea level rise that will ultimately occur after the Earth system fully adjusts to current levels of global warming.

Roughly 3 million years ago, during the Pliocene Epoch, the Earth witnessed a prolonged period of elevated temperatures (2.5°C–4°C higher than 1850–1900) and higher sea levels (5–25 m higher than 1850–1900), in combination with atmospheric carbon dioxide concentrations similar to those of the present day. The fact that Pliocene atmospheric carbon dioxide concentrations were similar to the present, while global temperatures and sea levels were significantly higher, reflects the difference between an Earth system that has fully adjusted to changes in natural drivers (the Pliocene) and one where greenhouse gases concentrations, temperature, and sea level rise are still increasing (present day). Much about the transition into the Pliocene climate state – in terms of key causes, the role of cycles that hastened or slowed the transition, and the rate of change in climate indicators such as sea level – remain topics of intense study by climate researchers, using a combination of paleoclimate observations and Earth system models. Insights from such studies may help to reduce the large uncertainties around estimates of global sea level rise by 2300, which range from 0.3 m to 3 m above 1850–1900 (in a low-emissions scenario) to as much as 16 m higher than 1850–1900 (in a very high-emissions scenario that includes accelerating structural disintegration of the polar ice sheets).

While present-day warming is unusual in the context of the recent geologic past in several different ways (FAQ 2.1), past warm climate states present a stark reminder that the long-term adjustment to present-day atmospheric carbon dioxide concentrations has only just begun. That adjustment will continue over the coming centuries to millennia.

FAQ 1.3 (continued)

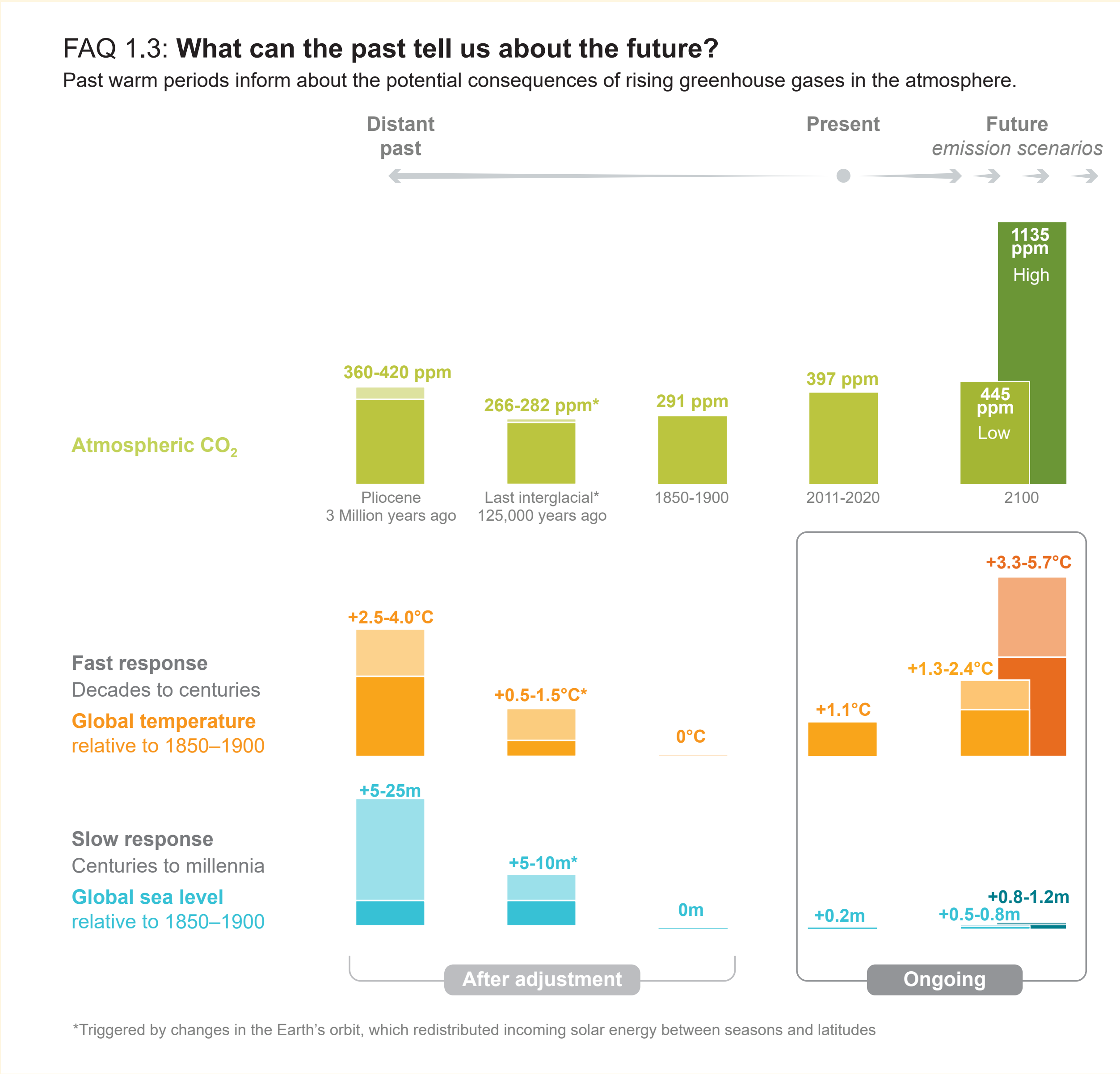

FAQ 1.3, Figure 1 | Comparison of past, present and future. Schematic of atmospheric carbon dioxide concentrations, global temperature, and global sea level during previous warm periods as compared to 1850–1900, present-day (2011–2020), and future (2100) climate change scenarios corresponding to low-emissions scenarios (SSP1-2.6; lighter colour bars) and very high-emissions scenarios (SSP5-8.5; darker colour bars).

Frequently Asked Questions

FAQ 2.1 | The Earth's Temperature Has Varied Before. How Is the Current Warming Any Different?

Earth's climate has always changed naturally, but both the global extent and rate of recent warming are unusual. The recent warming has reversed a slow, long-term cooling trend, and research indicates that global surface temperature is higher now than it has been for millennia.

While climate can be characterized by many variables, temperature is a key indicator of the overall climate state, and global surface temperature is fundamental to characterizing and understanding global climate change, including Earth's energy budget. A rich variety of geological evidence shows that temperature has changed throughout Earth's history. A variety of natural archives from around the planet, such as ocean and lake sediments, glacier ice and tree rings, shows that there were times in the past when the planet was cooler, and times when it was warmer. While our confidence in quantifying large-scale temperature changes generally decreases the farther back in time we look, scientists can still identify at least four major differences between the recent warming and those of the past.

It's warming almost everywhere. During decades and centuries of the past 2000 years, some regions warmed more than the global average while, at the same time, other regions cooled. For example, between the 10th and 13th centuries, the North Atlantic region warmed more than many other regions. In contrast, the pattern of recent surface warming is globally more uniform than for other decadal to centennial climate fluctuations over at least the past two millennia.

It's warming rapidly. Over the past 2 million years, Earth's climate has fluctuated between relatively warm interglacial periods and cooler glacial periods, when ice sheets grew over vast areas of the northern continents. Intervals of rapid warming coincided with the collapse of major ice sheets, heralding interglacial periods such as the present Holocene Epoch, which began about 12,000 years ago. During the shift from the last glacial period to the current interglacial, the total temperature increase was about 5°C. That change took about 5000 years, with a maximum warming rate of about 1.5°C per thousand years, although the transition was not smooth. In contrast, Earth's surface has warmed approximately 1.1°C since 1850–1900. However, even the best reconstruction of global surface temperature during the last deglacial period is too coarsely resolved for direct comparison with a period as short as the past 150 years. But for the past 2000 years, we have higher-resolution records that show that the rate of global warming during the last 50 years has exceeded the rate of any other 50-year period.

Recent warming reversed a long-term global cooling trend. Following the last major glacial period, global surface temperature peaked by around 6500 years ago, then slowly cooled. The long-term cooling trend was punctuated by warmer decades and centuries. These fluctuations were minor compared with the persistent and prominent warming that began in the mid-19th century when the millennial-scale cooling trend was reversed.

It's been a long time since it's been this warm. Averaged over the globe, surface temperatures of the past decade were probably warmer than when the long cooling trend began around 6500 years ago. If so, we need to look back to at least the previous interglacial period, around 125,000 years ago, to find evidence for multi-centennial global surface temperatures that were warmer than now.

Previous temperature fluctuations were caused by large-scale natural processes, while the current warming is largely due to human causes (see, for example, FAQ 1.3, FAQ 3.1). But understanding how and why temperatures have changed in the past is critical for understanding the current warming and how human and natural influences will interact to determine what happens in the future. Studying past climate changes also makes it clear that, unlike previous climate changes, the effects of recent warming are occurring on top of stresses that make humans and nature vulnerable to changes in ways that they have never before experienced (for example, see FAQ 11.2, FAQ12.3).

FAQ 2.1 (continued)

FAQ 2.1, Figure 1 | Evidence for the unusualness of recent warming.

Frequently Asked Questions

FAQ 2.2 | What Is the Evidence for Climate Change?

The evidence for climate change rests on more than just increasing surface temperatures. A broad range of indicators collectively leads to the inescapable conclusion that we are witnessing rapid changes to many aspects of our global climate. We are seeing changes in the atmosphere, ocean, cryosphere, and biosphere. Our scientific understanding depicts a coherent picture of a warming world.

We have long observed our changing climate. From the earliest scientists taking meteorological observations in the 16th and 17th centuries to the present, we have seen a revolution in our ability to observe and diagnose our changing climate. Today we can observe diverse aspects of our climate system from space, from aircraft and weather balloons, using a range of ground-based observing technologies, and using instruments that can measure to great depths in the ocean.

Observed changes in key indicators point to warming over land areas. Global surface temperature over land has increased since the late 19th century, and changes are apparent in a variety of societally relevant temperature extremes. Since the mid-1950s the troposphere (i.e., the lowest few km of the atmosphere) has warmed, and precipitation over land has increased. Near-surface specific humidity (i.e., water vapour) over land has increased since at least the 1970s. Aspects of atmospheric circulation have also evolved since the mid-20th century, including a poleward shift of mid-latitude storm tracks.

Changes in the global ocean point to warming as well. Global average sea surface temperature has increased since the late 19th century. The heat content of the global ocean has increased since the 19th century, with more than 90% of the excess energy accumulated in the climate system being stored in the ocean. This ocean warming has caused ocean waters to expand, which has contributed to the increase in global sea level in the past century. The relative acidity of the ocean has also increased since the early 20th century, caused by the uptake of carbon dioxide from the atmosphere, and oxygen loss is evident in the upper ocean since the 1970s.

Significant changes are also evident over the cryosphere – the portion of the Earth where water is seasonally or continuously frozen as snow or ice. There have been decreases in Arctic sea ice area and thickness and changes in Antarctic sea ice extent since the mid-1970s. Spring snow cover in the Northern Hemisphere has decreased since the late-1970s, along with an observed warming and thawing of permafrost (perennially frozen ground). The Greenland and Antarctic ice sheets are shrinking, as are the vast majority of glaciers worldwide, contributing strongly to the observed sea level rise.

Many aspects of the biosphere are also changing. Over the last century, long-term ecological surveys show that many land species have generally moved poleward and to higher elevations. There have been increases in green leaf area and/or mass (i.e., global greenness) since the early 1980s, and the length of the growing season has increased over much of the extratropical Northern Hemisphere since at least the mid-20th century. There is also strong evidence that various phenological metrics (such as the timing of fish migrations) for many marine species have changed in the last half century.

Change is apparent across many components of the climate system. It has been observed using a very broad range of techniques and analysed independently by numerous groups around the world. The changes are consistent in pointing to a climate system that has undergone rapid warming since the industrial revolution.

FAQ 2.2 (continued)

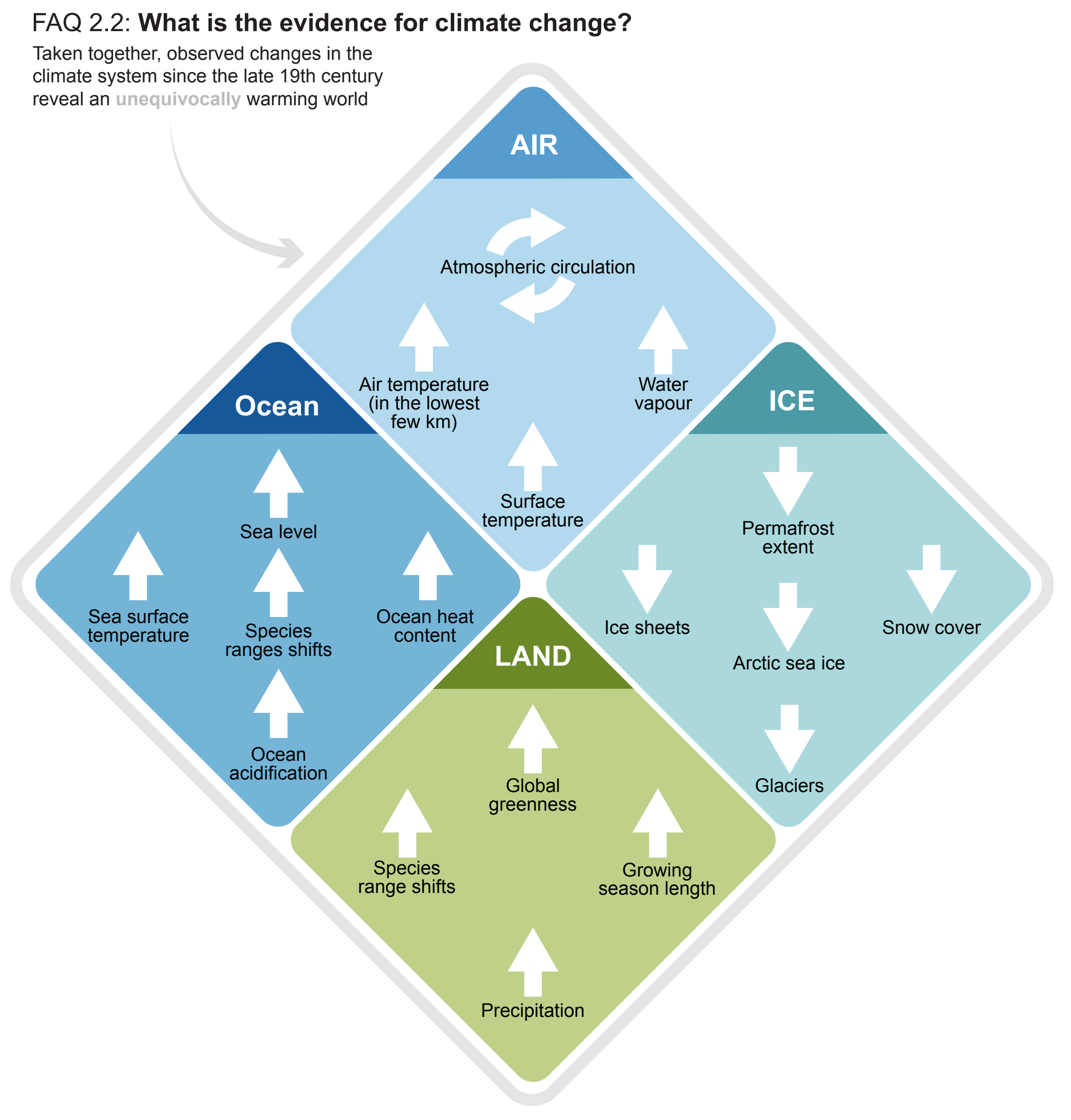

FAQ 2.2, Figure 1 | Synthesis of significant changes observed in the climate system over the past several decades. Upwards, downwards and circling arrows indicate increases, decreases and changes, respectively. Independent analyses of many components of the climate system that would be expected to change in a warming world exhibit trends consistent with warming. Note that this list is not comprehensive.

Frequently Asked Questions

FAQ 3.1 | How Do We Know Humans Are Responsible for Climate Change?

The dominant role of humans in driving recent climate change is clear. This conclusion is based on a synthesis of information from multiple lines of evidence, including direct observations of recent changes in Earth's climate; analyses of tree rings, ice cores, and other long-term records documenting how the climate has changed in the past; and computer simulations based on the fundamental physics that governs the climate system.

Climate is influenced by a range of factors. There are two main natural drivers of variations in climate on time scales of decades to centuries. The first is variations in the sun's activity, which alter the amount of incoming energy from the sun. The second is large volcanic eruptions, which increase the number of small particles (aerosols) in the upper atmosphere that reflect sunlight and cool the surface–an effect that can last for several years (see also FAQ 3.2). The main human drivers of climate change are increases in the atmospheric concentrations of greenhouse gases and of aerosols from burning fossil fuels, land use and other sources. The greenhouse gases trap infrared radiation near the surface, warming the climate. Aerosols, like those produced naturally by volcanoes, on average cool the climate by increasing the reflection of sunlight. Multiple lines of evidence demonstrate that human drivers are the main cause of recent climate change.

The current rates of increase of the concentration of the major greenhouse gases (carbon dioxide, methane and nitrous oxide) are unprecedented over at least the last 800,000 years. Several lines of evidence clearly show that these increases are the results of human activities. The basic physics underlying the warming effect of greenhouse gases on the climate has been understood for more than a century, and our current understanding has been used to develop the latest generation climate models (see FAQ 3.3). Like weather forecasting models, climate models represent the state of the atmosphere on a grid and simulate its evolution over time based on physical principles. They include a representation of the ocean, sea ice and the main processes important in driving climate and climate change.

Results consistently show that such climate models can only reproduce the observed warming (black line in FAQ 3.1, Figure 1) when including the effects of human activities (grey band in FAQ 3.1, Figure 1), in particular the increasing concentrations of greenhouse gases. These climate models show a dominant warming effect of greenhouse gas increases (red band, which shows the warming effects of greenhouse gases by themselves), which has been partly offset by the cooling effect of increases in atmospheric aerosols (blue band). By contrast, simulations that include only natural processes, including internal variability related to El Niño and other similar variations, as well as variations in the activity of the sun and emissions from large volcanoes (green band in FAQ 3.1, Figure 1), are not able to reproduce the observed warming. The fact that simulations including only natural processes show much smaller temperature increases indicates that natural processes alone cannot explain the strong rate of warming observed. The observed rate can only be reproduced when human influence is added to the simulations.

Moreover, the dominant effect of human activities is apparent not only in the warming of global surface temperature, but also in the pattern of warming in the lower atmosphere and cooling in the stratosphere, warming of the ocean, melting of sea ice, and many other observed changes. An additional line of evidence for the role of humans in driving climate change comes from comparing the rate of warming observed over recent decades with that which occurred prior to human influence on climate. Evidence from tree rings and other paleoclimate records shows that the rate of increase of global surface temperature observed over the past fifty years exceeded that which occurred in any previous 50-year period over the past 2000 years (see FAQ 2.1).

Taken together, this evidence shows that humans are the dominant cause of observed global warming over recent decades.

FAQ 3.1 (continued)

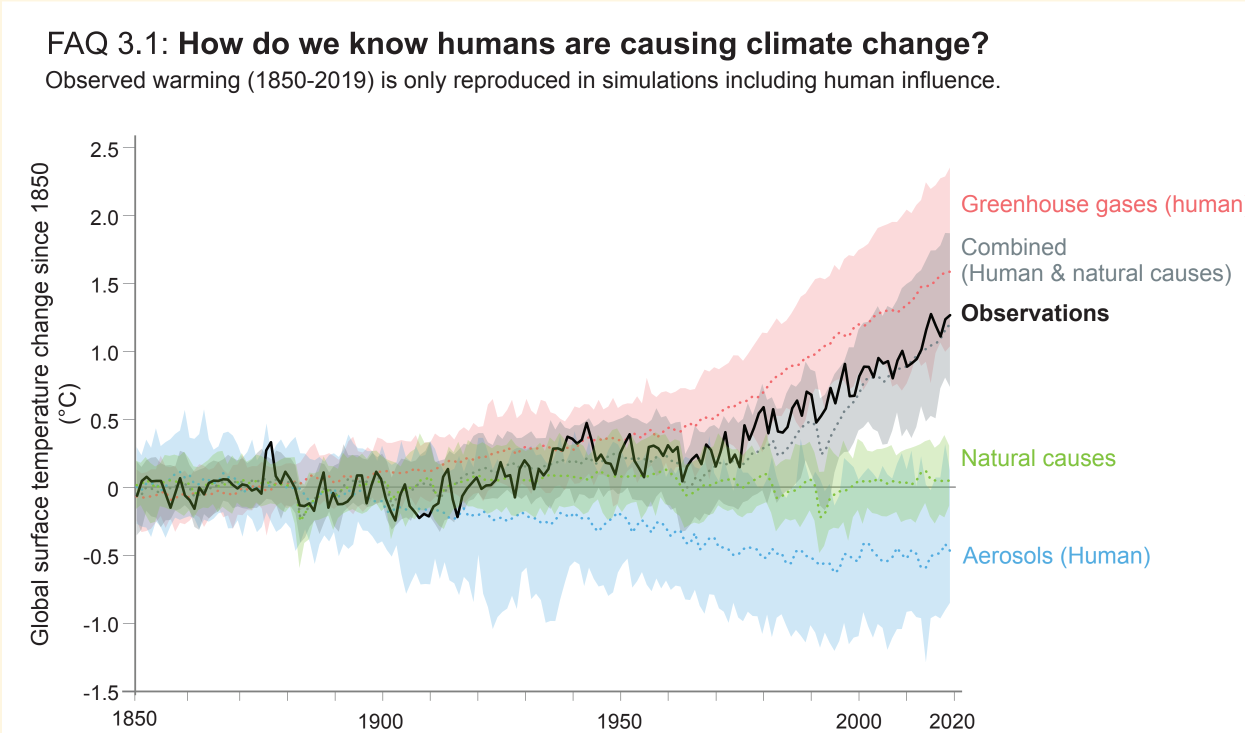

FAQ 3.1, Figure 1 | Observed warming (1850–2019) is only reproduced in simulations including human influence. Global surface temperature changes in observations, compared to climate model simulations of the response to all human and natural forcings (grey band), greenhouse gases only (red band), aerosols and other human drivers only (blue band) and natural forcings only (green band). Solid coloured lines show the multi-model mean, and coloured bands show the 5–95% range of individual simulations.

Frequently Asked Questions

FAQ 3.2 | What is Natural Variability and How Has it Influenced Recent Climate Changes?

Natural variability refers to variations in climate that are caused by processes other than human influence. It includes variability that is internally generated within the climate system and variability that is driven by natural external factors. Natural variability is a major cause of year-to-year changes in global surface climate and can play a prominent role in trends over multiple years or even decades. But the influence of natural variability is typically small when considering trends over periods of multiple decades or longer. When estimated over the entire historical period (1850–2020), the contribution of natural variability to global surface warming of –0.23°C to +0.23°C is small compared to the warming of about 1.1°C observed during the same period, which has been almost entirely attributed to the human influence.

Paleoclimatic records (indirect measurements of climate that can extend back many thousands of years) and climate models all show that global surface temperatures have changed significantly over a wide range of time scales in the past. One of these reasons is *natural variability*, which refers to variations in climate that are either *internally* generated within the climate system or *externally* driven by natural changes. Internal natural variability corresponds to a redistribution of energy within the climate system (for example via atmospheric circulation changes similar to those that drive the daily weather) and is most clearly observed as regional, rather than global, fluctuations in surface temperature. External natural variability can result from changes in the Earth's orbit, small variations in energy received from the sun, or from major volcanic eruptions. Although large orbital changes are related to global climate changes of the past, they operate on very long time scales (i.e., thousands of years). As such, they have displayed very little change over the past century and have had very little influence on temperature changes observed over that period. On the other hand, volcanic eruptions can strongly cool the Earth, but this effect is short-lived and their influence on surface temperatures typically fades within a decade of the eruption.

To understand how much of observed recent climate change has been caused by natural variability (a process referred to as attribution), scientists use climate model simulations. When only natural factors are used to force climate models, the resulting simulations show variations in climate on a wide range of time scales in response to volcanic eruptions, variations in solar activity, and internal natural variability. However, the influence of natural climate variability typically decreases as the time period gets longer, such that it only has mild effects on multi-decadal and longer trends (FAQ 3.2, Figure 1).

Consequently, over periods of a couple of decades or less, natural climate variability can dominate the human-induced surface warming trend – leading to periods with stronger or weaker warming, and sometimes even cooling (FAQ 3.2, Figure 1, left and centre). Over longer periods, however, the effect of natural variability is relatively small (FAQ 3.2, Figure 1, right). For instance, over the entire historical period (1850–2019), natural variability is estimated to have caused between –0.23°C and +0.23°C of the observed surface warming of about 1.1°C. This means that the bulk of the warming has been almost entirely attributed to human activities, particularly emissions of greenhouse gases (FAQ 3.1).

Another way to picture natural variability and human influence is to think of a person walking a dog. The path of the walker represents the human-induced warming, while their dog represents natural variability. Looking at global surface temperature changes over short periods is akin to focusing on the dog. The dog sometimes moves ahead of the owner and other times behind. This is similar to natural variability that can weaken or amplify warming on the short term. In both cases it is difficult to predict where the dog will be or how the climate will evolve in the near future. However, if we pull back and focus on the slow steady steps of the owner, the path of the dog is much clearer and more predictable, as it follows the path of its owner. Similarly, human influence on the climate is much clearer over longer time periods.

FAQ

FAQ 3.2 (continued)

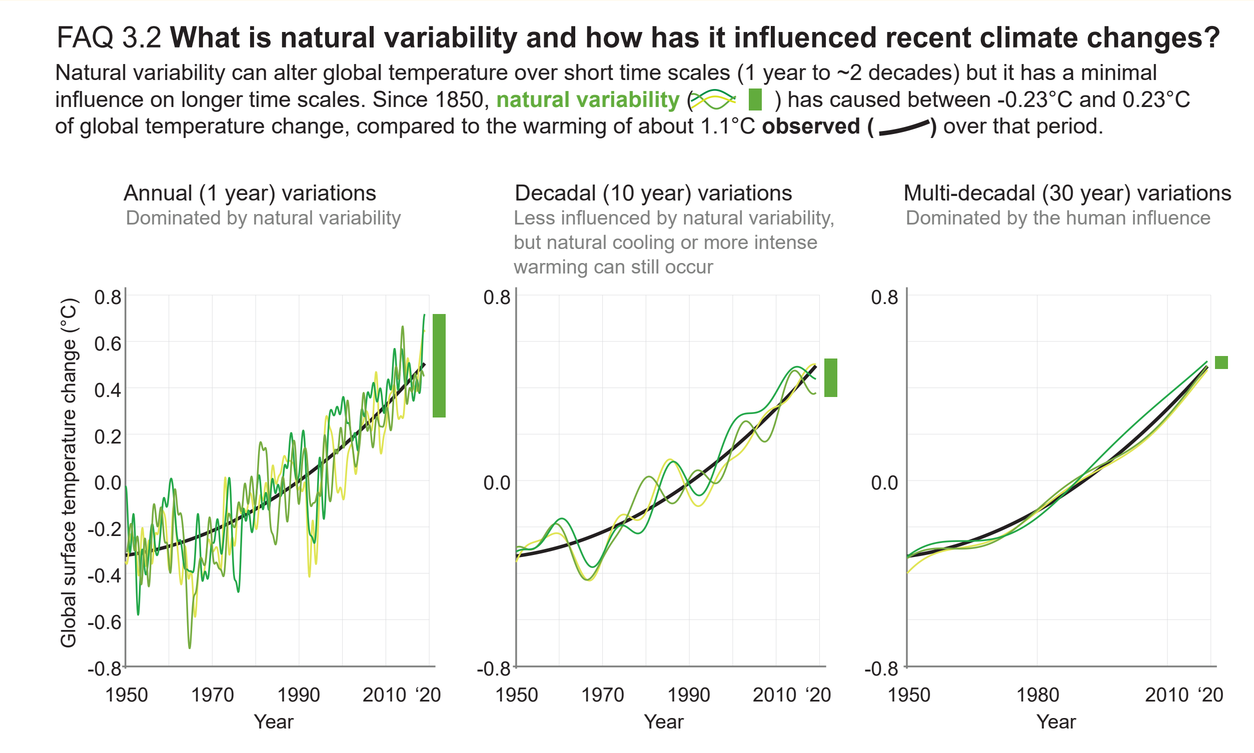

FAQ 3.2, Figure 1 | Annual (left), decadal (middle) and multi-decadal (right) variations in average global surface temperature. The thick black line is an estimate of the human contribution to temperature changes, based on climate models, whereas the green lines show the combined effect of natural variations and human-induced warming, different shadings of green represent different simulations, which can be viewed as showing a range of potential pasts. The influence of natural variability is shown by the green bars, and it decreases on longer time scales. The data is sourced from the CESM1 large ensemble.

Frequently Asked Questions

FAQ 3.3 | Are Climate Models Improving?

Yes, climate models have improved and continue to do so, becoming better at capturing complex and small-scale processes and at simulating present-day mean climate conditions. This improvement can be measured by comparing climate simulations against historical observations. Both the current and previous generations of models show that increases in greenhouse gases cause global warming. While past warming is well simulated by the new generation models as a group, some individual models simulate past warming that is either below or above what is observed. The information about how well models simulate past warming, as well as other insights from observations and theory, are used to refine this Report's projections of global warming.

Climate models are important tools for understanding past, present and future climate change. They are sophisticated computer programs that are based on fundamental laws of physics of the atmosphere, ocean, ice, and land. Climate models perform their calculations on a three-dimensional grid made of small bricks or 'gridcells' of about 100 km across. Processes that occur on scales smaller than the model grid cells (such as the transformation of cloud moisture into rain) are treated in a simplified way. This simplification is done differently in different models. Some models include more processes and complexity than others; some represent processes in finer detail (smaller grid cells) than others. Hence the simulated climate and climate change vary between models.

Climate modelling started in the 1950s and, over the years, models have become increasingly sophisticated as computing power, observations and our understanding of the climate system have advanced. The models used in the IPCC First Assessment Report published in 1990 correctly reproduced many aspects of climate (FAQ 1.1). The actual evolution of the climate since then has confirmed these early projections, when accounting for the differences between the simulated scenarios and actual emissions. Models continue to improve and get better and better at simulating the large variety of important processes that affect climate. For example, many models now simulate complex interactions between different aspects of the Earth system, such as the uptake of carbon dioxide by vegetation on land and by the ocean, and the interaction between clouds and air pollutants. While some models are becoming more comprehensive, others are striving to represent processes at higher resolution, for example to better represent the vortices and swirls in currents responsible for much of the transport of heat in the ocean.

Scientists evaluate the performance of climate models by comparing historical climate model simulations to observations. This evaluation includes comparison of large-scale averages as well as more detailed regional and seasonal variations. There are two important aspects to consider: (i) how models perform individually and (ii) how they perform as a group. The average of many models often compares better against observations than any individual model, since errors in representing detailed processes tend to cancel each other out in multi-model averages.

As an example, FAQ 3.3 Figure 1 compares simulations from the three most recent generations of models (available around 2008, 2013 and 2021) with observations of three climate variables. It shows the correlation between simulated and observed patterns, where a value of 1 represents perfect agreement. Many individual models of the new generation perform significantly better, as indicated by values closer to 1. As a group, each generation out-performs the previous generation: the multi-model average (shown by the longer lines) is progressively closer to 1. The vertical extent of the colored bars indicates the range of model performance across each group. The top of the bar moves up with each generation, indicating improved performance of the best performing models from one generation to the next. In the case of precipitation, the performance of the worst performing models is similar in the two most recent model generations, increasing the spread across models.

Developments in the latest generation of climate models, including new and better representation of physical, chemical and biological processes, as well as higher resolution, have improved the simulation of many aspects of the Earth system. These simulations, along with the evaluation of the ability of the models to simulate past warming as well as the updated assessment of the temperature response to a doubling of CO_2 in the atmosphere, are used to estimate the range of future global warming (FAQ 7.3).

FAQ 3.3 (continued)

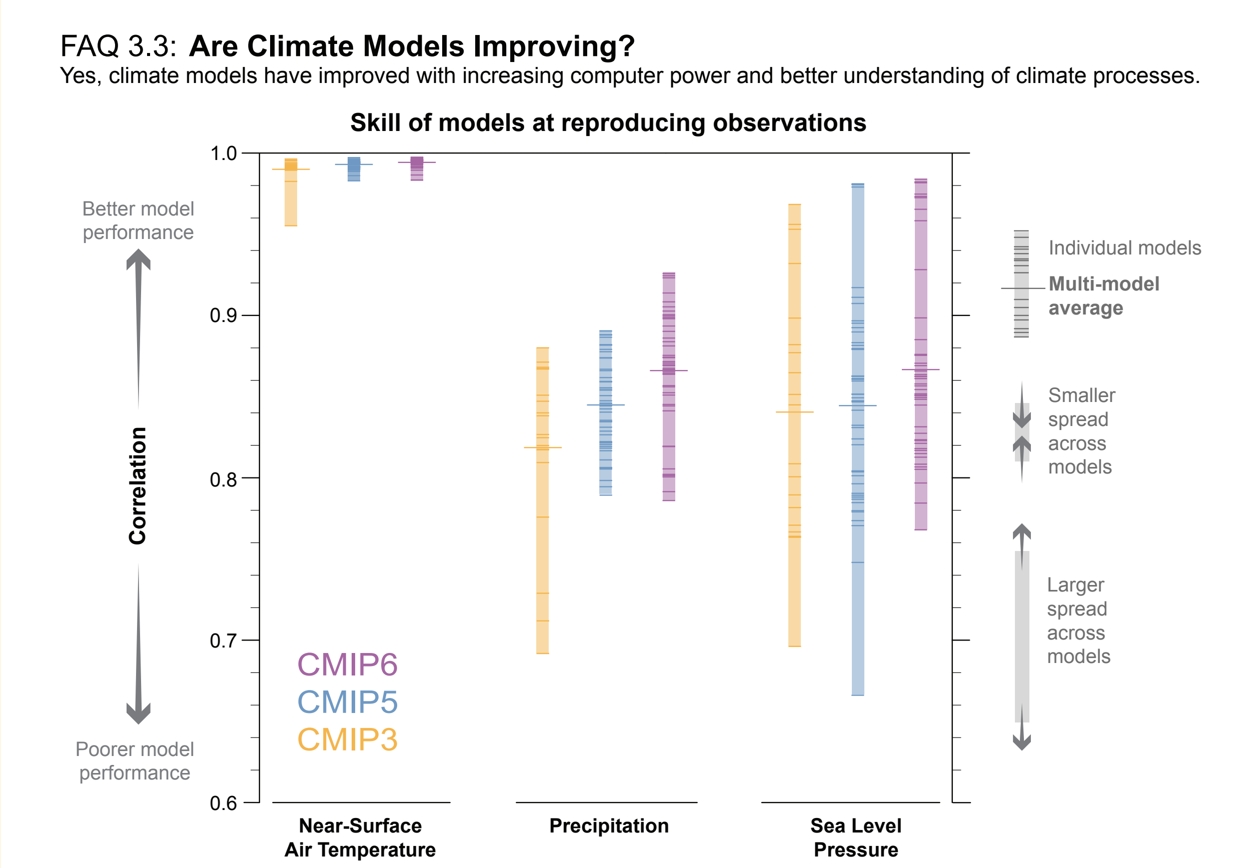

FAQ 3.3, Figure 1 | Pattern correlations between models and observations of three different variables: surface air temperature, precipitation and sea level pressure. Results are shown for the three most recent generations of models, from the Coupled Model Intercomparison Project (CMIP): CMIP3 (orange), CMIP5 (blue) and CMIP6 (purple). Individual model results are shown as short lines, along with the corresponding ensemble average (long line). For the correlations the yearly averages of the models are compared with the reference observations for the period 1980–1999, with 1 representing perfect similarity between the models and observations. CMIP3 simulations performed in 2004-2008 were assessed in the IPCC Fourth Assessment, CMIP5 simulations performed in 2011–2013 were assessed in the IPCC Fifth Assessment, and CMIP6 simulations performed in 2018–2021 are assessed in this Report.

Frequently Asked Questions

FAQ 4.1 | How Will the Climate Change Over the Next Twenty Years?

The parts of the climate system that have shown clear increasing or decreasing trends in recent decades will continue these trends for at least the next twenty years. Examples include changes in global surface temperature, Arctic sea ice cover, and global average sea level. However, over a period as short as twenty years, these trends are substantially influenced by natural climate variability, which can either amplify or attenuate the trend expected from the further increase in greenhouse gas concentrations.

Twenty years are a long time by human standards but a short time from a climate point of view. Emissions of greenhouse gases will continue over the next twenty years, as assumed in all the scenarios considered in this Report, albeit with varying rates. These emissions will further increase concentrations of greenhouse gases in the atmosphere (see FAQ 4.2), leading to continued trends in global surface warming and other parts of the climate system, including Arctic sea ice and global average sea level (see FAQ 9.2). FAQ 4.1, Figure 1 shows that both global surface temperature rise and the shrinking of sea ice in the Arctic will continue, with little difference between high- and low-emissions scenarios over the next 20 years (that is, between the red and blue lines).

However, these expected trends will be overlain by natural climate variability (see FAQ 3.2). First, a major volcanic eruption might occur, such as the 1991 eruption of Mt. Pinatubo on the Philippines; such an eruption might cause a global surface cooling of a few tenths of a degree Celsius lasting several years. Second, both atmosphere and ocean show variations that occur spontaneously, without any external influence. These variations range from localized weather systems to continent- and ocean-wide patterns and oscillations that change over months, years, or decades. Over a period of twenty years, natural climate variability strongly influences many climate quantities, when compared to the response to the increase in greenhouse gas concentrations from human activities. The effect of natural variability is illustrated by the very different trajectories that individual black, red or blue lines can take in FAQ 4.1, Figure 1. Whether natural variability would amplify or attenuate the human influence cannot generally be predicted out to twenty years into the future. Natural climate variability over the next twenty years thus constitutes an uncertainty that at best can be quantified accurately but that cannot be reduced.

Locally, the effect of natural variability would be much larger still. Simulations (not shown here) indicate that, locally, a cooling trend over the next twenty years cannot be ruled out, even under the high-emissions scenario – at a small number of locations on Earth, but these might lie anywhere. Globally, though, temperatures would rise under all scenarios.

In summary, while the direction of future change is clear for the two important climate quantities shown here – the global surface temperature and the Arctic sea ice area in September – the magnitude of the change is much less clear because of natural variability.

FAQ 4.1 (continued)

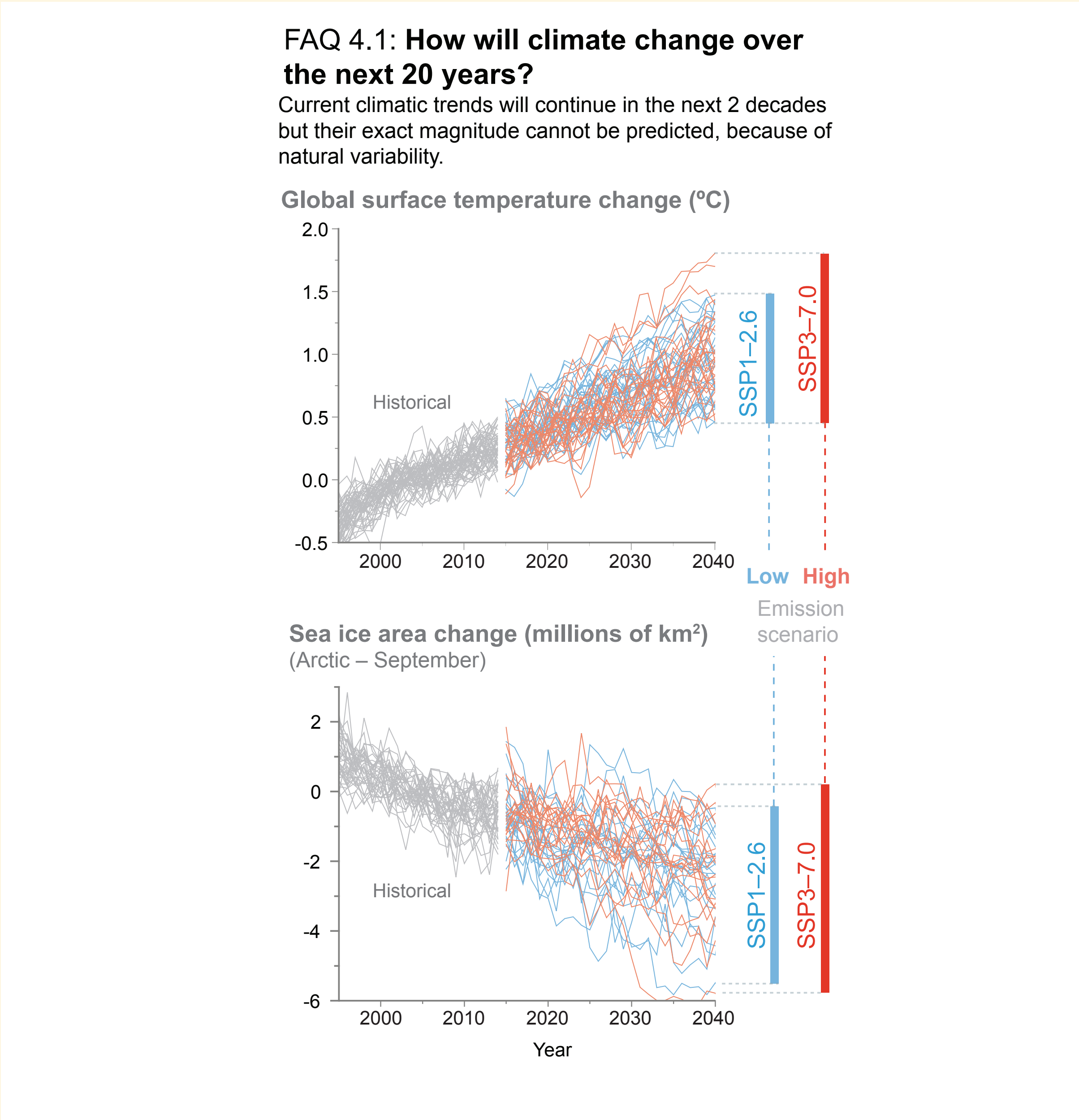

FAQ 4.1, Figure 1 | Simulations over the period 1995–2040, encompassing the recent past and the next twenty years, of two important indicators of global climate change. (Top) Global surface temperature, and **(bottom)**, the area of Arctic sea ice in September. Both quantities are shown as deviations from the average over the period 1995–2014. The grey curves are for the historical period ending in 2014; the blue curves represent a low-emissions scenario (SSP1-2.6) and the red curves one high-emissions scenario (SSP3-7.0).

Frequently Asked Questions

FAQ 4.2 | How Quickly Would We See the Effects of Reducing Carbon Dioxide Emissions?

The effects of substantial reductions in carbon dioxide emissions would not be apparent immediately, and the time required to detect the effects would depend on the scale and pace of emissions reductions. Under the lower-emissions scenarios considered in this Report, the increase in atmospheric carbon dioxide concentrations would slow visibly after about five to ten years, while the slowing down of global surface warming would be detectable after about twenty to thirty years. The effects on regional precipitation trends would only become apparent after several decades.

Reducing emissions of carbon dioxide (CO_2) – the most important greenhouse gas emitted by human activities – would slow down the rate of increase in atmospheric CO_2 concentration. However, concentrations would only begin to decrease when net emissions approach zero, that is, when most or all of the CO_2 emitted into the atmosphere each year is removed by natural and human processes (see FAQ 5.1 and FAQ 5.3). This delay between a peak in emissions and a decrease in concentration is a manifestation of the very long lifetime of CO_2 in the atmosphere; part of the CO_2 emitted by humans remains in the atmosphere for centuries to millennia.

Reducing the rate of increase in CO_2 concentration would slow down global surface warming within a decade. But this reduction in the rate of warming would initially be masked by natural climate variability and might not be detected for a few decades (see FAQ 1.2, FAQ 3.2 and FAQ 4.1). Detecting whether surface warming has indeed slowed down would thus be difficult in the years right after emissions reductions begin.

The time needed to detect the effect of emissions reductions is illustrated by comparing low- and high-emissions scenarios (FAQ 4.2, Figure 1). In the low-emissions scenario (SSP1-2.6), CO_2 emissions level off after 2015 and begin to fall in 2020, while they keep increasing throughout the 21st century in the high-emissions scenario (SSP3-7.0). The uncertainty arising from natural internal variability in the climate system is represented by simulating each scenario ten times with the same climate model but starting from slightly different initial states back in 1850 (thin lines). For each scenario, the differences between individual simulations are caused entirely by simulated natural internal variability. The average of all simulations represents the climate response expected for a given scenario. The climate history that would actually unfold under each scenario would consist of this expected response combined with the contribution from natural internal variability and the contribution from potential future volcanic eruptions (the latter effect is not represented here).

FAQ 4.2, Figure 1 shows that the atmospheric CO_2 concentrations differ noticeably between the two scenarios about five to ten years after the emissions have begun to diverge in year 2015. In contrast, the difference in global surface temperatures between the two scenarios does not become apparent until later – about two to three decades after the emissions histories have begun to diverge in this example. This time would be longer if emissions were reduced more slowly than in the low-emissions scenario illustrated here and shorter in the case of stronger reductions. Detection would take longer for regional quantities and for precipitation changes, which vary more strongly from natural causes. For instance, even in the low-emissions scenario, the effect of reduced CO_2 emissions would not become visible in regional precipitation until late in the 21st century.

In summary, it is only after a few decades of reducing CO_2 emissions that we would clearly see global temperatures starting to stabilize. By contrast, short-term reductions in CO_2 emissions, such as during the COVID-19 pandemic, do not have detectable effects on either CO_2 concentration or global temperature. Only sustained emissions reductions over decades would have a widespread effect across the climate system.

FAQ 4.2 (continued)

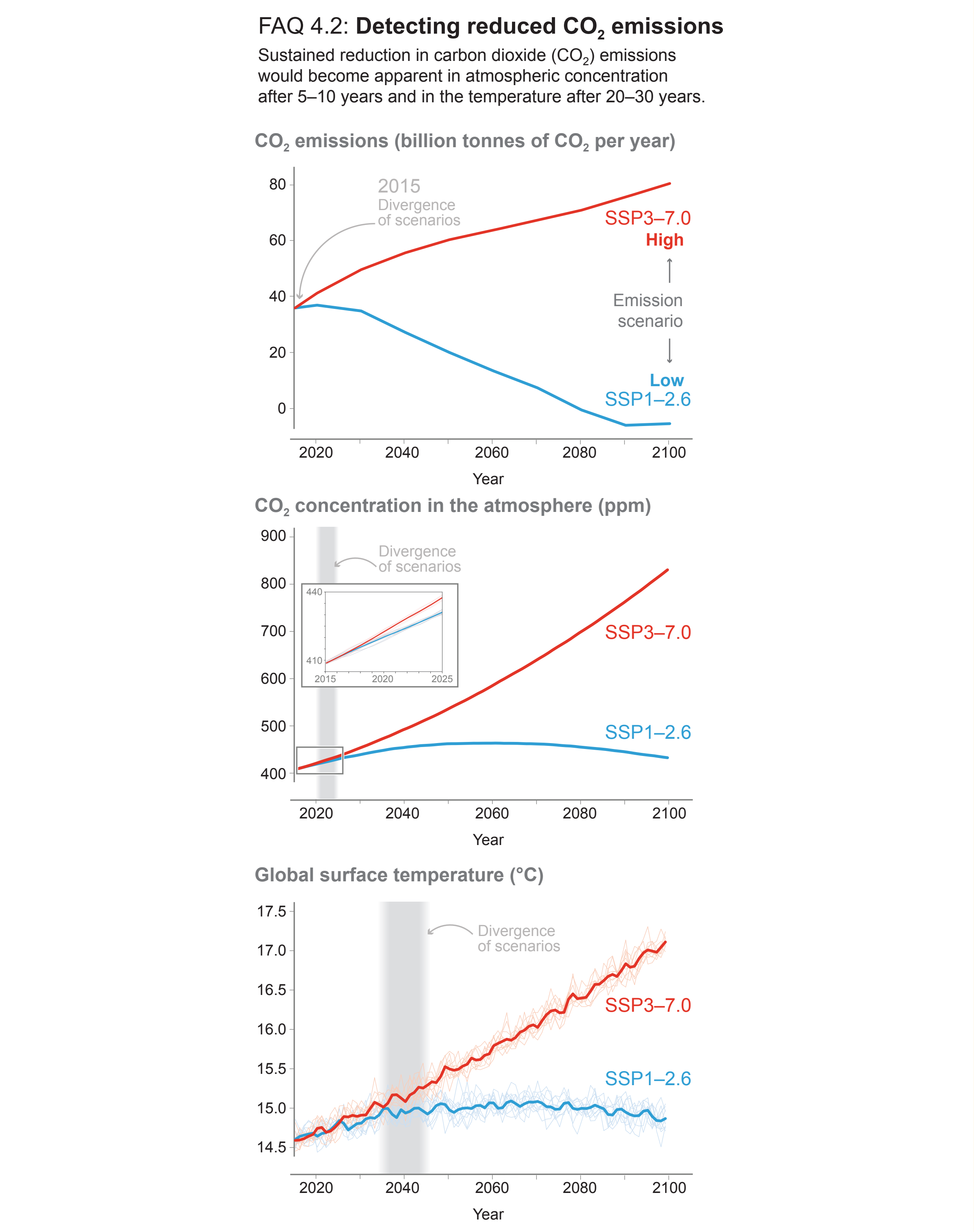

FAQ 4.2, Figure 1 | Observing the benefits of emissions reductions. (Top) Carbon dioxide (CO_2) emissions, **(middle)** CO_2 concentration in the atmosphere and **(bottom)** effect on global surface temperature for two scenarios: a low-emissions scenario (SSP1-2.6, blue) and a high-emissions scenario (SSP3-7.0). In the low-emissions scenario, CO_2 emissions begin to decrease in 2020 whereas they keep increasing throughout the 21st century in the high-emissions scenario. The thick lines are the average of the 10 individual simulations (thin line) for each scenario. Differences between individual simulations reflect natural variability.

FAQ

Frequently Asked Questions

FAQ 4.3 | At a Given Level of Global Warming, What Are the Spatial Patterns of Climate Change?

As the planet warms, climate change does not unfold uniformly across the globe, but some patterns of regional change show clear, direct and consistent relationships to increases in global surface temperature. The Arctic warms more than other regions, land areas warm more than the ocean surface, and the Northern Hemisphere more than the Southern Hemisphere. Precipitation increases over high latitudes, tropics and large parts of the monsoon regions, but decreases over the subtropics. For cases like these, we can infer the direction and magnitude of some regional changes – particularly temperature and precipitation changes – for any given level of global warming.

The intensity of climate change will depend on the level of global warming. It is possible to identify certain patterns of regional climate change that occur consistently, but increase in amplitude, across increasing levels of global warming. Such robust spatial patterns of climate change are largely independent of the specific scenario (and pathway in time) that results in a given level of global warming. That is, as long as different scenarios result in the same global warming level, irrespective of the time when this level is attained in each scenario, we can infer the patterns of regional change that would result from this warming. When patterns of changes are robust, regional consequences can be assessed for all levels of global warming, for all future time periods, and for all scenarios. Temperature and precipitation show such robust patterns of changes that are particularly striking.

The high latitudes of the Northern Hemisphere are projected to warm the most, by two to four times the level of global warming – a phenomenon referred to as Arctic amplification (FAQ 4.3, Figure 1, left). Several processes contribute to this high rate of warming, including increases in the absorption of solar radiation due to the loss of reflective sea ice and snow in a warmer world. In the Southern Hemisphere, Antarctica is projected to warm faster than the mid-latitude Southern Ocean, but the Southern Hemisphere high latitudes are projected to warm at a reduced amplitude compared to the level of global warming (FAQ 4.3, Figure 1, left). An important reason for the relatively slower warming of the Southern Hemisphere high latitudes is the upwelling of Antarctic deep waters that drives a large surface heat uptake in the Southern Ocean.

The warming is generally stronger over land than over the ocean, and in the Northern Hemisphere compared to the Southern Hemisphere, and with less warming over the central subpolar North Atlantic and the southernmost Pacific. The differences are the result of several factors, including differences in how land and ocean areas absorb and retain heat, the fact that there is more land area in the Northern Hemisphere than in the Southern Hemisphere, and the influence of ocean circulation. In the Southern Hemisphere, robust patterns of relatively high warming are projected for subtropical South America, southern Africa, and Australia. The relatively strong warming in subtropical southern Africa arises from strong interactions between soil moisture and temperature and from increased solar radiation as a consequence of enhanced subsidence.

Precipitation changes are also proportional to the level of global warming (FAQ 4.3, Figure 1, right), although uncertainties are larger than for the temperature change. In the high latitudes of both the Southern and Northern Hemispheres, increases in precipitation are expected as the planet continues to warm, with larger changes expected at higher levels of global warming (FAQ 4.3, Figure 1, right). The same holds true for the projected precipitation increases over the tropics and large parts of the monsoon regions. General drying is expected over the subtropical regions, particularly over the Mediterranean, southern Africa and parts of Australia, South America, and south-west North America, as well as over the subtropical Atlantic and parts of the subtropical Indian and Pacific Oceans. Increases in precipitation over the tropics and decreases over the subtropics amplify with higher levels of global warming.

Some regions that are already dry and warm, such as southern Africa and the Mediterranean, are expected to become progressively drier and drastically warmer at higher levels of global warming.

In summary, climate change will not affect all the parts of the globe evenly. Rather, distinct regional patterns of temperature and precipitation change can be identified, and these changes are projected to amplify as the level of global warming increases.

FAQ 4.3 (continued)

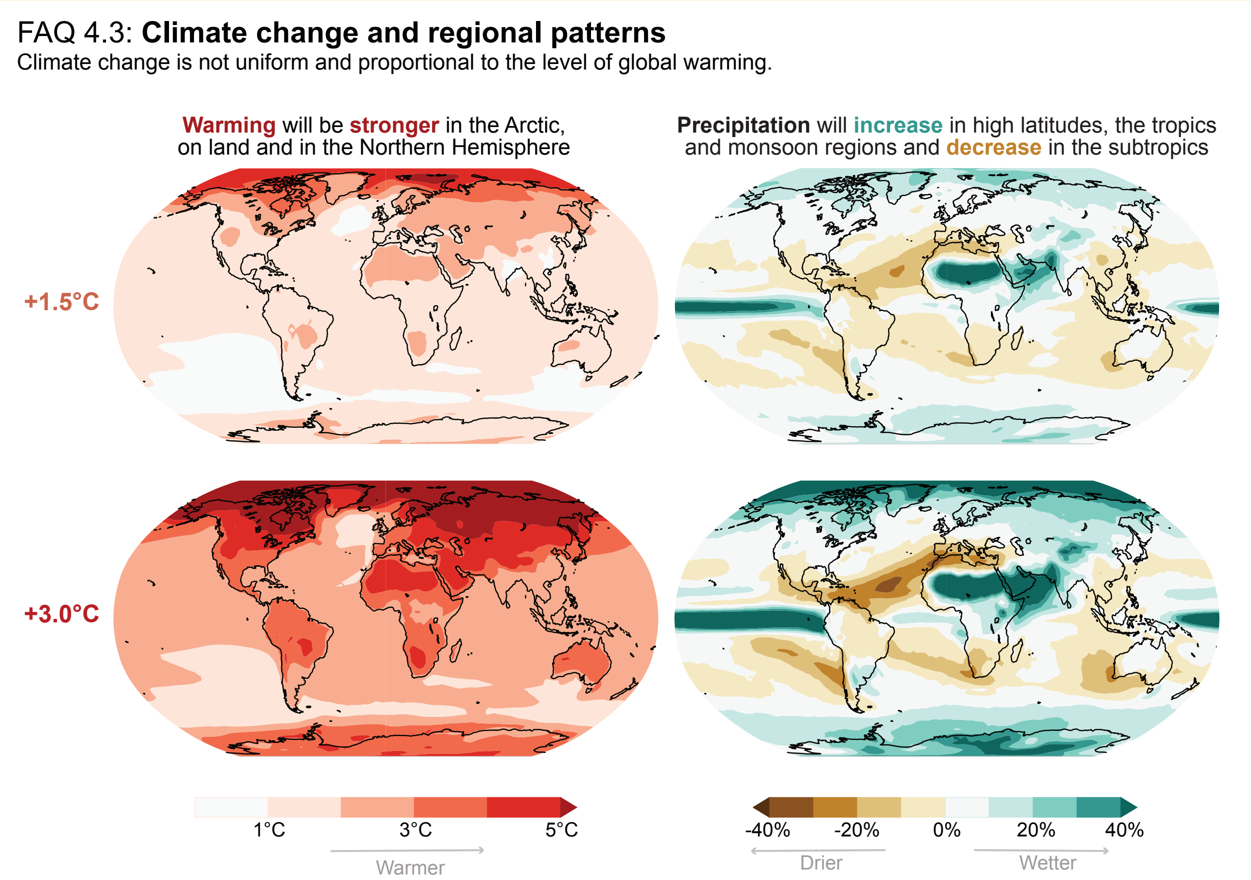

FAQ 4.3, Figure 1 | Regional changes in temperature (left) and precipitation (right) are proportional to the level of global warming, irrespective of the scenario through which the level of global warming is reached. Surface warming and precipitation change are shown relative to the 1850–1900 climate, and for time periods over which the globally averaged surface warming is 1.5°C **(top)** and 3°C **(bottom)**, respectively. Changes presented here are based on 31 CMIP6 models using the high-emissions scenario SSP3-7.0.

FAQ

Frequently Asked Questions

FAQ 5.1 | Is the Natural Removal of Carbon From the Atmosphere Weakening?

For decades, about half of the carbon dioxide (CO_2) that human activities have emitted to the atmosphere has been taken up by natural carbon sinks in vegetation, soils and oceans. These natural sinks of CO_2 have thus roughly halved the rate at which atmospheric CO_2 concentrations have increased, and therefore slowed down global warming. However, observations show that the processes underlying this uptake are beginning to respond to increasing CO_2 in the atmosphere and climate change in a way that will weaken nature's capacity to take up CO_2 in the future. Understanding of the magnitude of this change is essential for projecting how the climate system will respond to future emissions and emissions reduction efforts.

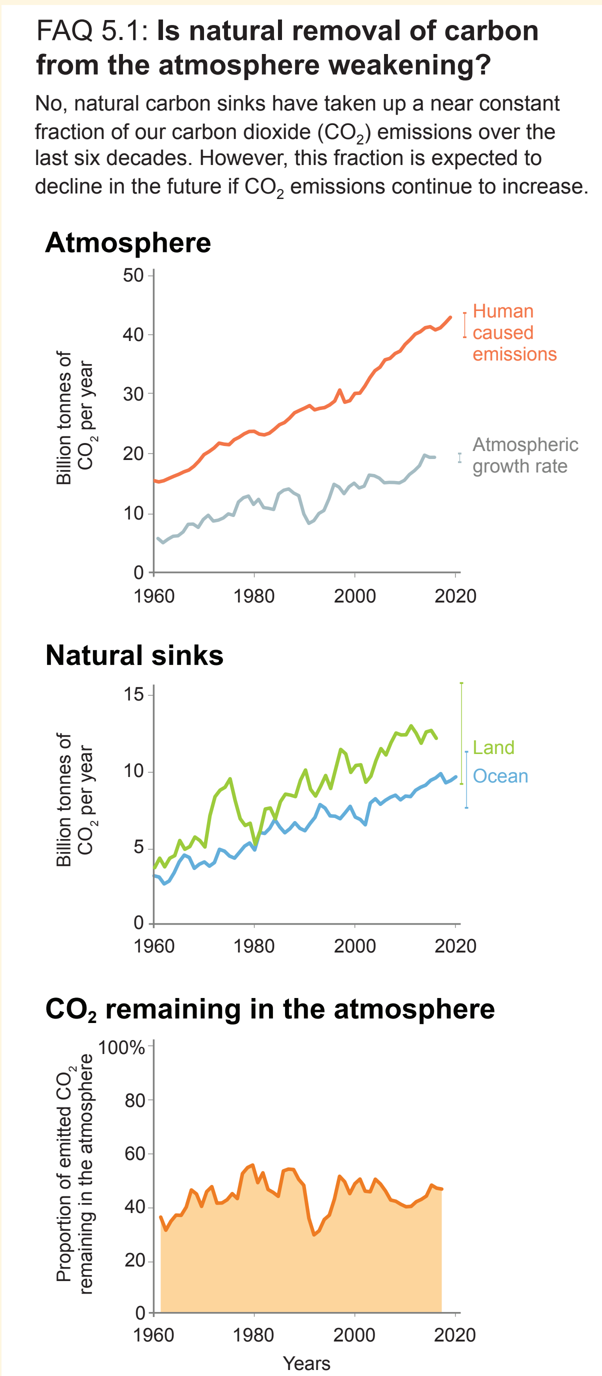

Direct observations of CO_2 concentrations in the atmosphere, which began in 1958, show that the atmosphere has only retained roughly half of the CO_2 emitted by human activities, due to the combustion of fossil fuels and land-use change such as deforestation (FAQ 5.1, Figure 1). Natural carbon cycle processes on land and in the oceans have taken up the remainder of these emissions. These land and ocean removals or 'sinks' have grown largely in proportion to the increase in CO_2 emissions, taking up 31% (land) and 23% (ocean) of the emissions in 2010–2019, respectively (FAQ 5.1, Figure 1). Therefore, the average proportion of yearly CO_2 emissions staying in the atmosphere has remained roughly stable at 44% over the last six decades, despite continuously increasing CO_2 emissions from human activities.

On land, it is mainly the vegetation that captures CO_2 from the atmosphere through *plant photosynthesis*, which ultimately accumulates both in vegetation and soils. As more CO_2 accumulates in the atmosphere, plant carbon capture increases through the *CO_2 fertilization effect* in regions where plant growth is not limited by, for instance, nutrient availability. Climate change affects the processes responsible for the uptake and release of CO_2 on land in multiple ways. Land CO_2 uptake is generally increased by longer growing seasons due to global warming in cold regions and by nitrogen deposition in nitrogen-limited regions. Respiration by plants and soil organisms, natural disturbances such as fires, and human activities such as deforestation all release CO_2 back into the atmosphere. The combined effect of climate change on these processes is to weaken the future land sink. In particular, extreme temperatures and droughts as well as permafrost thaw (see FAQ 5.2) tend to reduce the land sink regionally. In the ocean,

FAQ 5.1, Figure 1 | Atmospheric carbon dioxide (CO_2) and natural carbon sinks. (Top) Global emissions of CO_2 from human activities and the growth rate of CO_2 in the atmosphere; **(middle)** the net land and ocean CO_2 removal (natural sinks); and **(bottom)** the fraction of CO_2 emitted by human activities remaining in atmosphere from 1960 to 2019. Lines are the five years running mean, error bars denote the uncertainty of the mean estimate. See Table 5.SM.6 for more information on the data underlying this figure.

FAQ 5.1 (continued)

several factors control how much CO_2 is captured: the difference in CO_2 partial pressure between the atmosphere and the surface ocean; wind speeds at the ocean surface; the chemical composition of seawater (that is, its *buffering capacity*), which affects how much CO_2 can be taken up; and the use of CO_2 in photosynthesis by seawater microalgae. The CO_2-enriched surface ocean water is transported to the deep ocean in specific zones around the globe (such as the Northern Atlantic and the Southern Ocean), effectively storing the CO_2 away from the atmosphere for many decades to centuries. The combined effect of warmer surface ocean temperatures on these processes is to weaken the future ocean CO_2 sink.

The ocean carbon sink is better quantified than the land sink, thanks to direct ocean and atmospheric carbon observations. The land carbon sink is more challenging to monitor globally, because it varies widely, even regionally. There is currently no direct evidence that the natural sinks are slowing down, because observable changes in the fraction of human emissions stored on land or in oceans are small compared to year-to-year and decadal variations of these sinks. Nevertheless, it is becoming more obvious that atmospheric and climate changes are affecting the processes controlling the land and ocean sinks.

Since the land and ocean sinks respond to the rise in atmospheric CO_2 and to human-induced global warming, the absolute amount of CO_2 taken up by land and ocean will be affected by future CO_2 emissions. This also implies that, if countries manage to strongly reduce global CO_2 emissions, or even remove CO_2 from the atmosphere, these sinks will take up less CO_2 because of the reduced human perturbation of the carbon cycle. Under future high-warming scenarios, it is expected that the global ocean and land sinks will stop growing in the second half of the century as climate change increasingly affects them. Thus, the total amount of CO_2 emitted to the atmosphere and the responses of the natural CO_2 sinks will both determine what efforts are required to limit global warming to a certain level (see FAQ 5.4), underscoring how important it is to understand the evolution of these natural CO_2 sinks.

FAQ 5.2 | Can Thawing Permafrost Substantially Increase Global Warming?

In the Arctic, large amounts of organic carbon are stored in permafrost – ground that remains frozen throughout the year. If significant areas of permafrost thaw as the climate warms, some of that carbon may be released into the atmosphere in the form of carbon dioxide or methane, resulting in additional warming. Projections from models of permafrost ecosystems suggest that future permafrost thaw will lead to some additional warming – enough to be important, but not enough to lead to a 'runaway warming' situation, where permafrost thaw leads to a dramatic, self-reinforcing acceleration of global warming.

The Arctic is the biggest climate-sensitive carbon pool on Earth, storing twice as much carbon in its frozen soils, or *permafrost*, than is currently stored in the atmosphere. As the Arctic region warms faster than anywhere else on Earth, there are concerns that this warming could release greenhouse gases to the atmosphere and therefore significantly amplify climate change.

The carbon in the permafrost has built up over thousands of years, as dead plants have been buried and accumulated within layers of frozen soil, where the cold prevents the organic material from decomposing. As the Arctic warms and soils thaw, the organic matter in these soils begins to decompose rapidly and return to the atmosphere as either carbon dioxide or methane, which are both important greenhouse gases. Permafrost can also thaw abruptly in a given place, due to melting ice in the ground reshaping Arctic landscapes, lakes growing and draining, and fires burning away insulating surface soil layers. Thawing of permafrost carbon has already been observed in the Arctic, and climate models project that much of the shallow permafrost (<3 m depth) throughout the Arctic would thaw under moderate to high amounts of global warming (2°C–4°C).

While permafrost processes are complex, they are beginning to be included in models that represent the interactions between the climate and the carbon cycle. The projections from these permafrost carbon models show a wide range in the estimated strength of a carbon–climate vicious circle, from both carbon dioxide and methane, equivalent to 14–175 billion tonnes of carbon dioxide released per 1°C of global warming. By comparison, in 2019, human activities have released about 40 billion tonnes of carbon dioxide into the atmosphere. This has two implications. First, the extra warming caused by permafrost thawing is strong enough that it must be considered when estimating the total amount of remaining emissions permitted to stabilize the climate at a given level of global warming (i.e., the remaining carbon budget, see FAQ 5.4). Second, the models do not identify any one amount of warming at which permafrost thaw becomes a 'tipping point' or threshold in the climate system that would lead to a runaway global warming. However, models do project that emissions would continuously increase with warming, and that this trend could last for hundreds of years.

Permafrost can also be found in other cold places (e.g., mountain ranges), but those places contain much less carbon than in the Arctic. For instance, the Tibetan plateau contains about 3% as much carbon as is stored in the Arctic. There is also concern about carbon frozen in shallow ocean sediments. These deposits are known as *methane hydrates* or *clathrates*, which are methane molecules locked within a cage of ice molecules. They formed as frozen soils that were flooded when sea levels rose after the last ice age. If these hydrates thaw, they may release methane that can bubble up to the surface. The total amount of carbon in permafrost-associated methane hydrates is much less than the carbon in permafrost soils. Global warming takes millennia to penetrate into the sediments beneath the ocean, which is why these hydrates are still responding to the last deglaciation. As a result, only a small fraction of the existing hydrates could be destabilised during the coming century. Even when methane is released from hydrates, most of it is expected to be consumed and oxidised into carbon dioxide in the ocean before reaching the atmosphere. The most complete modelling of these processes to date suggests a release to the atmosphere at a rate of less than 2% of current human-induced methane emissions.

Overall, thawing permafrost in the Arctic appears to be an important additional source of heat-trapping gases to the atmosphere, more so than undersea hydrates. Climate and carbon cycle models are beginning to consider permafrost processes. While these models disagree on the exact amount of the heat-trapping gases that will be released into the atmosphere, they agree that: (i) the amount of such gases released from permafrost will increase with the amount of global warming; and (ii) the warming effect of thawing permafrost is significant enough to be considered in estimates of the remaining carbon budgets for limiting future warming.

FAQ 5.2 (continued)

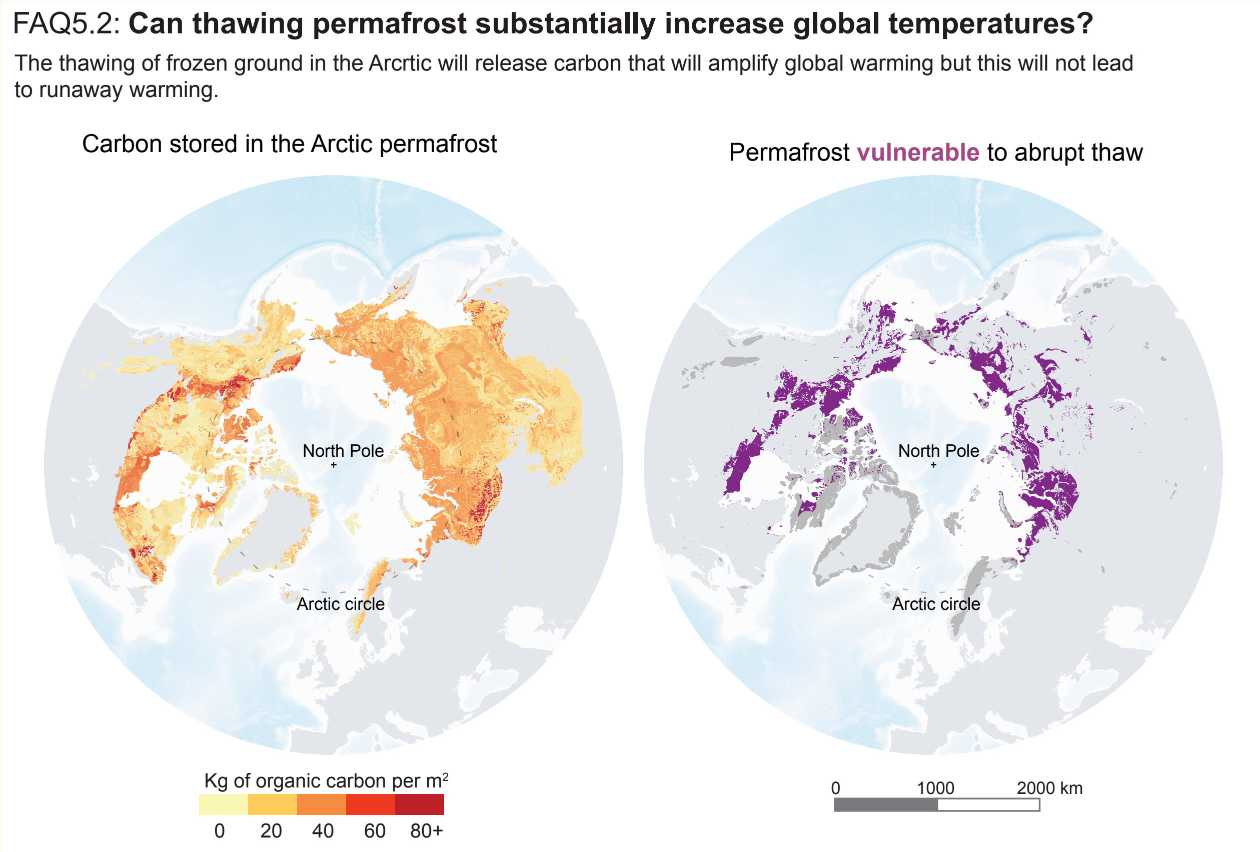

FAQ 5.2, Figure 1 | The Arctic permafrost is a big pool of carbon that is sensitive to climate change. (Left) Quantity of carbon stored in the permafrost, to 3 m depth (NCSCDv2 dataset) and **(right)** area of permafrost vulnerable to abrupt thaw (Circumpolar Thermokarst Landscapes dataset).

Frequently Asked Questions

FAQ 5.3 | Could Climate Change Be Reversed By Removing Carbon Dioxide From the Atmosphere?

Deliberate removal of carbon dioxide (CO_2) from the atmosphere could reverse (i.e., change the direction of) some aspects of climate change. However, this will only happen if it results in a net reduction in the total amount of CO_2 in the atmosphere, that is, if deliberate removals are larger than emissions. Some climate change trends, such as the increase in global surface temperature, would start to reverse within a few years. Other aspects of climate change would take decades (e.g., permafrost thawing) or centuries (e.g., acidification of the deep ocean) to reverse, and some, such as sea level rise, would take centuries to millennia to change direction.

The term *negative carbon dioxide (CO_2) emissions* refers to the removal of CO_2 from the atmosphere by deliberate human activities, in addition to removals that occur naturally, and is often used as synonymous with *carbon dioxide removal*. Negative CO_2 emissions can compensate for the release of CO_2 into the atmosphere by human activities. They could be achieved by strengthening natural CO_2 sequestration processes on land (e.g., by planting trees or through agricultural practices that increase the carbon content of soils) and/or in the ocean (e.g., by restoration of coastal ecosystems) or by removing CO_2 directly from the atmosphere. If CO_2 removals are greater than human-caused CO_2 emissions globally, emissions are said to be *net negative*. It should be noted that CO_2 removal technologies are unable, or not yet ready, to achieve the scale of removal that would be required to compensate for current levels of emissions, and most have undesired side effects.

In the absence of deliberate CO_2 removal, the CO_2 concentration in the atmosphere (a measure of the amount of CO_2 in the atmosphere) results from a balance between human-caused CO_2 release and the removal of CO_2 by natural processes on land and in the ocean (natural 'carbon sinks'; see FAQ 5.1). If CO_2 release exceeds removal by carbon sinks, the CO_2 concentration in the atmosphere would increase;

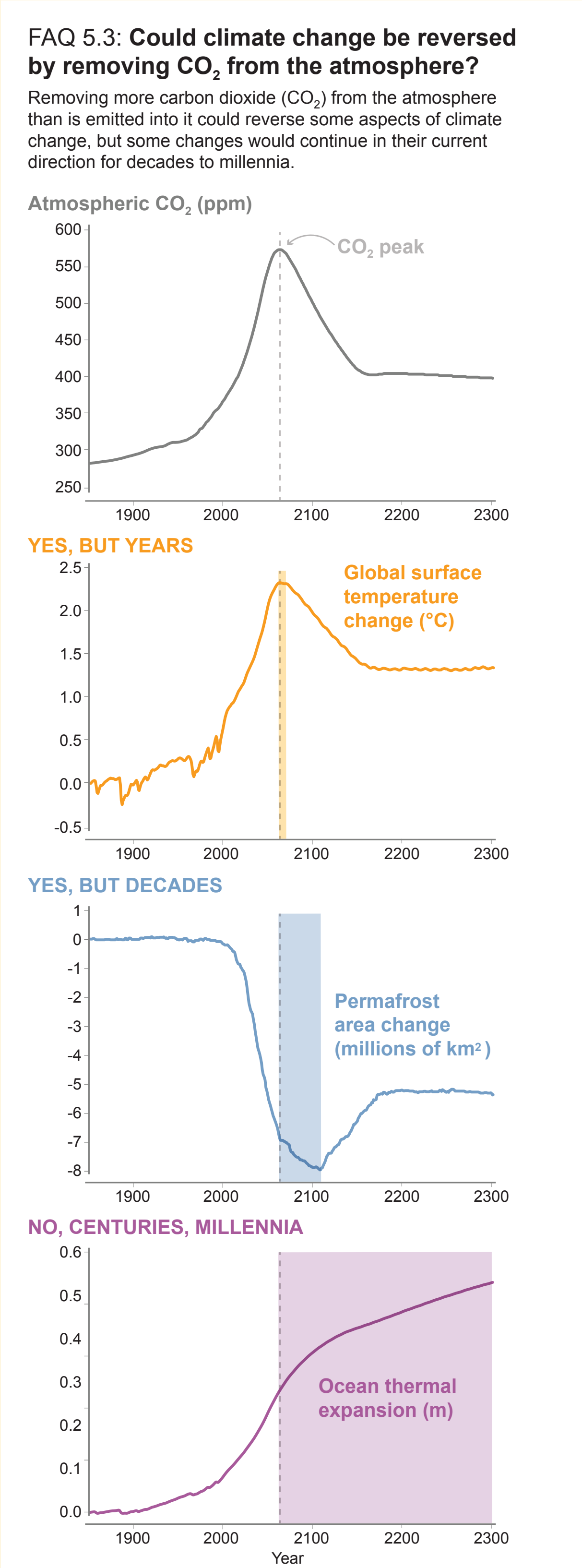

FAQ 5.3, Figure 1 | Changes in aspects of climate change in response to a peak and decline in the atmospheric CO_2 concentration (top panel). The vertical grey dashed line indicates the time of peak CO_2 concentration in all panels. It shows that the reversal of global surface warming lags the decrease in the atmospheric CO_2 concentration by a few years, the reversal of permafrost area decline lags the decrease in atmospheric CO_2 by decades, and ocean thermal expansion continues for several centuries. The quantitative information in the figure (i.e., numbers on vertical axes) is not to be emphasized as it results from simulations with just one model and will be different for other models. The qualitative behaviour, however, can be expected to be largely model independent.

FAQ

FAQ 5.3 (continued)

if CO_2 release equals removal, the atmospheric CO_2 concentration would stabilize; and if CO_2 removal exceeds release, the CO_2 concentration would decline. This applies in the same way to *net* CO_2 emissions – that is, the sum of human-caused releases and deliberate removals.

If the CO_2 concentration in the atmosphere starts to go down, the Earth's climate would respond to this change (FAQ 5.3, Figure 1). Some parts of the climate system take time to react to a change in CO_2 concentration, so a decline in atmospheric CO_2 as a result of net negative emissions would not lead to immediate reversal of all climate change trends. Recent studies have shown that global surface temperature starts to decline within a few years following a decline in atmospheric CO_2, although the decline would not be detectable for decades due to natural climate variability (see FAQ 4.2). Other consequences of human-induced climate change, such as reduction in permafrost area, would take decades; yet others, such as warming, acidification and oxygen loss of the deep ocean, would take centuries to reverse following a decline in the atmospheric CO_2 concentration. Sea level would continue to rise for many centuries to millennia, even if large deliberate CO_2 removals were successfully implemented.

'Overshoot' scenarios are a class of future scenarios that are receiving increasing attention, particularly in the context of ambitious climate goals, such as the global warming limits of 1.5°C or 2°C included in the Paris Agreement. In these scenarios, a slow rate of reduction in emissions in the near term is compensated by net negative CO_2 emissions in the later part of this century, which results in a temporary breach or 'overshoot' of a given warming level. Due to the delayed reaction of several climate system components, it follows that the temporary overshoot would result in additional climate changes compared to a scenario that reaches the goal without overshoot. These changes would take decades to many centuries to reverse, with the reversal taking longer for scenarios with larger overshoot.

Removing more CO_2 from the atmosphere than is emitted into it would indeed begin to reverse some aspects of climate change, but some changes would still continue in their current direction for decades to millennia. Approaches capable of large-scale removal of CO_2 are still in the state of research and development or unproven at the scales of deployment necessary to achieve a net reduction in atmospheric CO_2 levels. CO_2 removal approaches, particularly those deployed on land, can have undesired side effects on water, food production and biodiversity.

Frequently Asked Questions

FAQ 5.4 | What Are Carbon Budgets?

There are several types of carbon budgets. Most often, the term refers to the total net amount of carbon dioxide (CO_2) that can still be emitted by human activities while limiting global warming to a specified level (e.g., 1.5°C or 2°C above pre-industrial levels). This is referred to as the 'remaining carbon budget'. Several choices and value judgements have to be made before it can be unambiguously estimated. When the remaining carbon budget is combined with all past CO_2 emissions to date, a 'total carbon budget' compatible with a specific global warming limit can also be defined. A third type of carbon budget is the 'historical carbon budget', which is a scientific way to describe all past and present sources and sinks of CO_2.

The term *remaining carbon budget* is used to describe the total net amount of CO_2 that human activities can still release into the atmosphere while keeping global warming to a specified level, like 1.5°C or 2°C relative to pre-industrial temperatures. Emissions of CO_2 from human activities are the main cause of global warming. A remaining carbon budget can be defined because of the specific way CO_2 behaves in the Earth system. That is, global warming is roughly linearly proportional to the total net amount of CO_2 emissions that are released into the atmosphere by human activities – also referred to as cumulative anthropogenic CO_2 emissions. Other greenhouse gases behave differently and have to be accounted for separately.

The concept of a remaining carbon budget implies that, to stabilize global warming at any particular level, global emissions of CO_2 need to be reduced to net zero levels at some point. 'Net zero CO_2 emissions' describes a situation where all the anthropogenic emissions of CO_2 are counterbalanced by deliberate anthropogenic removals so that, on average, no CO_2 is added or removed from the atmosphere by human activities. Atmospheric CO_2 concentrations in such a situation would gradually decline to a long-term stable level as excess CO_2 in the atmosphere is taken up by ocean and land sinks (see FAQ 5.1). The concept of a remaining carbon budget also means that, if CO_2 emissions reductions are delayed, deeper and faster reductions are needed later to stay within the same budget. If the remaining carbon budget is exceeded, this will result in either higher global warming or a need to actively remove CO_2 from the atmosphere to reduce global temperatures back down to the desired level (see FAQ 5.3).

Estimating the size of remaining carbon budgets depends on a set of choices. These choices include: (1) the global warming level that is chosen as a limit (for example, 1.5°C or 2°C relative to pre-industrial levels); (2) the probability with which we want to ensure that warming is held below that limit (for example, a one-in-two, two-in-three, or higher chance), and (3) how successful we are in limiting emissions of other greenhouse gases that affect the climate, such as methane or nitrous oxide. These choices can be informed by science, but ultimately represent subjective choices. Once these choices have been made, to estimate the remaining carbon budget for a given temperature goal, we can combine knowledge about: how much our planet has warmed already; the amount of warming per cumulative tonne of CO_2; and the amount of warming that is still expected once global net CO_2 emissions are brought down to zero. For example, to limit global warming to 1.5°C above pre-industrial levels with either a one-in-two (50%) or two-in-three (67%) chance, the remaining carbon budgets amount to 500 and 400 billion tonnes of CO_2, respectively, from 1 January 2020 onward (FAQ 5.4, Figure 1). Currently, human activities are emitting around 40 billion tonnes of CO_2 into the atmosphere in a single year.

The remaining carbon budget depends on how much the world has already warmed to date. This past warming is caused by historical emissions, which are estimated by looking at the *historical carbon budget* – a scientific way to describe all past and present sources and sinks of CO_2. It describes how the CO_2 emissions from human activities have redistributed across the various CO_2 reservoirs of the Earth system. These reservoirs are the ocean, the land vegetation, and the atmosphere (into which CO_2 was emitted). The share of CO_2 that is not taken up by the ocean or the land, and that thus increases the concentration of CO_2 in the atmosphere, causes global warming. The historical carbon budget tells us that, of the about 2560 billion tonnes of CO_2 that were released into the atmosphere by human activities between the years 1750 and 2019, about a quarter were absorbed by the ocean (causing ocean acidification) and about a third by the land vegetation. About 45% of these emissions remain in the atmosphere (see FAQ 5.1). Adding these historical CO_2 emissions to estimates of remaining carbon budgets allows an estimate of the *total carbon budget* consistent with a specific global warming level.

FAQ 5.4 (continued)

In summary, determining a remaining carbon budget – that is, how much CO_2 can be released into the atmosphere while stabilizing global temperature below a chosen level – is well understood but relies on a set of choices. However, it is clear that, for limiting warming below 1.5°C or 2°C, the remaining carbon budget from 2020 onwards is much smaller than the total CO_2 emissions released to date.

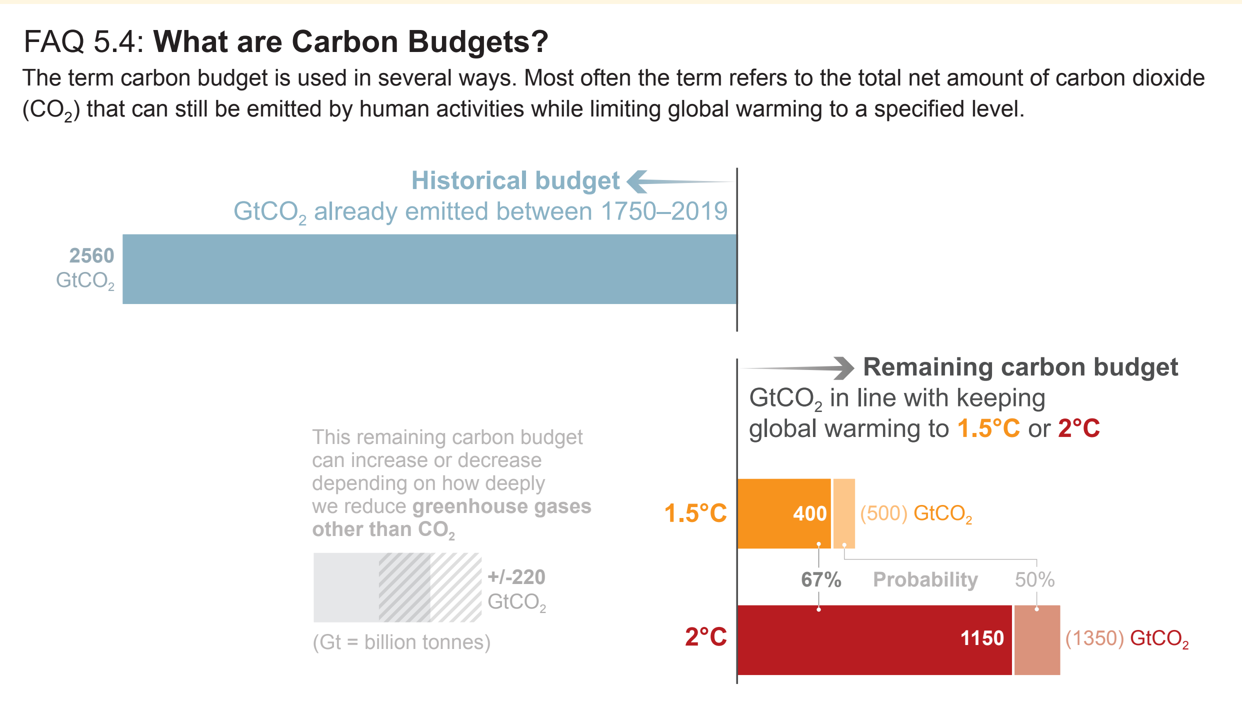

FAQ 5.4, Figure 1 | Various types of carbon budgets. Historical cumulative carbon dioxide (CO_2) emissions determine to a large degree how much the world has warmed to date, while the remaining carbon budget indicates how much CO_2 could still be emitted while keeping warming below specific temperature thresholds. Several factors limit the precision with which the remaining carbon budget can be estimated. Therefore, estimates need to specify the probability with which they aim at limiting warming to the intended target level (e.g., limiting warming to 1.5°C with a 67% probability).

Frequently Asked Questions

FAQ 6.1 | What Are Short-lived Climate Forcers and How Do They Affect the Climate?

Short-lived climate forcers (SLCFs) are compounds such as methane and sulphate aerosols that warm or cool the Earth's climate over shorter time scales – from days to years – than greenhouse gases like carbon dioxide, whose climatic effect lasts for decades, centuries or more. Because SLCFs do not remain in the atmosphere for very long, their effects on the climate are different from one region to another and can change rapidly in response to changes in SLCF emissions. As some SLCFs also negatively affect air quality, measures to improve air quality have resulted in sharp reductions in emissions and concentrations of those SLCFs in many regions over the few last decades.

The SLCFs include gases as well as tiny particles called *aerosols*, and they can have a warming or cooling effect on the climate (FAQ 6.1, Figure 1). Warming SLCFs are either greenhouse gases (e.g., ozone or methane) or particles like black carbon (also known as soot), which warm the climate by absorbing energy and are sometimes referred to as *short-lived climate pollutants.* Cooling SLCFs, on the other hand, are mostly made of aerosol particles (e.g., sulphate, nitrate and organic aerosols) that cool down the climate by reflecting away more incoming sunlight.

Some SLCFs do not directly affect the climate but produce climate-active compounds and are referred to as precursors. SLCFs are emitted both naturally and as a result of human activities, such as agriculture or extraction of fossil fuels. Many of the human sources, particularly those involving combustion, produce SLCFs at the same time as carbon dioxide and other long-lived greenhouse gases. Emissions have increased since the start of industrialization, and humans are now the dominant source for several SLCFs and SLCF precursors, such as sulphur dioxide (which produces sulphate aerosols) and nitrogen oxides (which produce nitrate aerosols and ozone), despite strong reductions over the last few decades in some regions due to efforts to improve air quality.

The climatic effect of a chemical compound in the atmosphere depends on two things: (i) how effective it is at cooling or warming the climate (its *radiative efficiency*) and (ii) how long it remains in the atmosphere (its *lifetime*). Because they have high radiative efficiencies, SLCFs can have a strong effect on the climate even though they have relatively short lifetimes of up to about two decades after emission. Today, there is a balance between warming and cooling from SLCFs, but this can change in the future.

The short lifetime of SLCFs constrains their effects in both space and time. First, of all the SLCFs, methane and the short-lived halocarbons persist the longest in the atmosphere: up to two decades (FAQ 6.1, Figure 1). This is long enough to mix in the atmosphere and to spread globally. Most other SLCFs only remain in the atmosphere for a few days to weeks, which is generally too short for mixing in the atmosphere, sometimes even regionally. As a result, the SLCFs are unevenly distributed and their effects on the climate are more regional than those of longer-lived gases. Second, rapid (but sustained) changes in emissions of SLCFs can result in rapid climatic effects.

In addition to the direct warming and cooling effects, SLCFs have many other consequences for the climate system and for air quality (see FAQ 6.2). For instance, deposition of black carbon on snow darkens its surface, which subsequently absorbs more solar energy, leading to more melting and more warming. Aerosols also modify the properties of clouds, which has indirect cooling effects on the climate and causes changes in local rainfall (see FAQ 7.2). Climate models indicate that SLCFs have altered atmospheric circulation on local and even hemispheric scales (e.g., monsoons) as well as regional precipitation. For instance, recent observations show that regional weather is influenced by strong regional contrasts in the evolution of aerosol concentrations, particularly over South and East Asia.

Although policies to limit climate change and discussions of the so-called *remaining carbon budgets* primarily focus on carbon dioxide (see FAQ 5.4), SLCFs can significantly affect temperature changes. It is therefore important to understand how SLCFs work and to quantify their effects. Because reducing some of the SLCF emissions, such as methane, can simultaneously reduce warming effects and adverse effects on air quality as well as help attaining Sustainable Development Goals, mitigation of SLCFs is often viewed as a favourable 'win-win' policy option.

FAQ 6.1 (continued)

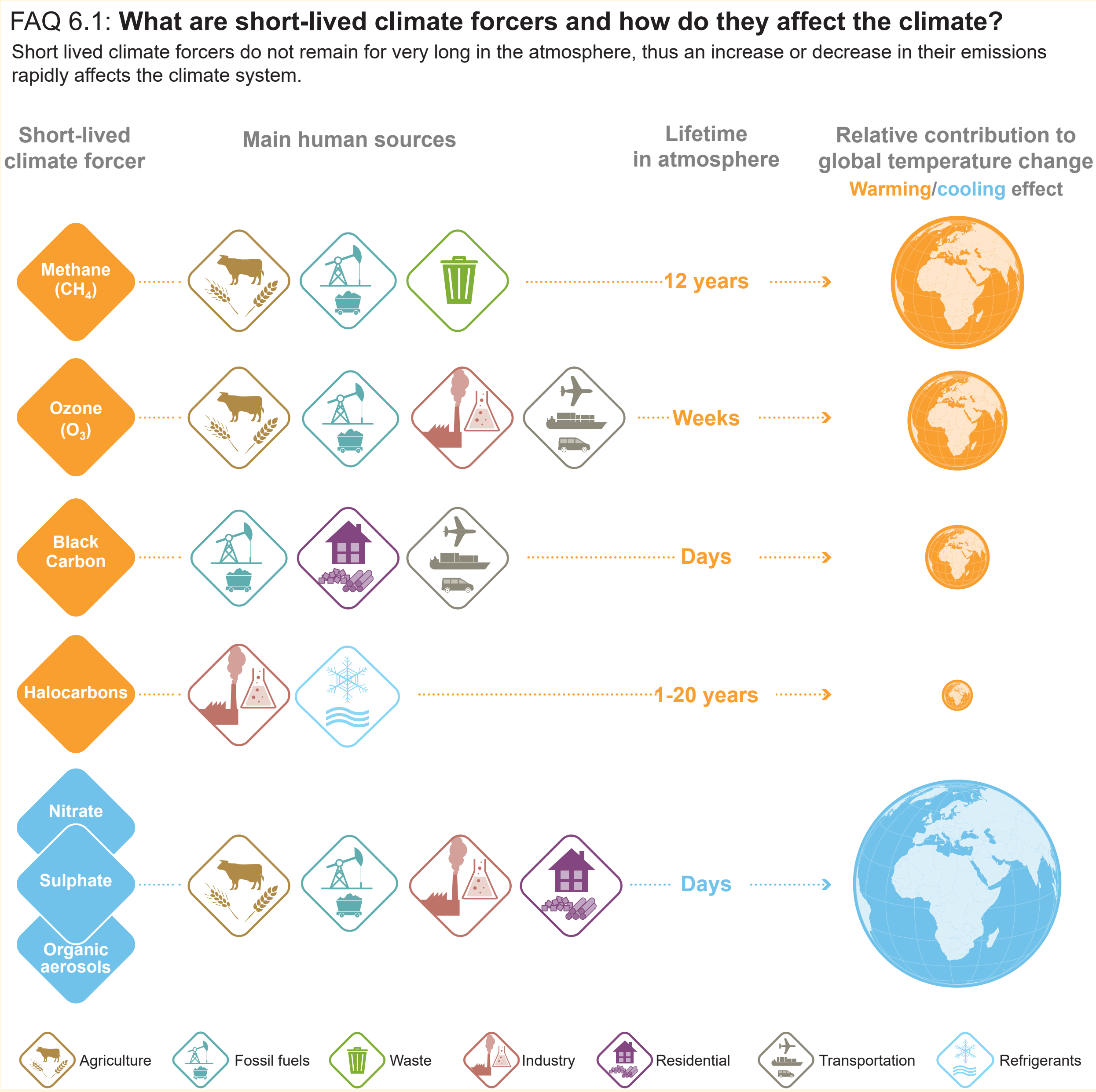

FAQ 6.1, Figure 1 | Main short-lived climate forcers, their sources, how long they exist in the atmosphere, and their relative contribution to global surface temperature changes between 1750 and 2019 (area of the globe). By definition this contribution depends on the lifetime, the warming/cooling potential (radiative efficiency), and the emissions of each compound in the atmosphere. Blue indicates cooling and orange indicates warming. Note that, between 1750 and 2019, the cooling contribution from aerosols (blue diamonds and globe) was approximately half the warming contribution from carbon dioxide.

Frequently Asked Questions

FAQ 6.2 | What Are the Links Between Limiting Climate Change and Improving Air Quality?

Climate change and air quality are intimately linked. Many of the human activities that produce long-lived greenhouse gases also emit air pollutants, and many of these air pollutants are also 'short-lived climate forcers' that affect the climate. Therefore, many options for improving air quality may also serve to limit climate change and vice versa. However, some options for improving air quality cause additional climate warming, and some actions that address climate change can worsen air quality.

Climate change and air pollution are both critical environmental issues that are already affecting humanity. In 2016, the World Health Organization attributed 4.2 million deaths worldwide every year to ambient (outdoor) air pollution. Meanwhile, climate change impacts water resources, food production, human health, extreme events, coastal erosion, wildfires, and many other phenomena.

Most human activities, including energy production, agriculture, transportation, industrial processes, waste management and residential heating and cooling, result in emissions of gaseous and particulate pollutants that modify the composition of the atmosphere, leading to degradation of air quality as well as to climate change. These air pollutants are also *short-lived climate forcers* – substances that affect the climate but remain in the atmosphere for shorter periods (days to decades) than long-lived greenhouse gases like carbon dioxide (see FAQ 6.1). While this means that the issues of air pollution and climate change are intimately connected, air pollutants and greenhouse gases are often defined, investigated and regulated independently of one another in both the scientific and policy arenas.

Many sources simultaneously emit carbon dioxide and air pollutants. When we drive our fossil fuel vehicles or light a fire in the fireplace, it is not just carbon dioxide or air pollutants that are emitted, but always both. It is therefore not possible to separate emissions into two clearly distinct groups. As a result, policies aiming at addressing climate change may have benefits or side effects for air quality, and vice versa.

For example, some short-term 'win-win' policies that simultaneously improve air quality and limit climate change include the implementation of energy efficiency measures, methane capture and recovery from solid-waste management and the oil and gas industry, zero-emissions vehicles, efficient and clean stoves for heating and cooking, filtering of soot (particulate matter) for diesel vehicles, cleaner brick-kiln technology, practices that reduce burning of agricultural waste, and the eradication of burning of kerosene for lighting.

There are, however, also 'win-lose' actions. For example, wood burning is defined as carbon neutral because a tree accumulates the same amount of carbon dioxide throughout its lifetime as is released when wood from that tree is burned. However, burning wood can also result in significant emissions of air pollutants, including carbon monoxide, nitrogen oxides, volatile organic compounds, and particulate matter, that locally or regionally affect the climate, human health and ecosystems (FAQ 6.2, Figure 1). Alternatively, decreasing the amount of sulphate aerosols produced by power and industrial plants, and from maritime transport, improves air quality but results in a warming influence on the climate, because those sulphate aerosols contribute to cooling the atmosphere by blocking incoming sunlight.

Air quality and climate change represent two sides of the same coin, and addressing both issues together could lead to significant synergies and economic benefits while avoiding policy actions that mitigate one of the two issues but worsen the other.

FAQ 6.2 (continued)

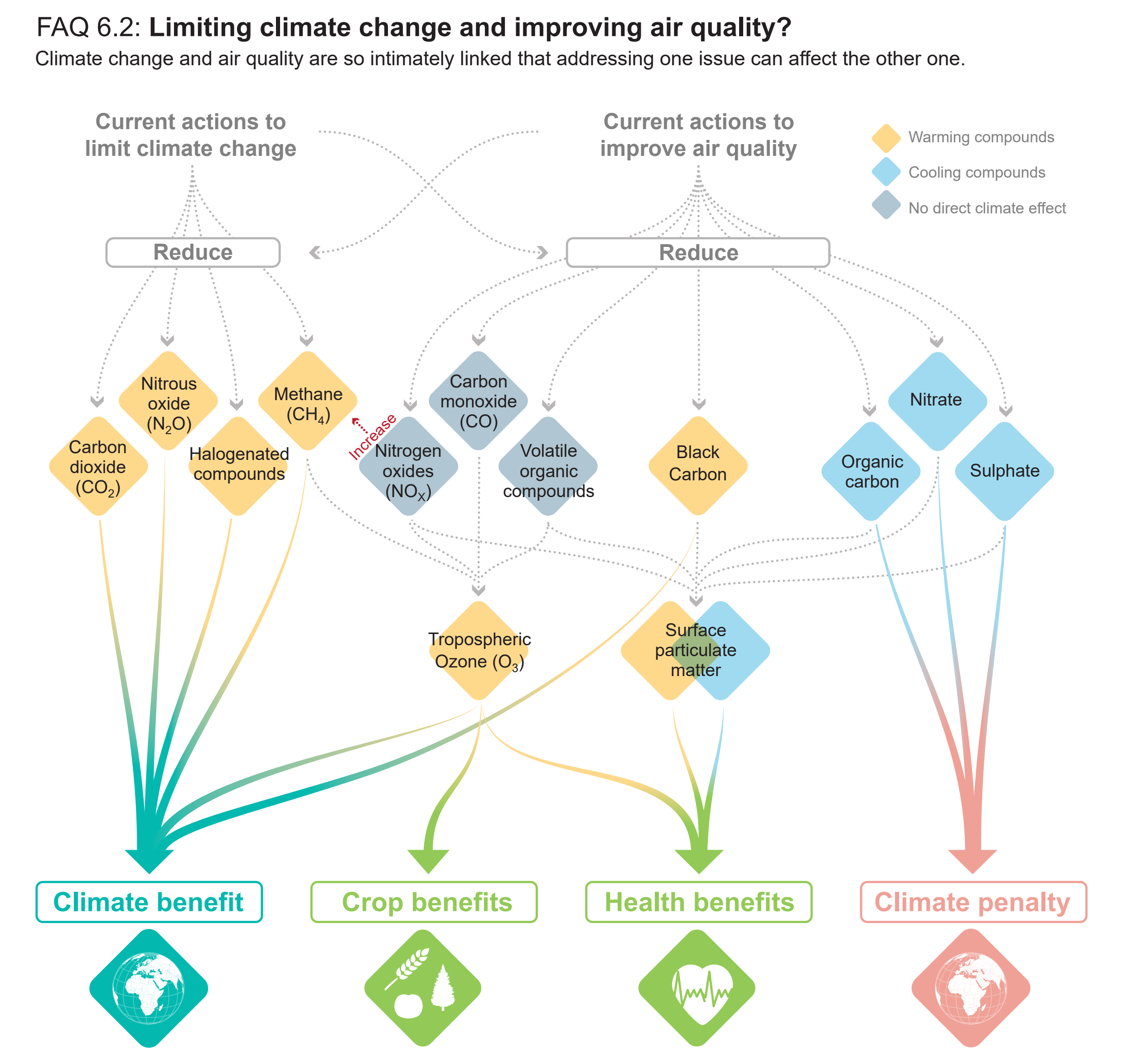

FAQ 6.2, Figure 1 | Links between actions aiming to limit climate change and actions to improve air quality. Greenhouse gases (GHGs) and aerosols (orange and blue) can affect climate directly. Air pollutants (bottom) can affect human health, ecosystems and climate. All these compounds have common sources and sometimes interact with each other in the atmosphere which makes it impossible to consider them separately (dotted grey arrows).

FAQ

Frequently Asked Questions

FAQ 7.1 | What Is the Earth's Energy Budget, and What Does It Tell Us About Climate Change?

The Earth's energy budget describes the flow of energy within the climate system. Since at least 1970 there has been a persistent imbalance in the energy flows that has led to excess energy being absorbed by the climate system. By measuring and understanding these energy flows and the role that human activities play in changing them, we are better able to understand the causes of climate change and project future climate change more accurately.

Our planet receives vast amounts of energy every day in the form of sunlight. Around a third of the sunlight is reflected back to space by clouds, by tiny particles called *aerosols*, and by bright surfaces such as snow and ice. The rest is absorbed by the ocean, land, ice and atmosphere. The planet then emits energy back out to space in the form of thermal radiation. In a world that was not warming or cooling, these energy flows would balance. Human activity has caused an imbalance in these energy flows.

We measure the influence of various human and natural factors on the energy flows at the top of our atmosphere in terms of *radiative forcings*, where a positive radiative forcing has a warming effect and a negative radiative forcing has a cooling effect. In response to these forcings, the Earth system will either warm or cool, so as to restore balance through changes in the amount of outgoing thermal radiation (the warmer the Earth, the more radiation it emits). Changes in Earth's temperature in turn lead to additional changes in the climate system (known as *climate feedbacks*) that either amplify or dampen the original effect. For example, Arctic sea ice has been melting as the Earth warms, reducing the amount of reflected sunlight and adding to the initial warming (an amplifying feedback). The most uncertain of those climate feedbacks are clouds, as they respond to warming in complex ways that affect both the emission of thermal radiation and the reflection of sunlight. However, we are now more confident that cloud changes, taken together, will amplify climate warming (see FAQ 7.2).

Human activities have unbalanced these energy flows in two main ways. First, increases in greenhouse gas levels have led to more of the emitted thermal radiation being absorbed by the atmosphere, instead of being released to space. Second, increases in pollutants have increased the amount of aerosols such as sulphates in the atmosphere (see FAQ 6.1). This has led to more incoming sunlight being reflected away, by the aerosols themselves and through the formation of more cloud drops, which increases the reflectivity of clouds (see FAQ 7.2).

Altogether, the global energy flow imbalance since the 1970s has been just over half a watt per square metre of the Earth's surface. This sounds small, but because the imbalance is persistent and because Earth's surface is large, this adds up to about 25 times the total amount of primary energy consumed by human society, compared over 1971 to 2018. Compared to the IPCC Fifth Assessment Report (AR5), we are now better able to quantify and track these energy flows from multiple lines of evidence, including satellite data, direct measurements of ocean temperatures, and a wide variety of other Earth system observations (see FAQ 1.1). We also have a better understanding of the processes contributing to this imbalance, including the complex interactions between aerosols, clouds and radiation.

Research has shown that the excess energy since the 1970s has mainly gone into warming the ocean (91%), followed by the warming of land (5%) and the melting of ice sheets and glaciers (3%). The atmosphere has warmed substantially since 1970, but because it is comprised of thin gases it has absorbed only 1% of the excess energy (FAQ 7.1, Figure 1). As the ocean has absorbed the vast majority of the excess energy, especially within its top two kilometres, the deep ocean is expected to continue to warm and expand for centuries to millennia, leading to long-term sea level rise – even if atmospheric greenhouse gas levels were to decline (see FAQ 5.3). This is in addition to the sea level rise expected from melting ice sheets and glaciers.

Understanding the Earth's energy budget al.o helps to narrow uncertainty in future projections of climate. By testing climate models against what we know about the Earth's energy budget, we can make more confident projections of surface temperature changes we might expect this century and beyond.

FAQ 7.1 (continued)

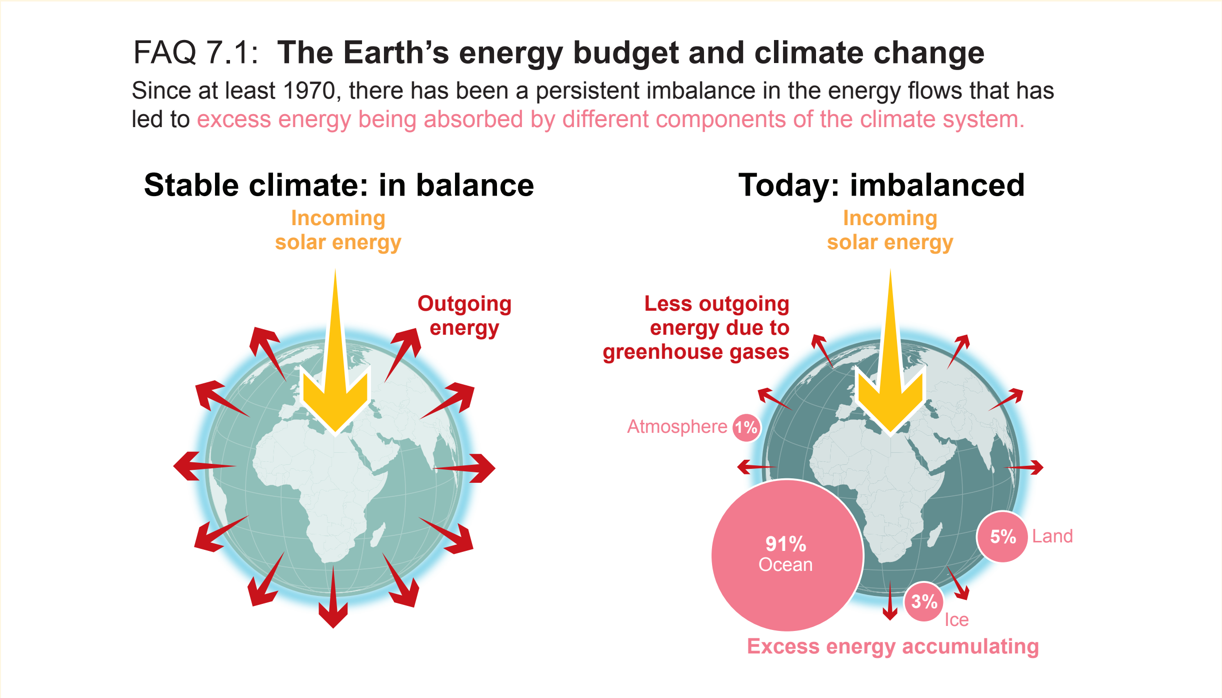

FAQ 7.1, Figure 1 | The Earth's energy budget compares the flows of incoming and outgoing energy that are relevant for the climate system. Since at least the 1970s, less energy is flowing out than is flowing in, which leads to excess energy being absorbed by the ocean, land, ice and atmosphere, with the ocean absorbing 91%.

FAQ

Frequently Asked Questions

FAQ 7.2 | What Is the Role of Clouds in a Warming Climate?

One of the biggest challenges in climate science has been to predict how clouds will change in a warming world and whether those changes will amplify or partially offset the warming caused by increasing concentrations of greenhouse gases and other human activities. Scientists have made significant progress over the past decade and are now more confident that changes in clouds will amplify, rather than offset, global warming in the future.

Clouds cover roughly two-thirds of the Earth's surface. They consist of small droplets and/or ice crystals, which form when water vapour condenses or deposits around tiny particles called *aerosols* (such as salt, dust, or smoke). Clouds play a critical role in the Earth's *energy budget* at the top of our atmosphere and therefore influence Earth's surface temperature (see FAQ 7.1). The interactions between clouds and the climate are complex and varied. Clouds at low altitudes tend to reflect incoming solar energy back to space, creating a cooling effect by preventing this energy from reaching and warming the Earth. On the other hand, higher clouds tend to trap (i.e., absorb and then emit at a lower temperature) some of the energy leaving the Earth, leading to a warming effect. On average, clouds reflect back more incoming energy than the amount of outgoing energy they trap, resulting in an overall net cooling effect on the present climate. Human activities since the pre-industrial era have altered this climate effect of clouds in two different ways: by changing the abundance of the aerosol particles in the atmosphere and by warming the Earth's surface, primarily as a result of increases in greenhouse gas emissions.

The concentration of aerosols in the atmosphere has markedly increased since the pre-industrial era, and this has had two important effects on clouds. First, clouds now reflect more incoming energy because cloud droplets have become more numerous and smaller. Second, smaller droplets may delay rain formation, thereby making the clouds last longer, although this effect remains uncertain. Hence, aerosols released by human activities have had a cooling effect, counteracting a considerable portion of the warming caused by increases in greenhouse gases over the last century (see FAQ 3.1). Nevertheless, this cooling effect is expected to diminish in the future, as air pollution policies progress worldwide, reducing the amount of aerosols released into the atmosphere.

Since the pre-industrial period, the Earth's surface and atmosphere have warmed, altering the properties of clouds, such as their altitude, amount and composition (water or ice), thereby affecting the Earth's energy budget and, in turn, changing temperature. This cascading effect of clouds, known as the *cloud feedback,* could either amplify or offset some of the future warming and has long been the biggest source of uncertainty in climate projections. The problem stems from the fact that clouds can change in many ways and that their processes occur on much smaller scales than global climate models can explicitly represent. As a result, global climate models have disagreed on how clouds, particularly over the subtropical ocean, will change in the future and whether the change will amplify or suppress the global warming.

Since the last IPCC Report in 2013 (the Fifth Assessment Report, or AR5), understanding of cloud processes has advanced with better observations, new analysis approaches and explicit high-resolution numerical simulation of clouds. Also, current global climate models simulate cloud behaviour better than previous models, due both to advances in computational capabilities and process understanding. Altogether, this has helped to build a more complete picture of how clouds will change as the climate warms (FAQ 7.2, Figure 1). For example, the amount of low-clouds will reduce over the subtropical ocean, leading to less reflection of incoming solar energy, and the altitude of high-clouds will rise, making them more prone to trapping outgoing energy; both processes have a warming effect. In contrast, clouds in high latitudes will be increasingly made of water droplets rather than ice crystals. This shift from fewer, larger ice crystals to smaller but more numerous water droplets will result in more of the incoming solar energy being reflected back to space and produce a cooling effect. Better understanding of how clouds respond to warming has led to more confidence than before that future changes in clouds will, overall, cause additional warming (i.e., by weakening the current cooling effect of clouds). This is called a *positive net cloud feedback*.

In summary, clouds will amplify rather than suppress the warming of the climate system in the future, as more greenhouse gases and fewer aerosols are released to the atmosphere by human activities.

FAQ 7.2 (continued)

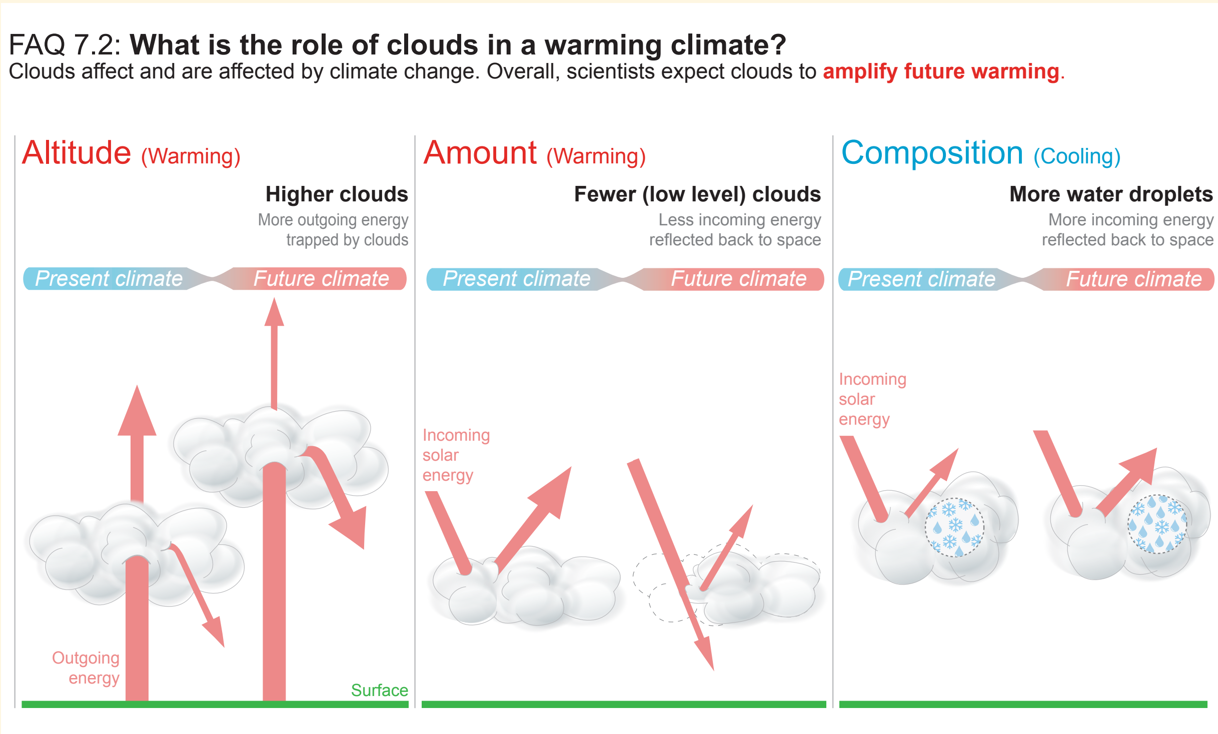

FAQ 7.2, Figure 1 | Interactions between clouds and the climate, today and in a warmer future. Global warming is expected to alter the altitude **(left)** and the amount **(centre)** of clouds, which will amplify warming. On the other hand, cloud composition will change **(right)**, offsetting some of the warming. Overall, clouds are expected to amplify future warming.

Frequently Asked Questions

FAQ 7.3 | What Is Equilibrium Climate Sensitivity and How Does It Relate to Future Warming?

For a given future scenario, climate models project a range of changes in global surface temperature. This range is closely related to equilibrium climate sensitivity, or ECS, which measures how climate models respond to a doubling of carbon dioxide in the atmosphere. Models with high climate sensitivity project stronger future warming. Some climate models of the new generation are more sensitive than the range assessed in the IPCC Sixth Assessment Report. This leads to end-of-century global warming in some simulations of up to 2°C–3°C above the current IPCC best estimate. Although these higher warming levels are not expected to occur, high-ECS models are useful for exploring low-likelihood, high-impact futures.

The *equilibrium climate sensitivity* (ECS) is defined as the long-term global warming caused by a doubling of carbon dioxide above its pre-industrial concentration. For a given emissions scenario, much of the uncertainty in projections of future warming can be explained by the uncertainty in ECS (FAQ 7.3, Figure 1). The significance of equilibrium climate sensitivity has long been recognized, and the first estimate was presented by Swedish scientist Svante Arrhenius in 1896.

This Sixth Assessment Report concludes that there is a 90% or more chance (*very likely*) that the ECS is between 2°C and 5°C. This represents a significant reduction in uncertainty compared to the Fifth Assessment Report, which gave a 66% chance (*likely*) of ECS being between 1.5°C and 4.5°C. This reduction in uncertainty has been possible not through a single breakthrough or discovery but instead by combining evidence from many different sources and by better understanding their strengths and weaknesses.

There are four main lines of evidence for ECS.

- The self-reinforcing processes, called *feedback loops*, that amplify or dampen the warming in response to increasing carbon dioxide are now better understood. For example, warming in the Arctic melts sea ice, resulting in more open ocean area, which is darker and therefore absorbs more sunlight, further intensifying the initial warming. It remains challenging to represent realistically all the processes involved in these feedback loops, particularly those related to clouds (see FAQ 7.2). Such identified model errors are now taken into account, and other known, but generally weak, feedback loops that are typically not included in models are now included in the assessment of ECS.
- Historical warming since early industrialisation provides strong evidence that climate sensitivity is not small. Since 1850, the concentrations of carbon dioxide and other greenhouse gases have increased, and as a result the Earth has warmed by about 1.1°C. However, relying on this industrial-era warming to estimate ECS is challenging, partly because some of the warming from greenhouse gases was offset by cooling from aerosol particles and partly because the ocean is still responding to past increases in carbon dioxide.
- Evidence from ancient climates that had reached equilibrium with greenhouse gas concentrations, such as the coldest period of the last ice age around 20,000 years ago, or warmer periods further back in time, provide useful data on the ECS of the climate system (see FAQ 1.3).
- Statistical approaches linking model ECS values with observed changes, such as global warming since the 1970s, provide complementary evidence.

All four lines of evidence rely, to some extent, on climate models, and interpreting the evidence often benefits from model diversity and spread in modelled climate sensitivity. Furthermore, high-sensitivity models can provide important insights into futures that have a low likelihood of occurring but that could result in large impacts. But, unlike in previous assessments, climate models are not considered a line of evidence in their own right in the IPCC Sixth Assessment Report.

The ECS of the latest climate models is, on average, higher than that of the previous generation of models and also higher than this Report's best estimate of 3.0°C. Furthermore, the ECS values in some of the new models are both above and below the 2°C to 5°C *very likely* range, and although such models cannot be ruled out as implausible solely based on their ECS, some simulations display climate change that is inconsistent with the observed changes when tested with ancient climates. A slight mismatch between models and this Report's assessment is only natural because this Report's assessment is largely based on observations and an improved understanding of the climate system.

FAQ 7.3 (continued)

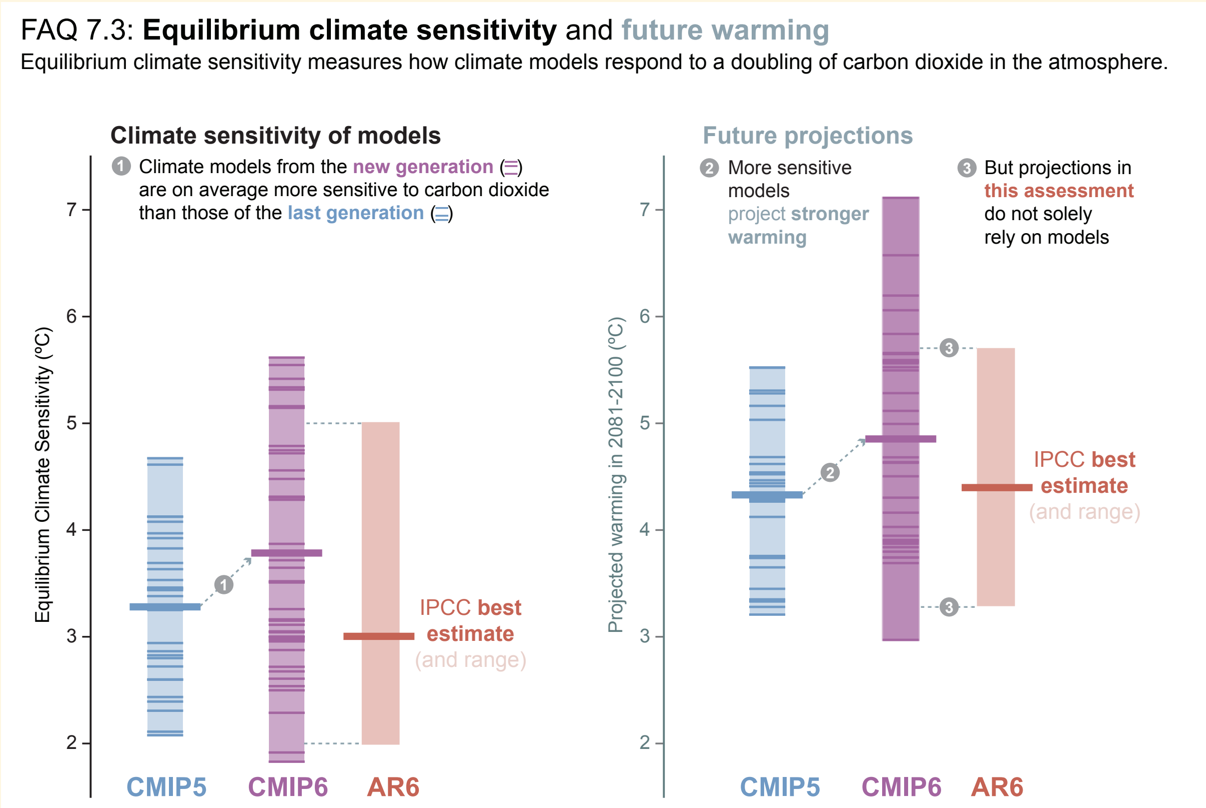

FAQ 7.3, Figure 1 | Equilibrium climate sensitivity and future warming. (left) Equilibrium climate sensitivities for the current generation (Coupled Model Intercomparison Project Phase 6, CMIP6) climate models, and the previous (CMIP5) generation. The assessed range in this Report (AR6) is also shown. **(right)** Climate projections of CMIP5, CMIP6 and AR6 for the very high-emissions scenarios RCP8.5, and SSP5-8.5, respectively. The thick horizontal lines represent the multi-model average and the thin horizontal lines represent the results of individual models. The boxes represent the model ranges for CMIP5 and CMIP6 and the range assessed in AR6.

FAQ

Frequently Asked Questions

FAQ 8.1 | How Does Land Use Change Alter the Water Cycle?

The ways in which humans use and change land cover, for example by converting fields to urban areas or clearing forests, can affect every aspect of the water cycle. Land-use changes can alter precipitation patterns and how water is absorbed into the ground, flows into streams and rivers, or floods the land surface, as well as how moisture evaporates back into the air. Changes in any of these aspects of the interconnected water cycle can affect the entire cycle and the availability of freshwater resources.

Land use describes the combination of activities and ground cover defining each area of the Earth's continental surface. Altering land use can modify the exchange of water between the atmosphere, soil and subsurface (FAQ 8.1, Figure 1).

For instance, changes in land cover can affect the ability of soils to soak up surface water (infiltration). When soil loses its capacity to soak up water, precipitation that would normally infiltrate and contribute to groundwater reserves will instead overflow, increasing surface water (runoff) and the likelihood of flooding. For example, changing from vegetation to urban cover can cause water to flow rapidly over buildings, roads and driveways and into drains rather than soaking into the ground. Deforestation over wide areas can also directly reduce soil moisture, evaporation and rainfall locally but can also cause regional temperature changes that affect rainfall patterns.

Extracting water from the ground and river systems for agriculture, industry and drinking water depletes groundwater and can increase surface evaporation because water that was previously in the ground is now in direct contact with the atmosphere, being available for evaporation.

Changing land use can also alter how wet the soil is, influencing how quickly the ground heats up and cools down and the local water cycle. Drier soils evaporate less water into the air but heat up more in the day. This can lead to warmer, more buoyant plumes of air that can promote cloud development and precipitation if there is enough moisture in the air.

Changes in land use can also modify the amount of tiny aerosol particles in the air. For instance, industrial and domestic activities can contribute to aerosol emissions, as do natural environments such as forests or salt lakes. Aerosols cool down global temperature by blocking out sunlight but can also affect the formation of clouds and therefore the occurrence of precipitation (see FAQ 7.2).

Vegetation plays an important role in soaking up soil moisture and evaporating water into the air (*transpiration*) through tiny holes (*stomata*) that allow the plants to take in carbon dioxide. Some plants are better at retaining water than others, so changes in vegetation can affect how much water infiltrates into the ground, flows into streams and rivers, or is evaporated.

More globally, land-use change is currently responsible for about 15% of the emissions of carbon dioxide from human activities, leading to global warming, which in turn affects precipitation, evaporation, and plant transpiration. In addition, higher atmospheric concentrations of carbon dioxide due to human activities can make plants more efficient at retaining water because the stomata do not need to open so widely. Improved land and water management (e.g., reforestation, sustainable irrigation) can also contribute to reducing climate change and adapting to some of its adverse consequences.

In summary, there is abundant evidence that changes in land use and land cover alter the water cycle globally, regionally and locally, by changing precipitation, evaporation, flooding, groundwater, and the availability of freshwater for a variety of uses. Since all the components of the water cycle are connected (and linked to the carbon cycle), changes in land use trickle down to many other components of the water cycle and climate system.

FAQ 8.1 (continued)

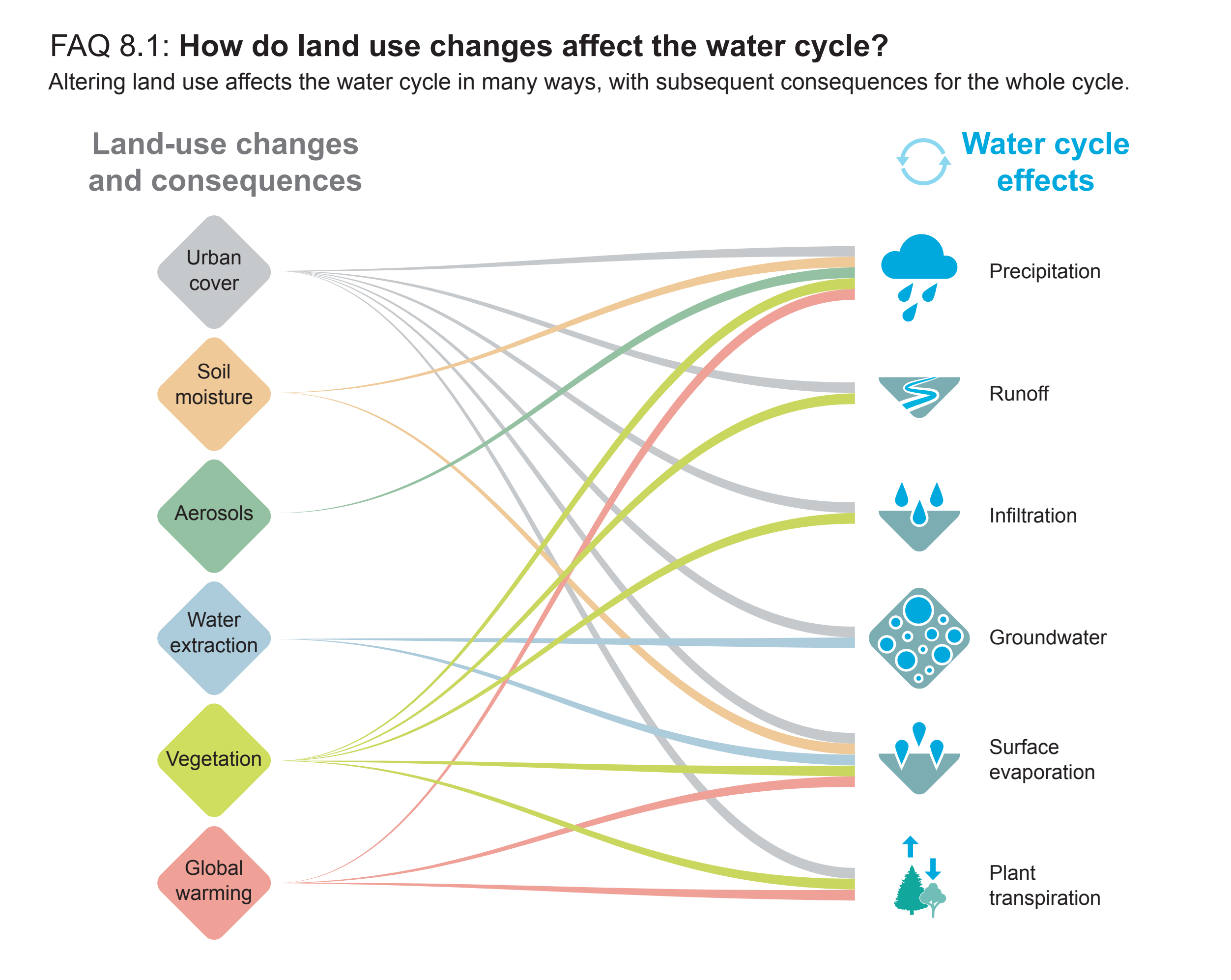

FAQ 8.1, Figure 1 | Land-use changes and their consequences on the water cycle. As all the components or the water cycle are tightly connected, changes in one aspect of the cycle affects almost all the cycle.

Frequently Asked Questions

FAQ 8.2 | Will Floods Become More Severe or More Frequent as a Result of Climate Change?

A warmer climate increases the amount and intensity of rainfall during wet events, and this is expected to amplify the severity of flooding. However, the link between rainfall and flooding is complex, so while the most severe flooding events are expected to worsen, floods could become rarer in some regions.

Floods are a natural and important part of the water cycle but they can also threaten lives and safety, disrupt human activities, and damage infrastructure. Most inland floods occur when rivers overtop their banks (*fluvial* flooding) or when intense rainfall causes water to build up and overflow locally (*pluvial* flooding). Flooding is also caused by coastal inundation by the sea, rapid seasonal melting of snow, and the accumulation of debris, such as vegetation or ice, that stops water from draining away.

Climate change is already altering the location, frequency and severity of flooding. Close to the coasts, rising sea levels increasingly cause more frequent and severe coastal flooding, and the severity of these floods is exacerbated when combined with heavy rainfall. The heavy and sustained rainfall events responsible for most inland flooding are becoming more intense in many areas as the climate warms because air near Earth's surface can carry around 7% more water in its gas phase (vapour) for each 1°C of warming. This extra moisture is drawn into weather systems, fueling heavier rainfall (FAQ 8.2, Figure 1).

A warming climate also affects wind patterns, how storms form and evolve, and the pathway those storms usually travel. Warming also increases condensation rates, which in turn releases extra heat that can energize storm systems and further intensify rainfall. On the other hand, this energy release can also inhibit the uplift required for cloud development, while increases in particle pollution can delay rainfall but invigorate storms. These changes mean that the character of precipitation events (how often, how long lasting and how heavy they are) will continue to change as the climate warms.

In addition to climate change, the location, frequency and timing of the heaviest rainfall events and worst flooding depend on natural fluctuations in wind patterns that make some regions unusually wet or dry for months, years, or even decades. These natural variations make it difficult to determine whether heavy rainfall events are changing locally as a result of global warming. However, when natural weather patterns bring heavy and prolonged rainfall in a warmer climate, the intensity is increased by the larger amount of moisture in the air.

An increased intensity and frequency of record-breaking daily rainfall has been detected for much of the land surface where good observational records exist, and this can only be explained by human-caused increases in atmospheric greenhouse gas concentrations. Heavy rainfall is also projected to become more intense in the future for most places. So, where unusually wet weather events or seasons occur, the rainfall amounts are expected to be greater in the future, contributing to more severe flooding.

However, heavier rainfall does not always lead to greater flooding. This is because flooding also depends upon the type of river basin, the surface landscape, the extent and duration of the rainfall, and how wet the ground is before the rainfall event (FAQ 8.2, Figure 1). Some regions will experience a drying in the soil as the climate warms, particularly in subtropical climates, which could make floods from a rainfall event less probable because the ground can potentially soak up more of the rain. On the other hand, less frequent but more intense downpours can lead to dry, hard ground that is less able to soak up heavy rainfall when it does occur, resulting in more runoff into lakes, rivers and hollows. Earlier spring snowmelt combined with more precipitation falling as rain rather than snow can trigger flood events in cold regions. Reduced winter snow cover can, in contrast, decrease the chance of flooding arising from the combination of rainfall and rapid snowmelt. Rapid melting of glaciers and snow in a warming climate is already increasing river flow in some regions, but as the volumes of ice diminish, flows will peak and then decline in the future. Flooding is also affected by changes in the management of the land and river systems. For example, clearing forests for agriculture or building cities can make rainwater flow more rapidly into rivers or low-lying areas. On the other hand, increased extraction of water from rivers can reduce water levels and the likelihood of flooding.

FAQ 8.2 (continued)

A mix of both increases and decreases in flooding have been observed in some regions and these changes have been attributed to multiple causes, including changes in snowmelt, soil moisture and rainfall. Although we know that a warming climate will intensify rainfall events, local and regional trends are expected to vary in both direction and magnitude as global warming results in multiple, and sometimes counteracting, influences. However, even accounting for the many factors that generate flooding, when weather patterns cause flood events in a warmer future, these floods will be more severe.

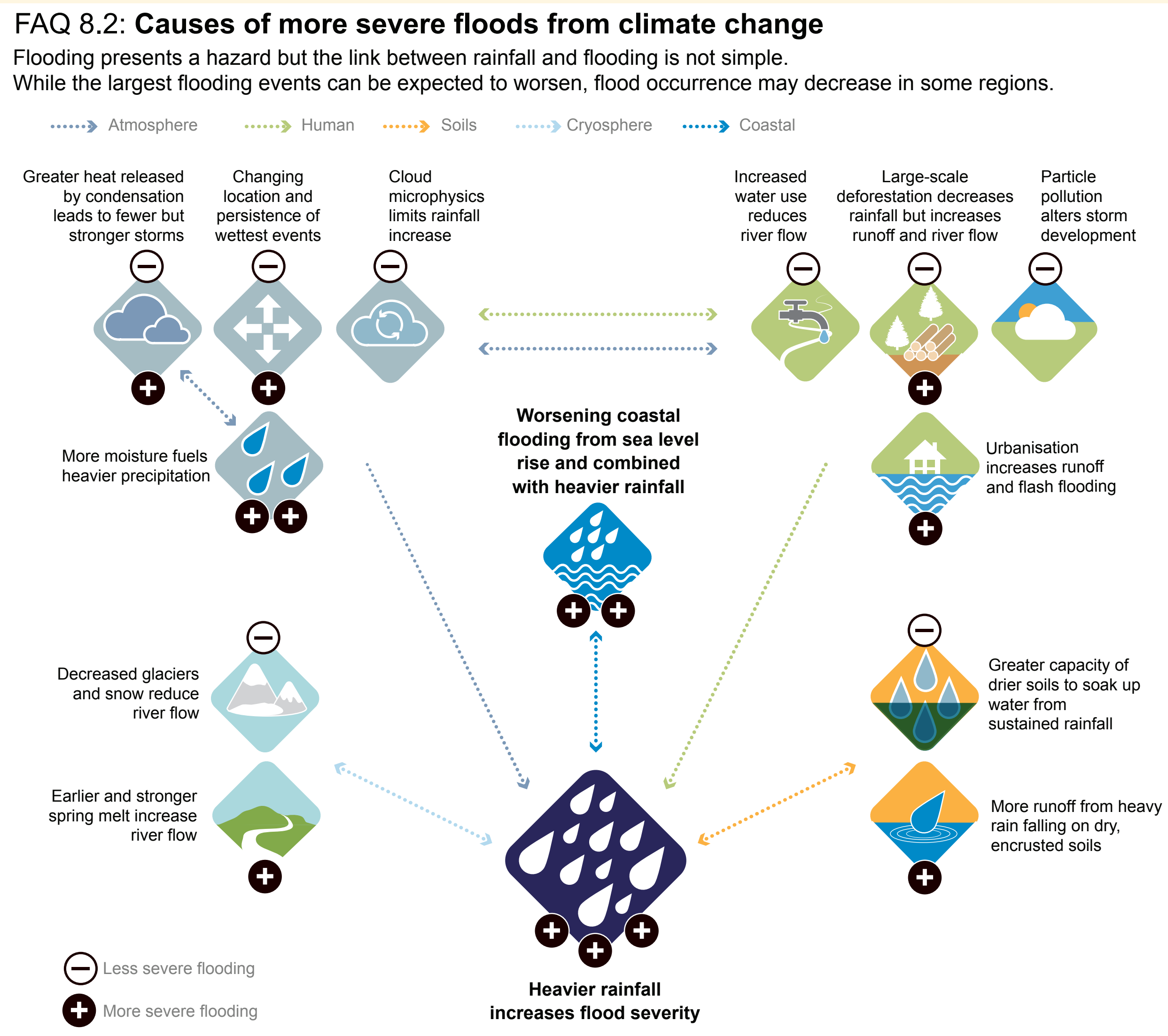

FAQ 8.2, Figure 1 | Schematic illustrating factors important in determining changes in heavy precipitation and flooding.

FAQ

Frequently Asked Questions

FAQ 8.3 | What Causes Droughts, and Will Climate Change Make Them Worse?

Droughts usually begin as a deficit of precipitation, but then propagate to other parts of the water cycle (soils, rivers, snow/ice and water reservoirs). They are also influenced by factors like temperature, vegetation and human land and water management. In a warmer world, evaporation increases, which can make even wet regions more susceptible to drought.

A drought is broadly defined as drier than normal conditions; that is, a moisture deficit relative to the average water availability at a given location and season. Since they are locally defined, a drought in a wet place will not have the same amount of water deficit as a drought in a dry region. Droughts are divided into different categories based on where in the water cycle the moisture deficit occurs: meteorological drought (precipitation), hydrological drought (runoff, streamflow, and reservoir storage), and agricultural or ecological drought (plant stress from a combination of evaporation and low soil moisture). Special categories of drought also exist. For example, a snow drought occurs when winter snowpack levels are below average, which can cause abnormally low streamflow in subsequent seasons. And while many drought events develop slowly over months or years, some events, called flash droughts, can intensify over the course of days or weeks. One such event occurred in 2012 in the Midwestern region of North America and had a severe impact on agricultural production, with losses exceeding $30 billion US dollars. Droughts typically only become a concern when they adversely affect people (reducing water available for municipal, industrial, agricultural, or navigational needs) and/or ecosystems (adverse effects on natural flora and fauna). When a drought lasts for a very long time (more than two decades) it is sometimes called a megadrought.

Most droughts begin when precipitation is below normal for an extended period of time (meteorological drought). This typically occurs when high pressure in the atmosphere sets up over a region, reducing cloud formation and precipitation over that area and deflecting away storms. The lack of rainfall then propagates across the water cycle to create agricultural drought in soils and hydrological drought in waterways. Other processes act to amplify or alleviate droughts. For example, if temperatures are abnormally high, evaporation increases, drying out soils and streams and stressing plants beyond what would have occurred from the lack of precipitation alone. Vegetation can play a critical role because it modulates many important hydrologic processes (soil water, evapotranspiration, runoff). Human activities can also determine how severe a drought is. For example, irrigating croplands can reduce the socio-economic impact of a drought; at the same time, depletion of groundwater in aquifers can make a drought worse.

The effect of climate change on drought varies across regions. In the subtropical regions like the Mediterranean, southern Africa, south-western Australia and south-western South America, as well as tropical Central America, western Africa and the Amazon basin, precipitation is expected to decline as the world warms, increasing the possibility that drought will occur throughout the year (FAQ 8.3, Figure 1). Warming will decrease snowpack, amplifying drought in regions where snowmelt is an important water resource (such as in south-western South America). Higher temperatures lead to increased evaporation, resulting in soil drying, increased plant stress, and impacts on agriculture, even in regions where large changes in precipitation are not expected (such as central and northern Europe). If emissions of greenhouse gases are not curtailed, about a third of global land areas are projected to suffer from at least moderate drought by 2100. On the other hand, some areas and seasons (such as high-latitude regions in North America and Asia, and the South Asian monsoon region) may experience increases in precipitation as a result of climate change, which will decrease the likelihood of droughts. FAQ 8.3, Figure 1 highlights the regions where climate change is expected to increase the severity of droughts.

FAQ 8.3 (continued)

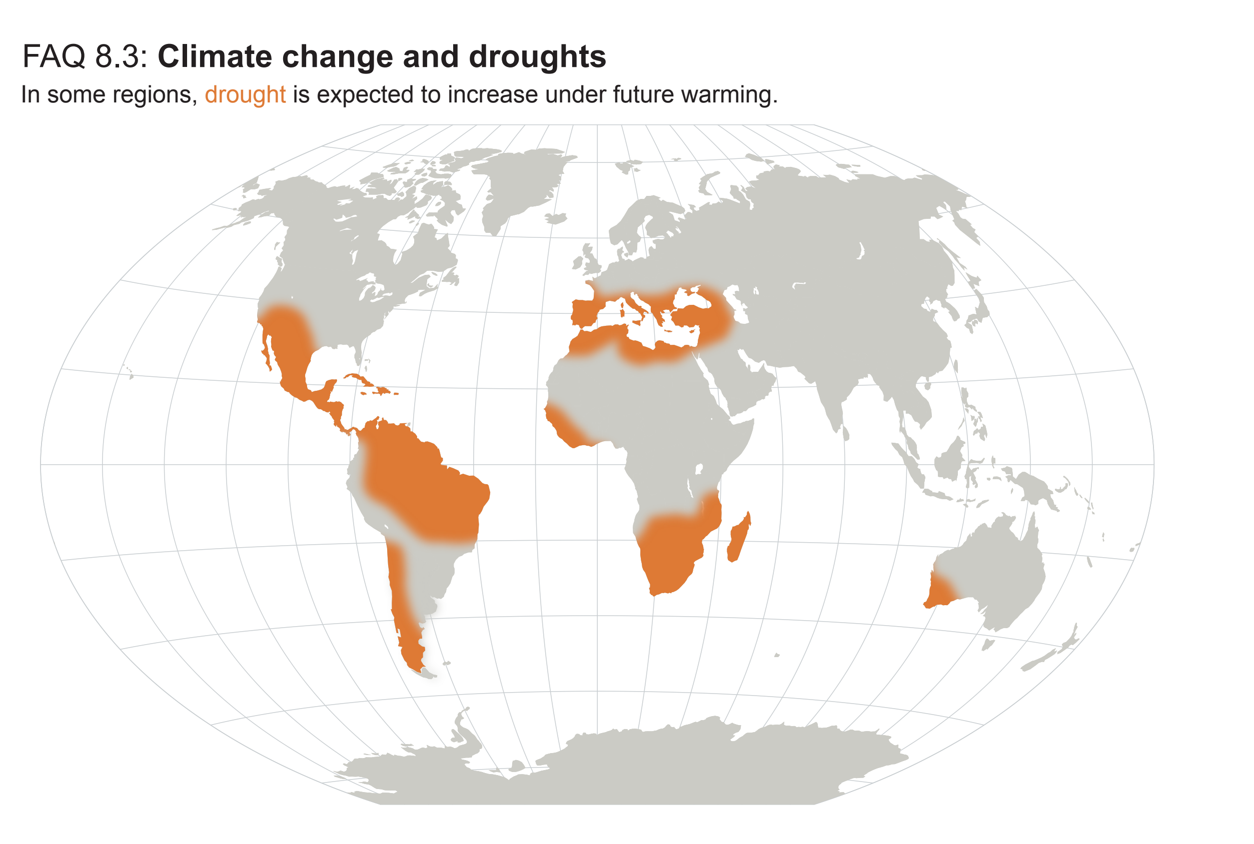

FAQ 8.3, Figure 1 | Schematic map highlighting in brown the regions where droughts are expected to become worse as a result of climate change. This pattern is similar regardless of the emissions scenario; however, the magnitude of change increases under higher emissions.

Frequently Asked Questions

FAQ 9.1 | Can Continued Melting of the Greenland and Antarctic Ice Sheets Be Reversed? How Long Would It Take for Them to Grow Back?

Evidence from the distant past shows that some parts of the Earth system might take hundreds to thousands of years to fully adjust to changes in climate. This means that some of the consequences of human-induced climate change will continue for a very long time, even if atmospheric heat-trapping gas levels and global temperatures are stabilized or reduced in the future. This is especially true for the Greenland and Antarctic ice sheets, which grow much more slowly than they retreat. If the current melting of these ice sheets continues for long enough, it becomes effectively irreversible on human time scales, as does the sea level rise caused by that melting.

Humans are changing the climate and there are mechanisms that amplify the warming in the polar regions (Arctic and Antarctic). The Arctic is already warming faster than anywhere else (see FAQ 4.3). This is significant because these colder high latitudes are home to our two remaining ice sheets: Antarctica and Greenland. Ice sheets are huge reservoirs of frozen freshwater, built up by tens of thousands of years of snowfall. If they were to completely melt, the water released would raise global sea level by about 65 m. Understanding how these ice sheets are affected by warming of nearby ocean and atmosphere is therefore critically important. The Greenland and Antarctic ice sheets are already slowly responding to recent changes in climate, but it takes a long time for these huge masses of ice to adjust to changes in global temperature. That means that the full effects of a warming climate may take hundreds or thousands of years to play out. An important question is whether these changes can eventually be reversed, once levels of greenhouse gases in the atmosphere are stabilized or reduced by humans and natural processes. Records from the past can help us answer this question.

For at least the last 800,000 years, the Earth has followed cycles of gradual cooling followed by rapid warming caused by natural processes. During cooling phases, more and more ocean water is gradually deposited as snowfall, causing ice sheets to grow and sea level to slowly decrease. During warming phases, the ice sheets melt more quickly, resulting in more rapid rises in sea level (FAQ 9.1, Figure 1). Ice sheets build up very slowly because growth relies on the steady accumulation of falling snow that eventually compacts into ice. As the climate cools, areas that can accumulate snow expand, reflecting back more sunlight that otherwise would keep the Earth warmer. This means that, once started, glacial climates develop rapidly. However, as the climate cools, the amount of moisture that the air can hold tends to decrease. As a result, even though glaciations begin quite quickly, it takes tens of thousands of years for ice sheets to grow to a point where they are in balance with the colder climate.

Ice sheets retreat more quickly than they grow because of processes that, once triggered, drive self-reinforcing ice loss. For ice sheets that are mostly resting on bedrock *above* sea level – like the Greenland Ice Sheet – the main self-reinforcing loop that affects them is the 'elevation–mass balance feedback' (FAQ 9.1, Figure 1, right). In this situation, the altitude of the ice-sheet surface decreases as it melts, exposing the sheet to warmer air. The lowered surface then melts even more, lowering it faster still, until eventually the whole ice sheet disappears. In places where the ice sheet rests instead on bedrock that is *below* sea level, and which also deepens inland, including many parts of the Antarctic Ice Sheet, an important process called 'marine ice sheet instability' is thought to drive rapid retreat (FAQ 9.1, Figure 1, left). This happens when the part of the ice sheet that is surrounded by sea water melts. That leads to additional thinning, which in turn accelerates the motion of the glaciers that feed into these areas. As the ice sheet flows more quickly into the ocean, more melting takes place, leading to more thinning and even faster flow that brings ever-more glacier ice into the ocean, ultimately driving rapid deglaciation of whole ice-sheet drainage basins.

These (and other) self-reinforcing processes explain why relatively small increases in temperature in the past led to very substantial sea level rise over centuries to millennia, compared to the many tens of thousands of years it takes to grow the ice sheets that lowered the sea level in the first place. These insights from the past imply that, if human-induced changes to the Greenland and Antarctic ice sheets continue for the rest of this century, it will take thousands of years to reverse that melting, even if global air temperatures decrease within this or the next century. In this sense, these changes are therefore irreversible, since the ice sheets would take much longer to regrow than the decades or centuries for which modern society is able to plan.

FAQ

FAQ 9.1 (continued)

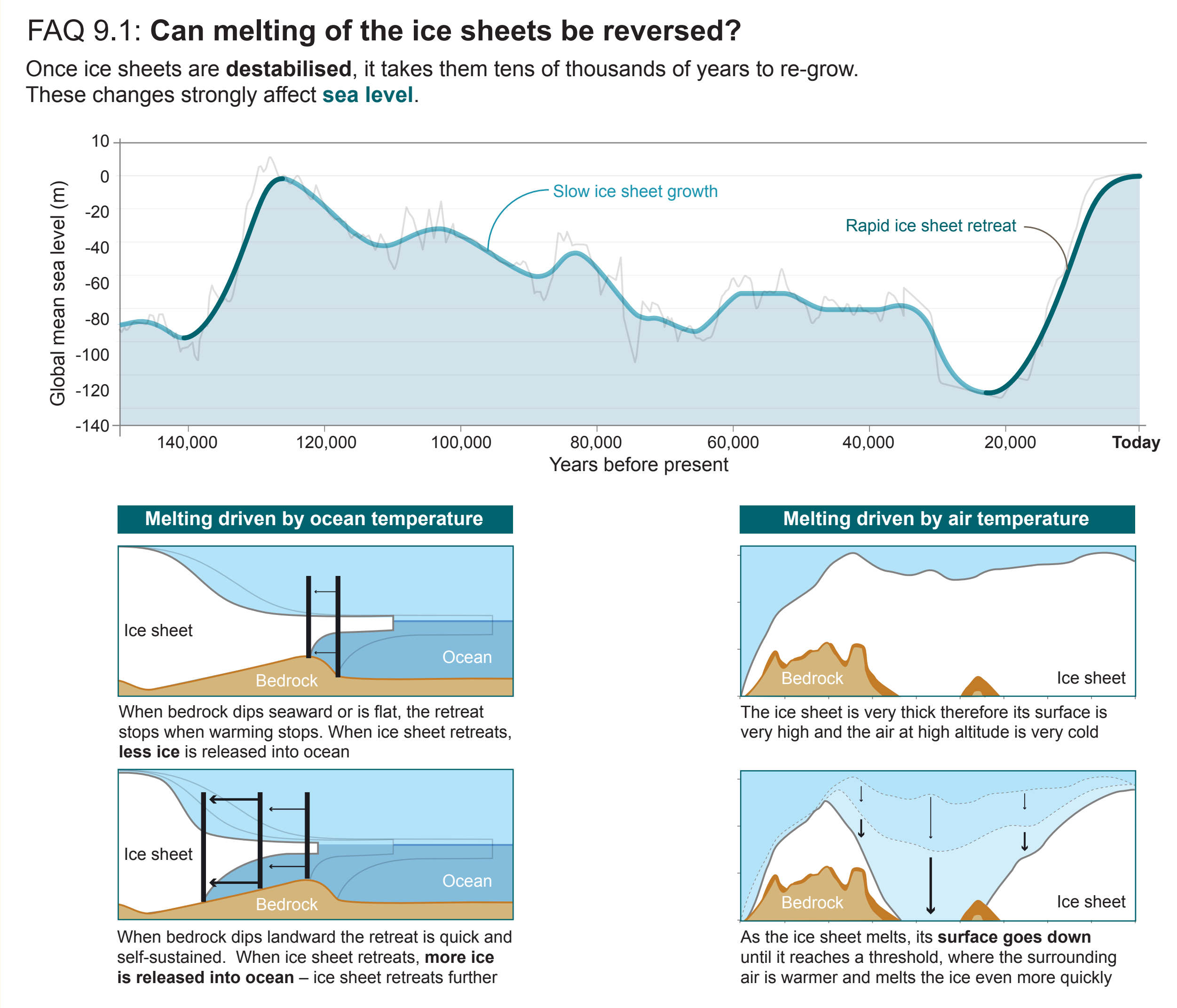

FAQ 9.1, Figure 1 | Ice sheets growth and decay. (Top) Changes in ice-sheet volume modulate sea level variations. The grey line depicts data from a range of physical environmental sea level recorders such as coral reefs while the blue line is a smoothed version of it. **(Bottom left)** Example of destabilization mechanism in Antarctica. **(Bottom right)** Example of destabilization mechanism in Greenland.

Frequently Asked Questions

FAQ 9.2 | How Much Will Sea Level Rise in the Next Few Decades?

As of 2018, global average sea level was about 15–25 cm higher than in 1900, and 7–15 cm higher than in 1971. Sea level will continue to rise by an additional 10–25 cm by 2050. The major reasons for this ongoing rise in sea level are the thermal expansion of seawater as its temperature increases, and the melting of glaciers and ice sheets. Local sea level changes can be larger or smaller than the global average, with the smallest changes in formerly glaciated areas, and the largest changes in low-lying river delta regions.

Across the globe, sea level is rising, and the rate of increase has accelerated. Sea level increased by about 4 mm per year from 2006 to 2018, which was more than double the average rate over the 20th century. Rise during the early 1900s was due to natural factors, such as glaciers catching up to warming that occurred in the Northern Hemisphere during the 1800s. However, since at least 1970, human activities have been the dominant cause of global average sea level rise, and they will continue to be for centuries into the future.

Sea level rises either through warming of ocean waters or the addition of water from melting ice and bodies of water on land. Expansion due to warming caused about 50% of the rise observed from 1971 to 2018. Melting glaciers contributed about 22% over the same period. Melting of the two large ice sheets in Greenland and Antarctica has contributed about 13% and 7%, respectively, during 1971 to 2018, but melting has accelerated in the recent decades, increasing their contribution to 22% and 14% since 2016. Another source is changes in land-water storage: reservoirs and aquifers on land have reduced, which contributed about an 8% increase in sea level.

By 2050, sea level is expected to rise an additional 10–25 cm whether or not greenhouse gas emissions are reduced (FAQ 9.2, Figure 1). Beyond 2050, the amount by which sea level will rise is more uncertain. The accumulated total emissions of greenhouse gases over the upcoming decades will play a big role beyond 2050, especially in determining where sea level rise and ice-sheet changes eventually level off.

Even if net zero emissions are reached, sea level rise will continue because the deep ocean will continue to warm and ice sheets will take time to catch up to the warming caused by past and present emissions: ocean and ice sheets are slow to respond to environmental changes (see FAQ 5.3). Some projections under low emissions show sea level rise continuing as net zero is approached at a rate comparable to today (3–8 mm per year by 2100 versus 3–4 mm per year in 2015), while others show substantial acceleration to more than five times the present rate by 2100, especially if emissions continue to be high and processes that accelerate retreat of the Antarctic Ice Sheet occur widely (FAQ 9.1).

Sea level rise will increase the frequency and severity of extreme sea level events at coasts (see FAQ 8.2), such as storm surges, wave inundation and tidal floods: risk can be increased by even small changes in global average sea level. Scientists project that, in some regions, extreme sea level events that were recently expected once in 100 years will occur annually at 20–25% of locations by 2050 regardless of emissions, but by 2100 emissions choice will matter: annually at 60% of locations for low emissions, and at 80% of locations under strong emissions.

In many places, local sea level change will be larger or smaller than the global average. From year to year and place to place, changes in ocean circulation and wind can lead to local sea level change. In regions where large ice sheets, such as the Fennoscandian in Eurasia and the Laurentide and Cordilleran in North America, covered the land during the last ice age, the land is still slowly rising up now that the extra weight of the ice sheets is gone. This local recovery is compensating for global sea level rise in these regions and can even lead to local decrease in sea level. In regions just beyond where the former ice sheets reached and the Earth bulged upwards, the land is now falling and, as a result, local sea level rise is faster than the global rate. In many regions within low-lying delta regions (such as New Orleans and the Ganges–Brahmaputra delta), the land is rapidly subsiding (sinking) because of human activities such as building dams or groundwater and fossil fuel extraction. Further, when an ice sheet melts, it has less gravitational pull on the ocean water nearby. This reduction in gravitational attraction causes sea level to fall close to the (now less-massive) ice sheet while causing sea level to rise farther away. Melt from a polar ice sheet therefore raises sea level most in the opposite hemisphere or in low latitudes – amounting to tens of centimetres difference in rise between regions by 2100.

FAQ 9.2 (continued)

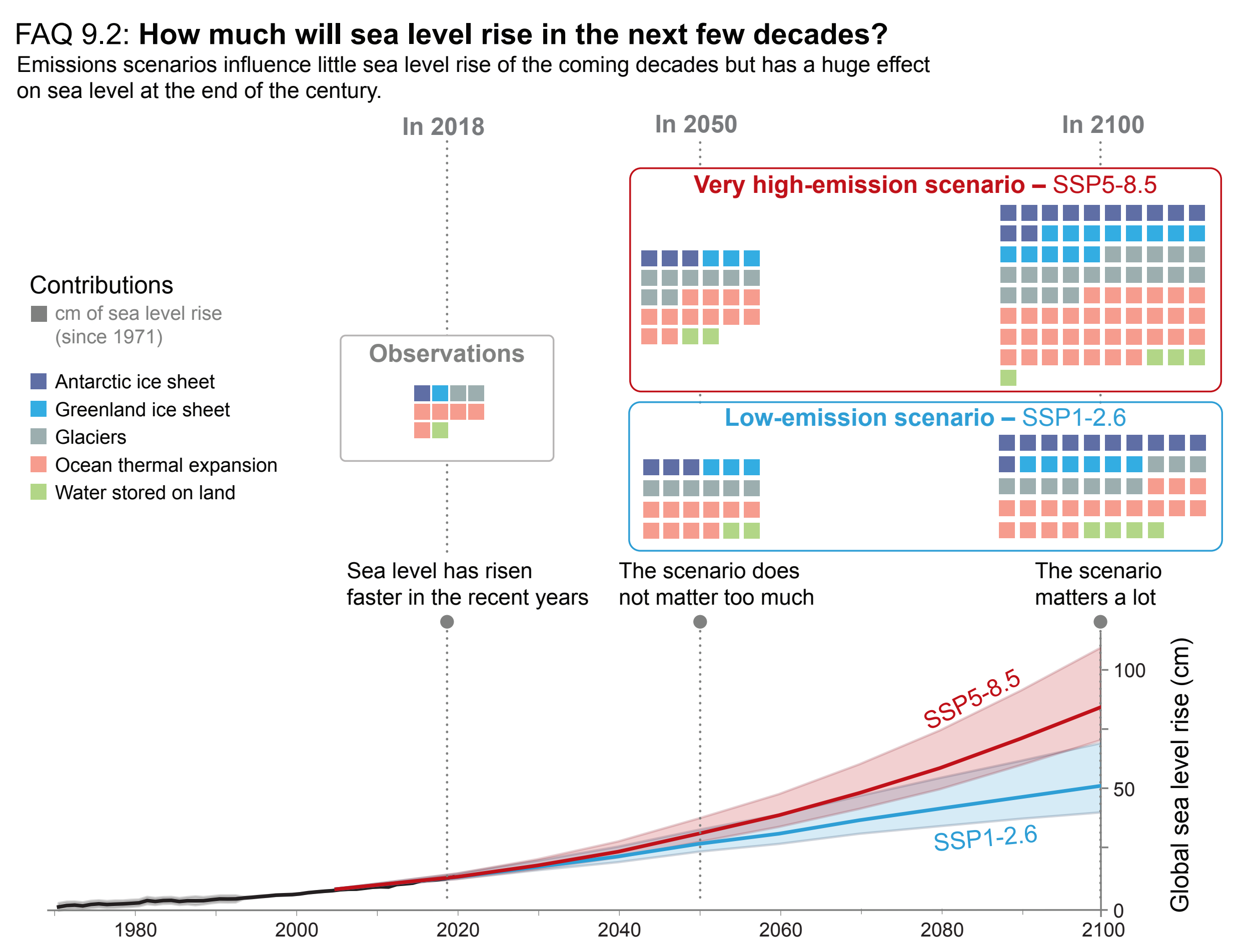

FAQ 9.2, Figure 1 | Observed and projected global mean sea level rise and the contributions from its major constituents.

Frequently Asked Questions

FAQ 9.3 | Will the Gulf Stream Shut Down?

The Gulf Stream is part of two circulation patterns in the North Atlantic: the Atlantic Meridional Overturning Circulation (AMOC) and the North Atlantic subtropical gyre. Based on models and theory, scientific studies indicate that, while the AMOC is expected to slow in a warming climate, the Gulf Stream will not change much and would not shut down totally, even if the AMOC did. Most climate models project that the AMOC slows in the later 21st century under most emissions scenarios, with some models showing it slowing even sooner. The Gulf Stream affects the weather and sea level, so if it slows, North America will see higher sea levels and Europe's weather and rate of relative warming will be affected.

The Gulf Stream is the biggest current in the North Atlantic Ocean. It transports about 30 billion kilograms of water per second northward past points on the east coast of North America. It is a warm current, with temperatures 5°C to 15°C warmer than surrounding waters, so it carries warmer water (thermal energy) from its southern origins and releases warmth to the atmosphere and surrounding water.

The Gulf Stream is part of two major circulation patterns, the Atlantic Meridional Overturning Circulation (AMOC) and the North Atlantic Subtropical Gyre (FAQ 9.3, Figure 1). The rotation of the Earth causes the big currents in both circulations to stay on the western side of their basin, which in the Atlantic means the circulations combine to form the Gulf Stream. Other large currents contribute to gyres, such as the Kuroshio in the North Pacific and the East Australian Current in the South Pacific, but the Gulf Stream is special in its dual role. There is no comparable deep overturning circulation in the North Pacific to the AMOC, so the Kuroshio plays only one role as part of a gyre.

The gyres circulate surface waters and result primarily from winds driving the circulation. These winds are not expected to change much and so neither will the gyres, which means the gyre portion of the Gulf Stream and the Kuroshio will continue to transport thermal energy poleward from the equator much as they do now. The gyre contribution to the Gulf Stream is 2 to 10 times larger than the AMOC contribution.

The Gulf Stream's role in the AMOC is supplying surface source water that cools, becomes denser and sinks to form cold, deep waters that travel back equatorward, spilling over features on the ocean floor and mixing with other deep Atlantic waters to form a southward current at a depth of about 1500 metres beneath the Gulf Stream. This overturning flow is the AMOC, with the Gulf Stream in the upper kilometre flowing northward, and the colder deep water flowing southward.

The AMOC is expected to slow over the coming centuries. One reason why is freshening of the ocean waters: by meltwater from Greenland, changing Arctic sea ice, and increased precipitation over warmer northern seas. An array of moorings across the Atlantic has been monitoring the AMOC since 2004, with recently expanded capabilities. The monitoring of the AMOC has not been long enough for a trend to emerge from variability and detect long-term changes that may be underway (see FAQ 1.2). Other indirect signs may indicate slowing overturning – for example, slower warming where the Gulf Stream's surface waters sink. Climate models show that this 'cold spot' of slower-than-average warming occurs as the AMOC weakens, and they project that this will continue. Paleoclimate evidence indicates that the AMOC changed significantly in the past, especially during transitions from colder climates to warmer ones, but that it has been stable for 8000 years.

What happens if the AMOC slows in a warming world? The atmosphere adjusts somewhat by carrying more heat, compensating partly for the decreases in heat carried by AMOC. But the 'cold spot' makes parts of Europe warm more slowly. Models indicate that weather patterns in Greenland and around the Atlantic will be affected, with reduced precipitation in the mid-latitudes, changing strong precipitation patterns in the tropics and Europe, and stronger storms in the North Atlantic storm track. The slowing of this current combined with the rotation of the Earth means that sea level along North America rises as the AMOC contribution to the Gulf Stream slows.

The North Atlantic is not the only site of sensitive meridional overturning. Around Antarctica, the world's densest seawater is formed by freezing into sea ice, leaving behind salty, cold water that sinks to the bottom and spreads northward. Recent studies show that melting of the Antarctic Ice Sheet and changing winds over the Southern Ocean can affect this southern meridional overturning, affecting regional weather.

FAQ 9.3 (continued)

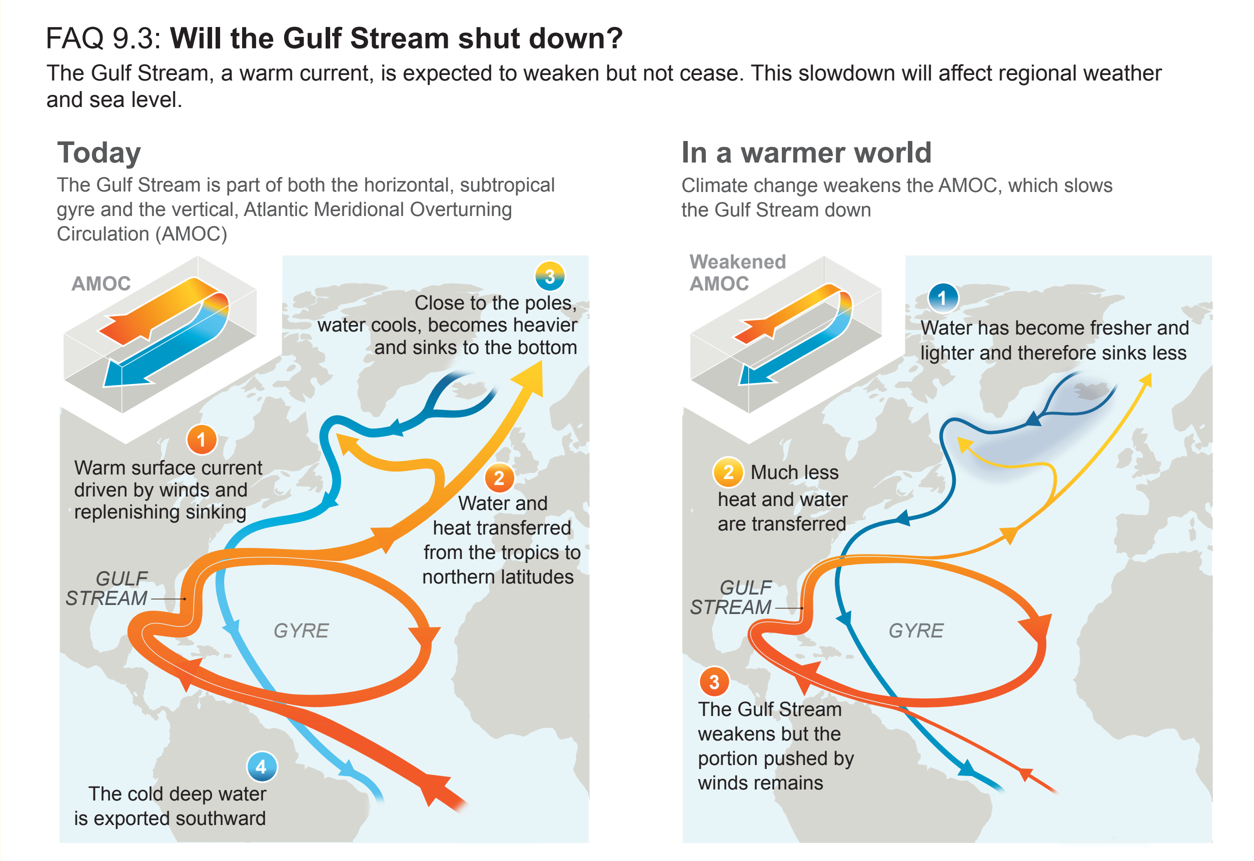

FAQ 9.3, Figure 1 | Horizontal (gyre) and vertical (Atlantic Meridional Overturning Circulation, AMOC) circulations in the Atlantic today (left) and in a warmer world (right). The Gulf Stream is a warm current composed of both circulations.

Frequently Asked Questions

FAQ 10.1 | How Can We Provide Useful Climate Information for Regional Stakeholders?

The world is physically and culturally diverse, and the challenges posed by climate change vary by region and location. Because climate change affects so many aspects of people's daily work and living, climate change information can help with decision-making, but only when the information is relevant for the people involved in making those decisions. Users of climate information may be highly diverse, ranging from professionals in areas such as human health, agriculture or water management to a broader community that experiences the impacts of changing climate. Providing information that supports response actions thus requires engaging all relevant stakeholders, their knowledge and their experiences, formulating appropriate information, and developing a mutual understanding of the usefulness and limitations of the information.

The development, delivery, and use of climate change information requires engaging all parties involved: those producing the climate data and related knowledge, those communicating it, and those who combine that information with their knowledge of the community, region or activity that climate change may impact. To be successful, these parties need to work together to explore the climate data and thus co-develop the climate information needed to make decisions or solve problems, distilling output from the various sources of climate knowledge into relevant climate information. Effective partnerships recognize and respond to the diversity of all parties involved (including their values, beliefs and interests), especially when they involve culturally diverse communities and their indigenous and local knowledge of weather, climate and their society. This is particularly true for climate change – a global issue posing challenges that vary by region. By recognizing this diversity, climate information can be relevant and credible, most notably when conveying the complexity of risks for human systems and ecosystems and for building resilience.

Constructing useful climate information requires considering all available sources in order to capture the fullest possible representation of projected changes and distilling the information in a way that meets the needs of the stakeholders and communities impacted by the changes. For example, climate scientists can provide information on future changes by using simulations of global and/or regional climate and inferring changes in the weather behaviour influencing a region. An effective distillation process (FAQ 10.1, Figure 1) engages with the intended recipients of the information, especially stakeholders whose work involves non-climatic factors, such as human health, agriculture or water resources. The distillation evaluates the accuracy of all information sources (observations, simulations, expert judgement), weighs the credibility of possible conflicting information, and arrives at climate information that includes estimating the confidence a user should have in it. Producers of climate data should further recognize that the geographic regions and time periods governing stakeholders' interest (for example, the growing season of an agricultural zone) may not align well with the time and space resolution of available climate data; thus additional model development or data processing may be required to extract useful climate information.

One way to distil complex information for stakeholder applications is to connect this information to experiences stakeholders have already had through storylines as plausible unfoldings of weather and climate events related to stakeholders' experiences. Dialogue between stakeholders and climate scientists can determine the most relevant experiences to evaluate for possible future behaviour. The development of storylines uses the experience and expertise of stakeholders, such as water-resource managers and health professionals, who seek to develop appropriate response measures. Storylines are thus a pathway through the distillation process that can make climate information more accessible and physically comprehensible. For example, a storyline may take a common experience like an extended drought, with depleted water availability and damaged crops, and show how droughts may change in the future, perhaps with even greater precipitation deficits or longer duration. With appropriate choices, storylines can engage nuances of the climate information in a meaningful way by building on common experiences, thus enhancing the information's usefulness.

Forging partnerships among all involved with producing, exploring and distilling climate data into climate information is at the centre of creating stakeholder-relevant information. These partnerships can occur through direct interaction between climate scientists and stakeholders as well as through organizations that have emerged to facilitate this process, such as climate services, national and regional climate forums, and consulting firms providing specialized climate information. These so-called 'boundary organizations' can serve the varied needs of all who would fold climate information into their decision processes. All of these partnerships are vital

FAQ 10.1 (continued)

for arriving at climate information that responds to physical and cultural diversity and to challenges posed by climate change that can vary region-by-region around the world.

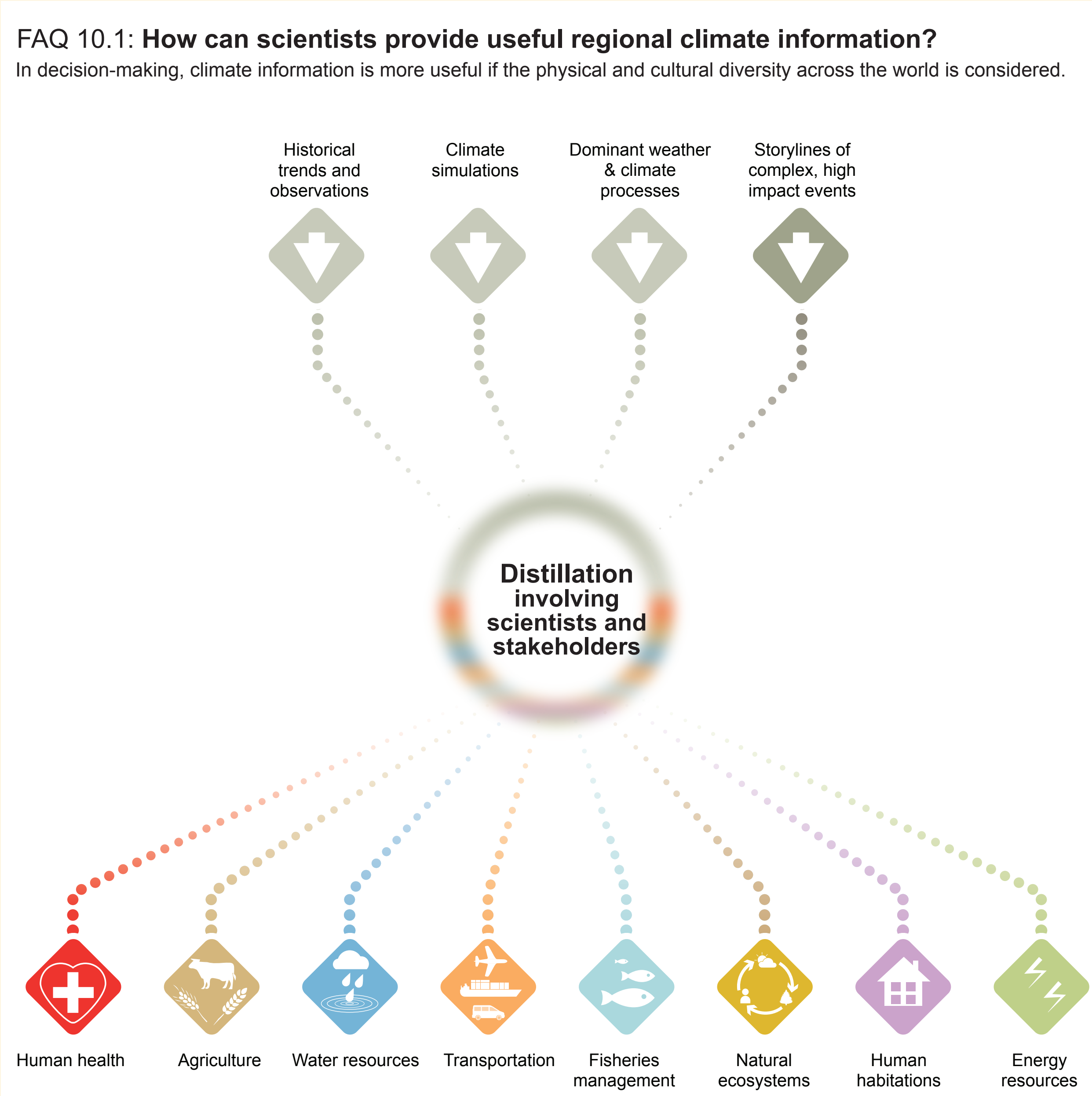

FAQ 10.1, Figure 1 | Climate information for decision makers is more useful if the physical and cultural diversity across the world is considered. The figure illustrates schematically the broad range of knowledge that must be blended with the diversity of users to distil information that will have relevance and credibility. This blending or distillation should engage the values and knowledge of both the stakeholders and the scientists. The bottom row contains examples of stakeholders' interests and is not all-inclusive. As part of the distillation, the outcomes can advance the United Nations' Sustainable Development Goals, covered in part by these examples.

FAQ

Frequently Asked Questions

FAQ 10.2 | Why Are Cities Hotspots of Global Warming?

Urban areas experience air temperatures that can be several degrees Celsius warmer than surrounding areas, especially during the night. This 'urban heat island' effect results from several factors, including reduced ventilation and heat trapping due to the close proximity of tall buildings, heat generated directly from human activities, the heat-absorbing properties of concrete and other urban building materials, and the limited amount of vegetation. Continuing urbanization and increasingly severe heatwaves under climate change will further amplify this effect in the future.

Today, cities are home to 55% of the world's population. This number is increasing, and every year cities welcome 67 million new residents, 90% of whom are moving to cities in developing countries. By 2030, almost 60% of the world's population is expected to live in urban areas. Cities and their inhabitants are highly vulnerable to weather and climate extremes, particularly heatwaves, because urban areas already are local hotspots. Cities are generally warmer – up to several degrees Celsius at night – than their surroundings. This warming effect, called the urban heat island, occurs because cities both receive and retain more heat than the surrounding countryside areas and because natural cooling processes are weakened in cities compared to rural areas.

Three main factors contribute to amplify the warming of urban areas (orange bars in FAQ 10.2, Figure 1). The strongest contribution comes from urban geometry, which depends on the number of buildings, their size and their proximity. Tall buildings close to each other absorb and store heat and also reduce natural ventilation. Human activities, which are very concentrated in cities, also directly warm the atmosphere locally, due to heat released from domestic and industrial heating or cooling systems, running engines, and other sources. Finally, urban warming also results directly from the heat-retaining properties of the materials that make up cities, including concrete buildings, asphalt roadways, and dark rooftops. These materials are very good at absorbing and retaining heat, and then re-emitting that heat at night.

The urban heat island effect is further amplified in cities that lack vegetation and water bodies, both of which can strongly contribute to local cooling (green bars in FAQ 10.2, Figure 1). This means that when enough vegetation and water are included in the urban fabric, they can counterbalance the urban heat island effect, to the point of even cancelling out the urban heat island effect in some neighbourhoods.

The urban heat island phenomenon is well-known and understood. For instance, temperature measurements from thermometers located in cities are corrected for this effect when global warming trends are calculated. Nevertheless, observations, including long-term measurements of the urban heat island effect are currently too limited to allow a full understanding of how the urban heat island varies across the world and across different types of cities and climatic zones, or how this effect will evolve in the future.

As a result, it is hard to assess how climate change will affect the urban heat island effect, and various studies disagree. Two things are, however, very clear. First, future urbanization will expand the urban heat island areas, thereby amplifying future warming in many places all over the world. In some places, the nighttime warming from the urban heat island effect could even be on the same order of magnitude as the warming expected from human-induced climate change. Second, more intense, longer and more frequent heatwaves caused by climate change will more strongly impact cities and their inhabitants, because the extra warming from the urban heat island effect will exacerbate the impacts of climate change.

In summary, cities are currently local hotspots because their structure, material and activities trap and release heat and reduce natural cooling processes. In the future, climate change will, on average, have a limited effect on the magnitude of the urban heat island itself, but ongoing urbanization together with more frequent, longer and warmer heatwaves will make cities more exposed to global warming.

FAQ 10.2 (continued)

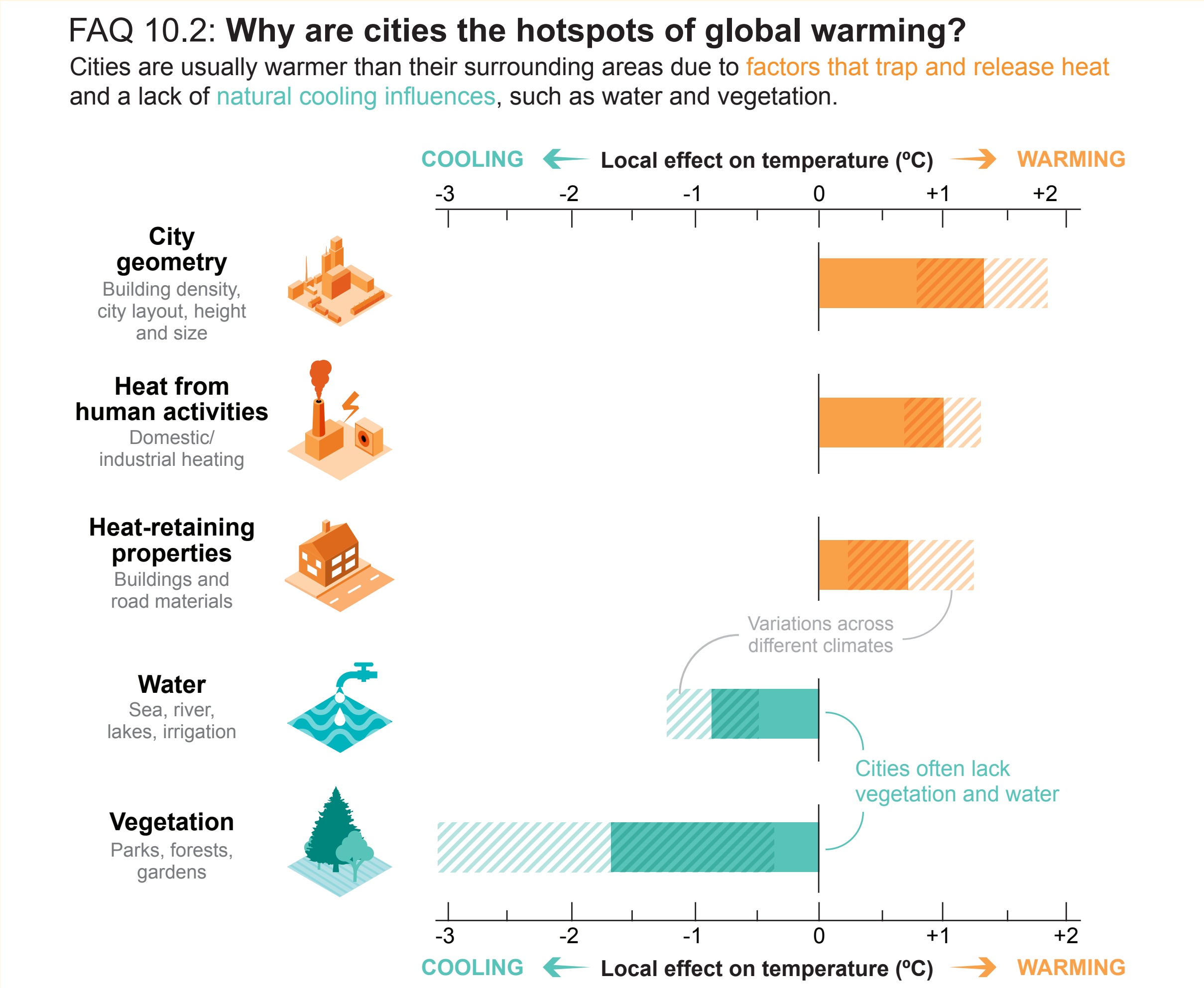

FAQ 10.2, Figure 1 | Efficiency of the various factors at warming up or cooling down neighbourhoods of urban areas. Overall, cities tend to be warmer than their surroundings. This is called the 'urban heat island' effect. The hatched areas on the bars show how the strength of the warming or cooling effects of each factor varies depending on the local climate. For example, vegetation has a stronger cooling effect in temperate and warm climates. Further details on data sources are available in the chapter data table (Table 10.SM.11).

FAQ

Frequently Asked Questions

FAQ 11.1 | How Do Changes In Climate Extremes Compare With Changes In Climate Averages?

Human-caused climate change alters the frequency and intensity of climate variables (e.g., surface temperature) and phenomena (e.g., tropical cyclones) in a variety of ways. We now know that the ways in which average and extreme conditions have changed (and will continue to change) depend on the variable and the phenomenon being considered. Changes in local surface temperature extremes closely follow the corresponding changes in local average surface temperatures. On the contrary, changes in precipitation extremes (heavy precipitation) generally do not follow those in average precipitation, and can even move in the opposite direction (e.g., with average precipitation decreasing but extreme precipitation increasing).

Climate change will manifest very differently depending on which region, season and variable we are interested in. For example, over some parts of the Arctic, temperatures will warm at rates about three to four times higher during winter compared to summer months. And in summer, most of northern Europe will experience larger temperatures increases than most places in south-east South America and Australasia, with differences that can be larger than 1°C, depending on the level of global warming. In general, differences across regions and seasons arise because the underlying physical processes differ drastically across regions and seasons.

Climate change will also manifest differently for different weather regimes and can lead to contrasting changes in average and extreme conditions. Observations of the recent past and climate model projections show that, in most places, changes in daily temperatures are dominated by a general warming where the climatological average and extreme values are shifted towards higher temperatures, making warm extremes more frequent and cold extremes less frequent. The top panels in FAQ 11.1, Figure 1 show projected changes in surface temperature for long-term average conditions (left) and for extreme hot days (right) during the warm season (summer in mid- to high latitudes). Projected increases in long-term average temperature differ substantially between different places, varying from less than 3°C in some places in central South Asia and southern South America to over 7°C in some places in North America, North Africa and the Middle East. Changes in extreme hot days follow changes in average conditions quite closely, although, in some places, the warming rates for extremes can be intensified (e.g., southern Europe and the Amazon basin) or weakened (e.g., northern Asia and Greenland) compared to average values.

Recent observations and global and regional climate model projections point to changes in precipitation extremes (including both rainfall and snowfall extremes) differing drastically from those in average precipitation. The bottom panels in FAQ 11.1, Figure 1 show projected changes in the long-term average precipitation (left) and in heavy precipitation (right). Averaged precipitation changes show striking regional differences, with substantial drying in places such as southern Europe and northern South America and wetting in places such as the Middle East and southern South America. Changes in extreme precipitation are much more uniform, with systematic increases over nearly all land regions. The physical reasons behind the different responses of averaged and extreme precipitation are now well understood. The intensification of extreme precipitation is driven by the increase in atmospheric water vapour (about 7% per 1°C of warming near the surface), although this is modulated by various dynamical changes. In contrast, changes in average precipitation are driven not only by moisture increases but also by slower processes that constrain future changes over the globe to only 2–3% per 1°C of warming near the surface.

In summary, the specific relationship between changes in average and extreme conditions strongly depends on the variable or phenomenon being considered. At the local scale, average and extreme surface temperature changes are strongly related, while average and extreme precipitation changes are often weakly related. For both variables, the changes in average and extreme conditions vary strongly across different places due to the effect of local and regional processes.

FAQ 11.1 (continued)

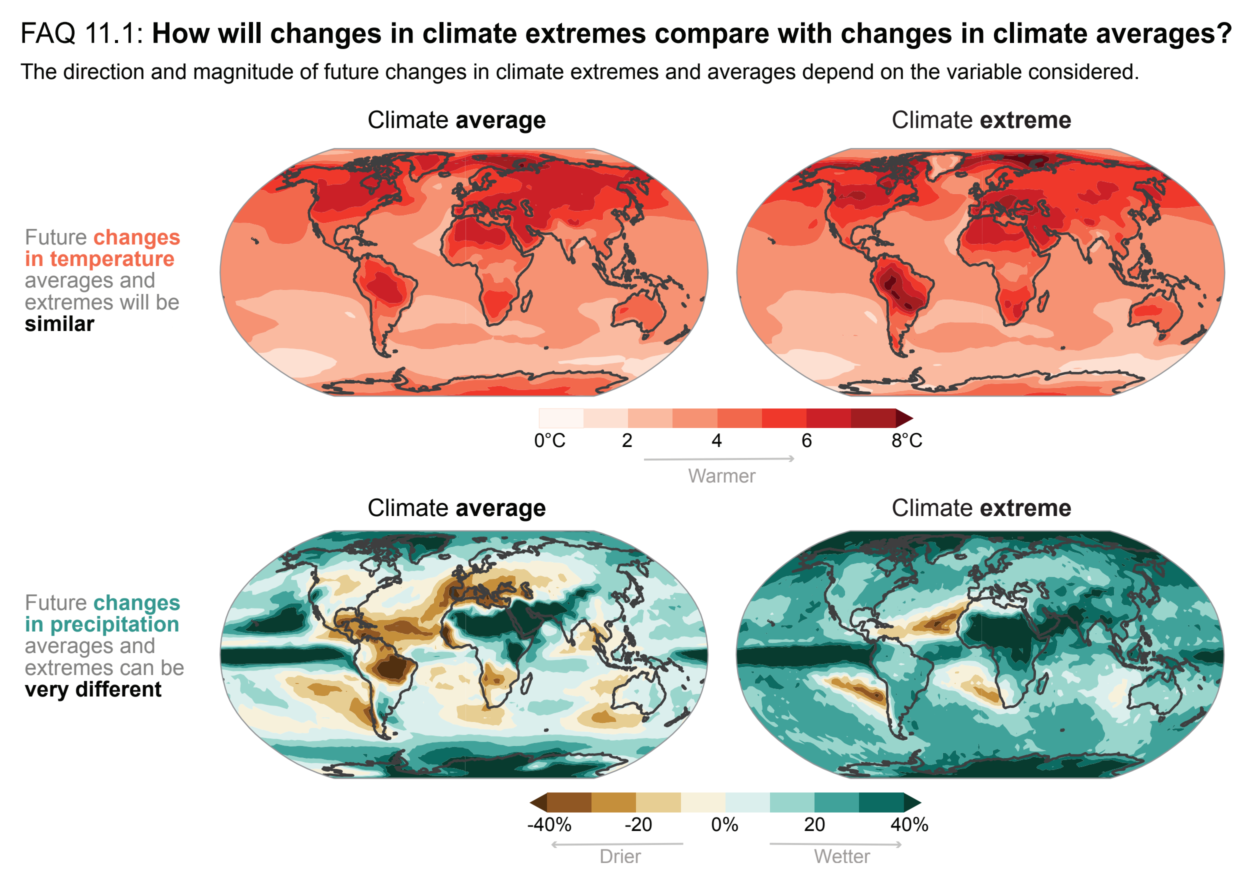

FAQ 11.1, Figure 1 | Global maps of future changes in surface temperature (top panels) and precipitation (bottom panels) for long-term average (left) and extreme conditions (right). All changes were estimated using the Coupled Model Intercomparison Project Phase 6 (CMIP6) ensemble median for a scenario with a global warming of 4°C relative to 1850–1900 temperatures. Average surface temperatures refer to the warmest three-month season (summer in mid- to high latitudes) and extreme temperatures refer to the hottest day in a year. Precipitation changes, which can include both rainfall and snowfall changes, are normalized by 1850–1900 values and shown as a percentage; extreme precipitation refers to the largest daily precipitation in a year.

Frequently Asked Questions

FAQ 11.2 | Will Unprecedented Extremes Occur As a Result Of Human-Induced Climate Change?

Climate change has already increased the magnitude and frequency of extreme hot events and decreased the magnitude and frequency of extreme cold events, and, in some regions, intensified extreme precipitation events. As the climate moves away from its past and current states, we will experience extreme events that are unprecedented, either in magnitude, frequency, timing or location. The frequency of these unprecedented extreme events will rise with increasing global warming. Additionally, the combined occurrence of multiple unprecedented extremes may result in large and unprecedented impacts.

Human-induced climate change has already affected many aspects of the climate system. In addition to the increase in global surface temperature, many types of weather and climate extremes have changed. In most regions, the frequency and intensity of hot extremes have increased and those of cold extremes have decreased. The frequency and intensity of heavy precipitation events have increased at the global scale and over a majority of land regions. Although extreme events such as land and marine heatwaves, heavy precipitation, drought, tropical cyclones, and associated wildfires and coastal flooding have occurred in the past and will continue to occur in the future, they often come with different magnitudes or frequencies in a warmer world. For example, future heatwaves will last longer and have higher temperatures, and future extreme precipitation events will be more intense in several regions. Certain extremes, such as extreme cold, will be less intense and less frequent with increasing warming.

Unprecedented extremes – that is, events not experienced in the past – will occur in the future in five different ways (FAQ 11.2, Figure 1). First, events that are considered to be extreme in the current climate will occur in the future with unprecedented magnitudes. Second, future extreme events will also occur with unprecedented frequency. Third, certain types of extremes may occur in regions that have not previously encountered those types of events. For example, as the sea level rises, coastal flooding may occur in new locations, and wildfires are already occurring in areas, such as parts of the Arctic, where the probability of such events was previously low. Fourth, extreme events may also be unprecedented in their timing. For example, extremely hot temperatures may occur either earlier or later in the year than they have in the past.

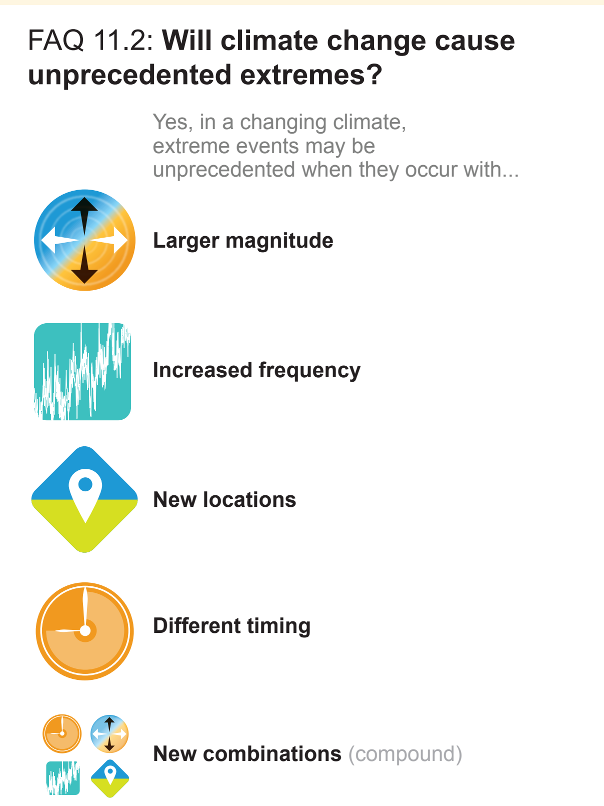

FAQ 11.2, Figure 1 | New types of unprecedented extremes that will occur as a result of climate change.

Finally, compound events – where multiple extreme events of either different or similar types occur simultaneously and/or in succession – may be more probable or severe in the future. These compound events can often impact ecosystems and societies more strongly than when such events occur in isolation. For example, a drought along with extreme heat will increase the risk of wildfires and agriculture damages or losses. As individual extreme events become more severe as a result of climate change, the combined occurrence of these events will create unprecedented compound events. This could exacerbate the intensity and associated impacts of these extreme events.

Unprecedented extremes have already occurred in recent years, relative to the 20th century climate. Some recent extreme hot events would have had very little chance of occurring without human influence on the climate (see FAQ 11.3). In the future, unprecedented extremes will occur as the climate continues to warm. Those extremes will happen with larger magnitudes and at higher frequencies than previously experienced. Extreme events may also appear in new locations, at new times of the year, or as unprecedented compound events. Moreover, unprecedented events will become more frequent with higher levels of warming, for example at 3°C of global warming compared to 2°C of global warming.

Frequently Asked Questions

FAQ 11.3 | Did Climate Change Cause That Recent Extreme Event In My Country?

While it is difficult to identify the exact causes of a particular extreme event, the relatively new science of event attribution is able to quantify the role of climate change in altering the probability and magnitude of some types of weather and climate extremes. There is strong evidence that characteristics of many individual extreme events have already changed because of human-driven changes to the climate system. Some types of highly impactful extreme weather events have occurred more often and have become more severe due to these human influences. As the climate continues to warm, the observed changes in the probability and/or magnitude of some extreme weather events will continue as the human influences on these events increase.

It is common to question whether human-caused climate change caused a major weather- and climate-related disaster. When extreme weather and climate events do occur, both exposure and vulnerability play an important role in determining the magnitude and impacts of the resulting disaster. As such, it is difficult to attribute a specific disaster directly to climate change. However, the relatively new science of event attribution enables scientists to attribute aspects of specific extreme weather and climate events to certain causes. Scientists cannot answer directly whether a particular event was caused by climate change, as extremes do occur naturally, and any specific weather and climate event is the result of a complex mix of human and natural factors. Instead, scientists quantify the relative importance of human and natural influences on the magnitude and/or probability of specific extreme weather events. Such information is important for disaster risk reduction planning, because improved knowledge about changes in the probability and magnitude of relevant extreme events enables better quantification of disaster risks.

On a case-by-case basis, scientists can now quantify the contribution of human influences to the magnitude and probability of many extreme events. This is done by estimating and comparing the probability or magnitude of the same type of event between the current climate – including the increases in greenhouse gas concentrations and other human influences – and an alternate world where the atmospheric greenhouse gases remained at pre-industrial levels. FAQ 11.3 Figure 1 illustrates this approach using differences in temperature and probability between the two scenarios as an example. Both the pre-industrial (blue) and current (red) climates experience hot extremes, but with different probabilities and magnitudes. Hot extremes of a given temperature have a higher probability of occurrence in the warmer current climate than in the cooler pre-industrial climate. Additionally, an extreme hot event of a particular probability will be warmer in the current climate than in the pre-industrial climate. Climate model simulations are often used to estimate the occurrence of a specific event in both climates. The change in the magnitude and/or probability of the extreme event in the current climate compared to the pre-industrial climate is attributed to the difference between the two scenarios, which is the human influence.

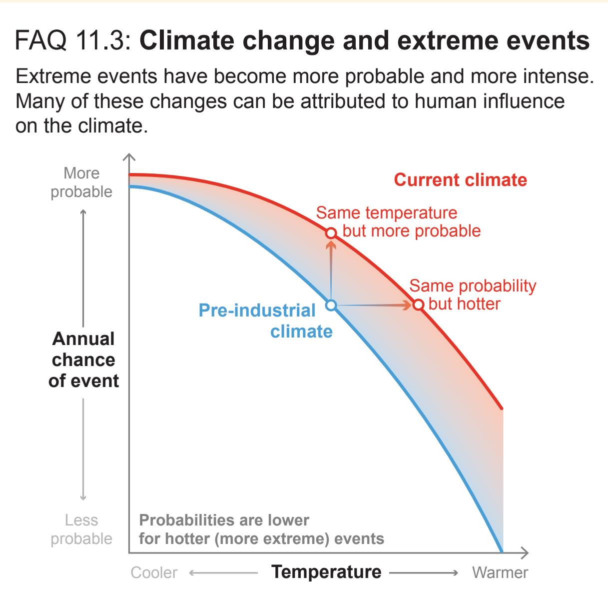

FAQ 11.3, Figure 1 | Changes in climate result in changes in the magnitude and probability of extremes. Example of how temperature extremes differ between a climate with pre-industrial greenhouse gases (shown in blue) and the current climate (shown in orange) for a representative region. The horizontal axis shows the range of extreme temperatures, while the vertical axis shows the annual chance of each temperature event's occurrence. Moving towards the right indicates increasingly hotter extremes that are more rare (less probable). For hot extremes, an extreme event of a particular temperature in the pre-industrial climate would be more probable (vertical arrow) in the current climate. An event of a certain probability in the pre-industrial climate would be warmer (horizontal arrow) in the current climate. While the climate under greenhouse gases at the pre-industrial level experiences a range of hot extremes, such events are hotter and more frequent in the current climate.

Attributable increases in probability and magnitude have been identified consistently for many hot extremes. Attributable increases have also been found for some extreme precipitation events, including hurricane rainfall events, but these results can vary among events. In some cases, large natural variations in the climate system prevent attributing changes in the probability or magnitude of a specific extreme to human influence. Additionally, attribution of certain classes of extreme weather (e.g., tornadoes) is beyond current modelling and theoretical capabilities. As the climate continues to warm, larger changes in

FAQ 11.3 (continued)

probability and magnitude are expected and, as a result, it will be possible to attribute future temperature and precipitation extremes in many locations to human influences. Attributable changes may emerge for other types of extremes as the warming signal increases.

In conclusion, human-caused global warming has resulted in changes in a wide variety of recent extreme weather events. Strong increases in probability and magnitude, attributable to human influence, have been found for many heatwaves and hot extremes around the world.

Frequently Asked Questions

FAQ 12.1 | What Is a Climatic Impact-driver (CID)?

A climatic impact-driver is a physical climate condition that directly affects society or ecosystems. Climatic impact-drivers may represent a long-term average condition (such as the average winter temperatures that affect indoor heating requirements), a common event (such as a frost that kills off warm-season plants), or an extreme event (such as a coastal flood that destroys homes). A single climatic impact-driver may lead to detrimental effects for one part of society while benefiting another, while others are not affected at all. A climatic impact-driver (or its change caused by climate change) is therefore not universally hazardous or beneficial, but we refer to it as a 'hazard' when experts determine it is detrimental to a specific system.

Climate change can alter many aspects of the climate system, but efforts to identify impacts and risks usually focus on a smaller set of changes known to affect, or potentially affect, things that society cares about. These *climatic impact-drivers* (CIDs) are formally defined in this Report as 'physical climate system conditions (e.g., means, events, extremes) that affect an element of society or ecosystems. Depending on system tolerance, CIDs and their changes can be detrimental, beneficial, neutral, or a mixture of each across interacting system elements and regions'. Because people, infrastructure and ecosystems interact directly with their immediate environment, climate experts assess CIDs locally and regionally. CIDs may relate to temperature, the water cycle, wind and storms, snow and ice, oceanic and coastal processes or the chemistry and energy balance of the climate system. Future impacts and risk may also be directly affected by factors unrelated to the climate (such as socio-economic development, population growth, or a viral outbreak) that may also alter the vulnerability or exposure of systems.

CIDs capture important characteristics of the average climate and both common and extreme events that shape society and nature (see FAQ 12.2). Some CIDs focus on aspects of the average climate (such as the seasonal progression of temperature and precipitation, average winds or the chemistry of the ocean) that determine, for example, species distribution, farming systems, the location of tourist resorts, the availability of water resources and the expected heating and cooling needs for buildings in an average year. CIDs also include common episodic events that are particularly important to systems, such as thaw events that can trigger the development of plants in spring, cold spells that are important for fruit crop chill requirements, or frost events that eliminate summer vegetation as winter sets in. Finally, CIDs include many extreme events connected to impacts such as hailstorms that damage vehicles, coastal floods that destroy shoreline property, tornadoes that damage infrastructure, droughts that increase competition for water resources, and heatwaves that can strain the health of outdoor labourers.

Many aspects of our daily lives, businesses and natural systems depend on weather and climate, and there is great interest in anticipating the impacts of climate change on the things we care about. To meet these needs, scientists engage with companies and authorities to provide climate services – meaningful and possibly actionable climate information designed to assist decision-making. Climate science and services can focus on CIDs that substantially disrupt systems to support broader risk management approaches. A single CID change can have dramatically different implications for different sectors or even elements of the same sector, so engagement between climate scientists and stakeholders is important to contextualize the climate changes that will come. Climate services responding to planning and optimization of an activity can focus on more gradual changes in operating climate conditions.

FAQ 12.1, Figure 1 tracks example outcomes of seasonal snow cover changes that connect climate science to the need for mitigation, adaptation and regional risk management. The length of the season with snow on the ground is just one of many regional climate conditions that may change in the future, and it becomes a CID because there are many elements of society and ecosystems that rely on an expected seasonality of snow cover. Climate scientists and climate service providers examining human-driven climate change may identify different regions where the length of the season with snow cover could increase, decrease, or stay relatively unaffected. In each region, change in seasonal snow cover may affect different systems in beneficial or detrimental ways (in the latter case, changing seasonal snow cover would be a 'hazard'), although systems such as coastal aquaculture remain relatively unaffected. The changing profile of benefits and hazards connected to these changes in the seasonal snow cover CID affects the profile of impacts, risks and benefits that stakeholders in the region will grapple with in response to climate change.

FAQ 12.1 (continued)

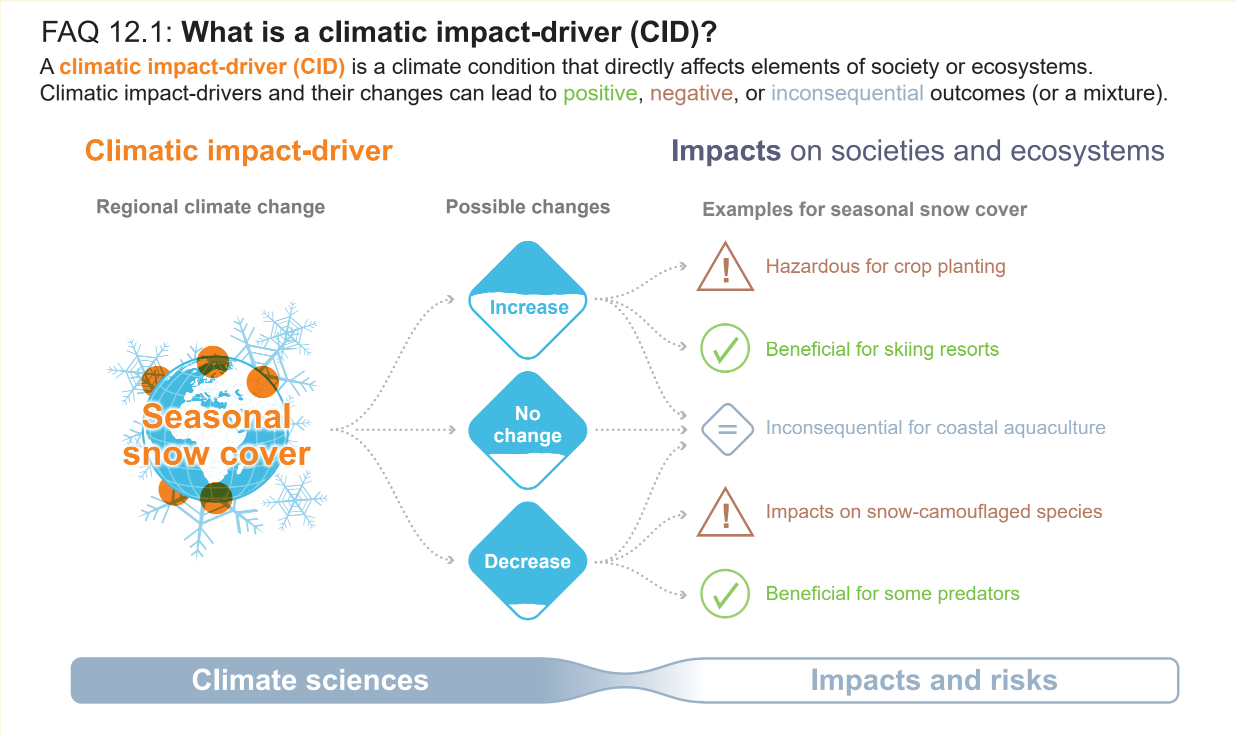

FAQ 12.1, Figure 1 | A single climatic impact-driver can affect ecosystems and society in different ways. A variety of impacts from the same climatic impact-driver change, illustrated with the example of regional seasonal snow cover.

FAQ

Frequently Asked Questions

FAQ 12.2 | What Are Climatic Thresholds and Why Are They Important?

Climatic thresholds tell us about the tolerance of society and ecosystems so that we can better scrutinize the types of climate changes that are expected to impact things we care about. Many systems have natural or structural thresholds. If conditions exceed those thresholds, the result can be sudden changes or even collapses in health, productivity, utility or behaviour. Adaptation and risk management efforts can change these thresholds, altering the profile of climate conditions that would be problematic and increasing overall system resilience.

Decision makers have long observed that certain weather and climate conditions can be problematic, or hazardous, for things they care about (i.e., things with socio-economic, cultural or intrinsic value). Many elements of society and ecosystems operate in a suitable climate zone selected naturally or by stakeholders considering the expected climate conditions. However, as climate change moves conditions beyond expected ranges, they may cross a climatic 'threshold' – a level beyond which there are either gradual changes in system behaviour or abrupt, non-linear and potentially irreversible impacts.

Climatic thresholds can be associated with either natural or structural tolerance levels. Natural thresholds, for instance, include heat and humidity conditions above which humans cannot regulate their internal temperatures through sweat, drought durations that heighten competition between species, and winter temperatures that are lethal for pests or disease-carrying vector species. Structural thresholds include engineered limits of drainage systems, extreme wind speeds that limit wind turbine operation, the height of coastal protection infrastructure, and the locations of irrigation infrastructure or tropical cyclone sheltering facilities.

Thresholds may be defined according to raw values (such as maximum temperature exceeding 35°C) or percentiles (such as the local 99th percentile daily rainfall total). They also often have strong seasonal dependence (see FAQ 12.3). For example, the amount of snowfall that a deciduous tree can withstand depends on whether the snowfall occurs before or after the tree sheds its leaves. Most systems respond to changes in complex ways, and those responses are not determined solely or precisely by specific thresholds of a single climate variable. Nonetheless, thresholds can be useful indicators of system behaviours, and an understanding of these thresholds can help inform risk management decisions.

FAQ 12.2 Figure 1 illustrates how threshold conditions can help us understand climate conditions that are suitable for normal system operation and the thresholds beyond which impacts occur. Crops tend to grow most optimally within a suitable range of daily temperatures that is influenced by the varieties being cultivated and the way the farm is managed. As daily temperatures rise above a 'critical' temperature threshold, plants begin to experience heat stress that reduces growth and may lower resulting yields. If temperatures reach a higher 'limiting' temperature threshold, crops may suffer leaf loss, pollen sterility, or tissue damage that can lead to crop failure. Farmers typically select a cropping system with some consideration to the probability of extreme temperature events that may occur within a typical season, and so identifying hot temperature thresholds helps farmers select their seed and field management strategies as part of their overall risk management. Climate experts may therefore aim to assist farm planning by providing information about the climate change-induced shifts to the expected frequency of daily heat extremes that exceed crop tolerance thresholds.

Adaptation and other changes in societies and environment can shift climatic thresholds by modifying vulnerability and exposure. For example, adaptation efforts may include breeding new crops with higher heat tolerance levels so that corresponding dangerous thresholds occur less frequently. Likewise, increasing the height of a flood embankment protecting a given community can increase the level of river flow that may be tolerated without flooding, reducing the frequency of damaging floods. Stakeholders therefore benefit from climate services that are based on a co-development process, with scientists identifying system-relevant thresholds and developing tailored climatic impact-driver indices that represent these thresholds (FAQ 12.1). These thresholds help focus the provision of action-relevant climate information for adaptation and risk management.

FAQ 12.2 (continued)

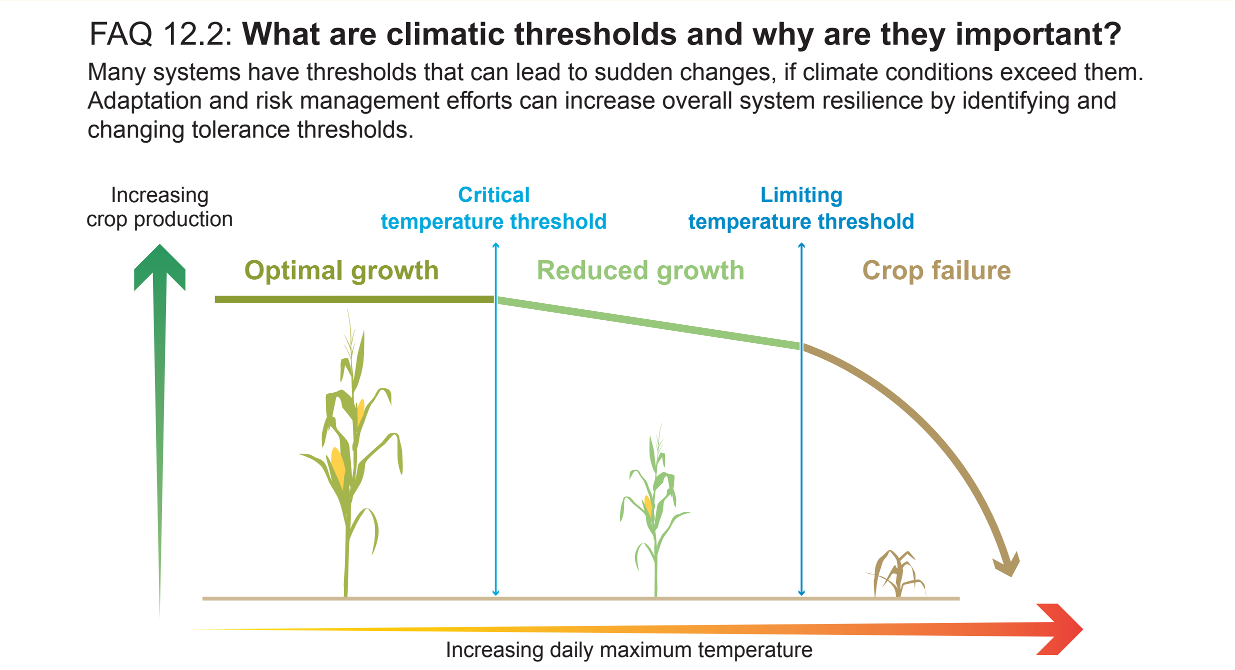

FAQ 12.2, Figure 1 | Crop response to maximum temperature thresholds. Crop growth rate responds to daily maximum temperature increases, leading to reduced growth and crop failure as temperatures exceed critical and limiting temperature thresholds, respectively. Note that changes in other environmental factors (such as carbon dioxide and water) may increase the tolerance of plants to increasing temperatures.

FAQ

Frequently Asked Questions

FAQ 12.3 | How Will Climate Change Affect the Regional Characteristics of a Climate Hazard?

Human-driven climate change can alter the regional characteristics of a climate hazard by changing the magnitude or intensity of the climate hazard, the frequency with which it occurs, the duration that hazardous conditions persist, the timing when the hazard occurs, or the spatial extent threatened by the hazard. By examining each of these aspects of a hazard's profile change, climate services may provide climate risk information that allows decision makers to better tailor adaptation, mitigation and risk management strategies.

A *climate hazard* is a climate condition with the potential to harm natural systems or society. Examples include heatwaves, droughts, heavy snowfall events and sea level rise. Climate scientists look for patterns in climatic impact-drivers to detect the signature of changing hazards that may influence stakeholder planning (FAQ 12.1). Climate service providers work with stakeholders and impacts experts to identify key system responses and tolerance thresholds (FAQ 12.2) and then examine historical observations and future climate projections to identify associated changes to the characteristics of a regional hazard's profile. Climate change can alter at least five different characteristics of the hazard profile of a region (FAQ 12.3, Figure 1):

Magnitude or intensity is the raw value of a climate hazard, such as an increase in the maximum yearly temperature or in the height of flooding that results from a coastal storm with a 1% change of occurring each year.

Frequency is the number of times that a climate hazard reaches or surpasses a threshold over a given period. For example, increases to the number of heavy snowfall events, tornadoes, or floods experienced in a year or in a decade.

Duration is the length of time over which hazardous conditions persist beyond a threshold, such as an increase in the number of consecutive days where maximum air temperature exceeds 35°C, the number of consecutive months of drought conditions, or the number of days that a tropical cyclone affects a location.

Timing captures the occurrence of a hazardous event in relation to the course of a day, season, year, or other period in which sectoral elements are evolving or co-dependent (such as the time of year when migrating animals expect to find a seasonal food supply). Examples include a shift towards an earlier day of the year when the last spring frost occurs or a delay in the typical arrival date for the first seasonal rains, the length of the winter period when the ground is typically covered by snow, or a reduction in the typical time needed for soil moisture to move from normal to drought conditions.

Spatial extent is the region in which a hazardous condition is expected, such as the area currently threatened by tropical cyclones, geographical areas where the coldest day of the year restricts a particular pest or pathogen, terrain where permafrost is present, the area that would flood following a common storm, zones where climate conditions are conducive to outdoor labour, or the size of a marine heatwave.

Hazard profile changes are often intertwined or stem from related physical changes to the climate system. For example, changes in the frequency and magnitude of extreme events are often directly related to each other as a result of atmospheric dynamics and chemical processes. In many cases, one aspect of hazard change is more apparent than others, which may provide a first emergent signal indicating a larger set of changes to come (FAQ 1.2).

Information about how a hazard has changed or will change helps stakeholders prioritize more robust adaptation, mitigation and risk management strategies. For example, allocation of limited disaster relief resources may be designed to recognize that tropical cyclones are projected to become more intense even as the frequency of those storms may not change. Planning may also factor in the fact that even heatwaves that are not record-breaking in their intensity can still be problematic for vulnerable populations when they persist over a long period. Likewise, firefighters recognize new logistical challenges in the lengthening of the fire weather season and an expansion of fire conditions into parts of the world where fires were not previously a great concern. Strong engagement between climate scientists and stakeholders therefore helps climate services tailor and communicate clear information about the types of changing climate hazards to be addressed in resilience efforts.

FAQ 12.3 (continued)

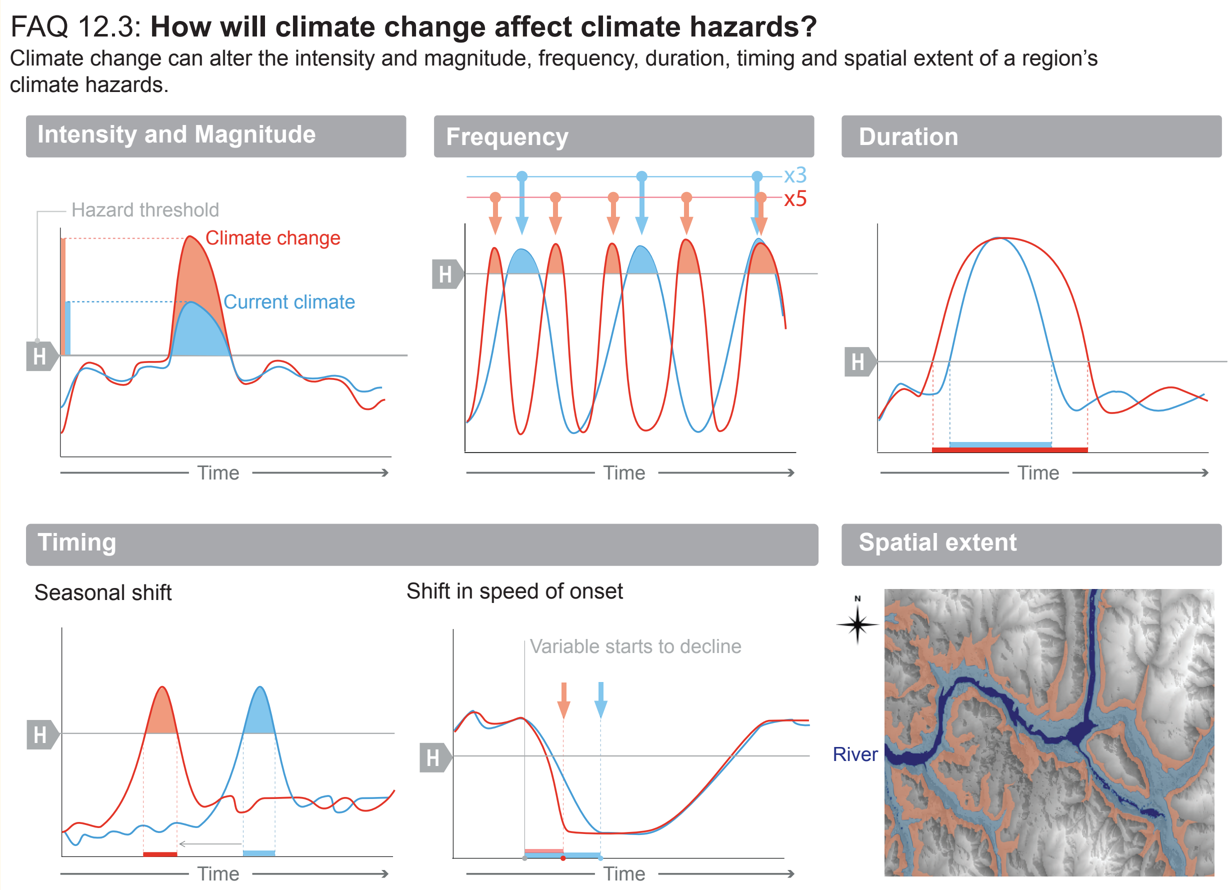

FAQ 12.3, Figure 1 | Types of changes to a region's hazard profile. The first five panels illustrate how climate changes can alter a hazard's intensity (or magnitude), frequency, duration, and timing (by seasonality and speed of onset) in relation to a hazard threshold (horizontal grey line, marked 'H'). The difference between the historical climate (blue) and future climate (red) shows the changing aspects of climate change that stakeholders will have to manage. The bottom right-hand panel shows how a given climate hazard (such as a current once-in-100-year river flood, geographic extent in blue) may reach new geographical areas under a future climate change (extended area in red).

FAQ

Glossary

Glossary

Coordinating Editors:

J.B. Robin Matthews (France/United Kingdom), Vincent Möller (Germany), Renée van Diemen (The Netherlands/United Kingdom), Jan S. Fuglestvedt (Norway), Valérie Masson-Delmotte (France), Carlos Méndez (Venezuela), Sergey Semenov (Russian Federation), Andy Reisinger (New Zealand)

Editorial Team:

Rondrotiana Barimalala (South Africa/Madagascar), Roxana Bojariu (Romania), Annalisa Cherchi (Italy), Peter M. Cox (United Kingdom), Sergio Henrique Faria (Spain/Brazil), Piers Forster (United Kingdom), Christopher Jones (United Kingdom), Nana Ama Browne Klutse (Ghana), Charles Koven (United States of America), Svitlana Krakovska (Ukraine), Sawsan K. Mustafa (Sudan), Friederike Otto (United Kingdom/Germany), Matthew D. Palmer (United Kingdom), Tamzin Palmer (United Kingdom), Wilfried Pokam Mba (Cameroon), Roshanka Ranasinghe (The Netherlands/Sri Lanka, Australia), Pedro Scheel Monteiro (South Africa), Joeri Rogelj (United Kingdom/ Belgium), Sharon L. Smith (Canada), Ying Sun (China), Andrew Turner (United Kingdom), Bart van den Hurk (The Netherlands), Émilie Vanvyve (United Kingdom/Belgium), Martin Wild (Switzerland), Cunde Xiao (China), Prodromos Zanis (Greece)

Note:

This glossary defines some specific terms as the Lead Authors intend them to be interpreted in the context of this report. Italicized words in definitions indicate that the italicized term is defined in the Glossary.

Subterms appear in italics beneath main terms.

This annex should be cited as:

IPCC, 2021: Annex VII: Glossary [Matthews, J.B.R., V. Möller, R. van Diemen, J.S. Fuglestvedt, V. Masson-Delmotte, C. Méndez, S. Semenov, A. Reisinger (eds.)]. *In Climate Change 2021: The Physical Science Basis. Contribution of Working Group I to the Sixth Assessment Report of the Intergovernmental Panel on Climate Change* [Masson-Delmotte, V., P. Zhai, A. Pirani, S.L. Connors, C. Péan, S. Berger, N. Caud, Y. Chen, L. Goldfarb, M.I. Gomis, M. Huang, K. Leitzell, E. Lonnoy, J.B.R. Matthews, T.K. Maycock, T. Waterfield, O. Yelekçi, R. Yu, and B. Zhou (eds.)]. Cambridge University Press, Cambridge, United Kingdom and New York, NY, USA, pp. 2215–2256, doi:10.1017/9781009157896.022.

1.5°C pathway See *Pathways*.

Ablation (of glaciers, ice sheets, or snow cover) See *Mass balance/budget (of glaciers or ice sheets)*.

Abrupt change A change in the system that is substantially faster than the typical rate of the changes in its history. See also *Abrupt climate change* and *Tipping point*.

Abrupt climate change A large-scale *abrupt change* in the climate system that takes place over a few decades or less, persists (or is anticipated to persist) for at least a few decades and causes substantial impacts in human and/or natural systems. See also *Abrupt change* and *Tipping point*.

Accumulation (of glaciers, ice sheets, or snow cover) See *Mass balance/budget (of glaciers or ice sheets)*.

Active layer Layer of ground above *permafrost* subject to annual thawing and freezing.

Adaptation In *human systems*, the process of adjustment to actual or expected *climate* and its effects, in order to moderate harm or exploit beneficial opportunities. In *natural systems*, the process of adjustment to actual climate and its effects; human intervention may facilitate adjustment to expected climate and its effects. See also *Adaptation options*, *Adaptive capacity* and *Maladaptive actions (Maladaptation)*.

Adaptation options The array of strategies and measures that are available and appropriate for addressing *adaptation*. They include a wide range of actions that can be categorized as structural, institutional, ecological or behavioural.

Adaptive capacity The ability of systems, institutions, humans and other organisms to adjust to potential damage, to take advantage of opportunities, or to respond to consequences (MA, 2005).

Added value Improvement of the representation of some climatic aspects by one methodology compared to another methodology. For instance, *downscaling* a coarse resolution global *climate model* may improve the representation of regional *climate* in complex terrain.

Adjustments (in relation to effective radiative forcing) The response to an agent perturbing the *climate system* that is driven directly by the agent, independently of any change in *global surface temperature*. For example, *carbon dioxide* and *aerosols*, by altering internal heating and cooling rates within the *atmosphere*, can each cause changes to cloud cover and other variables thereby producing an *effective radiative forcing* even in the absence of any surface warming or cooling. Adjustments are usually rapid in the sense that they begin to occur right away, before *climate feedbacks* which are driven by global surface warming (although some adjustments may still take significant time to proceed to completion, for example those involving vegetation or *ice sheets*).

Adjustment time See *Response time or adjustment time*.

Advection Transport of water or air along with its properties (e.g., temperature, chemical tracers) by winds or currents. Regarding the general distinction between advection and *convection*, the former describes transport by large-scale motions of the *atmosphere* or *ocean*, while convection describes the predominantly vertical, locally induced motions.

Aerosol A suspension of airborne solid or liquid particles, with typical particle size in the range of a few nanometres to several tens of micrometres and *atmospheric lifetimes* of up to several days in the *troposphere* and up to years in the *stratosphere*. The term aerosol, which includes both the particles and the suspending gas, is often used in this report in its plural form to mean 'aerosol particles'. Aerosols may be of either natural or *anthropogenic* origin in the troposphere; stratospheric aerosols mostly stem from volcanic eruptions. Aerosols can cause an *effective radiative forcing* directly through scattering and absorbing radiation (*aerosol–radiation interaction*), and indirectly by acting as *cloud condensation nuclei* or ice nucleating particles that affect the properties of clouds (*aerosol–cloud interaction*), and upon deposition on snow- or ice-covered surfaces. Atmospheric aerosols may be either emitted as primary particulate matter or formed within the atmosphere from gaseous *precursors* (secondary production). Aerosols may be composed of sea salt, organic carbon, *black carbon (BC)*, mineral species (mainly desert dust), sulphate, nitrate and ammonium or their mixtures. See also *Short-lived climate forcers (SLCFs).*

Aerosol effective radiative forcing (ERFari+aci) See *Aerosol–radiation interaction*.

Aerosol optical depth (AOD) Wavelength-dependent aerosol optical depth is a measure of the *aerosol* contribution to extinction of top-of-the-atmosphere solar intensity measured at the ground. AOD is unitless.

Fine-mode aerosol optical depth
Aerosol optical depth due to *aerosol* particles smaller than 1 μm in radius.

Aerosol–cloud interaction A process by which a perturbation to *aerosol* affects the microphysical properties and evolution of clouds through the aerosol role as *cloud condensation nuclei* or ice nuclei, particularly in ways that affect radiation or precipitation; such processes can also include the effect of clouds and precipitation on aerosol. The aerosol perturbation can be *anthropogenic* or come from some natural *source*. The *radiative forcing* from such interactions has traditionally been attributed to numerous indirect aerosol effects, but in this report, only two levels of radiative forcing (or effect) are distinguished:

Effective radiative forcing (or effect) due to aerosol–cloud interactions (ERFaci)
The final *radiative forcing* (or effect) from the *aerosol* perturbation, including the adjustments to the initial change in droplet or crystal formation rate. These adjustments include changes in the strength of *convection*, precipitation efficiency, cloud fraction, *lifetime* or water content of clouds, and the formation or suppression of clouds in remote areas due to altered circulations.

Instantaneous radiative forcing (or effect) due to aerosol–cloud interactions (IRFaci)
The *radiative forcing* (or radiative effect, if the perturbation is internally generated) due to the change in number or size distribution of cloud droplets or ice crystals that is the proximate result of an

aerosol perturbation, with other variables (in particular total cloud water content) remaining equal. In liquid clouds, an increase in cloud droplet concentration and surface area would increase the cloud *albedo*. This effect is also known as the cloud albedo effect, first indirect effect, or Twomey effect. It is a largely theoretical concept that cannot readily be isolated in observations or comprehensive process models due to the ubiquity of adjustments.

See also *Aerosol–radiation interaction*.

Aerosol–radiation interaction An interaction of *aerosol* directly with radiation produces radiative effects. In this report, two levels of *radiative forcing* (or effect) are distinguished:

Aerosol effective radiative forcing (ERFari+aci)
The total effective *radiative forcing* due to both *aerosol*–cloud and aerosol–radiation interactions is denoted aerosol effective radiative forcing (ERFari+aci).

Effective radiative forcing (or effect) due to aerosol–radiation interactions (ERFari)
The final *radiative forcing* (or effect) from the *aerosol* perturbation, including adjustments to the initial change in radiation. These adjustments include changes in cloud caused by the impact of the radiative heating on convective or larger-scale atmospheric circulations, traditionally known as semi-direct aerosol forcing (or effect).

Instantaneous radiative forcing (or effect) due to aerosol–radiation interactions (IRFari)
The *radiative forcing* (or radiative effect, if the perturbation is internally generated) of an *aerosol* perturbation due directly to aerosol–radiation interactions, with all environmental variables remaining unaffected. Traditionally known in the literature as the direct aerosol forcing (or effect).

See also *Aerosol–cloud interaction*.

Afforestation Conversion to *forest* of land that historically has not contained forests. [Note: For a discussion of the term forest and related terms such as afforestation, *reforestation* and *deforestation*, see the 2006 IPCC Guidelines for National Greenhouse Gas Inventories and their 2019 Refinement, and information provided by the United Nations Framework Convention on Climate Change (IPCC, 2006, 2019; UNFCCC, 2021a, b).] See also *Deforestation*, *Reforestation*, *Anthropogenic removals* and *Carbon dioxide removal (CDR)*.

Agreement In this Report, the degree of agreement within the scientific body of knowledge on a particular finding is assessed based on multiple lines of *evidence* (e.g., mechanistic understanding, theory, data, models, expert judgement) and expressed qualitatively (Mastrandrea et al., 2010). See also *Confidence*, *Likelihood*, *Uncertainty* and *Evidence*.

Agricultural and ecological drought See *Drought*.

Air mass A widespread body of air, the approximately homogeneous properties of which (i) have been established while that air was situated over a particular *region* of the Earth's surface, and (ii) undergo specific modifications while in transit away from the source region (AMS, 2021).

Air pollution Degradation of air quality with negative effects on human health or the natural or built environment due to the introduction, by natural processes or human activity, into the *atmosphere* of substances (gases, *aerosol*) which have a direct (primary pollutants) or indirect (secondary pollutants) harmful effect. See also *Short-lived climate forcers (SLCFs)*.

Airborne fraction The fraction of total *carbon dioxide* (CO_2) emissions (from *fossil fuels* and *land-use change*) remaining in the *atmosphere*.

Albedo The proportion of sunlight (*solar radiation*) reflected by a surface or object, often expressed as a percentage. Clouds, snow and ice usually have high albedo; soil surfaces cover the albedo range from high to low; vegetation in the dry season and/or in *arid zones* can have high albedo, whereas photosynthetically active vegetation and the *ocean* have low albedo. The Earth's planetary albedo changes mainly through changes in cloudiness and of snow, ice, leaf area and *land cover*.

Alkalinity See *Total alkalinity*.

Altimetry A technique for measuring the height of the Earth's surface with respect to the geocentre of the Earth within a defined terrestrial reference frame (geocentric sea level). See also *Geocentric sea level change*.

Annular modes Hemispheric scale patterns of atmospheric variability characterized by opposing and synchronous fluctuations in sea level pressure between the polar caps and mid-latitudes, with a structure exhibiting a high degree of zonal symmetry, and with no real preferred time scales ranging from days to decades. In each hemisphere, these fluctuations reflect changes in the latitudinal position and strength of the mid-latitude jets and associated storm tracks. Annular modes are defined as the leading mode of variability of extratropical sea level pressure or geopotential heights and are known as the *Northern Annular Mode (NAM)* and *Southern Annular Mode (SAM)* in the two hemispheres, respectively.

Northern Annular Mode (NAM)
A see-saw latitudinal fluctuation in Northern Hemisphere sea level pressure or geopotential height between the Arctic and the mid-latitudes. The NAM has some links with the *stratospheric polar vortex* and is related to the fluctuation in strength and latitude of the mean westerlies. Its variance is maximum in winter and its pattern has a strong regional expression in the North Atlantic, being strongly correlated with the *North Atlantic Oscillation* index. The NAM is also known as the Arctic Oscillation (AO). In its positive phase, the NAM is characterized by anomalously low pressure over the Arctic and high pressure over the mid-latitudes/subtropics, with a strengthening of the zonally averaged westerly winds on their polar flank that confines colder air across the Arctic. The negative NAM phase is characterized by a more distorted wind pattern and jet meanders that increase storminess in the mid-latitude regions. See Section AIV.2.1 in Annex IV of the AR6 WGI report.

Southern Annular Mode (SAM)
The leading mode of *climate variability* of Southern Hemisphere sea level pressure and geopotential height, which is associated with the strength and latitudinal shifts in the mid- to high-latitudes westerly wind belt. The SAM is also known as the Antarctic Oscillation (AAO).

A positive SAM phase is defined as lower-than-normal pressures over the polar regions and higher-than-normal pressures in the southern mid-latitudes, with a contraction towards Antarctica and strengthening of the westerly wind belt. The negative SAM phase exhibits positive high-latitude pressure anomalies, negative mid-latitude pressure anomalies and a weaker westerly flow expanded towards the equator. See Section AIV.2.2 in Annex IV of the AR6 WGI report. See also *Annular modes*.

Anomaly The deviation of a variable from its value averaged over a *reference period*.

Antarctic amplification See *Polar amplification*.

Antarctic Ice Sheet (AIS) See *Ice sheet*.

Antarctic oscillation (AAO) See *Southern Annular Mode (SAM)* (under *Annular modes*).

Anthropocene A proposed new geological epoch resulting from significant human-driven changes to the structure and functioning of the Earth System, including the *climate system*. Originally proposed in the Earth system science community in 2000, the proposed new epoch is undergoing a formalization process within the geological community based on the stratigraphic *evidence* that human activities have changed the Earth system to the extent of forming geological deposits with a signature that is distinct from those of the *Holocene*, and which will remain in the geological record. Both the stratigraphic and Earth system approaches to defining the Anthropocene consider the mid-20th century to be the most appropriate starting date (Steffen et al., 2016), although others have been proposed and continue to be discussed. The Anthropocene concept has already been informally adopted by diverse disciplines and the public to denote the substantive influence of humans on the Earth system.

Anthropogenic Resulting from or produced by human activities.

Anthropogenic emissions Emissions of *greenhouse gases (GHGs)*, *precursors* of GHGs and *aerosols* caused by human activities. These activities include the burning of *fossil fuels*, *deforestation*, *land use* and *land-use changes* (LULUC), livestock production, fertilization, waste management, and industrial processes. See also *Anthropogenic* and *Anthropogenic removals*.

Anthropogenic removals The withdrawal of *greenhouse gases (GHGs)* from the *atmosphere* as a result of deliberate human activities. These include enhancing biological *sinks* of CO_2 and using chemical engineering to achieve long-term removal and storage. Carbon dioxide capture and storage (CCS), which alone does not remove CO_2 from the atmosphere, can help reduce atmospheric CO_2 from industrial and energy-related sources if it is combined with bioenergy production (BECCS), or if CO_2 is captured from the air directly and stored (DACCS). [Note: In the 2006 IPCC Guidelines for national GHG Inventories (IPCC, 2006), which are used in reporting of emissions to the UNFCCC, 'anthropogenic' land-related GHG fluxes are defined as all those occurring on 'managed land', i.e., 'where human interventions and practices have been applied to perform production, ecological or social functions'. However, some removals (e.g., removals associated with CO_2 fertilization and N deposition) are not considered as 'anthropogenic', or are referred to as 'indirect' anthropogenic effects, in some of the scientific literature assessed in this report. As a consequence, the land-related net GHG emission estimates from global models included in this report are not necessarily directly comparable with land use, land-use change and forestry (LULUCF) estimates in national GHG Inventories.] See also *Carbon dioxide removal (CDR)*, *Afforestation*, *Enhanced weathering*, *Ocean alkalinization/Ocean alkalinity enhancement* and *Reforestation*.

Anthropogenic subsidence Downward motion of the land surface induced by *anthropogenic* drivers (e.g., loading, extraction of hydrocarbons and/or groundwater, drainage, mining activities) causing sediment compaction or subsidence/deformation of the sedimentary sequence, or oxidation of organic material, thereby leading to relative *sea level rise*.

Apparent hydrological sensitivity (η_a) The change in global mean precipitation per degree Celsius of *global mean surface air temperature (GSAT)* change with units of % per °C, although it can also be calculated as W m^{-2} per °C. See also *Hydrological sensitivity (η)*.

Arctic amplification See *Polar amplification*.

Arctic oscillation (AO) See *Northern Annular Mode (NAM)* (under *Annular modes*).

Arid zone Areas where vegetation growth is severely constrained due to limited water availability. For the most part, the native vegetation of arid zones is sparse. There is high rainfall variability, with annual averages below 300 mm. Crop farming in arid zones requires irrigation.

Aridity The state of a long-term climatic feature characterized by low average precipitation or available water in a *region*. Aridity generally arises from widespread persistent atmospheric subsidence or anticyclonic conditions, and from more localized subsidence in the lee side of mountains (adapted from Gbeckor-Kove, 1989; Türkeş, 1999). See also *Drought*.

Artificial ocean upwelling (AOUpw) A potential *carbon dioxide removal (CDR)* method that aims to artificially pump up cooler, nutrient-rich waters from deep in the *ocean* to the surface. The aim is to stimulate phytoplankton activity and thereby increase ocean CO_2 uptake.

Assets Natural or human-made resources that provide current or future utility, benefit, economic or intrinsic value to natural or human systems.

Atlantic Equatorial Mode See *Atlantic Zonal Mode (AZM)* under *Tropical Atlantic Variability (TAV)*.

Atlantic Meridional Mode (AMM) See *Tropical Atlantic Variability (TAV)*.

Atlantic Meridional Overturning Circulation (AMOC) See *Meridional overturning circulation (MOC)*.

Atlantic Multi-decadal Oscillation (AMO) See *Atlantic Multi-decadal Variability (AMV)*.

Atlantic Multi-decadal Variability (AMV) Large-scale fluctuations observed from one decade to the next in a variety of instrumental records and *proxy* reconstructions over the entire North Atlantic ocean and surrounding continents. Fingerprints of

AMV can be found at the surface *ocean*, which is characterized by swings in basin-scale *sea surface temperature* anomalies reflecting the interaction with the *atmosphere*. The positive phase of the AMV is characterized by anomalous warming over the entire North Atlantic, with the strongest amplitude in the subpolar gyre and along sea ice margin zones in the Labrador Sea and Greenland/Barents Sea and in the subtropical North Atlantic basin to a lower extent. In the AR6 WGI report, the term AMV is preferred to *Atlantic Multi-decadal Oscillation (AMO)* used in previous IPCC reports because there is no preferred time scale of *decadal variability* as the term oscillation would indirectly imply. See Section AIV.2.7 in Annex IV of the AR6 WGI report.

Atlantic Niño See *Atlantic Zonal Mode (AZM)* under *Tropical Atlantic Variability (TAV)*.

Atlantic Zonal Mode (AZM) See *Tropical Atlantic Variability (TAV)*.

Atmosphere The gaseous envelope surrounding the Earth, divided into five layers – the *troposphere* which contains half of the Earth's atmosphere, the *stratosphere*, the mesosphere, the thermosphere and the exosphere, which is the outer limit of the atmosphere. The dry atmosphere consists almost entirely of nitrogen (78.1% volume mixing ratio) and oxygen (20.9% volume mixing ratio), together with a number of trace gases, such as argon (0.93% volume mixing ratio), helium and radiatively active *greenhouse gases (GHGs)* such as *carbon dioxide (CO_2)* (0.04% volume mixing ratio), *methane (CH_4)*, *nitrous oxide (N_2O)* and *ozone (O_3)*. In addition, the atmosphere contains the GHG water vapour (H_2O), whose concentrations are highly variable (0–5% volume mixing ratio) as the sources (*evapotranspiration*) and sinks (precipitation) of water vapour show large spatio-temporal variations, and atmospheric temperature exerts a strong constraint on the amount of water vapour an air parcel can hold. The atmosphere also contains clouds and *aerosols*. See also *Hydrological cycle*, *Stratosphere* and *Troposphere*.

Atmosphere–ocean general circulation model (AOGCM) See *General circulation model (GCM)*.

Atmospheric boundary layer The atmospheric layer adjacent to the Earth's surface that is affected by friction against that boundary surface, and possibly by transport of heat and other variables across that surface (AMS, 2021). The lowest 100 m of the boundary layer (about 10% of the boundary layer thickness), where mechanical generation of turbulence is dominant, is called the surface boundary layer or surface layer.

Atmospheric lifetime See *Lifetime*.

Atmospheric rivers (ARs) Long, narrow (up to a few hundred km wide), shallow (up to a few km deep) and transient corridors of strong horizontal water vapour transport that are typically associated with a low-level jet stream ahead of the cold front of an *extratropical cyclone (ETC)* (Ralph et al., 2018).

Attribution Attribution is defined as the process of evaluating the relative contributions of multiple causal factors to a change or event with an assessment of *confidence*.

Australian and Maritime Continent monsoon (AusMCM) See *Global monsoon*.

Autotrophic respiration *Respiration* by photosynthetic (see *photosynthesis*) organisms (e.g., plants and algae).

Avalanche A mass of snow, ice, earth or rocks, or a mixture of these, falling down a mountainside.

Barystatic See *Sea level change (sea level rise/sea level fall)*.

Basal lubrication Reduction of friction at the base of an *ice sheet* or *glacier* due to lubrication by meltwater. This can allow the glacier or ice sheet to slide over its base. Meltwater may be produced by pressure-induced melting, friction or geothermal heat, or surface melt may drain to the base through holes in the ice.

Baseline/reference See *Reference scenario* (under *Scenario*) and *Reference period*.

Baseline scenario See *Reference scenario* (under *Scenario*).

Bifurcation point See *Tipping point*.

Biodiversity Biodiversity or biological diversity means the variability among living organisms from all sources including, among other things, terrestrial, marine and other aquatic *ecosystems*, and the ecological complexes of which they are part; this includes diversity within species, between species, and of ecosystems (UN, 1992). See also *Ecosystem*.

Bioenergy with carbon dioxide capture and storage (BECCS) *Carbon dioxide capture and storage (CCS)* technology applied to a bioenergy facility. Note that depending on the total emissions of the BECCS supply chain, *carbon dioxide (CO_2)* can be removed from the *atmosphere*. See also *Carbon dioxide capture and storage (CCS)*, *Anthropogenic removals* and *Carbon dioxide removal (CDR)*.

Biogenic volatile organic compounds (BVOCs) See *Volatile organic compounds (VOCs)*.

Biogeophysical potential See *Mitigation potential*.

Biological (carbon) pump A series of *ocean* processes through which inorganic carbon (as *carbon dioxide, CO_2*) is fixed as organic matter by *photosynthesis* in sunlit surface water and then transported to the ocean interior, and possibly the sediment, resulting in the storage of carbon.

Biomass Organic material excluding the material that is fossilized or embedded in geological formations. Biomass may refer to the mass of organic matter in a specific area (ISO, 2014).

Biosphere (terrestrial and marine) The part of the Earth system comprising all *ecosystems* and living organisms, in the *atmosphere*, on land (terrestrial biosphere) or in the *oceans* (marine biosphere), including derived dead organic matter, such as litter, soil organic matter and oceanic detritus.

Bipolar seesaw (also inter-hemispheric seesaw, inter-hemispheric asymmetry, hemispheric asymmetry) A phenomenon in which temperature changes in the Northern and Southern hemispheres are related but out of phase, generally inferred to represent a change in the magnitude or sign of net heat transport across the equator. Originally called hemispheric asymmetry and linked to changes in thermohaline overturning circulation on multi-millennial scales (Mix et al., 1986), later named bipolar seesaw and applied to millennial scales (Broecker, 1998) with a similar thermohaline mechanism (Stocker and Johnsen, 2003). See also *Meridional overturning circulation (MOC)* and *Deglacial or deglaciation or glacial termination*.

Black carbon (BC) A relatively pure form of carbon, also known as soot, arising from the incomplete combustion of fossil fuels, biofuel, and biomass. It only stays in the *atmosphere* for days or weeks. BC is a climate *forcing* agent with strong warming effect, both in the atmosphere and when deposited on snow or ice. See also *Aerosol* and *Atmosphere*.

Blocking Associated with persistent, slow-moving high-pressure systems that obstruct the prevailing westerly winds in the middle and high latitudes and the normal eastward progress of extratropical transient storm systems. It is an important component of the intra-seasonal *climate variability* in the extratropics and can cause long-lived weather conditions such as cold spells in winter and summer *heatwaves*.

Blue carbon Biologically driven carbon fluxes and storage in marine systems that are amenable to management. Coastal blue carbon focuses on rooted vegetation in the coastal zone, such as tidal marshes, mangroves and seagrasses. These *ecosystems* have high carbon burial rates on a per unit area basis and accumulate carbon in their soils and sediments. They provide many non-climatic benefits and can contribute to *ecosystem*-based adaptation. If degraded or lost, coastal blue carbon ecosystems are likely to release most of their carbon back to the *atmosphere*. There is current debate regarding the application of the blue carbon concept to other coastal and non-coastal processes and ecosystems, including the open *ocean*. See also *Sequestration*.

Brewer–Dobson circulation The meridional overturning circulation of the *stratosphere* transporting air upward in the tropics, poleward to the winter hemisphere, and downward at polar and subpolar latitudes. The Brewer–Dobson circulation is driven by the interaction between upward propagating planetary waves and the mean flow.

Burden The total mass of a substance of concern in the *atmosphere*.

Business as usual (BAU) The term business as usual scenario has been used to describe a *scenario* that assumes no additional policies beyond those currently in place and that patterns of socio-economic development are consistent with recent trends. The term is now used less frequently than in the past. See also *Reference scenario* (under *Scenario*).

^{13}C Stable *isotope* of carbon having an atomic weight of approximately 13. Measurements of the ratio of $^{13}C/^{12}C$ in *carbon dioxide (CO_2)* molecules are used to infer the importance of different *carbon cycle* and *climate* processes and the size of the terrestrial carbon *reservoir*.

^{14}C Unstable *isotope* of carbon having an atomic weight of approximately 14 and a half-life of about 5700 years. It is often used for dating purposes going back some 40 kyr. Its variation in time is affected by the magnetic fields of the Sun and Earth, which influence its production from cosmic rays.

Calcification The process of biologically precipitating calcium carbonate minerals to create organism shells, skeletons, otoliths, or other body structures. The chemical equation describing calcification is Ca^{2+} (aq) + $2HCO_3^-$ (aq) $\rightarrow$ $CaCO_3$(s) + CO_2 + H_2O. Aragonite and calcite are two common crystalline forms of biologically precipitated calcium carbonate minerals that have different solubilities.

Calving (of glaciers or ice sheets) The breaking off of discrete pieces of ice from a *glacier*, *ice sheet* or an *ice shelf* into lake or seawater, producing *icebergs*. This is a form of mass loss from an ice body.

Canopy temperature The temperature within the canopy of a vegetation structure.

Carbon budget Refers to two concepts in the literature: (i) an assessment of carbon cycle *sources* and *sinks* on a global level, through the synthesis of evidence for *fossil fuel* and cement emissions, emissions and removals associated with *land use* and *land-use change*, *ocean* and natural land sources and sinks of *carbon dioxide (CO_2)*, and the resulting change in atmospheric CO_2 concentration. This is referred to as the global carbon budget; (ii) the maximum amount of cumulative net global *anthropogenic* CO_2 emissions that would result in limiting *global warming* to a given level with a given probability, taking into account the effect of other anthropogenic climate forcers. This is referred to as the total carbon budget when expressed starting from the *pre-industrial* period, and as the remaining carbon budget when expressed from a recent specified date.

Note 1: Net anthropogenic CO_2 emissions are anthropogenic CO_2 emissions minus anthropogenic CO_2 removals. See also *Carbon dioxide removal (CDR)*.

Note 2: The maximum amount of cumulative net global anthropogenic CO_2 emissions is reached at the time that annual net anthropogenic CO_2 emissions reach zero.

Note 3: The degree to which anthropogenic climate forcers other than CO_2 affect the total carbon budget and remaining carbon budget depends on human choices about the extent to which these forcers are mitigated and their resulting *climate* effects.

Note 4: The notions of a total carbon budget and remaining carbon budget are also being applied in parts of the scientific literature and by some entities at regional, national, or sub-national levels. The distribution of global budgets across individual different entities and emitters depends strongly on considerations of equity and other value judgements.

Carbon cycle The flow of carbon (in various forms, e.g., as *carbon dioxide (CO_2)*, carbon in biomass, and carbon dissolved in the *ocean* as carbonate and bicarbonate) through the *atmosphere*, *hydrosphere*, terrestrial and marine *biosphere* and *lithosphere*. In this report, the reference unit for the global carbon cycle is $GtCO_2$ or GtC (one Gigatonne = 1 Gt = 10^{15} grams; 1 GtC corresponds to 3.664 $GtCO_2$). See also *Ocean carbon cycle*.

Carbon dioxide (CO_2) A naturally occurring gas, CO_2 is also a by-product of burning *fossil fuels* (such as oil, gas and coal), of burning *biomass*, of *land-use change* (LUC) and of industrial processes (e.g., cement production). It is the principal anthropogenic *greenhouse gas (GHG)* that affects the Earth's radiative balance. It is the reference gas against which other GHGs are measured and therefore has a *global warming potential (GWP)* of 1.

Carbon dioxide (CO_2) fertilization The increase of plant *photosynthesis* and water-use efficiency in response to increased atmospheric *carbon dioxide (CO_2)* concentration. Whether this increased photosynthesis translates into increased plant growth and carbon storage on land depends on the interacting effects of temperature, moisture and nutrient availability.

Carbon dioxide capture and storage (CCS) A process in which a relatively pure stream of *carbon dioxide (CO_2)* from industrial and energy-related sources is separated (captured), conditioned, compressed and transported to a storage location for long-term isolation from the *atmosphere*. Sometimes referred to as carbon capture and storage. See also *Bioenergy with carbon dioxide capture and storage (BECCS)*, *Sequestration*, *Anthropogenic removals* and *Carbon dioxide removal (CDR)*.

Carbon dioxide removal (CDR) *Anthropogenic* activities removing *carbon dioxide (CO_2)* from the *atmosphere* and durably storing it in geological, terrestrial, or *ocean* reservoirs, or in products. It includes existing and potential anthropogenic enhancement of biological or geochemical CO_2 *sinks* and direct air carbon dioxide capture and storage (DACCS), but excludes natural CO_2 *uptake* not directly caused by human activities. See also *Anthropogenic removals*, *Afforestation*, *Enhanced weathering*, *Ocean alkalinization/Ocean alkalinity enhancement*, *Reforestation*, *Bioenergy with carbon dioxide capture and storage (BECCS)* and *Carbon dioxide capture and storage (CCS)*.

Carbon neutrality Condition in which *anthropogenic* CO_2 emissions associated with a subject are balanced by anthropogenic CO_2 removals. The subject can be an entity such as a country, an organization, a district or a commodity, or an activity such as a service and an event. Carbon neutrality is often assessed over the life cycle including indirect ('scope 3') emissions, but can also be limited to the emissions and removals, over a specified period, for which the subject has direct control, as determined by the relevant scheme.

Note 1: Carbon neutrality and *net zero CO_2 emissions* are overlapping concepts. The concepts can be applied at global or sub-global scales (e.g., regional, national and sub-national). At a global scale, the terms carbon neutrality and net zero CO_2 emissions are equivalent. At sub-global scales, net zero CO_2 emissions is generally applied to emissions and removals under direct control or territorial responsibility of the reporting entity, while carbon neutrality generally includes emissions and removals within and beyond the direct control or territorial responsibility of the reporting entity. Accounting rules specified by GHG programmes or schemes can have a significant influence on the quantification of relevant CO_2 emissions and removals.

Note 2: In some cases, achieving carbon neutrality may rely on the supplementary use of offsets to balance emissions that remain after actions by the reporting entity are taken into account.

See also *Greenhouse gas neutrality* and *Net zero CO_2 emissions*.

Carbon sequestration See *Sequestration*.

Carbon sink See *Sink*.

Carbon source See *Source*.

Carbon–climate feedback See *Climate–carbon cycle feedback*.

Carbonaceous aerosol *Aerosol* consisting predominantly of organic substances and *black carbon*.

Carbonate counter pump See *Carbonate pump*.

Carbonate pump Ocean carbon fixation through the biological formation of carbonates, primarily by plankton that generate bio-mineral particles that sink to the *ocean* interior, and possibly the sediment. It is also called carbonate counter-pump, since the formation of calcium carbonate ($CaCO_3$) is accompanied by the release of *carbon dioxide (CO_2)* to surrounding water and subsequently to the *atmosphere*.

Catchment An area that collects and drains precipitation.

Cenozoic Era The third and current geological Era, which began 66.0 Ma. It comprises the Paleogene, Neogene and *Quaternary* Periods.

Central Pacific El Niño See *El Niño–Southern Oscillation (ENSO)*.

Chaotic A *dynamical system* such as the *climate system*, governed by non-linear deterministic equations, may exhibit erratic or chaotic behaviour in the sense that very small changes in the initial state of the system lead to large and apparently unpredictable changes in its temporal evolution. Such chaotic behaviour limits the *predictability* of the state of a non-linear dynamical system at specific future times, although changes in its statistics may still be predictable given changes in the system parameters or boundary conditions.

Charcoal Material resulting from charring of *biomass*, usually retaining some of the microscopic texture typical of plant tissues; chemically it consists mainly of carbon with a disturbed graphitic structure, with lesser amounts of oxygen and hydrogen.

Chlorofluorocarbons (CFCs) An organic compound that contains chlorine, carbon, hydrogen and fluorine and is used for refrigeration, air conditioning, packaging, plastic foam, insulation, solvents or aerosol propellants. Because they are not destroyed in the lower *atmosphere*, CFCs drift into the upper *atmosphere* where, given suitable conditions, they lead to *ozone (O_3)* depletion. They are some of the *greenhouse gases (GHGs)* covered under the 1987 *Montreal Protocol*, as a result of which manufacturing of these gases has been phased out, and they are being replaced by other compounds, including *hydrofluorocarbons (HFCs)*.

Chronology Arrangement of events according to dates or times of occurrence.

Cirrus cloud thinning (CCT) See *Solar radiation modification (SRM)*.

Clathrate (methane) A partly frozen slushy mix of *methane* gas and ice, usually found in sediments.

Clausius–Clapeyron equation/relationship The thermodynamic relationship between temperature and the vapour pressure of a substance in which two phases of the substance are in equilibrium (e.g., liquid water and water vapour). For gases such as water vapour, this relation gives the increase in equilibrium (or saturation) vapour pressure per unit change in air temperature.

Climate Climate in a narrow sense is usually defined as the average weather, or more rigorously as the statistical description in terms of the mean and variability of relevant quantities over a period of time ranging from months to thousands or millions of years. The classical period for averaging these variables is 30 years, as defined by the World Meteorological Organization (WMO). The relevant quantities are most often surface variables such as temperature, precipitation and wind. Climate in a wider sense is the state, including a statistical description, of the *climate system*.

Climate change A change in the state of the *climate* that can be identified (e.g., by using statistical tests) by changes in the mean and/or the variability of its properties and that persists for an extended period, typically decades or longer. Climate change may be due to natural internal processes or external *forcings* such as modulations of the solar cycles, volcanic eruptions and persistent *anthropogenic* changes in the composition of the *atmosphere* or in *land use*. Note that the *United Nations Framework Convention on Climate Change (UNFCCC)*, in its Article 1, defines climate change as: 'a change of climate which is attributed directly or indirectly to human activity that alters the composition of the global atmosphere and which is in addition to natural climate variability observed over comparable time periods'. The UNFCCC thus makes a distinction between climate change attributable to human activities altering the atmospheric composition and *climate variability* attributable to natural causes. See also *Climate variability*, *Detection and attribution*, *Global warming* and *Ocean acidification (OA)*.

Climate change commitment Climate change commitment is defined as the unavoidable future *climate change* resulting from inertia in the geophysical and socio-economic systems. Different types of climate change commitment are discussed in the literature (see subterms). Climate change commitment is usually quantified in terms of the further change in temperature, but it includes other future changes, for example in the *hydrological cycle*, in *extreme weather events*, in extreme climate events, and in sea level.

Constant composition commitment
The constant composition commitment is the remaining *climate change* that would result if atmospheric composition, and hence *radiative forcing*, were held fixed at a given value. It results from the thermal inertia of the *ocean* and slow processes in the *cryosphere* and land surface.

Constant emissions commitment
The constant emissions commitment is the committed *climate change* that would result from keeping *anthropogenic emissions* constant.

Zero emissions commitment
The zero emissions commitment is an estimate of the subsequent *global warming* that would result after *anthropogenic emissions* are set to zero. It is determined by both inertia in physical *climate system* components (*ocean*, *cryosphere*, land surface) and *carbon cycle* inertia. In its widest sense it refers to emissions of each climate forcer, including *greenhouses gases*, *aerosols* and their *precursors*. The climate response to this can be complex due to the different time scale of response of each climate forcer. A specific subcategory of zero emissions commitment is the Zero CO_2 Emissions Commitment which refers to the climate system response to CO_2 emissions after setting these to net zero. The CO_2-only definition is of specific use in estimating *remaining carbon budgets*.

Climate extreme (extreme weather or climate event) The occurrence of a value of a weather or *climate* variable above (or below) a threshold value near the upper (or lower) ends of the range of observed values of the variable. By definition, the characteristics of what is called *extreme weather* may vary from place to place in an absolute sense. When a pattern of extreme weather persists for some time, such as a season, it may be classified as an extreme climate event, especially if it yields an average or total that is itself extreme (e.g., high temperature, *drought*, or heavy rainfall over a season). For simplicity, both extreme weather events and extreme climate events are referred to collectively as 'climate extremes'.

Climate feedback An interaction in which a perturbation in one *climate* quantity causes a change in a second, and the change in the second quantity ultimately leads to an additional change in the first. A negative feedback is one in which the initial perturbation is weakened by the changes it causes; a positive feedback is one in which the initial perturbation is enhanced. The initial perturbation can either be externally forced or arise as part of *internal variability*. See also *Climate–carbon cycle feedback*, *Cloud feedback* and *Ice–albedo feedback*.

Climate feedback parameter A way to quantify the radiative response of the *climate system* to a change induced by a *radiative forcing*. It is quantified as the change in net energy flux at the top of atmosphere for a given change in annual global surface temperature. It has units of W m^{-2} $°C^{-1}$.

Climate forecast See *Climate prediction*.

Climate index A time series constructed from *climate* variables that provides an aggregate summary of the state of the *climate system*. For example, the difference between sea level pressure in Iceland and the Azores provides a simple yet useful historical *North Atlantic Oscillation (NAO)* index. Because of their optimal properties, climate indices are often defined using principal components – linear combinations of climate variables at different locations that have maximum variance subject to certain normalization constraints (e.g., the *Northern Annular Mode (NAM)* and *Southern Annular Mode (SAM)* indices, which are principal components of Northern Hemisphere and Southern Hemisphere gridded pressure anomalies, respectively). Definitions of observational indices for *Modes of climate variability* can be found in Annex IV of the AR6 WGI report.

Climate indicator Measures of the *climate system*, including large-scale variables and climate *proxies*. See also *Climate metrics*.

Key climate indicators
Key indicators constitute a finite set of distinct variables that may collectively point to important overall changes in the *climate system* of broad societal relevance across the atmospheric, oceanic, cryospheric and biospheric domains, with land as an implicit cross-cutting theme. Taken together, these indicators would be expected to both have changed and continue to change in the future in a

coherent and consistent manner. See Cross-Chapter Box 2.2, Table 1 in the AR6 WGI report.

Climate information Information about the past, current state or future of the *climate system* that is relevant for *mitigation*, *adaptation* and *risk management*. It may be tailored or 'co-produced' for specific contexts, taking into account users' needs and values.

Climate metrics Measures of aspects of the overall *climate system* response to *radiative forcing*, such as *equilibrium climate sensitivity (ECS)*, *transient climate response (TCR)*, *transient climate response to cumulative CO_2 emissions (TCRE)* and the *airborne fraction* of *anthropogenic* carbon dioxide. See also *Greenhouse gas emission metric*, *Climate indicator* and *Key climate indicators* (under *Climate indicator*).

Climate model A qualitative or quantitative representation of the *climate system* based on the physical, chemical and biological properties of its components, their interactions and feedback processes and accounting for some of its known properties. The climate system can be represented by models of varying complexity; that is, for any one component or combination of components, a spectrum or hierarchy of models can be identified, differing in such aspects as the number of spatial dimensions, the extent to which physical, chemical or biological processes are explicitly represented, or the level at which empirical parametrizations are involved. There is an evolution towards more complex models with interactive chemistry and biology. Climate models are applied as a research tool to study and simulate the *climate* and for operational purposes, including monthly, seasonal and interannual *climate predictions*. See also *Earth system model (ESM)*, *Earth system model of intermediate complexity (EMIC)*, *Energy balance model (EBM)*, *Simple climate model (SCM)*, *Regional climate model (RCM)*, *Dynamic global vegetation model (DGVM)*, *General circulation model (GCM)* and *Emulators*.

Climate pattern A set of spatially varying coefficients obtained by 'projection' (regression) of *climate* variables onto a *climate index* time series. When the climate index is a principal component, the climate pattern is an eigenvector of the covariance matrix, referred to as an empirical orthogonal function (EOF) in climate science.

Climate prediction A climate prediction or climate forecast is the result of an attempt to produce (starting from a particular state of the *climate system*) an estimate of the actual evolution of the *climate* in the future, for example, at seasonal, interannual or decadal time scales. Because the future evolution of the climate system may be highly sensitive to initial conditions, has *chaotic* elements and is subject to *natural variability*, such predictions are usually probabilistic in nature.

Climate projection Simulated response of the *climate system* to a *scenario* of future emissions or concentrations of *greenhouse gases (GHGs)* and *aerosols* and changes in *land use*, generally derived using *climate models*. Climate projections are distinguished from *climate predictions* by their dependence on the emission/concentration/ *radiative forcing* scenario used, which is in turn based on assumptions concerning, for example, future socio-economic and technological developments that may or may not be realized.

Climate response A general term for how the *climate system* responds to a *radiative forcing*.

Climate sensitivity The change in the surface temperature in response to a change in the atmospheric *carbon dioxide (CO_2)* concentration or other *radiative forcing*. See also *Climate feedback parameter*.

Earth system sensitivity
The equilibrium surface temperature response of the coupled *atmosphere–ocean–cryosphere*–vegetation–*carbon cycle* system to a doubling of the atmospheric *carbon dioxide (CO_2)* concentration is referred to as Earth system sensitivity. Because it allows *ice sheets* to adjust to the external perturbation, it may differ substantially from the *equilibrium climate sensitivity* derived from coupled atmosphere–ocean models.

Effective equilibrium climate sensitivity
An estimate of the surface temperature response to a doubling of the atmospheric *carbon dioxide (CO_2)* concentration that is evaluated from model output or observations for evolving non-equilibrium conditions. It is a measure of the strengths of the *climate feedbacks* at a particular time and may vary with *forcing* history and climate state, and therefore may differ from *equilibrium climate sensitivity*.

Equilibrium climate sensitivity (ECS)
The equilibrium (steady state) change in the surface temperature following a doubling of the atmospheric *carbon dioxide (CO_2)* concentration from *pre-industrial* conditions.

Transient climate response (TCR)
The surface temperature response for the hypothetical scenario in which atmospheric *carbon dioxide (CO_2)* increases at 1% yr^{-1} from *pre-industrial* to the time of a doubling of atmospheric CO_2 concentration (year 70).

Transient climate response to cumulative CO_2 emissions (TCRE)
The transient surface temperature change per unit cumulative *carbon dioxide (CO_2)* emissions, usually 1000 GtC. TCRE combines both information on the *airborne fraction* of cumulative CO_2 emissions (the fraction of the total CO_2 emitted that remains in the *atmosphere*, which is determined by *carbon cycle* processes) and on the *transient climate response (TCR)*.

Climate services Climate services involve the provision of *climate information* in such a way as to assist decision-making. The service includes appropriate engagement from users and providers, is based on scientifically credible information and expertise, has an effective access mechanism and responds to user needs (Hewitt et al., 2012).

Climate simulation ensemble A group of parallel model simulations characterizing historical *climate* conditions, *climate predictions*, or *climate projections*. Variation of the results across the ensemble members may give an estimate of modelling-based uncertainty. Ensembles made with the same model but different initial conditions characterize the uncertainty associated with internal *climate variability*, whereas multi-model ensembles including simulations by several models also include the effect of model differences. Perturbed parameter ensembles, in which model parameters are varied in a systematic manner, aim to assess the uncertainty resulting from internal model specifications within a single model. Remaining sources of uncertainty unaddressed with model ensembles are related to systematic model errors or biases, which may be assessed from systematic comparisons of model simulations with observations wherever available.

Climate system The global system consisting of five major components: the *atmosphere*, the *hydrosphere*, the *cryosphere*, the *lithosphere* and the *biosphere* and the interactions between them. The climate system changes in time under the influence of its own internal dynamics and because of *external forcings* such as volcanic eruptions, solar variations, *orbital forcing*, and *anthropogenic* forcings such as the changing composition of the atmosphere and *land-use change*.

Climate threshold A limit within the *climate system* (or its *forcing*) beyond which the behaviour of the system is qualitatively changed. See also *Abrupt climate change* and *Tipping point*.

Climate variability Deviations of *climate* variables from a given mean state (including the occurrence of extremes, etc.) at all spatial and temporal scales beyond that of individual weather events. Variability may be intrinsic, due to fluctuations of processes internal to the *climate system* (*internal variability*), or extrinsic, due to variations in natural or anthropogenic *external forcing* (forced variability). See also *Climate change* and *Modes of climate variability*.

Decadal variability
Decadal variability refers to *climate variability* on decadal time scales. See also *Pacific Decadal Variability (PDV)*, *Atlantic Multi-decadal Oscillation/Variability (AMO/AMV)* and *Pacific Decadal Oscillation (PDO)* (under *Pacific Decadal Variability (PDV)*).

Internal variability
Fluctuations of the climate dynamical system when subject to a constant or periodic *external forcing* (such as the annual cycle). See also *Climate variability*.

Natural variability
Natural variability refers to climatic fluctuations that occur without any human influence, that is, *internal variability* combined with the response to external natural factors such as volcanic eruptions, changes in *solar activity* and, on longer time scales, orbital effects and plate tectonics. See also *Orbital forcing*.

Climate velocity The speed at which isolines of a specified *climate* variable travel across landscapes or seascapes due to changing climate. For example, climate velocity for temperature is the speed at which isotherms move due to changing climate (km yr^{-1}) and is calculated as the temporal change in temperature (°C yr^{-1}) divided by the current spatial gradient in temperature (°C km^{-1}). It can be calculated using additional climate variables such as precipitation or can be based on the climatic niche of organisms.

Climate–carbon cycle feedback A *climate feedback* involves changes in the properties of the land and ocean *carbon cycle* in response to *climate change*. In the *ocean*, changes in oceanic temperature and circulation could affect the *atmosphere*–ocean *carbon dioxide (CO_2)* flux; on the continents, *climate change* could affect plant *photosynthesis* and soil microbial *respiration* and hence the flux of CO_2 between the atmosphere and the land *biosphere*.

Climatic impact-driver (CID) Climatic impact-drivers (CIDs) are physical *climate system* conditions (e.g., means, events, extremes) that affect an element of society or *ecosystems*. Depending on system tolerance, CIDs and their changes can be detrimental, beneficial, neutral or a mixture of each across interacting system elements and *regions*. See also *Risk*, *Hazard* and *Impacts (consequences, outcomes)*.

Cloud condensation nuclei (CCN) The subset of *aerosol* particles that serve as an initial site for the condensation of liquid water, which can lead to the formation of cloud droplets, under typical cloud formation conditions. The main factor that determines which *aerosol* particles are CCN at a given supersaturation is their size.

Cloud feedback A *climate feedback* involving changes in any of the properties of clouds as a response to a change in the local or global surface temperature. Understanding cloud feedbacks and determining their magnitude and sign requires an understanding of how a change in *climate* may affect the spectrum of cloud types, the cloud fraction and height, the radiative properties of clouds, and finally the Earth's radiation budget.

Cloud radiative effect The radiative effect of clouds relative to the identical situation without clouds.

Cloud-resolving models (CRMs) Numerical models that are that are of high enough *resolution* and have the necessary physics to represent the dynamical and physical processes of cloud formation.

CMIP6 See *Coupled Model Intercomparison Project (CMIP)*.

CO_2 equivalent (CO_2-eq) emission The amount of *carbon dioxide (CO_2)* emission that would have an equivalent effect on a specified key measure of *climate change*, over a specified time horizon, as an emitted amount of another *greenhouse gas (GHG)* or a mixture of other GHGs. For a mix of GHGs, it is obtained by summing the CO_2-equivalent emissions of each gas. There are various ways and time horizons to compute such equivalent emissions (see *greenhouse gas emission metric*). CO_2-equivalent emissions are commonly used to compare emissions of different GHGs, but should not be taken to imply that these emissions have an equivalent effect across all key measures of climate change. [Note: Under the Paris Rulebook (Decision 18/CMA.1, annex, paragraph 37), parties have agreed to use GWP-100 values from the IPCC AR5 or GWP-100 values from a subsequent IPCC Assessment Report to report aggregate emissions and removals of GHGs. In addition, parties may use other metrics to report supplemental information on aggregate emissions and removals of GHGs.]

Coast The land near to the sea. The term 'coastal' can refer to that land (e.g., as in 'coastal communities'), or to that part of the marine environment that is strongly influenced by land-based processes. Thus, coastal seas are generally shallow and near-shore. The landward and seaward limits of the coastal zone are not consistently defined, either scientifically or legally. Thus, coastal waters can either be considered as equivalent to territorial waters (extending 12 nautical miles/22.2 km from mean low water), or to the full Exclusive Economic Zone, or to shelf seas, with less than 200 m water depth.

Common era (CE) CE (Common Era) and BCE (Before the Common Era) are alternative names for AD (Anno Domini) and BC (Before Christ) in the Gregorian international standard calendar-year system. CE/BCE are preferred in an international context because they are neutral with respect to religion. The numbering of calendar years is the same under both terminologies. The CE began in year AD 1 and extends to the present day.

Compatible emissions *Earth system models* that simulate the land and ocean *carbon cycle* can calculate *carbon dioxide (CO_2)* emissions that are compatible with a given atmospheric CO_2 concentration trajectory. The compatible emissions over a given period of time are equal to the increase of carbon over that same period of time in the sum of the three active *reservoirs*: the *atmosphere*, the land and the *ocean*.

Compound events See *Compound weather/climate events*.

Compound weather/climate events The terms 'compound events', 'compound extremes' and 'compound extreme events' are used interchangeably in the literature and this report and refer to the combination of multiple drivers and/or *hazards* that contributes to societal and/or environmental *risk* (Zscheischler et al., 2018).

Concentrations scenario See *Scenario*.

Confidence The robustness of a finding based on the type, amount, quality and consistency of *evidence* (e.g., mechanistic understanding, theory, data, models, expert judgement) and on the degree of *agreement* across multiple lines of evidence. In this report, confidence is expressed qualitatively (Mastrandrea et al., 2010).

Constant composition commitment See *Climate change commitment*.

Constant emissions commitment See *Climate change commitment*.

Convection Vertical motion driven by buoyancy forces arising from static instability, usually caused by near-surface cooling or increases in salinity in the case of the *ocean* and near-surface warming or cloud-top radiative cooling in the case of the *atmosphere*. In the atmosphere, convection gives rise to cumulus clouds and precipitation and is effective at both scavenging and vertically transporting chemical species. In the ocean, convection can carry surface waters to deep within the ocean.

Convection-permitting models See *Cloud-resolving models (CRMs)*.

Coral bleaching Loss of coral pigmentation through the loss of intracellular symbiotic algae (known as zooxanthellae) and/or loss of their pigments.

Coral reef An underwater *ecosystem* characterised by structure-building stony corals. Warm-water coral reefs occur in shallow seas, mostly in the tropics, with the corals (animals) containing algae (plants) that depend on light and relatively stable temperature conditions. Cold-water coral reefs occur throughout the world, mostly at water depths of 50–500 m. In both kinds of reef, living corals frequently grow on older, dead material, predominantly made of calcium carbonate ($CaCO_3$). Both warm- and cold-water coral reefs support high *biodiversity* of fish and other groups and are considered to be especially vulnerable to *climate change*.

Coupled Model Intercomparison Project (CMIP) A *climate* modelling activity from the World Climate Research Programme (WCRP), which coordinates and archives *climate model* simulations based on shared model inputs by modelling groups from around the world. The CMIP Phase 3 (CMIP3) multi-model dataset includes projections using Special Report on Emissions Scenarios (SRES) scenarios. The CMIP Phase 5 (CMIP5) dataset includes projections using the *Representative Concentration Pathways (RCP)*. The CMIP6 phase involves a suite of common model experiments as well as an ensemble of CMIP-endorsed Model Intercomparison Projects (MIPs).

Cryosphere The components of the Earth system at and below the land and *ocean* surface that are frozen, including snow cover, *glaciers*, *ice sheets*, *ice shelves*, *icebergs*, *sea ice*, lake ice, river ice, *permafrost* and seasonally *frozen ground*.

Cumulative emissions The total amount of emissions released over a specified period of time. See also *Carbon budget* and *Transient climate response to cumulative CO_2 emissions (TCRE)* (under *Climate sensitivity*).

Dansgaard–Oeschger events (D-O events) Millennial-scale events first characterized in Greenland *ice cores* as abrupt warming from a cold *stadial* state to a warmer *interstadial* state, followed by a return to a cold stadial state (Dansgaard et al., 1993), and traced in the *ocean* via deposits of ice-rafted sand grains (Bond and Lotti, 1995). Named after Willi Dansgaard and Hans Oeschger by Bond and Lotti (1995). An example of a D–O event during the most recent *deglacial* transition is the Bølling–Allerød interstadial. Warm D–O events in Greenland are associated with cooling events in Antarctica (Blunier and Brook, 2001) through ocean *thermohaline circulation* (Stocker and Johnsen, 2003). See also *Bipolar seesaw (also interhemispheric seesaw, interhemispheric asymmetry, hemispheric asymmetry)*.

Data assimilation Mathematical method used to combine different sources of information in order to produce the best possible estimate of the state of a system. This information usually consists of observations of the system and a numerical model of the system evolution. Data assimilation techniques are used to create initial conditions for weather forecast models and to construct *reanalyses* describing the trajectory of the *climate system* over the time period covered by the observations.

Dead zones Extremely *hypoxic* (i.e., low-oxygen) areas in *oceans* and lakes, caused by excessive nutrient input from human activities coupled with other factors that deplete the oxygen required to support many marine organisms in bottom and near-bottom water.

Decadal predictability Refers to the notion of *predictability* of the *climate system* on a decadal time scale. See also *Climate prediction*, *Predictability* and *Decadal prediction*.

Decadal prediction A *climate prediction* on decadal time scales. See also *Predictability* and *Decadal predictability*.

Decadal variability See *Climate variability*.

Deep uncertainty See *Uncertainty*.

Deforestation Conversion of *forest* to non-forest. [Note: For a discussion of the term forest and related terms such as *afforestation*, *reforestation* and deforestation, see the 2006 IPCC Guidelines for National Greenhouse Gas Inventories and their 2019 Refinement, and information provided by the United Nations Framework Convention on Climate Change (IPCC, 2006, 2019; UNFCCC, 2021a, b).] See also *Afforestation* and *Reforestation*.

Deglacial or deglaciation or glacial termination The period of transition from *glacial* conditions at the end of a glacial period to *interglacial* conditions characterized by a reduction in land ice volume. Gradual changes can be punctuated by *abrupt changes* linked to *stadial*/*interstadial* events and *bipolar seesaw* aspect. The last deglacial transition occurred between about 18,000 and 11,000 years ago. It encompasses rapid events such as *Meltwater Pulse 1A (MWP-1A)* and millennial-scale fluctuations such as the *Younger Dryas*. See also *Glacial–interglacial cycles* and *Ice age*.

Detection Detection of change is defined as the process of demonstrating that *climate* or a system affected by climate has changed in some defined statistical sense, without providing a reason for that change. An identified change is detected in observations if its *likelihood* of occurrence by chance due to *internal variability* alone is determined to be small, for example, <10%.

Detection and attribution See *Detection* and *Attribution*.

Diatoms Microscopic (2–200 µm) unicellular photosynthetic algae that live in surface waters of lakes, rivers and *oceans* and form shells of opal. In the global ocean, marine diatom species distribution is primarily driven by nutrient availability. On regional scales, their species distribution in ocean sediment cores can be related to past *sea surface temperatures* (Abrantes et al., 2013).

Dimensions of integration In IPCC AR6, concepts used to synthesize the knowledge of *climate change* across not just the physical sciences, but also across *impacts*, *adaptation* and *mitigation* research. The concept of 'dimensions of integration' includes (i) emission and *concentration scenarios* underlying the climate change *projections* assessed in this report, (ii) levels of projected global mean temperature change and (iii) total amounts of cumulative carbon emissions for projections.

Direct (aerosol) effect See *Aerosol–radiation interaction*.

Direct air capture (DAC) Chemical process by which a pure *carbon dioxide (CO_2)* stream is produced by capturing CO_2 from the ambient air. See also *Anthropogenic removals* and *Carbon dioxide removal (CDR)*.

Disaster A 'serious disruption of the functioning of a community or a society at any scale due to hazardous events interacting with conditions of exposure, vulnerability and capacity, leading to one or more of the following: human, material, economic and environmental losses and impacts' (UNGA, 2016). See also *Exposure*, *Hazard*, *Risk* and *Vulnerability*.

Discharge (of ice) See *Mass balance/budget (of glaciers or ice sheets)*.

Dissolved inorganic carbon The combined total of different types of non-organic carbon in (seawater) solution, comprising carbonate (CO_3^{2-}), bicarbonate (HCO_3^-), carbonic acid (H_2CO_3) and *carbon dioxide (CO_2)*.

Diurnal temperature range (DTR) The difference between the maximum and minimum temperature during a 24-hour period.

Dobson unit (DU) A unit to measure the total amount of *ozone* in a vertical column above the Earth's surface (total column ozone). The number of Dobson units is the thickness in units of 10^{-5} m that the *ozone* column would occupy if compressed into a layer of uniform density at a pressure of 1013 hPa and a temperature of 0°C. One DU corresponds to a column of ozone containing 2.69×10^{20} molecules per square metre. A typical value for the amount of ozone in a column of the Earth's *atmosphere*, although very variable, is 300 DU.

Downscaling A method that derives local- to regional-scale information from larger-scale models or data analyses. Two main methods exist: dynamical downscaling and empirical/statistical downscaling. The dynamical method uses the output of *regional climate models*, global models with variable spatial *resolution*, or high-resolution global models. The empirical/statistical methods are based on observations and develop statistical relationships that link the large-scale atmospheric variables with local/regional climate variables. In all cases, the quality of the driving model remains an important limitation on quality of the downscaled information. The two methods can be combined, for example, applying empirical/statistical downscaling to the output of a regional climate model consisting of a dynamical downscaling of a global climate model.

Drought An exceptional period of water shortage for existing *ecosystems* and the human population (due to low rainfall, high temperature, and/or wind). See also *Plant evaporative stress*.

Agricultural and ecological drought
Depending on the affected biome: a period with abnormal *soil moisture* deficit, which results from combined shortage of precipitation and excess *evapotranspiration*, and during the growing season impinges on crop production or *ecosystem* function in general.

Hydrological drought
A period with large *runoff* and water deficits in rivers, lakes and reservoirs.

Meteorological drought
A period with an abnormal precipitation deficit.

Dynamic global vegetation model (DGVM) A model that simulates vegetation development and dynamics through space and time, as driven by *climate* and other environmental changes.

Dynamical downscaling See *Downscaling*.

Dynamical system A process or set of processes whose evolution in time is governed by a set of deterministic physical laws. The *climate system* is a dynamical system.

Early Eocene Climatic Optimum (EECO) The EECO is a period of geological time that occurred about 53 to 49 million years ago, during the Eocene Epoch. Continental positions at this time were somewhat different to present due to tectonic plate movements. Geological data indicate that the EECO was a period of relatively high atmospheric CO_2 concentrations (about 1150–2500 ppmv) and relative warmth (*global mean surface temperature* was about 10–18°C above the 1850–1900 reference), and polar *ice sheets* were absent.

Earth system model (ESM) A coupled *atmosphere–ocean general circulation model (AOGCM)* in which a representation of the *carbon cycle* is included, allowing for interactive calculation of atmospheric *carbon dioxide (CO_2)* or *compatible emissions*. Additional components (e.g., atmospheric chemistry, *ice sheets*, dynamic vegetation, nitrogen cycle, but also urban or crop models) may be included. See also *Earth system model of intermediate complexity (EMIC)*.

Earth system model of intermediate complexity (EMIC) EMICs represent *climate* processes at a lower *resolution* or in a simpler, more idealized fashion than an *Earth system model (ESM)*.

Earth's energy budget encompasses the major energy flows of relevance for the *climate system*: the top-of-atmosphere energy budget; the surface energy budget; changes in the global energy inventory and internal flows of energy within the climate system that characterize the climate state.

Top-of-atmosphere energy budget
Comprises the energy fluxes associated with incoming *solar radiation*, reflected solar radiation and emitted thermal radiation. Typical units: W m^{-2}.

Surface energy budget
Comprises the exchanges of heat at the surface of the Earth associated with both radiative and non-radiative processes. Typical units: W m^{-2}.

Global energy inventory
Quantifies the excess energy absorbed or lost by the Earth system (*ocean*, land, *atmosphere* and *cryosphere*), mostly in the form of heat, associated with *radiative forcing* of the *climate*. Typical units: Joules.

Global energy budget
For a given time period, the global energy budget expresses the balance between change in the global energy inventory, the time-integrated *effective radiative forcing* and time-integrated *radiative response of the climate system*. Typical units: Joules.

See also *Earth's energy imbalance*.

Earth's energy imbalance The persistent and positive (downward) net top of atmosphere energy flux associated with greenhouse gas *forcing* of the *climate system*. See also *Earth's energy budget* and *Radiative response (of the climate system)*.

Earth system sensitivity See *Climate sensitivity*.

Effective equilibrium climate sensitivity See *Climate sensitivity*.

East Antarctic Ice Sheet (EAIS) See *Ice sheet*.

East Asian monsoon (EAsiaM) See *Global monsoon*.

Eastern boundary upwelling systems (EBUS) Eastern boundary upwelling systems (EBUS) are located at the eastern (landward) edges of major *ocean* basins in both hemispheres, where equatorward winds drive upwelling currents that bring cool, nutrient-rich (and often oxygen-poor) waters from the deep ocean to the surface near the coast.

Eastern Pacific El Niño See *El Niño–Southern Oscillation (ENSO)*.

Economic potential See *Mitigation potential*.

Ecosystem A functional unit consisting of living organisms, their non-living environment and the interactions within and between them. The components included in a given ecosystem and its spatial boundaries depend on the purpose for which the ecosystem is defined: in some cases, they are relatively sharp, while in others they are diffuse. Ecosystem boundaries can change over time. Ecosystems are nested within other ecosystems, and their scale can range from very small to the entire *biosphere*. In the current era, most ecosystems either contain people as key organisms or are influenced by the effects of human activities in their environment.

Effective radiative forcing (ERF) See *Radiative forcing*, *Aerosol effective radiative forcing (ERFari+aci)* (under *Aerosol–radiation interaction*), *Effective radiative forcing (or effect) due to aerosol–cloud interactions (ERFaci)* (under *Aerosol–cloud interaction*) and *Effective radiative forcing (or effect) due to aerosol–radiation interactions (ERFari)* (under *Aerosol–radiation interaction*).

Ekman transport The total transport resulting from a balance between the Coriolis force and the frictional stress due to the action of the wind on the *ocean* surface.

El Niño See *El Niño–Southern Oscillation (ENSO)*.

El Niño–Southern Oscillation (ENSO) The term El Niño was initially used to describe a warm-water current that periodically flows along the coast of Ecuador and Peru, disrupting the local fishery. It has since become identified with warming of the tropical Pacific Ocean east of the dateline. This oceanic event is associated with a fluctuation of a global-scale tropical and subtropical surface pressure pattern called the Southern Oscillation. This coupled *atmosphere*–*ocean* phenomenon, with preferred time scales of two to about seven years, is known as the El Niño–Southern Oscillation (ENSO). The warm and cold phases of ENSO are called El Niño and La Niña, respectively. ENSO is often measured by the surface pressure anomaly difference between Tahiti and Darwin and/or the *sea surface temperatures* in the central and eastern equatorial Pacific. This phenomenon has a great impact on the wind, sea surface temperature and precipitation patterns in the tropical Pacific. It has climatic effects throughout the Pacific region and in many other parts of the world through global *teleconnections*. See Section AIV.2.3 in Annex IV of the AR6 WGI report.

Central Pacific El Niño
An El Niño event in which *sea surface temperature* anomalies are stronger in the central equatorial Pacific than in the east. Also known as a Modoki El Niño event.

Eastern Pacific El Niño
An El Niño event in which *sea surface temperature* anomalies are largest in the eastern tropical Pacific.

Electromagnetic spectrum Wavelength, frequency or energy range of all electromagnetic radiation. In terms of *solar radiation*, the spectral irradiance is the power arriving at the Earth per unit area, per unit wavelength.

Elevation-dependent warming (EDW) Characteristic of many regions where mountains are located, in which past and/or future surface air temperature changes vary neither uniformly nor linearly with elevation. In many cases, warming is enhanced within or above a certain elevation range.

Emergence (of the climate signal) Emergence of a *climate change* signal or trend refers to when a change in *climate* (the 'signal') becomes larger than the amplitude of natural or internal variations (defining the 'noise'), This concept is often expressed as a 'signal-to-noise' ratio and emergence occurs at a defined threshold of this ratio (e.g., S/N > 1 or 2). Emergence can refer to changes relative to a historical or modern baseline (usually at least 20 years long) and can also be expressed in terms of time (*time of emergence*) or in terms of a global warming level. Emergence is also used to refer to a time when we can expect to see a response to reducing *greenhouse gas (GHG)* emissions (emergence with respect to *mitigation*). Emergence can be estimated using observations and/or model simulations. See also *Time of emergence (ToE)*.

Emergent constraint An attempt to reduce the uncertainty in *climate projections*, using an ensemble of *Earth system models (ESMs)* to relate a specific feedback or future change to an observation of the past or current *climate* (typically some trend, variability or change in variability).

Emission factor/Emissions intensity A coefficient that quantifies the emissions or removals of a gas per unit activity. Emission factors are often based on a sample of measurement data, averaged to develop a representative rate of emission for a given activity level under a given set of operating conditions.

Emission pathways See *Pathways*.

Emissions See *Cumulative emissions*, *Anthropogenic emissions*, *Fossil fuel emissions*, *Non-CO_2 emissions and radiative forcing* and *Negative greenhouse gas emissions*. See also *Emissions scenario* (under *Scenario*), and *Emission pathways.*

Emulation Reproducing the behaviour of complex, process-based models (namely, *Earth system models, ESMs*) via simpler approaches, using either *emulators* or *simple climate models (SCMs)*. The computational efficiency of emulating approaches opens new analytical possibilities given that ESMs take a lot of computational resources for each simulation. See also *Emulators* and *Simple climate model (SCM)*.

Emulators A broad class of heavily parametrized models ('simple climate models'), statistical methods like neural networks, genetic algorithms or other artificial intelligence approaches designed to reproduce the responses of more complex, process-based *Earth system models (ESMs)*. The main application of emulators is to extrapolate insights from ESMs and observational constraints to a larger set of *emission scenarios*. See also *Emulation* and *Simple climate model (SCM)*.

Energy balance model (EBM) An energy balance model is a simplified climate model that is typically used as an emulator of climate to analyse the energy budget of the Earth to compute changes in the *climate*. In its simplest form, there is no explicit spatial dimension, and the model then provides an estimate of the changes in globally averaged temperature computed from the changes in radiation. This zero-dimensional energy balance model can be extended to a one-dimensional or two-dimensional model if changes to the energy budget with respect to latitude, or both latitude and longitude, are explicitly considered.

Energy balance The difference between the total incoming and total outgoing energy. If this balance is positive, warming occurs; if it is negative, cooling occurs. Averaged over the globe and over long time periods, this balance must be zero. Because the *climate system* derives virtually all its energy from the Sun, zero balance implies that, globally, the absorbed *solar radiation*, that is, *incoming solar radiation* minus reflected *solar radiation* at the top of the *atmosphere* and *outgoing longwave radiation* emitted by the *climate system* are equal.

Energy budget (of the Earth) The Earth is a physical system with an energy budget that includes all gains of incoming energy and all losses of outgoing energy. The Earth's energy budget is determined by measuring how much energy comes into the Earth system from the Sun, how much energy is lost to space, and accounting for the remainder on Earth and its *atmosphere*. *Solar radiation* is the dominant source of energy into the Earth system. Incoming solar energy may be scattered and reflected by clouds and *aerosols* or absorbed in the atmosphere. The transmitted radiation is then either absorbed or reflected at the Earth's surface. The average *albedo* of the Earth is about 0.3, which means that 30% of the incident solar energy is reflected into space, while 70% is absorbed by the Earth. Radiant solar or shortwave energy is transformed into sensible heat, latent energy (involving different water states), potential energy, and kinetic energy before being emitted as *infrared radiation*. With the average surface temperature of the Earth of about 15°C (288 K), the main outgoing energy flux is in the infrared part of the spectrum. See also *Sensible heat flux* and *Latent heat flux*.

Enhanced weathering A proposed method to increase the natural rate of removal of *carbon dioxide (CO_2)* from the *atmosphere* using silicate and carbonate rocks. The active surface area of these minerals is increased by grinding, before they are actively added to soil, beaches or the open *ocean*. See also *Carbon dioxide removal (CDR)* and *Anthropogenic removals*.

Ensemble A collection of comparable datasets that reflect variations within the bounds of one or more sources of *uncertainty* and that, when averaged, can provide a more robust estimate of underlying behaviour. Ensemble techniques are used by the observational, *reanalysis* and modelling communities. See also *Climate simulation ensemble*.

Equilibrium and transient climate experiment An equilibrium climate experiment is a *climate model* experiment in which the model is allowed to fully adjust to a change in *radiative forcing*. Such experiments provide information on the difference between the initial and final states of the model, but not on the time-dependent response. If the forcing is allowed to evolve gradually according to a prescribed *emissions scenario*, the time-dependent response of a climate model may be analysed. Such an experiment is called a transient climate experiment.

Equilibrium climate sensitivity (ECS) See *Climate sensitivity*.

Equilibrium line The spatially averaged boundary at a given moment, usually chosen as the seasonal *mass budget* minimum at the end of summer, between the region on a *glacier* where there is a net annual loss of ice mass (ablation area) and that where there is a net annual gain (*accumulation* area). The altitude of this boundary is referred to as equilibrium line altitude (ELA).

Equivalent carbon dioxide (CO_2) emission See *CO_2 equivalent (CO_2-eq) emission*.

Eutrophication Over-enrichment of water by nutrients such as nitrogen and phosphorus. It is one of the leading causes of water quality impairment. The two most acute symptoms of eutrophication are *hypoxia* (or oxygen depletion) and harmful algal blooms.

Evaporation The physical process by which a liquid (e.g., water) becomes a gas (e.g., water vapour).

Evapotranspiration The combined processes through which water is transferred to the *atmosphere* from open water and ice surfaces, bare soil, and vegetation that make up the Earth's surface.

Potential evapotranspiration The potential rate of water loss from wet soils and from plant surfaces, without any limits imposed by the water supply.

Evidence Data and information used in the scientific process to establish findings. In this report, the degree of evidence reflects the amount, quality and consistency of scientific/technical information on which the Lead Authors are basing their findings. See also *Agreement*, *Confidence*, *Likelihood* and *Uncertainty*.

Exposure The presence of people; *livelihoods*; species or *ecosystems*; environmental functions, services, and resources; infrastructure; or economic, social, or cultural assets in places and settings that could be adversely affected.

Extended concentration pathways (ECPs) See *Representative concentration pathways (RCPs)* (under *Pathways*).

External forcing External forcing refers to a *forcing* agent outside the *climate system* causing a change in the climate system. Volcanic eruptions, solar variations and changes in Earth's orbit, as well as *anthropogenic* changes in the composition of the *atmosphere* or in *land use* are external forcings. See also *Orbital forcing*.

Extratropical cyclone (ETC) Any cyclonic-scale storm that is not a *tropical cyclone*. Usually refers to a mid- or high-latitude migratory storm system formed in regions of large horizontal temperature variations. Sometimes called extratropical storm or extratropical low.

Extratropical jets Extratropical jets are wind maxima in the upper *troposphere* marking zones of baroclinic instability. Anomalies in the position of these jets are often associated with storms, *blocking*, and weather extremes.

Extreme climate event See *Climate extreme (extreme weather or climate event)*.

Extreme coastal water level (ECWL) See *Extreme sea level (ESL)*.

Extreme sea level (ESL) The occurrence of an exceptionally low or high local sea surface height, arising from (a combination of) short-term phenomena (e.g., *storm surges*, tides and waves). *Relative sea level changes* affect extreme sea levels directly by shifting the mean water levels and indirectly by modulating the propagation of tides, waves and/or surges due to increased water depth. In addition, extreme sea levels can be influenced by changes in the frequency, tracks or strength of weather systems and storms, or due to anthropogenically induced changes such as the modification of coastlines or dredging. In turn, changes in any or all of the contributions to extreme sea levels may lead to long–term relative sea level changes. Alternate expressions for ESL may be used depending on the processes resolved.

Extreme still water level (ESWL) refers to the combined contribution of relative sea level change, tides and storm-surges. Wind-waves also contribute to coastal sea level via three processes: infragravity waves (lower frequency gravity waves generated by the wind waves), wave setup (time-mean sea level elevation due to wave energy dissipation), and swash (vertical displacement up the shore-face induced by individual waves). Extreme total water level (ETWL) is the ESWL plus wave setup. When considering coastal impacts, swash is also important, and Extreme coastal water level (ECWL) is used. See also *Storm surge* and *Sea level change (sea level rise/sea level fall)*.

Extreme still water level (ESWL) See *Extreme sea level (ESL)*.

Extreme total water level (ETWL) See *Extreme sea level (ESL)*.

Extreme weather event An event that is rare at a particular place and time of year. Definitions of 'rare' vary, but an extreme weather event would normally be as rare as or rarer than the 10th or 90th percentile of a probability density function estimated from observations. By definition, the characteristics of what is called extreme weather may vary from place to place in an absolute sense. See also *Climate extreme (extreme weather or climate event)*.

Extreme/heavy precipitation event An extreme/heavy precipitation event is an event that is of very high magnitude with a very rare occurrence at a particular place. Types of extreme precipitation may vary depending on its duration (hourly, daily or multi-days (e.g., 5 days)) though all of them qualitatively represent high magnitude. The intensity of such events may be defined with a block maxima approach such as annual maxima or with a peaks over threshold approach, such as rainfall above the 95th or 99th percentile at a particular place.

Faculae Bright patches on the Sun. The area covered by faculae is greater during periods of high *solar activity*.

Feedback See *Climate feedback*.

Fine-mode aerosol optical depth See *Aerosol optical depth (AOD)*.

Fingerprint The *climate* response pattern in space and/or time to a specific *forcing* is commonly referred to as a fingerprint. The spatial patterns of sea level response to melting of *glaciers* or *ice sheets* (or other changes in surface loading) are also referred to as fingerprints. Fingerprints are used to detect the presence of this response in observations and are typically estimated using forced *climate model* simulations. See also *Detection* and *attribution*.

Fire weather Weather conditions conducive to triggering and sustaining wildfires, usually based on a set of indicators and combinations of indicators including temperature, *soil moisture*, humidity, and wind. Fire weather does not include the presence or absence of fuel load.

Firn Snow that has survived at least one *ablation* season but has not been transformed to *glacier* ice. Its pore space is at least partially interconnected, allowing air and water to circulate. Firn densities typically are 400–830 kg m^{-3}.

Fitness-for-purpose The suitability of a model (or other resource, such as a dataset or method) for a particular task, such as quantifying the contribution of increased *greenhouse gas* concentrations to recent changes in *global mean surface temperature* or projecting changes in *drought* frequency in a region under a given *scenario*. Assessment of a model's fitness-for-purpose can be informed both by how the model represents relevant physical processes and by how it scores on relevant performance metrics.

Flaring Open air burning of waste gases and volatile liquids, through a chimney, at oil wells or rigs, in refineries or chemical plants, and at landfills.

Flood The overflowing of the normal confines of a stream or other water body, or the accumulation of water over areas that are not normally submerged. Floods can be caused by unusually heavy rain, for example during storms and cyclones. Floods include river (fluvial) floods, flash floods, urban floods, rain (pluvial) floods, sewer floods, *coastal* floods and *glacial lake outburst floods (GLOFs)*.

Flux A movement (a flow) of matter (e.g., water vapour, particles), heat or energy from one place to another, or from one medium (e.g., land surface) to another (e.g., atmosphere).

Foraminifera Single-celled, sand-sized marine organisms (protists) that possess a hard test mainly composed of agglutinated walls (detrital grains glued together with organic cement) or calcium carbonate (predominantly calcite). They are used to reconstruct a range of (paleo)environmental variables such as salinity, temperature, oxygenation, oxygen isotope composition and organic and nutrient flux.

Forcing See *Radiative forcing*.

Forest A vegetation type dominated by trees. Many definitions of the term forest are in use throughout the world, reflecting wide differences in biogeophysical conditions, social structure and economics. [Note: For a discussion of the term forest in the context of National GHG inventories, see the 2006 IPCC Guidelines for National GHG Inventories and their 2019 Refinement, and information provided by the United Nations Framework Convention on Climate Change (IPCC, 2006, 2019; UNFCCC, 2021a, b).] See also *Afforestation*, *Deforestation* and *Reforestation*.

Fossil fuel emissions Emissions of *greenhouse gases (GHGs)* (in particular *carbon dioxide (CO_2)*), other trace gases and *aerosols* resulting from the combustion of fuels from fossil carbon deposits such as oil, gas and coal.

Fossil fuels Carbon-based fuels from fossil hydrocarbon deposits, including coal, oil and natural gas.

Free atmosphere The atmospheric layer that is negligibly affected by friction against the Earth's surface, and which is above the *atmospheric boundary layer*.

Frozen ground Soil or rock in which part or all of the pore water consists of ice. See also *Active layer* and *Permafrost*.

General circulation The large-scale motions of the *atmosphere* and the *ocean* as a consequence of differential heating on a rotating Earth. General circulation contributes to the *energy balance* of the system through transport of heat and momentum.

General circulation model (GCM) A numerical representation of the *atmosphere–ocean–sea ice* system based on the physical, chemical and biological properties of its components, their interactions and feedback processes. General circulation models are used for weather forecasts, seasonal to *decadal prediction*, and *climate projections*. They are the basis of the more complex *Earth system models (ESMs)*. See also *Climate model*.

Geocentric sea level change See *Sea level change (sea level rise/sea level fall)*.

Geoid The equipotential surface having the same geopotential at each latitude and longitude around the world (geodesists denote this potential W0) that best approximates the mean sea level. It is the surface of reference for measurement of altitude. In practice, several variations of definitions of the geoid exist depending on the way the permanent tide (the zero-frequency gravitational tide due to the Sun and Moon) is considered in geodetic studies.

Geostrophic winds or currents A wind or current that is in balance with the horizontal pressure gradient and the Coriolis force, and thus is outside of the influence of friction. Thus, the wind or current is directly parallel to isobars and its speed is proportional to the horizontal pressure gradient.

Glacial isostatic adjustment (GIA) The ongoing changes in *gravity, rotation and viscoelastic solid Earth deformation (GRD)* in response to past changes in the distribution of ice and water on Earth's surface. On a time scale of decades to tens of millennia following mass redistribution, Earth's mantle flows viscously as it evolves toward isostatic equilibrium, causing solid Earth movement and *geoid* changes, which can result in regional-to-local sea level variations. See also *Sea level change (sea level rise/sea level fall)*.

Glacial lake outburst flood (GLOF)/Glacier lake outburst A sudden release of water from a glacier lake, including any of the following types – a glacier-dammed lake, a pro-glacial moraine-dammed lake or water that was stored within, under or on the *glacier*.

Glacial or glaciation A period characterized by the establishment of expanded *ice sheets* and *glaciers*, and associated with global mean sea level (GMSL) substantially lower than present; generally coincides with even-numbered *marine isotope stages*. Glacial intervals were interrupted by *interglacial* intervals. The Last Glacial Maximum (LGM) is a specific interval within the most recent glaciation, when ice sheets were near their global maximum volume (Clark et al., 2009; Gowan et al., 2021) and GMSL was nearly at its lowest level (Lambeck et al., 2014; Yokoyama et al., 2018). Local or regional glacial maxima may be diachronous, for example ranging from about 29,000 years ago and 16,000 years ago. For purposes of global synthesis, IPCC AR6 adopts a practical chronostratigraphic definition of LGM of 23,000–19,000 years BP (before 1950; chronozone level 1 of Mix et al., 2001). For modelling purposes, LGM is defined by the model time step nearest to the centre of this interval, 21,000 years ago (Kageyama et al., 2017). See also *Deglacial or deglaciation or glacial termination*, *Glacial–interglacial cycles*, *Ice age* and *Interglacial or interglaciation*.

Glacial termination See *Deglacial or deglaciation or glacial termination*.

Glacial–interglacial cycles Phase of the Earth's history marked by large changes in continental ice volume and global sea level. See also *Glacial or glaciation*, *Deglacial or deglaciation or glacial termination*, *Interglacial or interglaciation* and *Ice age*.

Glaciated State of a surface that was covered by *glacier* ice in the past, but not at present. See also *Glacierized*.

Glacier A perennial mass of ice, and possibly firn and snow, originating on the land surface by accumulation and compaction of snow and showing evidence of past or present flow. A glacier typically gains mass by *accumulation* of snow and loses mass by *ablation*. Land ice masses of continental size (>50,000 km^2) are referred to as *ice sheets* (Cogley et al., 2011).

Outlet glacier A *glacier*, usually between rock walls, that is part of, and drains, an *ice sheet*. See also *Ice stream*.

Glacierized A surface that is currently covered by *glacier* ice. See also *Glaciated*.

Global carbon budget See *Carbon budget*.

Global dimming Global dimming refers to the observed widespread reduction in the amount of *solar radiation* received at the Earth's surface from the 1950s to the 1980s, with an increase in *anthropogenic* aerosol emissions appearing to have contributed. This was followed by a partial recovery since the 1990s ('brightening'), particularly in industrialized areas, coincident with a reduction in anthropogenic *aerosol* emissions.

Global mean sea level (GMSL) change See *Sea level change (sea level rise/sea level fall)*.

Global mean surface air temperature (GSAT) Global average of near-surface air temperatures over land, *oceans* and *sea ice*. Changes in GSAT are often used as a measure of global temperature change in *climate models*. See also *Global mean surface temperature (GMST)*.

Global mean surface temperature (GMST) Estimated global average of near-surface air temperatures over land and *sea ice*, and *sea surface temperature (SST)* over ice-free *ocean* regions, with changes normally expressed as departures from a value over a specified *reference period*. See also *Global mean surface air temperature (GSAT)*.

Global monsoon The global monsoon (GM) is a global-scale solstitial mode that dominates the annual variation of tropical and sub-tropical precipitation and circulation. The GM domain is defined as the area where the annual range of precipitation (local summer minus winter mean precipitation rate) is greater than 2.5 mm day^{-1}, following on from the definition as in Kitoh et al. (2013). Further details on how the GM is defined, used and related to regional monsoons throughout the Report are provided by Annex V in the AR6 WGI report.

Australian and Maritime Continent monsoon (AusMCM)
The Australian–Maritime Continent monsoon (AusMCM) occurs during December–January–February, with the large-scale shift of the *Inter-tropical Convergence Zone* into the Southern Hemisphere and covering northern Australia and the Maritime Continent up to 10°N. The AusMCM is characterized by the seasonal reversal of prevailing easterly winds to westerly winds and the onset of periods of active *convection* and heavy rainfall. Over northern Australia, the monsoon season generally lasts from December to March and is associated with west to north-westerly inflow of moist winds, producing convection and heavy precipitation. Over the Maritime Continent, the main rainy season south of the equator is centred on December to February with north-westerly monsoon flow at low levels. Further details on how AusMCM is defined and used throughout the Report are provided in Annex V.

East Asian monsoon (EAsiaM)
The East Asian monsoon (EAsiaM) is the seasonal reversal in wind and precipitation occurring over East Asia, including eastern China, Japan and the Korean peninsula. In contrast to the other monsoons it extends quite far north, out of the tropical belt, and it is largely influenced by subtropical systems and by disturbances from the mid-latitudes. The EAsiaM manifests during boreal summer with warm and wet southerly winds, but also during boreal winter with cold and dry northerly winds. In late April/early May, rainfall onsets in the central Indochina Peninsula, and in mid-June the rainy season arrives over East Asia with the formation of the Meiyu front along the Yangtze River valley, Changma in Korea and Baiu in Japan. In July, the monsoon advances up to North China, the Korean peninsula and central Japan. During boreal winter, strong north-westerlies manifest over north and north-east China, Korea and Japan, while strong north-easterlies arrive along the coast of East Asia. Further details on how EAsiaM is defined and used throughout the Report are provided in Annex V.

North American monsoon (NAmerM)
The North American monsoon (NAmerM) is a regional-scale atmospheric circulation system with increases in summer precipitation over northwestern Mexico and southwest United States. The monsoonal characteristics of the region include a pronounced annual maximum of precipitation in boreal summer (June–July–August) accompanied by a surface low pressure system and an upper-level anticyclone, although seasonal reversal of the surface winds is primarily limited to the northern Gulf of California. Further details on how NAmerM is defined and used throughout the Report are provided in Annex V.

South American monsoon (SAmerM)
The South American monsoon (SAmerM) is a regional circulation characterized by inflow of low-level winds from the Atlantic to South America, including Brazil, Peru, Bolivia and northern Argentina, associated with the development of surface pressure gradients (and intense precipitation) during austral summer (December–January–February). During September–October–November, areas of intense *convection* migrate from northwestern South America to the south. Associated with this regime, an upper-tropospheric anticyclone (a.k.a. the Bolivian High) forms over the Altiplano region during the monsoon onset. The SAmerM then retreats during March–April–May with a northeastward migration of the convection. Further details on how SAmerM is defined and used throughout the Report are provided in Annex V.

South and South East Asian monsoon (SAsiaM)
The South and South East Asian monsoon (SAsiaM) is characterized by pronounced seasonal reversals of wind and precipitation. The SAsiaM region extends across vast geographical areas and several countries, including India, Bangladesh, Nepal, Myanmar, Sri Lanka,

Pakistan, Thailand, Laos, Cambodia, Vietnam and the Philippines. The SAsiaM starts in late May/early June and progresses towards the northeast, ending in late September/early October. During the core monsoon season, maxima of SAsiaM precipitation are located over the west coast, north-east and central north India, Myanmar and Bangladesh, whereas minima are located over north-west and south-eastern India, western Pakistan, and south-eastern and northern Sri Lanka. Further details on how SAsiaM is defined and used throughout the Report are provided in Annex V.

West African monsoon (WAfriM)
The West African monsoon (WAfriM) is a seasonal reversal in wind and precipitation whose domain includes Benin, Burkina-Faso, northern Cameroon, Cape Verde, northern Central African Republic, Chad, Gambia, Ghana, Guinea, Guinea Bissau, Ivory Coast, Liberia, Mali, Mauritania, Niger, Nigeria, Senegal, Sierra Leone and Togo. The WAfriM is characterized by the northward progression from May to September of moist low-level south-westerlies from the Gulf of Guinea. In May and June, rainfall essentially remains along the Guinean coast with a maximum occurring near 5°N, followed by a sudden decrease of rainfall, marking the 'short dry season' in the Guinean coast and the monsoon onset in the Sahel. Then rainfall continues to progress northward up to about 18–20°N, with a maximum near 12°N in late August/September, until it retreats starting from October towards the Guinean coast for a second maximum. Further details on how WAfriM is defined and used throughout the Report are provided in Annex V.

Global surface temperature See *Global mean surface temperature (GMST)* and *Global mean surface air temperature (GSAT)*. See also *Global warming*.

Global warming Global warming refers to the increase in *global surface temperature* relative to a baseline *reference period*, averaging over a period sufficient to remove interannual variations (e.g., 20 or 30 years). A common choice for the baseline is 1850–1900 (the earliest period of reliable observations with sufficient geographic coverage), with more modern baselines used depending upon the application. See also *Climate change* and *Climate variability*.

Global warming potential (GWP) An index measuring the *radiative forcing* following an emission of a unit mass of a given substance, accumulated over a chosen time horizon, relative to that of the reference substance, *carbon dioxide* (CO_2). The GWP thus represents the combined effect of the differing times these substances remain in the *atmosphere* and their effectiveness in causing radiative forcing. See also *Lifetime* and *Greenhouse gas emission metric*.

Gravitational, rotational and deformational (GRD) effects See *Sea level change (sea level rise/sea level fall)*.

Gravity Recovery and Climate Experiment (GRACE) A pair of satellites that measured the Earth's gravity field anomalies from 2002 to 2017. These fields have been used, among other things, to study mass changes of the polar *ice sheets* and *glaciers*.

Greenhouse effect The infrared radiative effect of all infrared-absorbing constituents in the *atmosphere*. *Greenhouse gases (GHGs)*, clouds, and some *aerosols* absorb *terrestrial radiation* emitted by the Earth's surface and elsewhere in the atmosphere. These substances emit *infrared radiation* in all directions, but, everything else being equal, the net amount emitted to space is normally less than would have been emitted in the absence of these absorbers because of the decline of temperature with altitude in the *troposphere* and the consequent weakening of emission. An increase in the concentration of GHGs increases the magnitude of this effect; the difference is sometimes called the enhanced greenhouse effect. The change in a GHG concentration because of *anthropogenic emissions* contributes to an instantaneous radiative forcing. Earth's surface temperature and *troposphere* warm in response to this *forcing*, gradually restoring the radiative balance at the top of the atmosphere.

Greenhouse gas emission metric A simplified relationship used to quantify the effect of emitting a unit mass of a given *greenhouse gas* on a specified key measure of *climate change*. A relative GHG emission metric expresses the effect from one gas relative to the effect of emitting a unit mass of a reference GHG on the same measure of climate change. There are multiple emission metrics, and the most appropriate metric depends on the application. GHG emission metrics may differ with respect to (i) the key measure of climate change they consider, (ii) whether they consider climate outcomes for a specified point in time or integrated over a specified time horizon, (iii) the time horizon over which the metric is applied, (iv) whether they apply to a single emission pulse, emissions sustained over a period of time, or a combination of both, and (v) whether they consider the climate effect from an emission compared to the absence of that emission or compared to a reference emissions level or climate state.

Notes: Most relative GHG emission metrics (such as the *global warming potential (GWP)*, global temperature change potential (GTP), global damage potential, and GWP*) use *carbon dioxide* (CO_2) as the reference gas. Emissions of non-CO_2 gases, when expressed using such metrics, are often referred to as 'carbon dioxide equivalent' emissions. A metric that establishes equivalence regarding one key measure of the *climate system* response to emissions does not imply equivalence regarding other key measures. The choice of a metric, including its time horizon, should reflect the policy objectives for which the metric is applied.

Greenhouse gas neutrality Condition in which metric-weighted anthropogenic *greenhouse gas (GHG)* emissions associated with a subject are balanced by metric-weighted anthropogenic GHG removals. The subject can be an entity such as a country, an organization, a district or a commodity, or an activity such as a service or an event. GHG neutrality is often assessed over the life cycle, including indirect ('scope 3') emissions, but can also be limited to the emissions and removals, over a specified period, for which the subject has direct control, as determined by the relevant scheme. The quantification of GHG emissions and removals depends on the GHG emission metric chosen to compare emissions and removals of different gases, as well as the time horizon chosen for that metric.

Note 1: GHG neutrality and net zero GHG emissions are overlapping concepts. The concepts can be applied at global or sub-global scales (e.g., regional, national and sub-national). At a global scale, the terms greenhouse gas neutrality and net zero greenhouse gas emissions are equivalent. At sub-global scales, net zero greenhouse gas emissions is generally applied to emissions and removals under direct control or territorial responsibility of the reporting entity, while greenhouse gas neutrality generally includes emissions and removals within and beyond the direct control or territorial responsibility of the reporting entity. Accounting rules specified by GHG programmes or schemes can have a significant influence on the quantification of relevant emissions and removals.

Note 2. Under the Paris Rulebook (Decision 18/CMA.1, annex, paragraph 37), parties have agreed to use GWP100 values from the IPCC AR5 or GWP100 values from a subsequent IPCC Assessment Report to report aggregate emissions and removals of GHGs. In addition, parties may use other metrics to report supplemental information on aggregate emissions and removals of GHGs.

Note 3: In some cases, achieving greenhouse gas neutrality may rely on the supplementary use of offsets to balance emissions that remain after actions by the reporting entity are taken into account.

See also *Carbon neutrality*, *Greenhouse gas emission metric* and *Net zero greenhouse gas emissions*.

Greenhouse gases (GHGs) Gaseous constituents of the *atmosphere*, both natural and *anthropogenic*, that absorb and emit radiation at specific wavelengths within the spectrum of radiation emitted by the Earth's surface, by the atmosphere itself, and by clouds. This property causes the *greenhouse effect*. Water vapour (H_2O), *carbon dioxide (CO_2)*, *nitrous oxide (N_2O)*, *methane (CH_4)* and *ozone (O_3)* are the primary GHGs in the Earth's atmosphere. Human-made GHGs include *sulphur hexafluoride (SF_6), hydrofluorocarbons (HFCs)*, *chlorofluorocarbons (CFCs)* and perfluorocarbons (PFCs); several of these are also O_3-depleting (and are regulated under the *Montreal Protocol*). See also *Well-mixed greenhouse gas*.

Greenland Ice Sheet (GrIS) See *Ice sheet*.

Gross Primary Production (GPP) See *Primary production*.

Ground-level ozone Atmospheric *ozone (O_3)* is formed naturally or from human-emitted *precursors* near Earth's surface, thus affecting human health, agriculture and *ecosystems*. Ozone is a *greenhouse gas (GHG)*, but ground-level ozone, unlike stratospheric ozone, also directly affects organisms at the surface. Ground-level ozone is sometimes referred to as tropospheric ozone, although much of the *troposphere* is well above the surface and thus does not directly expose organisms at the surface.

Grounding line The junction between a *glacier* or *ice sheet* and an *ice shelf*; the place where ice starts to float. This junction normally occurs over a zone, rather than at a line.

Gyre Basin-scale *ocean* horizontal circulation pattern with slow flow circulating around the ocean basin, closed by a strong and narrow (100 to 200 km wide) boundary current on the western side. The subtropical gyres in each ocean are associated with high pressure in the centre of the gyres; the subpolar gyres are associated with low pressure.

Hadley cell See *Hadley circulation*.

Hadley circulation A direct, thermally driven overturning cell in the *atmosphere* consisting of poleward flow in the upper *troposphere*, subsiding air into the subtropical anticyclones, return flow as part of the trade winds near the surface, and with rising air near the equator in the so-called *Inter-tropical Convergence Zone*.

Halocarbons A collective term for the group of partially halogenated organic species, which includes the *chlorofluorocarbons (CFCs)*, hydrochlorofluorocarbons (HCFCs), *hydrofluorocarbons (HFCs)*, halons, methyl chloride and methyl bromide. Many of the halocarbons have large *global warming potentials*. The chlorine and bromine-containing halocarbons are also involved in the depletion of the *ozone layer*.

Halocline A layer in the oceanic water column in which salinity changes rapidly with depth. Generally, saltier water is denser and lies below less salty water. In some high-latitude *oceans* the surface waters may be colder than the deep waters, and the halocline is responsible for maintaining water column stability and isolating the surface waters from the deep waters.

Halosteric See *Sea level change (sea level rise/sea level fall)*.

Halosteric sea level change See *Sea level change (sea level rise/sea level fall)*.

Hazard The potential occurrence of a natural or human-induced physical event or trend that may cause loss of life, injury, or other health *impacts*, as well as damage and loss to property, infrastructure, *livelihoods*, service provision, *ecosystems* and environmental resources. See also *Impacts (consequences, outcomes)* and *Risk*.

Heat index A measure of how hot the air feels to the human body. The index is mainly based on surface air temperature and *relative humidity*; thus it reflects the combined effect of high temperature and humidity on human physiology and provides a relative indication of potential health risks.

Heat stress A range of conditions in, for example, terrestrial or aquatic organisms when the body absorbs excess heat during overexposure to high air or water temperatures or thermal radiation. In aquatic water-breathing animals, hypoxia and acidification can exacerbate *vulnerability* to heat. Heat stress in mammals (including humans) and birds, both in air, is exacerbated by a detrimental combination of ambient heat, high humidity and low wind speeds, causing regulation of body temperature to fail.

Heatwave A period of abnormally hot weather, often defined with reference to a relative temperature threshold, lasting from two days to months. Heatwaves and warm spells have various and, in some cases, overlapping definitions. See also *Marine heatwave*, *Blocking*, *Heat index* and *Heat stress*.

Heavy precipitation event See *Extreme/heavy precipitation event*.

Heinrich event Distinct layers of coarse-grained sediments comprised of ice-rafted debris identified across marine sediment cores in the North Atlantic. These sedimentary layers are closely associated with millennial-scale cooling events in the North Atlantic and a distinct pattern of global temperature and hydrological changes that are largely consistent with evidence for a slowdown, or even near-collapse, of the *Atlantic Meridional Overturning Circulation (AMOC)* during these times.

Heterotrophic respiration The conversion of organic matter to *carbon dioxide (CO_2)* by organisms other than autotrophs.

Holocene The current *interglacial* geological epoch, the second of two epochs within the *Quaternary* Period, the preceding being the *Pleistocene*. The International Commission on Stratigraphy (ICS) defines the start of the Holocene Epoch at 11,700 years before 2000 (Walker et al., 2019) spanning the interval from 11,700 yr to the present day. Together with the subadjacent Pleistocene, it comprises the Quaternary System/Period. The Holocene record contains diverse geomorphological, biological, climatological and archaeological evidence, within sequences that are often continuous and extremely well-preserved at decadal, annual and even seasonal resolution. As a consequence, the Holocene is perhaps the most intensively studied series/epoch within the entire Geological Time Scale. Yet until recently little attention had been paid to a formal subdivision of the Holocene. Here we describe an initiative by the Subcommission on Quaternary Stratigraphy (SQS. It encompasses the mid-Holocene (MH), the 1000-year-long interval centred at 6000 years before 1950; a period of long-standing focus for climate modelling, with enhanced seasonality in the Northern Hemisphere and decreased seasonality in the Southern Hemisphere. The early part of the Holocene is marked by the late stages of *deglaciation* of Pleistocene land ice, sea level rise, and the occurrence of warm phases that affected different regions at different times, often referred to as the 'Holocene Thermal Maximum'. In addition, the epoch includes the post-glacial interval, which began approximately 7000 years ago when the fundamental features of the modern *climate system* were essentially in place, as the influence of remnant Pleistocene *ice sheets* waned. See also *Anthropocene*.

Holocene Thermal Maximum (HTM) See *Holocene*.

Human influence on the climate system Human-driven activities that lead to changes in the *climate system* due to perturbations of the Earth's energy budget (also called anthropogenic *forcing*). Human influence results from emissions of *greenhouse gases*, *aerosols*, *ozone-depleting substances (ODSs)*, and *land-use change*. See also *Anthropogenic*, *Anthropogenic emissions* and *Anthropogenic removals*.

Human system Any system in which human organizations and institutions play a major role. Often, but not always, the term is synonymous with society or social system. Systems such as agricultural systems, urban systems, political systems, technological systems and economic systems are all human systems in the sense applied in this Report.

Hurricane See *Tropical cyclone*.

Hydroclimate Part of the *climate* pertaining to the hydrology of a *region*.

Hydrofluorocarbons (HFCs) A type of *greenhouse gas (GHG)*, HFCs are organic compounds that contain fluorine, carbon and hydrogen atoms and they are produced commercially as a substitute for *chlorofluorocarbons (CFCs)*. They are mainly used in refrigeration and semiconductor manufacturing.

Hydrological cycle The cycle in which water evaporates from the *ocean* and the land surface, is carried over the Earth in atmospheric circulation as water vapour, condenses to form clouds, precipitates over the ocean and land as rain or snow, which on land can be intercepted by trees and vegetation, potentially accumulating as snow or ice, provides runoff on the land surface, infiltrates into soils, recharges groundwater, discharges into streams, and ultimately, flows into the oceans as rivers, polar *glaciers* and *ice sheets*, from which it will eventually evaporate again. The various systems involved in the hydrological cycle are usually referred to as hydrological systems.

Hydrological drought See *Drought*.

Hydrological sensitivity (η) The linear change in global mean precipitation per degree Celsius of *global mean surface air temperature (GSAT)* change once precipitation changes related to fast atmospheric and land surface adjustments to *radiative forcings* have occurred. Units are % per °C although it can also be calculated as W m^{-2} per °C. See also *Apparent hydrological sensitivity (η_a)*.

Hydrosphere The component of the *climate system* comprising liquid surface and subterranean water, such as in *oceans*, seas, rivers, freshwater lakes, underground water, *wetlands*, etc.

Hypoxic Conditions of low dissolved oxygen in shallow water *ocean* and freshwater environments. There is no universal threshold for hypoxia. A value around 60 µmol kg^{-1} has commonly been used for some estuarine systems, although this does not necessarily directly translate into biological impacts. Anoxic conditions occur where there is no oxygen present at all. See also *Eutrophication*.

Hypsometry The distribution of land or ice surface as a function of altitude.

Ice age An informal term for a geological period characterized by a long-term reduction in the temperature of the Earth's *climate*, resulting in the presence or expansion of *ice sheets* and *glaciers*. Among the Earth's ice ages is the current *Quaternary* Period, characterized by alternating *glacial* and *interglacial* intervals. See also *Deglacial or deglaciation or glacial termination* and *Glacial–interglacial cycles*.

Ice core A cylinder of ice drilled out of a *glacier* or *ice sheet* to determine the physical properties of the ice body and to gain information on past changes in *climate* and composition of the *atmosphere* that are preserved in the ice or in air trapped in the ice.

Ice sheet An ice body originating on land that covers an area of continental size, generally defined as covering >50,000 km^2, and that has formed over thousands of years through *accumulation* and compaction of snow. An ice sheet flows outward from a high central ice plateau with a small average surface slope. The margins usually slope more steeply, and most ice is *discharged* through fast-flowing ice streams or *outlet glaciers*, often into the sea or into *ice shelves* floating on the sea. There are only two ice sheets in the modern world, one on Greenland and one on Antarctica. The latter is divided into the East Antarctic Ice Sheet (EAIS), the West Antarctic Ice Sheet (WAIS) and the Antarctic Peninsula Ice Sheet. During *glacial* periods, there were other ice sheets.

Ice shelf A floating slab of ice originating from land of considerable thickness extending from the coast (usually of great horizontal extent with a very gently sloping surface), resulting from the flow of *ice sheets*, initially formed by the accumulation of snow, and often filling embayments in the coastline of an ice sheet. Nearly all ice shelves are in Antarctica, where most of the ice *discharged* into the *ocean* flows via ice shelves.

Ice stream A stream of ice with strongly enhanced flow that is part of an *ice sheet*. It is often separated from surrounding ice by strongly sheared, crevassed margins.

Ice–albedo feedback A *climate feedback* involving changes in the Earth's surface *albedo*. Snow and ice have an albedo much higher (up to ~0.8) than the average planetary albedo (~0.3). With increasing temperatures, it is anticipated that snow and ice extent will decrease, the Earth's overall albedo will decrease and more *solar radiation* will be absorbed, warming the Earth further.

Iceberg Large piece of freshwater ice broken off from a *glacier* or an *ice shelf* during *calving* and floating in open water (at least 5 m height above sea level). Smaller pieces of floating ice known as 'bergy bits' (less than 5 m above sea level) or 'growlers' (less than 2 m above sea level) can originate from glaciers or ice shelves, or from the breaking up of a large iceberg. Icebergs can also be classified by shape, most commonly being either tabular (steep sides and a flat top) or non-tabular (varying shapes, with domes and spires) (NOAA, 2021). In lakes, icebergs can originate by breaking off shelf ice, which forms through freezing of a lake surface.

Impacts The consequences of realized *risks* on natural and human systems, where risks result from the interactions of climate-related *hazards* (including extreme weather/climate events), *exposure*, and *vulnerability*. Impacts generally refer to effects on lives, *livelihoods*, health and well-being, *ecosystems* and species, economic, social and cultural assets, services (including ecosystem services), and infrastructure. Impacts may be referred to as consequences or outcomes and can be adverse or beneficial. See also *Adaptation*, *Exposure*, *Hazard*, *Vulnerability* and *Risk*.

Incoming solar radiation See *Insolation*.

Indian Ocean basin (IOB) mode A mode of interannual variability characterized by a temporal alternation of basin-wide warming and cooling of the Indian Ocean sea surface. It mostly develops in response to *El Niño–Southern Oscillation (ENSO)*, but often persists after ENSO's equatorial eastern Pacific signal has dissipated. The IOB affects atmospheric circulation, temperature, and precipitation in South, South East, and East Asia as well as Africa, and modulates *tropical cyclone* activity in the north-western Pacific. See Section AIV.2.4 in Annex IV of the AR6 WGI report. See also *Modes of climate variability* and *Indian Ocean Dipole (IOD)*.

Indian Ocean Dipole (IOD) A mode of interannual variability that features an east–west dipole of *sea surface temperature* anomalies in the tropical Indian Ocean. Its positive phase shows concurrent sea surface cooling off Sumatra and Java and warming off Somalia in the west, combined with anomalous surface easterlies along the equator, while the opposite anomalies are seen in the negative phase. The IOD typically develops in boreal summer and matures in boreal autumn and controls part of the rainfall interannual variability in Australia, South Eastern Asia and Eastern Africa. See Section AIV.2.4 in Annex IV of the AR6 WGI report. See also *Indian Ocean Basin (IOB) mode*.

Indirect aerosol effect See *Aerosol–cloud interaction*.

Indirect land-use change (iLUC) See *Land-use change (LUC)*.

Industrial revolution A period of rapid industrial growth with far-reaching social and economic consequences, beginning in Britain during the second half of the 18th century and spreading to Europe and later to other countries including the United States. The invention of the steam engine was an important trigger of this development. The industrial revolution marks the beginning of a strong increase in the use of *fossil fuels*, initially coal, and hence emission of *carbon dioxide (CO_2)*.

Infrared radiation See *Terrestrial radiation*.

Initial condition ensemble (ICE) See *Climate simulation ensemble*.

Insolation The amount of *solar radiation* reaching the Earth by latitude and by season measured in W m^{-2}. Usually, insolation refers to the radiation arriving at the top of the *atmosphere*. Sometimes it is specified as referring to the radiation arriving at the Earth's surface. See also *Orbital forcing* and *Total solar irradiance (TSI)*.

Instantaneous radiative forcing (or effect) due to aerosol–cloud interactions (IRFaci) See *Aerosol–cloud interaction*.

Instantaneous radiative forcing (or effect) due to aerosol–radiation interactions (IRFari) See *Aerosol–radiation interaction*.

Integrated assessment model (IAM) Models that integrate knowledge from two or more domains into a single framework. They are one of the main tools for undertaking integrated assessments. One class of IAM used with respect to climate change *mitigation* may include representations of: multiple sectors of the economy, such as energy, *land use* and *land-use change*; interactions between sectors; the economy as a whole; associated *greenhouse gas (GHG)* emissions and *sinks*; and reduced representations of the *climate system*. This class of model is used to assess linkages between economic, social and technological development and the evolution of the climate system. Another class of IAM additionally includes representations of the costs associated with climate change *impacts*, but includes less detailed representations of economic systems. These can be used to assess impacts and mitigation in a cost–benefit framework and have been used to estimate the social cost of carbon.

Inter-decadal Pacific Oscillation (IPO) See *Pacific Decadal Variability (PDV)*.

Inter-tropical Convergence Zone (ITCZ) The Inter-tropical Convergence Zone is an equatorial zonal belt of low pressure, strong *convection* and heavy precipitation near the equator where the north-east trade winds meet the south-east trade winds. This band moves seasonally. See also *South Pacific Convergence Zone (SPCZ)*.

Interglacial or interglaciation A globally warm period lasting thousands of years between *glacial* periods within an *ice age*. Generally coincides with odd-numbered *marine isotope stages (MIS)* when mean sea level was close to present. The Last Interglacial (LIG) occurred between about 129 and 116 ka (thousand years) before present (defined as 1950) although the warm period started in some areas a few thousand years earlier. In terms of MIS, *interglaciations* are defined as the interval between the midpoint of the preceding termination and the onset of the next glaciation. The LIG coincides with MIS 5e. The present interglaciation, the *Holocene*, started at 11,700 years before 2000 CE, although global mean sea level did not approach its present position until roughly 7000 years ago. See also

Deglacial or deglaciation or glacial termination, *Glacial-interglacial cycles*, *Glacial or glaciation* and *Ice age*.

Internal climate variability See *Internal variability* (under *Climate variability*).

Interstadial or interstade A brief period of regional climatic warming during a *glacial* or *interglacial* interval, often characterized by transient glacial retreats. Interstadials are generally of short duration (hundreds to a few thousand years) compared to glacial or interglacial intervals (lasting many thousands to tens of thousands of years). One example of a regional interstadial event is based on millennial scale warming recorded by oxygen *isotope* ratios in Greenland *ice cores*, the so called "Greenland Interstadials" (Johnsen et al., 1992). See also *Stadial or stade*.

Irreversibility A perturbed state of a *dynamical system* is defined as irreversible on a given time scale if the recovery from this state due to natural processes takes substantially longer than the time scale of interest. See also *Tipping point*.

Isostatic or Isostasy Isostasy refers to the response of the Earth to changes in surface load. It includes the deformational and gravitational response. This response is elastic on short time scales, as in the Earth–*ocean* response to recent changes in mountain glaciation, or viscoelastic on longer time scales, as in the response to the last *deglaciation* following the *Last Glacial Maximum*.

Isotopes Atoms of the same chemical element that have the same the number of protons but differ in the number of neutrons. Some proton–neutron configurations are stable (stable isotopes), others are unstable undergoing spontaneous radioactive decay (radioisotopes). Most elements have more than one stable isotope. Isotopes can be used to trace transport processes or to study processes that change the isotopic ratio. Radioisotopes provide, in addition, time information that can be used for radiometric dating. See also *^{13}C* and *^{14}C*.

Key climate indicators See *Climate indicator*.

Kriging Kriging is a method of interpolation (normally spatial interpolation when used with atmospheric or oceanographic data) in which the interpolated values are estimated using a Gaussian process governed by prior covariances.

La Niña See *El Niño–Southern Oscillation (ENSO)*.

Land The terrestrial portion of the biosphere that comprises the natural resources (soil, near-surface air, vegetation and other biota, and water), the ecological processes, topography, and human settlements and infrastructure that operate within that system (UNCCD, 1994; FAO, 2007).

Land cover The biophysical coverage of *land* (e.g., bare soil, rocks, *forests*, buildings and roads or lakes). Land cover is often categorized in broad land-cover classes (e.g., deciduous forest, coniferous forest, mixed forest, grassland, bare ground). [Note: In some literature, land cover and *land use* are used interchangeably, but the two represent distinct classification systems. For example, the land cover class woodland can be under various land uses such as livestock grazing, recreation, conservation, or wood harvest.]

Land–cover change Change from one *land cover* class to another, due to change in *land use* or change in natural conditions (Pongratz et al., 2018). See also *Land-use change (LUC)*.

Land surface air temperature (LSAT) The near-surface air temperature over land, typically measured at 1.25–2 m above the ground using standard meteorological equipment.

Land use The total of arrangements, activities and inputs applied to a parcel of *land*. The term land use is also used in the sense of the social and economic purposes for which land is managed (e.g., grazing, timber extraction, conservation and city dwelling). In national *greenhouse gas (GHG)* inventories, land use is classified according to the IPCC land-use categories of forest land, cropland, grassland, wetlands, settlements, other lands (see the 2006 IPCC Guidelines for National GHG Inventories and their 2019 Refinement for details (IPCC, 2006, 2019)).

Land-use change (LUC) The change from one *land use* category to another. Note that in some scientific literature, land-use change encompasses changes in land-use categories as well as changes in land management. See also *Afforestation, Deforestation* and *Reforestation*.

Indirect land-use change (iLUC) Land-use change outside the area of focus that occurs as a consequence of change in use or management of land within the area of focus, such as through market or policy drivers. For example, if agricultural land is diverted to biofuel production, *forest* clearance may occur elsewhere to replace the former agricultural production. See *Land-use change (LUC)*.

Land water storage (LWS) Land water storage (LWS) includes all surface water, *soil moisture*, groundwater storage and snow, but excludes water stored in *glaciers* and *ice sheets*. Changes in LWS can be caused either by direct human intervention in the water cycle (e.g., storage of water in reservoirs by building dams in rivers, groundwater extraction from groundwater reservoirs for consumption and irrigation, or *deforestation*) or by *climate* variations (e.g., changes in the amount of water in endorheic lakes and *wetlands*, the canopy, the soil, the *permafrost* and the snowpack). Land water storage changes caused by climate variations may also be indirectly affected by *anthropogenic* influences. See also *Sea level change (sea level rise/sea level fall)*.

Lapse rate The rate of change of an atmospheric variable, usually temperature, with height. The lapse rate is considered positive when the variable decreases with height.

Large-scale The *climate system* involves process interactions from the micro- to the global-scale. Any threshold for defining 'large-scale' is arbitrary. Understanding of large-scale *climate variability* and change requires knowledge of both the response to external *forcings* and the role of *internal variability*. Many external forcings have substantial hemispheric or continental scale variations. *Modes of climate variability* are driven by *ocean*-basin-scale processes. Thus we define large-scale to include ocean-basin and continental scales as well as hemispheric and global scales.

Last deglacial transition See *Deglacial or deglaciation or glacial termination* and *Younger Dryas*.

Last Glacial Maximum (LGM) See *Glacial or glaciation*.

Last Interglacial (LIG) See *Interglacial or interglaciation*.

Last millennium The interval of the *Common Era (CE)* between 1001 and 2000 CE. Encompasses the Little Ice Age, a roughly defined period characterized by multiple expansions of mountain *glaciers* worldwide, the timing of which differs among regions but generally occurred between 1400 CE and 1900 CE. The last millennium also mostly encompasses the Medieval Warm Period (also called the Medieval Climate Anomaly), a roughly defined period of relatively warm conditions or other *climate* excursions such as extensive *drought*, the timing and magnitude of which differ among regions, but generally occurred between 900 and 1400 CE. Transient *climate model* experiments by the Paleoclimate Modelling Intercomparison Project (PMIP) for the last millennium extend from 850–1849 CE.

Latent heat flux The turbulent *flux* of heat from the Earth's surface to the *atmosphere* that is associated with *evaporation* or condensation of water vapour at the surface; a component of the surface energy budget. See also *Sensible heat flux*.

Lifetime Lifetime is a general term used for various time scales characterizing the rate of processes affecting the concentration of trace gases. The following lifetimes may be distinguished:

Response time or adjustment time (T_a)
Response time or adjustment time (T_a) is the time scale characterizing the decay of an instantaneous pulse input into the *reservoir*. The term adjustment time is also used to characterize the adjustment of the mass of a reservoir following a step change in the *source* strength. Half-life or decay constant is used to quantify a first-order exponential decay process. See *Response time or adjustment time* for a different definition pertinent to *climate* variations.

The term lifetime is sometimes used, for simplicity, as a surrogate for adjustment time.

In simple cases, where the global removal of the compound is directly proportional to the total mass of the reservoir, the adjustment time equals the *turnover time*: $T = T_a$. An example is CFC-11, which is removed from the *atmosphere* only by photochemical processes in the *stratosphere*. In more complicated cases, where several reservoirs are involved or where the removal is not proportional to the total mass, the equality $T = T_a$ no longer holds.

Carbon dioxide (CO_2) is an extreme example. Its turnover time is only about 4 years because of the rapid exchange between the atmosphere and the *ocean* and terrestrial biota. However, a large part of that CO_2 is returned to the atmosphere within a few years. The adjustment time of CO_2 in the atmosphere is determined from the rates of removal of carbon by a range of processes with time scales from months to hundreds of thousands of years. As a result, 15 to 40% of an emitted CO_2 pulse will remain in the atmosphere longer than 1,000 years, 10 to 25% will remain about ten thousand years, and the rest will be removed over several hundred thousand years.

In the case of *methane (CH_4)*, the adjustment time is different from the turnover time because the removal is mainly through a chemical reaction with the hydroxyl radical (OH), the concentration of which itself depends on the CH_4 concentration. Therefore, the CH_4 removal rate S is not proportional to its total mass M.

Turnover time (T) (also called global atmospheric lifetime) is the ratio of the mass M of a *reservoir* (e.g., a gaseous compound in the *atmosphere*) and the total rate of removal S from the *reservoir*: T = M/S. For each removal process, separate turnover times can be defined. In soil carbon biology, this is referred to as mean residence time.

Light-absorbing particles Light-absorbing particles (LAP), for example, *black carbon (BC)*, brown carbon and dust, are particles that absorb *solar radiation* and convert it into internal energy, thus raising the particle's temperature and emitting thermal-infrared radiation that is selectively absorbed by the surrounding medium. LAP affect the energy balance of the *atmosphere* and clouds, and when deposited on snow and ice, they reduce snow/ice albedo, increasing heating and accelerating melting. These particles have a warming effect on *climate*.

Likelihood The chance of a specific outcome occurring, where this might be estimated probabilistically. Likelihood is expressed in this report using a standard terminology (Mastrandrea et al., 2010). See also *Agreement*, *Confidence*, *Evidence* and *Uncertainty*.

Lithosphere The upper layer of the solid Earth, both continental and oceanic, which comprises all crustal rocks and the cold, mainly elastic part of the uppermost mantle. Volcanic activity, although part of the *lithosphere*, is not considered as part of the *climate system*, but acts as an *external forcing* factor.

Livelihood The resources used and the activities undertaken in order for people to live. Livelihoods are usually determined by the entitlements and assets to which people have access. Such assets can be categorized as human, social, natural, physical or financial.

Local sea level change See *Sea level change (sea level rise/sea level fall)*.

Long-lived greenhouse gases (LLGHGs) A set of *well-mixed greenhouse gases* with long atmospheric *lifetimes*. This set of compounds includes *carbon dioxide (CO_2)* and *nitrous oxide (N_2O)*, together with some halogenated compounds. They have a warming effect on *climate*. These compounds accumulate in the *atmosphere* at decadal to centennial time scales, and their effect on climate hence persists for decades to centuries after their emission. On time scales of decades to a century, already emitted emissions of long-lived climate forcers can only be abated by greenhouse gas removal.

Longwave radiation See *Terrestrial radiation*.

Low-likelihood, high impact outcomes Outcomes/events whose probability of occurrence is low or not well known (as in the context of *deep uncertainty*) but whose potential *impacts* on society and *ecosystems* could be high. To better inform *risk assessment* and decision-making, such low-*likelihood* outcomes are considered if they are associated with very large consequences and may therefore constitute material *risks*, even though those consequences do not necessarily represent the most likely outcome.

Madden–Julian Oscillation (MJO) The largest mode of tropical atmospheric intra-seasonal variability with typical periods ranging from 20 to 90 days. The MJO corresponds to planetary-scale disturbances of pressure, wind and deep *convection* moving predominantly eastward along the equator. As it progresses, the MJO is associated with the temporal alternation of large-scale enhanced and suppressed rainfall, with maximum loading over the Indian and western Pacific oceans, although influences of the MJO can be tracked over the Atlantic/Africa in dynamical fields. See Section AIV.2.8 in Annex IV of the AR6 WGI report.

Maladaptive actions (Maladaptation) Actions that may lead to increased *risk* of adverse *climate*-related outcomes, including via increased *greenhouse gas (GHG)* emissions, increased *vulnerability* to *climate change*, or diminished welfare, now or in the future. Maladaptation is usually an unintended consequence.

Marine cloud brightening (MCB) See *Solar radiation modification (SRM)*.

Marine heatwave A period during which water temperature is abnormally warm for the time of the year relative to historical temperatures, with that extreme warmth persisting for days to months. The phenomenon can manifest in any place in the *ocean* and at scales of up to thousands of kilometres. See also *Heatwave*.

Marine ice cliff instability (MICI) A hypothetical mechanism of an ice cliff failure. In case a marine-terminated *ice sheet* loses its buttressing *ice shelf*, an ice cliff can be exposed. If the exposed ice cliff is tall enough (about 800 m of the total height, or about 100 m of the above-water part), the stresses at the cliff face exceed the strength of the ice, and the cliff fails structurally in repeated *calving* events. See also *Marine ice sheet instability (MISI)*.

Marine ice sheet instability (MISI) A mechanism of *irreversible* (on the decadal to centennial time scale) retreat of a *grounding line* for the marine-terminating *glaciers*, in case the glacier bed slopes towards the *ice sheet* interior. See also *Marine ice cliff instability (MICI)*.

Marine isotope stage (MIS) Geological periods of alternating *glacial* and *interglacial* conditions, each typically lasting tens of thousands of years as inferred from the oxygen *isotope* composition of microfossils from deep sea sediment cores. MIS numbers increase back in time from the present, which is MIS 1. Even-number MISs coincide with glacial periods, and odd-numbered MISs are interglacials.

Marine-based ice sheet An *ice sheet* containing a substantial region that rests on a bed lying below sea level and whose perimeter is in contact with the *ocean*. The best known example is the West Antarctic Ice Sheet.

Mass balance/budget (of glaciers or ice sheets) Difference between the mass input (*accumulation*) and the mass loss (*ablation*) of an ice body (e.g., a *glacier* or *ice sheet*) over a stated time period, which is often a year or a season. Surface mass balance refers to the difference between surface accumulation and surface ablation.

Ablation (of glaciers, ice sheets, or snow cover)
All processes that reduce the mass of a *glacier*, *ice sheet*, or *snow cover*. The main processes are melting, and for glaciers also *calving* (or, when the glacier nourishes an *ice shelf*, *discharge of ice* across the *grounding line*), but other processes such as sublimation and loss of wind-blown snow can also contribute to ablation. Ablation also refers to the mass lost by any of these processes.

Accumulation (of glaciers, ice sheets, or snow cover)
All processes that add to the mass of a *glacier*, an *ice sheet*, or *snow cover*. The main process of accumulation is snowfall. Accumulation also includes deposition of hoar, freezing rain, other types of solid precipitation, gain of wind-blown snow, avalanching, and basal accumulation (often beneath floating ice).

Discharge (of ice)
Rate of the flow of ice through a vertical section of a *glacier* perpendicular to the direction of the flow of ice. Often used to refer to the loss of mass at marine-terminating glacier fronts (mostly *calving* of *icebergs* and submarine melt), or to mass flowing across the *grounding line* of a floating *ice shelf*.

Mean sea level The surface level of the *ocean* at a particular point averaged over an extended period of time such as a month or year. Mean sea level is often used as a national datum to which heights on land are referred.

Megacity Urban agglomerations with 10 million inhabitants or more.

Meltwater Pulse 1A (MWP-1A) A particular interval of rapid global *sea level rise* between about 14,700 and 14,300 years ago, associated with the end of the last *ice age* and attributed to freshwater *flux* to the *ocean* from accelerated melting of *ice sheets* and *glaciers*. First defined based on oxygen *isotope* data (Duplessy et al., 1981), and later shown to be reflected by high rates of sea level rise (Fairbanks, 1989). See also *Deglacial or deglaciation or glacial termination*.

Meridional overturning circulation (MOC) Meridional (north–south) overturning circulation in the *ocean* quantified by zonal (east–west) sums of mass transports in depth or density layers. In the North Atlantic, away from the subpolar regions, the MOC (which is in principle an observable quantity) is often identified with the thermohaline circulation (THC), which is a conceptual and incomplete interpretation. The MOC is also driven by wind, and can also include shallower overturning cells such as occur in the upper ocean in the tropics and subtropics, in which warm (light) waters moving poleward are transformed to slightly denser waters and subducted equatorward at deeper levels.

Atlantic Meridional Overturning Circulation (AMOC)
The main current system in the South and North Atlantic Oceans. AMOC transports warm upper-*ocean* water northwards and cold, deep water southwards, as part of the global ocean circulation system. Changes in the strength of AMOC can affect other components of the *climate system*.

Meteorological drought See *Drought*.

Methane (CH_4) The greenhouse gas methane is the major component of natural gas and associated with all hydrocarbon fuels. Significant *anthropogenic emissions* also occur as a result of animal husbandry and paddy rice production. Methane is also produced naturally where organic matter decays under anaerobic conditions, such as in *wetlands*. Under future *global warming*, there is potential for increased methane emissions from thawing *permafrost*, *wetlands* and sub-sea gas hydrates. See also *Short-lived climate forcers (SLCFs)*.

Microclimate Local *climate* at or near the Earth's surface.

Microwave sounding unit (MSU) A microwave sounder on U.S. National Oceanic and Atmospheric Administration (NOAA) polar orbiter satellites that estimates the temperature of thick layers of the *atmosphere* by measuring the thermal emission of oxygen molecules from a complex of emission lines near 60 GHz. A series of nine MSUs began making this kind of measurement in late 1978. Beginning in mid-1998, a follow-on series of instruments, the Advanced Microwave Sounding Units (AMSUs), began operation.

Mid-Holocene (MH) See *Holocene*.

Mid-Pliocene Warm Period (MPWP) See *Pliocene*.

Mineralization/Remineralization The conversion of an element from its organic form to an inorganic form as a result of microbial decomposition. In nitrogen mineralization, organic nitrogen from decaying plant and animal residues (proteins, nucleic acids, amino sugars and urea) is converted to ammonia (NH_3) and ammonium (NH_4^+) by biological activity.

Mitigation (of climate change) A human intervention to reduce emissions or enhance the *sinks* of *greenhouse gases*.

Mitigation pathways See *Pathways*.

Mitigation potential The quantity of net *greenhouse gas* emission reductions that can be achieved by a given *mitigation* option relative to specified emission baselines. [Note: Net greenhouse gas emission reductions is the sum of reduced emissions and/or enhanced *sinks*.] See also *Sequestration potential*.

Biogeophysical potential
The mitigation potential constrained by biological, geophysical and geochemical limits and thermodynamics, without taking into account technical, social, economic and/or environmental considerations.

Economic potential
The portion of the technical potential for which the social benefits exceed the social costs, taking into account a social discount rate and the value of externalities.

Technical potential
The mitigation potential constrained by biogeophysical limits as well as availability of technologies and practices. Quantification of technical potentials takes into account primarily technical considerations, but social, economic and/or environmental considerations are occasionally also included, if these represent strong barriers for the deployment of an option.

Mitigation scenario See *Scenario*.

Mixing ratio See *Mole fraction or mixing ratio*.

Model ensemble See *Climate simulation ensemble*. See also *Ensemble*.

Model initialization A *climate prediction* typically proceeds by integrating a *climate model* forward in time from an initial state that is intended to reflect the actual state of the *climate system*. Available observations of the climate system are assimilated into the model. Initialization is a complex process that is limited by available observations, observational errors and, depending on the procedure used, may be affected by *uncertainty* in the history of climate *forcing*. The initial conditions will contain errors that grow as the forecast progresses, thereby limiting the time period over which the forecast will be useful.

Model spread The range or spread in results from *climate models*, such as those assembled for Coupled Model Intercomparison Project Phase 6 (CMIP6). Does not necessarily provide an exhaustive and formal estimate of the *uncertainty* in *feedbacks*, *forcing* or *projections* even when expressed numerically, for example, by computing a standard deviation of the models' responses. In order to quantify uncertainty, information from observations, physical constraints and expert judgement must be combined, using a statistical framework.

Modes of climate variability Recurrent space-time structures of *natural variability* of the *climate system* with intrinsic spatial patterns, seasonality and time scales. Modes can arise through the dynamical characteristics of the atmospheric circulation but also through coupling between the *ocean* and the *atmosphere*, with some interactions with land surfaces and *sea ice*. Many modes of variability are driven by internal climate processes and are a critical potential source of climate *predictability* on sub-seasonal to decadal time scales. See Annex IV of the AR6 WGI report. See also *Annular modes*, *Tropical Atlantic Variability (TAV)*, *Indian Ocean Dipole (IOD)*, *Indian Ocean Basin (IOB) mode*, *Pacific Decadal Variability (PDV)*, *Pacific Decadal Oscillation (PDO)* (under *Pacific Decadal Variability (PDV)*), *El Niño–Southern Oscillation (ENSO)*, *North Atlantic Oscillation (NAO)*, *Northern Annular Mode (NAM)* (under *Annular modes*), *Southern Annular Mode (SAM)* (under *Annular modes*), *Atlantic Meridional Mode (AMM)* (under *Tropical Atlantic Variability (TAV)*), *Atlantic Zonal Mode (AZM)* (under *Tropical Atlantic Variability (TAV)*), *Madden–Julian Oscillation (MJO)*, *Atlantic Multi-decadal Variability (AMV)* and *Inter-decadal Pacific Oscillation (IPO)* (under *Pacific Decadal Variability (PDV)*).

Mole fraction or mixing ratio Mole fraction, or mixing ratio, is the ratio of the number of moles of a constituent in a given volume to the total number of moles of all constituents in that volume. It is usually reported for dry air. Typical values for *well-mixed greenhouse gases* are in the order of μmol mol^{-1} (parts per million: ppm), nmol mol^{-1} (parts per billion: ppb), and fmol mol^{-1} (parts per trillion: ppt). Mole fraction differs from volume mixing ratio, often expressed in ppmv, etc., by the corrections for non-ideality of gases. This correction is significant relative to measurement precision for many *greenhouse gases* (Schwartz and Warneck, 1995).

Monsoon See *Global monsoon*.

Montreal Protocol The Montreal Protocol on Substances that Deplete the Ozone Layer was adopted in Montreal in 1987, and subsequently adjusted and amended (including London (1990), Copenhagen (1992), Vienna (1995), Montreal (1997), Beijing (1999) and Kigali (2016)). It controls the consumption and production of chlorine- and bromine-containing chemicals that destroy *stratospheric ozone (O_3)*, such as *chlorofluorocarbons (CFCs)*, methyl chloroform, carbon tetrachloride and many others. Since the Kigali Amendment in 2016, *hydrofluorocarbons (HFCs)*, which were used as alternatives to *ozone-depleting substances (ODSs)*, have been targeted for a phase-down due to their *climate* effect as *greenhouse gases (GHGs)*.

Multi-model ensemble (MME) See *Climate simulation ensemble*. See also *Ensemble*.

Narrative See *Storyline*. See also *Pathways*.

Natural systems The dynamic physical, physicochemical and biological components of the Earth system that would operate independently of human activities.

Natural variability See *Climate variability*.

Near-surface permafrost See *Permafrost*.

Negative greenhouse gas emissions Removal of *greenhouse gases (GHGs)* from the *atmosphere* by deliberate human activities, that is, in addition to the removal that would occur via natural *carbon cycle* or atmospheric chemistry processes. See also *Carbon dioxide removal (CDR)*, *Net negative greenhouse gas emissions*, *Net zero CO_2 emissions* and *Net zero greenhouse gas emissions*.

Net negative greenhouse gas emissions A situation of net negative greenhouse gas emissions is achieved when metric-weighted anthropogenic *greenhouse gas (GHG)* removals exceed metric-weighted anthropogenic GHG emissions. Where multiple GHG are involved, the quantification of net emissions depends on the metric chosen to compare emissions of different gases (such as *global warming potential*, global temperature change potential, and others, as well as the chosen time horizon). See also *Net zero CO_2 emissions*, *Net zero greenhouse gas emissions*, *Negative greenhouse gas emissions*, *Carbon dioxide removal (CDR)* and *Greenhouse gas emission metric*.

Net primary production (NPP) See *Primary production*.

Net zero CO_2 emissions Condition in which anthropogenic *carbon dioxide (CO_2)* emissions are balanced by anthropogenic CO_2 removals over a specified period.

Note: Carbon neutrality and net zero CO_2 emissions are overlapping concepts. The concepts can be applied at global or sub-global scales (e.g., regional, national and sub-national). At a global scale, the terms carbon neutrality and net zero CO_2 emissions are equivalent. At sub-global scales, net zero CO_2 emissions is generally applied to emissions and removals under direct control or territorial responsibility of the reporting entity, while carbon neutrality generally includes emissions and removals within and beyond the direct control or territorial responsibility of the reporting entity. Accounting rules specified by GHG programmes or schemes can have a significant influence on the quantification of relevant CO_2 emissions and removals.

See also *Net zero greenhouse gas emissions* and *Carbon neutrality*.

Net zero greenhouse gas emissions Condition in which metric-weighted anthropogenic *greenhouse gas (GHG)* emissions are balanced by metric-weighted anthropogenic GHG removals over a specified period. The quantification of net zero GHG emissions depends on the GHG emission metric chosen to compare emissions and removals of different gases, as well as the time horizon chosen for that metric.

Note 1: GHG neutrality and net zero GHG emissions are overlapping concepts. The concept of net zero GHG emissions can be applied at global or sub-global scales (e.g., regional, national and sub-national). At a global scale, the terms GHG neutrality and net zero GHG emissions are equivalent. At sub-global scales, net zero GHG emissions is generally applied to emissions and removals under direct control or territorial responsibility of the reporting entity, while GHG neutrality generally includes anthropogenic emissions and anthropogenic removals within and beyond the direct control or territorial responsibility of the reporting entity. Accounting rules specified by GHG programmes or schemes can have a significant influence on the quantification of relevant emissions and removals.

Note 2: Under the Paris Rulebook (Decision 18/CMA.1, annex, paragraph 37), parties have agreed to use GWP100 values from the IPCC AR5 or GWP100 values from a subsequent IPCC Assessment Report to report aggregate emissions and removals of GHGs. In addition, parties may use other metrics to report supplemental information on aggregate emissions and removals of GHGs.

See also *Net zero CO_2 emissions*, *Greenhouse gas emission metric* and *Greenhouse gas neutrality)*.

Nitrogen deposition Nitrogen deposition is defined as the nitrogen transferred from the *atmosphere* to the Earth's surface by the processes of wet deposition and dry deposition.

Nitrous oxide (N_2O) The main *anthropogenic* source of N_2O, a greenhouse gas (GHG), is agriculture (soil and animal manure management), but important contributions also come from sewage treatment, *fossil fuel* combustion, and chemical industrial processes. N_2O is also produced naturally from a wide variety of biological sources in soil and water, particularly microbial action in wet tropical *forests*.

Non-CO_2 emissions and radiative forcing Non-CO_2 emissions included in this report are all *anthropogenic emissions* other than *carbon dioxide (CO_2)* that result in *radiative forcing*. These include *short-lived climate forcers*, such as *methane (CH_4)*, some fluorinated gases, *ozone (O_3)* precursors, *aerosols* or aerosol *precursors*, such as *black carbon* and sulphur dioxide, respectively, as well as long-lived *greenhouse gases*, such as *nitrous oxide (N_2O)* or other fluorinated gases. The radiative forcing associated with non-CO_2 emissions and changes in surface *albedo* (e.g., resulting from *land-use change*) is referred to as non-CO_2 radiative forcing.

Non-linearity A process is called non-linear when there is no simple proportional relation between cause and effect. The *climate system* contains many such non-linear processes, resulting in a system with potentially very complex behaviour. Such complexity may lead to *abrupt climate change* and *tipping points*.

Non-methane volatile organic compounds (NMVOCs) See *Volatile organic compounds (VOCs)*.

Non-overshoot pathways See *Pathways*.

North American monsoon (NAmerM) See *Global monsoon*.

Northern Annular Mode (NAM) See *Annular modes*.

North Atlantic Oscillation (NAO) The leading mode of large-scale atmospheric variability in the North Atlantic basin characterized by alternating (see-saw) variations in sea level pressure or geopotential height between the Azores High in the subtropics and the Icelandic Low in the mid- to high latitudes, with some northward extension deep into the Arctic. It is associated with fluctuations in the strength and latitudinal position of the main westerly winds across a vast North Atlantic–Europe domain, and thus with fluctuations in the embedded *extratropical cyclones* and associated frontal systems leading to strong *teleconnection* over the entire North Atlantic adjacent continents. The positive and negative phases of the NAO show similar characteristics described for the *Northern Annular Mode (NAM)*. See Section AIV.2.1 in Annex IV of the AR6 WGI report.

Northern polar vortex See *Stratospheric polar vortex*.

Ocean The interconnected body of saline water that covers 71% of the Earth's surface, contains 97% of the Earth's water and provides 99% of the Earth's biologically habitable space. It includes the Arctic, Atlantic, Indian, Pacific and Southern Oceans, as well as their marginal seas and coastal waters.

Ocean acidification (OA) A reduction in the *pH* of the *ocean*, accompanied by other chemical changes (primarily in the levels of carbonate and bicarbonate ions), over an extended period, typically decades or longer, which is caused primarily by *uptake* of *carbon dioxide* (CO_2) from the *atmosphere*, but can also be caused by other chemical additions or subtractions from the ocean. *Anthropogenic* OA refers to the component of pH reduction that is caused by human activity (IPCC, 2011, p. 37).

Ocean alkalinization/Ocean alkalinity enhancement A proposed *carbon dioxide removal (CDR)* method that involves deposition of alkaline minerals or their dissociation products at the *ocean* surface. This increases surface *total alkalinity*, and may thus increase ocean *carbon dioxide* (CO_2) uptake and ameliorate surface *ocean acidification*. See also *Anthropogenic removals*.

Ocean carbon cycle The ocean *carbon cycle* is the set of processes that exchange carbon between various *pools* within the *ocean*, as well as between the *atmosphere*, Earth's interior, *cryosphere*, and the sea-floor. See also *Carbon cycle*.

Ocean deoxygenation The loss of oxygen in the *ocean*. It results from ocean warming, which reduces oxygen solubility and increases oxygen consumption and *stratification*, thereby reducing the mixing of oxygen into the ocean interior. Deoxygenation can also be exacerbated by the addition of excess nutrients in the *coastal* zone.

Ocean dynamic sea level change See *Sea level change (sea level rise/sea level fall)*.

Ocean fertilization A proposed *carbon dioxide removal (CDR)* method that relies on the deliberate increase of nutrient supply to the near-surface *ocean* with the aim of *sequestering* additional CO_2 from the *atmosphere* through biological production. Methods include direct addition of micro-nutrients or macro-nutrients. To be successful, the additional carbon needs to reach the deep ocean where it has the potential to be sequestered on climatically relevant time scales. See also *Anthropogenic removals* and *Carbon dioxide removal (CDR)*.

Ocean heat uptake efficiency This is a measure ($W\ m^{-2}\ °C^{-1}$) of the rate at which heat storage by the global *ocean* increases as global surface temperature rises. It is a useful parameter for *climate change* simulations in which the *radiative forcing* is changing monotonically, when it can be compared with the *climate feedback parameter* to gauge the relative importance of radiative response and ocean heat *uptake* in determining the rate of *climate change*. It can be estimated from such an experiment as the ratio of the rate of increase of ocean heat content to the surface temperature change.

Ocean stratification See *Stratification*.

Orbital forcing Orbital *forcing* is the influence of slow, systematic and predictable changes in orbital parameters (eccentricity, obliquity and precession of the equinox) on incoming *solar radiation* (*insolation*), especially its latitudinal and seasonal distribution. It is an *external forcing* and a key driver of *glacial–interglacial cycles*.

Organic aerosol Component of the *aerosol* that consists of organic compounds, mainly carbon, hydrogen, oxygen and lesser amounts of other elements.

Outgoing longwave radiation Net outgoing radiation in the infrared part of the spectrum at the top of the *atmosphere.*

Outlet glacier See *Glacier*.

Overshoot pathways See *Pathways*.

Oxygen minimum zone (OMZ) The midwater layer (200–1000 m) in the open *ocean* in which oxygen saturation is the lowest in the ocean. The degree of oxygen depletion depends on the largely bacterial consumption of organic matter, and the distribution of the OMZs is influenced by large-scale ocean circulation. In coastal oceans, OMZs extend to the shelves and may also affect benthic *ecosystems*.

Ozone (O_3) The triatomic form of oxygen, and a gaseous *atmospheric* constituent. In the *troposphere*, O_3 is created both naturally and by photochemical reactions involving gases resulting from human activities (e.g., smog). Tropospheric O_3 acts as a *greenhouse gas (GHG)*. In the *stratosphere*, O_3 is created by the interaction between solar ultraviolet radiation and molecular oxygen (O_2). Stratospheric O_3 plays a dominant role in the stratospheric radiative balance. Its concentration is highest in the *ozone layer*. See also *Ground-level ozone*, *Ozone hole*, *Ozone-depleting substances (ODSs)*, *Ozonesonde* and *Short-lived climate forcers (SLCFs)*.

Ozone layer A layer of Earth's *stratosphere* that absorbs most of the Sun's ultraviolet radiation. It contains high concentrations of *ozone* (O_3) in relation to other parts of the *atmosphere*, although still small in relation to other gases in the *stratosphere*. The ozone layer contains less than 10 parts per million of ozone, while the average ozone concentration in Earth's atmosphere as a whole is about 0.3 parts per million. The ozone layer is mainly found in the lower portion of the stratosphere, from approximately 15 to 35 kilometres (9.3 to 21.7 miles) above Earth, although its thickness varies seasonally and geographically. See also *Ozone hole* and *Ozone-depleting substances (ODSs)*.

Ozone-depleting substances (ODSs) Man-made gases that destroy *ozone* (O_3) once they reach the *ozone layer* in the *stratosphere*. Ozone-depleting substances include: *chlorofluorocarbons (CFCs)*, hydrochlorofluorocarbons (HCFCs), hydrobromofluorocarbons (HBFCs), halons, methyl bromide, carbon tetrachloride and methyl chloroform. They are used as refrigerants in commercial, home and vehicle air conditioners and refrigerators, foam blowing agents, components in electrical equipment, industrial solvents, solvents for cleaning (including dry cleaning), aerosol spray propellants and fumigants. See also *Ozone layer*, *Ozone* (O_3) and *Stratospheric ozone*.

Ozonesonde An ozonesonde is a radiosonde measuring *ozone (O_3)* concentrations. The radiosonde is usually carried on a weather balloon and transmits measured quantities by radio to a ground-based receiver.

Pacific Decadal Oscillation (PDO) See *Pacific Decadal Variability (PDV)*.

Pacific Decadal Variability (PDV) Coupled decadal-to-inter-decadal variability of the atmospheric circulation and underlying *ocean* that is typically observed over the entire Pacific Basin beyond the *El Niño–Southern Oscillation (ENSO)* time scale. In the AR6 WGI report, PDV encapsulates the *Pacific Decadal Oscillation (PDO)*, the South Pacific Decadal Oscillation (SPDO), tropical Pacific decadal variability (also called decadal ENSO), and the Inter-decadal Pacific Oscillation (IPO). Typically, the positive phase of the PDV is characterized by anomalously high *sea surface temperatures* in the central-eastern tropical Pacific that extend to the extratropical North and South Pacific along the American coasts, encircled to the west by cold sea surface *anomalies* in the mid-latitude North and South Pacific. The negative phase is accompanied by sea surface temperature anomalies of the opposite sign. Those sea surface temperature anomalies are linked to anomalies in atmospheric and oceanic circulation throughout the whole Pacific Basin. The PDV is associated with decadal modulations in the relative occurrence of El Niño and La Niña. See Section AIV.2.6 in Annex IV of the AR6 WGI report.

Inter-decadal Pacific Oscillation (IPO)
An equatorially symmetric pattern of *sea surface temperature* variability at decadal-to-inter-decadal time scales. While the *Pacific Decadal Oscillation (PDO)* and its South Pacific counterpart, the South Pacific Decadal Oscillation (SPDO), are considered as physically distinct modes, the tropical Pacific decadal–inter-decadal variability can drive both the PDO and SPDO, forming the IPO as a synchronized pan-Pacific variability. Its spatial pattern of sea surface temperature *anomalies* is similar to that of the *El Niño–Southern Oscillation (ENSO)*, but with a broader meridional extent in the tropical signal and more weights in the extratropics compared to the tropics. In the AR6 WGI report, it is encapsulated within the definition and description of *Pacific Decadal Variability (PDV)*. See also Section AIV.2.6 in Annex IV of the AR6 WGI report.

Pacific Decadal Oscillation (PDO)
The leading mode of variability obtained from decomposition in empirical orthogonal function of *sea surface temperature* over the North Pacific north of 20°N, and characterized by a strong decadal component. The positive phase of the PDO features a dipole of sea surface temperature *anomalies* in the North Pacific, with a cold lobe near the centre of the basin and extending westward along the Kuroshio, encircled by warmer conditions along the coast of North America and in the subtropics. A positive PDO is accompanied by an intensified Aleutian Low and an associated cyclonic circulation enhancement leading to *teleconnections* over the continents adjacent to the North Pacific. In the AR6 WGI report, the PDO is encapsulated within the definition and description of *Pacific Decadal Variability (PDV)*. See also Section AIV.2.6 in Annex IV of the AR6 WGI report.

Pacific-North American (PNA) pattern An atmospheric large-scale wave pattern featuring a sequence of tropospheric high and low pressure *anomalies* stretching from the subtropical west Pacific to the east coast of North America.

Palaeocene–Eocene Thermal Maximum (PETM) The PETM is a transient event that occurred between 55.9 and 55.7 million years ago. Continental positions at this time were somewhat different to present due to tectonic plate movements. Geological data indicate that the PETM was characterised by a warming (*global mean surface temperature* rose to about 4°C–7°C warmer than the preceding mean state), and an increase in atmospheric CO_2 (from about 900 to about 2000 ppmv). In addition, ocean *pH* and oxygen content decreased; many deep-sea species went extinct and tropical *coral reefs* diminished.

Paleoclimate *Climate* during periods prior to the development of measuring instruments, including historic and geologic time, for which only *proxy* climate records are available.

Parameterization In *climate models*, this term refers to the technique of representing processes that cannot be explicitly resolved at the spatial or temporal *resolution* of the model (sub-grid scale processes) by relationships between model-resolved larger-scale variables and the area- or time-averaged effect of such sub-grid scale processes.

Pathways The temporal evolution of natural and/or human systems towards a future state. Pathway concepts range from sets of quantitative and qualitative *scenarios* or *narratives* of potential futures to solution-oriented decision-making processes to achieve desirable societal goals. Pathway approaches typically focus on biophysical, techno-economic, and/or socio-behavioural trajectories and involve various dynamics, goals, and actors across different scales. See also *Scenario* and *Scenario storyline* (under *Storyline*).

1.5°C pathway
A pathway of emissions of *greenhouse gases* and other climate forcers that provides an approximately one-in-two to two-in-three chance, given current knowledge of the climate response, of *global warming* either remaining below 1.5°C or returning to 1.5°C by around 2100 following an overshoot.

Emission pathways
Modelled trajectories of global *anthropogenic emissions* over the 21st century.

Mitigation pathways
A temporal evolution of a set of *mitigation scenario* features, such as *greenhouse gas (GHG)* emissions and socio-economic development.

Non-overshoot pathways
Pathways that stay below a specified concentration, *forcing*, or global warming level during a specified period of time (e.g., until 2100).

Overshoot pathways
Pathways that first exceed a specified concentration, *forcing*, or global warming level, and then return to or below that level again before the end of a specified period of time (e.g., before 2100). Sometimes the magnitude and *likelihood* of the overshoot is also characterized. The overshoot duration can vary from one pathway to the next, but in most overshoot pathways in the literature and referred to as overshoot pathways in the AR6, the overshoot occurs over a period of at least one decade and up to several decades.

Representative Concentration Pathways (RCPs)
Scenarios that include time series of *emissions* and concentrations of the full suite of *greenhouse gases (GHGs)* and *aerosols* and chemically active gases, as well as *land use*/*land cover* (Moss et al., 2010). The word representative signifies that each RCP provides only one of many possible scenarios that would lead to the specific *radiative forcing* characteristics. The term pathway emphasises that not only the long-term concentration levels are of interest, but also the trajectory taken over time to reach that outcome (Moss et al., 2010).

RCPs usually refer to the portion of the concentration pathway extending up to 2100, for which *integrated assessment models* produced corresponding *emission scenarios*. Extended concentration pathways describe extensions of the RCPs from 2100 to 2300 that were calculated using simple rules generated by stakeholder consultations, and do not represent fully consistent scenarios. Four RCPs produced from integrated assessment models were selected from the published literature and used in the Fifth IPCC Assessment, and are also used in this Assessment for comparison, spanning the range from approximately below 2°C warming to high (>4°C) warming best-estimates by the end of the 21st century: RCP2.6, RCP4.5 and RCP6.0 and RCP8.5.

- RCP2.6: One pathway where radiative forcing peaks at approximately 3 W m^{-2} and then declines to be limited at 2.6 W m^{-2} in 2100 (the corresponding Extended Concentration Pathway, or ECP, has constant emissions after 2100).
- RCP4.5 and RCP6.0: Two intermediate stabilization pathways in which radiative forcing is limited at approximately 4.5 W m^{-2} and 6.0 W m^{-2} in 2100 (the corresponding ECPs have constant concentrations after 2150).
- RCP8.5: One high pathway which leads to >8.5 W m^{-2} in 2100 (the corresponding ECP has constant emissions after 2100 until 2150 and constant concentrations after 2250).

See also *Coupled Model Intercomparison Project (CMIP)* and *Shared Socio-economic Pathways (SSPs)* (under *Pathways*).

Shared Socio-economic Pathways (SSPs)
Shared Socio-economic Pathways (SSPs) have been developed to complement the *Representative Concentration Pathways (RCPs)*. By design, the RCP emission and concentration pathways were stripped of their association with a certain socio-economic development. Different levels of emissions and *climate change* along the dimension of the RCPs can hence be explored against the backdrop of different socio-economic development pathways (SSPs) on the other dimension in a matrix. This integrative SSP-RCP framework is now widely used in the climate *impact* and policy analysis literature, where *climate projections* obtained under the RCP scenarios are analysed against the backdrop of various SSPs. As several emissions updates were due, a new set of emissions scenarios was developed in conjunction with the SSPs. Hence, the abbreviation SSP is now used for two things: On the one hand SSP1, SSP2, …, SSP5 are used to denote the five socio-economic scenario families. On the other hand, the abbreviations SSP1-1.9, SSP1-2.6, …, SSP5-8.5 are used to denote the newly developed emissions scenarios that are the result of an SSP implementation within an *integrated assessment model*. Those SSP scenarios are bare of climate policy assumption, but in combination with so-called shared policy assumptions (SPAs), various approximate *radiative forcing* levels of 1.9, 2.6, …, or 8.5 W m^{-2} are reached by the end of the century, respectively.

Pattern scaling Techniques used to represent the spatial variations in *climate* at a given increase in *global mean surface air temperature (GSAT)* are referred to as 'pattern scaling'.

Peat Soft, porous or compressed, sedimentary deposit of which a substantial portion is partly decomposed plant material with high water content in the natural state (up to about 90%).

Peatlands Peatland is a land where soils are dominated by *peat*.

Percentile A partition value in a population distribution that a given percentage of the data values are below or equal to. The 50th percentile corresponds to the median of the population. Percentiles are often used to estimate the extremes of a distribution. For example, the 90th (10th) percentile may be used to refer to the threshold for the upper (lower) extremes.

Permafrost Ground (soil or rock, and included ice and organic material) that remains at or below 0°C for at least two consecutive years (Harris et al., 1988). Note that permafrost is defined via temperature rather than ice content and, in some instances, may be ice-free.

Near-surface permafrost
Permafrost within about 3–4 m of the ground surface. The depth is not precise, but describes what commonly is highly relevant for people and *ecosystems*. Deeper permafrost is often progressively less ice-rich and responds more slowly to warming than near-surface permafrost. The presence or absence of near-surface permafrost is not the only significant metric of permafrost change, and deeper permafrost may persist when near-surface permafrost is absent.

Permafrost degradation
Decrease in the thickness and/or areal extent of permafrost.

Permafrost thaw
Progressive loss of ground ice in permafrost, usually due to input of heat. Thaw can occur over decades to centuries over the entire depth of permafrost ground, with impacts occurring while thaw progresses. During thaw, temperature fluctuations are subdued because energy is transferred by phase change between ice and water. After the transition from permafrost to non-permafrost, ground can be described as thawed.

Perturbed parameter ensemble See *Climate simulation ensemble*.

pH A dimensionless measure of the acidity of a dilute solution (e.g., seawater) based on the activity, or effective concentration, of hydrogen ions (H^+) in the solution. pH is measured on a logarithmic scale where $pH = -\log_{10}(H^+)$. Thus, a pH decrease of 1 unit corresponds to a 10-fold increase in the acidity, or the activity of H^+.

Phenology The relationship between biological phenomena that recur periodically (e.g., development stages, migration) and *climate* and seasonal changes.

Photosynthesis The production of carbohydrates in plants, algae and some bacteria using the energy of light. *Carbon dioxide (CO_2)* is used as the carbon source.

Physical climate storyline See *Storyline*.

Piacenzian warm period See *Pliocene*.

Plankton Free-floating organisms living in the upper layers of aquatic systems. Their distribution and migration are primarily determined by water currents. A distinction is made between phytoplankton, which depend on *photosynthesis* for their energy supply, and zooplankton, which feed on phytoplankton, other zooplankton, and bacterioplankton.

Plant evaporative stress Plant evaporative stress in both crops and natural vegetation can result from the combination of a high atmospheric evaporative demand and limited available water to supply this demand by means of *evapotranspiration*, further enhancing *agricultural and ecological drought*.

Pleistocene The Pleistocene Epoch is the earlier of two epochs in the *Quaternary* System, extending from 2.59 Ma to the beginning of the *Holocene* at approximately 11.7 ka.

Pliocene The Pliocene Epoch is the more recent of two epochs of the Neogene Period within the *Cenozoic Era*. It extends from 5.33 Ma to the beginning of the *Pleistocene* Epoch at 2.59 Ma. The Neogene Period precedes the current geological period, the *Quaternary* Period, which is one of several *ice ages* that have occurred during Earth's geological history. It encompasses the mid-Pliocene warm period (MPWP), also known as the Piacenzian warm period, which occurred from approximately 3.3 to 3.0 Ma. The MPWP, in turn, encompasses the *interglacial* episode, *marine isotope stage (MIS)* KM5c, which peaked at 3.205 Ma, when *orbital forcing* was similar to modern (Haywood et al., 2016).

Polar amplification Polar amplification describes the phenomenon where surface temperature change at high latitudes exceeds the global average surface temperature change. The terms Arctic amplification or Antarctic amplification are used when describing the phenomenon occurring at one of the poles.

Pollen analysis A technique of both relative dating and environmental *reconstruction*, consisting of the identification and counting of pollen types preserved in *peat*, lake sediments and other deposits.

Pool, carbon and nitrogen A *reservoir* in the Earth system where elements, such as carbon and nitrogen, reside in various chemical forms for a period of time. See also *Reservoir*, *Sequestration, Sequestration potential, Sink, Source* and *Uptake*.

Post-glacial period See *Holocene*.

Potential evapotranspiration See *Evapotranspiration*.

Pre-industrial (period) The multi-century period prior to the onset of large-scale industrial activity around 1750. The *reference period* 1850–1900 is used to approximate pre-industrial *global mean surface temperature (GMST)*. See also *Industrial revolution*.

Precipitable water The total amount of atmospheric water vapour in a vertical column of unit cross-sectional area. It is commonly expressed in terms of the height of the water if completely condensed and collected in a vessel of the same unit cross section.

Precursors Atmospheric compounds that are not *greenhouse gases (GHGs)* or *aerosols*, but that have an effect on GHG or aerosol concentrations by taking part in physical or chemical processes regulating their production or destruction rates.

Predictability The extent to which future states of a system may be predicted based on knowledge of current and past states of the system. Because knowledge of the *climate system*'s past and current states is generally imperfect, as are the models that utilize this knowledge to produce a *climate prediction*, and because the *climate system* is inherently *non-linear* and *chaotic*, predictability of the climate system is inherently limited. Even with arbitrarily accurate models and observations, there may still be limits to the predictability of such a non-linear system (AMS, 2021). See also *Climate prediction* and *Prediction quality/skill*.

Prediction quality/skill Measures of the success of a prediction against observationally based information. No single measure can summarize all aspects of forecast quality, and a suite of *metrics* is considered. Metrics will differ for forecasts given in deterministic and probabilistic form. See also *Climate prediction* and *Predictability*.

Primary production The synthesis of organic compounds by plants and microbes, on land or in the *ocean*, primarily by *photosynthesis* using light and *carbon dioxide (CO_2)* as sources of energy and carbon respectively. It can also occur through chemosynthesis, using chemical energy, for example, in deep sea vents.

Gross primary production (GPP)
The total amount of carbon fixed by *photosynthesis* over a specified time period.

Net primary production (NPP)
The amount of carbon fixed by *photosynthesis* minus the amount lost by *respiration* over a specified time period.

Probability density function (PDF) A probability density function is a function that indicates the relative chances of occurrence of different outcomes of a variable. The function integrates to unity over the domain for which it is defined and has the property that the integral over a sub-domain equals the probability that the outcome of the variable lies within that sub-domain. For example, the probability that a temperature *anomaly* defined in a particular way is greater than zero is obtained from its PDF by integrating the PDF over all possible temperature anomalies greater than zero. Probability density functions that describe two or more variables simultaneously are similarly defined.

Process-based model Theoretical concepts and computational methods that represent and simulate the behaviour of real-world systems derived from a set of functional components and their interactions with each other and the system environment, through physical and mechanistic processes occurring over time.

Projection A potential future evolution of a quantity or set of quantities, often computed with the aid of a model. Unlike predictions, projections are conditional on assumptions concerning, for example, future socio-economic and technological developments that may or may not be realized. See also *Climate projection*, *Pathways* and *Scenario*.

Proxy A proxy *climate indicator* is any biophysical property of materials formed during the past that is interpreted to represent some combination of climate-related variations back in time. Climate-related data derived in this way are referred to as proxy data, and time series of proxy data are proxy records. Examples of proxy types include pollen assemblages, *tree ring* widths, speleothem and coral geochemistry, and various data derived from marine sediments and *glacier* ice. Proxy data can be calibrated to provide quantitative *climate information*.

Proxy records See *Proxy*.

Quasi-Biennial Oscillation (QBO) A near-periodic oscillation of the equatorial zonal wind between easterlies and westerlies in the tropical *stratosphere* with a mean period of around 28 months. The alternating wind maxima descend from the base of the mesosphere down to the *tropopause* and are driven by wave energy that propagates up from the *troposphere*.

Quaternary The Quaternary Period is the last of three periods that make up the *Cenozoic Era* (66 Ma to present), extending from 2.58 Ma to the present, and includes the *Pleistocene* and *Holocene* Epochs.

Radiative forcing The change in the net, downward minus upward, radiative *flux* (expressed in W m^{-2}) due to a change in an external driver of *climate change*, such as a change in the concentration of *carbon dioxide* (CO_2), the concentration of volcanic *aerosols* or the output of the Sun. The stratospherically adjusted radiative forcing is computed with all tropospheric properties held fixed at their unperturbed values, and after allowing for stratospheric temperatures, if perturbed, to readjust to radiative-dynamical equilibrium. Radiative forcing is called instantaneous if no change in stratospheric temperature is accounted for. The radiative forcing once both stratospheric and tropospheric adjustments are accounted for is termed the effective radiative forcing.

Radiative response (of the climate system) The net top-of-atmosphere radiative flux that opposes a change in *radiative forcing* as a result of *climate feedbacks*. Typical units: W m^{-2}. See also *Earth's energy budget and Climate feedback parameter*.

Rapid dynamical change (of glaciers or ice sheets) Changes in *glacier* or *ice sheet* mass controlled by changes in flow speed and *discharge* rather than by *accumulation* or *ablation*. This can result in a rate of mass change larger than that due to any imbalance between accumulation and ablation. Rapid dynamical change may be initiated by a climatic trigger, such as incursion of warm *ocean* water beneath an *ice shelf*, or thinning of a grounded tide-water terminus, which may lead to reactions within the glacier system that may result in rapid ice loss.

Reanalysis Reanalyses are created by processing past meteorological or oceanographic data using fixed state-of-the-art weather forecasting or *ocean* circulation models with *data assimilation* techniques. They are used to provide estimates of variables such as historical atmospheric temperature and wind or oceanographic temperature and currents, and other quantities. Using fixed data assimilation avoids effects from the changing analysis system that occur in operational analyses. Although continuity is improved, global reanalyses still suffer from changing coverage and biases in the observing systems.

Reasons for concern (RFCs) Elements of a classification framework, first developed in the IPCC Third Assessment Report, which aims to facilitate judgements about what level of *climate change* may be dangerous (in the language of Article 2 of the UNFCCC; UNFCCC, 1992) by aggregating *risks* from various sectors, considering *hazards*, *exposures*, *vulnerabilities*, capacities to adapt, and the resulting *impacts*.

Reconstruction (of climate variable) Approach to reconstructing the past temporal and spatial characteristics of a *climate* variable from predictors. The predictors can be instrumental data if the reconstruction is used to infill missing data or *proxy* data if it is used to develop *paleoclimate* reconstructions. Various techniques have been developed for this purpose: linear multivariate regression-based methods and non-linear Bayesian and analogue methods.

Reference period A time period of interest, or a period over which some relevant statistics are calculated. A reference period can be used as a baseline period or as a comparison to a baseline period.

Baseline period
A time period against which differences are calculated (e.g., expressed as *anomalies* relative to a baseline).

Reference scenario See *Scenario*.

Reforestation Conversion to *forest* of land that has previously contained forests but that has been converted to some other use. [Note: For a discussion of the term forest and related terms such as *afforestation*, reforestation and *deforestation*, see the 2006 IPCC Guidelines for National Greenhouse Gas Inventories and their 2019 Refinement, and information provided by the United Nations Framework Convention on Climate Change (IPCC, 2006, 2019; UNFCCC, 2021a, b).] See also *Afforestation*, *Deforestation*, *Anthropogenic removals* and *Carbon dioxide removal (CDR)*.

Region *Land* and/or *ocean* area characterized by specific geographical and/or climatological features. The *climate* of a region emerges from a multi-scale combination of its own features, remote influences from other regions, and global climate conditions.

Regional climate model (RCM) A *climate model* at higher *resolution* over a limited area. Such models are used in *downscaling* global *climate* results over specific regional domains.

Regional sea level change See *Sea level change (sea level rise/sea level fall)*.

Relative humidity The ratio of actual water vapour pressure to that at saturation with respect to liquid water or ice at the same temperature. See also *Specific humidity*.

Relative sea level (RSL) change See *Sea level change (sea level rise/sea level fall)*.

Remaining carbon budget See *Carbon budget*.

Representative Concentration Pathways (RCPs) See *Pathways*.

Reservoir A component or components of the *climate system* where a *greenhouse gas (GHG)* or a *precursor* of a greenhouse gas is stored (UNFCCC Article 1.7 (UNFCCC, 1992)). See also *Pool, carbon and nitrogen*, *Sequestration*, *Sequestration potential, Sink, Source* and *Uptake*.

Resilience The capacity of interconnected social, economic and ecological systems to cope with a hazardous event, trend or disturbance, responding or reorganizing in ways that maintain their essential function, identity and structure. Resilience is a positive attribute when it maintains capacity for *adaptation*, learning and/or transformation (Arctic Council, 2016). See also *Hazard*, *Risk* and *Vulnerability*.

Resolution In *climate models*, this term refers to the physical distance (metres or degrees) between each point on the grid used to compute the equations. Temporal resolution refers to the time step or time elapsed between each model computation of the equations.

Respiration The process whereby living organisms convert organic matter to *carbon dioxide (CO_2)*, releasing energy and consuming molecular oxygen.

Response time or adjustment time In the context of *climate* variations, the response time or adjustment time is the time needed for the *climate system* or its components to re-equilibrate to a new state, following a *forcing* resulting from external processes. It is very different for various components of the climate system. The response time of the *troposphere* is relatively short, from days to weeks, whereas the *stratosphere* reaches equilibrium on a time scale of typically a few months. Due to their large heat capacity, the *oceans* have a much longer response time: typically decades, but up to centuries or millennia. The response time of the strongly coupled surface–troposphere system is, therefore, slow compared to that of the stratosphere, and mainly determined by the oceans. The *biosphere* may respond quickly (e.g., to *droughts*), but also very slowly to imposed changes.

In the context of *lifetimes*, response time or adjustment time (T_a) is the time scale characterizing the decay of an instantaneous pulse input into the *reservoir*. See *Response time or adjustment time (T_a)* under *Lifetime*.

Return period An estimate of the average time interval between occurrences of an event (e.g., flood or extreme rainfall) of (or below/above) a defined size or intensity.

Return value The highest (or, alternatively, lowest) value of a given variable, on average occurring once in a given period of time (e.g., in 10 years).

Risk The potential for adverse consequences for human or ecological systems, recognizing the diversity of values and objectives associated with such systems. In the context of *climate change*, risks can arise from potential *impacts* of climate change as well as human responses to climate change. Relevant adverse consequences include those on lives, *livelihoods*, health and well-being, economic, social and cultural assets and investments, infrastructure, services (including ecosystem services), *ecosystems* and species.

In the context of climate change impacts, risks result from dynamic interactions between climate-related *hazards* with the *exposure* and *vulnerability* of the affected human or ecological system to the hazards. Hazards, exposure and vulnerability may each be subject to uncertainty in terms of magnitude and *likelihood* of occurrence, and each may change over time and space due to socio-economic changes and human decision-making (see also *risk management*, *adaptation* and *mitigation*).

In the context of climate change responses, risks result from the potential for such responses not achieving the intended objective(s), or from potential trade-offs with, or negative side-effects on, other societal objectives, such as the Sustainable Development Goals (SDGs) (see also *risk trade-off*). Risks can arise, for example, from *uncertainty* in implementation, effectiveness or outcomes of climate policy, climate-related investments, technology development or adoption, and system transitions. See also *Hazard* and *Impacts (consequences, outcomes)*.

Risk assessment The qualitative and/or quantitative scientific estimation of *risks*. See also *Risk management* and *Risk perception*.

Risk framework A common framework for describing and assessing *risk* across all three Working Groups is adopted to promote clear and consistent communication of risks and to better inform *risk assessment* and decision-making related to *climate change*.

Risk management Plans, actions, strategies or policies to reduce the *likelihood* and/or magnitude of adverse potential consequences, based on assessed or perceived *risks*. See also *Risk assessment* and *Risk perception*.

Risk perception The subjective judgement that people make about the characteristics and severity of a *risk*. See also *Risk assessment* and *Risk management*.

Risk trade-off The change in the portfolio of *risks* that occurs when a countervailing risk is generated (knowingly or inadvertently) by an intervention to reduce the target risk (Wiener and Graham, 2009).

River discharge See *Streamflow*.

Rock glacier A debris landform (mass of rock fragments and finer material that contains either an ice core or an ice-cemented matrix) generated by a former or current gravity-driven creep of *permafrost* in mountain slopes (Harris et al., 1988; Giardino et al., 2011; IPA-RG, 2020). It is detectable in the landscape due to the occurrence of (i) a steep slope delimiting the terminal part, (ii) generally well-defined lateral margins in a continuation of the front, and (iii) transversal or longitudinal ridges and furrows (ridge and furrow topography). These are geomorphological indicators of the occurrence of permafrost conditions. Although it is an ice storage feature, it is not a type of *glacier* since it does not originate at the surface by the recrystallization of snow.

Runoff The flow of water over the surface or through the subsurface, which typically originates from the part of liquid precipitation and/or snow/ice melt that does not evaporate, transpire or refreeze, and returns to water bodies.

Sampling uncertainty See *Uncertainty*.

Scenario A plausible description of how the future may develop based on a coherent and internally consistent set of assumptions about key driving forces (e.g., rate of technological change (TC), prices) and relationships. Note that scenarios are neither predictions nor forecasts, but are used to provide a view of the implications of developments and actions. See also *Pathways* and *Scenario storyline* (under *Storyline*).

Baseline scenario
See *Reference scenario* (under *Scenario*).

Concentrations scenario
A plausible representation of the future development of atmospheric concentrations of substances that are radiatively active (e.g., *greenhouse gases (GHGs)*, *aerosols*, tropospheric *ozone*), plus human-induced *land–cover changes* that can be radiatively active via *albedo* changes, and often used as input to a *climate model* to compute *climate projections.*

Emissions scenario
A plausible representation of the future development of emissions of substances that are radiatively active (e.g., *greenhouse gases (GHGs)* or *aerosols*), plus human-induced *land-cover changes* that can be radiatively active via *albedo* changes, based on a coherent and internally consistent set of assumptions about driving forces (such as demographic and socio-economic development, technological change, energy and *land use*) and their key relationships. *Concentration scenarios*, derived from emission scenarios, are often used as input to a *climate model* to compute *climate projections*.

Mitigation scenario
A plausible description of the future that describes how the (studied) system responds to the implementation of *mitigation* policies and measures.

Reference scenario
Scenario used as starting or reference point for a comparison between two or more scenarios.

[Note 1: In many types of *climate change* research, reference scenarios reflect specific assumptions about patterns of socio-economic development and may represent futures that assume no climate policies or specified climate policies, for example those in place or planned at the time a study is carried out. Reference scenarios may also represent futures with limited or no climate *impacts* or *adaptation*, to serve as a point of comparison for futures with impacts and adaptation. These are also referred to as baseline scenarios in the literature.

Note 2: Reference scenarios can also be climate policy or impact scenarios, which in that case are taken as a point of comparison to explore the implications of other features, for example, of delay, technological options, policy design and strategy or to explore the effects of additional impacts and adaptation beyond those represented in the reference scenario.

Note 3: The term business as usual scenario has been used to describe a scenario that assumes no additional policies beyond those currently in place and that patterns of socio-economic development are consistent with recent trends. The term is now used less frequently than in the past.

Note 4: In climate change *attribution* or impact attribution research, reference scenarios may refer to counterfactual historical scenarios assuming no anthropogenic *greenhouse gas (GHG)* emissions (climate change attribution) or no climate change (impact attribution).]

Socio-economic scenario
A scenario that describes a plausible future in terms of population, gross domestic product (GDP), and other socio-economic factors relevant to understanding the implications of *climate change*.

Scenario storyline See *Storyline*.

Sea ice Ice found at the sea surface that has originated from the freezing of seawater. Sea ice may be discontinuous pieces (ice floes) moved on the *ocean* surface by wind and currents (pack ice), or a motionless sheet attached to the *coast* (land-fast ice). Sea ice concentration is the fraction of the ocean covered by ice. Sea ice less than one year old is called first-year ice. Perennial ice is sea ice that survives at least one summer. It may be subdivided into second-year ice and multi-year ice, where multi-year ice has survived at least two summers.

Sea ice area (SIA)
Sea ice area is the area covered by sea ice. In contrast to *sea ice extent*, it is a linear measure of sea ice coverage that does not depend on grid resolution.

Sea ice concentration
Sea ice concentration is the fraction of the *ocean* covered by ice.

Sea ice extent (SIE) Sea ice extent is calculated for gridded data products as the total area of all grid cells with *sea ice concentration* above a given threshold, usually 15 %. It hence is a grid-dependent, non-linear measure of sea ice coverage.

Sea level change (sea level rise/sea level fall) Change to the height of sea level, both globally and locally (*relative sea level* change) at seasonal, annual, or longer time scales due to (i) a change in *ocean* volume as a result of a change in the mass of water in the ocean (e.g., due to melt of *glaciers* and *ice sheets*), (ii) changes in ocean volume as a result of changes in ocean water density (e.g., expansion under warmer conditions), (iii) changes in the shape of the ocean basins and changes in the Earth's gravitational and rotational fields, and (iv) local subsidence or uplift of the land. *Global mean sea level (GMSL) change* resulting from change in the mass of the ocean is called barystatic. The amount of barystatic sea level change due to the addition or removal of a mass of water is called its *sea level equivalent (SLE)*. Sea level changes, both globally and locally, resulting from changes in water density are called steric. Density changes induced by temperature changes only are called thermosteric, while density changes induced by salinity changes are called halosteric. Barystatic and steric sea level changes do not include the effect of changes in the shape of ocean basins induced by the change in the ocean mass and its distribution. See also *Vertical land motion (VLM)*, *Land water storage*, *Glacial isostatic adjustment (GIA)*, *Extreme sea level (ESL)* and *Storm surge*.

Geocentric sea level change
The change in local mean sea surface height with respect to the terrestrial reference frame; it is the sea level change observed with instruments from space. See also *Altimetry*.

Global mean sea level (GMSL) change
The increase or decrease in the volume of the *ocean* divided by the ocean surface area. It is the sum of changes in ocean density through temperature changes (global mean *thermosteric sea level change*) and changes in the ocean mass as a result of changes in the *cryosphere* or *land water storage* (barystatic sea level change).

Gravitational, rotational and deformational (GRD) effects
Changes in Earth gravity, Earth rotation and viscoelastic solid Earth deformation (GRD) result from the redistribution of mass between terrestrial ice and water reservoirs and the *ocean*. Contemporary terrestrial mass loss leads to elastic solid Earth uplift and a nearby relative sea level fall (for a single source of terrestrial mass loss this is within ~2000 km, for multiple sources the distance depends on the interaction of the different relative sea level patterns). Farther away (more than ~7000 km for a single source of terrestrial mass loss), relative sea level rises more than the global average, due (to first order) to gravitational effects. Earth deformation associated with adding water to the oceans and a shift of the Earth's rotation axis towards the source of terrestrial mass loss leads to second-order effects that increase spatial variability of the pattern globally. GRD effects due to the redistribution of ocean water within the ocean itself are referred to as self-attraction and loading effects.

Halosteric sea level change
Halosteric sea level change occurs as a result of salinity variations: higher salinity leads to higher density and decreases the volume per unit of mass. Although both processes can be relevant on regional to local scales, only thermosteric changes impact the *global mean sea level (GMSL) change*, whereas the global mean halosteric change is negligible (Gregory et al., 2019).

Local sea level change
Change in sea level relative to a datum (such as present-day *mean sea level*) at spatial scales smaller than 10 km.

Ocean dynamic sea level change
Change in mean sea level relative to the *geoid* associated with circulation and density-driven changes in the *ocean*. Ocean dynamic sea level change is regionally varying but by definition has a zero global mean and conventionally is inverse-barometer corrected (i.e., the effect of the hydrostatic depression of the sea surface by atmospheric pressure changes is removed). Changes in ocean currents occur due to variations in heating and cooling, variability in winds and changes in seasonally to annually averaged air temperature and humidity.

Regional sea level change
Change in sea level relative to a datum (such as present-day *mean sea level*) at spatial scales of about 100 km.

Relative sea level (RSL) change
The change in local mean sea surface height (SSH) relative to the local solid surface, that is, the sea floor, as measured by instruments that are fixed to the Earth's surface, such as *tide gauges*. This reference frame is used when considering coastal *impacts*, *hazards* and *adaptation* needs.

Steric sea level change
Steric sea level change is caused by changes in *ocean* density and is composed of *thermosteric sea level change* and *halosteric sea level change*.

Thermosteric sea level change
Thermosteric sea level change (where thermosteric sea level rise may also be referred to as thermal expansion) occurs as a result of changes in *ocean* temperature: increasing temperature reduces ocean density and increases the volume per unit of mass.

Sea level equivalent (SLE) The SLE of a mass of water, ice, or water vapour is that mass, converted to a volume using a density of 1000 kg m^{-3}, and divided by the present-day *ocean* surface area of 3.625 × 1000 m^2. Thus, 362.5 Gt of water mass added to the ocean correspond to 1 mm of global mean sea level rise.

Sea level rise (SLR) See *Sea level change (sea level rise/sea level fall)*.

Sea surface temperature (SST) The subsurface bulk temperature in the top few metres of the *ocean*, measured by ships, buoys and drifters. From ships, measurements of water samples in buckets were mostly switched in the 1940s to samples from engine intake water. Satellite measurements of skin temperature (uppermost layer; a fraction of a millimetre thick) in the infrared or the top centimetre or so in the microwave are also used, but must be adjusted to be compatible with the bulk temperature.

Semi-direct (aerosol) effect See *Aerosol–radiation interaction*.

Semi-empirical model Model in which calculations are based on a combination of observed associations between variables and theoretical considerations relating variables through fundamental principles (e.g., conservation of energy). For example, in sea level studies, semi-empirical models refer specifically to transfer functions formulated to project future *global mean sea level (GMSL) change*, or contributions to it, from future *global surface temperature* change or *radiative forcing*.

Sensible heat flux The turbulent or conductive flux of heat from the Earth's surface to the *atmosphere* that is not associated with phase changes of water; a component of the surface energy budget. See also *Latent heat flux*.

Sequestration The process of storing carbon in a carbon *pool*. See also *Pool, carbon and nitrogen*, *Reservoir*, *Sequestration potential, Sink, Source* and *Uptake*.

Sequestration potential The quantity of *greenhouse gases* that can be removed from the *atmosphere* by *anthropogenic* enhancement of *sinks* and stored in a *pool*. See *Mitigation potential* for different subcategories of sequestration potential. See also *Pool, carbon and nitrogen*, *Reservoir*, *Sequestration*, *Source* and *Uptake*.

Shared policy assumptions (SPAs) See *Shared Socio-economic Pathways (SSPs)* (under *Pathways*).

Shared Socio-economic Pathways (SSPs) See *Pathways*.

Short-lived climate forcers (SLCFs) A set of chemically reactive compounds with short (relative to *carbon dioxide* (CO_2)) atmospheric *lifetimes* (from hours to about two decades) but characterized by different physiochemical properties and environmental effects. Their emission or formation has a significant effect on *radiative forcing* over a period determined by their respective atmospheric lifetimes. Changes in their emissions can also induce long-term *climate* effects via, in particular, their interactions with some biogeochemical cycles. SLCFs are classified as direct or indirect, with direct SLCFs exerting climate effects through their radiative forcing and indirect SLCFs being the *precursors* of other direct climate forcers. Direct SLCFs include *methane (CH_4)*, *ozone (O_3)*, primary *aerosols* and some halogenated species. Indirect SLCFs are precursors of ozone or secondary aerosols. SLCFs can be cooling or warming through interactions with radiation and clouds. They are also referred to as near-term climate forcers. Many SLCFs are also air pollutants. A subset of exclusively warming SLCFs is also referred to as short-lived climate pollutants (SLCPs), including methane, ozone, and *black carbon (BC)*.

Short-lived climate pollutants (SLCP) See *Short-lived climate forcers (SLCFs)*.

Shortwave radiation See *Solar radiation*.

Significant wave height The average trough-to-crest height of the highest one-third of the wave heights (sea and swell) occurring in a particular time period.

Simple climate model (SCM) A broad class of lower-dimensional models of the *energy balance*, radiative transfer, *carbon cycle,* or a combination of such physical components. SCMs are also suitable for performing *emulations* of *climate*-mean variables of *Earth system models (ESMs)*, given that their structural flexibility can capture both the parametric and structural uncertainties across process-oriented ESM responses. They can also be used to test consistency across multiple lines of *evidence* with regard to *climate sensitivity* ranges, *transient climate responses (TCRs)*, *transient climate response to cumulative CO_2 emissions (TCREs)* and carbon cycle *feedbacks*. See also *Emulators* and *Earth system model of intermediate complexity (EMIC)*.

Sink Any process, activity or mechanism which removes a *greenhouse gas*, an *aerosol* or a *precursor* of a greenhouse gas from the *atmosphere* (UNFCCC Article 1.8 (UNFCCC, 1992)). See also *Pool, carbon and nitrogen*, *Reservoir*, *Sequestration*, *Sequestration potential, Source* and *Uptake*.

Small Island Developing States (SIDS) Small Island Developing States (SIDS), as recognized by the United Nations OHRLLS (UN Office of the High Representative for the Least Developed Countries, Landlocked Developing Countries and Small Island Developing States), are a distinct group of developing countries facing specific social, economic and environmental vulnerabilities (UN-OHRLLS, 2011). They were recognized as a special case both for their environment and development at the Rio Earth Summit in Brazil in 1992. Fifty-eight countries and territories are presently classified as SIDS by the UN OHRLLS, with 38 being UN member states and 20 being Non-UN Members or Associate Members of the Regional Commissions (UN-OHRLLS, 2018).

Snow cover Snow cover refers to all the snow that has accumulated on the ground at a given time (UNESCO/IASH/WMO, 1970).

Snow cover duration (SCD)
How long snow continuously remains on the land surface, or the period between snow-on and snow-off dates.

Snow cover extent (SCE)
The areal extent of snow covered ground.

Snow water equivalent (SWE)
The depth of liquid water that would result if a mass of snow melted completely.

Socio-economic scenario See *Scenario*.

Soil moisture Water stored in the soil in liquid or frozen form. Root-zone soil moisture is of most relevance for plant activity.

Soil temperature The temperature of the soil. This can be measured or modelled at multiple levels within the depth of the soil.

Solar activity General term collectively describing a variety of magnetic phenomena on the Sun such as *sunspots*, *faculae* (bright areas), and flares (emission of high-energy particles). It varies on time scales from minutes to millions of years. The *solar cycle*, with an average duration of 11 years, is an example of a quasi-regular change in solar activity.

Solar cycle (11-year) A quasi-regular modulation of *solar activity* with varying amplitude and a period of between 8 and 14 years.

Solar radiation Electromagnetic radiation emitted by the Sun with a spectrum close to that of a black body with a temperature of 5770 K. The radiation peaks in visible wavelengths. When compared to the *terrestrial radiation* it is often referred to as shortwave radiation. See also *Insolation* and *Total solar irradiance (TSI)*.

Solar radiation modification (SRM) Refers to a range of radiation modification measures not related to greenhouse gas (GHG) *mitigation* that seek to limit *global warming*. Most methods involve reducing the amount of incoming *solar radiation* reaching the surface, but others also act on the *longwave radiation* budget by reducing optical thickness and cloud lifetime.

Cirrus cloud thinning (CCT)
One of several radiation modification approaches to counter the warming caused by *greenhouse gases (GHGs)*. In this approach, it is proposed to reduce the amount of cirrus clouds by injecting ice nucleating substances in the upper *troposphere*. The reduction in cirrus clouds is expected to increase the amount of longwave cooling to space resulting in a planetary cooling. Although cirrus cloud thinning primarily affects the *longwave radiation* budget of our planet, it is often identified as one of the *solar radiation modification (SRM)* approaches in the literature.

Marine cloud brightening (MCB)
One of several solar radiation modification (SRM) approaches to increase the planetary *albedo*. In this approach, it is proposed to inject sea salt *aerosols* into persistent marine low clouds. This is expected to increase the cloud droplet concentration of these clouds and their reflectivity.

Stratospheric aerosol injection (SAI)
One of several solar radiation modification (SRM) approaches to increase the planetary *albedo*. In the approach, it is proposed to inject highly reflective *aerosols* such as sulphates into the lower *stratosphere*. This is expected to increase the fraction of *solar radiation* deflected to space resulting in a planetary cooling.

Solubility pump A physicochemical process that transports *dissolved inorganic carbon* from the *ocean*'s surface to its interior. The solubility pump is primarily driven by the solubility of *carbon dioxide (CO_2)* (with more CO_2 dissolving in colder water) and the large-scale, thermohaline patterns of ocean circulation.

Source Any process or activity which releases a *greenhouse gas*, an *aerosol* or a *precursor* of a greenhouse gas into the *atmosphere* (UNFCCC Article 1.9 (UNFCCC, 1992)). See also *Pool, carbon and nitrogen*, *Reservoir*, *Sequestration*, *Sequestration potential, Sink* and *Uptake*.

South American monsoon (SAmerM) See *Global monsoon*.

South and Southeast Asian monsoon (SAsiaM) See *Global monsoon*.

Southern Annular Mode (SAM) See *Annular modes*.

South Pacific Convergence Zone (SPCZ) A band of low-level convergence, cloudiness and precipitation ranging from the west Pacific warm pool south-eastwards towards French Polynesia. It is one of the most significant features of subtropical Southern Hemisphere *climate*. It shares some characteristics with the *Inter-tropical Convergence Zone (ITCZ)*, but is more extratropical in nature, especially east of the International Date Line.

Southern Oscillation See *El Niño–Southern Oscillation (ENSO)*.

Specific humidity The specific humidity specifies the ratio of the mass of water vapour to the total mass of moist air. See also *Relative humidity*.

Stadial or stade A brief period of regional climatic cooling during a *glacial* or *interglacial* interval, often characterized by transient glacial advances. Stadials are generally of short duration (hundreds to a few thousand years) compared to glacial or interglacial intervals (lasting many thousands to tens of thousands of years). One example of a regional stadial event is based on millennial scale cooling recorded by oxygen *isotope* ratios in Greenland *ice cores*, the so called "Greenland Stadials" (Johnsen et al., 1992). See also *Interstadial or interstade*.

Statistical downscaling See *Downscaling*.

Steric sea level change See *Sea level change (sea level rise/sea level fall)*.

Storm surge The temporary increase, at a particular locality, in the height of the sea due to extreme meteorological conditions (low atmospheric pressure and/or strong winds). The storm surge is defined as being the excess above the level expected from the tidal variation alone at that time and place. See also *Sea level change (sea level rise/sea level fall)* and *Extreme sea level (ESL)*.

Storm tracks Originally, a term referring to the tracks of individual cyclonic weather systems, but now often generalized to refer to the main *regions* where the tracks of extratropical disturbances occur as sequences of low (cyclonic) and high (anticyclonic) pressure systems.

Storyline A way of making sense of a situation or a series of events through the construction of a set of explanatory elements. Usually, it is built on logical or causal reasoning. In *climate* research, the term storyline is used both in connection to *scenarios* as related to a future trajectory of the climate and *human systems* or to a weather or climate event. In this context, storylines can be used to describe plural, conditional possible futures or explanations of a current situation, in contrast to single, definitive futures or explanations.

Physical climate storyline
A self-consistent and plausible unfolding of a physical trajectory of the *climate system*, or a weather or climate event, on time scales from hours to multiple decades (Shepherd et al., 2018). Through this, storylines explore, illustrate and communicate *uncertainties* in the *climate system* response to *forcing* and in *internal variability*.

Scenario storyline
A narrative description of a *scenario* (or family of scenarios), highlighting the main scenario characteristics, relationships between key driving forces and the dynamics of their evolution.

Stratification Process of forming of layers of (*ocean*) water with different properties such as salinity, density and temperature that act as barrier for water mixing. The strengthening of near-surface stratification generally results in warmer surface waters, decreased oxygen levels in deeper water, and intensification of *ocean acidification (OA)* in the upper ocean.

Stratosphere The highly stratified region of the atmosphere above the *tropopause*, extending to about 50 km altitude. See also *Troposphere*.

Stratospheric aerosol injection (SAI) See *Solar radiation modification (SRM)*.

Stratosphere–troposphere exchange (STE) *Stratosphere–troposphere* exchange (STE) is understood as the *flux* of air or trace constituents across the *tropopause*, including both directions: the stratosphere to troposphere transport (STT) and troposphere to stratosphere transport (TST). STE is one of the key factors controlling the budgets of *ozone*, water vapour and other substances in both the *troposphere* and the lower *stratosphere*.

Stratospheric ozone Stratospheric ozone describes the *ozone (O_3)* that resides in the *stratosphere*, the region of the *atmosphere* which exists between 10 and 50 kilometres above the surface of the earth. Ninety percent of total-column ozone resides in the stratosphere. See also *Ozone layer* and *Ozone-depleting substances (ODSs)*.

Stratospheric polar vortex A large-scale region of cold air poleward of approximately 60 degrees that is contained by a strong westerly jet from the *tropopause* (8–10 km) to the stratopause (50–60 km) and that forms in each hemisphere during the winter half-year. Planetary waves can temporarily disrupt the vortex, producing easterly winds and rapid warming over polar regions in the *stratosphere*, and leading to substantial weakening or breakdown of the vortex.

Stratospheric sounding unit (SSU) A three-channel infrared sounder on operational U.S. National Oceanic and Atmospheric Administration (NOAA) polar-orbiting satellites. The three channels are used to determine profiles of temperature in the *stratosphere* (AMS, 2021).

Streamflow Water flow within a river channel, for example, expressed in $m^3 s^{-1}$. A synonym for river discharge.

Subduction *Ocean* process in which surface waters enter the ocean interior from the surface mixed layer through Ekman pumping and lateral *advection*. The latter occurs when surface waters are advected to a region where the local surface layer is less dense and therefore must slide below the surface layer, usually with no change in density.

Sudden stratospheric warming (SSW) A phenomena of rapid warming in the *stratosphere* at high latitudes (sometimes more than 50°C in 1–2 days) that can cause breakdown of *stratospheric polar vortices*.

Sulphur hexafluoride (SF_6) SF_6, a *greenhouse gas (GHG)*, is mainly used in heavy industry to insulate high-voltage equipment and to assist in the manufacturing of cable-cooling systems and semiconductors.

Sunspots Dark areas on the Sun where strong magnetic fields reduce the convection, causing a temperature reduction of about 1500 K compared to the surrounding regions. The number of sunspots is higher during periods of higher *solar activity* and varies in particular with the *solar cycle*.

Surface air temperature See *Land surface air temperature (LSAT)* and *Global mean surface air temperature (GSAT)*.

Surface mass balance (SMB) See *Mass balance/budget (of glaciers or ice sheets)*.

Surface temperature See *Global mean surface air temperature (GSAT)*, *Global mean surface temperature (GMST)*, *Land surface air temperature (LSAT)* and *Sea surface temperature (SST)*.

Surprises A class of *risk* that can be defined as low-*likelihood* but well-understood events and events that cannot be predicted with current understanding (see Section 1.4.4.3 in AR6 WGI Chapter 1).

Swash See *Extreme sea level (ESL)*.

Talik A layer or body of unfrozen ground in a *permafrost* area due to a local anomaly in thermal, hydrological, hydrogeological or hydrochemical conditions (IPA, 2005).

Technical potential See *Mitigation potential*.

Teleconnection Association between *climate* variables at widely separated, geographically fixed locations related to each other through physical processes and oceanic and/or atmospheric dynamical pathways. Teleconnections can be caused by several climate phenomena, such as Rossby wave-trains, mid-latitude jet and *storm track* displacements, fluctuations of the *Atlantic Meridional Overturning Circulation (AMOC)*, fluctuations of the *Walker circulation*, etc. They can be initiated by *modes of climate variability*, thus providing the development of remote climate *anomalies* at various temporal lags. See also *Teleconnection pattern*.

Teleconnection pattern Spatial structure of climate *anomalies* that are linked to each other through *teleconnection* processes or that are the *large-scale* fingerprint of *modes of climate variability*. Teleconnection patterns can be visualized using correlation and/or regression maps of *climate* variables with some *climate indices* (i.e., those derived from the temporal variation of the main modes of climate variability). They can also be obtained from principal component analysis, singular value decomposition/maximum covariance analysis, clustering based on spatial recurrence criteria, etc. See also Section Atlas.3.1 of the AR6 WGI report and *Teleconnection*.

Temperature overshoot Exceedance of a specified global warming level, followed by a decline to or below that level during a specified period of time (e.g., before 2100). Sometimes the magnitude and *likelihood* of the overshoot is also characterized. The overshoot duration can vary from one *pathway* to the next, but in most *overshoot pathways* in the literature and as referred to as overshoot pathways in the AR6, the overshoot occurs over a period of at least one decade and up to several decades. See also *Pathways*.

Terrestrial radiation Radiation emitted by the Earth's surface, the *atmosphere* and clouds. It is also known as thermal infrared or longwave radiation and is to be distinguished from the near-infrared radiation that is part of the solar spectrum. Infrared radiation, in general, has a distinctive range of wavelengths (spectrum) longer than the wavelength of the red light in the visible part of the spectrum. The spectrum of terrestrial radiation is almost entirely distinct from that of shortwave or *solar radiation* because of the difference in temperature between the Sun and the Earth–atmosphere system.

Thermal expansion See *Steric sea level change* (under *Sea level change (sea level rise/sea level fall)*).

Thermocline The layer of maximum vertical temperature gradient in the *ocean*, lying between the surface ocean and the abyssal ocean. In subtropical regions, its source waters are typically surface waters at higher latitudes that have subducted (see *Subduction*) and moved equatorward. At high latitudes, it is sometimes absent, replaced by a *halocline*, which is a layer of maximum vertical salinity gradient.

Thermohaline circulation (THC) See *Meridional overturning circulation (MOC)*.

Thermokarst Process by which characteristic landforms result from thawing of ice-rich *permafrost* or melting of massive ice (IPA, 2005).

Thermosteric See *Sea level change (sea level rise/sea level fall)*.

Tide gauge A device at a coastal or deep-sea location that continuously measures the level of the sea with respect to the adjacent land. Time averaging of the sea level so recorded gives the observed secular changes of the relative sea level.

Time of emergence (ToE) Time when a specific *anthropogenic* signal related to *climate change* is statistically detected to emerge from the background noise of natural *climate variability* in a *reference period*, for a specific *region* (Hawkins and Sutton, 2012). See also *Emergence (of the climate signal)*.

Tipping element A component of the Earth system that is susceptible to a *tipping point*.

Tipping point A critical threshold beyond which a system reorganizes, often abruptly and/or irreversibly. See also *Tipping element*, *Irreversibility* and *Abrupt change*.

Total alkalinity Total Alkalinity (AT) is a measurable parameter of the seawater acid–base system which, when expressed in micromoles per kilogram of seawater, is a conservative variable both on mixing and for changes in temperature and/or pressure. Changes in total alkalinity in the *oceans* can result from a variety of biogeochemical processes that affect the acid–base composition of the seawater itself. However, its value is not affected by the exchange of *carbon dioxide* gas between seawater and the *atmosphere*. Measurements of total alkalinity can thus be used to help study these biogeochemical processes and can also be used to help calculate the state of the seawater acid–base system. Total alkalinity is most commonly measured using an acidimetric titration technique that determines how much acid is required to titrate a seawater sample to a specified equivalence point.

Total carbon budget See *Carbon budget*.

Total solar irradiance (TSI) The total amount of *solar radiation* in watts per square metre received outside the Earth's *atmosphere* on a surface normal to the incident radiation and at the Earth's mean distance from the Sun. Reliable measurements of solar radiation can only be made from space, and the precise record extends back only to 1978. Variations of a few tenths of a percent are common, usually associated with the passage of *sunspots* across the solar disk. The *solar cycle* variation of TSI is of the order of 0.1% (AMS, 2021). See also *Insolation*.

Total water level See *Extreme sea level (ESL)*.

Trace gas A minor constituent of the *atmosphere*, next to nitrogen and oxygen that together make up 99% of all volume. The most important trace gases contributing to the *greenhouse effect* are *carbon dioxide (CO_2)*, *ozone (O_3)*, *methane (CH_4)*, *nitrous oxide (N_2O)*, perfluorocarbons (PFCs), *chlorofluorocarbons (CFCs)*, *hydrofluorocarbons (HFCs)*, *sulphur hexafluoride (SF_6)* and water vapour (H_2O).

Transient climate response (TCR) See *Climate sensitivity*.

Transient climate response to cumulative CO_2 emissions (TCRE) See *Climate sensitivity*.

Tree rings Concentric rings of secondary wood evident in a cross section of the stem of a woody plant. The difference between the dense, small-celled late wood of one season and the wide-celled early wood of the following spring enables the age of a tree to be estimated, and the ring widths or density can be related to *climate* parameters such as temperature and precipitation.

Tropical Atlantic modes See *Tropical Atlantic Variability (TAV)*.

Tropical Atlantic Variability (TAV) A generic term to describe the *climate variability* of the tropical Atlantic which is dominated at interannual to decadal time scales by two main climate modes: the *Atlantic Zonal Mode (AZM)* and the *Atlantic Meridional Mode (AMM)*. The Atlantic Zonal Mode, also commonly referred to as the Atlantic Niño or Atlantic equatorial mode, is associated with *sea surface temperature* anomalies near the equator, peaking in the eastern basin, while the Atlantic meridional mode is characterized by an inter-hemispheric gradient of sea surface temperature and wind anomalies. Both modes are associated with significant *teleconnections* over Africa and South America.

Atlantic Meridional Mode (AMM) The Atlantic Meridional Mode (AMM) refers to the interannual to *decadal variability* of the cross-equatorial *sea surface temperature* gradients and surface wind anomalies in the tropical Atlantic. It modulates the strength and latitudinal shifts of the *Inter-tropical Convergence Zone (ITCZ)*, which impacts regional rainfall over Northeast Brazil and Atlantic *hurricane* activity. See Section AIV.2.5 in Annex IV of the AR6 WGI report.

Atlantic Zonal Mode (AZM) An equatorial coupled mode in the Atlantic similar to *El Niño–Southern Oscillation (ENSO)* in the Pacific, and therefore sometimes referred to as the Atlantic Niño. The AZM is associated with *sea surface temperature* anomalies near the equatorial Atlantic and rainfall disturbances over the African monsoon domain. Its variations are mostly observed in the interannual scale. It is called also Atlantic equatorial mode. See Section AIV.2.5 in Annex IV of the AR6 WGI report.

Tropical cyclone The general term for a strong, cyclonic-scale disturbance that originates over tropical *oceans*. Distinguished from weaker systems (often named tropical disturbances or depressions) by exceeding a threshold wind speed. A tropical storm is a tropical cyclone with one-minute average surface winds between 18 and 32 m s^{-1}. Beyond 32 m s^{-1}, a tropical cyclone is called a hurricane, typhoon, or cyclone, depending on geographic location.

Tropopause The boundary between the *troposphere* and the *stratosphere*. It ranges from 8–9 km at high latitudes to 15–16 km in the tropics.

Troposphere The lowest part of the *atmosphere*, below the *tropopause*, where clouds and weather phenomena occur. In the troposphere, temperatures generally decrease with height. See also *Stratosphere*.

Tropospheric ozone See *Ozone (O_3)* and *Ground-level ozone*.

Tundra A treeless biome characteristic of polar and alpine regions.

Turnover time (T) See *Lifetime*.

Typhoon See *Tropical cyclone*.

Typological domains See *Typological regions*.

Typological regions Regions of the Earth that share one or more specific features (known as 'typologies'), such as geographic location (e.g., coastal), physical processes (e.g., *monsoons*), and biological (e.g., *coral reefs*, tropical *forests*), geological (e.g., mountains) or *anthropogenic* (e.g., *megacities*) formation, and for which it is useful to consider the common *climate* features. Typological regions are smaller than climatic zones (e.g., a mountain region) and can be discontinuous (e.g., a group of megacities affected by the *urban heat island* effect, or monsoon regions).

Uncertainty A state of incomplete knowledge that can result from a lack of information or from disagreement about what is known or even knowable. It may have many types of sources, from imprecision in the data to ambiguously defined concepts or terminology, incomplete understanding of critical processes, or uncertain *projections* of human behaviour. Uncertainty can therefore be represented by quantitative measures (e.g., a *probability density function*) or by qualitative statements (e.g., reflecting the judgement of a team of experts) (see Moss and Schneider, 2000; IPCC, 2004; Mastrandrea et al., 2010). See also *Confidence* and *Likelihood*.

Deep uncertainty
A situation of deep uncertainty exists when experts or stakeholders do not know or cannot agree on: (1) appropriate conceptual models that describe relationships among key driving forces in a system; (2) the probability distributions used to represent uncertainty about key variables and parameters; and/or (3) how to weigh and value desirable alternative outcomes (Lempert et al., 2003).

Interpolation uncertainty
Uncertainty arising from a statistical or physical model-based interpolation of a field between available estimates to create a more spatio-temporally complete estimate.

Sampling uncertainty
Uncertainty arising from incomplete or uneven availability of measurements in either space or time or both.

Trend estimates uncertainty
Uncertainty arising from data fitting to a time-series with potential non-linear and autoregressive character.

United Nations Framework Convention on Climate Change (UNFCCC) The UNFCCC was adopted in May 1992 and opened for signature at the 1992 Earth Summit in Rio de Janeiro. It entered into force in March 1994 and as of September 2020 had 197 Parties (196 States and the European Union). The Convention's ultimate objective is the 'stabilization of greenhouse gas concentrations in the atmosphere at a level that would prevent dangerous anthropogenic interference with the climate system' (UNFCCC, 1992). The provisions of the Convention are pursued and implemented by two further treaties: the Kyoto Protocol and the Paris Agreement.

Uptake The transfer of substances (such as carbon) or energy (e.g., heat) from one compartment of a system to another; for example, in the Earth system from the *atmosphere* to the *ocean* or to the land. See also *Pool, carbon and nitrogen*, *Reservoir*, *Sequestration*, *Sequestration potential, Sink* and *Source*.

Upwelling region A region of an *ocean* where cold, typically nutrient-rich waters well up from the deep ocean.

Urban heat island (UHI) The relative warmth of a city compared with surrounding rural areas, associated with heat trapping due to the close proximity of tall buildings, the heat-absorbing properties of urban building materials, reduced ventilation, and heat generated directly from human activities. See also *Urbanization*.

Urbanization In the WGI report, urbanization is used to mean the process of soil sealing with the change of natural *land cover* to built environment and urban areas, together with its associated *albedo* changes, and increased surface *runoff* and elevated warming. See also *Urban heat island (UHI)*.

Ventilation The exchange of *ocean* properties with the atmospheric surface layer such that property concentrations are brought closer to equilibrium values with the *atmosphere* (AMS, 2021), and the processes that propagate these properties into the ocean interior.

Vertical land motion (VLM) The change in height of the land surface or the sea floor and can have several causes in addition to elastic deformation associated with contemporary changes in *gravity, rotation and viscoelastic solid Earth deformation (GRD)* and viscoelastic deformation associated with *glacial isostatic adjustment (GIA)*. Subsidence (sinking of the land surface or sea floor) can, for instance, occur through compaction of alluvial sediments in deltaic regions, removal of fluids such as gas, oil, and water, or drainage of peatlands. Tectonic deformation of the Earth's crust can occur as a result of earthquakes and volcanic eruptions. See also *Sea level change (sea level rise/sea level fall)*.

Very short-lived halogenated substances (VSLSs) Very short-lived halogenated substances (VSLSs) are considered to include source gases (very short-lived halogenated substances present in the *atmosphere* in the form they were emitted from natural and *anthropogenic* sources), halogenated product gases arising from source gas degradation, and other sources of *tropospheric* inorganic halogens. VSLSs have tropospheric *lifetimes* of around 0.5 years or less.

Volatile organic compounds (VOCs) Important class of organic chemical air pollutants that are volatile at ambient air conditions. Other terms used to represent VOCs are hydrocarbons (HCs), reactive organic gases (ROGs) and non-methane volatile organic compounds (NMVOCs). NMVOCs are major contributors – together with nitrogen oxides (NO_x), and carbon monoxide (CO) – to the formation of photochemical oxidants such as *ozone* (O_3).

Biogenic volatile organic compounds (BVOCs)
Organic gas-phase compounds emitted from terrestrial and aquatic ecosystems that are critical in ecology and plant physiology, from abiotic and biotic stress functions to integrated components of metabolism. BVOCs are important in atmospheric chemistry as *precursors* for *ozone* (O_3) and secondary organic aerosol formation. Other terms used to represent BVOCs are hydrocarbons (HCs), reactive organic gases (ROGs) and non-methane volatile organic compounds (NMVOCs).

Vulnerability The propensity or predisposition to be adversely affected. Vulnerability encompasses a variety of concepts and elements including sensitivity or susceptibility to harm and lack of capacity to cope and adapt. See also *Exposure*, *Hazard* and *Risk*.

Walker circulation Direct thermally driven zonal overturning circulation in the *atmosphere* over the tropical Pacific Ocean, with rising air in the western and sinking air in the eastern Pacific.

Warm spell See *Heatwave*.

Water cycle See *Hydrological cycle*.

Water mass A body of *ocean* water with identifiable properties (temperature, salinity, density, chemical tracers) resulting from its unique formation process. Water masses are often identified through a vertical or horizontal extremum of a property such as salinity. North Pacific Intermediate Water (NPIW) and Antarctic Intermediate Water (AAIW) are examples of water masses.

Water security 'The capacity of a population to safeguard sustainable access to adequate quantities of acceptable quality water for sustaining livelihoods, human well-being, and socio-economic development, for ensuring protection against water-borne pollution and water-related disasters, and for preserving ecosystems in a climate of peace and political stability' (UN-Water, 2013).

Wave run-up See *Extreme sea level (ESL)*.

Wave setup See *Extreme sea level (ESL)*.

Weathering The gradual removal of atmospheric *carbon dioxide (CO_2)* through dissolution of silicate and carbonate rocks. Weathering may involve physical processes (mechanical weathering) or chemical activity (chemical weathering).

Well-mixed greenhouse gas A *greenhouse gas (GHG)* that has an atmospheric *lifetime* long enough (greater than several years) to be homogeneously mixed in the *troposphere*, and as such the global average mixing ratio can be determined from a network of surface observations. For many well-mixed greenhouse gases, measurements made in remote regions differ from the global mean by <15%.

West African monsoon (WAfriM) See *Global monsoon*.

West Antarctic Ice Sheet (WAIS) See *Ice sheet*.

Wetland Land that is covered or saturated by water for all or part of the year (e.g., *peatland*).

Younger Dryas The period from approximately 12.9 to 11.7 ka (thousand years before 1950), during the *last deglacial transition*, characterized by a temporary return to colder conditions in many locations, especially around the North Atlantic. See also *Stadial* and *Last deglacial transition*.

Zero emissions commitment See *Climate change commitment*.

References

AMS, 2021: Glossary of Meteorology. American Meteorological Society (AMS), Boston, MA, USA. Retrieved from: http://glossary.ametsoc.org.

Carson, M. and G. Peterson (eds.), 2016: *Arctic Resilience Report 2016*. Stockholm Environment Institute and Stockholm Resilience Centre, Stockholm, Sweden, 218 pp.

Blunier, T. and E.J. Brook, 2001: Timing of Millennial-Scale Climate Change in Antarctica and Greenland During the Last Glacial Period. *Science*, **291(5501)**, 109 LP – 112, doi:10.1126/science.291.5501.109.

Bond, G.C. and R. Lotti, 1995: Iceberg Discharges into the North Atlantic on Millennial Time Scales During the Last Glaciation. *Science*, **267(5200)**, 1005 LP – 1010, doi:10.1126/science.267.5200.1005.

Broecker, W.S., 1998: Paleocean circulation during the Last Deglaciation: A bipolar seesaw? *Paleoceanography*, 13(2), 119–121, doi:10.1029/97pa03707.

Clark, P.U. et al., 2009: The Last Glacial Maximum. *Science*, **325(5941)**, 710–714, doi:10.1126/science.1172873.

Cogley, J.G. et al., 2011: *Glossary of Glacier Mass Balance and Related Terms*. IHP-VII Technical Documents in Hydrology No. 86, IACS Contribution No. 2, UNESCO-IHP, Paris, France, 114 pp.

Dansgaard, W. et al., 1993: Evidence for general instability of past climate from a 250-kyr ice-core record. *Nature*, **364(6434)**, 218–220, doi:10.1038/364218a0.

Duplessy, J.C., G. Delibrias, J.L. Turon, C. Pujol, and J. Duprat, 1981: Deglacial warming of the northeastern Atlantic ocean: correlation with the paleoclimatic evolution of the european continent. *Palaeogeography, Palaeoclimatology, Palaeoecology*, **35(C)**, 121–144, doi:10.1016/0031-0182(81)90096-1.

Fairbanks, R.G., 1989: A 17,000-year glacio-eustatic sea level record: influence of glacial melting rates on the Younger Dryas event and deep-ocean circulation. *Nature*, **342(6250)**, 637–642, doi:10.1038/342637a0.

FAO, 2007: *Land evaluation: Towards a revised framework.* Land and Water Discussion Paper 6, Food and Agriculture Organisation of the United Nations (FAO), Rome, Italy, 124 pp., www.fao.org/nr/lman/docs/lman_070601_en.pdf.

Gbeckor-Kove, N., 1989: Lectures on Drought and Desertification Delivered at the Training Session in Agrometeorology (Crop–Weather Modelling) – 14–24 November 1988, Munoz, Nueva Ecija, Philippines, by Mr. N. Gbeckor-Kove, WMO Secretariat. In: *Drought and Desertification.* WMO/TD-No.286, World Meteorological Organization (WMO), Geneva, Switzerland, pp. 41–73, https://library.wmo.int/doc_num.php?explnum_id=9500.

Giardino, J.R., N.R. Regmi, and J.D. Vitek, 2011: Rock Glaciers. In: *Encyclopedia of Snow, Ice and Glaciers*. Springer Netherlands, Dordrecht, The Netherlands, pp. 943–948, doi:10.1007/978-90-481-2642-2_453.

Gowan, E.J. et al., 2021: A new global ice sheet reconstruction for the past 80 000 years. *Nature Communications*, **12(1)**, 1199, doi:10.1038/s41467-021-21469-w.

Gregory, J.M. et al., 2019: Concepts and Terminology for Sea Level: Mean, Variability and Change, Both Local and Global. *Surveys in Geophysics*, **40(6)**, 1251–1289, doi:10.1007/s10712-019-09525-z.

Harris, S.A. et al., 1988: *Glossary of Permafrost and Related Ground-Ice Terms*. Technical Memorandum No. 142, Permafrost Subcommittee, Associate Committee on Geotechnical Research, National Research Council of Canada, Ottawa, ON, Canada, 159 pp., doi:10.4224/20386561.

Hawkins, E. and R. Sutton, 2012: Time of emergence of climate signals. *Geophysical Research Letters*, **39(1)**, doi:10.1029/2011gl050087.

Haywood, A.M. et al., 2016: The Pliocene Model Intercomparison Project (PlioMIP) Phase 2: scientific objectives and experimental design. *Climate of the Past*, **12(3)**, 663–675, doi:10.5194/cp-12-663-2016.

Hewitt, C., S. Mason, and D. Walland, 2012: The Global Framework for Climate Services. *Nature Climate Change*, **2(12)**, 831–832, doi:10.1038/nclimate1745.

IPA, 2005: *Multi-language Glossary of Permafrost and Related Ground-Ice Terms*. International Permafrost Association (IPA), 159 pp., https://globalcryospherewatch.org/reference/glossary_docs/Glossary_of_Permafrost_and_Ground-Ice_IPA_2005.pdf.

Delaloye, R. and T. Echelard (eds.), 2020: *Towards standard guidelines for inventorying rock glaciers: Baseline concepts (Version 4.0)*. International Permafrost Association (IPA) Action Group Rock glacier inventories and kinematics, Longyearbyen, Svalbard, 13 pp., https://bigweb.unifr.ch/Science/Geosciences/Geomorphology/Pub/Website/IPA/Guidelines/V4/200117_Baseline_Concepts_Inventorying_Rock_Glaciers_V4.pdf.

IPCC, 2004: IPCC Workshop on Describing Scientific Uncertainties in Climate Change to Support Analysis of Risk and of Options [Manning, M.R., M. Petit, D. Easterling, J. Murphy, A. Patwardhan, H.-H. Rogner, R. Swart, and G. Yohe (eds.)]. Intergovernmental Panel on Climate Change (IPCC), Geneva, Switzerland, 138 pp., https://www.ipcc.ch/event/ipcc-workshop-on-describing-scientific-uncertainties-in-climate-change-to-support-analysis-of-risk-and-of-options.

IPCC, 2006: 2006 IPCC Guidelines for National Greenhouse Gas Inventories, Prepared by the National Greenhouse Gas Inventories Programme. [Eggleston, H.S., L. Buendia, K. Miwa, T. Ngara, and K. Tanabe (eds.)]. Institute for Global Environmental Strategies (IGES), Hayama, Japan, www.ipcc-nggip.iges.or.jp/public/2006gl/index.html.

IPCC, 2011: Workshop Report of the Intergovernmental Panel on Climate Change Workshop on Impacts of Ocean Acidification on Marine Biology and Ecosystems. [Field, C.B., V. Barros, T.F. Stocker, D. Qin, K.J. Mach, G.-K. Plattner, M.D. Mastrandrea, M. Tignor, and K.L. Ebi (eds.)]. IPCC Working Group II Technical Support Unit, Carnegie Institution, Stanford, California, United States of America, 164 pp., www.ipcc.ch/publication/ipcc-workshop-on-ocean-acidification-on-marine-biology-and-ecosystems.

IPCC, 2019: 2019 Refinement to the 2006 IPCC Guidelines for National Greenhouse Gas Inventories. [Calvo Buendia, E., K. Tanabe, A. Kranjc, J. Baasansuren, M. Fukuda, S. Ngarize, A. Osako, Y. Pyrozhenko, P. Shermanau, and S. Federici (eds.)]. Intergovernmental Panel on Climate Change (IPCC), Geneva, Switzerland, www.ipcc-nggip.iges.or.jp/public/2019rf/index.html.

ISO, 2014: ISO 16559:2014(en). Solid biofuels – Terminology, definitions and descriptions. International Standards Organisation (ISO). Retrieved from: www.iso.org/obp/ui/#iso:std:iso:16559:ed-1:v1:en.

Johnsen, S.J. et al., 1992: Irregular glacial interstadials recorded in a new Greenland ice core. *Nature*, **359(6393)**, 311–313, doi:10.1038/359311a0.

Kageyama, M. et al., 2017: The PMIP4 contribution to CMIP6 – Part 4: Scientific objectives and experimental design of the PMIP4-CMIP6 Last Glacial Maximum experiments and PMIP4 sensitivity experiments. *Geoscientific Model Development*, **10(11)**, 4035–4055, doi:10.5194/gmd-10-4035-2017.

Kitoh, A. et al., 2013: Monsoons in a changing world: A regional perspective in a global context. *Journal of Geophysical Research Atmospheres*, **118(8)**, 3053–3065, doi:10.1002/jgrd.50258.

Lambeck, K., H. Rouby, A. Purcell, Y. Sun, and M. Sambridge, 2014: Sea level and global ice volumes from the Last Glacial Maximum to the Holocene. *Proceedings of the National Academy of Sciences*, **111(43)**, 15296–15303, doi:10.1073/pnas.1411762111.

Lempert, R.J., S.W. Popper, and S.C. Bankes, 2003: *Shaping the Next One Hundred Years: New Methods for Quantitative, Long-Term Policy Analysis*. RAND Corporation, Santa Monica, CA, USA, 186 pp.

MA, 2005: Appendix D: Glossary. In: *Ecosystems and Human Well-being: Current States and Trends. Findings of the Condition and Trends Working Group* [Hassan, R., R. Scholes, and N. Ash (eds.)]. Millennium Ecosystem Assessment (MA). Island Press, Washington, DC, USA, pp. 893–900.

Mastrandrea, M.D. et al., 2010: *Guidance Note for Lead Authors of the IPCC Fifth Assessment Report on Consistent Treatment of Uncertainties*. Intergovernmental Panel on Climate Change (IPCC), Geneva, Switzerland, 6 pp., www.ipcc.ch/publication/ipcc-cross-working-group-meeting-on-consistent-treatment-of-uncertainties.

Mix, A.C., W.F. Ruddiman, and A. McIntyre, 1986: Late Quaternary paleoceanography of the Tropical Atlantic, 1: Spatial variability of annual mean sea-surface temperatures, 0–20,000 years B.P.. *Paleoceanography*, **1(1)**, 43–66, doi:10.1029/pa001i001p00043.

Mix, A.C., E. Bard, and R. Schneider, 2001: Environmental processes of the ice age: land, oceans, glaciers (EPILOG). *Quaternary Science Reviews*, **20(4)**, 627–657, doi:10.1016/s0277-3791(00)00145-1.

Moss, R.H. and S.H. Schneider, 2000: Uncertainties in the IPCC TAR: Recommendations to Lead Authors for More Consistent Assessment and Reporting. In: *Guidance Papers on the Cross Cutting Issues of the Third Assessment Report of the IPCC* [Pachauri, R., T. Taniguchi, and K. Tanaka (eds.)]. Intergovernmental Panel on Climate Change (IPCC), Geneva, Switzerland, pp. 33–51.

Moss, R.H. et al., 2010: The next generation of scenarios for climate change research and assessment. *Nature*, **463(7282)**, 747–756, doi:10.1038/nature08823.

NOAA, 2021: What is an iceberg? National Oceanic and Atmospheric Administration (NOAA). National Ocean Service website. Retrieved from: https://oceanservice.noaa.gov/facts/iceberg.html.

Pongratz, J. et al., 2018: Models meet data: Challenges and opportunities in implementing land management in Earth system models. *Global Change Biology*, **24(4)**, 1470–1487, doi:10.1111/gcb.13988.

Ralph, F.M., M.D. Dettinger, M.M. Cairns, T.J. Galarneau, and J. Eylander, 2018: Defining "Atmospheric River": How the Glossary of Meteorology Helped Resolve a Debate. *Bulletin of the American Meteorological Society*, **99(4)**, 837–839, doi:10.1175/bams-d-17-0157.1.

Schwartz, S.E. and P. Warneck, 1995: Units for use in atmospheric chemistry (IUPAC Recommendations 1995). *Pure and Applied Chemistry*, **67(8/9)**, 1377–1406, http://publications.iupac.org/pac/1995/pdf/6708x1377.pdf.

Shepherd, T.G. et al., 2018: Storylines: an alternative approach to representing uncertainty in physical aspects of climate change. *Climatic Change*, **151(3–4)**, 555–571, doi:10.1007/s10584-018-2317-9.

Steffen, W. et al., 2016: Stratigraphic and Earth System approaches to defining the Anthropocene. *Earth's Future*, **4(8)**, 324–345, doi:10.1002/2016ef000379.

Stocker, T.F. and S.J. Johnsen, 2003: A minimum thermodynamic model for the bipolar seesaw. *Paleoceanography*, **18(4)**, 1087, doi:10.1029/2003pa000920.

Türkeş, M., 1999: Vulnerability of Turkey to Desertification With Respect to Precipitation and Aridity Conditions. *Turkish Journal of Engineering and Environmental Sciences*, **23**, 363–380.

UN, 1992: Article 2: Use of Terms. In: *Convention on Biological Diversity*. United Nations (UN), pp. 3–4, www.cbd.int/doc/legal/cbd-en.pdf.

UNCCD, 1994: *United Nations Convention to Combat Desertification in countries experiencing serious drought and/or desertification, particularly in Africa*. 58 pp., https://treaties.un.org/doc/Treaties/1996/12/19961226%2001-46%20PM/Ch_XXVII_10p.pdf.

UNESCO/IASH/WMO, 1970: *Seasonal snow cover: A guide for measurement, compilation and assemblage of data*. United Nations Educational, Scientific and Cultural Organization (UNESCO), Paris, France, 38 pp.

UNFCCC, 1992: *United Nations Framework Convention on Climate Change*. FCCC/INFORMAL/84, United Nations Framework Convention on Climate Change (UNFCCC), 24 pp., https://unfccc.int/resource/docs/convkp/conveng.pdf.

UNFCCC, 2021a: Reporting and accounting of LULUCF activities under the Kyoto Protocol. United Nations Framework Convention on Climate Change (UNFCCC). Retrieved from: https://unfccc.int/topics/land-use/workstreams/land-use-land-use-change-and-forestry-lulucf/reporting-and-accounting-of-lulucf-activities-under-the-kyoto-protocol.

UNFCCC, 2021b: Reporting and Review under the Paris Agreement. United Nations Framework Convention on Climate Change (UNFCCC). Retrieved from: https://unfccc.int/process-and-meetings/transparency-and-reporting/reporting-and-review-under-the-paris-agreement.

UNGA, 2016: *Report of the open-ended intergovernmental expert working group on indicators and terminology relating to disaster risk reduction*. A/71/644, United Nations General Assembly (UNGA), 41 pp., https://digitallibrary.un.org/record/852089.

UN-OHRLLS, 2011: *Small Island Developing States: Small Islands Big(ger) Stakes*. Office for the High Representative for the Least Developed Countries, Landlocked Developing Countries and Small Island Developing States (UN-OHRLLS), New York, NY, USA, 32 pp.

UN-OHRLLS, 2018: Small Island Developing States: Country profiles. Office for the High Representative for the Least Developed Countries, Landlocked Developing Countries and Small Island Developing States (UN-OHRLLS). Retrieved from: http://unohrlls.org/about-sids/country-profiles.

UN-Water, 2013: What is Water Security? Infographic. UN-Water, Geneva, Switzerland. Retrieved from: www.unwater.org/publications/water-security-infographic.

Walker, M. et al., 2019: Formal Subdivision of the Holocene Series/Epoch: A Summary. *Journal of the Geological Society of India*, **93(2)**, 135–141, doi:10.1007/s12594-019-1141-9.

Wiener, J.B. and J.D. Graham (eds.), 2009: *Risk vs Risk: Tradeoffs in Protecting Health and the Environment*. Harvard University Press, Cambridge, MA, USA, 352 pp.

Yokoyama, Y. et al., 2018: Rapid glaciation and a two-step sea level plunge into the Last Glacial Maximum. *Nature*, **559(7715)**, 603–607, doi:10.1038/s41586-018-0335-4.

Zscheischler, J. et al., 2018: Future climate risk from compound events. *Nature Climate Change*, **8(6)**, 469–477, doi:10.1038/s41558-018-0156-3.